Reinhard Brandner

Stochastic System Actions and Effects in Engineered Timber Products and Structures

Monographic Series TU Graz

Timber Engineering & Technology

Series Editors

G. Schickhofer Institute of Timber Engineering and Wood Technology
R. Brandner Institute of Timber Engineering and Wood Technology

Monographic Series TU Graz

Timber Engineering & Technology **Volume 2**

Reinhard Brandner

Stochastic System Actions and Effects in Engineered Timber Products and Structures

---

This work is based on the dissertation *"Stochastic System Actions and Effects in Engineered Timber Products and Structures"*, presented by Reinhard Brandner at Graz University of Technology, Institute of Timber Engineering and Wood Technology in June 2012.
Supervisors: G. Schickhofer (Graz University of Technology), E. Stadlober (Graz University of Technology)

Bibliographic information published by Die Deutsche Bibliothek.
Die Deutsche Bibliothek lists this publication in the Deutsche Nationalbibliografie; detailed bibliographic data are available at http://dnb.ddb.de.

The promotion of the Land Steiermark, Referat für Wissenschaft und Forschung, Abteilung 8 Wissenschaft und Gesundheit by funding the costs for printing and publication has to be gratefully acknowledged.

Das Land Steiermark
➔ Wissenschaft

Cover photo Wenner Bridge at St. Georgen, Styria / A (source: Gerhard Schickhofer

Layout Wolfgang Karl, TU Graz / Universitätsbibliothek
Printed by TU Graz / Büroservice

Verlag der Technischen Universität Graz
www.ub.tugraz.at/Verlag
ISBN: 978-3-85125-263-7 (print)

PREFACE OF THE MONOGRAPHIC SERIES

Composing a scientific work in terms of a dissertation constitutes a supremely personal concern of a cognition-oriented extension of knowledge. After having finalised and published such a work it is the aim to conduct a liberal, scientific discourse with an interested and objective scientific community. This circumstance together with the associated possibility to discuss this scientific work have to be accentuated especially in times were the amount of applied research is increasing. In this spirit: **The personal liberty in research starts at that point where the externally demanded applicability ends**.

With the monographic series **Timber Engineering & Technology (TET)** of the Institute of Timber Engineering and Wood Technology the publishers aim on providing the community with fundamental works of the area of expertise. With regards to content this is judged as a contribution for an outstanding and open-minded scientific discourse among experts. Citing **B. von Chartes** (freely translated): **"…we are like dwarfs on the shoulders of giants, so that we can see more than they, and things at a greater distance, not by virtue of any sharpness of sight on our part, or any physical distinction, but because we are carried high and raised up by their giant size."**. Following this, today's state-of-the-art together with the own scientific work counts as basis of the next generations, thereby providing those fundamentals what from innovations can be derived in succession.

Graz, February 2013, Univ.-Prof. Dipl.-Ing. Dr.techn. Gerhard Schickhofer

Content

Abstract

Stochastic System Actions and Effects in Engineered Timber Products and Structures

Within the last decades and supported by progress made in adhesive technology high performing and versatile applicable engineered timber products have been developed. After classification and subsequent bonding of the raw material these products show high resistance in strength and stiffness and allow column-free overspan of large areas. The connection of these system products to structures is made by nodes which itself mostly consist of connectors arranged in groups. Thus the composition of elements to systems can be observed at least on three hierarchies: (1) within the hierarchical structure of wood and timber, (2) within engineered timber products and groups of connectors, and (3) within the bearing structure, consisting of primary, secondary and tertiary structural elements. Despite common aspects between these hierarchies in respect to arrangement and common action of elements a general consideration is currently not available. Engineered timber products or the group action of connectors are in particular described by empirical models which are mostly established by fitting test data. Thereby and due to partly pronounced variations in material characteristics of timber significant influences on the group action of elements within systems can be observed.

In this thesis stochastic system actions and related effects of serial, parallel or serial-parallel arranged elements are analysed and the most influencing parameters are captured. Based on a comprehensive survey of literature on the three most important stochastic material models for linear-elastic brittle (WEIBULL, 1939; DANIELS, 1945; a.o.) and ideally linear-elastic-plastic material behaviour it is the aim to derive general laws for the description of serial and parallel system behaviour with the help of stochastic simulations. Based on these investigations and completed by additionally elaborated material specific facts of wood and timber on several hierarchies these general laws together with proposed models are exemplarily applied to and explained on engineered timber products. Thereby the aim is to show the relevance of stochastic methods as part of material and structure modelling, and additionally to provide the engineer with simplified models for the estimation of system behaviour.

Zusammenfassung (in German)

Stochastische Betrachtung von Systemprodukten und –strukturen aus Holz

In den letzten Jahrzehnten kam es, unterstützt durch die Fortschritte in der Klebetechnologie, zur Entwicklung leistungsfähiger und vielseitig einsetzbarer Bauprodukte aus Holz. Diese ermöglichen, nach gezielter Klassifizierung des Grundmaterials und anschließender Fügung, das Abtragen hoher Lasten und das stützenfreie Überspannen weiter Flächen. Die Fügung dieser Systemprodukte zu Tragstrukturen erfolgt über Verbindungsknoten aus meist zu Gruppen angeordneten Stiften. Das Fügen von Elementen zu Systemen kann somit auf zumindest drei Ebenen beobachtet werden: (1) innerhalb der hierarchischen Materialstruktur Holz, (2) in Systemprodukten aus Holz bzw. in der Gruppenwirkung von Verbindungsmitteln, und (3) in der Tragstruktur, bestehend aus primären, sekundären und tertiären Tragelementen. Trotz Gemeinsamkeiten zwischen den Systemebenen hinsichtlich der Anordnung und des gemeinsamen Wirkens der Elemente ist gegenwärtig eine übergeordnete Betrachtung nicht gegeben. Insbesondere bei Systemprodukten aus Holz oder der Gruppenwirkung von Verbindungsmitteln wird in der Beschreibung auf empirische, meist an Versuchsdaten gefittete Modelle, zurückgegriffen. Hierbei kommt es, bedingt durch die zum Teil ausgeprägten Streuungen in den Materialkennwerten von Holz, zu erheblichen Beeinflussungen auf die beobachtbare Gruppenwirkung der Elemente in Systemen.

Inhalt dieser Arbeit ist es die Anteile stochastischer Systemwirkungen seriell, parallel oder seriell-parallel gefügter Elemente allgemein zu studieren und wesentliche Einflussgrößen zu erfassen. Aufbauend auf einer umfangreichen Literaturrecherche betreffend die drei wesentlichen stochastischen Materialmodelle für linear-elastisch sprödes (WEIBULL, 1939; DANIELS, 1945; u.a.) und ideal linear-elastisch-plastisches Werkstoffverhalten gilt es mit Hilfe von stochastischen Simulationen allgemeine Gesetzmäßigkeiten aus seriellem sowie parallelem Systemverhalten abzuleiten. Darauf aufbauend und ergänzt durch erarbeitete spezifische Fakten zum Material Holz entlang seiner Hierarchiekette werden diese allgemein anwendbaren Gesetzmäßigkeiten und davon abgeleitete Modelle an ausgewählten Beispielen für Systemprodukte aus Holz angewendet und dargelegt. Hierbei ist es insbesondere das Ziel, einerseits die Relevanz der Stochastik in der Material- und Strukturmodellierung aufzuzeigen, und andererseits

dem Ingenieur vereinfachte Modelle zur Abschätzung des Systemverhaltens zur Verfügung zu stellen.

Preface

Timber is a natural, sustainable raw material. It is optimised for load bearing, nutrients and water transport and storage in the living tree. It is also outstanding for a remarkable variety of applications as building material in engineered light-weight structures with exhaustive strength vs. density ratios. It has shown its outstanding abilities since thousands of years and has thereby remarkably influenced the evolution of mankind including also the industrial revolution and nowadays art in construction and living. Timber constitutes a high efficient, porous raw material. It is used for various applications utilising single tissues or just chemical constituents for e.g. medicine and food industry up to cellulose fibres for high efficient composites and many more. Nevertheless, the main application worldwide in regard to deployed volume, beside about 50% share for energy, lies in the building industry sector, especially for load bearing purposes. In that field timber remarkable constitutes a material enabling slender, sophisticated and architectural appealing structures and art. Current developments in production techniques widen the product range further from primary linear elements to two dimensional structural components like cross laminated timber (CLT).

Nevertheless, in competition with building and construction materials like concrete and steel timber and timber products have to be on the edge of current and future requirements defined by the daily business and use. Generally spoken, building products have to be:

- economically affordable and compatible in respect to
  - price per unit volume / mass;
  - costs during the erection;
  - costs during life time and disposal / recycling;
- available in respect to time, quantity and quality;
- multifunctional in structural application and over the whole life time;
- reliable, safe and uniform and / or predictable in quality concerning its characteristics and behaviour in interaction with its environment.

Timber and timber products exhibit good and even best performance in nearly all categories listed above if the material is applied considering its natural characteristics. In the last decades and concerning the last three mentioned requirements the performance of timber was in particular pushed by the development of adhesive systems. These enable **bonding** of timber elements side-by-side, face-by-face or also lengthwise (cross-bonding) to linear, two- and three-dimensional system products which act as one unit and can be produced in practically every desired dimension. These developments together with advancements in **quality assurance** of timber in respect to grading or classification of the raw material enabled a revolution in the development of high efficient timber products for load bearing purposes characterised e.g. by

- classified base material of a defined and standardised quality according international standards (e.g. EN 14081, EN 338);
- internationally standardised material and product characteristics (e.g. EN 338, EN 1194, PREN 14080 and several technical approvals);
- defined, regulated and limited product and material characteristics in respect to dimension, moisture content, surface and appearance.

This revolution lead to product developments like finger jointed construction timber (FJCT), duo- and trio-beams, glued laminated timber (GLT), cross laminated timber (CLT), laminated veneer lumber (LVL) and oriented strand boards (OSB). All these products are characterisable as systems composed of elements and components like beams, boards, veneers or strands which are forced to interact within the product due to a rigid or quasi-rigid connection performed by bonding. Even the material itself act as a system composed of elements as representatives of lower hierarchical levels of the material structure. Through this interaction homogenisation effects are activated which reduce the variability of characteristic properties, e.g. physical properties like strength, stiffness and density. This enables firstly a higher reliability in compliance of product characteristics, and secondly an enhancement of performance especially of the bearing capacity. The last one follows from increasing design relevant properties on lower quantile levels (e.g. 5 %-quantiles). The development and advances in the field of engineered **connection techniques** (e.g. dowel-type fasteners for shearing, self-tapping full-threaded screws for withdrawl) enable efficient and high performing erection and establishment of timber constructions leading further to system interaction on the level of load bearing structures.

Beside all these essential impacts and developments consistent characterisation of raw, graded and classified material is lacking. There exists no consistent modelling of timber products for example with starting point at the performance of the base material. Nevertheless, this is required if the obvious interactions of positive and negative system effects are recognised as worthful for consideration.

The main focus of this work is on one specific topic of all possible applications of timber. It concentrates on the load bearing behaviour of timber and timber products and tries to span the scientific work from bar-shaped linear members like trusses and beams, to two dimensional slab- and plate-like elements up to connection systems. It concentrates on the term “system”, characterised by the arrangement of elements and their interactions observable as system behaviour or “system action”, divided into “serial” and “parallel” actions and serial and parallel “system effects” as logical consequences, the output of the system action. Nevertheless, the more general work concerning parallel and serial system actions and effects is also applicable to other materials as well as familiar applications described in this manuscript. It has to be clarified that this manuscript focuses on the stochastic description of system behaviour. Nevertheless, the material behaviour and mechanics in respect to stresses and strains plays a major role and influence consequences of system action. As will be outlined in more detail afterwards perfect brittle failure characteristics in combination with perfect linear elastic material behaviour can be defined as the simplest case of material description. It can be modelled sufficiently by consideration of stochastic system effects under mechanical constraints. However, the system action itself will be always an interaction of mechanics and stochastics. In the opposite, perfect plastic material behaviour leads to a reduction of stochastic system effects on expectable values leading to a balancing of all effected and interacting elements in the system.

More generally, the interaction of elements can be treated (i) as a function of system size, (ii) in respect to the element arrangement in the system in respect to its stresses and strains, (iii) and in dependency of the material behaviour in the elastic / plastic region.

The present work supports the interested reader partially with simplified equations enabling considerations of treated system effects in standardised design procedures having in mind the theoretical background and descriptive boundary conditions of stochastics. The aim is to support the engineer with decisive and important information concerning system actions and effects and to provide to a certain degree the possibility to take into account the stochastics nature of materials.

A brief overview of the content: The thesis is subdivided in chapters which mirror the above mentioned aspects in a broader sense. The **first chapter** concentrates on the relevance of dispersion / statistical spread in general and discusses why it is impossible to neglect one of the main parameters for the description of materials, material behaviour and natural phenomena in general. In addition some statements and general definitions are given. **Chapter two** gives a brief overview and introduction to statistics and probability theory and delivers tools concentrating on definitions of some selected probability distributions, statistical theories and general statistical models. The reader familiar with this topic may skip this chapter. Nevertheless and in the opinion of the author the importance of the presented theory dedicates this chapter to the general part of the work and not to the annex. The **third chapter** focuses on serial and parallel system actions and related effects. After a general overview both aspects – serial and parallel – are discussed in detail concentrating on stochastic effects. The results are applicable also for other materials as wood and even for serial and parallel systems in general. **Chapter four** gives some comments on scaling and hierarchical levels of wood and timber and its tissues at first time concentrating on the focused material timber. Some general thoughts on scaling and analogies between hierarchical levels are discussed. **Chapter five** exemplarily demonstrates the application of so far compiled work and gives information on modelling of various effects in timber and timber products with respect to its main characteristics strength, stiffness and density. Starting with an introductory section, a review of literature concerning spatial correlation as well as serial and parallel effects, this chapter provides the basis for the stochastic consideration of system effects in structural timber and system products. Chaper five may be seen as the most important chapter of the work presenting applications and equations relevant to practical aspects and standardisation. The manuscript finishes with a closing **chapter six** reflecting and displaying some general outcomes and conclusions of the work.

Acknowledgments: The herein presented thesis would not have been possible without support by a number of persons to whom I owe gratidude for a diversity of reasons.

First of all I would like to express my sincere gratidude to Univ.-Prof. Dipl.-Ing. Dr.techn. Gerhard Schickhofer for offering me an assistant professor position at the Institute of Timber Engineering and Wood Technology at Graz University of Technology as well as for the opportunity to lead and conduct numerous research projects within the last eight years mainly performed at or in collaboration with the competence centre holz.bau forschungs gmbh. His inspiring and motivating character which enthusiasticly

directed me to the field of science with focus on timber engineering, the time for discussions and for taking over the supervision have to be especially acknowledged. In this respect I would also like to express my sincere gratidude to Univ.-Prof. Dipl.-Ing. Dr.techn. Ernst Stadlober as co-supervisor, but in particular for inspiring me to deepen my knowledge in statistics and probability theory and to combine both research fields of timber engineering and stochastics with focus on stochastic material modelling. The numerous fruitful discussions, time and effort conducted for reading and reviewing my work and his enthusiasm during our meetings are highly appreciated. I want to express my general gratidude again to both for encouraging me to new perceptions and view on topics and scientific challenges. I would like to express my great thank to my colleague Dipl.-Ing. Dr.-techn. Alexandra Thiel for her willingness to spend time for discussions and for her support in programming as well as her patience when I was reporting on progress and latest findings of my work.

The research performed would partly not have been done without the financial support in particular of research projects MMSM 2.2.1 stoch_mod and 2.2.3 sfem_mat of the K-Project “timber.engineering” (01/2008 till 12/2012) conducted at the competence centre holz.bau forschungs gmbh and performed in collaboration with the Institute of Timber Engineering and Wood Technology at Graz Unversity of Technology and the industrial partners involved in these research projects. The research projects are fostered through the funds of the Federal Ministry of Economics, Family and Youth, the Federal Ministry of Transport, Innovation and Technology, the Styrian Business Promotion Agency Association and the Province of Styria (A14).

Finally, I would like to express my sincere gratidude, my greatest thank to my closest relatives, my wife Martina, my parents and parents in law Maria, Gerhard, Elisabeth and Manfred and to all of mine and my wife’s family members who kept on encouraging me to conduct this work, who supported me in progress and regress just by understanding and just for being here and jointly went the way with me. Special thanks go to my love Martina. I thank you especially for your continuous motivation, understanding, patience and for listening to me when I was enthusiastically refering on my work or just destroyed after recognising mistakes or suffering from regress or too slow progress, for keeping me in contact with life in particular in periods of intensive focus on work. Thank you just for standing behind me and being on my side …

Chapter 1

Introduction

The variability, dispersion or statistical spread of natural phenomena and in particular of natural materials defines a critical feature and the driving force of this work. This chapter concentrates on the general topic of varying properties and delivers some essential background in demonstrating the necessity of stochastics as an important part, in but least important as the mechanics for the description of materials and their structural behaviour. The chapter starts with a general introduction on motivation and relevance of this work for timber engineering and for primary as well as secondary timber industry. The general applicability of some outcomes is discussed also for other materials and system considerations. A subsequent section concentrates in more detail on the dispersion, the statistical spread or variability and how these uncertainties can be classified and eventually influenced as well. The last section is dedicated to a short and general discussion on systems and to impacts on their modelling.

1.1 General Introduction and Overview of the Work

Wood and timber are fascinating natural materials designed by nature and designed as load bearing material, optimised on nano, micro and macro structural level. The material provides maximum resistance and multifunctionality in respect to mechanical characteristics, e.g. strength, stiffness, nutrients and water transport and storage with a minimum of mass. These features are consequences of an optimisation process provided by nature focusing on minimisation of used material (→ resource prevention). Thereby parts and tissues like the shape of a tree, branches and cells are optimised in form and function. Some examples are the conical shape of the trunk, the inclusion of branches in

the structure of the trunk and the internal system able to react on externally applied stresses, by being generally pre-stressed (internal stresses) on the outside (MATTHECK AND BRELOER, 1994), and the generation of special tissues or cell types like reaction wood. These are only a few fascinating and inspiring characteristics relevant for and studied in the fields of wood technology, biomechanics and bionics. Due to its cellular, fragile material structure wood is often compared with bone. Nevertheless, whereas bone is able to react on externally applied stresses by restructuring and stiffening high stressed areas by more or less constant total volume (despite of growth of a human or animal) wood cells are once differentiated manifested in their structure and characteristics during the whole life until degradation, aside from the conversion from sap- to heartwood. In contrast to bone trees have the ability to react on external stresses in every next cell generation till the end of life.

Growth and optimisation of the structure in the living tree is rather individually in respect to species, genetics, attitude, nutrients, social position within the forest, and other influencing parameters. This leads to a huge variety of individuals with a high statistical spread in their characteristics even if considering trees of the same species and from the same growth region, or even in particular timber elements taken from the same tree. Hence it is not surprising that wood and timber which is gained by harvesting and breakdown of the trees to logs and further to boards, scantlings, and beams show a distinctive statistical spread in their characteristics. This spread may be even increased due to conversion of the tree-internal optimised material structure with respect to the natural structure by arbitrarily choosen cutting patterns which are optimised primary according further applications and optical appearance, e.g. knots, knot clusters and decay. Only the breakdown process of logs to structural timber leads for example to about 20% reduction (loss) in bending and compression strength.

Thus it is no surprise that structural timber (e.g. boards, scantlings, beams) exhibit large variability in their characteristics, especially in strengths. Last is due to the fact that physical characteristics required for the design of timber structures are strength, stiffness and density. Hereby the latter two characteristics are more or less of interest as averaged properties of timber in reference dimensions and thereby not significantly affected by localised changes. In contrast, strength itself is an absolutely locally defined characteristic. The weakest cross section or weakest layer in a specimen dominates and determines decisively the whole strength potential. Nevertheless, there are also more than one application examples where also local characteristics of density and stiffness are

required, e.g. if considering the influence of locally placed fasteners in respect to their bearing capacity mainly influenced by local density, or stiffness in conjunction with stability e.g. in the half length of a hingh-supported column under compression.

In general, design and erection of constructions require reliable and thereby homogenised products characterised by well predictable properties exhibiting low statistical spread enabling e.g. wide applicability, dood-natured failure behaviour, durability and affordability. In respect to timber some of these characteristics are fulfilled already naturally. Beside the natural ability to be used as structural, load bearing element, timber products are predominantely associated with "natural appearance", "heat insulation" and other non-structural aspects. Maybe, as already stated by J. E. GORDON, "timber is too simple to be used", meaning that the basic and oldest building material of mankind offers too less challenge to operate more intensively with timber in modern engineered structures. Other engineeres may be frightened of the statistical spread, the variety of characteristics and special features of timber and prefere nowadays common materials like steel, concrete and reinforced concrete, used to work with in daily business. For example timber shows in contrast to concrete material high performance in tension and compression in grain direction being additionally sustainable and durable if used adequately. Enforced by current discussions like the global CO_2 problematic, timber experiencies some kind of renaissance, being more and more recognised as chance, as solution for some of our big environmental and economical challenges. Nevertheless, to increase further the attractiveness of timber to be used for engineering purposes it is necessary to decrease the statistical spread observable in characteristics, e.g. by the development of homogenised products. In timber homogenisation can be done on several ways, e.g.

- homogenisation of swelling and shrinkage (e.g. by activating cross laminating effects);
- homogenisation of quality, moisture, etc. by classification (grading) and quality assurance;
- homogenisation of physical (mechanical) characteristics like strength, stiffness and density by activation and utilisation of system actions and related effects.

The **first way** focuses on cross laminated products which show a reduction of swelling and shrinkage as consequence of activated cross laminating effects (locking effects) suffering from the negligible shrinkage rate in axial direction which is rougly about 1/100 and 1/50 of tangential and radial direction, respectively. Furthermore, cross laminating

additionally balance properties and bearing capacities in longitudinal and transverse direction. Products which suffer already from these considerations are e.g. plywood, LVL, OSB and CLT in plane direction.

The **second way** focuses on a certain homogenisation by quality assurance and classification (grading) of timber. Nevertheless, due to limited predictability or even impossible determination of some most important growth characteristics which decisively determine strength capacity (e.g. local and global grain deviation) decades of intensive international research shows only limited progress in strength grading. This leads to an insufficient and unreliable reduction of statistical spread and restricted predictability of strength classes (extractable from recent results published e.g. by RANTA-MAUNUS AND DENZLER, 2009; STAPEL ET AL., 2010). Thereby, grading enables only direct homogenisation in case of direct determinable characteristics. If a characteristic has to be classified by means of predictions and predictive parameters (e.g. strength estimated by means of eigenfrequency, density and knot share ratios) the possibilities in achieving reliable results and in particular for a reliable fulfilment of a certain degree of homogenisation itself are significantly affected by the degree of predictability. In general only a minor portion of indirect influence on a target homogenisation is realised. Even if grading would work perfectly the question is still open how to react on the grading result within industrial processes. Due to observable spatial correlation within specimens a repetitive grading result in every subsequent increment (e.g. defined by the knot cluster distance in softwoods with approximately 400 to 600 mm) has to be expected. Once the whole specimen is rejected a distinctive downgrading of the material and a high percentage of loss (reject) in raw material graded for a specific purpose has to be expected. Trimming every increment leads also to a high share of rejected specimen segments being additionally uneconomically due to high amount of required finger jointing. Nevertheless, fast and reliable on-line and on-site determination of density and stiffness (e.g. based on eigenfrequency measurements) enables the determination of also important global design characteristics.

The **third way** of homogenisation allows for direct reduction of statistical spread by activation of system effects due to common actions of sufficiently connected sub-elements, elements and components in systems. In contrast to grading (level two) enforced interaction between elements in parallel systems balances characteristics due to the fact that neighbouring elements can be assumed to be distributed independently in

respect to strength and stiffness. This leads to a maximum of homogenisation in physical properties.

The focus of the present work is on modelling and quantification of these system actions and effects, of the common action of elements in a system in respect to their individual but expectable characteristics, their arrangement in the system (serial vs. parallel), the system size and the type of loading. Thereby, utilisation and activation of system action (common action) is a direct and reliable method for controlling the degree of homogenisation also in characteristics which cannot be classified (graded) non-destructively (e.g. strength of natural materials). Thus system products are also simplier in production and handling considering the additionally required efforts in classification procedures. Nevertheless, a certain degree of secured quality and expectable characteristics of the base material is necessary and support a reliable production of system products and reliable activation of system effects. The influence of statistical spread of the base material is sharply reduced by homogenisation which leads to a balancing of base material characteristics and grading deficiencies. Some system products which benefit from these actions and effects are already available, in timber e.g. duo, trio, GLT, CLT, but also in other materials and environmental aspects, e.g computer systems, clusters and networks.

Analysing the current design, product and test standards partly non consistent regulations of the base material (EN 338 vs. EN 1194 or PREN 14080), minor and if than often not explicit consideration of system effects as function of their main parameters, e.g. system size (technical approval of duo and trio beams e.g. Z-9.1-0623 and Z-9.1-0440 as well as PREN 14080), not conform regulations, e.g. of size effects in product and design standards (e.g. EN 384 vs. EN 1194 vs. EN 1995-1-1) are given. Furthermore, inconsistent determination of characteristic values by means of contradicting statistical methods or even so called statistical tools with unclear or minor statistical background or justification (e.g. EN 384 or EN 14080 vs. EN 14358) can be found. These facts, which for sure are not only valid for European standards and the material timber itself prevent any coherent modelling and design of products, system products and structures or any optimisation of already existent or newly invented products and structures. Perhaps it is simple to analyse and criticize above facts but for sure the ideal condition of an absolutely coherent system of standards is nearly impossible to reach beside the fact that consens is the driving force of codification in general.

The aim of this work is to elaborate additional background of system action and related effects as a result of homogenisation, the reduction of statistical spread in the main physical characteristics, e.g. strength, stiffness and density. Hereby, the systems are split into serial and parallel systems. These are further analysed separately for providing the basis for later examination and application of so far gained knowledge, especially for current timber system products and structures as well as for some improvements of existing products and design of new products by taken into account the necessity of combining stochastics and mechanics. The first one (stochastics) is for consideration of variability (statistical spread) and the second one (mechanics) is for consideration of stresses and strains and their mechanical contribution within an element, component, system or structure. The analysis of system effects in timber products is perhaps especially worthwhile due to remarkable amount of statistical spread in characteristics, in particular strength, delivering a huge potential for homogenisation. For example, considering the tensile strength of boards with an expectable coefficient of variation $\mathrm{CoV}(f_{t,0}) = 30\%$. Due to the design of strength on the 5%-quantile only 59.1% of the average strength potential (mean value) is used as basis for design calculations assuming $f_{t,0} \sim$ lognormal. If it is possible to reduce this spread to an amount of say $\mathrm{CoV}(f_{t,0}) = 10\%$, without affecting the average in total 84.4% of mean potential can be realised on 5%-quantile design level. This enables an increase in the utilisation ratio (performance) of $\eta_{sys} / \eta_1 = 42.9\%$. For quantification of these system effects analysis focuses on three system levels (Fig. 1.1),

- Level I: material;
- Level II: system products;
- Level III: system bearing structures.

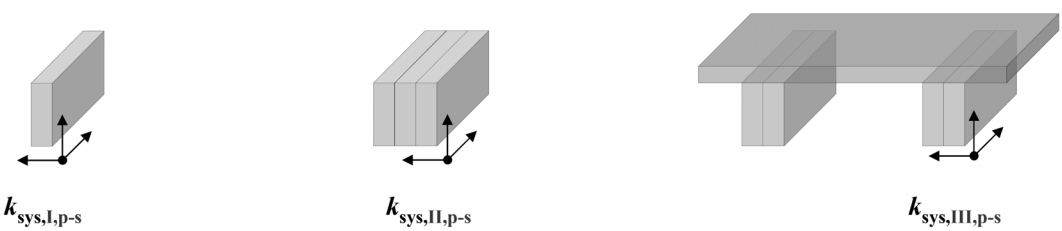

Fig. 1.1: Examples of systems on level I, II and III: structural material (I); system products (II); system structures (III); $p \equiv$ parallel, $s \equiv$ serial system action

Level I concentrates on a simplified stochastic description of the base material structure, e.g. a board analysed as a series of discrete increments of zones with and without local

strength reducing growth characteristics. In the sense of stochastics the examinations concentrate on spatial correlation and distribution of local material characteristics by means of a stochastic process.

Level II deals with the influence of serial and / or parallel system action by connecting elements and / or components in a way that they are forced to common (parallel) or at least simultaneous (serial) action under external load. These examinations are especially of interest for the design of system products and for the development of engineered "bearing models". Hereby type and degree of connection (punctiform – continuous; loose – flexible – rigid) play a decisive role.

Level III focus on quantification of system actions and effects in bearing structures composed of system products and material from level I and II, e.g. roof, floor and wall structures, bridge decks and frameworks.

This thesis concentrates mainly on level II, in particular on (quasi) rigid connected systems, deriving some essential basics on level I and showing some aspects for applications on level III. The variability (statistical spread), relationships and correlations between characteristics are thereby essential. Together with the interaction of elements in systems they are the driving forces of the work. Beforehand a clarification of the term "system" is required. Therefore the next two introductory sections give some comments on the main aspects, variability and systems.

1.2 The Nature of dispersing Properties

Any material and any characteristic property exhibit a certain amount of variation in its manifested characteristics. This can be observed already in the variable and dynamic behaviour of electron's position on discrete energy levels within atoms up to the (static and dynamic) behaviour of environment and universe as well.

In particular natural materials like wood, timber and soil properties show partly large variabilities. Examples of variabilities expressed by the coefficients of variation (CoV) (see section 2.3.1) are given in Tab. 1.1. In fact variability is the key of evolution, of the adaptation of life and nature in general to new challenges of the environment by supporting a huge variety of specifications at any time. During the selection process, as inherent in life, the best adapted individuums in living nature, in respect to time and space, survive.

Tab. 1.1: Some examples of coefficients of variation (CoV)

property	**CoV [%]**
structural steel: yield stress f_y (JCSS:2001)	7%
structural steel: tension strength f_u (JCSS:2001)	4%
timber: bending strength f_m (JCSS:2006)	25%
timber: E-modulus $E_{m,0}$ (JCSS:2006)	13%
timber: tensile strength parallel to grain $f_{t,0}$ (JCSS:2006)	30%

1.2.1 Typology of Uncertainties and Sources of Dispersion

Uncertainties and thereby sources of dispersion can be classified as being in nature either **aleatoric** or **epistemic** (THOMA, 2004).

Tab. 1.2: Overview and comparison of aleatoric and epistemic uncertainties / sources of spread

aleatoric uncertainties	**epistemic uncertainties**
▪ natural inherent variability → can not be influenced	▪ model uncertainties ▪ statistical uncertainties ▪ measurement uncertainties ▪ human uncertainties → can be influenced and reduced

Aleatoric uncertainties are dedicated to the randomness / the fortuity of events inherent in each physical phenomenon. It can be expressed as the non-influencable natural variability. The epistemic part classifies uncertainties which include model uncertainties, statistical uncertainties, measurement and human errors. It represents that part of variability which can be reduced to a certain (economically meaningful and technical possible) amount. This reduction can be done by improving models, progressing performance of quality assurance and / or repetition of tests and measurements, as well as intensified training, supervision and the implementation of controlling and regulating systems. Both, aleatoric and epistemic uncertainties should take part in stochastic models and both types of uncertainty are influenced by system action. An overview of aleatoric and epistemic uncertainties is given in Tab. 1.2.

1.2.2 Specifics on Timber Engineering and Comments on Mechanics vs. Stochastics

In case of materials for engineering purposes variability in load bearing structures has to be considered especially in (i) judgement of reliability and (ii) in decision making processes concerning the safety of elements, components and consequently of the whole system structure as well. Up to now design procedures given in standards consider the variability of actions and resistances on different levels. Deterministic design codes base on allowed / accepted design values of actions and resistances by including safety factors which were established during decades or even hundreds of years by practical experiences of trials and errors. In contrast, probabilistic design enables in principle an individual design by direct consideration of the stochastic nature of actions and resistances in each specific case. It provides a more specific decision tool than possible by means of generally applicable approaches. Nevertheless, probabilistic design requires the knowledge of all specific characteristics relevant for design, in particular the full stochastic description of actions and resistances. It may be argued that knowledge of a general trend acceptable on average provides accurate and sufficient information relevant for decision making processes, e.g. the design of structures. However, there are several aspects and effects which can only occur due to the occurrence of dispersion, e.g. system effects as discussed within this work. These system effects show to be in magnitude dependent on e.g. the quantile level of interest. Furthermore, dispersion of action and resistance influences the failure probability and hence the reliability of structures significantly. This fact may be even more decisive if series productions of structures instead of single structure types are intended.

The relevance of stochastics and mechanics are often controversially discussed. Mechanics thereby is an important and physically based theory for derivation of stresses and strains within elements, components, systems and structures as reaction on externally applied actions. Nevertheless mechanics alone can not explain the differences between material properties on various hierarchical levels, e.g. from atomistic to engineering scale. Thereby stochastics, a mathematical theory, plays a dominating role in judgement and explanation of these differences, which are caused by the nature of scaling in characteristics, structures and randomness of occurence. The inclusion of stochastics in mechanical calculations enables higher order modelling under correct consideration of average relationships and trends as well as the consideration of variability as inherent part of characteristics. As every property needs to be characterised by at least expectation and

variance, modelling of materials and structures relies on mechanics and stochastics. This at least for judgement if a certain representative volume element (RVE) is large enough such that the variability of a property of interest is reduced to an acceptable residual amount for specific calculations in continuum mechanics.

In the sense of this manuscript dealing with stochastic system actions and effects, the structure, arrangement of the elements and its interaction in the system define the focus of the work with special emphasis on the stochastic description of the system behaviour. This enables a quantitative registration in daily designing procedures of engineers and in the business of product design and decision finding processes.

1.3 General Aspects of Systems

The term „system“ (ancient greek: “*systema*”) in general characterises a structure, its composition as a collective of elements that interact with each other but appear and function externally as one unit (e.g. DUDEN, 2001 and MATTHIES, 2002). In the sense of ARISTOTLE (384-322 b.C.) “*... the assembly is more than the sum of its components ...*” the number of single elements without any connection and interrelationship do not form a system; elsewise systems are not comparable if only the number, type and arrangement of its elements are consistent but the interrelationships are not.

The system must be differentiated from its environment by the definition of system boundaries. This specification, the compilation of the system out of its environment, e.g. the universe of nature, is not trivial and has to be done in correspondence with the scope of examination, i.e. the scope of the modelling process. In general, the definition of system boundaries is a subjective process and depends on the observers’ perspective leading to generalisations and therefore to exemplary reproductions of natural processes. The approach to segment complex procedures and systems that may consist of sub-systems or may be a sub-system of a higher-ranking complex is perhaps limited by restricted human intelligence. Systems described by humans are simplified models of natural processes which perhaps enable and support the understanding of these processes to a certain degree.

However, it is difficult to entirely observe the structure of a system from the outside but it can be observed and ascertained by the effects, appearance and operation of the system resulting from the system action (e.g. MATTHIES, 2002). In that respect, the **system**

structure, the functionality of a system which is defined by the arrangement of and relationships between elements and components (in contrast to aggregates or assemblies which are only arranged without structure) has to be differentiated from the **system action** which depends on the **activity** (in- or extrinsic) in respect to the system structure, e.g. the external impact on systems by forces leading to stresses in systems and perhaps to stress transfer between the elements in dependency of the elements which are arranged side by side or consecutive, defined by the interaction between elements. In that respect system action depends on the system structure, the in- or extrinsic activity, and on the interaction of elements and components within the system. The consequence of system action observed externally is herein defined as **system effect**.

The artificially assembled system structures of engineered wood and timber products are specified, i.e. by the industrial production process, the design of products and by the system structure. Detection, identification and description of interactions and relationships, the system actions and related system effects, summarise the targets addressed in the present work. Thus, the focus lies on the external perception of a system which has been analysed by variation of system structure, the examined characteristic properties and the arrangement of elements within the system structure. The structuring of elements and their relationships within the system serves solely the aims of segmentation and demonstration of complex processes, the examination and the collection of knowledge about effects on macro-scale (system-level) and micro-scale (level of elements and their interactions) (see e.g. HUBRIG AND HERRMANN, 2005).

In general, the representation of systems is accomplished by models. The evaluation of models is always a judgement about being more or less accurate but ever about wrong models. No model is able to mirror reality completely as it is a simplification of reality under certain constraints and assumptions. Hence, the explanatory power of a model is based on the simplification representing the core structure under realistic assumptions.

Chapter 2

General Remarks concerning Probability Theory and Statistics

This chapter is a brief summary of essential stochastic definitions and discusses some background knowledge and basics concerning statistics and probability theory. A general section on definitions and basics of probability theory and statistics is following a section which concentrates on statistical distribution models relevant for timber engineering. In that respect some comments concerning the definition of representative statistical distribution models (RSDMs) are included. The chapter ends with a section addressing regression and hierarchical models and gives an overview of stochastic processes, essential functions and transformations in stochastics as well.

2.1 Some Definitions and Basics of Stochastics

Within this section some general definitions with respect to probability theory and statistics are given. Readers who are familiar with these topics may skip this section.

Stochastics or the "art of guessing" is a special field of mathematics and combines the two areas of probability theory and statistics (see Fig. 2.1). The term "stochastics" origin from old Greek language and means "random" the "fortune of actions". The opposite behaviour would be deterministic (according BURY, 1975 corresponding to the boarder case of stochastics with variation $\equiv 0$), expressing that each individual outcome of processes, the action, can be directly calculated and foreseen, whereas the outcome of stochastic processes (development in time and / or space) can only be defined by judgements or predictions, so called expectations, with a certain probability of

occurrence. That means that each individual outcome can be predicted to occur with a certain probability but can not be foreseen explicitly.

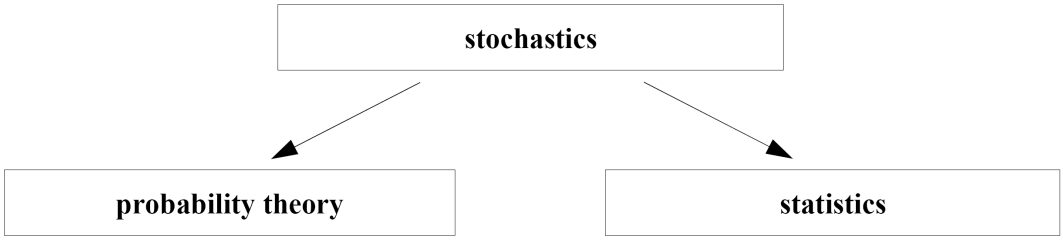

Fig. 2.1: Stochastics: visualisation of divisions

The **theory of statistics** combines a doctrine of methods to operate with quantitative data in information. It contains the collection, analysis and interpretation (inference) as well as graphical procedures for densification and presentation of data. Statistics and its methods can be subdivided into (see for illustrative purposes also Fig. 2.2):

- descriptive statistics (describing, empirical statistics for data preparation and data densification → data mining);
- explorative statistics (hypotheses generating statistics);
- inductive statistics (mathematical, conclusive, inference statistics).

The **probability theory** decribes the probability of the occurrence of certain events, e.g. defined as A, B, … The union of all possible (elementary) events of a certain experiment defines the event space Ω. Thereby the probability space consists of the event space Ω, the collection of subsets $\mathcal{A}$ and the measure P which is standardised on [0, 1]. The measure P assigns a probability to all events $A, B, \ldots$ ($\subseteq \Omega$) within the system $\mathcal{A}$. Thus probability theory analyses the behaviour and regularity of random variables X which is defined as projection of $\mathcal{A} \mapsto \mathbb{R}$ (further definition see section 2.2 and e.g. STADLOBER, 2011A).

Fig. 2.2 shows an overview of statistical inference by illustrating the relationships between theoretical models and observations. The definitions of elements in the figure are given in the next sections.

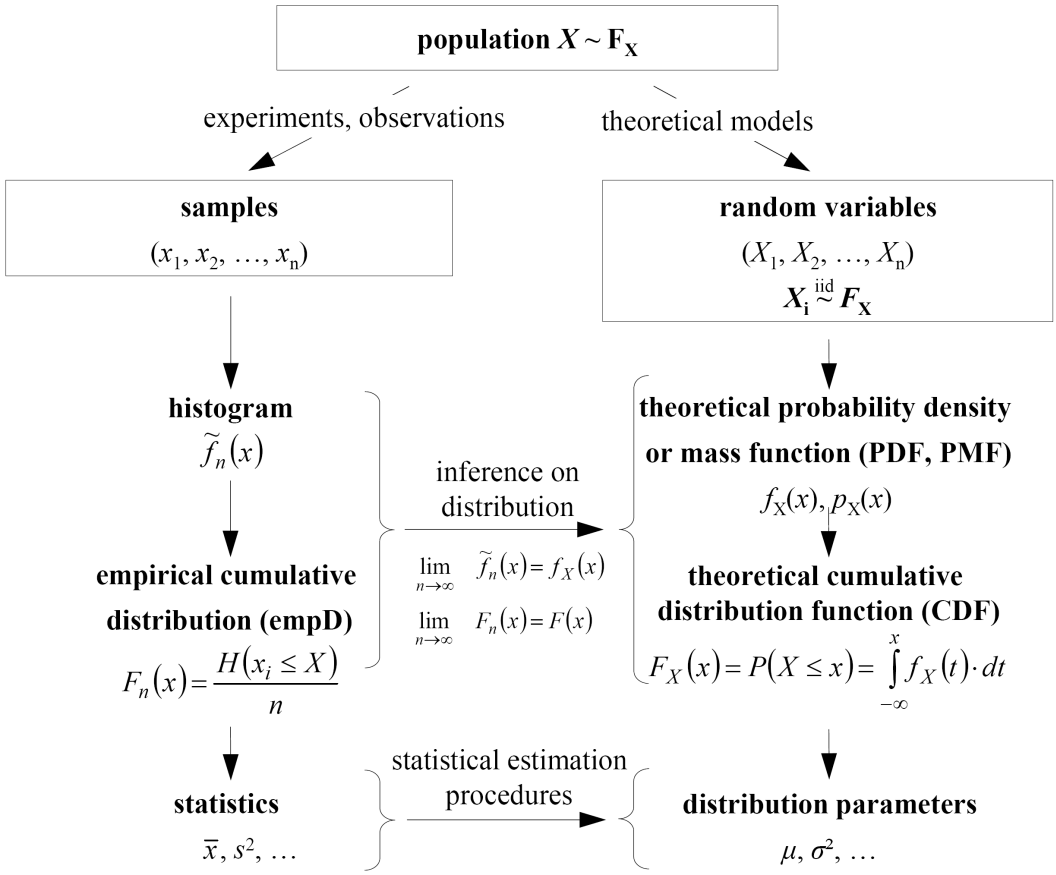

Fig. 2.2: Statistical inference: relationship between samples, empirical distributions, statistics and random variables, theoretical distribution models and parameters (adapted; SCHUËLLER, 1981)

2.1.1 Definition of Probability

The general definition of probability is given by the axioms of KOLMOGOROV. Let Ω be the event space and $\mathcal{A}$ the σ-Algebra over Ω. Then the probability function P: $\Omega \mapsto [0, 1]$ is defined as

- $0 \le P(A) \le 1, \forall A \in \mathcal{A}$ (axiom of mass);
- $P(\Omega) = 1$; $P(\emptyset) = 0$ (axiom of normalisation);
- for a sequence A_n of pairwise disjoint events in $\mathcal{A}$ (i.e. $A_i \cap A_j = \emptyset$) it follows

$$P\left(\bigcup_{i=1}^{\infty} A_i\right) = \sum_{i=1}^{\infty} P(A_i). \qquad \text{(axiom of addition).}$$

Thus a probability function P (.) has domain σ-Algebra and satisfies the axioms of KOLOMOGOROV, the axioms of probability (CASELLA AND BERGER, 2002).

There are two important special cases of probability. The first one is the classical definition according LAPLACE or BERNOULLI (1713). Both defined probability as the ratio between favourable and possible cases, (2.1). This definition traces back to combinatorial statistics and gambling theory, assuming equal probabilities for occurrence of all elementary events,

$$P(A) = \frac{N_A}{N}. \tag{2.1}$$

The second definition is a frequentistic one (according to R. VON MISES, 1919) and is given by the limiting value of the relative frequency of occurrence of a certain event after (in)finite independent experiments have been performed under constant conditions,

$$P(A) = \lim_{N\to\infty} H(A,N) = \lim_{N\to\infty} \frac{N_A}{N}, \tag{2.2}$$

with H(A, N) as relative frequency, the occurrence of event A in N trials (e.g. CASELLA AND BERGER, 2002; ROHLING, 2007).

Tab. 2.1: Combinatorics: some basic equations

	with replacement	without replacement
ordered	n^r	$\frac{n!}{(n-r)!}$
unordered	$\binom{n+r-1}{r} = \frac{(n+r-1)!}{r! \cdot (n-1)!}$	$\binom{n}{r} = \frac{n!}{r! \cdot (n-r)!}$

To take into account the total number of possible events the arrangement of an experiment has to be differentiated into experiments “with” and “without” replacement of already occured events and in respect to required or not required knowledge of the order

of outcomes ("ordered" and "unordered"). Thus the number of possible arrangements of taking r from n possible events is given in Tab. 2.1 (e.g. CASELLA AND BERGER, 2002; DURETT, 1994).

An additional definition of probability is given by the English priest and statistician THOMAS BAYES (e.g. cit. in CASELLA AND BERGER, 2002; STADLOBER, 2011A) who defined probability subjective as a degree of belief. His theorem was developed by means of conditional and total probability. The **conditional probability** as probability that event E given event A may occur is defined as

$$P(E \mid A) = \frac{P(A \cap E)}{P(A)}, \text{ with } P(A) > 0. \tag{2.3}$$

With $P(A \cap E) = P(A) \cdot P(E \mid A) = P(E) \cdot P(A \mid E)$, with $P(A)$, $P(E) > 0$, it follows that

$$P(E \mid A) = \frac{P(A \mid E) \cdot P(E)}{P(A)}, \; P(A) > 0, \text{ and } P(A \mid E) = \frac{P(E \mid A) \cdot P(A)}{P(E)}, \; P(E) > 0. \tag{2.4}$$

Assuming pairwise disjoint events ($E_i \cap E_j = \emptyset$, $\forall\, i \neq j$, with $E_1 \cup E_2 \cup \ldots \cup E_n = \Omega$, with $i, j = 1, \ldots, n$, $A \subset \cup_i E_i$, the theorem of **total probability** is given as

$$P(A) = \sum_{i=1}^{n} P(A \cap E_i) = \sum_{i=1}^{n} P(A \mid E_i) \cdot P(E_i). \tag{2.5}$$

In the special case of $\Omega = A \cup \overline{B}$ it follows (STADLOBER, 2011A)

$$P(A) = P(B) \cdot P(A|B) + P(\overline{B}) \cdot P(A|\overline{B}). \tag{2.6}$$

The **theorem of BAYES** follows from combining both theorems of conditional probability and of total probability, and is given as

$$P(E_i \mid A) = \frac{P(A \mid E_i) \cdot P(E_i)}{\sum_{j=1}^{n} P(A \mid E_j) \cdot P(E_j)}, \tag{2.7}$$

with $P(E_i)$ as prior probability, $P(A \mid E_i)$ as likelihood, $P(A)$ as normalising constant and $P(E_i \mid A)$ as posterior probability (see e.g. CASELLA AND BERGER, 2002; THOMA, 2004; ROHLING, 2007). Thus BAYES's formula provides updating on existing (prior) state of

knowledge of a relevant event or the *"... guessing of prior probabilities in case of missing data*" (BURY, 1975).

2.1.2 Addititive Law of Probability for arbitrary Events

In general, the probability of the union of events A and B is given by $P(A \cup B) = P(A) + P(B) - P(A \cap B)$. In case of A, B being disjoint the calculation can be simplified to $P(A \cup B) = P(A) + P(B)$ (e.g. DURRETT, 1994).

2.1.3 Multiplicative Law of Probability

The probability of the intersection between A and B given by $P(A \cap B)$ can be calculated according to $P(A \cap B) = P(A) \cdot P(B \mid A)$. Due to the equality of $(A \cap B) = (B \cap A)$ it follows that $P(A) \cdot P(B \mid A) = P(B) \cdot P(A \mid B)$. In case of three events A, B and C the multiplicative law lead to $P(A \cap B \cap C) = P(A) \cdot P(B \mid A) \cdot P(C \mid A \cap B)$. In case of n events the probability can be derived by (e.g. STADLOBER, 2005)

$$P\left(\bigcap_{i=1}^{n} A_i\right) = P(A_1) \cdot P(A_2 \mid A_1) \cdot P(A_3 \mid A_1 \cap A_2) \cdot \ldots \cdot P\left(A_n \mid \bigcap_{i=1}^{n-1} A_i\right), \quad \text{with } P\left(\bigcap_{i=1}^{n-1} A_i\right) > 0 . \tag{2.8}$$

In case of statistically independent events A, B, … the probability of their intersection can be calculated by simple multiplication, $P(A \cap B \cap \ldots) = P(A) \cdot P(B) \cdot \ldots$ (e.g. DURRETT, 1994). Furthermore, the information concerning a **dependency** between the probabilities of certain events is essential for judgement of the usability of some probability theorems and calculation procedures. In general, independency is mostly assumed to simplify the calculation of probabilities. Statistical independence, defined by $P(A \cap B) = P(A) \cdot P(B)$, has to be proved. According CASELLA AND BERGER (2002) mutually independency of a certain collection of events $A_1, A_2, \ldots, A_n$ holds if any subcollection $A_{i_1}, \ldots, A_{i_k}$ has probability

$$P\left(\bigcap_{j=1}^{k} A_{i_j}\right) = \prod_{j=1}^{k} P\left(A_{i_j}\right). \tag{2.9}$$

2.2 Definition of a Random Variable and its Distribution

A **random variable** is defined as a function which assigns every elementary event ω from the event space Ω of a random experiment exactly one real number $X(\omega)$ (e.g. DURRETT, 1994; CASELLA AND BERGER, 2002). In other words, the projection X of elements in Ω in elements in $\mathbb{R}$ (X: $\Omega \mapsto \mathbb{R}$) is named a random variable. The probability measure P_X is named the distribution of X (STADLOBER, 2011A). Possible values x of $X = X(\omega)$, $\omega \in \Omega$ X are named as realisations of X.

Generally, a **probability distribution** describes the character, the random occurence of data by means of parameters for location as center of probability mass and spread as well as the shape of the distribution of the data on a specific range. A differentiation according the type of data which has to be described is required, e.g. between discrete and continuous data. Discrete data can only take specific values whereas continuous data can take any value within a defined domain. Furthermore, the statistical distribution can be classified as bounded or unbounded distribution expressing the occurrence of a certain limit on one or both sides of the distribution domain $\neq (\pm\infty)$ or not (e.g. VAN HAUWERMEIREN AND VOSE, 2009). To simplify the representation of data's statistical distribution various families of numerous statistical distribution models are available. Thus a sufficient description of a data set requires (i) the knowledge of the underlying statistical distribution model and (ii) its associated parameters. Additional information about the statistical uncertainties inherent in estimates of statistical parameters should be provided.

A statistical **cumulative distribution function (CDF)** of a random variable X, defined as $F_X(x) = P_X(X \leq x)$, $\forall\, x$ is defined as right continuous function if following three conditions are fulfilled (e.g. CASELLA AND BERGER, 2002)

- $\lim_{x \to -\infty} F_X(x) = 0$; $\lim_{x \to +\infty} F_X(x) = 1$;
- $F_X(x)$ is a nondecreasing function of x;
- $F_X(x)$ is right-continuous ($\rightarrow \lim_{x \downarrow x0} F_X(x) = F_X(x_0)$, $\forall\, x_0$).

A **probability mass function (PMF)** describes the probability of occurrence of discrete random variables X, defined as $p_X(x) = P(X = x)$, $\forall\, x$. A **probability density function (PDF)** $f_X(x)$, $\forall\, x$ describes continuous random variables X defined by

$$f_X(x) = \frac{dF_X(x)}{dx}. \tag{2.10}$$

Both, PMF and PDF have to fulfill the conditions

- $p_X(x) \geq 0$ and $f_X(x) \geq 0$, $\forall\, x$;
- PMF: $\sum_x p_X(x) = 1$; PDF: $\int_x f_X(x) \cdot dx = 1$.

A random variable X is named a **discrete random variable** X if it can accept a finite or at least a countable infinite number of values. Its distribution is completely defined by $p_i = P(X = i)$, $i = 0, 1, 2, \ldots$, with the step-wise function (e.g. STADLOBER, 2011A)

$$F_X(x) = \sum_{i=0}^{\lfloor x \rfloor} p_i \text{, with } \sum_{i=0}^{\infty} p_i = 1. \tag{2.11}$$

A random variable X is named a **continuous random variable** X if there exists a function $f_X(x) \geq 0$ with (e.g. STADLOBER, 2011A)

$$F_X(x) = \int_{-\infty}^{\infty} f_X(t) \cdot dt \text{, with } f_X(x) \text{ as PDF of } X. \tag{2.12}$$

Additionally, according CASELLA AND BERGER (2002)

$$w(x \mid \mu, \sigma^2) = \frac{1}{\sigma} \cdot f_Z\left(z = \frac{x - \mu}{\sigma}\right) \tag{2.13}$$

defines a PDF if and only if Z is a random variable with PDF $f_Z(z)$ and $X = \sigma \cdot Z + \mu$, $E[Z] = 0$ and $Var[Z] = 1^2$, with $E[X] = \sigma \cdot E[Z] + \mu$ and $Var[X] = \sigma^2 \cdot Var[Z]$.

Bi- or multivariate models involve more than one random variable. The **joint PMF** exemplarily for two variables X and Y is given as (see e.g. STADLOBER, 2011A)

$$\begin{aligned} p_{ij}(x, y) &= P(X = i, Y = j) = \\ &= P(Y = j \mid X = i) \cdot P(X = i) = P(X = i \mid Y = j) \cdot P(Y = j). \end{aligned} \tag{2.14}$$

The **joint PDF** exemplarily for two variables X and Y is given as

$$f_{X,Y}(x,y) = f_{Y|X}(y \mid x) \cdot f_X(x) = f_{X|Y}(x \mid y) \cdot f_Y(y). \tag{2.15}$$

The **joint CDFs** for discrete and continuous variables X, Y are given as

$$\begin{aligned} F_{X,Y}(x,y) &= \sum_{i \le \lfloor x \rfloor} \sum_{j \le \lfloor y \rfloor} p_{ij} \text{ , with } p_{ij} = P(X = i, Y = j) && \text{… if } X, Y \text{ are discrete;} \\ F_{X,Y}(x,y) &= \int_{-\infty}^{x} \int_{-\infty}^{y} f_{X,Y}(u,v) \cdot dv \cdot du && \text{… if } X, Y \text{ are continuous.} \end{aligned} \tag{2.16}$$

The **marginal PMF**s are given as

$$\begin{aligned} P(X = i) &= \sum_y P(X = i, Y = j) = \sum_y P(X = i \mid Y = j) \cdot P(Y = j); \\ P(Y = j) &= \sum_x P(X = i, Y = j) = \sum_x P(Y = j \mid X = i) \cdot P(X = i). \end{aligned} \tag{2.17}$$

In case of (X, Y) being stochastically independent it follows that

$$\begin{aligned} P(X = i, Y = j) &= P(X = i) \cdot P(Y = j), \forall\, i, j && \text{… if } X, Y \text{ are discrete;} \\ f_{X,Y}(x,y) &= f_X(x) \cdot f_Y(y) && \text{… if } X, Y \text{ are continuous.} \end{aligned} \tag{2.18}$$

The **marginal PDF**s are given as

$$f_X(x) = \int_{-\infty}^{\infty} f_{X,Y}(x,y) \cdot dy \,;\; f_Y(y) = \int_{-\infty}^{\infty} f_{X,Y}(x,y) \cdot dx \,. \tag{2.19}$$

The **conditional PDF** of Y given that $X = x$ is defined by

$$f_{Y|X}(y \mid x) = \frac{f_{X,Y}(x,y)}{f_X(x)}, \text{ with } f_X(x) > 0 \,. \tag{2.20}$$

2.3 Characteristics of Statistical Distributions

The distribution of random variables is sufficiently represented by the distribution model and its parameters. The parameters or characteristic figures can be classified as (e.g. VAN HAUWERMEIREN AND VOSE, 2009)

- **location parameters:**

  They give information about the position of the center of the probability mass or density function. They have a direct influence on statistics like mean and mode.
- **scale parameters:**

  They contain information about the spread of the probability mass or density function. If squared, this set of parameters constitutes a part of the variance of the describing variable.
- **shape parameters:**

  These parameters deliver information about the shape, e.g. the skewness or kurtosis of the probability mass or density function. This class of parameters shows a nonlinear influence on the variable and is usually defined as a coefficient of the variable.

Let X be a random variable with X: $(\Omega, \mathcal{A}) \to (\mathbb{R}, \mathcal{B})$, with $\mathcal{B}$ as Borel σ-Algebra, and g a real function g: $\mathbb{R} \to \mathbb{R}$, with $g^{-1}(-\infty, y] \in \mathcal{B}$, then $Y = g(X)$ is also a random variable.

2.3.1 The Expected Value

In general, the **expected value** of a random variable defines an average value, a measure of the center (the center of gravity) of the distribution of random variables. The expected value E[g(X)] of the function Y = g(X) is given by

$$E[g(X)] = \sum_{x \in \chi} g(x) \cdot p_X(x), \text{ if } X \text{ is discrete;}$$
$$E[g(X)] = \int_{-\infty}^{\infty} g(x) \cdot f_X(x) \cdot dx, \text{ if } X \text{ is continuous.} \tag{2.21}$$

There are some special cases for $Y = g(X)$ which are discussed briefly. Let $\boldsymbol{g(X) = X^k}$. The expected value E[X^k] is named the $\boldsymbol{k^{th}}$ **moment of the random variable** $\boldsymbol{X}$ with CDF $F_X(x)$ and given as

$$\mu_k = E\left[X^k\right]. \tag{2.22}$$

In case of $\boldsymbol{k = 1}$, $g(X) = X$ it follows the **expected value of the random variable** $\boldsymbol{X}$ given as

$$\mu_1 = \mu = E[X] \ . \tag{2.23}$$

For example, the expected value E[X] can be calculated by

$$\begin{aligned} E[X] &= \sum_{i=1}^{n} x_i \cdot p_X(x_i), \text{ if } X \text{ is discrete,} \\ E[X] &= \int_{-\infty}^{\infty} x \cdot f_X(x) \cdot dx \text{ , if } X \text{ is continuous.} \end{aligned} \tag{2.24}$$

Due to linearity of E[X] the expected value of function g(X) = $a \cdot X + b$, with a, b as constant (deterministic) values, is given by E[g(X)] = $a \cdot$ E[X] + b. For g(X, Y) = $a \cdot X + b \cdot Y$ the expected value is thus E[g(X, Y)] = $a \cdot$ E[X] + $b \cdot$ E[Y]. In particular in case of a multiplication of independent variables X_i with g(X_i) = $X_1 \cdot X_2 \cdot \ldots \cdot X_n$, $i = 1, \ldots, n$, the expectation can be easily derived by calculating the product of all expectations,

$$E[X_i \cdot \ldots \cdot X_n] = \prod_{i=1}^{n} E[X_i]. \tag{2.25}$$

Let $\boldsymbol{g(X) = (X - \mu)^k}$. The expected value E[$(X - \mu)^k$] is named the **$k^{th}$ central moment of the random variable X** with CDF $F_X(x)$ and given as

$$\alpha_k = E\left[(X - \mu)^k\right] \ . \tag{2.26}$$

In case of $\boldsymbol{k = 2}$ it follows the **variance of the random variable X** given as

$$\alpha_2 = E[X - \mu]^2 = Var[X] = \sigma^2 . \tag{2.27}$$

The variance σ^2 of the random variable X constitutes a measure of the degree of dispersion of the distribution of X around μ, the probability of values occurring around the expected value. The moment of inertia of the corresponding distribution of a unit mass around its center of gravity can be seen as analogical description as known from mechanics (e.g. SCHUËLLER, 1981).

In case of the continuous random variable X the variance Var[X] can be calculated as

$$Var[X] = \int_{-\infty}^{\infty} [x-\mu]^2 \cdot f_X(x) \cdot dx = \int_{-\infty}^{\infty} x^2 \cdot f_X(x) \cdot dx - \mu^2 . \tag{2.28}$$

The variance Var[g(X)] with g(X) = $a \cdot X + b$, with a, b as constants, is given by Var[g(X)] = $a^2 \cdot$ Var[X]. According the Theorem of BIENAYMÉ the variance of the sum of independent random variables X_i is given by the sum of the variances of X_i,

$$Var\left[\sum_{i=1}^{n} X_i\right] = \sum_{i=1}^{n} Var[X_i], \text{ with } i = 1, \ldots, n. \tag{2.29}$$

An alternative calculation of Var[X] is given by STEINER's displacement law, defined as (e.g. STADLOBER, 2011A)

$$Var[X] = E[X^2] - E^2[X] \ . \tag{2.30}$$

The square root of variance is named **standard deviation σ**.

The variance of a sum of variables X_i with constant factors c_i and CoVar as covariance are given by

$$Var\left[\sum_{i=1}^{n} c_i \cdot X_i\right] = \sum_{i=1}^{n} c_i^2 \cdot Var[X_i] + \sum_{i=1}^{n} \sum_{\substack{j=1 \\ j \neq i}}^{n} c_i \cdot c_j \cdot CoVar[X_i, X_j]. \tag{2.31}$$

The variance of a linear function of two random variables X and Y with two constants a, b is therefore given by

$$Var[a \cdot X + b \cdot Y] = a^2 \cdot Var[X] + b^2 \cdot Var[Y] + 2 \cdot a \cdot b \cdot CoVar[X, Y]. \tag{2.32}$$

A relative measure of dispersion is given by the **coefficient of variation CoV** defined as

$$CoV[X] = \frac{\sigma}{\mu} . \tag{2.33}$$

The **skewness γ_1 [X] = skew [X]** is as measure of symmetry or asymmetry of the distribution of the random variable X and given as

$$\gamma_1[X] = skew[X] = \frac{E\left[(X-\mu)^3\right]}{[Var[X]]^{3/2}} = \frac{\alpha_3}{\sigma^3}. \tag{2.34}$$

In case of skew $[X] = 0$ the distribution is symmetric, in case of skew $[X] < 0$ and skew $[X] > 0$ the distribution of X is named left- and right-skewed, respectively.

The **kurtosis γ_2 [X] = kurt [X]** is as measure of the shape in the center and at the tails of the distribution of the random variable X and herein given as

$$\gamma_2[X] = kurt[X] = \frac{E\left[(X-\mu)^4\right]}{[Var[X]]^{2}} = \frac{\alpha_4}{\sigma^4}. \tag{2.35}$$

2.3.2 The Mode

The **mode of a random variable *X***, abbreviated mode[X], is the value which is most likely to occur (e.g. VAN HAUWERMEIREN AND VOSE, 2009). This means that the mode of a given variable corresponds to the value at the maximum of the probability mass or density function of discrete or continuous variables, respectively. In case of mean[X] = mode[X] the variable shows symmetrical distribution, whereas in case of mode[X] < mean[X] and mode[X] > mean[X] the variable X is right- and left-skewed, respectively.

2.3.3 The Moment Generating Function (MGF)

Let X be a random variable with CDF $F_X(x)$, than the moment generating function $M_X(t)$ of X (MGF) is given as (CASELLA AND BERGER, 2002)

$$M_X(t) = E\left[e^{t \cdot X}\right], \tag{2.36}$$

if the expected value exists near 0.

$M_X(t)$ represents the LAPLACE-transform of $f_X(x)$. $M_X(t)$ can be calculated by

$$M_X(t) = \int_{-\infty}^{\infty} e^{t \cdot x} \cdot f_X(x) \cdot dx \text{, if } X \text{ is continuous,}$$
$$M_X(t) = \sum_x e^{t \cdot x} \cdot P(X = x) \text{, if } X \text{ is discrete.} \tag{2.37}$$

The kth moment of X can be easily derived by means of $M_X(t)$ with

$$E\left[X^k\right] = M_X^k(0) \text{, with } M_X^k(0) = \frac{d^k}{dt^k} M_X(t) \Big|_{t=0}. \tag{2.38}$$

Thus the kth moment is equal to the kth derivative of $M_X(t)$ at $t = 0$.

2.3.4 The Characteristic Function

The characteristic function $\phi_X(t)$ is given as

$$\phi_X(t) = E\left[e^{i \cdot t \cdot X}\right] \text{, with } i = \sqrt{-1} \text{ as the imaginary number.} \tag{2.39}$$

It is unique for every CDF and does always exist even if MGF does not. It completely determines the distribution of random variables.

2.3.5 Characteristics of Conditional Distributions

Let g(Y) be a function of Y given that $X = x$. The variance of Y given that $X = x$ is given as (e.g. DURRETT, 1994)

$$Var[Y \mid X = x] = E\left[\left\{ Y - E[Y \mid X = x] \right\}^2 \mid X = x\right] = E\left[Y^2 \mid X = x\right] - E^2[Y \mid X = x], \tag{2.40}$$

whereby the variance Var[Y] is defined as

$$Var[Y] = E\left[Var[Y \mid X = x]\right] + Var\left[E[Y \mid X = x]\right]. \tag{2.41}$$

The expected value and variance in case of **conditional PDF** under consideration of g(Y) as function of Y given that $X = x$ can be derived by

$$E[g(Y) \mid X = x] = \int_{-\infty}^{\infty} g(y) \cdot f_{Y|X}(y \mid x) \cdot dy \,, \tag{2.42}$$

and

$$Var[Y \mid X = x] = E\left[Y^2 \mid X = x\right] - E^2[Y \mid X = x]. \tag{2.43}$$

In case of a **conditional PMF** the variance Var[X] can be calculated as

$$Var[X] = E\left[Var[X \mid Y = y]\right] + Var\left[E[X \mid Y = y]\right] \,. \tag{2.44}$$

2.3.6 The Covariance

The covariance of two random variables X and Y is given by

$$CoVar[X,Y] = E[(X - \mu_X) \cdot (Y - \mu_Y)] = E[X \cdot Y] - \mu_X \cdot \mu_Y \,. \tag{2.45}$$

2.3.7 The Correlation Coefficient according Pearson

The correlation coefficient $\rho_{XY}(x,y) = \rho_{XY}$ according PEARSON is a direct and normalised measure of the strongness of a linear relationship between X and Y and defined as

$$\rho_{XY}(xy) = \rho_{XY} = \frac{CoVar[X,Y]}{\sqrt{Var[X] \cdot Var[Y]}} = \frac{CoVar[X,Y]}{\sigma_X \cdot \sigma_Y}, \text{ with } -1 \le \rho_{XY} \le 1. \tag{2.46}$$

2.4 Representatives of Univariate Statistical Distribution Models of Continuous Variables

In general a statistical distribution constitutes a model representing the main features and characteristics, a property or an aggregate of properties of interest. In that respect the statistical distribution constitutes a simplification, an abstraction in respect to the nature of the underlying variety and randomness of a certain variable. For characterisation of a property or natural phenomenon the statistical distribution model has to be chosen with caution and in respect to the scope of the model. Within this work statistical distribution models which representatively characterise the distribution of a property or action in

respect to the scope of the model are called **representative statistical distribution models** (**RSDM**s). The accurate choice of an RSDM demands on the definition of the scope of the model. Thus it demands on the decision of representing the whole range of a variable or only a part of it. Aspects like (i) how scaling and changes in actions can be considered and incorporated in further modelling processes, (ii) the analysis of the asymptotic behaviour of the distribution model, as well as (iii) the incorporation of physical constraints and boarder conditions in respect to the underlying physical phenomena and the nature of the property or action have to be considered to enable representative and accurate modelling. As mentioned, it is not always necessary to represent the statistical nature, especially with focus on the location and the distribution characteristics, over the whole range of possible outcomes. In particular in case of reliability analysis it can be sufficient to represent the nature of resistance in the lower quantile range and that of action within the upper quantile range. In contrast, modelling of system effects or actions generally requires the best and physical compatible knowledge of a representative statistical distribution model over the whole range due to given interactions between model variables along the whole distributions.

The necessity for modelling of stochastic nature by statistical distribution models consequences from the in general insufficient available knowledge about the behaviour of the total population. Only finite test series and data as random outcomes are available. Representing the whole empirical distribution is practically impossible and theoretically questionable because only each specific random sample used for inference may be represented accurately. Considering the nature of phenomena, representatives and inference based on data should be sufficient and accurate in respect to the scope of the model. Hereby the quantity of key figures or distribution parameters should be also choosen carefully. They should be physically justifiable and empirically as well as practically manageable. In particular, information about statistical uncertainties of the parameters enables performance of parameter studies analysing their influence on the outcomes. Thus best possible reduction of uncertainties is due to cumulative errors for sure more important in case of stochastic processes or modelling of large systems than in case of representation of single outcomes.

According SCHUËLLER (1981) continuous statistical distribution models follow from the examination of boarder constraints of the relationship between the random variable which describes the physical phenomenon and its singular mechanisms, whereby their singular contribution on total dispersion of the variable cannot be determined definitely. By

knowledge of how singular mechanisms or constituted, statements regarding the distribution of variables are possible. Thus three main cases are given:

- additive acting singular mechanisms;
- multiplicative acting singular mechanisms;
- behaviour of their extreme values (minima, maxima).

The first two cases are often associated and represented by normal and lognormal distribution models, respectively, and will be discussed within the next sections 2.4.1 and 2.4.2. The third case is in particular the topic of extreme value theory (see section 2.6.2). Concerning strengths of brittle materials this case is often associated with the WEIBULL distribution model (WD) as presented in sections 2.4.3 and 3.2.1.

In general, stochastic modelling concentrates on eliminating outliers. This is perhaps sufficient for modelling the average behaviour of a variable. Nevertheless, the outliers can in particular support the analysis and the predictive quality of models because they often contribute an added value for the explanation of the underlying phenomena, even more than the mass of averages can do. Therefore rejecting outliers from data should be done with caution and never without a careful and comprehensive proof beforehand.

2.4.1 The Normal (Gauss) Distribution Model (ND)

The normal distribution (ND) constitutes the most famous and widest applied statistical distribution model. It follows directly from the Central Limit Theorem (see section 2.6.1) and from the arithmetic series. It specifies the distribution model for characterisation of sums of independent but not necessarily identical distributed variables. In that sense ND is especially applicable for modelling of arithmetic, additive processes (e.g. LIMPERT, 2001; SCHUËLLER, 1981).

A variable X with $X \sim \mathrm{ND}\,(X \mid \boldsymbol{\theta})$ and $\boldsymbol{\theta} = (\mu, \sigma^2)$ as parameter vector is known as being normally distributed, if it has the density function

$$f_X(x) = \frac{1}{\sigma \cdot \sqrt{2 \cdot \pi}} \cdot \exp\left[-\frac{1}{2} \cdot \left(\frac{x-\mu}{\sigma}\right)^2\right], X \in \mathbb{R}. \tag{2.47}$$

Through standardisation of ND variables by

$$Z = \frac{X - \mu}{\sigma} \tag{2.48}$$

it leads to the standard normal distribution (SND) of Z, with $Z \sim \text{SND}\,(Z \mid \boldsymbol{\theta})$ and $\boldsymbol{\theta} = (0, 1^2)$, with PDF

$$f_Z(z \mid \theta) = \phi(z) = \frac{1}{\sqrt{2 \cdot \pi}} \cdot \exp\left[-\frac{z^2}{2}\right], \tag{2.49}$$

and CDF

$$F_Z(z \mid \theta) = P[Z \le z] = \Phi(z) = \int_{-\infty}^{z} \phi(u) \cdot du \text{, with } \Phi(z) = 1 - \Phi(-z). \tag{2.50}$$

On the basis of (2.47), (2.48), (2.49) and (2.50) the PDF and CDF of normally distributed variables can also be written as

$$f_X(x \mid \theta) = \frac{1}{\sigma} \cdot \phi(z)\text{; } F_X(x \mid \theta) = P[X \le x] = \Phi\left(\frac{x - \mu}{\sigma}\right) = \Phi(z). \tag{2.51}$$

The parameters of ND correspond to expected value E[.] = μ and the variance Var[.] = σ^2, with E[.] and Var[.] as the expectation and variance operator, respectively. Thus ND constitutes a statistical distribution model whereby the distribution parameters coincide with the first and second central moments E[.] and Var[.].

The distribution parameters can be estimated from empirical data sets by calculating the empirical arithmetic mean $\overline{X}$ and standard deviation S or variance S^2 as

$$\overline{X} = \frac{1}{n} \cdot \sum_{i=1}^{n} X_i \text{ , } S^2 = \frac{1}{n-1} \cdot \sum_{i=1}^{n} \left(\overline{X} - X_i\right)^2 \text{ and } S = \sqrt{S^2} \text{ ,} \tag{2.52}$$

or by means of likelihood estimators as well as on the basis of empirical determined quantiles Q_p, e.g. the median with

$$\hat{Q}_{0.50} = med[X]. \tag{2.53}$$

In case of parameters estimated by means of maximum likelihood the variance-covariance matrix $[V_{ij}]$ of the parameters $\overline{X}$ and S_L, with

$$\overline{X} = \frac{1}{n} \cdot \sum_{i=1}^{n} X_i \text{ and } S_L = \sqrt{\frac{1}{n} \cdot \sum_{i=1}^{n} \left(\overline{X} - X_i\right)^2}\,, \tag{2.54}$$

is given as (BURY, 1975)

$$\left[V_{ij}\right] = \begin{bmatrix} \dfrac{\sigma^2}{n} & 0 \\ 0 & \dfrac{\sigma^2}{2 \cdot n} \end{bmatrix}, \tag{2.55}$$

with $[V_{ij}]$ as the inverse of the information matrix $[I_{ij}]$ given by

$$\left[V_{ij}\right] = \left[I_{ij}\right]^{-1}. \tag{2.56}$$

The information matrix corresponds to the expectation of the 2nd partial derivative of the log-likelihood function $\ln(L)$ and is given as

$$\left[I_{ij}\right] = \left[-E\left[\frac{\partial^2 \ln(L)}{\partial\theta_i \cdot \partial\theta_j}\right]\right]. \tag{2.57}$$

The log-likelihood function $\ln(L)$ is defined as

$$\ln(L \mid \theta) = \ln\left(\prod_{i=1}^{n} f_{X_i}(x_i \mid \theta)\right) = \sum_{i=1}^{n} \ln\left[f_{X_i}(x_i \mid \theta)\right], \tag{2.58}$$

with $f_X(x|\boldsymbol{\theta})$ from (2.51). The maximum likelihood estimates $\hat{\theta}$ are obtained as solution of

$$\ln\left[L\left(\hat{\theta}\right)\right] = \max_{\theta} \ \ln\left[L(\theta)\right]. \tag{2.59}$$

Thus the variance of $\overline{X}$ is given by $\mathrm{Var}[\overline{X}] = \sigma^2 / n$ and that of S_L is given by $\mathrm{Var}[S_L] = \sigma^2 / (2 \cdot n)$.

The mode of ND variables or the value representing the argument of the maximum of the density, is given by

$$\arg\left[f_X(x\,|\,\theta)_{\max}\right] = \arg\left[f_X(\mu\,|\,\theta)\right] = \arg\left[\frac{1}{\sigma_x \cdot \sqrt{2\cdot\pi}}\right] = \mu\,. \tag{2.60}$$

The inflexion points of the distribution are well known at $\mu \pm \sigma$. Herein defined probabilities within a span of k-times the standard deviation are given e.g. by

$k = 1$: $\mu \pm 1 \cdot \sigma$ → $P(\mu - \sigma \le X \le \mu + \sigma) = \Phi(1) - \Phi(-1) = 2 \cdot \Phi(1) - 1 = 68.3$ %;

$k = 2$: $\mu \pm 2 \cdot \sigma$ → $P(\mu - 2\cdot\sigma \le X \le \mu + 2\cdot\sigma) = \Phi(2) - \Phi(-2) = 2 \cdot \Phi(2) - 1 = 95.5$ %;

$k = 3$: $\mu \pm 3 \cdot \sigma$ → $P(\mu - 3\cdot\sigma \le X \le \mu + 3\cdot\sigma) = \Phi(3) - \Phi(-3) = 2 \cdot \Phi(3) - 1 = 99.7$ %.

The ND is invariant in convolution. Thus sums of independent ND variates are also normally distributed, see

$$\sum_{i=1}^{n} X_i \sim ND\left(\sum_{i=1}^{n}\mu_i, \sum_{i=1}^{n}\sigma_i^2\right), \text{ for } X_i \overset{i}{\sim} ND\left(\mu_i, \sigma_i^2\right). \tag{2.61}$$

According CRAMÉR this relationship holds also for the inverse situation. In case of normally distributed sums the summands are also normally distributed.

The skewness skew[X] of ND variables equals 0 (→ symmetrical distribution model) whereas the kurtosis kurt[X] equals 3.0 (BURY, 1975).

The ratio of two independent SND-variables X and Y, with $U = X / Y$ follows a Cauchy distribution (CASELLA AND BERGER, 2002) with

$$f_U(u) = \frac{1}{\pi \cdot \left(u^2 + 1\right)}, \text{ with } -\infty < u < \infty \text{ and non-existing moments.} \tag{2.62}$$

Beside univariate ND also bi- and multivariate ND models are available. In the general case of two dependent (correlated) ND-variables the bivariate ND-model is defined as

$$\begin{bmatrix} X_1 \\ X_2 \end{bmatrix} \sim ND\left(\begin{bmatrix} \mu_1 \\ \mu_2 \end{bmatrix}, \begin{bmatrix} \sigma_1^2 & \rho\cdot\sigma_1\cdot\sigma_2 \\ \rho\cdot\sigma_1\cdot\sigma_2 & \sigma_2^2 \end{bmatrix}\right), \tag{2.63}$$

with $\rho = \rho_{XY}$ as (PEARSON) correlation coefficient and CoVar[X_1, X_2] = $\rho \cdot \sigma_1 \quad \sigma_2$. In case of independent variables ($\rho = 0$) the bivariate ND simplifies to

$$\begin{bmatrix} X_1 \\ X_2 \end{bmatrix} \sim ND\left(\begin{bmatrix} \mu_1 \\ \mu_2 \end{bmatrix}, \begin{bmatrix} \sigma_1^2 & 0 \\ 0 & \sigma_2^2 \end{bmatrix}\right), \tag{2.64}$$

with joint PDF

$$f_{X_1,X_2}(x_1,x_2) = \frac{1}{2\cdot\pi\cdot\sigma_1\cdot\sigma_2}\cdot\exp\left[-\frac{1}{2}\cdot\left[\left(\frac{x_1-\mu_1}{\sigma_1}\right)^2+\left(\frac{x_2-\mu_2}{\sigma_2}\right)^2\right]\right], \tag{2.65}$$

for $\forall\, x_1, x_2 \in \mathbb{R}$.

Independent SND variables Z_1, Z_2 can be easily transformed to

$$\begin{bmatrix} Y_1 \\ Y_2 \end{bmatrix} \sim SND\left(\begin{bmatrix} 0 \\ 0 \end{bmatrix}, \begin{bmatrix} 1 & \rho \\ \rho & 1 \end{bmatrix}\right), \text{ by } \begin{bmatrix} Y_1 \\ Y_2 \end{bmatrix} = \begin{bmatrix} Z_1 \\ \rho\cdot Z_1 + \sqrt{1-\rho^2}\cdot Z_2 \end{bmatrix} \tag{2.66}$$

and hence to

$$\begin{bmatrix} X_1 \\ X_2 \end{bmatrix} = \begin{bmatrix} \sigma_1\cdot Y_1+\mu_1 \\ \sigma_2\cdot Y_2+\mu_2 \end{bmatrix} \sim ND\left(\begin{bmatrix} \mu_1 \\ \mu_2 \end{bmatrix}, \begin{bmatrix} \sigma_1^2 & \rho\cdot\sigma_1\cdot\sigma_2 \\ \rho\cdot\sigma_1\cdot\sigma_2 & \sigma_2^2 \end{bmatrix}\right). \tag{2.67}$$

In case of n-dimensional normally distributed variables the multivariate normal PDF is given by

$$f_{(X_1,..,X_n)}(x_1,..,x_n) = \frac{1}{(2\cdot\pi)^{n/2}\cdot|\Sigma|^{1/2}}\cdot\exp\left[-\frac{1}{2}\cdot(x-\mu)^T\cdot\Sigma^{-1}(x-\mu)\right], \tag{2.68}$$

with $|\Sigma|$ as determinant of the covariance matrix Σ = CoVar, with elements CoVar[X_i, X_j].

2.4.2 The Logarithmic Normal Distribution Model (LND)

The basis of the logarithmic normal distribution (lognormal, LND) traces back to works of GIBRAT (1930, 1931) who derived the distribution function by means of theoretically qualitative assumptions which are well known under the name of "**law of proportionate effect**". In short, the law states that the product of proportional identical changes, which are assumed to be normally distributed, tends with increasing changes to LND, independent of the starting point. KOLMOGOROFF derived the LND model in 1941 on

basis of the description of the distribution of particle sizes, whereby the particles are independently subdivided which leads to two independent sized parts each. LIMPERT ET AL. (2001) described in general, that additive and multiplicative actions and effects on continuous variables tend to be normally and lognormally distributed, respectively. Additionally, SCHUËLLER (1981) stressed the appropriateness of LND to describe the stochastic nature of multiplicative processes. He reports about frequent use for representation of the microscopic behaviour of fatigue mechanisms in raw materials. Especially in the fields of physics, natural, social and engineering sciences the relevance of LND is seen similar to the ND model (JOHNSON ET AL., 1994). The advantage of the approximation of empirical data by a two-parametric LND (2pLND) is beside the theoretical background of "the theory of proportionate effects" in particular given by the constraint of only positive values which can be observed in many physical aspects and properties like strengths and stiffness. In case of low dispersion within the values of about $\mathrm{CoV}[Y] \approx (15 \div 20)\%$ the difference in shape between ND and LND may appear negligible especially if expectations are far away from zero thresholds. Nevertheless, the extreme values in the upper distribution area, e.g. the 95%-quantiles, are clearly different (e.g. AHRENS, 1954).

In general, a variable Y is defined as being lognormally distributed ($Y \sim$ LND) if its logarithm $X = \ln(Y)$ is normally distributed ($X \sim$ ND). The density of 2pLND is given by

$$f_Y(y) = \frac{1}{y \cdot \sigma_X \cdot \sqrt{2 \cdot \pi}} \cdot \exp\left[-\frac{1}{2} \cdot \left(\frac{\ln(y) - \mu_X}{\sigma_X} \right)^2 \right]. \tag{2.69}$$

The distribution parameters can be estimated from empirical data by the method of moments on the basis of the empirical arithmetic mean and the empirical variance (e.g. ZUPAN AND TURK, 2004; THOMOPOULOS AND JOHNSON, 2004; SCHUËLLER, 1981), see

$$\mu_X = \ln\left(\frac{\mu_Y^2}{\sqrt{\mu_Y^2 + \sigma_Y^2}} \right), \; \sigma_X^2 = \ln\left(\frac{\sigma_Y^2}{\mu_Y^2} + 1 \right) = \ln\left[CoV(Y)^2 + 1 \right], \tag{2.70}$$

as well as by means of the maximum likelihood method. In case of parameter estimations based on log-likelihood the variance-covariance matrix of the estimates $\hat{\mu}_X$ and $\hat{\sigma}_X$ is given as (BURY, 1975)

$$\left[V_{ij}\right]=\begin{bmatrix} \frac{\sigma_X^2}{n} & 0 \\ 0 & \frac{\sigma_X^2}{2\cdot n} \end{bmatrix}. \tag{2.71}$$

Thus the variances of $\hat{\mu}_X$ and $\hat{\sigma}_X$ are given respectively by Var[$\hat{\mu}_X$] = σ_X^2 / n and Var[$\hat{\sigma}_X$] = $\sigma_X^2 / (2 \cdot n)$.

The expectation E[Y] and variance Var[Y] are given as

$$E[Y]=\mu_Y=\exp\left(\mu_X+\frac{\sigma_X^2}{2}\right)=\sqrt{\exp\left(2\cdot\mu_X+\sigma_X^2\right)}\ , \tag{2.72}$$

$$Var[Y]=\sigma_Y^2=\exp\left(2\cdot\mu_X+\sigma_X^2\right)\cdot\left[\exp\left(\sigma_X^2\right)-1\right]=E^2[Y]\cdot\left[\exp\left(\sigma_X^2\right)-1\right]\ . \tag{2.73}$$

By means of the transformation

$$W=\frac{\ln(Y)-\mu_X}{\sigma_X} \tag{2.74}$$

THOMA (2004) states that the CDF of lognormals can be expressed by means of the normal distribution operator, with $F_Y(y) = P\,[Y \le y] = \Phi(w)$. Further characteristic values of LND, e.g. median med[Y], coefficient of variation CoV[Y], skewness skew[Y] and kurtosis kurt[Y] can be derived as (see AITCHISON AND BROWN, 1981)

$$med[Y]=\tilde{Y}=\exp(\mu_X), \tag{2.75}$$

$$CoV[Y]=\frac{\sigma_Y}{\mu_Y}=\sqrt{\exp\left(\sigma_X^2\right)\ -1}\ , \tag{2.76}$$

$$skew[Y]=CoV^3[Y]+3\cdot CoV[Y], \tag{2.77}$$

$$kurt[Y]=CoV^8[Y]+6\cdot CoV^6[Y]+15\cdot CoV^4[Y]+16\cdot CoV^2[Y]. \tag{2.78}$$

Hereby skew[Y] and kurt[Y] are both positive and increase with increasing variance Var[Y]. Concerning the location parameters it can be proved that mod[Y] $\le$ med[Y] $\le$ E[Y], whereby according to CROW AND SHIMIZU (1988) the mode mod[Y] can be derived by

$$\mathrm{mod}[Y] = \exp\left(\mu_X - \sigma_X^2\right). \tag{2.79}$$

The quantiles of LND variables can be derived by means of parameter z_p corresponding to the pth-quantile of a SND variable, see

$$y_p = \exp\left(\mu_X + z_p \cdot \sigma_X\right). \tag{2.80}$$

In case of $p = 5\%$ the required 5%-quantile is given by $z_{05} = \Phi^{-1}(0.05) = -1.645$, with $\Phi^{-1}(p)$ as the inverse standard normal distribution operator. Consequently in the limiting case with $\sigma_X \to 0$ quantiles y_p and other statistics tend to $\to \exp(\mu_X) = \mathrm{med}[Y]$ corresponding to the expected value $\mathrm{E}[Y]$, with $\sigma_X = 0$.

If the 5 %-quantile y_{05} and $\mathrm{CoV}[Y]$ are known the distribution parameter μ_Y can be derived as

$$\mu_Y = y_{05} \cdot \exp\left[-\Phi^{-1}(0.05) \cdot \sqrt{\ln\left(CoV[Y]^{\,2} + 1\right)}\right] \cdot \sqrt{CoV[Y]^{\,2} + 1}\,. \tag{2.81}$$

The product of independent (ind.) distributed LND variables can be seen in analogy to the sum of independent ND variables (SHARPE, 2004; CROW AND SHIMIZU, 1988). The distribution of the product of independent 2pLND variables follows also a lognormal distribution, with

$$\prod_{i=1}^{n} Y_i \sim 2pLND\left(\sum_{i=1}^{n} \mu_{X,i}, \sum_{i=1}^{n} \sigma_{X,i}^2\right). \tag{2.82}$$

In case of iid LND variables (2.82) simplifies to

$$\prod_{i=1}^{n} Y_i \sim 2pLND\left(n \cdot \mu_X, n \cdot \sigma_X^2\right). \tag{2.83}$$

A more general case of products of iid 2pLND variables is given in CROW AND SHIMIZU (1988). For Y_i, with $i = 1, \ldots, n$ and the constant values b_i and $c > 0$ (e.g. $c = \exp(a)$; $a > 0$) it follows

$$c \cdot \prod_{i=1}^{n} X_i^{b_i} \sim 2pLND\left(a + \sum_{i=1}^{n} b_i \cdot \mu_{ND,i}, \sum_{i=1}^{n} b_i^2 \cdot \sigma_{ND,i}^2\right). \tag{2.84}$$

Consequently, also 1 / Y and Y_1 / Y_2 are lognormally distributed, with

$$\left(\frac{1}{Y}\right) \sim \mathrm{LND}\left(-\mu_X, \sigma_X^2\right) \quad \text{and} \quad \left(\frac{Y_1}{Y_2}\right) \sim \mathrm{LND}\left(\mu_{X,1} - \mu_{X,2}, \sigma_{X,1}^2 + \sigma_{X,2}^2\right). \tag{2.85}$$

In case of iid Y_i with $i = 1, \ldots, n$ the geometric mean of Y_i is also lognormally distributed, with (AITCHINSON AND BROWN, 1981)

$$\left(\prod_{i=1}^{n} Y_i\right)^{1/n} \sim \mathrm{LND}\left(\mu_X, \frac{\sigma_X^2}{n}\right). \tag{2.86}$$

In case of dependent (correlated) bivariate 2pLND variables Y_1 and Y_2 with LND (μ, Σ) the expectation vector μ and variance-covariance matrix Σ are given by (LAW AND KELTON, 2000)

$$\mu = \left[\mu_{X,1}, \mu_{X,2}\right]^T \; ; \; \Sigma = \begin{bmatrix} \sigma_{X,1}^2 & \sigma_{X,1} \cdot \sigma_{X,2} \cdot \rho_{X,1;X,2} \\ \sigma_{X,1} \cdot \sigma_{X,2} \cdot \rho_{X,1;X,2} & \sigma_{X,2}^2 \end{bmatrix}, \tag{2.87}$$

with covariance

$$CoVar\left[Y_1, Y_2\right] = \exp\left(\sigma_{X,1} \cdot \sigma_{X,2} - 1\right) \cdot \exp\left(\mu_{X,1} + \mu_{X,2} + \frac{\sigma_{X,1}^2 + \sigma_{X,2}^2}{2}\right), \tag{2.88}$$

and correlation coefficient

$$\rho_{Y_1,Y_2} = \frac{\exp\left(\rho_{X,1;X,2} \cdot \sigma_{X,1} \cdot \sigma_{X,2}\right) - 1}{\sqrt{\left[\exp\left(\sigma_{X,1}^2\right) - 1\right] \cdot \left[\exp\left(\sigma_{X,2}^2\right) - 1\right]}}. \tag{2.89}$$

The covariance of corresponding bivariate ND-variables is given by (LAW AND KELTON, 2000)

$$CoVar\left[X_1, X_2\right] = \ln\left(1 + \frac{CoVar\left[Y_1, Y_2\right]}{\left|\mu_{Y,1} \cdot \mu_{Y,2}\right|}\right). \tag{2.90}$$

The distribution of the product of two 2pLND variables is given by

$$Y_1 \cdot Y_2 \sim 2pLND\left(\mu_{X,1} + \mu_{X,2}, \sigma_{X,1}^2 + 2 \cdot \sigma_{X,1} \cdot \sigma_{X,2} \cdot \rho + \sigma_{X,2}^2\right) , \tag{2.91}$$

whereas the distribution of the quotient follows

$$Y_1 / Y_2 \sim 2pLND\left(\mu_{X,1} - \mu_{X,2}, \sigma_{X,1}^2 - 2 \cdot \sigma_{X,1} \cdot \sigma_{X,2} \cdot \rho + \sigma_{X,2}^2\right) . \tag{2.92}$$

In that sense the central limit theorem can also be applied for products of independent positive variables Y_i, with both existing central moments $E[\ln(Y_i)] = \mu_X$ and $Var[\ln(Y_i)] = \sigma_X^2$, given as

$$\prod_{i=1}^{n} Y_i \overset{asympt.}{\sim} 2pLND\left(n \cdot \mu_X, n \cdot \sigma_X^2\right), \text{ with } i = 1, .., n, \tag{2.93}$$

which implies that the geometric mean follows asymptotically a LND according (2.86).

2.4.3 The Weibull Distribution Model (WD)

In 1939 WEIBULL derived the statistical distributions called two- and three-parameter WEIBULL distributions (2pWD, 3pWD). These models are based on physically driven assumptions in combination with stochastics and especially rank statistics, including the extreme value theory of minima. In short, he modelled (brittle) materials as aggregates of a large number of elements with iid strengths. Thereby the strength of the aggregate reduces with increasing size due to the assumption that a failure of the weakest element initiates a sudden failure of the whole aggregate. This led to the well known “weakest link theory” according WEIBULL (WLT) although he was not the first who published the principle idea behind WLT. Further details on this theory are given in section 3.2.1. In contrast to ND and LND the WD provides a statistical distribution model in analytical closed form but requires additional efforts in determining the WD parameters. The WD is the only statistical distribution model which stays in principle the same in limiting cases, e.g. in investigations concerning the minima and maxima of iid variables.

The PDF of the three parameter WEIBULL distribution (3pWD) is given by

$$f_X(x) = \frac{\beta}{\alpha} \cdot \left(\frac{x - x_0}{\alpha}\right)^{\beta - 1} \cdot \exp\left[-\left(\frac{x - x_0}{\alpha}\right)^{\beta}\right], \tag{2.94}$$

with location parameter x_0 within $0 \le x_0 \le x < \infty$ and scale and shape parameters $\alpha, \beta > 0$. The CDF follows from integration and is given by

$$F_X(x) = 1 - \exp\left[-\left(\frac{x - x_0}{\alpha}\right)^{\beta}\right]. \tag{2.95}$$

In case of $x_0 = 0$, equ. (2.94) and (2.95) simplify to the 2pWD, with PDF and CDF given as

$$f_X(x) = \frac{\beta}{\alpha} \cdot \left(\frac{x}{\alpha}\right)^{\beta-1} \cdot \exp\left[-\left(\frac{x}{\alpha}\right)^{\beta}\right], \; F_X(x) = 1 - \exp\left[-\left(\frac{x}{\alpha}\right)^{\beta}\right]. \tag{2.96}$$

The expectation E[X] and variance Var[X] can be calculated as

$$\begin{aligned} &\text{3pWD:} \qquad E[X] = x_0 + \alpha \cdot \Gamma\left(1 + \frac{1}{\beta}\right), \\ &\text{2pWD:} \qquad E[X] = \alpha \cdot \Gamma\left(1 + \frac{1}{\beta}\right), \end{aligned} \tag{2.97}$$

and

$$\text{3pWD and 2pWD:} \qquad Var[X] = \alpha^2 \cdot \left[\Gamma\left(1 + \frac{2}{\beta}\right) - \Gamma^2\left(1 + \frac{1}{\beta}\right)\right], \tag{2.98}$$

with location parameter $x_0 \ge x \ge 0$, scale and shape parameters $\alpha, \beta > 0$, respectively, and $\Gamma(.)$ expressing the complete gamma function defined by

$$\Gamma[z] = \int_0^{\infty} t^{z-1} \cdot \exp(-t) \cdot dt\,. \tag{2.99}$$

The variance-covariance matrix of parameter estimates $\hat{\alpha}$ and $\hat{\beta}$ based on maximum likelihood method is given by (BURY, 1975)

$$[V_{ij}] = \frac{1}{n} \cdot \begin{bmatrix} 1.10866 \cdot \dfrac{\alpha^2}{\beta^2} & 0.25702 \cdot \alpha \\ 0.25702 \cdot \alpha & 0.60793 \cdot \beta^2 \end{bmatrix}, \tag{2.100}$$

with $\mathrm{Var}[\hat{\alpha}] = 1.10866 \cdot \alpha^2 / (n \cdot \beta^2)$ and $\mathrm{Var}[\hat{\beta}] = 0.60793 \cdot \beta^2 / n$. As given in equ. (2.100) the estimates of α and β are not independent. The coefficient of variation CoV[X] can be derived as

$$\text{2pWD: } CoV[X] = \frac{\sqrt{Var(X)}}{E[X]} = \frac{\sqrt{\Gamma\left(1+\frac{2}{\beta}\right) - \Gamma^2\left(1+\frac{1}{\beta}\right)}}{\Gamma\left(1+\frac{1}{\beta}\right)},$$

$$\text{3pWD: } CoV[X] = \frac{\sqrt{\Gamma\left(1+\frac{2}{\beta}\right) - \Gamma^2\left(1+\frac{1}{\beta}\right)}}{\frac{x_0}{\alpha} + \Gamma\left(1+\frac{1}{\beta}\right)}. \tag{2.101}$$

Thus in case of 2pWD the coefficient of variation CoV[X] only depends on the WEIBULL module or shape parameter β and not on the scale parameter α. The WEIBULL module is also well known for the characterisation of failure rates according the bath-tube-curve, with $\beta < 1$ representing early (infant) failures, $\beta = 1$ representing random failures and $\beta > 1$ wear-out failures (WILKER, 2004).

Quantiles of 2pWD variables can be derived from (2.95) as

$$x_p = \alpha \cdot \left[\ln\left(\frac{1}{1-p}\right)\right]^{1/\beta} \quad \rightarrow \; med[X] = x_{50} = \alpha \cdot [\ln(2)]^{1/\beta}. \tag{2.102}$$

The mode is given by

$$\mathrm{mod}[X] = \alpha \cdot \left(\frac{\beta-1}{\beta}\right)^{1/\beta}, \text{ for } \beta > 1. \tag{2.103}$$

As shown in (2.101) CoV[X] of 2pWD only depends on the WEIBULL module β, and vice versa. A short study of CoV[X] as function of β in the range of CoV[X] = (1, 100)% leads to a well approximating equation (see Fig. 2.3, left) given as

$$CoV_{est}[X] \approx \beta^{-0.93}, \text{ for } 127.5 \geq \beta \geq 1.0. \tag{2.104}$$

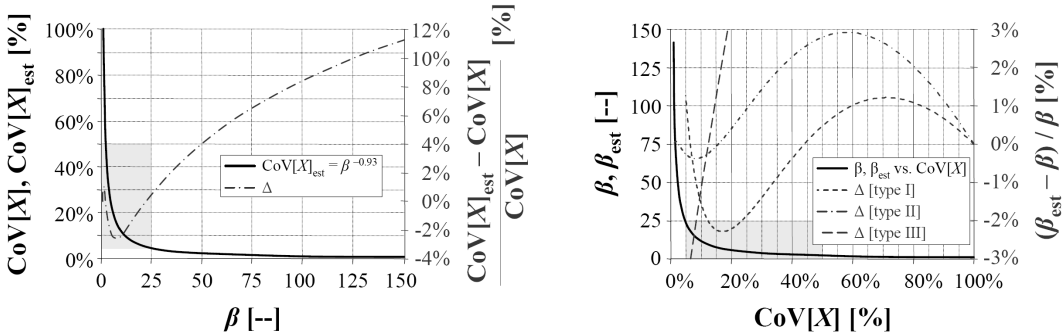

Fig. 2.3: WEIBULL shape parameter β vs. coefficient of variation CoV[X], comparison of approximations: (left) CoV[X], CoV[X]$_{\text{est}}$ vs. β; (right) β, β_{est} vs. CoV[X]; grey region mark common ranges of CoV[X] and β in material science

The estimation of β given a known or estimated CoV[X] is perhaps a bit tricky leading to unrealistic approximations especially at CoV[X] < 10%. Roughly spoken β can be estimated by calculating the inverse formulation of equ. (2.104) given by

$$\textbf{type I}: \beta_{est} \approx CoV\left[X\right]^{-1.078}, \text{ for } 10\% \leq \text{CoV}[X] \leq 100\% \tag{2.105}$$

with a maximum squared error $\varepsilon^2 = (\beta_{\text{est}} - \beta)^2$ of $\varepsilon^2 = 3.83\%$ and $10\% \leq \text{CoV}[X] \leq 100\%$ (see Fig. 2.3, right). An improved estimation of β is given by the function

$$\textbf{type II}: \beta_{est} \approx \Gamma\left(CoV\left[X\right]^{0.1104}\right)^{-3.2447} \cdot CoV\left[X\right]^{-1.3317}, \tag{2.106}$$

for $1\% \leq \text{CoV}[X] \leq 100\%$, with a maximum squared error $\varepsilon^2 = (\beta_{\text{est}} - \beta)^2$ of $\varepsilon^2 = 0.51\%$ with ε in the range of $\varepsilon = (-7.12\%, +6.14\%)$, for $1\% \leq \text{CoV}[X] \leq 100\%$ corresponding to $1.0 \leq \beta \leq 127.5$. In case of failure definition $\delta = (\beta_{\text{est}} - \beta) / \beta$ the failure range is given by $\delta = (-0.38\%, +2.92\%)$ (see Fig. 2.3, right).

Based on the above estimation of β the second distribution parameter α can be estimated by means of β_{est} and estimation of med[X] in case of a given sample. Thus the error in β_{est} is even reduced in calculating α_{est}. The procedure for predicting α has the advantage that rank statistics are more robust against outliers than empirical mean and variance. Nevertheless CoV[X] has to be estimated first and therefore also arithmetic mean and empirical variance are required. As mentioned in previous sections the knowledge on expectable ranges of CoV[X] provides further analysis in respect to parameter studies

supporting judgement of accuracy in prediction. For comparison, HITCHON AND PHILLIPS (1978) proposed that the relationship can be approximated by $\beta \approx 1.20 / \mathrm{CoV}[X]$ (**type III**) (see Fig. 2.3, right).

2.5 Order Statistics

Let $(X_1, \ldots, X_n)$ be a sample vector with identical and independent distributed (iid) X_i and CDF $F_X(x)$. Than the order statistics are the statistics of ordered events with defined order of occurence, denoted by $X_{(i)}$, with $X_{(1)} \leq X_{(2)} \leq \ldots \leq X_{(n)}$, with max $[X_{(i)}] = X_{(n)}$ and min $[X_{(i)}] = X_{(1)}$. Thus the **range R** is given by $R = X_{(n)} - X_{(1)}$. The order statistics of realisations of random variable X_i are given as $x_{(i)} = x_{(1)}, \ldots, x_{(n)}$.

Assuming an iid random variable X_i with density $f_X(x)$ and CDF $F_X(x)$ than the probability density function $f_k(x)$ as well as the cumulative distribution function $F_k(x)$ of $X_{(k)}$ at the position k are given as (e.g. ROHLING, 2007)

$$\begin{aligned} f_k(x) &= k \cdot \binom{n}{k} \cdot [1 - F_X(x)]^{n-k} \cdot F_X(x)^{k-1} \cdot f_X(x), \\ F_k(x) &= \sum_{j=k}^{n} \binom{n}{j} \cdot [F_X(x)]^{j} \cdot [1 - F_X(x)]^{n-j}. \end{aligned} \tag{2.107}$$

The PDF and CDF of extreme values, the minima and maxima, are given as

$$\begin{aligned} &\text{minima:} \quad f_1(x) = n \cdot [1 - F(x)]^{n-1} \cdot f(x) \text{ and } F_1(x) = 1 - [1 - F(x)]^{n}, \\ &\text{maxima:} \quad f_n(x) = n \cdot F(x)^{n-1} \cdot f(x) \text{ and } F_n(x) = F(x)^{n}. \end{aligned} \tag{2.108}$$

Note: The types of statistical distributions and equations for calculation of some key distribution characteristics of extremes in the limiting case with $n \to \infty$ are discussed in more detail in section 2.6.2.

The pth quantile x_p of a random variable represents a value which divides the probability mass in two parts where $P(X \leq x_p) = p$ (e.g. STADLOBER, 2008). In case of continuous random variables it follows

$$F_X(x_p) = P(X \le x_p) = p = \int_{-\infty}^{x_p} f_X(x) \cdot dx \rightarrow x_p = F_X^{-1}(p). \tag{2.109}$$

The theoretical quantile x_p can be estimated by empirical quantiles Q_p which are functions of order statistics $X_{(k)}$. There are numerous possibilities how to estimate the theoretical quantiles x_p by Q_p. Three common possibilities, as given in STADLOBER (2011B) are presented briefly.

<u>Type I: Q_p based on the inverse of the empirical distribution function</u>

In type I x_p is estimated by Q_p by means of the inverse of the empirical distribution function (empD). Thereby Q_p is a discrete estimator and given as

$$\begin{aligned} Q_p &= \frac{1}{2} \cdot \left[X_{(n \cdot p)} + X_{(n \cdot p+1)} \right] && \text{, if } (n \cdot p) \text{ is an integer,} \\ Q_p &= X_{(\lfloor n \cdot p \rfloor + 1)} && \text{, if } (n \cdot p) \text{ is not an integer.} \end{aligned} \tag{2.110}$$

<u>Type II: Estimator Q_p as implemented in statistical software packages e.g. SPSS, MiniTab</u>

In type II the continuous estimator Q_p is given as

$$\begin{aligned} Q_p &= X_{(1)} && , k = 1, \\ Q_p &= a \cdot X_{(k-1)} + (1-a) \cdot X_{(k)} && , 2 \le k \le n, \\ Q_p &= X_{(n)} && , k = n + 1, \end{aligned} \tag{2.111}$$

with

$$k = \lfloor (n+1)/p \rfloor + 1, \; a = k - (n+1) \cdot p \,. \tag{2.112}$$

<u>Type III: Estimator Q_p as implemented by default as type 7 in R (2009)</u>

In type III the continuous estimator Q_p with good smooting is given as

$$Q_p = (1-g) \cdot x_{(\lfloor (n-1) \cdot p \rfloor + 1)} + g \cdot x_{(\lfloor (n-1) \cdot p \rfloor + 2)}, \tag{2.113}$$

with

$$g = (n-1)\cdot p - \lfloor (n-1)\cdot p \rfloor. \tag{2.114}$$

The **median x_{50} = med(X)** as parameter of location halves the probability of events and is defined by

$$\begin{aligned} med(X) &= X_{[(n+1)/2]} && \text{, if } n \text{ is odd,} \\ med(X) &= \left[X_{(n/2)} + X_{(n/2+1)}\right] / 2 && \text{, if } n \text{ is even.} \end{aligned} \tag{2.115}$$

2.6 Some Theorems, Theories and Statistical Models

Following sections present additional stochastic background and discuss the Central Limit Theorem, major aspects of extreme value theory, regression and correlation analysis, hierarchical models, stochastic processes and time series as well as some functions and transformations helpful for further applications.

2.6.1 The Central Limit Theorem

The Central Limit Theorem states that in case of an iid sequence of random variables $X_1, X_2, \ldots$, with $E[X_i] = \mu$, $Var[X_i] = \sigma^2 > 0$ and the definition of the sample mean given by

$$\overline{X}_n = \frac{1}{n}\cdot\sum_{i=1}^{n} X_i\ , \tag{2.116}$$

the CDF Z_n given as

$$Z_n = \sqrt{n}\cdot\left(\frac{\overline{X}_n - \mu}{\sigma}\right), \tag{2.117}$$

converges in the limiting case

$$\lim_{n\to\infty}\ G_n(x) = \int_{-\infty}^{x} \frac{1}{\sqrt{2\cdot\pi}}\cdot\exp\left(-\frac{y^2}{2}\right)\cdot dy = \Phi(x), \tag{2.118}$$

to the standard normal distribution (SND). The normality follows herein from the sum of in respect to finite variance, small and independent disturbances. In general equ. (2.118) is a very usefull approximation also for finite but sufficient large number of summands.

Even if the number of variables is small, in the range of about 10 to 20, and even if the distribution of the variables is far away from normality (e.g. uniformly distributed) the distribution of the sum converges relatively fast to the normal distribution. The judgement whether or not the approximation is sufficiently accurate has to be done individually and in dependency of the type of the parent distribution(s) (CASELLA AND BERGER, 2002).

2.6.2 The Extreme Value Statistics and its Distribution Models

The extreme value theory (EVT) concentrates on the stochastic description and modelling of the behaviour of extreme values (e.g. maxima, minima) with focus on iid variables and processes. The extreme value distributions describe limiting distribution functions with system size $n \to \infty$. As generally known (see (2.107)), if X_1, X_2, …, X_n are iid random variables with CDF $F_X(x)$ the distribution of extremes for **minima** constitutes as

$$X_{(1)} \le X_{(2)} \le \ldots \le X_{(n)} \rightarrow F_{X,\min}(x) = F_{X_{(1)}}(x) = 1 - \left[1 - F_X(x)\right]^n,$$
$$\text{or inversely } F_X(x) = 1 - \left[1 - F_{X,\min}(x)\right]^{1/n}, \tag{2.119}$$

and for **maxima** as

$$X_{(n)} \ge \ldots \ge X_{(2)} \ge X_{(1)} \rightarrow F_{X,\max}(x) = F_{X_{(n)}}(x) = \left[F_X(x)\right]^n,$$
$$\text{or inversely } F_X(x) = \left[F_{X,\max}(x)\right]^{1/n}. \tag{2.120}$$

Tab. 2.2: Limiting distributions vs. parent distributions (KOTZ AND NADARAJAH, 2000)

type of parent distribution	**limiting distribution for extremes**	
	maxima	**minima**
$X_i \sim$ exponential $(x \mid \theta)$	type I	type III
$X_i \sim$ gamma $(x \mid \theta)$	type I	type III
$X_i \sim$ normal $(x \mid \theta)$	type I	type I
$X_i \sim$ lognormal $(x \mid \theta)$	type I	type I
$X_i \sim$ uniform $(x \mid \theta)$	type III	type III
$X_i \sim$ pareto $(x \mid \theta)$	type II	type III
$X_i \sim$ cauchy $(x \mid \theta)$	type II	type II

According GRIFITH's theory differences between the calculated strength of materials by means of classical strength theory and the observed strength can be traced back to strength reducing flaws in the material body.

PEIRCE (1926) was probably the first who connected the specimen strength with extreme value theory. Based on these previous works WEIBULL (1939) defined his well known stochastic strength theory on the basis of weakest link theory for brittle materials. A comprehensive and recommended summary of the developments regarding extreme value theory is given in KOTZ AND NADARAJAH (2000).

FISHER AND TIPETT (1928) showed that there are exactly three types of limiting extreme value distributions (KOTZ AND NADARAJAH, 2000). For maxima they are given by equ. (2.121) to (2.123), with $\boldsymbol{\theta} = (\mu, \sigma, \xi)^{\mathrm{T}}$ as parameter vector with $\sigma, \xi > 0$, $\mu \in \mathbb{R}$ as location parameter, σ as scaling parameter and ξ as shape parameter. The corresponding distributions for minima are derived by substitution of x by $(-x)$.

Type I is often treated as reference extreme value distribution (EVD). Variables distributed according type II or type III can be easily transformed to type I. If $X \sim$ type II with $F_X(x \mid 0, \sigma, \xi)$, substituting X by $\ln(X)$ leads to type I with $F_X(x \mid 0, \ln(\sigma), 1 / \xi)$. If $X \sim$ type III with $F_X(x \mid 0, \sigma, \xi)$, substituting X by $\ln(X)$ leads to type I with $F_X(x \mid 0, -\ln(\sigma), 1 / \xi)$.

Tab. 2.2 gives the limiting distributions in dependency of the parent distribution of X.

Type I (Gumbel-type):

$$P[X \le x] = F_X(x \mid \theta) = \exp\left[-\exp\left(-\frac{x-\mu}{\sigma}\right)\right], \tag{2.121}$$

with $x \in (-\infty, +\infty)$

→ exponential decrease of upper distribution tail (e.g. SCHUËLLER, 1981);

Type II (Fréchet-type):

$$P[X \le x] = F_X(x \mid \theta) = \begin{cases} 0 & x \le \mu \\ \exp\left[-\left(\frac{x-\mu}{\sigma}\right)^{-\xi}\right] & x > \mu \end{cases}, \tag{2.122}$$

with $x \in [\mu - \sigma / \xi, +\infty)$, $\xi > 0$

→ polynomial decrease of upper distribution tail (e.g. SCHUËLLER, 1981);

Type III (reversed Weibull-type):

$$P[X \le x] = F_X(x \mid \theta) = \begin{cases} \exp\left[-\left(-\dfrac{x-\mu}{\sigma}\right)^{\xi}\right] & x < \mu \\ 1 & x \ge \mu \end{cases}, \tag{2.123}$$

with $x \in (-\infty, \mu - \sigma / \xi]$, $\xi < 0$

→ for modelling of material's life time stressed in fatigue (e.g. SCHUËLLER, 1981).

All three types can be traced back to the generalised extreme value distribution (GEVD) with same domains of X with CDF

$$P[X \le x] = F_X(x \mid \theta) = \begin{cases} \exp\left[-\left(1+\xi \cdot \dfrac{x-\mu}{\sigma}\right)\right]^{-1/\xi} & -\infty < x \le \mu - \dfrac{\sigma}{\xi}, \quad \xi < 0 \\ & \mu - \dfrac{\sigma}{\xi} \le x < \infty, \quad \xi > 0 \\ \exp\left[-\exp\left(-\dfrac{x-\mu}{\sigma}\right)\right] & -\infty < x < \infty, \quad \xi = 0 \end{cases}, \tag{2.124}$$

and PDF

$$f_X(x \mid \theta) = \begin{cases} \dfrac{1}{\sigma} \cdot \exp\left[-\left(1+\xi \cdot \dfrac{x-\mu}{\sigma}\right)\right]^{-1/\xi} \cdot \left(1+\xi \cdot \dfrac{x-\mu}{\sigma}\right)^{-1/\xi-1} & \xi \ne 0 \\ \dfrac{1}{\sigma} \cdot \exp\left[-\exp\left(-\dfrac{x-\mu}{\sigma}\right)\right] \cdot \exp\left(-\dfrac{x-\mu}{\sigma}\right) & \xi = 0 \end{cases}. \tag{2.125}$$

The three types of EVD can be derived from GEVD with $\xi = 0$ → type I, $\xi > 0$ → type II and $\xi < 0$ → type III, whereby ξ is predominantly influenced by the functional form of the tail as already indicated in equ. (2.121) to (2.123). Hence $\xi = 0$ corresponds to an exponential decreasing function, $\xi > 0$ to a polynomial decreasing functional behaviour, in general expectable in case of long-tailed parent distributions, and $\xi < 0$ characterises distributions with short tails given in case of a finite upper limit. In the evaluation of ξ some problems may occur if $\xi < (-1/2)$ and $\xi > 1/2$ due to not existing likelihoods or not existent second and higher moments. Nevertheless, environmental data and data sets gained from natural processes show that parameter ξ is in general within the range of $[-1/2 < \xi < 1/2]$ (KOTZ AND NADARAJAH, 2000).

The central moments and some more figures of GEVD, case $\xi \neq 0$, can be derived by

$$E[X] = \mu - \frac{\sigma}{\xi} + \frac{\sigma}{\xi} \cdot \kappa_1 \text{, if } \xi \neq 0,\ \xi < 1, \tag{2.126}$$

$$Var[X] = \frac{\sigma^2}{\xi^2} \cdot \left(\kappa_2 - \kappa_1^{\,2}\right) \text{, if } \xi \neq 0,\ \xi < 1/2, \tag{2.127}$$

$$\mathrm{mod}[X] = \mu + \frac{\sigma}{\xi} \cdot \left[(1+\xi)^{-\xi} - 1\right] \text{, if } \xi \neq 0, \tag{2.128}$$

$$skew[X] = \frac{\kappa_3 - 3 \cdot \kappa_1 \cdot \kappa_2 + 2 \cdot \kappa_1^{\,3}}{\left(\kappa_2 - \kappa_1^{\,2}\right)^{3/2}} \text{, if } \xi \neq 0, \tag{2.129}$$

$$kurt[X] = \frac{\kappa_4 - 4 \cdot \kappa_1 \cdot \kappa_3 + 6 \cdot \kappa_2 \cdot \kappa_1^{\,2} - 3 \cdot \kappa_1^{\,4}}{\left(\kappa_2 - \kappa_1^{\,2}\right)^{2}} \text{, if } \xi \neq 0, \tag{2.130}$$

with $\kappa_k = \Gamma\,(1 - k \cdot \xi)$, for $k = 1, 2, \ldots$

By means of order statistics the probability distribution function of the rth order statistic $X_{(r)}$ of iid random variables with $-\infty < x < \infty$ is given by

$$f_{X_{(r)}}(x) = \frac{n\,!}{(r-1)\,!\cdot(n-r)\,!} \cdot \sum_{j=0}^{n-r} (-1)^j \cdot \binom{n-r}{j} \cdot \exp\left[-x - (j+r) \cdot \exp(-x)\right]. \tag{2.131}$$

The kth moment is given by

$$E\left[X_{(r)}^{\,k}\right] = \frac{n\,!}{(r-1)\,!\cdot(n-r)\,!} \cdot \sum_{j=0}^{n-r} (-1)^j \cdot \binom{n-r}{j} \cdot g_k(r+j),$$

$$\text{with } g_k(c) = \int_{-\infty}^{\infty} x^k \cdot \exp\left[-x - c \cdot \exp(-x)\right] \cdot dx. \tag{2.132}$$

Here it has to be remarked that ordered realisations are due to ranking not independent even if the realisations itself represent independent outcomes (BURY, 1975).

Some more Comments on Type I EVD

The EVD type I is perhaps the most common and preferably studied type of the EVD models and is also known as double-exponential or GUMBEL model. As given in Tab. 2.2

type I EVD is also the limiting distribution of variables with ND or 2pLND as parent distribution, for minima and maxima. The right-skewed PDF is given by

$$f_X(x \mid \theta) = \frac{1}{\sigma} \cdot \exp\left[-\frac{x-\mu}{\sigma} - \exp\left(-\frac{x-\mu}{\sigma}\right)\right], \text{ for maxima,}$$
$$f_X(x \mid \theta) = \frac{1}{\sigma} \cdot \exp\left[\frac{x-\mu}{\sigma} - \exp\left(\frac{x-\mu}{\sigma}\right)\right], \text{ for minima.} \tag{2.133}$$

If standardised by

$$Y = \frac{X-\mu}{\sigma}, \tag{2.134}$$

the PDFs simplify to

$$f_Y(y \mid \theta) = \exp[-y - \exp(-y)], \text{ for maxima,}$$
$$f_Y(y \mid \theta) = \exp[y - \exp(y)], \text{ for minima,} \tag{2.135}$$

with $\boldsymbol{\theta} = (\mu, \sigma)^{\mathrm{T}}$ as parameter vector. The CDFs are given as

$$F_X(x \mid \theta) = \exp\left[-\exp\left(-\frac{x-\mu}{\sigma}\right)\right], \text{ for maxima,}$$
$$F_X(x \mid \theta) = 1 - \exp\left[-\exp\left(\frac{x-\mu}{\sigma}\right)\right], \text{ for minima.} \tag{2.136}$$

By taking twice the logarithm of equ. (2.136) it follows

$$-\ln[-\ln(F_X(x \mid \theta))] = \frac{x-\mu}{\sigma} \text{ (maxima); } \ln[-\ln(1 - F_X(x \mid \theta))] = \frac{x-\mu}{\sigma} \text{ (minima).} \tag{2.137}$$

If the left side of equations in (2.137) (y-axis) is plotted against the right side of (2.137) (x-axis) a linear function with gradient $(1 / \sigma)$ and intersection with the x-axis at $x = \mu$ is given. This graph represents a probability paper which enables a quick qualitative judgement of a set of realisations of a specific variable whether or not being represented by type I. It is recommended to compute the empirical distribution empD by values $\mathrm{empD_i} = (i - 0.5) / n$, with $i = 1, \ldots, n$.

The first two central moments of EVD type I are given by

$$E[X] = \mu + \sigma \cdot \gamma \text{ (maxima); } E[X] = \mu - \sigma \cdot \gamma \text{ (minima),} \tag{2.138}$$

with $\gamma = 0.5772156\ldots$ as the EULER-MASCHERONI constant, and

$$Var[X] = \frac{1}{6} \cdot \pi^2 \cdot \sigma^2 \approx 1.64493 \cdot \sigma^2 \text{ (for maxima and minima).} \tag{2.139}$$

The skewness skew[X] = 1.1396 is independent of the distribution parameters μ and σ (SCHUËLLER, 1981). The location parameter μ conforms to mode[X]. The inflexion points are at

$$X = \mu \pm \sigma \cdot \ln\left[\frac{1}{2} \cdot \left(3 + \sqrt{5}\right)\right] \approx \mu \pm 0.96 \cdot \sigma\,. \tag{2.140}$$

The quantiles x_p, with $F_X(x_p) = p$ can be calculated simply as

$$x_p = \mu - \sigma \cdot \ln[-\ln(p)] \text{ (for maxima); } x_p = \mu + \sigma \cdot \ln\left[\ln\left(\frac{1}{p}\right)\right] \text{ (for minima).} \tag{2.141}$$

On the basis of the empirical mean $\overline{X}$ and standard deviation S the distribution parameters can be estimated by the method of moments given in LOWERY AND NASH (1970) as well as LANDWEHR ET AL. (1979) by

$$\hat{\mu} = \overline{X} - \gamma \cdot \hat{\sigma} \text{ (for maxima); } \hat{\mu} = \overline{X} + \gamma \cdot \hat{\sigma} \text{ (for minima) and } \hat{\sigma} = \frac{\sqrt{6}}{\pi} \cdot S\,. \tag{2.142}$$

According to TIAGO DE OLIVEIRA (1963) the variance of these estimated parameters can be evaluated with skew[X] = $\sqrt{\beta_1}$ (X) ≈ $\sqrt{1.29857}$ = 1.1396 and kurt[X] = β_2 (X) ≈ 5.4 by

$$Var[\hat{\mu}] = \frac{\hat{\sigma}^2}{n} \cdot \left[\frac{\pi^2}{6} + \frac{\gamma^2}{4} \cdot (\beta_2 - 1) - \frac{\pi}{\sqrt{6}} \cdot \gamma \cdot \sqrt{\beta_1}\right] \approx \frac{1.1678 \cdot \hat{\sigma}^2}{n}\,, \tag{2.143}$$

$$Var[\hat{\sigma}] = \frac{\hat{\sigma}^2}{4 \cdot n} \cdot (\beta_2 - 1) \approx \frac{1.1 \cdot \hat{\sigma}^2}{n}\,. \tag{2.144}$$

By means of maximum likelihood estimation technique (MLE) the distribution parameters can be derived by

$$\hat{\mu} = -\hat{\sigma} \cdot \ln\left[\frac{1}{n} \cdot \sum_{i=1}^{n} \exp\left(-\frac{X_i}{\hat{\sigma}}\right)\right] \quad \text{and} \quad \hat{\sigma} = \overline{X} - \frac{\sum_{i=1}^{n} X_i \cdot \exp\left(-\frac{X_i}{\hat{\sigma}}\right)}{\sum_{i=1}^{n} \exp\left(-\frac{X_i}{\hat{\sigma}}\right)}, \tag{2.145}$$

solving first the estimate for σ iteratively and than the equation for estimating μ.

Following BURY (1975) the variance-covariance matrix of MLE is given by

$$\left[V_{ij}\right] = \frac{6 \cdot \sigma^2}{n \cdot \pi^2} \cdot \begin{bmatrix} (1-\gamma)^2 + \frac{\pi^2}{6} & 1-\gamma \\ 1-\gamma & 1 \end{bmatrix} \approx \frac{\sigma^2}{n} \cdot \begin{bmatrix} 1.10866 & 0.25702 \\ 0.25702 & 0.60793 \end{bmatrix}, \tag{2.146}$$

with Var[$\hat{\mu}$] = 1.10866 · σ^2 / n and Var[$\hat{\sigma}$] = 0.60793 · σ^2 / n. Furthermore, BURY (1975) comments that samples of size n taken from an extreme value phenomenon following type I EVD show that the largest observation $X_{(n)}$ also follows type I EVD but with shifted location parameter $\mu(X_{(n)}) = \sigma_X \cdot \ln(n) + \mu_X$ and standard deviation $\sigma(X_{(n)}) = \sigma_X$.

2.6.3 Regression and Correlation Analysis

General regression analysis provides the description of a random variable (the dependent variable) by means of a functional relationship to expectation and variance of a (set) of values of the explaining random variable(s) (e.g. SCHUËLLER, 1981). Regression and correlation analysis enable a systematic examination of relationships but not necessary insight into the physics behind the phenomena. Thus extrapolations have to be done with caution (e.g. SCHUËLLER, 1981). BURY (1975) states that statistical dependencies are essentially symmetrical but due to physical considerations some asymmetry may occur due to the fact that statistical dependency does not automatically indicate a causal connection between two or more random variables.

The Simple Linear Regression Model and its Boarder Conditions

In general, the “classic linear models” given by the analysis of variance (ANOVA) and the simple linear regression model are based on an underlying linear model with ND errors (CASELLA AND BERGER, 2002).

According STADLOBER AND SCHAUER (2007) the simple linear regression model gives a first order relationship between two variables. The formulation is given by

$$Y = \alpha \cdot x + \beta + \varepsilon \rightarrow Y_i = \alpha \cdot x_i + \beta + \varepsilon_i \text{, with } i = 1, \ldots, n, \tag{2.147}$$

with Y as the dependent variable in relation to a fixed variable $X = x$ and parameters α and β. The stochastics, the randomness of a specific Y_i given x_i is considered by the random error ε_i. It is assumed that

$$\varepsilon_i \overset{iid}{\sim} ND\left(0,\ \sigma^2\right), \text{ hence } Y_i \overset{ind.}{\sim} ND\left(\mu_Y,\ \sigma^2\right), \text{ with } \mu_Y = \alpha \cdot x_i + \beta, \tag{2.148}$$

hence

$$E\left[Y_i \mid X = x_i\right] = \alpha + \beta \cdot x_i \text{ and } Var\left[\varepsilon_i \mid X = x_i\right] = \sigma^2 = Var\left[Y_i \mid X = x_i\right], \tag{2.149}$$

with constant variance σ^2 (homoscedasticity). Minimisation of the sum of squared errors given as

$$\sum_{i=1}^{n} \varepsilon_i^2 = \sum_{i=1}^{n} \left(y_i - \alpha - \beta \cdot x_i\right)^2 \text{, with estimator } \hat{\varepsilon}_i = e_i = y_i - \hat{y}_i = y_i - \left(\hat{\alpha} + \hat{\beta} \cdot x_i\right), \tag{2.150}$$

with e_i as the observable residuum, is done by means of least square method (LSM). The parameters and its estimators are given by

$$\beta = \frac{CoVar(X,Y)}{Var(X)} \rightarrow \hat{\beta} = \frac{\sum_{i=1}^{n} \left(x_i - \bar{x}\right) \cdot \left(Y_i - \bar{Y}\right)}{\sum_{i=1}^{n} \left(x_i - \bar{x}\right)^2}, \tag{2.151}$$

and

$$\alpha = E[Y] - \beta \cdot E[X] = \mu_Y - \beta \cdot \mu_X \rightarrow \hat{\alpha} = \bar{Y} - \hat{\beta} \cdot \bar{x}. \tag{2.152}$$

The degree of dependence of Y on X can be expressed by the PEARSON correlation coefficient $\rho_{X,Y}(x, y) = \rho_{X,Y}$ defined by

$$\rho_{X,Y}(x,y) = \frac{CoVar[X,Y]}{\sqrt{Var[X]\cdot Var[X]}} = \frac{CoVar[X,Y]}{\sigma_X \cdot \sigma_Y} = \beta \cdot \frac{\sigma_X}{\sigma_Y}, \text{ with } -1 \le \rho_{X,Y} \le 1. \tag{2.153}$$

The components of total squared sum SST of the observed values can be identified as

$$\underbrace{\sum_{i=1}^{n}(Y_i - \bar{Y})^2}_{SST} = \underbrace{\sum_{i=1}^{n}(\hat{y}_i - \bar{y})^2}_{SSR} + \underbrace{\sum_{i=1}^{n}(y_i - \hat{y}_i)^2}_{SSE}, \tag{2.154}$$

with SSR as sum of squared deviations from regression estimates $\hat{y}_i$ and $\bar{y}$ and SSE as the sum of squared deviations between data y_i and the regression estimates for $\hat{y}_i$ defined as residuum $e_i = y_i - \bar{y}_i$. Thus the coefficient of determination, in case of a simple linear regression model defined by $B_{X,Y} = \rho^2_{X,Y}$, expresses the fraction of variance of data which can be explained by the regression model and is defined by

$$B_{X,Y} = 1 - \frac{SSE}{SST} = \frac{SSR}{SST}. \tag{2.155}$$

By means of the transformation $t_i = x_i - \bar{x}$ the regression model becomes $Y = \beta_1 + \beta_2 \cdot t + \varepsilon$, $\beta_1 = E[Y]$ and $\beta_2 = \beta$, with independent regression parameters $\hat{\beta}_1$ and $\hat{\beta}_2$ (CoVar[$\hat{\beta}_1$, $\hat{\beta}_2$] = 0) and distributions

$$\beta_1 = E[Y] = \mu_Y \rightarrow \hat{\beta}_1 \sim ND\left(\bar{Y}, \frac{S_Y^2}{n}\right), \tag{2.156}$$

and

$$\beta_2 = \beta \rightarrow \hat{\beta}_2 \sim ND\left(\hat{\beta}_2, \frac{S_Y^2}{s_t^2}\right) = ND\left(\hat{\beta}_2, \frac{S_Y^2}{s_X^2}\right),$$

with $s_T^2 = \sum_{i=1}^{n} t_i^2 = \sum_{i=1}^{n}(x_i - \bar{x})^2 = s_X^2$. (2.157)

2.6.4 Hierarchical Models

Hierarchical models enable a sequential examination of complex processes by splitting the process into hierarchically simplier models (CASELLA AND BERGER, 2002). The simplest hierarchical model is given by a second order hierarchy, for example by splitting into $X \mid Y \sim \mathrm{DM}\,(X \mid Y)$ and $Y \sim \mathrm{DM}\,(Y)$ for computing the DM of X knowing that $\mathrm{E}[X \mid y] \rightarrow \mathrm{f}\,(y)$. The consequently computed "mixture distributions" are a sign of an underlying hierarchical structure.

For example, HOHENBICHLER AND RACKWITZ (1981) analysed a uniform correlation independent of the distance (time, space) between two or more events known as **equicorrelation**. In general, equicorrelation follows if all elements in a system depend on a common parameter Z whereby Z itself is defined as a random variable modelled by means of a hierarchical model, i.e. in case of a second order hierarchical model given by

$$X_i = Z \cdot Y_i\,, \tag{2.158}$$

with $R_\mathrm{N} = R_\mathrm{N}(X_1, \ldots, X_\mathrm{N})$ expressed by $R_\mathrm{N} = R_\mathrm{N}(Z \cdot Y_1, \ldots, Z \cdot Y_\mathrm{N})$, with Y_i iid and $(Z \cdot Y_1, \ldots, Z \cdot Y_\mathrm{N})$ being independent distributed.

With $(X_1, \ldots, X_\mathrm{N})$ and $(Z, Y_1, \ldots, Y_\mathrm{N})$ as i.e. equicorrelated lognormal random vectors and $\mathrm{E}[X_\mathrm{i}] = \mu$, $\mathrm{Var}[X_\mathrm{i}] = \sigma^2$ ($\rightarrow X_\mathrm{i}$ iid LND-variables) and $\rho[X_\mathrm{i}, X_\mathrm{j}] = \rho$ it follows that (JONES AND MILLER, 1966)

$$\begin{aligned}
&E[Y_i] = \mu / \sqrt{1+\gamma}\,,\ Var[Y_i] = \sigma^2 \cdot (1-\rho)/1+\gamma^2\,,\\
&E[Z] = \sqrt{1+\gamma}\,,\ Var[Z] = \gamma \cdot (1+\gamma)\,,\\
&\rho[Y_i, Y_j] = \rho[Y_i, Z] \ = 0\,,\\
&\text{with } \gamma = \rho \cdot \sigma^2 / \mu^2\,.
\end{aligned} \tag{2.159}$$

The CDF of Y_i becomes

$$\begin{aligned}
&Y_i \sim F_Y(y_i) = \Phi\left(\frac{\ln(y_i) - \eta}{\tau}\right),\\
&\text{with } \eta = 2 \cdot \ln(\mu) - \frac{1}{2} \cdot \ln\left(\mu^2 + \sigma^2\right) \text{ and } \tau^2 = \ln\left(\mu^2 + \sigma^2\right) - \ln\left(\mu^2 + \rho \cdot \sigma^2\right).
\end{aligned} \tag{2.160}$$

2.6.5 Stochastic Processes

A stochastic process constitutes the dynamic part of probability theory (e.g. SCHUËLLER, 1981). In other words, a stochastic process is a model for random processes, random e.g. in time or space, especially relevant if dependency on time or space is given (e.g. WINKLER, 2000). According GRÜN (2009) stochastic processes act as counterpart to empirical time series and constitute the basis for modelling of these. For comparison, a similar relationship between empirical data sets and random variables in classical statistics is given. Whereas in classical statistics the analysis of iid random variables is the core topic, stochastic processes focus on the description of discrete or continuous observations of random processes and therefore on modelling of dependent structures (STEINEBACH, 2006). The sequence of outcomes and occurrence of random variables is in general decisive in stochastic processes. According ROHLING (2007) stochastic processes do not concentrate on singulary iid variables with emphasis on the arithmetic mean, but concentrate on a range of variables with the aim to model time or space dependent dynamical aspects with focus on dependencies between variables with distances in time or space, expressed by their (spatial) correlation structure.

A stochastic process $X(t) = \{X_t(\omega), t \in T\}$ is defined as a family of random variables mapping $X: \Omega \times \tau \rightarrow \mathbb{R}$ which constitutes a real function x_t for each fixed $\omega \in \Omega$ and describes the random process of a sequence of random variables along t, e.g. time (e.g. HASSLER, 2002), space or objectively abstract (e.g. VOß ET AL., 2004). τ and E constitute the parameter domain and the event space, respectively. Especially the relationship of neighbouring random variables becomes important. In case of fixed elementary events $\omega = \omega_0$ realisations of the stochastic process $X(t)$, also known as trajectories or pattern functions, can be observed. The sum of all possible trajectories defines the population of a stochastic process (e.g. VOß ET AL., 2004). In case of fixed $t = t_0$ the random variables $X(t_0)$ shows realisations

$$X_{t_0}(\omega_1),\ X_{t_0}(\omega_2),\ \ldots,\ X_{t_0}(\omega_n). \tag{2.161}$$

The expected value function of $X(t)$ is given by $m_t = \mathrm{E}[X_t] = \mathrm{E}[X_t(\omega)] = \mu(t),\ t \in \tau$ and called trend or trend function (e.g. STADLOBER, 2005; ROHLING, 2007). It expresses the mean function, the average development of the stochastic process $X(t)$ over time or space. For characterisation of the relationship between random variables of a trend-free

stochastic process the **auto covariance function** of $X(t)$ is defined by (e.g. STADLOBER, 2005)

$$K_{XX}(t,s) = CoVar[X_t, X_s] = E[(X_t - m_t)\cdot(X_s - m_s)] = E[X_t, X_s] - m_t \cdot m_s\,, \tag{2.162}$$

with s, $t \in \tau$. This is a symmetrical function in s and t with $K_{XX}(s, t) = K_{XX}(t, s)$. In case of $K_{XX}(t, t)$ it is equal to the **variance** of the stochastic process given by

$$K_{XX}(t,t) = CoVar[X_t, X_t] = Var[X_t] = \sigma^2(t)\,,\ t \in \tau. \tag{2.163}$$

The **auto correlation function (ACF)** of $X(t)$ is given by

$$\rho_{XX}(t,s) = E[X_t \cdot X_s] = \frac{CoVar[X_t, X_s]}{\sqrt{Var[X_t]\ \cdot Var[X_s]}}\ . \tag{2.164}$$

The characteristics of ACF are as following:

- average power of the process

  $$\rho_{XX}(m) \le \rho_{XX}(0) = E\left[\ |X_m|^2\right] = \sigma_X^2 + \mu_X^2\,;$$

- real, even function

  $$\rho_{XX}(-m) = \rho_{XX}(m);$$

- convergence for non-periodic processes

  $$\rho_{XX}(m) = \lim_{N\to\infty} \frac{1}{2\cdot N+1} \sum_{n=-N}^{N} X_n \cdot X_{n+m}\ .$$

In case of a sufficient large value of $|t - s|$ it can be expected that X_s and X_t are only weakly correlated, with

$$\lim_{|t-s|\to\infty} K(s,t) = \lim_{|t-s|\to\infty} \rho(s,t) = 0\,. \tag{2.165}$$

In case of $Z_t(\omega) = [X_t(\omega), Y_t(\omega)]$ being a two-dimensional random variable of a stochastic process the **cross covariance function** as well as the **cross correlation function (CCF)** are given by

$$K_{XY}(t,s) = CoVar[X_t, Y_s],\ s,\ t \in \tau,\ K_{XY}(t,s) = K_{XY}(s,t), \tag{2.166}$$

and

$$\rho_{XY}(t,s) = \frac{CoVar[X_t, Y_s]}{\sqrt{Var[X_t]\ \cdot Var[Y_s]}}\ . \tag{2.167}$$

For an m-dimensional random variable

$$X_t(\omega) = \left[X_{t_1}(\omega),\ \ldots,\ X_{t_m}(\omega)\right] \tag{2.168}$$

of a stochastic process following notations are given:

mean function (vector): $\mu(t) = [\mu_1(t), \ldots, \mu_m(t)]$, (2.169)

variance function (matrix): $\sigma^2(t) = E\left[(X_t - \mu_t)\cdot(X_t - \mu_t)'\right]$, (2.170)

covariance function (matrix): $K(t_1, t_2) = E\left[(X_{t,1} - \mu_{t,1})\cdot(X_{t,2} - \mu_{t,2})'\right]$. (2.171)

Stationarity of Stochastic Processes

In case of <u>strong stationarity</u> the CDF shows invariance against time shifts, denoted by $X(t) = \{X_t, t \in T\}\ \forall\ n \in \mathbb{N}$: $\forall\ \tau, t_1, \ldots, t_n \in T$

$$F_{[X(t_1),\ldots,X(t_n)]}(x_1,\ldots,x_n) = F_{[X(t_1+\tau),\ldots,X(t_n+\tau)]}(x_1,\ldots,x_n). \tag{2.172}$$

Consequently, $E[X_t] = m_t = \mu = m$ and $Var[X_t] = \sigma^2$. Both are constant and independent of t. Also the covariance function depends only on the difference $\tau = t - s$, with $K(s, t) = E[X_s, X_t] - m^2 = K(0, \tau) = K(\tau) = CoVar[X_s, X_{\tau+s}] = K(-\tau)$, $K(0) = CoVar[X_s, X_s] = Var[X_s]$, $\rho(\tau) = \rho(s, t) = K(\tau) / K(0)$, $\lim_{|\tau|\to\infty} K(\tau) = 0$, and the smoothing- or trend-fitting function aligns parallel to time axis (e.g. STADLOBER, 2005; ROHLING, 2007).

<u>Weak stationarity</u> is defined by $E[X_t] = m_t = \mu = m$, $\forall\ t$, $Var[X_t] = \sigma^2 =$ constant (homoscedasticity) and $K(\tau) = K(s, s + \tau)$, $\forall\ s \in \tau$, $s + \tau \in \tau$ (STADLOBER, 2005). In case of weak stationary stochastic processes $\rho_{XX}(t, s)$ satisfies

$$\rho_{XX}(t,s) = \rho(\tau) = \frac{K(\tau)}{K(0)}. \tag{2.173}$$

A stochastic process ε_t is defined as "**white noise**" (pure random process) if expectation $E[\varepsilon_t] = 0$ and variance $Var[\varepsilon_t] = \sigma_\varepsilon^2$, for $\forall\, t \in \tau$, with $CoVar\,[\varepsilon_{t,1}, \varepsilon_{t,2}] = 0$, $\forall\, t_1 \neq t_2$. Consequently, all random variables are independent with a common and constant expectation $\mu = 0$ (or standardised for $\mu = 0$) and with constant variance. Sometimes the stronger condition $\varepsilon_t \sim$ iid $(0, \sigma^2)$ is assumed. The cummulative process of "white noise" is known as "**random walk**".

Ergodic Stochastic Processes

Ergodicity is an additional requirement on stationarity. It enables the derivation of a sufficient statistic based on only one trajectory instead of a band (number) of trajectories as it would be necessary in case of general or stationary stochastic processes. The assumption is that all ensemble average values $E[X_t]$ of $X(t)$ are identical and sufficient represented by each realised trajectory $x(t)$ expressed by

$$E[X(t)]^n = \int_{-\infty}^{\infty} \xi^n \cdot f_X(\xi) \cdot d\xi = \lim_{\tau \to \infty} \frac{1}{2 \cdot T} \int_{-T}^{T} x_t^n(t) \cdot dt\,,\ \forall\, n, \tag{2.174}$$

with $E[X(t_i)]$ as mean value (expectation) of the band corresponding to the average time value (ROHLING, 2007). Therefore and in case of weak stationary and ergodic processes $K_{XX}(t, s)$ is given by

$$K_{XX}(\tau) = \lim_{T \to \infty} \frac{1}{2 \cdot T} \int_{-T}^{T} X_t \cdot X_{t-\tau} \cdot dt\,. \tag{2.175}$$

The power of this stochastic process is given by $\rho_{XX}(0) = \rho_{XX}(0) + \rho_{YY}(0) + 2 \cdot \rho_{XY}(0)$. In case of time discrete, stationary and ergodic stochastic processes it follows

$$\rho_{XX}(m) = K_{XX}(m) = \lim_{N \to \infty} \frac{1}{2 \cdot N + 1} \sum_{n=-N}^{N} X_n \cdot X_{n+m}\,. \tag{2.176}$$

A discrete stochastic process can for example be described by means of a Poisson process or of Markov chains, whereas continuous stochastic processes follow e.g. a Gauss process (e.g. SCHUËLLER, 1981). The first two mentioned processes are further briefly discussed.

The Poisson Process

The Poisson process is one well known special case of stochastic processes and developed by theoretical analysis of queueing and arrival processes (ROHLING, 2007; STADLOBER, 2005). Thereby random variable Z_n describes the time lag (difference or distance) between arrivals n and $(n-1)$ which is assumed to be iid. The number of arrivals up to time point $t = t_0$ with time interval $[0, t_0]$, denoted by $N(t) = n$, is called counting process. The arrival process is assumed to be ergodic with (mean) arrival rate $\lambda = n_A / t_0$, with $n_A = N(t_0)$. The probability of k arrivals within time interval $[0, t_0]$ is assumed to be Poisson distributed,

$$P[N(t_0) = k] = \frac{(\lambda \cdot t_0)^k}{k!} \cdot \exp(-\lambda \cdot t_0),\ N(t_0) \sim \text{Poi}\ (\lambda \cdot t_0), \tag{2.177}$$

with $E[N(t_0)] = \text{Var}[N(t_0)] = \lambda \cdot t_0$. The distribution of the time-lag Z_n between two arrivals is assumed to be iid and expontially distributed with CDF and PDF

$$\begin{aligned} &F_{Z_n}(t) = P(Z_n \le t) = 1 - \exp(-\lambda \cdot t), \text{ with } t \ge 0,\ Z_n \sim \text{Exp}\ (\lambda), \\ &f_{Zn}(t) = \lambda \cdot \exp(-\lambda \cdot t), \end{aligned} \tag{2.178}$$

with $E[Z] = 1 / \lambda$ and $\text{Var}[Z] = 1 / \lambda^2$.

Markov Chains

The Markov characteristic is defined by the lack of memory, the Markov-property. Thus future values depend only on the current value but they are independent of past values, see (e.g. ROHLING, 2007)

$$P(X_{t+1} = j \mid X_t = i_t, X_{t-1} = i_{t-1}, \ldots, X_0 = i_0) = P(X_{t+1} = j \mid X_t = i_t),\ \forall\ (i_0, \ldots, i_t). \tag{2.179}$$

The main characteristics:

- the conditional probability $p_{ij}(t, t+1) = p_{i \mid j}(t, t+1) = P(X_{t+1} = j \mid X_t = i)$ is defined as single-step transition probability from i to j;
- Markov chains are homogenous if single-step transition probabilities are independent from the time of observation t, $p_{ij}(t, t+1) = p_{ij}$, corresponding to Markov chains with stationary transition probabilities.

WINKLER (2000) report that processes with events which only depend on their last state are very common in physical processes. The description of such a process starts with an arbitrary choosen initial state, gained from a pre-defined initial distribution, and develops according the defined transition probabilities. These describe the probability of occurrence of event j at time t in case that the event i at time $(t-1)$ has occured. These one-step dependencies of stochastic processes can also be modelled by 1st order autoregressive models, abbreviated by AR(1).

2.6.6 Time Series

HARTUNG ET AL. (2002), SCHERRER (2009) and GRÜN (2009) define time series as temporary (finite) sequences of quantitative, in respect to time ranked outcomes (measured values) of a specific event. These are performed (1) to gain knowledge about the event within a system, (2) to examine changes (trends), (3) to extract key figures, and (4) used for forecasting of probabilities of future events. Hereby the observation of a time series, the data acquisition, is in general made in equidistant time steps. These time steps shall be choosen short enough to enable the observation of all relevant phenomena in respect to the scope of the model (→ representative time step or time increment). The components $Y(t)$ of a time series can in general be split into three main components:

- flat time series component $G(t)$, as cyclical, wave-shaped component (trend component → estimation by means of least squares method (LSM) in case of robust (linear) trends; (weighted) moving average (MA) otherwise (→ illustration of intermediate-term developments);

- seasonal component $S(t)$ as periodical, wave-shaped component (→ estimation by filtering, smoothing, assuming an additive time series model with constant seasonal trend; → de-trendend) → e.g. moving averages (MA);

- random, irregular component $R(t)$ as sequence of short-time irregular changes with random fluctuation σ around $\mu = 0$.

Consequently, additive (classical) time series models are given as

$$Y(t) = G(t) + S(t) + R(t). \tag{2.180}$$

According GRÜN (2009) also multiplicative segmentation of time series as defined in (2.181) is possible. By logarithmisation they are transformed into additive time series as given by (2.180), see

$$Y(t) = G(t) \cdot S(t) \cdot R(t) \rightarrow \ln[Y(t)] = \ln[G(t)] + \ln[S(t)] + \ln[R(t)]. \tag{2.181}$$

The characteristics like autocovariance, autocorrelation and partial autocorrelation are important statistics of time series $y_1, \ldots, y_n$. They describe interrelationships between observations in determined distances between discrete time steps. Therefore lag(k) defines the relationship between y_t and y_{t+k}, for $t = k, \ldots, (n-k)$. The empirical autocovariance at lag(k) is given by

$$c(k) = \frac{1}{n-k} \cdot \sum_{t=1}^{n-k} (y_t - \bar{y}) \cdot (y_{t+k} - \bar{y}) = c(-k), \text{ for } k = 0, 1, \ldots, n-1, \tag{2.182}$$

whereby the standardisation with $1 / (n-k)$ is sometimes replaced by $1 / n$. Thus the empirical autocovariance at lag(k) is equal with c(k) = c(0), the variance of empirical time series. The empirical auto covariance serves as predictor of the autocovariance K(k) of the population.

The empirical autocorrelation $r(k)$ as predictor of $\rho(k)$ can be computed by standardising the empirical autocovariance by the empirical variance at lag(k), see

$$r(k) = \frac{c(k)}{c(0)} = \frac{\sum_{t=1}^{n-k} (y_t - \bar{y}) \cdot (y_{t+k} - \bar{y})}{\sum_{t=1}^{n-k} (y_t - \bar{y})^2} = r(-k), \text{ with } r(k{=}0) = r(0) = 1. \tag{2.183}$$

2.6.7 Functions and Transformations of Variables and their Distributions

In general, if X is a random variable with CDF given as $F_X(x)$ than any function of X, e.g. g(X) is also a random variable, e.g. Y = g(X) (CASELLA AND BERGER, 2002). Let χ be a domain defined by $\chi = \{x: f_X(x) > 0\}$ and γ be a domain defined by $\gamma = \{y: y = g(X)$, for some $x \in \chi\}$ then if X defines a continuous random variable the CDF of Y = g(X) given as $F_Y(y)$ is given by

$$F_Y(y) = \int_{\{x \in \chi : x \le g^{-1}(y)\}} f_X(x) \cdot dx = \int_{-\infty}^{g^{-1}(y)} f_X(x) \cdot dx = F_X\left[g^{-1}(y)\right] \quad \text{, if g}(x) \text{ increases,}$$

$$F_Y(y) = \int_{g^{-1}(y)}^{\infty} f_X(x) \cdot dx = 1 - F_X\left[g^{-1}(y)\right] \quad \text{, if g}(x) \text{ decreases.} \tag{2.184}$$

In case of a discrete random variable X the same holds by changing the integral by the sum operator. The PDF in case of a partly monotone function g(x) is given by

$$f_Y(y) = \begin{cases} \sum_{i=1}^{k} f_X\left[g_i^{-1}(y)\right] \cdot \left| \frac{d}{dy} g_i^{-1}(y) \right| & , \; y \in \gamma \\ 0 & , \; else \end{cases}, \tag{2.185}$$

with $g_1(x)$, …, $g_k(x)$, $i = 1, \ldots, k$, defined on A_1, …, A_k as monotone regions of g(x) and subspaces of the sample space (CASELLA AND BERGER, 2002; ROHLING, 2007). In case of a monotone function g(x) over the whole domain of X the PDF simplifies to

$$f_Y(y) = f_X[h(y)] \cdot \left| \frac{d}{dy} h(y) \right|, \tag{2.186}$$

with $Y = g(x)$ and $h(y) = g^{-1}(y) = X \rightarrow dx / dy = dh(y) / dy$.

For example, if two random variables X and Y with joint PDF $f_{X,Y}(x, y)$ are transformed according $u = g_1(x, y)$ and $v = g_2(x, y)$ the joint PDF of U and V is given by (CASELLA AND BERGER, 2002)

$$f_{U,V}(u,v) = f_{X,Y}\left[h_1(u,v), h_2(u,v)\right] \cdot |J|, \tag{2.187}$$

with |J| as the absolute value of the Jacobian determinand which is defined by

$$J = \begin{vmatrix} \frac{\partial x}{\partial u} & \frac{\partial x}{\partial v} \\ \frac{\partial y}{\partial u} & \frac{\partial y}{\partial v} \end{vmatrix} = \frac{\partial x}{\partial u} \cdot \frac{\partial y}{\partial v} - \frac{\partial y}{\partial u} \cdot \frac{\partial x}{\partial v},$$

$$\text{with } \frac{\partial x}{\partial u} = \frac{\partial h_1(u,v)}{\partial u}, \; \frac{\partial x}{\partial v} = \frac{\partial h_1(u,v)}{\partial v}, \; \frac{\partial y}{\partial u} = \frac{\partial h_2(u,v)}{\partial u}, \; \frac{\partial y}{\partial v} = \frac{\partial h_2(u,v)}{\partial v}. \tag{2.188}$$

Comments on Sums of Variables

The PDF of a sum of mutually independent random variables can be derived by means of calculating the product of existing MGFs (see section 2.3.3) given as (CASELLA AND BERGER, 2002)

$$M_Z(z) = \left(e^{t\cdot\sum b_i}\right)\cdot M_{X_1}(a_1\cdot t)\cdot\ldots\cdot M_{X_n}(a_n\cdot t), \text{ with } Z=\sum_{i=1}^{n}(a_i\cdot X_i+b_i), \tag{2.189}$$

with X_i as random variables and a_i, b_i as constants.

Another possibility of deriving the PDF of a sum of independent random variables is given by calculating the convolution of the PDFs. Assuming two independent random variables X and Y with PDF or PMF $f_X(x)$ or $p_X(x)$ and $f_Y(y)$ or $p_Y(y)$ than the PDF of $Z = X + Y$ is given by (DURRETT, 1994)

$$\begin{aligned} f_Z(z) &= \sum_x P(X=x)\cdot P(Y=z-x) = p_X(x) * p_Y(y), \text{ if } Z \text{ is discrete;} \\ f_Z(z) &= \int_{-\infty}^{\infty} f_X(x)\cdot f_Y(z-x)\cdot dx = f_X(x) * f_Y(y), \text{ if } Z \text{ is continuous.} \end{aligned} \tag{2.190}$$

Fourier transformation (FT) transforms the PDFs of variables X and Y into their spectrum FT [$f_X(x)$] and FT [$f_Y(y)$]. The spectrum of the PDF of Z is thus given by the product of the spectrums of the PDFs of X and Y, see

$$f_Z(z) = f_X(x) * f_Y(y) \xrightarrow{FT} FT[f_Z(z)] = FT[f_X(x)]\cdot FT[f_Y(y)]. \tag{2.191}$$

In probability theory the same calculation procedure can be performed by means of the characteristic function $\phi_X(t)$ (ROHLING, 2007; section 2.3.4).

In case of $Z = X_1 + X_2 + \ldots$ the PDF of Z is given by

$$f_Z(z) = f_{X_1}(x) * f_{X_2}(x) * \ldots \rightarrow \phi_Z(t) = \prod_{i=1}^{n}\phi_{X_i}(t), \tag{2.192}$$

and in case of $X_i \sim$ iid by

$$\phi_Z[t] = \left[\phi_{X_i}(t)\right]^n . \tag{2.193}$$

The backwards transformation is given by

$$f_Z(z) = \frac{1}{2 \cdot \pi} \cdot \int_{-\infty}^{\infty} \phi_Z(t) \cdot \exp(-i \cdot t \cdot z) \cdot dt \text{ , with } \phi_Z(0) = 1. \tag{2.194}$$

Comments on Products of Variables

In case of dependent random variables X and Y with existing moments for calculating E[.] and Var[.] the expected value and the variance of the ratio $Z = X / Y$ can be approximated by (CASELLA AND BERGER, 2002)

$$E[Z] \approx \frac{\mu_X}{\mu_Y} \text{ ; } Var[Z] \approx \left(\frac{\mu_X}{\mu_Y}\right)^2 \cdot \left(\frac{Var[X]}{\mu_X^2} + \frac{Var[Y]}{\mu_Y^2} - 2 \cdot \frac{CoVar[X,Y]}{\mu_X \cdot \mu_Y}\right). \tag{2.195}$$

Chapter 3

Serial and parallel System Actions and related Effects with Focus on Strength

This chapter presents some general notes concerning serial and parallel system actions and effects. After a brief introduction a comprehensive literature review about the state-of-the-art of current stochastic material (strength) models is given. In particular Weibull's weakest link theory, theory of plasticity and Daniels's fibre bundle theory are introduced followed by a section presenting latest developments gained by combining these theories to more realistic and broader applicable material and structure models. Thereafter serial and parallel stochastic effects are discussed in more detail, both theoretically and under support of comprehensive stochastic simulations relevant for finite system sizes. This chapter provides theoretical and general applicable background information concerning systems and gives the basis for further examinations relevant to timber system products and structures investigated in chapters 4 and 5. The focus is rather on a general description of material behaviour in systems composed of elements or components which form itself a system of elements.

3.1 General Overview and some Definitions

As already discussed in section 1.3 systems are defined by the arrangement and interaction of system elements and components whereby the system itself can even constitute a sub-system of higher-ranking systems. There are two main features which characterise and determine a system: firstly the quantity of interacting elements, herein expressed by N and M in case of parallel and serial arranged elements, respectively, and secondly the type of interaction between the elements in respect to their arrangement

relative to system exposure. The system action or reaction as a consequence of exposure in contrast to action and effects observable in single elements are called "system effects". In agreement with the specific notation of system size by N, M and $N \cdot M$ for parallel, serial and a combination of serial and parallel acting elements, respectively, these are also differentiated into parallel, serial and parallel-serial system effects. Whereas relative to loading direction serial arranged elements automatically incorporate serial system action, in systems composed of parallel arranged elements serial and parallel actions can be observed. The observable effects are in dependency of several facts which are discussed in more detail within the next sections.

In the following some general statements on probability theory theorems are introduced, basic features of serial and parallel system actions are compared and the state-of-the-art of stochastic strength theories dealing with serial and parallel system action under randomness of element characteristics are discussed, namely the "perfect brittle material model" according to WEIBULL (1939), the "perfect plastic material model" as well as the "fibre bundle model" according to DANIELS (1945). After that recent developments in stochastic modelling of system behaviour under more general assumptions are presented. A general graphical visualisation of serial and parallel acting systems is shown in Fig. 3.1 left (a) and right (b), respectively.

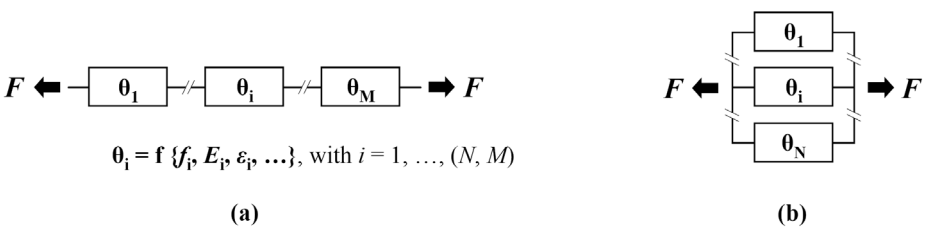

Fig. 3.1: Schematic illustration of systems: (a) serial acting system, (b) parallel acting system; F as external applied load, θ_i as parameter vector of random element characteristics (e.g. strength f_i, E-modulus E_i and strain ε_i) with $i = 1, \ldots, N, M$, with N and M as parallel and serial system size, respectively

Let E_i be the failure event of the ith element. Then the failure event of a serial system is given by (e.g. THOMA, 2004)

$$E_{serial} = E_1 \cup E_2 \cup \ldots E_n = \cup E_i \,, \tag{3.1}$$

and in case of an ideal parallel system by

$$E_{parallel} = E_1 \cap E_2 \cap ... E_n = \cap E_i \,. \tag{3.2}$$

Consequently, a series of parallel systems reads

$$E_{serial\_parallel} = \cup \cap E_{ij} \,, \tag{3.3}$$

and a parallel arrangement of serial systems leads to

$$E_{parallel\_serial} = \cap \cup E_{ij} \,. \tag{3.4}$$

In that respect the failure of one (the first) element in a serial system initiates immediately the failure of the whole system whereas in ideal parallel systems a collaps is given only if all elements fail. Let R_i be the event that the ith element K_i is intact and R_s the event that the whole system is intact with probabilities $p_i = P(R_i)$ and $p_s = P(R_s)$. If independent failure of the elements occurs with probability $q_i = 1 - p_i$ then the following statements concerning the reliability of systems can be made (e.g. STADLOBER, 2005; SCHUËLLER, 1981): The probability of survival or reliability of a serial system of M elements is given by

$$P\left(R_{s,serial}\right) = P\left(\bigcap_{i=1}^{M} R_i\right) = P\left(R_1 \cap R_2 \cap ... \cap R_n\right) \overset{R_i \text{ indep.}}{\rightarrow} \prod_{i=1}^{M} p_i \,, \tag{3.5}$$

with

$$P\left(\bigcap_{i=1}^{n} R_i\right) < \min_i P\left(R_i\right). \tag{3.6}$$

Thus the reliability of a serial system is always smaller than the reliability of the weakest element in the system.

The probability of survival or reliability of a parallel system of N elements is given by

$$P\left(R_{s,parallel}\right) = P\left(\bigcup_{i=1}^{N} R_i\right) = P\left(R_1 \cup R_2 \cup ... \cup R_n\right) \overset{R_i \text{ indep.}}{\rightarrow} 1 - \prod_{i=1}^{N}\left(1 - p_i\right), \tag{3.7}$$

with

$$P\left(\bigcup_{i=1}^{n} R_i\right) > \max_i P(R_i). \tag{3.8}$$

Here the reliability of an ideal parallel system is always larger than the reliability of the strongest element in the system.

Consequently, the failure probabilities P(R_f) of perfect serial and parallel systems assuming independency between the elements are given by

$$P(R_{f,serial}) = 1 - \prod_{i=1}^{M}(1-q_i) \text{ and } P(R_{f,parallel}) = \prod_{i=1}^{N}(q_i). \tag{3.9}$$

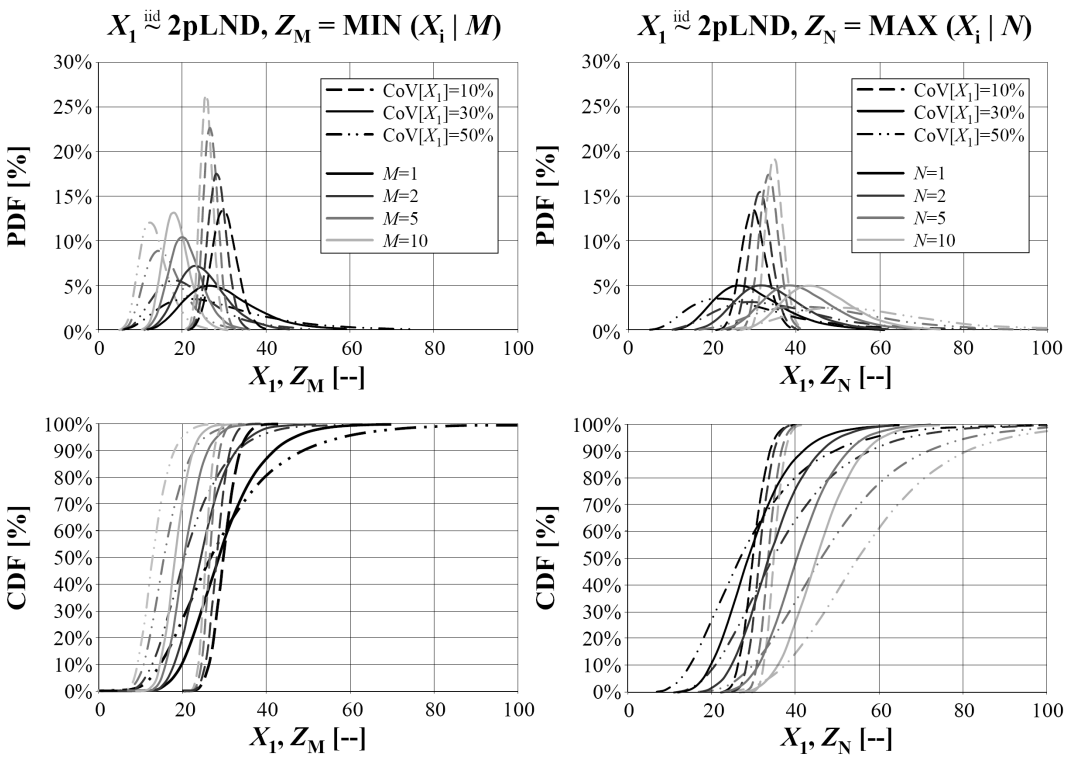

Fig. 3.2: Changes in PDF and CDF of ideal serial (left) and ideal parallel (right) acting iid elements assuming $X_1 \sim$ 2pLND; variation of CoV[X_1]; E[X_1] = 30, with X_1 as characteristic at M, N = 1

In the special case of iid elements the reliabilities P(R_s) and failure probabilities P(R_f) tend in the limiting case with $M, N \to \infty$ to the corresponding statistical models of extreme value theory (see section 2.6.2).

Reliabilities and failure probabilities of perfect serial and parallel systems provide bounds for calculation and judgement of probabilities of more complex systems which can only be estimated by simulations and / or under certain constraints. Nevertheless, these trivial bounds are very inefficient for most practical calculations enabling strict restricted evidence in reliability calculations. Improved bounds are for example discussed and given in GOLLWITZER (1986) with references on RACKWITZ (1978), DITLEVSEN (1979A,B), HOHENBICHLER (1980), GOLLWITZER AND RACKWITZ (1983) and others. It has to be noted that the requirement of iid variables fails already if for example reliabilities are calculated based on stochastic modelled action and resistance variables (GOLLWITZER, 1986). Some examples of changes in PDF and CDF of ideal serial and parallel systems of iid elements with $X \sim$ 2pLND are given in Fig. 3.2.

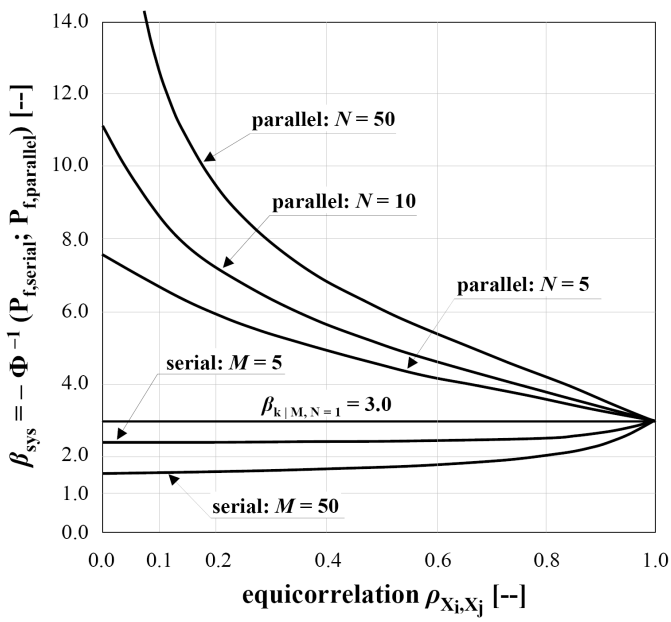

Fig. 3.3: Safety index β in dependency of system type, system size and magnitude of equicorrelation between interacting system elements based on reliability calculations by means of second order reliability method (SORM); adopted from GOLLWITZER (1986)

The comparison between the distribution of element characteristics and that of systems not only changes in location and shape. There is also a decrease in statistical spread and a distinctive influence on the reliability of these systems given. Therefore Fig. 3.3 provides a comparison of reliabilities by comparing safety index β of given systems depending on the system action, system size and the magnitude of equicorrelation between interacting elements (see GOLLWITZER, 1986). As already discussed in GOLLWITZER (1986) it can be observed that serial system action shows only minor influence in case of a certain dependency, roughly only above $\rho \approx 0.70$ and larger system size. In contrast, parallel acting systems show distinctive dependency on system size and correlation. Thus comprehensive knowledge of RSDM and correlation structure of elements is in particular decisive for accurate modelling of parallel system action.

In the following a general comparison of some principle differences and limiting conditions of serial and parallel system action are discussed:

Actions of Elements within the System

In serial systems each element has to carry the complete applied load. In contrast, parallel arranged elements in an ideal case of equal (uniform) load sharing on average only carry an equal share of load given by $1 / N$.

Whereas in serial acting systems the elements act more or less individually as being arranged intentionally in a row in respect to the loading direction, elements in parallel systems act intentionally as elements side by side and parallel in respect to the loading direction. Thus parallel acting systems suffer from balancing effects or homogenisation in characteristics of all involved elements by common activation of "averaging" effects due to balancing of differences between the characteristics, at least between the neighbouring elements. Consequently, the possibility and the amount of homogenisation is a function of statistical spread which is inherent in every characteristic.

The strength of serial acting systems is in general given by the weakest element according the "weakest link theory" often mentioned in conjunction to WEIBULL (1939). As the system size M increases the expected strength of the system decreases, in the limiting case $\lim_{M \to \infty} E[f_{sys,M}] \to 0$ or tends to a certain limit value defined by the strength distribution of the element (e.g. a treshhold value). Additionally to the shift of statistical strength distribution to minimum values also the variance $Var[f_{sys,M}]$ decreases, in the limiting case $\lim_{M \to \infty} Var[f_{sys,M}] \to 0$. Parallel system action, as discussed in more detail

afterwards, can be modelled by considering a bundle of elements. These elements are with or without interlinkages and constraint to work as one unit. The first major work on this topic can be traced back to the "fibre bundle theory" established by DANIELS (1945). Due to the common action of elements and homogenisation the expected system strength $E[f_{sys,N}]$ tends with $N \rightarrow \infty$ to a certain boundary value ≥ 0. The variance tends to $\lim_{N \rightarrow \infty} Var[f_{sys,N}] \rightarrow 0$.

Arrangement Dimensions

Serial and parallel systems also differ in respect to the possibilities how the elements can be arranged relative to the loading direction. Whereas serial arrangement only involves one dimension (1D), parallel arrangement can be done even two-dimensionally (1D, 2D).

Engineering Aspects

Statically determined structures in general and statically indetermined tower-like structures composed of brittle or ductile behaving elements can be described as serial systems. In case of serial systems of strongly correlated elements the upper boundary distribution is defined by the maximum of element's failure probability. In contrast statically indetermined, redundant structures can be modelled as parallel systems. In case of statically indetermined systems composed of ductile behaving elements the limiting case (system collaps) is perhaps already reached after subsequent failure of a few elements at the same time (avalanche) (e.g. SCHUËLLER, 1981). If robustness is considered it is generally adviseable to create redundant statically indetermined structures whenever load redistribution is in principle possible as in case of plastic material behaviour. In case of brittle material the erection of statically determined structures is adviced to confine the extension of damage in case of partial (element) failure.

Fig. 3.4 shows conceptionally possible arrangements of elements denoted as representative volume elements (RVEs) characterised by orthotropic material behaviour and characteristics with differentiation in longitudinal (long), radial (rad) and tangential (tan) direction. It discusses system actions on strengths (*f*) due to parallel (p) and / or serial (s) arrangement of elements relative to load direction and in respect to the main material directions (longitudinal / transversal) denoted by 0 / 90. Whereas three illustrations of possible 1D arrangements on the left show some possibilities for individual theoretical studies on system behaviour, the example on the right includes parallel and serial arrangements and actions in all structural directions. This makes clear

that within a real material structure a certain share of serial and parallel acting elements is always present.

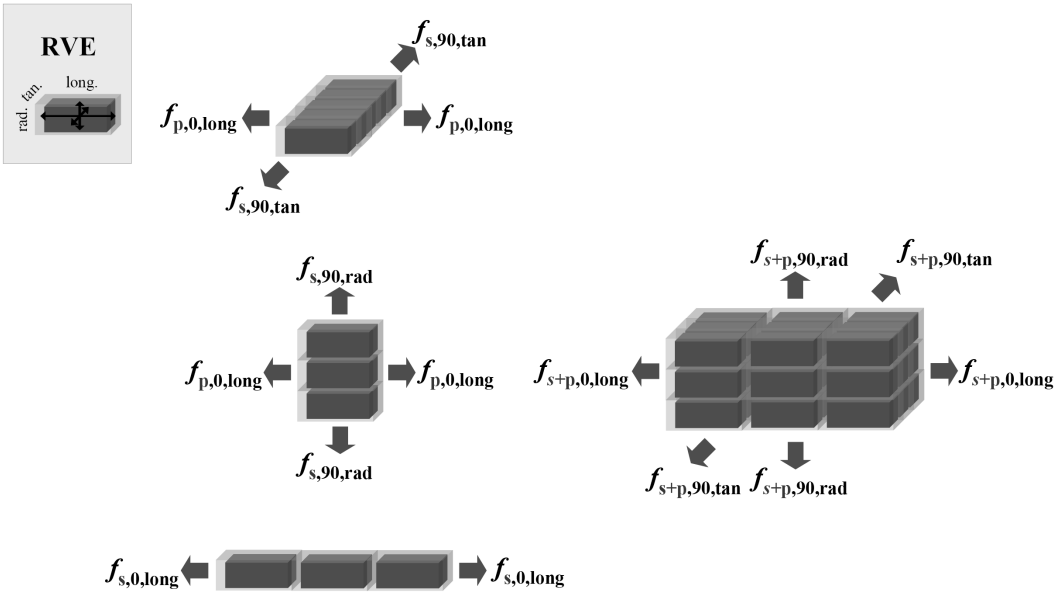

Fig. 3.4: Schematic illustration of various types of systems in respect to element arrangement and system action in parallel (p), serial (s) or serial-parallel (s+p), considering an orthotropic material with differing properties in radial (rad), tangential (tan) and longitudinal (long) direction

3.2 Material Modelling: Inclusion of Stochastics vs. Classical Mechanical Models

EPSTEIN (1948) states that stochastic models take GRIFFITH's theory as a starting point. According to this theory the differences between theoretical (calculated) and practically observable material strength comes from the fact that real materials include flaws which weaken the material structure whereby the worst flaws determine the strength. Thus extreme value theory (EVT) plays a major role in development of material strength models considering the limiting case of infinite system dimensions. The first researchers who recognised the connection between strength of materials and EVT were PEIRCE (1926) and WEIBULL (1939). Whereas the interest of fracture and serial systems concentrates on the weakest link failure in parallel systems (e.g. DANIELS's theory) the

focus lies on the problem of load redistribution after partial failures occurred. It is noted that in some cases of EVT it may be easier to reformulate the problem by means of the distribution of maxima instead of concentration on minima. The limitation to iid elements in EVT has to be mentioned too. Furthermore, the quantity of size effects not only depends on the volume under stress, the stress distribution and the coefficient of variation but also on the type of the underlying statistical distribution model.

As generally well known but often neglected, characteristics of natural but also technical materials require at least two parameters for a sufficient description, one for expressing the expectation and one for expressing the spread inherent in each characteristic. In that respect derivation of a model for an individual characteristic requires an appropriate representative statistical distribution model (RSDM) and associated distribution parameters. The RSDM and its parameters can be derived on basis of representative test data with or without the support of simulation results. The next step can be a model which expresses the description of a characteristic in dependency of explanatory variables, e.g. a regression model. These descriptive models have already been discussed in more detail in chapter 2.

Nevertheless, the biggest challenges in material modelling are given by (i) modelling the strength of materials on various hierarchical levels due to scaling effects, (ii) by modelling the strength capacities of materials of geometries and dimensions deviating from standardised test configurations, (iii) structures under arbitrary stress, or (iv) strength of systems exhibiting system effects. The last one requires a model dependent on size, arrangement, interconnection and relationship of elements in the system relative to loads applied externally. For an appropriate strength model the material behaviour along the whole stress-strain-relationship as well as the fracture behaviour becomes important and decisive. Three main theories in respect to system action can be differentiated:

- Strength Model for **Perfect Brittle Material**;
- Strength Model for **Perfect Plastic Material**;
- Strength Model for **Fibre Bundles**.

As mentioned above materials can be characterised on various hierarchical levels. For modelling the expected material behaviour on a certain hierarchical level the required accuracy has to be defined beforehand to provide the user with a handsome, sufficient accurate, reliable and tangible model for “daily business”. The focus of the present work is to support the engineer with some simplified definitions for some specific applications

as later discussed in chapter 5. Nevertheless, to enable a sufficient description of material behaviour on a certain hierarchical level the model has to start at one level before. In addition it requires at least the knowledge of the material behaviour of one further hierarchical level.

Most literature denotes the three following material strength models as "classical" models. However, for avoiding any confusion with classical mechanics this term is not used in the following description and only the general name of each theory is mentioned.

3.2.1 Stochastic Strength Model for Perfect Brittle Materials: Weibull's Weakest Link Theory

In case of perfect brittle material a uniform stressed volume (system) fails with achievement of the strength of the weakest sub-volume element. This failure behaviour corresponds to perfect serial systems. The system can be modelled as a chain of M serial acting elements under uniform tensile stress. After the "weakest link theory" of WEIBULL (1939A,B) this chain fails immediately after overloading of the weakest link, the weakest element. WEIBULL derived his theory empirically (WEIBULL, 1951) on the basis of several important assumptions which are discussed briefly within this section.

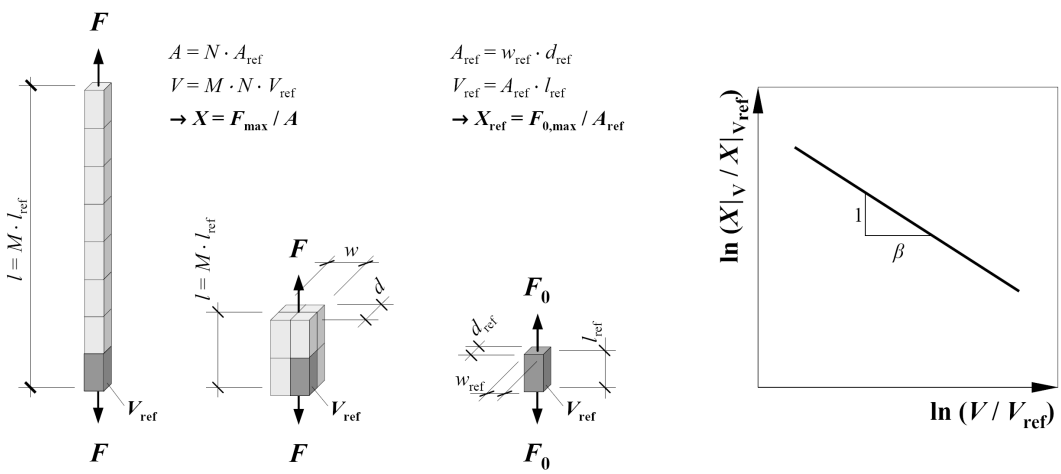

Fig. 3.5: Illustration of main assumptions and basics of "weakest link theory" according WEIBULL (1939)

WEIBULL assumed that all system elements are iid, uniformly stressed, small but finite and with volume dV as ewll as of isotropic material with risk of rupture given by

$$dB = -\ln(1 - S_0) \cdot dV = n(\sigma) \cdot dV \ , \tag{3.10}$$

with $n(\sigma)$ as specific material function and S_0 as probability of failure of a reference volume element (RVE). In case of a statistically isotropic material $n(\sigma)$ is independent of the position of finite volume element dV and of the direction of action of stress σ. In a statistically anisotropic material $n(\sigma)$ constitutes a function of the position of dV and the direction of the stress σ. The material function $n(\sigma)$ derived on the basis of GRIFFITH's theory and SMEKAL's terminology assumes perfect brittle material behaviour and the occurrence of n small but finite sized flaws (e.g. checks, cracks, flaws in the atomic structure of the material, etc.) within a volume V. These flaws are characterised as potential failure inducing characteristics in a volume V under stress σ. The isotropic and orthotropic cases require that flaws are small but finite in relation to a representative volume element (RVE). Consequently, the discrete occurrence of flaws can be smeared and considered as being continuously distributed. The probability of failure is assumed as being proportional to the stressed volume or system size with $B \approx V$. If n flaws in a RVE are concentrated on dV stress σ also concentrates on dV with probability of failure

$$dS = n \cdot dV \ . \tag{3.11}$$

In case of p-elements (p-RVEs) with volume dV and probability of failure dS the probability of failure of the system according the probability theory of perfect serial systems is given by (see also equ. (2.119) and (3.9))

$$S = 1 - (1 - n \cdot dV)^{p} \ . \tag{3.12}$$

Considering the whole volume V under stress σ with $V = p \cdot \mathrm{d}V$ and $\mathrm{d}V = V / p$ than (3.12) becomes

$$S = 1 - \left(1 - n \cdot \frac{V}{p}\right)^{p \cdot (n \cdot V)/(n \cdot V)} \ . \tag{3.13}$$

In the limiting case with $p \to \infty$ and $\mathrm{d}V \to 0$ so that volume $V =$ constant the boundary value of failure probability is given by

$$S = 1 - \lim_{p/(n\cdot V)\to\infty} \left(1 - n\cdot\frac{V}{p}\right)^{p\cdot(n\cdot V)/(n\cdot V)} \to 1 - \exp(-n\cdot V). \tag{3.14}$$

Thereby $n(\sigma)$ is equal to the quantity of flaws in a RVE ($V = 1$) provoking failure at stresses smaller or equal to σ_0. Thus a monotonically increasing function $n(\sigma)$ is required.

The risk of rupture B of an arbitrary stressed element with volume V follows from integration over the whole domain

$$B = \int n(\sigma)\cdot dV\,. \tag{3.15}$$

By means of a general distribution function WEIBULL gives the probability of failure of a volume element with

$$S = 1 - \exp(-B) = 1 - \exp\left[-\int n(\sigma)\cdot dV\right] \text{, with } B = -\ln(1-S). \tag{3.16}$$

Equ. (3.16) is called the "fundamental law of an isotropic brittle material" (WEIBULL, 1939A). The ultimate stress or strength at point of failure can be calculated considering the limit value of the quantity of experimental trials given by

$$\sigma_b = \int_0^\infty \exp\left[-\int n(\sigma)\cdot dV\right]\cdot d\sigma\,. \tag{3.17}$$

For identity between (3.16) and (3.17) the specific material function $n(\sigma)$ takes the form

$$n(\sigma) = \frac{dB}{dV} = \left(\frac{\sigma}{\sigma_0}\right)^m. \tag{3.18}$$

The specific material function $n(\sigma)$ in (3.18) can be reformulated to

$$n(\sigma) = k\cdot\sigma^m \text{, with } \sigma_0 = k^{-1/m} \rightarrow n(\sigma) = \left(\frac{\sigma}{\sigma_0}\right)^m, \tag{3.19}$$

and the probability of failure to

$$S = 1 - \exp\left[-V \cdot \left(\frac{\sigma}{\sigma_0} \right)^m \right], \tag{3.20}$$

with $S = 0.63 = 63\ \%$ in case of $V = 1$ and $\sigma = \sigma_0$. Thus, inserting (3.18) in (3.17) the strength is given by

$$\sigma_b = \int_0^\infty \exp\left[-\int \left(\frac{\sigma}{\sigma_0} \right)^m \cdot dV \right] \cdot d\sigma\,. \tag{3.21}$$

In case of an arbitrary stress situation with $\sigma \rightarrow \mathrm{f}(x, y, z)$ the stress function becomes $\sigma = \sigma_\mathrm{p} \cdot \mathrm{f}(x, y,\ z)$ which corresponds to a proportional stress increase in all three directions. The risk of rupture B (WEIBULL, 1939A) becomes

$$B = \int n \cdot \left[\sigma_p \cdot f(x,y,z) \right] \cdot dV\,, \tag{3.22}$$

and with $n(\sigma) = k \cdot \sigma^\mathrm{m}$

$$B = \int k \cdot \left[\sigma \cdot f(x,y,z) \right]^m \cdot dV\,, \tag{3.23}$$

which corresponds to a linear scaling of the system.

Exemplarily, in case of an equal stressed volume, e.g. uniaxial tension stress, the risk of rupture B becomes

$$B = \int k \cdot \left[\sigma \cdot f(x,y,z) \right]^m \cdot dV \rightarrow B = \int k \cdot \sigma^m \cdot dV = k \cdot V \cdot \sigma^m = V \cdot \left(\frac{\sigma}{\sigma_0} \right)^m, \tag{3.24}$$

with standard deviation a given by the square root of variance a^2

$$a^2 = Var[\sigma_b] = \int_0^\infty (\sigma - \sigma_b)^2 \cdot dS = \int_0^\infty \exp\left[-V \cdot \left(\frac{\sigma}{\sigma_0} \right)^m \right] \cdot d\left(\sigma^2\right) - \sigma_b^2\,, \tag{3.25}$$

with σ as one-dimensional tensile stress. Consequently, the expectation and standard deviation of strength increase with decreasing volume but the relative measure of dispersion given by the coefficient of variation (CoV) stays constant and independent of

the stressed volume and of parameter σ_0. Thus CoV is solely defined by power m as shape parameter of 2pWD. Furthermore, (3.16) constitutes a special case of the "statistical theory of strength". Considering this and the limiting case of $m \to \infty$ it follows that $S(\sigma) = S(\sigma_0)$ and $\sigma_b \to \sigma_0$. At the same time also the statistical spread expressed by a^2 tends to zero. Consequently, equivalence between the "statistical theory of strength" and the "classical strength theory" ($\sigma_b = \sigma_0$) is only given in the limiting case of theoretically deterministic strengths. In reality there is always a certain amount of variability inherent in all natural phenomena and characteristics. Thus, real materials and structures are represented insufficiently by means of the "classical theory of strength" which assumes deterministic characteristics and neglects volume effects (WEIBULL, 1939A).

Further considerations of WEIBULL include the definition of lower and upper boundary strengths of materials. Due to physics WEIBULL argues for the lower boundary value that $\sigma_1 \geq 0$. In (most) cases it can also be assumed that $\sigma_1 > 0$, e.g. due to proof loading or pre-stressing of materials during exploitation and production (→ 3pWD). In that case the strength is given by the three parameter model

$$S_b^{\,1} = \sigma_1 + h \cdot \int_{\sigma_1}^{\infty} \exp\left[-\int k \cdot \sigma^m \cdot dV\right] \cdot d\sigma \text{, with } \sigma_1 > 0,\ h = \frac{1}{1 - S_0}. \tag{3.26}$$

WEIBULL discusses also an upper boundary value σ_2. This is argued in reference to SMEKAL and the naturally inherent maximum strength of materials. This upper limit is defined by perfect materials free of flaws with a dimension equal to a RVE, representative for each relevant scale or at least defined by the maximum strength potential of a perfect molecular structure. Once a boundary value is introduced the relative dispersion CoV shows to be dependent on shape and scale parameter.

WEIBULL (1951) reports that the empirical derived statistical distribution model enables well representation of a wide range of different data sets of diverse materials and applications. In some cases well representation of data over the whole data range is given. In other cases a section-wise representation by section-wise fitting of WD parameters is advised. Concerning the latter statement the question is formulated if the WEIBULL model represents the data insufficiently or if natural and material inherent phenomena in the investigated data necessiate a section-wise data analysis.

To conclude, the failure probability is proportional to the stressed volume. The material itself is treated as continuum following the theory of elasticity. Furthermore, an isotropic

material composed of nearly infinite finite sized elements with iid strengths is assumed. These assumptions allow for smearing the material characteristics by smearing the discrete occurrence of flaws as required for treatment as continuum (WEIBULL, 1939A,B).

One main characteristic of WD is that its formulation is in principle the same in the limiting cases of minima and maxima as shown in extreme value theory (see section 2.6.2). Coming back to the notations for WD given in section 2.4.3 with $\sigma = x$, scale parameter $\sigma_0 = \alpha$, shape parameter $m = \beta$ and location parameter $\sigma_1 = x_0$ the statistical distribution model of minima (assuming a perfect serial system of iid strength values $X_i \sim$ WD, $i = 1, \ldots, M$ with M as system size) is in general given by a 3pWD with CDF (THOMA, 2004)

$$F_X(x) = 1 - \exp\left[-\frac{V}{V_0}\cdot\left(\frac{x - x_0}{\alpha}\right)^{\beta}\right] = 1 - \exp\left[-M\cdot\left(\frac{x - x_0}{\alpha}\right)^{\beta}\right], x \geq x_0, \tag{3.27}$$

with $M = V / V_0$ in case of known $V_0 = V_{\text{ref}}$. The first two central moments are given by

$$E[X] = x_0 + \alpha\cdot\Gamma\left(1 + \frac{1}{\beta}\right)\cdot\left(\frac{V}{V_0}\right)^{-1/\beta}, \tag{3.28}$$

$$Var[X] = \alpha^2\cdot\left[\Gamma\left(1 + \frac{2}{\beta}\right) - \Gamma^2\left(1 + \frac{1}{\beta}\right)\right]\cdot\left(\frac{V}{V_0}\right)^{-2/\beta}. \tag{3.29}$$

In case of an inhomogeneous stress distribution the CDF of a 2pWD ($x_0 = 0$, $X = \Sigma$) is given by

$$F_\Sigma(\sigma) = 1 - \exp\left[-\frac{1}{V_0}\cdot\left(\int_V \psi(x,y,z)^{\beta}\cdot dV\right)\cdot\left(\frac{\sigma}{\alpha}\right)^{\beta}\right], \sigma > 0. \tag{3.30}$$

In cases were the reference volume V_0 is not defined equ. (3.30) is reformulated to

$$F_\Sigma(\sigma) = 1 - \exp\left[-\int_V \left(\frac{\psi(x,y,z)}{\alpha}\right)^{\beta}\cdot dV\right], \sigma > 0, \tag{3.31}$$

with fullness parameter λ (e.g. ISAKSSON, 1999) given by

$$\lambda(x,y,z) = \lambda = \int_V \left(\frac{\psi(x,y,z)}{\alpha} \right)^{\beta} \cdot dV \,. \tag{3.32}$$

This parameter expresses the amount of stressed volume relative to the total volume element in respect to the mechanical and statistical stress distribution. This is in general done with reference to a uniform stressed volume, e.g. an element loaded in tension parallel to grain. A comparison of two elements with different volumes but identical stress distribution can be formulated by the well known relationship (e.g. SUTHERLAND ET AL., 1999)

$$\frac{\sigma_2}{\sigma_1} = \left(\frac{V_1}{V_2} \right)^{1/\beta} \,. \tag{3.33}$$

In case of differing stress distributions (3.33) can be reformulated to

$$\frac{\sigma_2}{\sigma_1} = \left(\frac{\lambda_1 \cdot V_1}{\lambda_2 \cdot V_2} \right)^{1/\beta} \,. \tag{3.34}$$

In case of an anisotropic material the theory can be adapted to the "modified weakest link theory" by segmenting the size effect in sub-dimensions, e.g. length (l), width (w) and depth (d), given as

$$\frac{\sigma_2}{\sigma_1} = \left(\frac{\lambda_1 \cdot l_1}{\lambda_2 \cdot l_2} \right)^{1/k_l} , \quad \frac{\sigma_2}{\sigma_1} = \left(\frac{\lambda_1 \cdot w_1}{\lambda_2 \cdot w_2} \right)^{1/k_w} , \quad \frac{\sigma_2}{\sigma_1} = \left(\frac{\lambda_1 \cdot d_1}{\lambda_2 \cdot d_2} \right)^{1/k_d} , \tag{3.35}$$

which represents length, width and depth effects with associated powers $1 / k_l$, $1 / k_w$ and $1 / k_d$, respectively.

Based on above formulations some calculations are presented analysing the fullness parameters of some exemplified loading situations. If not mentioned explicitely, linear elements of isotropic material with rectangular cross section are assumed.

Case I: Element loaded in uniaxial Tension parallel to Grain

In case of elements which are loaded uniaxially in tension parallel to grain the stress distribution in all three directions x, y, z (in direction of length, width and depth,

respectively, with point-of-origin in neutral axis) is constant and equal to σ, with $\sigma_{\max} = f_{t,0}$. Thus the fullness parameter $\lambda = \lambda_{\text{tension\_II}}$ (3.32) is given by

$$\lambda = \int_V \left(\frac{\psi(x,y,z)}{\alpha} \right)^{\beta} \cdot dV =$$

$$= \left(\frac{\sigma}{\alpha} \right)^{\beta} \cdot \int_{x=0}^{l} \int_{y=0}^{w} \int_{z=0}^{d} 1^{\beta} \cdot dz \cdot dy \cdot dx = \left(\frac{\sigma}{\alpha} \right)^{\beta} \cdot l \cdot w \cdot d = \left(\frac{\sigma}{\alpha} \right)^{\beta} \cdot V = \lambda_{tension\_II} \,. \tag{3.36}$$

This type of loading is often taken as reference stress distribution and as basis for comparing the influence of deviating stress distributions, e.g. bending and torsion.

Case II: Element under pure Bending Moment

In case of pure bending the stress distribution in direction of x and y is constant and equal to σ, whereas the bending stress distribution in z direction behaves linearly with $\sigma(z) = \sigma_z(z) / \sigma_{z,\max}(z = d / 2) = 2 \cdot z / d$ between $z = (0, d / 2)$ and $\sigma(z) = -2 \cdot z / d$ between $z = (0, -d / 2)$. The fullness parameter $\lambda = \lambda_{\text{bending}}$ is given by

$$\lambda = \int_V \left(\frac{\psi(x,y,z)}{\alpha} \right)^{\beta} \cdot dV =$$

$$= \left(\frac{\sigma}{\alpha} \right)^{\beta} \cdot \int_{x=0}^{l} \int_{y=0}^{w} 2 \cdot \int_{z=0}^{d/2} \left(\frac{2 \cdot z}{d} \right)^{\beta} \cdot dz \cdot dy \cdot dx = \left(\frac{\sigma}{\alpha} \right)^{\beta} \cdot \frac{l \cdot w \cdot d}{\beta + 1} = \tag{3.37}$$

$$= \left(\frac{\sigma}{\alpha} \right)^{\beta} \cdot \frac{V}{\beta + 1} = \lambda_{bending} \,.$$

The ratio bending vs. tension is given by $\lambda_{\text{bending}} / \lambda_{\text{tension\_II}} = 1 / (\beta + 1)$. In case of $\beta = 5.8$ corresponding to a CoV[X] ≈ 20% the ratio is ($\lambda_{\text{bending}} / \lambda_{\text{tension\_II}} \mid \beta = 5.8$) = 0.147 and in case of $\beta = 3.2$ corresponding to a CoV[X] ≈ 30% the same ratio gives 0.238. Thus the fullness parameter in case of pure bending only represents roughly 15% and 24% of elements loaded uniaxially in tension. This corresponds to expected maximum stress ratios according equ. (3.34) of 139.2% and 156.6% which implies that 39% and 57%

higher maximum stress in case of elements under pure bending moment than under pure tension can be expected if the same statistical distribution parameters α and β are used.

In case of timber under pure bending the integration over the whole stress field in z-direction is discussable due to the fact that timber in bending-compression zone shows a linear-elastic-plastic behaviour which contradicts the assumed brittle failure behaviour as it is for example given in the bending-tension zone.

Case III: Element under Three-Point Bending

In case of an element stressed in three-point bending the stress distribution in direction of y is constant and equal to σ, whereas the bending stress distribution in z direction is linear with $\sigma(z) = \sigma_z(z) / \sigma_{z,max}(z = d / 2) = 2 \cdot z / d$ between $z = (0, d / 2)$ and $\sigma(z) = -2 \cdot z / d$ between $z = (0, -d / 2)$. In x-direction the integration has to be split into $\sigma(x) = \sigma_x(x) / \sigma_{x,max}(x = l / 2) = 2 \cdot x / l$ between $x = (0, l / 2)$ and $\sigma(x) = 2 \cdot (l - x) / l$ between $x = (l / 2, l)$. Consequently, the fullness parameter $\lambda = \lambda_{3pB}$ is given as

$$\begin{aligned}\lambda &= \int_V \left(\frac{\psi(x,y,z)}{\alpha}\right)^\beta \cdot dV = \\ &= \left(\frac{\sigma}{\alpha}\right)^\beta \cdot \left[\int_{x=0}^{l/2}\int_{y=0}^{w} 2 \cdot \int_{z=0}^{d/2} \left(\frac{4 \cdot z \cdot x}{d \cdot l}\right)^\beta \cdot dz \cdot dy \cdot dx + \right. \\ &\left. + \int_{x=l/2}^{l}\int_{y=0}^{w} 2 \cdot \int_{z=0}^{d/2} \left(\frac{4 \cdot z \cdot (l-x)}{d \cdot l}\right)^\beta \cdot dz \cdot dy \cdot dx \right] = \left(\frac{\sigma}{\alpha}\right)^\beta \cdot \frac{V}{(\beta+1)^2} = \lambda_{3pB} \,.\end{aligned} \tag{3.38}$$

The ratio of three-point-bending vs. tension is given by $\lambda_{3pB} / \lambda_{tension\_II} = 1 / (\beta + 1)^2$, that of three-point bending vs. pure bending moment by $\lambda_{3pB} / \lambda_{bending} = 1 / (\beta + 1)$. In case of $\beta = 5.8$ corresponding to a CoV[X] ≈ 20% the ratio is $(\lambda_{3pB} / \lambda_{tension\_II} \mid \beta = 5.8) = 0.022$ and in case of $\beta = 3.2$ corresponding to a CoV[X] ≈ 30% the same ratio gives 0.057. Thus the fullness parameter in case of three-point-bending represents only about 2% to 6% of elements loaded uniaxially in tension. A comparison of ratios between three-point bending and pure bending shows $(\lambda_{3pB} / \lambda_{bending} \mid \beta = 5.8) = 0.147$ and $(\lambda_{3pB} / \lambda_{bending} \mid \beta = 3.2) = 0.238$. These values correspond to expected maximum stress ratios according equ. (3.34) of 193.7% and 245.2% which implies that 94% and 145% higher maximum stress in case of elements under three-point-bending than under pure tension can be expected, whereas maximum stress ratios according equ. (3.34) of 139.2%

and 156.6% imply that 39% and 57% higher maximum stress in case of elements under three-point bending than under pure bending moment are reachable if the same statistical distribution parameters α and β are used. The equality between the ratios of pure bending vs. tension and three-point bending vs. pure bending appears logical considering equal stress distribution and constant vs. linear stress distribution in longitudinal vs. cross section and cross section vs. longitudinal direction, respectively.

Case IV: Element under Four-Point Bending

In case of an element stressed in four-point bending the stress distribution in direction of y is constant and equal to σ, whereas the bending stress distribution in z direction is linear with $\sigma(z) = \sigma_z(z) / \sigma_{z,\max}(z = d / 2) = 2 \cdot z / d$ between $z = (0, d / 2)$ and $\sigma(z) = -2 \cdot z / d$ between $z = (0, -d / 2)$. In x-direction the integration has to be split into $\sigma(x) = \sigma_x(x) / \sigma_{x,\max}(x = l / 3) = 3 \cdot x / l$ between $x = (0, l / 3)$, $\sigma(x) = 1$ between $x = (l / 3, 2 \cdot l / 3)$ and $\sigma(x) = 3 \cdot (l - x) / l$ between $x = (2 \cdot l / 3, l)$. Herein the fullness parameter $\lambda = \lambda_{4pB}$ is given as

$$\begin{aligned}
\lambda &= \int_V \left(\frac{\psi(x,y,z)}{\alpha} \right)^\beta \cdot dV = \\
&= \left(\frac{\sigma}{\alpha} \right)^\beta \cdot \left[\int_{x=0}^{l/3} \int_{y=0}^{w} 2 \cdot \int_{z=0}^{d/2} \left(\frac{6 \cdot z \cdot x}{d \cdot l} \right)^\beta \cdot dz \cdot dy \cdot dx + \right. \\
&+ \int_{x=l/3}^{2/3 \cdot l} \int_{y=0}^{w} 2 \cdot \int_{z=0}^{d/2} \left(\frac{2 \cdot z}{d} \right)^\beta \cdot dz \cdot dy \cdot dx + \\
&\left. + \int_{x=2/3 \cdot l}^{l} \int_{y=0}^{w} 2 \cdot \int_{z=0}^{d/2} \left(\frac{6 \cdot z \cdot (l - x)}{d \cdot l} \right)^\beta \cdot dz \cdot dy \cdot dx \right] = \left(\frac{\sigma}{\alpha} \right)^\beta \cdot \frac{V}{3} \cdot \frac{3 + \beta}{(\beta + 1)^2} = \lambda_{4pB} \,.
\end{aligned} \tag{3.39}$$

Consequently, the ratios of four-point bending vs. tension and vs. pure bending moment are $\lambda_{4pB} / \lambda_{tension\_II} = (3 + \beta) / [3 \cdot (\beta + 1)^2]$ and $\lambda_{4pB} / \lambda_{bending} = (3 + \beta) / [3 \cdot (\beta + 1)]$, respectively. In case of $\beta = 5.8$ corresponding to a CoV[X] ≈ 20% the ratio is $(\lambda_{4pB} / \lambda_{tension\_II} \mid \beta = 5.8) = 0.063$ and in case of $\beta = 3.2$ corresponding to a CoV[X] ≈ 30% the same ratio gives 0.117. Thus the fullness parameter in case of four-point bending represents only roughly 6% to 12% of elements loaded uniaxially in tension. Comparison of ratios between four-point-bending and pure bending shows $(\lambda_{4pB} / \lambda_{bending} \mid \beta = 5.8) = 0.431$ and $(\lambda_{4pB} / \lambda_{bending} \mid \beta = 3.2) = 0.492$. These values

correspond to maximum expected stress ratios according equ. (3.34) of 160.9% and 195.4% which implies that 61% and 95% higher maximum stress in case of elements under four-point bending than under pure tension can be expected, whereas maximum stress ratios according equ. (3.34) of 115.6% and 124.8% imply that 16% and 25% higher maximum stress in case of elements under four-point bending than under pure bending moment are reachable if the same statistical distribution parameters α and β are used.

Case V: Element under constant Load in Bending

In case of an element under constant load stressed in bending the stress distribution in direction of y is constant and equal to σ, whereas the bending stress distribution in z direction behaves linearly with $\sigma(z) = \sigma_z(z) / \sigma_{z,\max}(z = d / 2) = 2 \cdot z / d$ between $z = (0, d / 2)$ and $\sigma(z) = -2 \cdot z / d$ between $z = (0, -d / 2)$. In x-direction the stress distribution is given by $\sigma(x) = \sigma_x(x) / \sigma_{x,\max}(x = l / 2) = 4 \cdot x \cdot (l - x) / l^2$ between $x = (0, l)$. Herein the fullness parameter $\lambda = \lambda_{\text{const.load}}$ is given by

$$\begin{aligned}
\lambda &= \int_V \left(\frac{\psi(x,y,z)}{\alpha} \right)^{\beta} \cdot dV = \\
&= \left(\frac{\sigma}{\alpha} \right)^{\beta} \cdot \int_{x=0}^{l} \int_{y=0}^{w} 2 \cdot \int_{z=0}^{d/2} \left(\frac{8 \cdot z \cdot x \cdot (l-x)}{l^2 \cdot d} \right)^{\beta} \cdot dz \cdot dy \cdot dx = \\
&= \left(\frac{\sigma}{\alpha} \right)^{\beta} \cdot \frac{V \cdot \sqrt{\pi}}{2} \cdot \frac{\Gamma(1+\beta)}{(1+\beta) \cdot \Gamma\left(\frac{3}{2} + \beta \right)} = \lambda_{const.load} \cdot
\end{aligned} \tag{3.40}$$

In case of $\beta = 5.8$ corresponding to a CoV[X] ≈ 20% the ratio is ($\lambda_{\text{const.load}} / \lambda_{\text{tension\_II}} \mid \beta = 5.8$) = 0.051 and in case of $\beta = 3.2$ corresponding to a CoV[X] ≈ 30% the same ratio gives 0.106. Thus the fullness parameter in case of elements under constant load in bending represents only roughly 5% to 11% of elements loaded uniaxially in tension. Comparison of ratios between constant load in bending and pure bending shows ($\lambda_{\text{const.load}} / \lambda_{\text{bending}} \mid \beta = 5.8$) = 0.346 and ($\lambda_{\text{const.load}} / \lambda_{\text{bending}} \mid \beta = 3.2$) = = 0.445. These values correspond to maximum stress ratios according equ. (3.34) of 167.1% and 201.6% which implies that 67% and 102% higher maximum expected stress in case of elements under constant load in bending than under pure tension can be expected, whereas maximum stress ratios according equ. (3.34) of 120.1% and 128.7% which implies 20% and 29% higher maximum stress in case of elements under constant

load in bending than under pure bending moment are reachable if the same statistical distribution parameters α and β are used.

Fig. 3.6 shows the relative expected strength $E[X] / E[X|_{\text{case I, II, IV}}]$ dependent on CoV[X] and the stress distribution within the cross section as well as along the element due to changing loading cases (see Fig. 3.6, right). Hereby the reference stress situation is varied and given as case I, II and IV. The graph outlines clearly the significant influence of stress distribution and CoV[X], emphasising the statements above.

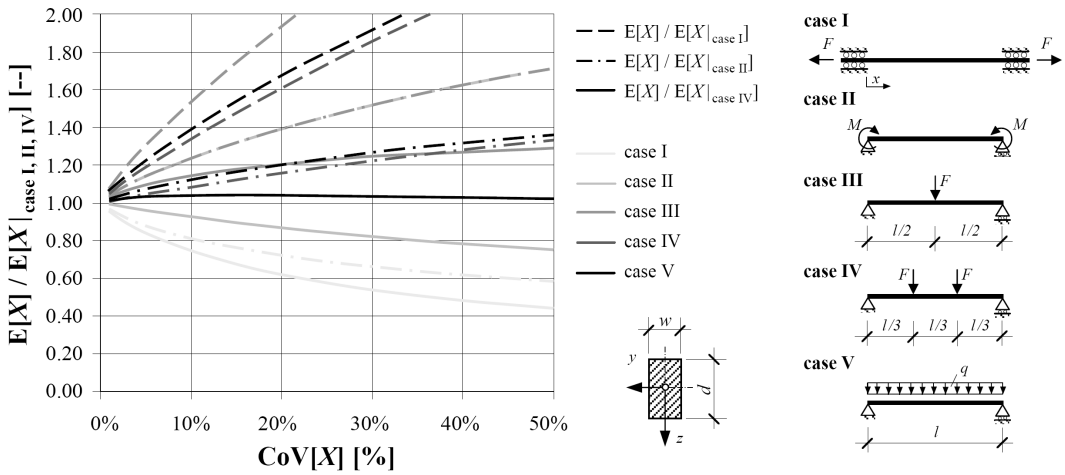

Fig. 3.6: Influence of stress distribution and type of loading on the expected strength capacity according WEIBULL's WLT: relative expected strengths under variation of the reference case (I, II, IV)

3.2.2 Strength Model for Perfect Plastic Materials

Elastic material behaviour can be easily described by means of HOOK's law, but for plastic material behaviour no simplified description is available. Perfect plastic or perfect elastic-plastic material behaviour is characterised by steadily increasing strain after the load or stress equals the yield load or stress. Consequently, perfect plastic material shows no hardening or softening after yielding (e.g. PRAGER AND HODGE, 1954). Unloading or reverse loading shows complete recovery of elastic deformations but persistence of plastic deformations until yielding of reverse yield stress and propagation of (infinite) plastic flow in reverse direction at constant maximum stress. According PRAGER (1959) a perfect plastic material model and its stress-strain function is given by Fig. 3.7, left (model of brittle, perfect plastic body). A perfect elastic-plastic material model can be

characterised by an additional elastic spring responsible for the elastic share as shown in Fig. 3.7, right (model of linear elastic perfect plastic body). With σ_0 as yield stress and $\sigma < \sigma_0$ the body behaves rigid (Fig. 3.7, left) or elastic. In case of $\sigma = \sigma_0$ = constant plastic flow under constant maximum stress can be observed.

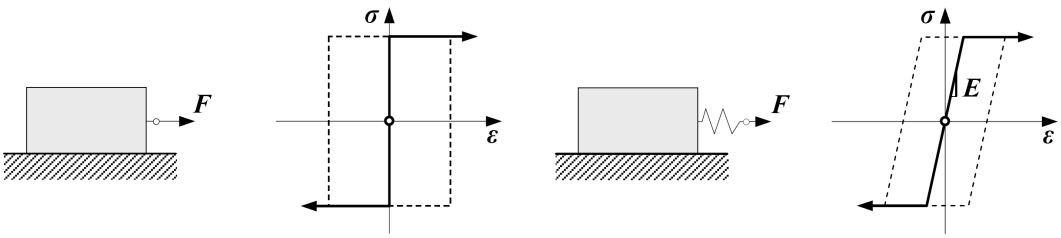

Fig. 3.7: Perfect plastic material behaviour according PRAGER (1959): (left) brittle, perfect plastic body; (right) perfect elastic-plastic body

One of the main differences between elastic and plastic behaviour is given by the lack of one-to-one correspondence between stress and strain. In a perfect linear elastic-plastic material behaviour changes in strain are composed of an elastic (e) and a plastic (p) share given by $d\varepsilon_i = d\varepsilon_i^{(e)} + d\varepsilon_i^{(p)}$, with ε_i as a set of generalised strains. The strain is therefore given by

$$\varepsilon = \varepsilon^{(p)} + \varepsilon^{(e)} = \varepsilon^{(p)} + \frac{\sigma}{E}, \tag{3.41}$$

with HOOK's law $\sigma = E \cdot \varepsilon^{(e)}$ and $\varepsilon^{(e)}$ as elastic strain and $\varepsilon^{(p)}$ as permanent strain. The same relationship is given for lateral contraction, see

$$\delta = \delta^{(p)} + \delta^{(e)} = \delta^{(p)} + \nu \cdot \frac{\sigma}{E}, \tag{3.42}$$

with ν as POISSON's ratio (PRAGER AND HODGE, 1954). In isotropic materials the relationship between lateral contraction and strain is given by

$$\frac{\delta}{\varepsilon} = \frac{\delta^{(p)} + \delta^{(e)}}{\varepsilon^{(p)} + \varepsilon^{(e)}} = \frac{2 \cdot \nu + \varepsilon^{(p)} / \varepsilon^{(e)}}{2 \cdot \left(1 + \varepsilon^{(p)} / \varepsilon^{(e)}\right)}, \tag{3.43}$$

which is equivalent to HOOK's law $\delta / \varepsilon = \nu$ within elastic region and $\varepsilon^{(p)} = 0$. In case of plastic flow elastic strain $\varepsilon^{(e)} = \sigma / E$ stays constant whereas $\varepsilon^{(p)}$ as well as the ratio δ / ε increases monotonically against the limit value $\delta / \varepsilon = \nu = 1 / 2$.

So far stresses are small the material shows elastic behaviour. With increasing loading small plastic zones develop and grow steadily. Therefore at the beginning only restricted local plastic flow is given whereby plastic zones are surrounded by elastic behaving material. After a while fusion of plastic zones occurs and leads to unrestricted plastic flow above the flow limit (PRAGER AND HODGE, 1954).

As a consequence of above basic characteristics of perfect plastic material, a parallel system composed of perfect plastic behaving elements shows load redistribution after elements reached their individual yield stress. Thereby, elements are capable to carry full load even after yielding, but every additional loading consequences in additional plastic flow until the load is sufficiently redistributed to elements which are still below the yield limit at particular load level. Consequently, the maximum system bearing capacity (system strength) $X_{\mathrm{sys,N}}$ of, e.g., a system under uniform tensile load is reached after all elements have reached their yield stress. It is defined by the weighted sum of element's yield stresses

$$X_{sys,N} = \frac{F_{sys,N}}{A_{sys,N}} = \frac{\sum_{i=1}^{N} A_i \cdot X_i}{\sum_{i=1}^{N} A_i} \xrightarrow{A_i = A = const.} \frac{1}{N} \cdot \sum_{i=1}^{N} X_i \,, \tag{3.44}$$

with $X_{\mathrm{i}} = F_{\mathrm{i}} / A_{\mathrm{i}}$ and $A_{\mathrm{i}} = A$ = constant as cross section of each element i, F_{i} as maximum (yield) load per element, $X_{\mathrm{i}} \sim \mathrm{DM}\,(\mathrm{E}[X_{\mathrm{i}}], \mathrm{Var}[X_{\mathrm{i}}])$ as yield stress per element i, with $i = 1, \ldots, N$. The expectation and variance of $X_{\mathrm{sys,N}}$ are given by

$$E\left[X_{sys,N}\right] = \frac{1}{N} \cdot \sum_{i=1}^{N} X_i \;\text{ and }\; Var\left[X_{sys,N}\right] = \frac{1}{N^2} \cdot \sum_{i=1}^{N} \sum_{j}^{N} CoVar\left[X_i, X_j\right]. \tag{3.45}$$

In case of large system sizes ($> N$) and small dependency between the element's yield stresses the system strength converges to the normal distribution following the central limit theorem (e.g. THOMA, 2004; KÖHLER, 2007). In case of perfect ductility the statistical distribution of strain is irrelevant (e.g. GOLLWITZER, 1986). In case of equicorrelated element strengths with correlation coefficient $\rho(X_{\mathrm{i}}, X_{\mathrm{j}})$ the variance $\mathrm{Var}[X_{\mathrm{sys,N}}]$ is given by (GOLLWITZER, 1986)

$$Var\left[X_{sys,N}\right] = Var\left[X_i\right] \cdot \frac{1 + \rho \cdot (N-1)}{N} \,. \tag{3.46}$$

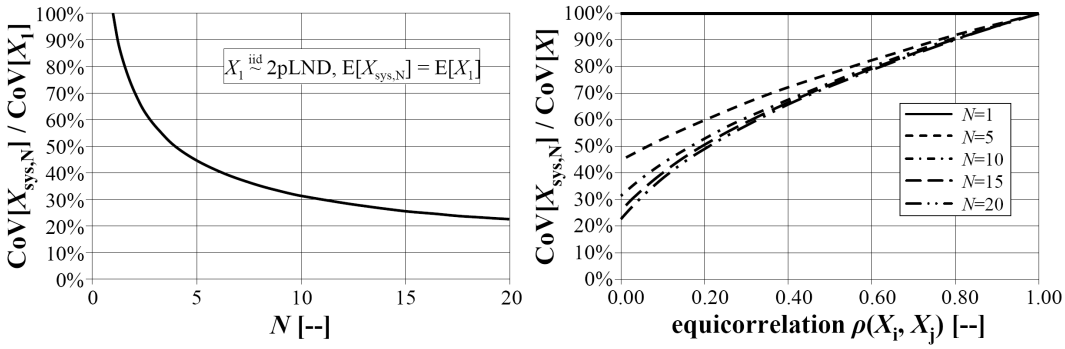

Fig. 3.8: $\mathrm{CoV}[X_{\mathrm{sys,N}}]$ in dependency of the system size N assuming iid elements $X \sim$ 2pLND (left) and $\mathrm{CoV}[X_{\mathrm{sys,N}}] / \mathrm{CoV}[X]$ in dependency of the system size N and the magnitude of equicorrelation calculated according equ. (3.46) (right)

Fig. 3.8 shows the dependency of $\mathrm{CoV}[X_{\mathrm{sys,N}}]$ on the system size N as well as on the magnitude of equicorrelation within and between the elements. Clearly visible is the decrease of homogenisation with decreasing system size and increasing correlation.

3.2.3 Strength Model for Parallel Systems with Load Redistribution: Daniels's Fibre Bundle Model

The fibre bundle model, also known as "**classical model of bundle of *N* parallel fibres stretched between two clamps**" (e.g. PARAMONOVA ET AL., 2006), goes back to the famous work of DANIELS (1945). He developed this theory on basis of PEIRCE (1926) who observed that materials can be considered as systems of elements arranged in serial and parallel, and the work of WEIBULL (1939) and his "weakest link theory".

In his study DANIELS examined a system of N parallel aligned and uniform stressed fibres (elements), loaded in pure tension in fibre direction. Contradicting to WEIBULL's theory which states that the system collapses as the weakest element fails DANIELS assumed that the system of parallel fibres is able to withstand a certain (critical) amount of element failures with intermediate equilibrium (steady) states in load redistribution between surviving fibres under increasing load until the system looses its equilibrium and fails totally. This is in principle in line with a perfect parallel system in stochastics. There systems fail with failure of all elements.

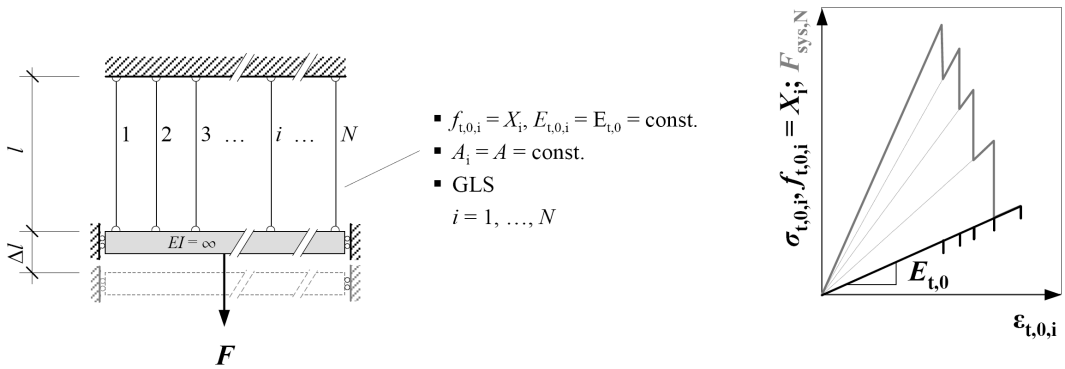

Fig. 3.9: Principles, basics and assumptions of DANIELS's fibre bundle model (FBM; DANIELS, 1945)

DANIELS (1945) derived the first and until now the most important of only a few available analytical solutions for the asymptotic statistical distribution of strength of fibre bundles. Thereby following assumptions are made:

- the parallel system is composed of N parallel fibres stretched uniformly between two controlled parallel moving clamping devices;
- the applicability of HOOK's law of perfect linear-elastic stress-strain-behaviour;
- the parallel aligned fibres are uniformly stressed with equal elongations and equal E-modulus ($E_i = E$ = constant) and thus characterised by identical load-deformation-curves but iid fibre strength values with $F_{max,i} = f_i = X_i \sim F_X(x)$;
- equal (uniform) or also called global load sharing (GLS) as a mean field approach is supposed after load from i partial failed fibres onto r survivors has been redistributed, with $i = 1, \ldots, N$, $r = N - i + 1$.

The last but one point argues an equal and constant E-modulus. This is based on DANIELS experience that the spread of E_1 appears negligible compared to that of the elongation at failure point $\varepsilon_{f,1}$. Considering E_1 as being independent from $\varepsilon_{f,1}$ (referencing observations made from PEIRCE, 1926) DANIELS (1945) argues further that the spread of E can be neglected in parallel systems assuming a mean field approach whereby $\mathrm{CoV}[E_{sys,N}] = \mathrm{CoV}[E_1] / \sqrt{N}$, with $E_{sys,N}$ as E-modulus of a parallel system composed of N fibres. Note: This is indeed a realistic assumption but says nothing about the load (re)distribution potential between the fibres which are forced to equal elongation in case of $\mathrm{CoV}[E_1] \neq 0$. This requires that the load is distributed proportional to the individual fibre stiffness values $E_i \cdot A_i$, with A_i as the fibre cross section which for simplicity can be

assumed to be constant and equal to one. Concerning the last assumption DANIELS (1945, 1989) already argued that GLS may be valid only in some practical cases.

With $X_{(1)} \leq X_{(2)} \leq \ldots \leq X_{(N)}$, $X_{(1)} = \min[X_i]$ and $X_{(N)} = \max[X_i]$, the ultimate load of the fiber bundle or resistance of the system $F_{max,sys} = X_{sys} \cdot N = R_N$ is defined by

$$\begin{aligned} R_N &= \max_{N \geq r \geq 1} \left[r \cdot X_{(r)} \right] = \\ &= \max_{1 \leq i \leq N} \left[N \cdot X_{(1)}, (N-1) \cdot X_{(2)}, \ldots, X_{(N)} \right] = \max_{1 \leq i \leq N} \left[(N-i+1) \cdot X_{(i)} \right] . \end{aligned} \tag{3.47}$$

In the simplest case when HOOK's law with $\sigma = E \cdot \varepsilon$ holds, with $E = 1$ without loss of generality, the load on each fiber (element) $F_i(\varepsilon)$ at extension ε is defined by

$$F_i(\varepsilon) = \varepsilon \cdot H(\varepsilon_f - \varepsilon), \tag{3.48}$$

with ε_f as the extension at point of fiber failure and parametrisation $H(w) = 1$ if $w \geq 0$ (fiber intact) and $H(w) = 0$ if $w < 0$ (fiber already failed). The total load on the fiber bundle at given extension ε is given by

$$R_N(\varepsilon) = \sum_{i=1}^{N} F_i(\varepsilon) = \varepsilon \cdot \sum_{i=1}^{N} H(\varepsilon_{f,i} - \varepsilon), \tag{3.49}$$

and the system stress $\sigma_{sys}(\varepsilon)$ at given extension ε is defined by

$$\sigma_{sys}(\varepsilon) = \frac{F_{sys}(\varepsilon)}{N} = \frac{1}{N} \cdot \sum_{i=1}^{N} F_i(\varepsilon). \tag{3.50}$$

The system strength $X_{sys} = f_{sys}$ is given by

$$f_{sys} = X_{sys} = \max\left[\sigma_{sys}(\varepsilon)\right] = \max\left[\frac{N \cdot F_{(1)}}{N}, \frac{(N-1) \cdot F_{(2)}}{N}, \ldots, \frac{F_{(N)}}{N} \right] . \tag{3.51}$$

The maximal resistance of the fibre bundle can be calculated by means of DANIELS's recursive formula (e.g. HOHENBICHLER AND RACKWITZ, 1981)

$$F_{R_N}(x) = S_N(x) = (-1)^{N+1} \cdot F_X^N\left(\frac{x}{N}\right) - \sum_{k=1}^{N-1} \left[(-1)^k \cdot \left(\frac{N}{k}\right) \cdot F_X^k\left(\frac{x}{N}\right) \cdot S_{N-k}(x) \right] , \tag{3.52}$$

which is analytically exact but difficult to handle in praxis.

DANIELS (1945) investigated the asymptotic behaviour ($N \to \infty$) of the maximum system load distribution under specifications given above. He concluded that with $\lim_{N \to \infty} y \cdot [1 - F_Y(y)] = 0$ the asymptotic maximum system load R_N follows a normal distribution (ND) given by

$$\lim_{N \to \infty} P\left(\frac{R_N - E[R_N]}{\sqrt{Var[R_N]}} \le x \right) = \Phi(x), \tag{3.53}$$

with expectation $E[R_N]$ and variance $Var[R_N]$

$$E[R_N] = N \cdot x_0 \cdot [1 - F_X(x_0)] \text{ and } Var[R_N] = x_0^{\,2} \cdot [N \cdot F_X(x_0) \cdot (1 - F_X(x_0))], \tag{3.54}$$

with x_0 as singular solution of $x \cdot [1 - F_X(x)] = \max[X]$. The expected value of the mean fibre bundle resistance and its standard deviation are given by (PARAMONOVA ET AL., 2006)

$$E[\overline{R}_N] = x_0 \cdot [1 - F_X(x_0)] \text{ and } \sqrt{Var[\overline{R}_N]} = x_0 \cdot \sqrt{F_X(x_0) \cdot [1 - F_X(x_0)]} \,/\, \sqrt{N}, \tag{3.55}$$

with r survivors and load on surviving fibres given by $(N - i + 1) \cdot X_{(i)}$. The average resistance of fibres in the fibre bundle is defined by

$$\overline{R} = \max_i \left[X_{(i)} \cdot \left(\frac{N - i + 1}{N} \right) \right] . \tag{3.56}$$

The convergence to the normal distribution follows from the fact that the probability for an element having strength $X \ge x_0$ for $x = x_0$ is given by $p = 1 - F_X(x_0)$. Consequently, the number of intact elements having at least strength x_0 follows the binomial distribution with $E[.] = N \cdot p$ and $Var[.] = N \cdot p \cdot (1 - p)$. According to the central limit theorem and with $N \to \infty$ this converges in probability to ND. The asymptotic result derived by DANIELS (1945) is also given for more complex systems, e.g. if X_i follows a Markov-chain. In general, convergence to the asymptotic distribution is very slow with rate $O(N^{-1/4})$. Beside this it was shown that DANIELS's result could be justified to work sufficiently for structural design purposes. In general and in case of very small system

sizes ($N \leq 5$) and medium variances (e.g. $\mathrm{CoV}[X] \leq 10\%$) it has been observed that the system behaviour can be approximated by a serial (weakest link) system. Note: This is logical due to the fact that in case of low dispersion and small system size ($<< N$) the chance of reaching a steady state after failure of the first element and initiated load redistribution is low. Additionally, DANIELS (1945) already remarked that the ability and amount of load distribution depends on the elastic properties of the elements.

As a more general conclusion of DANIELS's fibre bundle model (FBM) this theory may be treated as the most important enlargement of WEIBULL's weaket link theory (WLT). Whereas WEIBULL's theory assumes sudden system collaps at first element failure, DANIELS's model allows for load redistribution after partial failures and thus broadens the field of material strength and behaviour modelling in general.

3.2.4 Advances and further Developments on the Basis of Weibull's and Daniels's Theories and Generalisation of Material Behaviour

WEIBULL (1939) and DANIELS (1945) provide the fundamental basis for explicit consideration of stochastics in mechanical modelling of material strengths. Beside the fact that numerous assumptions are necessary to enable analytical solutions the theories provide a well defined basis for further developments enabled by mathematical description of pioneering thoughts driven from intensive observations of natural phenomena.

In the last decades these theories have been intensified and broadened. Efforts have been made in combining both FBM and WLT and in introducting and analysing finite, even small system sizes as well as in describing systems composed of elements of arbitrary material behaviour. DANIELS (DANIELS, 1974; DANIELS, 1989; DANIELS AND SKYRME, 1985) extended the fibre bundle model and justified the final result of system strength being asymptotically normally distributed by considering various approaches of modelling parallel systems but sticking to the main assumptions made in 1945. In the work of DANIELS (1974) the error of the mean function of the asymptotic fibre bundle strength distribution $R_\mathrm{N} \sim \mathrm{ND}\,(\mathrm{E}[R_\mathrm{N}], \mathrm{Var}[R_\mathrm{N}])$ for finite system sizes of N parallel elements was reduced by introduction of C_N as **additive term on the asymptotic expectation** with $\mathrm{E}[R_\mathrm{N}] \rightarrow \mathrm{E}[R_\mathrm{N}] + C_\mathrm{N}$ given as

$$C_N = 0.966 \cdot N^{1/3} \cdot a \text{, with } a^3 = \frac{f_X^2(x_0) \cdot x_0^{\,4}}{2 \cdot f_X(x_0) + x_0 \cdot f_X'(x_0)} = \frac{x_0^{\,4} \cdot f_X(x_0)}{2 + x_0 \cdot \dfrac{f_X'(x_0)}{f_X(x_0)}} \,. \tag{3.57}$$

SEN AND BHATTACHARYYA (1976) confirmed DANIELS's ND as asymptotic distribution of fibre bundle strength also under certain mixing conditions and in case of full correlated element strengths. PHOENIX (1979) modelled the strength of parallel systems by means of a **quantile process approach** investigating the time to failure and breakdown of the system as consequence of a fatigue failure. He used ordered down times on the basis of a probabilistic approach of the Palmgren-Miner-rule (PALMGREN, 1924 and MINER, 1945). A quantile process approach was also used by SMITH (1982). He inverted the fibre strength distribution to gain uniform distributed quantiles. He observed a much faster convergence to the asymptotic distribution with O ($N^{-1/6}$) expressing the error of the uniform distribution. SMITH (1980) and SMITH AND PHOENIX (1981) discussed the asymptotic distribution of fibre bundle strength in respect to solutions provided by extreme value theory (EVT). They showed that in case of GLS the strength distribution follows asymptotically the GUMBEL or double-exponential distribution model (type I, EVT). In case of local load sharing (LLS), which is discussed in more detail later, and iid element strengths with $X \sim$ WD also fibre bundle strength follows a WD (SMITH, 1983). In 1989 DANIELS modelled the asymptotic distribution of the maximum system load and breaking extension by considering an extension of a Gaussian process for Brownian motion based on the work of SMITH (1982) and PHOENIX AND TAYLOR (1973). PHOENIX AND TAYLOR (1973) already reformulated DANIELS's theory by analysing the asymptotic maximum of system load by assuming iid extensions of fibres (elements) rather than fibre load. The idea dealing with the extension was judged as being natural and more realistic especially for materials exhibiting elastic-plastic behaviour. In their work they further extended DANIELS's theory introducing a certain amount of **random slack** (iid for each fibre) as well as the possibility of some **plastic yield** (also independent from breaking extension and random for each fibre) enabling energy dissipation before fibres break. Therefore they made use of the asymptotic ND of the maximum system load capacity. The analysis of imperfect linear elastic load-extension curves of fibres due to iid random slack led to non-linear load-extension behaviour of the bundle and to a reduction of the mean asymptotic system strength. A certain amount of plasticity, modelled as plastic plateau after linear elasticity (bi-linear stress-strain relationship), led to an increase in system strength. The influence of imperfect loading which introduces unequal load

sharing in fibres was also investigated reflecting a reduction in the asymptotic system strength.

In their pioneering work ZWEBEN AND ROSEN (1970) described materials more generally as **"heterogenous continua composed of discrete volume elements whose characteristics are related to material structure and imperfections"**. They assumed a statistical distributed strength and partial failure of elements initiating localised stress concentrations until the system collapses. Former works confirmed the random occurrence of partial failures in fibre bundles and verified that local stress concentrations influence the system strength significantly. The localised stress concentrations require a broader definition of a **class of load sharing rules** given by the general term of **local load sharing (LLS)**. Note: In contrast to DANIELS assumption of global (uniform) load sharing (GLS) the class of LLS demonstrates the whole range of possible load sharing rules on the one hand with the limit and most optimistic case of GLS and on the other hand with the opposite limiting case of **extreme LLS (ELLS)**. In ELLS the load from partial failures is redistributed only to directly neighboured survivors. Consequently, LLS characterises load redistribution within a certain domain around failed fibres as center. The specification of each type of LLS is done by the **load enhancement factor *K***. In case of ELLS the direct survived neighbouring fibres have to carry $K_k \cdot X$, with factor K_k given by $K_k = 1 + k / 2$, with $K_0 = 1 < K_1 < K_2 < \ldots$ and with k as the amount of failed fibres in the neighbourhood of the survivor (HARLOW AND PHOENIX, 1979A,B, 1981A,B, 1982; SMITH, 1980; SMITH, 1983). HEDGEPETH AND VAN DYKE (1967) calculated K-factors which are slightly smaller than these in case of ELLS. Consequently a certain amount of extra load is also shared by fibres which are a bit farther away as the direct neighbours. SMITH (1983) assumed therein a non-linear load transfer and local stress concentrations with peak at the centre of failed fibre(s). ZWEBEN AND ROSEN (1970) already investigated a **serial-parallel fibre bundle model (s-p-FBM)** of M serial increments with N parallel elements per cross sectional unit with iid strengths $X \sim$ WD assuming ELLS due to local stress concentrations. The fibres were assumed to be embedded in a **matrix material** which is responsible for load transfer by shear after partial failures. The incremental length of M serial linked sub-systems is defined by the **ineffective length δ** necessary for shear transfer from failed fibres to survivors after partial failures (see also GÜCER AND GURLAND, 1962; IBNADELJALIL AND CURTIN, 1997; PHOENIX ET AL., 1997; SMITH, 1982; HARLOW ET AL., 1983; SUTHERLAND ET AL.,1999). Thereby the fibres have to carry full load in tension; a certain contribution by the matrix material is neglected. In their work ZWEBEN AND ROSEN (1970) concentrated on the definition of a

representative volume element (RVE), representative in shape (depending on the material), dimension and the quantity of expectable flaws under consideration of a corresponding stress enhancement factor K dependent on quantity and consequence of flaws. They also included crack growth in dependency on stress concentration parameters. Therefore the RVE was defined in dimension with length δ and diameter of the element (fibre) plus proportionate share of matrix material.

Concerning the **fibre-matrix interaction** SMITH (1983) noted that fibres embedded in a ductile matrix are not able to extend independently. In this and earlier works (e.g. SMITH, 1980, 1982) he observed that load transfer between failed and surviving fibres is solely performed by shearing as discussed e.g. in ZWEBEN AND ROSEN (1970). According IBNADELJALIL AND CURTIN (1997) and in reference to CHOU (1992) this type of load transfer through the matrix is called a "**shear-lag type model**". In contrast PHOENIX ET AL. (1997) analysed a fibre bundle embedded in a brittle matrix with GLS provided by **stress transfer through friction and shear**. They assumed a quasi periodical cracking of the matrix material perpendicular to fibre direction. Thereby a random occurrence of partial failures already before loading of the system (predamage) is considered to follow a Poisson distribution. Consequently, matrix material is only responsible for load transfer from failed to surviving fibres by shear whereby the fibres solely carry the full externally applied load in tension. Another possibility which was considered is that load-redistribution is performed by friction with loss of connectivity between fibres and matrix material. IBNADELJALIL AND CURTIN (1997) analysed the influence of matrix material by investigations on a 3D-fibre matrix modelled as 3D-lattice model. Brittle matrix material (e.g. fibre reinforced ceramics) was observed to develop cracks transversely to fibre direction. Thus fibres are responsible to carry the full externally applied load. In case of plastic matrix material (e.g. metals) yielding is given already long before reaching the maximum bearing capacity of the bundles. Once more the fibres are responsible to carry the load. In case of a linear-elastic-plastic matrix behaviour it can also be assumed that the bearing capacity of matrix material is reached before fibres fail. All these discussed possibilities of matrix material behaviour conclude that the fibres are exclusively responsible for transferring the system load. Nevertheless, matrix material contributes decisively to or even enables load sharing between fibres after partial failures occurred. This justifies the disregard of matrix material in modelling the maximum bearing capacity of fibre bundles.

As already discussed in ZWEBEN AND ROSEN (1970) one main expansion of WEIBULL's and DANIELS's theories was the explicit combination of both theories to the **serial-parallel fibre bundle model (s-p-FBM)**. There are numerous scientific papers addressing this subject, e.g. GÜCER AND GURLAND (1962), MISTLER (1979), HARLOW AND PHOENIX (1979A,B; 1981A,B; 1982), SMITH (1980, 1982, 1983), HARLOW ET AL., (1983) and PHOENIX ET AL. (1997). SMITH (1982, 1983) investigated the s-p-FBM of GÜCER AND GURLAND (1962) assuming a ductile matrix and GLS (SMITH, 1982) or ELLS (SMITH, 1983) and iid fibre strength with $X_1 \sim$ WD. The serial system size M is given by $M = l / \delta$ with l as fibre length (e.g. HARLOW ET AL., 1983) and N parallel fibres per serial system (increment). The system strength was defined as the maximum stress the weakest serial increment is able to withstand. Thereby the serial system effect was modelled by means of EVT for minima. Consequently, load redistribution was only allowed for (as expectable) within N parallel elements, whereas the system of M serial linked increments fails with failure of the first link (weakest sub-system) and thus follows the WLT, e.g. WEIBULL (1939). The first failure immediately initiates system collaps due to lack of the possibility that the residual fibres take additional load. Nevertheless, weakest link failure can also occur in parallel arranged DANIELS systems if the strength values of N fibres are distributed in proportion to a harmonic series, e.g. [1, 1 / 2, 1 / 3, …, 1 / N] which is called "**domino phenomenon**" (PARAMONOVA ET AL., 2006). In 1982 SMITH stated that s-p-FBM is also of interest for polymer fibrils which consist of molecular chains with alternating cristalline and amorphous regions (note: e.g. cellulose; see chapter 4). SMITH (1983) references HARLOW ET AL. (1983) who developed an approximation for the strength of s-p-FBM under varying load sharing rules. It is recommended that this model works well only for very small N but very large M due to the dominating contribution of serial (weakest link) system behaviour. The approximative CDF for the critical value of k fibre failures as maximum number of fibre failures before the system collapses is given by (HARLOW ET AL., 1983)

$$H_{M,N}(x) \approx 1 - \exp\left[-\left(\frac{x}{a_{M,N}}\right)^{N \cdot \beta}\right], \text{ with } x > 0, \tag{3.58}$$

with $H_{M,N}(x)$ as CDF of fibre bundle resistance of M serial linked increments each of N parallel fibres, X as load per fibre with $X \sim \mathrm{WD}(a, \beta)$, $a_{M,N}$ as normalising constant with $a_{M,N} = x_0 \cdot (M \cdot c_N)^{-1/(N \cdot \beta)}$ and c_N as constant depending on the load sharing rule (note: the dependency on the load sharing rule is not stated explicitly). In their model HARLOW

AND PHOENIX (1979A,B; 1981A,B; 1982) investigated s-p-FBMs under ELLS by means of load enhancement factor K. They found an approximative CDF given by

$$H_{M,N}(x) \approx H_{M,N}^{(k)}(x) = 1 - \left[1 - H_N^{(k)}(x)\right]^M \approx 1 - \exp\left[-\left(\frac{x}{a_{M,N}^{(k)}}\right)^{k\cdot\beta}\right], \text{ with } x > 0, \tag{3.59}$$

with $H_N^{(k)}$ as the probability of k-failures in a fibre bundle of N parallel fibres at load X, $H_{M,N}^{(k)}$ as the probability of k-failures in a fibre bundle of M serial increments with N parallel fibres each, X as iid fibre strength with $X \sim \mathrm{WD}(a, \beta)$ and $a_{M,N}^{(k)}$ as normalising constant. Whereas the **size effect**, the change in (system) strength with increasing (system) size, of serial linked single fibres follows a WD and is given by O ($N^{-1/\beta}$), the fibre bundle strength follows O ($N^{-1/(k\cdot\beta)}$). Therefore, the decrease in strength is less pronounced in parallel fibre systems than in serial linked single fibres, whereby the critical value itself depends on N. Because k being a function of N the size effect of fibre bundles in the limiting case $M, N \to \infty$ can be expressed by O [1 / ln(N)] or O [1 / ln($N \cdot M$)] (see e.g. SMITH, 1980) which serves as asymptotically lower bound of the size effect of parallel or serial-parallel systems, respectively. Thus k represents physically the "**critical crack size**" or "**critical failure sequence**", i.e. the maximum number of consecutive failures before a total system collaps occurs. SMITH (1983) concludes that a simple WEIBULL-approximation of the lower distribution tail as proposed e.g. by HARLOW ET AL. (1983) is not adequate for most practical applications. This is because the assumption of negligible load redistribution effects in case of serial-parallel systems and thus a focus solely on serial size effect does not hold in real composites. For a good choice of k, SMITH (1980) proposed to use the inequality

$$\gamma(k-1) < \frac{\ln(N\cdot M)}{\beta} < \gamma(k), \tag{3.60}$$

with $\gamma(0) = 0$ and $\gamma(k)|_{k\geq 1}$ as defined by

$$\gamma(k)\Big|_{k\geq 1} = k\cdot\ln(K_k) - \sum_{j=1}^{k-1}\ln(K_j). \tag{3.61}$$

MISTLER (1979) investigated size effects on tensile strength perpendicular to grain of glued laminated timber beams focusing on end notches on the bending-tension side. He observed that the exclusive consideration of weakest link theory which implies the failure

of a system after first incipient cracking is not always verifyable in tests. In particular, in testing specimens with a relatively large surface under tension stress perpendicular to grain a certain amount of load redistribution after partial failure can be observed. Based on his experiments he developed the so called "**rope-wire-model**" (note: corresponding to a **s-p-FBM**) assuming serial "weakest link" behaviour ("chain") with increasing number of laminations in stress direction and parallel system behaviour ("rope") with increasing dimension of stressed cross section. Assuming iid strengths $f_1 = X_1 \sim \mathrm{WD}\,(\alpha, \beta)$, E-modulus $E_1 = E =$ constant and GLS (note: DANIELS's system) MISTLER studied by means of probability theory (inclusion-exclusion formula and combinatorics) the expectable strength distribution parameters of (small and finite) systems of N parallel elements. He concluded that the system strength also follows WD with $f_{\mathrm{sys}} = X_{\mathrm{N}} \sim \mathrm{WD}\,(\alpha_{\mathrm{N}}, \beta_{\mathrm{N}})$ and parameters given by

$$\begin{aligned} &\alpha_N \approx \alpha \cdot \left[1 + 0.71 \cdot \beta^{-0.355} \cdot \left(N^{0.012 \cdot \beta - 0.64} - 1\right)\right] , \\ &\beta_N = c_1 + c_2 \cdot \sqrt{N} \text{ , with } c_1 \approx \beta - b_0 \cdot \ln(\beta),\ c_2 \approx b_0 \cdot \ln(\beta) \text{ with default } b_0 = 1 . \end{aligned} \tag{3.62}$$

MISTLER verified his model by destructive tests observing a huge influence of statistical spread within and between the elements and showed that in case of WEIBULL's theory $\mathrm{CoV}[X_{\mathrm{M}}]$ is constant and independent of M with $\lim_{\mathrm{M} \to \infty} \mathrm{E}[X_{\mathrm{M}}] \to 0$, but in case of a parallel system $\mathrm{CoV}[X_{\mathrm{N}}]$ decreases with increasing N and $\lim_{\mathrm{N} \to \infty} \mathrm{E}[X_{\mathrm{N}}] \to L$ with $L > 0$. Note: Beside the fact that MISTLER (1979) analysed a finite DANIELS system no references to DANIELS or to literature regarding FBMs in general were made in his thesis.

Other papers concentrated on functions for size effects and formulation of power laws to describe the decrease of expectation and variance of system strength and resistance with increasing system size in respect to the underlying load sharing rule. For example, simulations of SMITH (1980) confirmed DANIELS's result that in case of GLS the standard deviation decreases with increasing system size proportional to $\sim 1 / \sqrt{N}$ which follows directly from the average process approach. In case of LLS SMITH (1980) observed that the standard deviation decreases proportional to $a / \ln(N)$ with a as some constant value. DUXBURY AND LEATH (1994) investigated fibre bundles under ELLS by means of lattice models. They found that the size effect behaves proportional to $[1 + k \cdot \ln(L)] - 1$, with k as number of failures and $L = \sqrt{N}$ in case of a square lattice. ZHANG AND DING (1994) studied the distribution of the **critical average load per fibre x_{C}** of a fibre bundle which immediately initiates a total system collaps. In general, $\lim_{\mathrm{N} \to \infty} x_{\mathrm{C}} \to 0$. The distribution of the **burst size D(Δ)**, the size of elements (fibres) which fail simultaneously, follows

asymptotically a **power law** with $D(\Delta) \propto \Delta^{-\xi}$. The power ξ shows in general (e.g. LLS) dependency on CDF of fibre strength and system size N. In case of GLS ξ only depends on CDF. In the limiting case $N \to \infty$ for GLS ξ was found to be independent of CDF with **universal (avalanche) power $\xi = 2.5$** (e.g. HEMMER AND HANSEN, 1992; HANSEN AND HEMMER, 1994; KUN ET AL., 2000). In case of LLS the burst distribution can be approximated by a power law of type $D(\Delta) / N \propto \Delta^{-\xi}$ with power ξ non-universal and positively correlated with N being dependent on CDF of fibre strength. Also KLOSTER ET AL. (1997) confirmed that the asymptotic power model of burst size distribution in case of LLS and GLS are not in the same universality class. They observed that **the maximum load a fibre bundle is able to withstand increases in case of GLS proportional to N and in case of LLS proportional to $N / \ln(N)$.**

Further research on FBMs concentrated on **critical cluster sizes which initiate system collaps as avalanche successive breakdown** of fibre failures until reaching a steady state. Some papers postulate a certain transition area where the system behaviour shows independency from the load sharing rule. IBNADELJALIL AND CURTIN (1997) assumed that a critical cluster size $<< N$ exists with bundle strength being independent of the underlying load sharing rule GLS or LLS. The assumption is based on the occurrence of a certain cluster of fibres (the weakest cluster) within the parallel system decisive for the system which provokes system collaps (note: this can be seen as formulation of an RVE). IBNADELJALIL AND CURTIN (1997) assumed a fibre bundle with poor matrix-fibre interface determined by shear capacity (slipping and friction). They defined the ratio $\Omega = G_{090} / E_{t,0}$ as the ratio between shear and tensile E-modulus of matrix and fibres, respectively, with $\Omega \to 0$ representing ELLS, $\Omega \to \infty$ for GLS and $0 \leq \Omega < \infty$ for cases in between. Searching for this critical cluster size necessiates the definition of a sub-system of N_l fibres with length δ_l and smearing of boundary and correlation effects (note: similar to the definition of an RVE) to enable the extrapolation to systems multiple-times larger than the critical cluster (RVE) with system size $N = N_f / N_l$ times $M = L / \delta_l$, with N_f as total quantity of parallel fibres and L as length of bundle or fibre length. Based on the work of PHOENIX ET AL. (1997) and in case of GLS it was concluded that length δ_l is given by $\delta_l = 0.4 \cdot \delta_c$, with δ_c as the critical length. It was assumed that δ_l is independent of the load sharing rule but dependent on local fibre-matrix interactions. Consequently, the definition is assumed to be also representative in case of LLS. With fibre strength $f_l = X_l \sim$ WD it was stated that n_l is a function of WEIBULL shape parameter β and parameter Ω, with n_l being smaller if β gets larger (note: the higher the variance of X_l the greater the RVE necessary to smear the influence of size, statistical spread and

correlation). HIDALGO ET AL. (2002) developed a **stress transfer function** to account for load sharing in between GLS and ELLS. They considered first thermodynamical aspects where materials show a finite critical strength (≥ 0) in the limiting case of $N \to \infty$. Without such a critical point $\lim_{N \to \infty} \sim 1 / \ln(N)$ conform to LLS. In elastic materials and following fracture mechanics the stress increase σ_{add} of an element with distance r from crack tip shows a proportional relationship $\sigma_{add} \sim r^{-\gamma}$, in case of GLS with $\gamma \to 0$ and in case of ELLS with $\gamma \to \infty$. On basis of these power laws and under the conditions of fibre strength $X_1 \sim$ WD, stress σ, statically increasing load increments (no dynamical effects), load sharing in dependency of the radial distance between the intact fibre i and the failed fibre j and of elastic interaction between the fibres HIDALGO ET AL. (2002) developed the stress transfer function

$$F(r_{ij}, \gamma) = Z \cdot r_{ij}^{-\gamma} \text{, with normalising constant } Z = \left(\sum_{i \in I} r_{ij}^{-\gamma}\right)^{-1}, \tag{3.63}$$

with I as the set of all intact fibres and the periodical boarder condition of the system with $R_{max} = \sqrt{2} \cdot (L - 1) / 2$, with L as linear size of the system (width and / or depth of the cross section of the fibre bundle). Thus parameter γ determines the "**effective range of interaction**" between failed and intact fibres with stress increase within the intact fibre i after failing of fibre j given by

$$\sigma_i(t + \tau) = \sigma_i(t + \tau - 1) + \sum_{j \in B(\tau)} \sigma_j(t + \tau - 1) \cdot F(r_{ij}, \gamma), \tag{3.64}$$

with τ as time (stress) increment and $B(\tau)$ as the set of all fibres which failed within the time (stress) increment τ and where

$$\sigma_i(t_0 + T) = \sum_{\tau=1}^{T} \sigma_i \cdot (t_0 + \tau), \tag{3.65}$$

is the total stress on element i during an avalanche in the time span (t_0, $t_0 + T$). An analysis of parameter γ shows that $\gamma = 0$ represents "pure" GLS but $0 \leq \gamma \leq (\approx 2.2 \pm 0.1)$ also represents GLS with σ_c being independent of N and γ. In case of $\gamma > \gamma_c$ LLS is given, with σ_c dependent on N and γ up to a possible second transition area around $\gamma \approx 7$ with $\sigma_c|_{\gamma \geq \approx 7}$ only depending on N with $\sigma_c(N) \sim \alpha / \ln(N)$ for $\gamma >> \gamma_c$ and $N \to \infty$, and $\sigma_c = (\beta \cdot e)^{-1/\beta}$ for $\sigma \sim$ WD, $0 \leq \gamma \leq (2.2 \pm 0.1)$, $\gamma_c \approx (2.2 \pm 0.1)$ and σ_c as the ultimate strength of the system (see Fig. 3.10). Therefore, **fibre breakdown in GLS occurs completely randomly without any correlated crack growth within the system.** The

system failure occurs at a random position within the system. **In case of LLS random fibre breakdown occurs initially but due to increasing localised stress concentration more and more correlated growth of clusters of failed fibres occurs and propagates until an avalanche breakdown (instability), initiated in the dominant cluster, causes system collaps**. Note: These observations confirm the assumptions made by IBNADELJALIL AND CURTIN (1997) who assumed similar system behaviour up to a certain cluster size independent of the load sharing rule. The transition parameter γ_c is observed to become smaller with increasing WEIBULL shape parameter β. Note: This corresponds to a decrease of CoV[σ] leading to a decrease of RVE representing cluster size as already published previously in IBNADELJALIL AND CURTIN (1997). To conclude, the existence of a finite limit value for $\sigma_c > 0$ at $N \to \infty$ was confirmed in case of GLS but in case of LLS asymptotic analysis gives $\lim_{N \to \infty} \sigma_c \to 0$ as consequence of localised stress concentrations initiating system collaps.

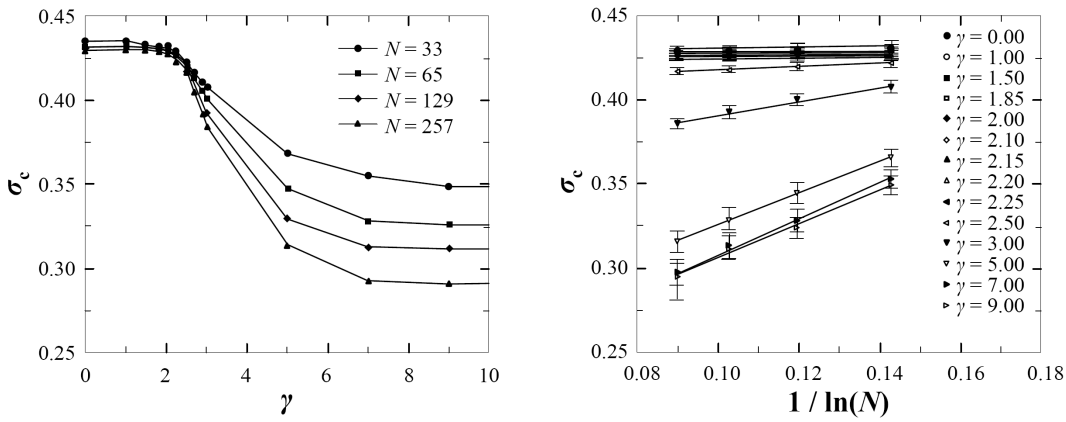

Fig. 3.10: Ultimate system strength σ_c in dependency of linear system size N and load sharing factor γ: (left) σ_c vs. γ and N; (right) σ_c vs. 1 / ln(N) and γ (HIDALGO ET AL., 2002)

Beside above mentioned literature focusing on the influence of load sharing rules (GLS vs. ELLS) and the interaction of elements in s-p-FBMs with and without matrix material the basic assumptions of identical perfect linear elastic stress-strain behaviour of fibres and constant E-modulus as given in DANIELS (1945) were in general left. Therefore **correlation between material characteristics within and between fibres** was in general neglected. HOHENBICHLER AND RACKWITZ (1983) reported with reference on RACKWITZ (1978) that already a minor correlation between the strengths of elements in a parallel system can influence the system strength significantly. In their paper they enlarged DANIELS's FBM by investigating an "**imposed strain approach**" for brittle

materials. Considering a parallel system of N elements under uniform load with total system load L and uniform imposed extension of each element with $\varepsilon_1 = \varepsilon_{sys} = \varepsilon =$ constant, the stress $S_i(\varepsilon)$ in each element i, $i = 1, \ldots, N$ given ε is defined by

$$S_i(\varepsilon) = \begin{cases} \varepsilon \cdot \dfrac{X_i}{Y_i} & , \ 0 \le \varepsilon \le Y_i = \varepsilon_f \\ 0 & , \ else \end{cases} , \tag{3.66}$$

with X_i as random distributed strength of the ith element and $Y_i = \varepsilon_{f,i}$ as the corresponding ultimate strain. The bearing capacity and maximum system resistance are given by

$$R_N(\varepsilon) = \sum_{i=1}^{N} S_i(\varepsilon) \text{ and } R_N = \max_{\varepsilon \ge 0}\left[\sum_{i=1}^{N} S_i(\varepsilon)\right] . \tag{3.67}$$

The probability of failure P_f of the system under load L follows

$$\begin{aligned} P_f = P(R_N \le L) &= P\left\{\max_{\varepsilon \ge 0}\left[\sum_{i=1}^{N} S_i(\varepsilon)\right] \le L\right\} = \\ &= P\left\{\bigcap_{\varepsilon \ge 0}\left[\sum_{i=1}^{N} S_i(\varepsilon) - L \le 0\right]\right\} \le \min_{\varepsilon \ge 0}\left\{P\left[\sum_{i=1}^{N} S_i(\varepsilon) - L \le 0\right]\right\}, \end{aligned} \tag{3.68}$$

with the last inequality as upper bound according probability theory, with $P(\cap_\varepsilon A_\varepsilon) \le \min_\varepsilon \{P(A_\varepsilon)\}$. Under consideration of ordered Y_i's with $Y_{(1)} \le Y_{(2)} \le \ldots \le Y_{(N)}$ it follows that

$$R_N(\varepsilon = Y_{(k)}) = \sum_{i=k}^{N} S_{(i)}(\varepsilon) = \sum_{i=k}^{N} Y_{(k)} \cdot \frac{X_{(i)}}{Y_{(i)}} , \tag{3.69}$$

with $X_{(i)}$ and $S_{(i)}$ corresponding to $Y_{(i)}$. The maximum resistance of the system is given by

$$R_N = \max_{k=1}^{N}\left[\sum_{i=k}^{N} Y_{(k)} \cdot \frac{X_{(i)}}{Y_{(i)}}\right] . \tag{3.70}$$

Investigating the special case e.g. analysed bei DANIELS (1945) with $E = X_i / Y_i =$ constant $= X_{(i)} / Y_{(i)}$ it follows

$$R_N = \max_{1\le k\le N}\left[\sum_{i=k}^{N} Y_{(k)}\cdot E\right] = \max_{1\le k\le N}\left[\sum_{i=k}^{N} X_{(k)}\right] = \max_{1\le k\le N}\left[(N-k+1)\cdot X_{(k)}\right]. \tag{3.71}$$

Given that $R_N \ge (N-k+1)\cdot X_{(k)}$ for every k the probability of failure according the general definition of parallel (redundant) systems which fail if all elements have been failed is given by

$$\begin{aligned} P_f &= P(R_N \le L) = P\left\{\max_{\varepsilon\ge 0}\left[\sum_{i=1}^{N} S_i(\varepsilon)\right] \le L\right\} = \\ &= P\left\{\bigcap_k \left[(N-k+1)\cdot X_{(k)} - L \le 0\right]\right\} \le \min_k \left\{P\left[(N-k+1)\cdot X_{(k)} - L \le 0\right]\right\}. \end{aligned} \tag{3.72}$$

In particular the last term corresponds to the upper bound, the highest possible strength of a parallel (redundant) system given as failure probability of the strongest element. HOHENBICHLER AND RACKWITZ (1983) performed some analysis by means of first-order reliability method (FORM) investigating also the influence of correlated elements. They concluded that FORM may be sufficient in many engineering applications. Nevertheless, the linearisation and implication of some error already in modelling of single elements accumulate to multiple errors calculating the failure probability of large parallel systems. Therefore the application of higher order reliability analysis (e.g. second-order reliability method, SORM) is proposed. Few years later GOLLWITZER AND RACKWITZ (1990) note that the rate of convergence of asymptotic results of fibre bundle strength distribution is in general very poor leading to unrealistic results for finite and in particular very small system sizes. In general GLS enables maximum of redundancy in parallel systems. Dynamical effects which may occur during partial failures are described as being dependent on the status of the system, the damping behaviour and the rate of energy dissipation during partial failure, e.g.

$$P_f = P(R_N \le L) = P\left\{\bigcap_{k=1}^{N}\left[(N-k+1)\cdot X_{(k)} - X_{(k-1)} - L \le 0\right]\right\}. \tag{3.73}$$

Nevertheless, dynamical effects (expressed by the term $X_{(k-1)}$) which seem to be decisive for finite systems vanish with $N \to \infty$. GOLLWITZER (1986) and GOLLWITZER AND RACKWITZ (1990) delivered some numerical results for finite (small) systems. Simulations based on the assumptions of GLS and equicorrelation neglected also time-effects. By means of the order statistics approach of HOHENBICHLER AND RACKWITZ

(1983) and GUERS AND RACKWITZ (1987) who performed FORM and SORM analysis, GOLLWITZER AND RACKWITZ (1990) modelled element's force $R_i(\varepsilon)$ at given deformation ε, in particular $R_i(Y_{(i)}, Q_i)$ at corresponding strain $\varepsilon = Y_{(i)}$ under consideration of a random parameter vector Q_i necessary for further description of load-strain-relationship given by

$$F_{sys} = \left\{ \max_{\varepsilon} \left[\sum_{i=1}^{N} R_i(\varepsilon) \right] - S \le 0 \right\} = \left\{ \bigcap_{\delta} \left(\sum_{i=1}^{N} R_i(\varepsilon) - S \le 0 \right) \right\} \le$$
$$\le \left\{ \max_{i=1}^{N} \left[R_i\left(Y_{(i)}, Q_i\right) + \sum_{k \ne i}^{N} R_k\left(Y_{(i)}, Q_k\right) \right] - S \le 0 \right\}. \tag{3.74}$$

The inequality on the right side results from the possibility that a maximum of system resistance can occur also in between the discretised force-strain relationships of elements in systems, i.e. between $[Y_{(i)}, Y_{(i+1)}]$, $i = 1, \ldots, N-1$. Within their numerical calculations a reliability index of $\beta_k = 2.0$ as reference value was used. Limiting cases like perfect parallel, perfect serial, perfect plastic and perfect brittle material behaviour were analysed. Beside the fact that perfect parallel systems fail in mechanical justification, both, perfect serial and perfect parallel systems offer studying of limiting cases of system reliability as well as bearing capacity calculations. Therefore GOLLWITZER (1986) and GOLLWITZER AND RACKWITZ (1990) modelled arbitrary stress-strain relationships by means of a more general formalism developed by GLOS (1978), see

$$\sigma(\varepsilon) = \frac{\varepsilon + K_1 \cdot \varepsilon^{\nu}}{K_2 + K_3 \cdot \varepsilon + K_4 \cdot \varepsilon^{\nu}},$$
$$T(\varepsilon) = \frac{K_2 + \nu \cdot K_1 \cdot K_2 \cdot \varepsilon^{\nu-1} + (\nu - 1) \cdot (K_1 \cdot K_3 - K_4) \cdot \varepsilon^{\nu}}{\left(K_2 + K_3 \cdot \varepsilon + K_4 \cdot \varepsilon^{\nu}\right)^2}, \tag{3.75}$$

with constraints

$$T(0) = \frac{d\sigma}{d\varepsilon}(\varepsilon = 0) = E_0, \; T(\varepsilon_0) = \frac{d\sigma}{d\varepsilon}(\varepsilon = \varepsilon_0) = 0,$$
$$\sigma(\varepsilon_0) = \sigma_{\max}, \; \lim_{\varepsilon \to \infty} \sigma(\varepsilon) = \sigma_{asym}, \tag{3.76}$$

with E_0 as E-modulus at $\varepsilon = 0$ and σ_{asym} as asymptotic stress at $\varepsilon \to \infty$. Consequently, parameters K_i, with $i = 1, \ldots, 4$, are given by

$$K_1 = \frac{\sigma_{asym}}{Z}\,,\; K_2 = \frac{1}{E_0}\,,\; K_3 = \frac{1}{\sigma_{\max}} - \frac{\nu \cdot K_2}{(\nu - 1)\cdot \varepsilon_0}\,,\; K_4 = \frac{1}{Z} \tag{3.77}$$

with

$$Z = (\nu - 1)\cdot E_0 \cdot \varepsilon_0{}^{\nu} \cdot \left(1 - \frac{\sigma_{asym}}{\sigma_{\max}}\right). \tag{3.78}$$

The parameter sets of various stress-strain relationships analysed by GOLLWITZER (1986) and GOLLWITZER AND RACKWITZ (1990) are given in Tab. 3.1.

Tab. 3.1: Cases and parameter sets of various stress-strain relationships discussed in GOLLWITZER (1986) and GOLLWITZER AND RACKWITZ (1990)

cases		$\sigma_{\max}$	ε_0	E_0	σ_{asym}	ν	$E[\varepsilon_0]$ / $E[\sigma_{\max}]$
case I:	elastic, perfect plastic	1.00	0.25	16	0.98	7	1 / 4
case II:	non-linear plastic, softening	1.00	1.00	4	0.25	7	--
case III:	elastic-plastic, sharp softening	1.00	0.25	16	0.25	7	1 / 4
case IV:	brittle, non-linear softening	1.00	0.25	16	0.00	20	1 / 4
case V:	brittle	1.00	0.25	4	0.00	20	1 / 4

As shown in Fig. 3.11 (left) parallel systems are in behaviour comparable to serial systems if $<< N$ due to the fact that load redistribution lacks existence of potential survivors. Note: This highly depends on the spread of element's potential with expectation of possible redistribution and further increase of load in case of higher spread (> CoV). **Consequently, in case of small system sizes it is proposed to design structures by single elements with high bearing capacity instead of parallel arranged elements of brittle material.** Furthermore, the degree of ductility plays a major and decisive role for the expectable potential of redundancy. GOLLWITZER (1986) and GOLLWITZER AND RACKWITZ (1990) defined the degree of ductility Δ as

$$\Delta = \frac{\int_0^{2\cdot\varepsilon_0} \sigma(\varepsilon)\cdot d\varepsilon - \frac{\sigma_{\max} - \varepsilon_0}{2}}{\sigma_{\max}\cdot\varepsilon_0}\,, \tag{3.79}$$

with upper limit of integration arbitrary chosen as $2 \cdot \varepsilon_0$, and ε_0 as strain at maximum stress $\sigma_{\max}$. A full positive correlation between deformation at maximum force of each

element and fracture deformation is assumed. As shown in Fig. 3.11 and Fig. 3.12 system reliability and the gain of redundancy increases with increasing ductility or plasticity in element's material behaviour with already remarkable increase even at low ductility measures if spread of ε_0 is small.

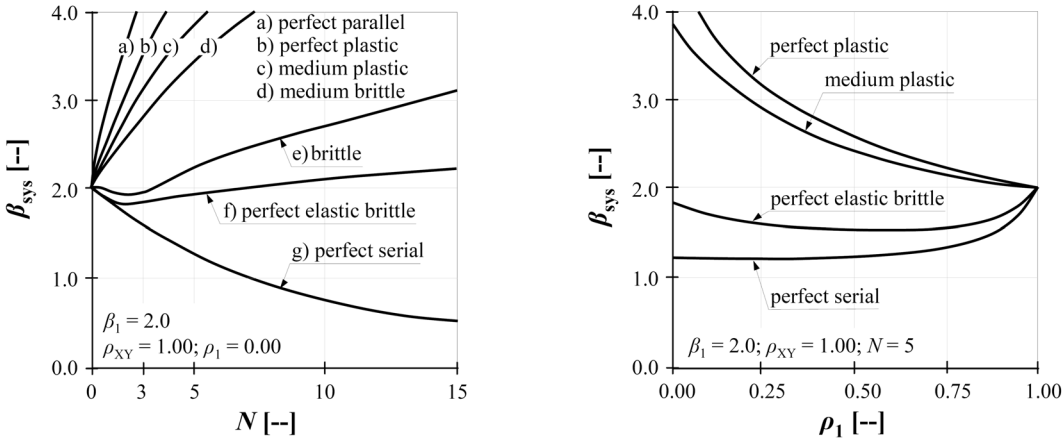

Fig. 3.11: System reliability index β_{sys} in comparison to element reliability index β_1 under various stress-strain relationships according GOLLWITZER (1986) and GOLLWITZER AND RACKWITZ (1990): (left) β_{sys} vs. N; (right) β_{sys} vs. ρ_1

Concerning the stochastic dependency between the element strengths the numerical results clearly show that the lower the correlation ($-1.0 \leq \rho \leq +1.0$) the higher the gain of redundancy in material with partly or full plastic behaving materials, but the higher the loss in the bearing capacity in serial systems or parallel systems built up of perfect elastic materials. Nevertheless, the reliability of serial systems increases with increasing correlation. In systems composed of full correlated elements the arrangement and interaction as well as the material behaviour plays no role. The correlation within elements shows only minor influence on system reliability beside systems composed of brittle material. Note: This seems to be obvious if the interaction between elements in parallel systems and relationships between these elements or between neighbouring sub-elements is considered as decisive. It determines the system action but not the correlation structure within the (sub-)elements due to the fact that redundancy originate from interactions between the elements. The analysis of the influence of relationships between coefficients of variation (CoV) of action and resistance (see Fig. 3.12, right) gives a decreasing reduction of redundancy in case of high CoV[S] with the tendency to provoke a more serial than parallel system action in case of >> CoV[S]. The increase of

redundancy above ≈ CoV[S] / CoV[X] ≥ 2.0 is negligible. In case of deterministic actions a higher CoV[X] (see Fig. 3.12, left) shows positive effects on the reliability of systems composed of ductile or brittle elements. For brittle systems with small N but large CoV[X] the negative effect disappears. Nevertheless, a higher CoV[X] corresponds to higher requirements on material classification to be able to reach the required design values which in case of strengths are normally given as 5%-quantile values.

Another influence is given by CoV[Y] as spread of deformation at maximum load on elements. The results show that the reliability of systems sharply decreases with increasing CoV[Y] and nearly vanish for CoV[Y] > 70%, with CoV[Y] → ∞ leading to a "quasi" serial acting system (GOLLWITZER, 1986). Perhaps for most materials CoV[Y] can be assumed as being small. Note: This is in contradiction to DANIELS assumptions who assumed negligible spread of E-modulus E_1 if compared to the high spread expectable for breaking extension $\varepsilon_{f,1}$. In their last study GOLLWITZER AND RACKWITZ (1990) analysed the influence of dynamical effects. They showed that dynamics plays a decisive role even in larger systems.

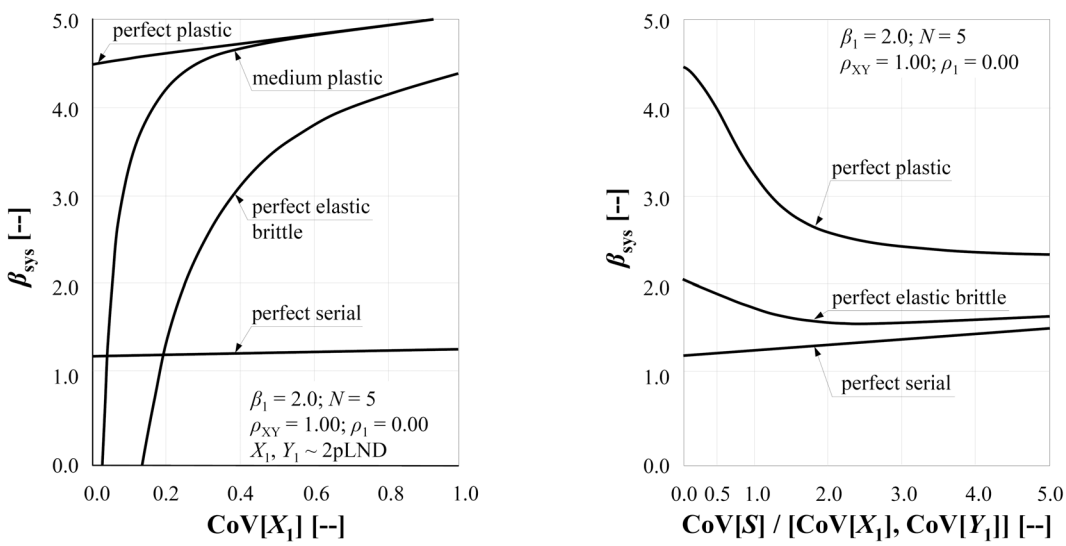

Fig. 3.12: Reliability index β_{sys} in comparison to β_1 under various stress-strain relationships according GOLLWITZER (1986) and GOLLWITZER AND RACKWITZ (1990): (left) β_{sys} vs. CoV[X_1]; (right) β_{sys} vs. CoV[S] / CoV[X_1] = CoV[S] / CoV[Y_1]

GOLLWITZER AND RACKWITZ (1990) conclude that DANIELS' system and his assumption of GLS show high redundancy effects which are negligible in case of high correlation

between the elements and in case of CoV[S] ≈ CoV[R]. Further, the influence of material behaviour plays an important role showing higher redundancy in case of elements with some amount of ductility. They note also that attention should be paid in transfer of discussed results for practical application due to the fact that most parallel systems exhibit LLS and therefore show a tendency to behave more like serial systems.

According IBNADELJALIL AND CURTIN (1997) GLS could be verified in case of brittle material behaviour but delivered poor estimates in case of metals and synthetics. Thereby GLS delivered the highest extra value of all load sharing rules. GURVICH AND PIPES (1995) investigated the influence of load sharing models as multi-step failure mechanisms on expectable system strength. A decrease of expected system strength (mean value) and of coefficient of variation CoV[X_N] with increasing N was more pronounced in case of higher initial CoV[X_1]. Furthermore, the variability of the E-modulus modelled independently of X_1 was analysed and showed that X_N decreases with increasing CoV[E] but only distinctively above CoV[X_1] > 10% and CoV[E] > 20%. Nevertheless GURVICH AND PIPES (1995) concluded that the influence of CoV[E] on X_N can be neglected for practical applications because of the predominant influence of parameters N and CoV[X_1].

Further papers with focus on the analysis of FBMs in respect to fibre characteristics, critical failure sequence and asymptotic power laws are published by KUN ET AL. (2000) and subsequent papers, e.g. HIDALGO ET AL. (2001). KUN ET AL. (2000) investigated a 2D fibre bundle structure of N parallel fibres by means of DANIELS's model. They discussed the introduction of some plasticity by reducing the E-modulus after yielding by a factor α, with $E_{pl} = E \cdot \alpha$, given $\varepsilon > \varepsilon_f$, with $0 \leq \alpha \leq 1$ and ε_f as the extension at yield point, transition between linear-elasticity and plasticity. In cases where each fibre can only fail once (note: e.g. in case of fibre bundle with length equal the ineffective length δ) the bundle stress is given by

$$\sigma_{sys} = \frac{F}{N} = \sigma \cdot [1 - P(f)] + a \cdot \sigma \cdot P(f), \tag{3.80}$$

with the first term expressing the load carried by intact fibres and the second term for the residual load carried by already failed fibres, with the total load on the fibre bundle F, σ as fibre stress, P(f) as share of failed fibres, [1 – P(f)] as share of survivors and a as parameter characterising the residual amount of stress potential in failed fibres. In case of a "dry" fibre bundle (without a matrix) $a = 0$, and with $a = 0.5$ the formulation represents

the micromechanical model for fibre reinforced ceramic matrix composites. For cases in which each fibre can fail k-times further differentiation is made in "quenched disorder" (maximum load of each fibre stays constant in all k-failures → constant failure treshold) and "annealed disorder" (maximum load of each fibre varies from failure to failure → iid failure tresholds considering possible microscopic re-arrangements in the material structure) to mirror the behaviour of fibres after $(k-1)$ failures. Note: This model is in principle a s-p-FBM with k possible fibre failures equal a serial segmentation of each fibre in sub-elements. The model represents a second order hierarchical model, which is differentiated in deterministic and stochastic strengths of sub-elements denoted by "quenched" and "annealed disorder", respectively, and stochastic strengths of elements. The fibre bundle stress in case of a maximum allowed failure quantity of $k_{\max}$ per fibre is in case of "quenched disorder" given by

$$\frac{F}{N} = f \cdot \left[1 - P(f)\right] + \sum_{i=1}^{k_{\max}-1} a^i \cdot f \cdot \left[P\left(a^{i-1} \cdot f\right) - P\left(a^i \cdot f\right)\right] + a^{k_{\max}} \cdot f \cdot P\left(a^{k_{\max}-1} \cdot f\right), \tag{3.81}$$

and in case of "annealed disorder" given by

$$\frac{F}{N} = \sum_{i=0}^{k_{\max}-1} a^i \cdot f \cdot \left[1 - P\left(a^i \cdot f\right)\right] \cdot \prod_{j=0}^{i-1}\left(a^j \cdot f\right) + a^{k_{\max}} \cdot f \cdot \prod_{i=0}^{k_{\max}-1}\left[P\left(a^i \cdot f\right)\right]. \tag{3.82}$$

Investigations with $f_1 = X_1 \sim$ WD confirmed that the avalanche power law (size of consecutive fibre failures) in case of GLS is universal and asymptotically given by the proportion $\Delta^{-5/2}$. In case of LLS, "dry" fibre bundle and continuous damage as well as annealed fibre bundles (independent from damage parameter a) the total number of clusters N_C in the fibre bundle follows the simple scaling law $N_C = L^2 \cdot g(F / L^2)$. Following KUN ET AL. (2000), HIDALGO ET AL. (2001) made some further investigations regarding quenched and annealed disordered failures of fibres within a fibre bundle. They showed that in general weaker fibres can break more often than stronger ones. HIDALGO ET AL. (2001) described the failure behaviour of a fibre bundle, considering it as disordered solid, as consequence of microscopic failure avalanches until the avalanche breakdown looses balance which immediately leads to system collaps. Furthermore the energy dissipation in fibres after k-failures as well as the influence of softening and hardening was analysed.

In some publications notes were made regarding the distribution model of fibre strengths and its influence on the distribution of bundle strength. For example HOHENBICHLER AND

RACKWITZ (1981) discussed the influence and modelling aspects of equicorrelation between elements in a parallel system. Assuming a second order hierarchical model with $X_i = Z \cdot Y_i$ with iid Y_i, independent distributed X_i and reliability $R_N = R_N(X_1, X_2, \ldots, X_N)$ of N elements with strength X_i, $i = 1, \ldots, N$, it follows that in case of iid $X_1 \sim$ LND the asymptotic CDF of the system strength considering DANIELS's fibre bundle converges to a LND given by

$$\lim_{N\to\infty} R_N(X_1,\ldots,X_N) \overset{asympt.}{\sim} LND(E[R_N], Var[R_N]),$$
$$\text{with } E[R_N] = \sqrt{1+\gamma}\cdot E'_N,\ Var[R_N] = \gamma\cdot(1+\gamma)\cdot E'^{\,2}_N, \tag{3.83}$$
$$\text{and } E'_N = N\cdot y_0\cdot[1-F_Y(y_0)],$$

with $y_0 = \exp(\eta - \tau \cdot x_0)$, $F_Y(y_0) = \Phi(x_0)$, x_0 as singular solution of $\tau \cdot \Phi(x_0) = \varphi(x_0)$ and CDF of Y_i

$$Y_i \sim F_Y(y_i) = \Phi\left(\frac{\ln(y_i)-\eta}{\tau}\right),$$
$$\text{with } \eta = 2\cdot\ln(\mu) - \frac{1}{2}\cdot\ln(\mu^2+\sigma^2) \text{ and } \tau^2 = \ln(\mu^2+\sigma^2) - \ln(\mu^2+\rho\cdot\sigma^2). \tag{3.84}$$

The rate of convergence was analysed by investigating the relative deviation Δ_N of $R_N(X_1, \ldots, X_N)$ and its limit value $Z \cdot E'_N$, with $\Delta_N = [R_N(X_1, \ldots, X_N) - Z \cdot E'_N] / (Z \cdot E'_N)$. It was shown that Δ_N decreases roughly with $N^{-1/2}$ and roughly proportional to CoV[X] and $(1-\rho)^{1/4}$. PARAMONOVA ET AL. (2006) remark that the general assumption that fiber strengths follows automatically $X_1 \sim$ WD is doubtful. They note that sometimes $X_1 \sim$ LND seems to be more appropriate for representation of fiber strength. HOHENBICHLER AND RACKWITZ (1981) noted that in materials with plastic behaviour in general as well as in parallel (redundant) systems with load redistribution the system reliability can be determined as appropriate weighted sum of the element strengths. They remarked that parallel fibre systems with brittle behaviour are often modelled to follow WEIBULL's weakest link theory. Beside the fact that this is done for simplification and instead of the often complex models the last one perhaps mirror the parallel system behaviour more accurately. SUTHERLAND ET AL. (1999) discussed the applicability of WLT for fibre bundles and concluded that the final failure of the bundle follows a certain **damage accumulation** which contradicts weakest link failure. In the discussion about the applicability of **linear-elastic fracture mechanics (LEFM)** for modelling fibre bundle

strength they postulated less usability. LEFM generally assumes that flaws, especially splits, are in their dimension proportional to that of the system under consideration. This seems to be not the case in praxis, e.g. in fibre bundles the characteristics are determined by fibres which behave constant in length even if the investigated volume of the fibre bundle is changed. Furthermore, LEFM does not allow for complex failure modes which are often observed in fibre bundles. In addition, it was generally concluded that with changes in dimension changes in characteristics are often expressed by a "**composite size effect**" which in reality constitutes a conglomerate of various effects determined by testing of composites of various dimensions, e.g. changes in material properties, changes in test method, changes of test parameters and changes in the material structure. CALARD AND LAMON (2004) investigated also a fibre bundle as DANIELS's system with failure probability of a fibre under constant stress distribution $P(\sigma) \sim WD(\alpha, \beta)$ with N as the number of parallel fibres of length l. **They differentiated between load and deformation controlled tests**. Whereby load-controlled failure of fibres immediately initiate load sharing and further processes to an unstable system failure, in case of deformation controlled tests load sharing has time to develop. The system does not necessarily fail immediately and may reach some steady state. In case of deformation controlled tests the share $P(\sigma)$ of failed fibres $r(\sigma)$ at stress σ is given by $r(\sigma) / N = P(\sigma)$. The maximum load a fibre bundle can withstand in case of stable failure (deformation controlled) is given by $dF(\sigma) / d\sigma = 0$, with $F(\sigma)$ as bundle load at state σ, and in case of instable failure (load controlled) maximum load on the bundle is given at $P = P_c$, with α_c as critical ratio $r(\sigma) / N$ which initiates total collaps of the fibre bundle. In case of deformation controlled testing it follows

$$\sigma_{\max} = \alpha \cdot \left(\beta \cdot \frac{V}{V_0} \right)^{-1/\beta},$$

$$P(\sigma_{\max}) = 1 - \exp\left(-\frac{1}{\beta} \right), \tag{3.85}$$

$$F_{\max} = F(\sigma_{\max}) = N \cdot S_f \cdot \alpha \cdot \left(\beta \cdot \frac{V}{V_0} \right)^{-1/\beta} \cdot \exp\left(-\frac{1}{\beta} \right),$$

with $F_{\max}$ as the maximum bundle load and S_f as the cross section of each fibre. In case of load controlled testing it follows

$$P_c = P(\sigma_{\max}) = 1 - \exp\left(-\frac{1}{\beta}\right),$$
$$F_{\max} = F(P_c) = N \cdot (1 - P_c) \cdot S_f \cdot \sigma_F, \tag{3.86}$$

with $\sigma_F = \sigma_{\max}$ as the strength of the fibre bundle at instable state. According a statistical definition the scatter of maximum force $F_{\max}$, naturally equal to the critical number of failed fibres r_c, can be derived by means of the binomial distribution BN [N, $P(\sigma_{\max})$]. Thus the expectation and variance of r_c are given by

$$E[r_c] = N(\sigma_{\max})$$
$$\rightarrow E[F_{\max}] = N \cdot [1 - P(\sigma_{\max})] \cdot S_f \cdot \sigma_{\max},$$
$$Var[r_c] = N \cdot [1 - P(\sigma_{\max})] \cdot P(\sigma_{\max}) \tag{3.87}$$
$$\rightarrow Var[F_{\max}] = (S_f \cdot \sigma_{\max})^2 \cdot N \cdot [1 - P(\sigma_{\max})] \cdot P(\sigma_{\max}),$$

with coefficient of variation CoV[$F_{\max}$] equal to that of DANIELS (1945), MCCARTNEY AND SMITH (1983) and GURVICH AND PIPE (1995), given by

$$CoV[F_{\max}] = \sqrt{\frac{P(\sigma_{\max})}{N \cdot [1 - P(\sigma_{\max})]}}. \tag{3.88}$$

Practical tests showed remarkable differences to model predictions. Despite the performance of deformation controlled tests unstable failures and high CoV[$F_{\max}$] were observed. The analysis under consideration of a certain amount of LLS (due to friction between fibres, shear transfer in case of fibres embedded in a matrix material or dynamical effects (stress waves due to partial failures) showed that solely an amount of about 35% LLS enabled matching of theoretical and practical results. PRADHAN AND CHAKRABARTI (2008) studied the fatigue behaviour of fibre bundles in case of GLS analytically and by means of simulations in case of LLS. They noted that a dynamical failure process can be observed already with the failure of the first fibre and proceeding load redistribution until a certain equilibrium (steady) state is reached or the system collapse. They called this type of failure behaviour in the system "**self-organising breaking dynamics**".

In two accompanying papers CHUDOBA ET AL. (2006) and VOŘECHOVSKÝ AND CHUDOBA (2006) investigated in detail the fibre bundle behaviour at varying conditions

of material and test configuration by means of comprehensive Monte-Carlo simulations. The material parameters like cross sectional area A_i of each element $i = 1, \ldots, N$, fibre (element) length l_i, amount of shear interaction between fibres as well as varying E-modulus E_i, fibre tensile strength f_i and the system size N based on basic assumptions made by DANIELS (1945). The influences of varying test configuration parameters like clamping conditions or initiated twists in fibres (elements) were analysed. Concerning shear interaction it was concluded that the more intensive the interaction the more brittle the system fails. A delayed activation in combination with increased shear interaction led to a faster activation of system stiffness. Varying fibre (element) length L_i assuming $L_i \sim$ uniformly distributed showed a decrease in system stiffness at maximum system load given by the factor $r_\lambda = \ln(1 + \lambda_{max}) / \lambda_{max}$, with λ as ratio of additional element length to its nominal length, $\lambda = L / l$, with $l = l_{min}$. In case of large elements this effect diminished in fibre bundle tests. The load-elongation diagram of the elements in the system shows constant maximum load but increasing elongation potential of fibres (elements) with increasing length L_i. Varying cross sectional diameter and thus varying cross sectional area consequences a constant level of elongation but a varying E-modulus and maximum load in load-elongation diagram. Thereby A_i was assumed to be distributed uniformly. Thus the system failed at failure of the first element, or in other words, all elements failed at the same elongation. The influence on system strength up to CoV[f_i] = 10% was found to be small but A_i initiates a certain amount of spread in load-elongation relationship and in maximum load of the system. Studies on varying fibre (element) activation strain (random slack), as already done by PHOENIX AND TAYLOR (1973), gave a load-elongation diagram with equidistant parallel shifted functions due to assumed uniform distributed slack with equal maximum load and E-modulus. CHUDOBA ET AL. (2006) split the system behaviour in three sections: The first section showed a non-linear increase of stiffness in the system due to successive activation of elements after initial slack. The second section was characterised on the one hand without further activations but no partial failures and on the other hand with further activations and partial failures. The third section was characterised by in- / decreasing of load bearing capacity of the system due to successive partial failures. Based on their first parameter studies CHUDOBA ET AL. (2006) concluded that spread in fibre length and / or random slack significantly reduce the load bearing efficiency of parallel acting systems, in particular if constituted of short elements ($< l$), considering the choosen model assumptions.

In their accompanying paper VOŘECHOVSKÝ AND CHUDOBA (2006) studied s-p_FBMs composed of elements with strength $f_1 \sim$ WD. They remarked that iid elements in serial

would lead to unrealistic infinite (expectation) of system strength if the element length l_1 in relation to reference length l_{ref}, required to account for length effects as implicitly given by WEIBULL distribution, is considerable shorter, with $l_1 \to 0$ and $l_1 / l_{ref} \to 0$. They included a certain correlation within the elements in length direction by means of an autocorrelation function (ACF) within a stationary, homogenous and ergodic stochastic process given by

$$R_{aa}(\Delta d) = \exp\left[-\left(\frac{|\Delta d|}{l_\rho}\right)^r\right], \tag{3.89}$$

with l_ρ as correlation length, d as distance between the serial increments and r as power with $r = 2$ in case of a GAUß-ACF. Consideration of autocorrelation leads to serial size effects which approach the expectation (mean value) of element's strength in case of $l << l_\rho$ and which asymptotically approach the size effect according WEIBULL (1939) in case of $l >> l_\rho$ and thus leads to a decrease in system strength with increasing serial system size with power $1 / m$, with m as WEIBULL shape parameter which depends on CoV[f_i]. Thus, in case of $l << l_\rho$ the random strength field is sufficiently represented by the mean value whereas in case of $l >> l_\rho$ the influence of serial correlation diminishes. With references to BAŽANT ET AL. (2004, 2007) the cross-over function is simplified by a bi-linear function with intersection at [l_ρ; $f_{i,mean}$]. Consequently, three functional areas of statistical length effect are given, first with $l / l_\rho \to 0 \to l << l_\rho$ with system strength $f_{sys} \sim$ ND, second the transition area with influence by the autocorrelation random field at $l / l_\rho \approx 1.00 \to l = l_\rho$, and the third area with $l / l_\rho \to \infty \to l >> l_\rho$ and iid $f_{sys} \sim$ WD. According VOŘECHOVSKÝ AND CHUDOBA (2006) this length effect corresponds to the energetic-statistical size effect of quasi-brittle structures failing at crack initiation as given in BAŽANT ET AL. (2004, 2007). Based on simulations performed in VOŘECHOVSKÝ AND CHUDOBA (2006) it was found that the bi-linear intersection point [l_ρ; $f_{i,mean}$] is independent of serial system size M. It was concluded that serial and parallel system effects can be investigated separately and their interrelationship in s-p_FBMs can be simply considered by multiplication of both effects. In s-p_FBMs it follows that the system strength decreases for $l >> l_\rho$ at expectation but with constant CoV[f_{sys}] whereas in case of $l << l_\rho$ E[f_{sys}] behaves constant but a distinctive decreases in CoV[f_{sys}] proportional to CoV[f_i] / $\sqrt{N}$ is given. Based on DANIELS's (1945) asymptotic system strength distribution VOŘECHOVSKÝ AND CHUDOBA (2006) give following extension

$$E\left[f_{sys,M,N}\right] = \alpha \cdot m^{-1/m} \cdot \exp\left(-\frac{1}{m}\right) \cdot \left(\frac{l_\rho}{l}\right)^{1/m}, \tag{3.90}$$

with α and m as scale and shape parameter of WD, l_ρ as correlation length and l as element and system length.

These statements show that perhaps in most realistic cases of material behaviour the assumptions as well as the bundle strength of finite size N, considering DANIELS's theory, lead to overestimations, especially in cases of linear-elastic load-extension behaviour of the individual fibres. Thus more realistic modelling in respect to (i) consideration of a certain amount of local load sharing (LLS), (ii) CoV[E], (iii) correlation within and between fibres, (iv) the enlargement to serial-parallel systems to account for the fibrous material structure, as well as (v) the consideration of embedment characteristics of fibres within a matrix or (vi) the consideration of friction between fibres and the material behaviour itself (elastic, plastic, …) are important aspects which have to be taken into account and clarified regarding their relevance. The necessity to examine serial-parallel fibre bundle models follows directly from the increasing possibility of occurrence of a defect along an individual fibre with increasing length, leading to a reduction of bearing capacity. Furthermore, the embedment of fibres within a matrix material enables that the same fibre can break more often. This is due to stress distribution over the matrix material. A comparable mechanism appears possible in case of friction as stress transfer between directly neighboured fibres. This leads to a stepwise three-dimensional damage accumulation of parallel aligned fibres in width and depth and in serial, along the fibre or fibre bundle. Hereby **the weakest serial increment of parallel bundles defines the system strength and directly links the DANIELS's system with that of WEIBULL**.

3.2.5 Intermediate Conclusions

At the end of the foregoing four sections and in particular as conclusion of the last section 3.2.4 some summarising remarks are made: The basic stochastic material (strength) models, namely the weakest link theory (WLT) of WEIBULL (1939), the perfect plastic material model and the fibre bundle model (FBM) according DANIELS (1945) constitute the fundamental basis for further developments and progress regarding strength models under inclusion of stochastics. Beside the fact that all these models base on very strict and ideal assumed material conditions they clearly outline the necessity for consideration of stochastics in material modelling. Therefore the consideration of variability inherent in

characteristics of materials and structures enables the examination of effects which cannot be explained by mechanics alone. The deepend knowledge of material and structure behaviour enhances not only the reliability in design processes but more, offer the engineer, producer and user to invent new combinations, to perform material design, optimise the production process, monitor and perform specific training of all persons in charge. Of course the ideal material performances seldom explain sufficiently the real material behaviour; advanced models and enlargements of presented fundamental models are required. Progressing development of these models has already been initiated and done in the last decades. The greatest progress is given by the combination of all three theories to serial-parallel material models (s-p_FBMs) under consideration of a broader range of material behaviour and under inclusion of interaction between system elements over the interface of a matrix material or by friction. Furthermore, the system behaviour after partial failures by definition of load sharing rules (GLS vs. LLS) has been introduced and studied. Some comprehensive analysis based on numerical simulations have been made to examine the influences of stochastic parameters, in particular the spread of load and resistance as well as various types of correlation and some imperfections like random slack, random element length or some plastic yielding.

In a first view it may appear that research in this field is comprehensive and sufficient. Nevertheless there are still many open questions and some model constraints which require a more detailed view and more detailed judgement like the serial and parallel system behaviour considering LND as RSDM of material strength and stiffness characteristics, the inclusion of spatial correlation structures (stochastic processes), the interaction of multi-variate or multi-modal RSDMs and the derivation of some simplified equations, which are accurate enough for engineering applications and ready for a rough material and structure design. For that the following sections are dedicated to perform additional calculations and simulations with the aim to deliver some first answers and advanced models ready for practical applications with focus on finite serial and parallel systems.

3.3 Stochastic Effects in serial acting Systems

Before starting with parameter studies and detailed analysis of some cases of serial systems some general considerations are made. If a perfect serial acting system of serial arranged elements in respect to loading direction is given, the maximum bearing capacity of this system is determined by the weakest element X_M with

$$X_M = \min_i(X_i),\ i = 1, \ldots, M. \tag{3.91}$$

The system strength depends only on the strength of the weakest element but not on material behaviour, stress-strain function, E-modulus or other characteristics. Even in serial systems composed of elements of perfect plastic material and were all elements in the system are exposed to total system load the system strength is determined by the yielding of the weakest element X_M. Considering the relationship between the bearing capacity and system size M a decrease of quantiles as well as expectation and variance with increasing M is expected. This follows from the focus on the minimum, e.g. the lower tail of the parent distribution of $X_1 \sim F_X(x)$, as illustrated in Fig. 3.13.

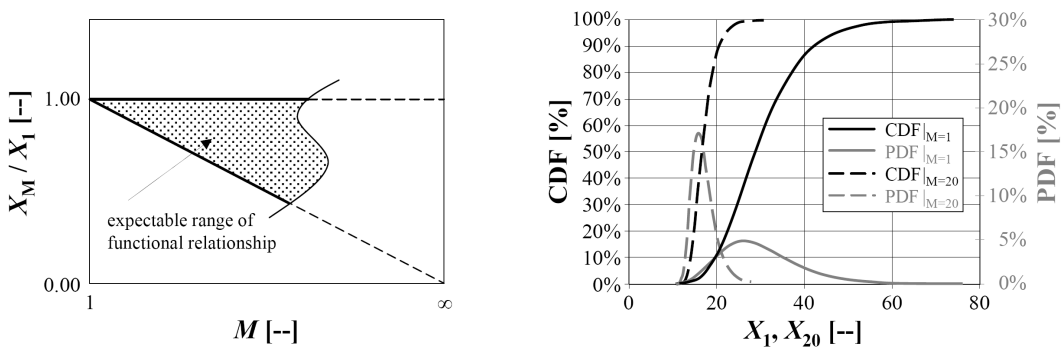

Fig. 3.13: Schematic visualisation of the expectable range of X_M / X_1 (left); example of a serial system of iid elements $X_1 \sim$ 2pLND with $E[X_1] = 30$ and $CoV[X_1] = 30\%$, $\min[X_{20}] \sim$ GUMBEL (15.84; 2.14^2) (right)

As a first guess it can be argued that $\lim_{M \to \infty} X_M / X_1 \to 0$. Of course extreme value theory (EVT) for iid elements gives limit distributions and expectations as limit values for $\lim_{M \to \infty} X_M / X_1 \to \geq 0$, see section 2.6.2. An approximation of $\lim_{M \to \infty} X_M / X_1 \to \approx 0$ appears accurate enough in most cases in particular if M is finite and not too large (see e.g. Fig. 3.14). Consequently, one possible simple function for the description of the relationship X_M / X_1 vs. M is provided by a general power model given by $X_M / X_1 = \alpha \cdot M^{-\beta}$, with α as scaling and β as power parameter depending on the parent distribution model, the analysed distribution characteristic and the parameter vector $\boldsymbol{\theta}$ of $X_i \sim F_X(x \mid \boldsymbol{\theta})$. Hereby both constraints $X_M / X_1 = 1.00$ and $X_M / X_1 \mid_{M \to \infty} \to 0$ are fulfilled. The power model is already linked with WEIBULL's weakest link theory (WLT) and his size effect in equ. (3.33) till (3.35). Nevertheless and as presented later, the power model is not always sufficient for simple modelling of effects in distribution characteristics.

Beside that even a minor correlation between the serial elements may affect the relationship X_M / X_1 vs. M significantly. Due to that a more detailed analysis of serial system effects is required.

This section is dedicated to modelling of stochastic effects in serial acting systems by means of ND, LND and WD as parent distributions (RSDMs) for the strength of elements. Having in mind that the limit distribution models of all these parent distributions are provided by EVT in case of iid elements the question still remains how to model the statistical distribution of finite, in particular small system sizes M. Of course, for WD analytical expressions are explicitly available and inherent in the distribution model with the special feature that the principle model can be used directly for the limiting cases of maxima and minima. ND or LND distributed elements suffer from not closed solvable DMs. In addition the convergence to the GUMBEL distribution (type I, EVT) with $M \to \infty$ is still unclear. Starting first with a brief overview by discussing the influence of each distribution model on the system behaviour, the following sub-sections are dedicated to define some simplified models for estimating the system distribution in dependency of system size M, the RSDM and the parameters of elements X_1. Serial systems composed of iid elements but also of correlated elements are analysed. Furthermore the influences on system behaviour as well as the simplified consideration in models are discussed.

3.3.1 Distribution of the Minimum in dependency of RSDM and Distribution Characteristics

Within this section effects from serial system action on distribution parameters and quantiles are discussed. In case of ND and LND as RSDMs random variates of elements X_1 were generated. The data was gained by performing Monte-Carlo simulations in R (2009). Thereby 10,000 serial systems with system size $M = 1, 2, \ldots, 10^3$ were generated according the parent distribution of X_1 and its parameters, with an arbitrary chosen $E[X_1] = 30$ (which has no influence on the normalised results) and varying $CoV[X_1] = 10\%, 20\%, \ldots, 50\%, 75\%, 100\%$. The random samples were created by sampling each system separately, 10,000 times for each system configuration. In case of WD as RSDM analytical expressions for elements are available (see sections 2.4.3 and 3.2.1). Fig. 3.14 shows the relative change of expectation, standard deviation and $CoV[X_M]$ as well as of some quantiles in relationship to M. As expected the system

capacity decreases with increasing system size M. This decrease is more pronounced in systems composed of elements with a high CoV[X_1].

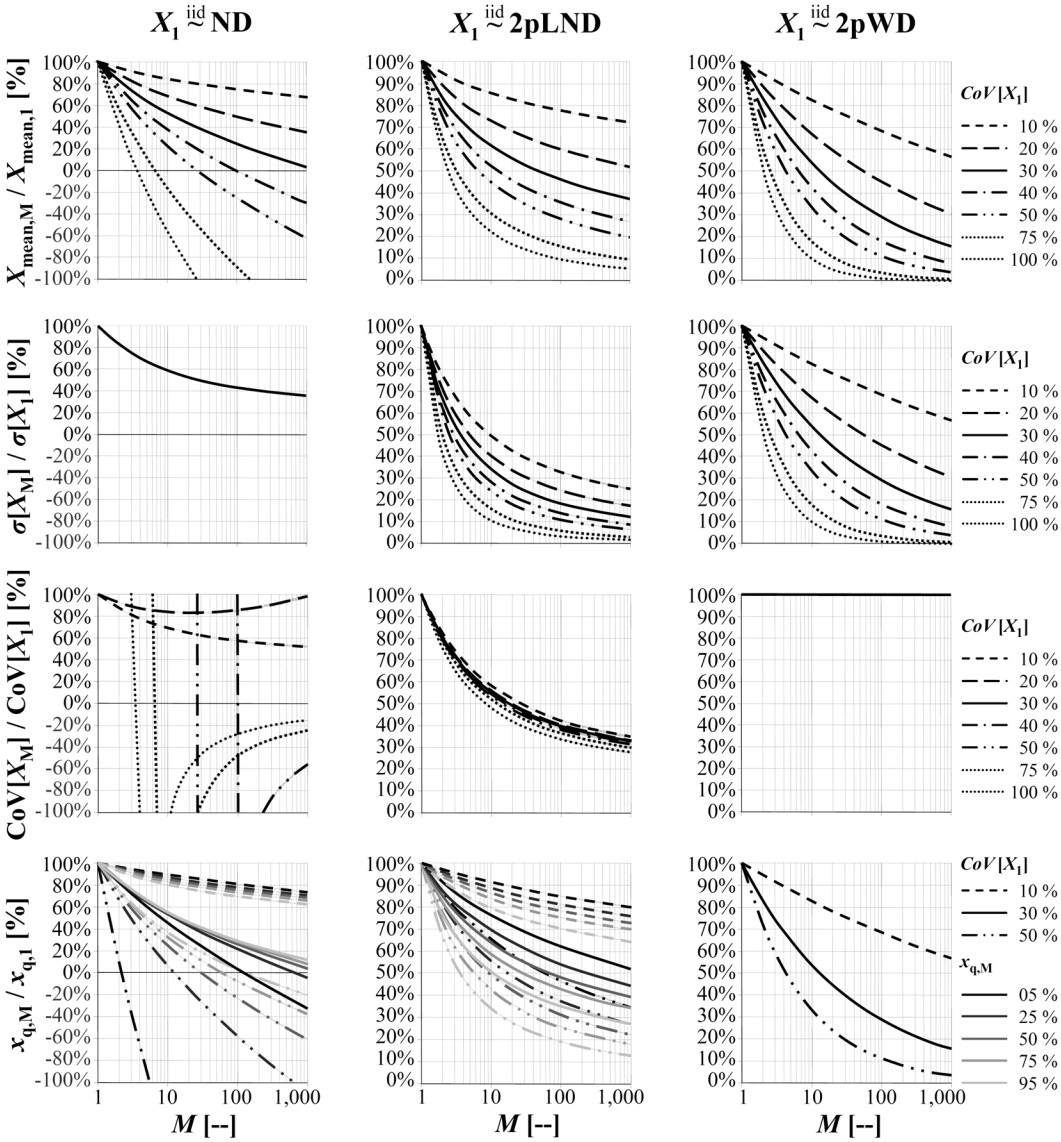

Fig. 3.14: Relative changes in distribution characteristics of X_M in dependency on serial system size M and the RSDM of elements X_1: (left) $X_1 \sim$ ND; (middle) $X_1 \sim$ 2pLND; (right) $X_1 \sim$ 2pWD

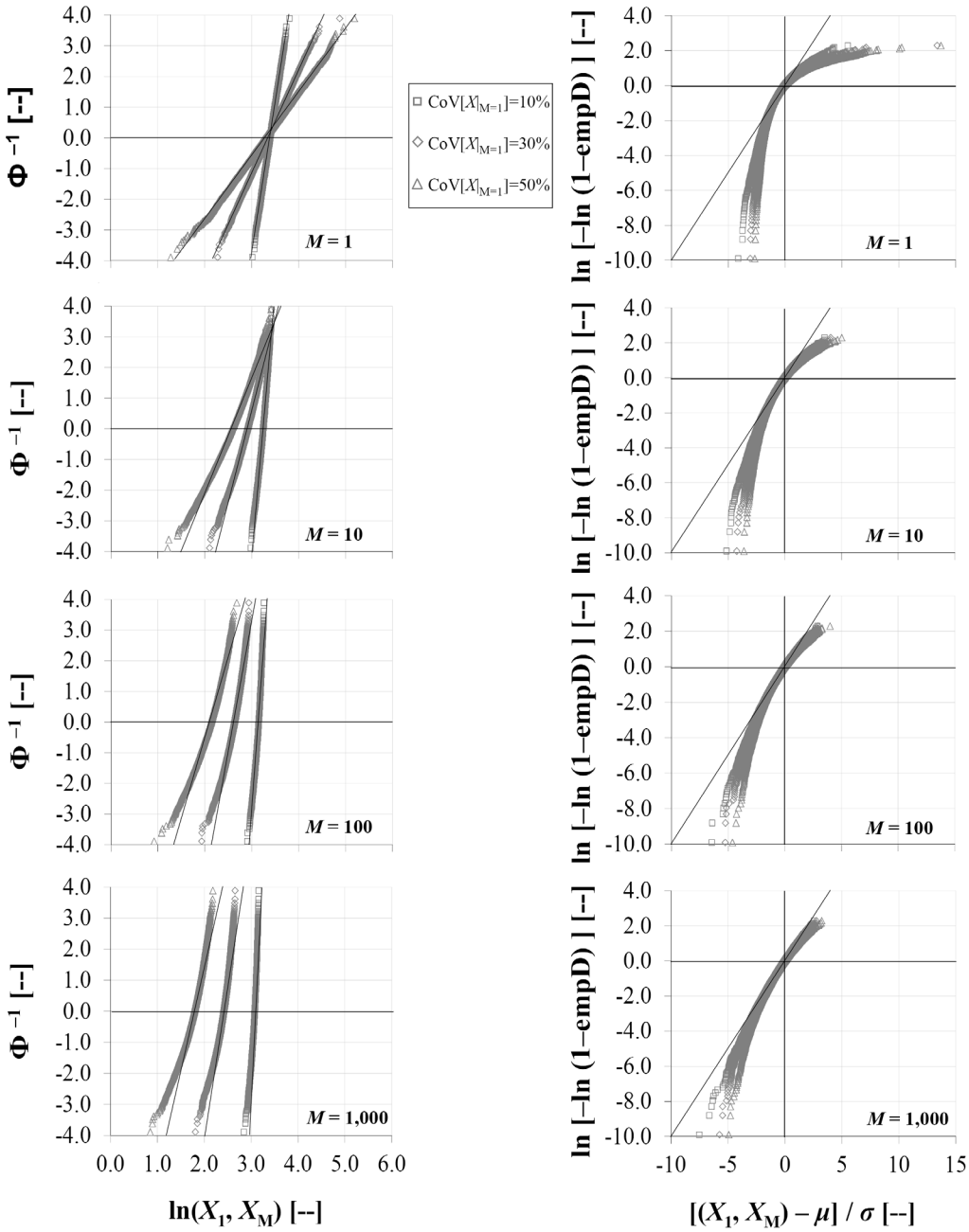

Fig. 3.15: Plots of probability paper for 2pLND (left) and GUMBEL distribution (right) gained from simulations of serial systems of iid elements $X_1 \sim$ 2pLND, E[X_1] = 30, CoV[X_1] = (10, 30, 50)% and system sizes M = 1, 10, 100, 1,000

In particular the decrease is steeper the higher the p-values of the underlying quantile calculation. This is due to the shift of system strength values to the minimum, the weakest element. Of course not only the distribution parameters change but also the characteristics of the distribution, as given by EVT. Following EVT the parent distributions ND and LND converge to GUMBEL or double-exponential distribution (type I, EVT) whereas WD as RSDM remains in principle the same but with adaptations in the distribution parameters as given in section 3.2.1.

Focusing on finite serial acting systems and thereby on their minimum the information of the limit distribution model does not help much without a supporting description of the converging process, e.g. from ND and 2pLND to GUMBEL distribution in dependency of M. Without such a description and / or without sufficiently reliable and accurate approximations, information about the limit distribution is even worthless. To get a first idea about this converging process Fig. 3.15 shows probability paper plots for 2pLND elements depending on various system sizes and CoV[X_1]. As visible, there is a significant influence on the distribution shape, the skewness and kurtosis. These plots show also that in serial systems of M = 1,000 iid elements representation of the strength distribution of X_M by 2pLND is even better than by GUMBEL distribution.

Due to statements above a simple and perhaps approximative description of the convergence process is not given on hand. Therefore, next section concentrates on the establishment and analysis of some approximative methods with the aim to cope with a sufficient accurate and simple description of the statistical distribution of minima of serial acting systems composed of a finite number of iid elements.

3.3.2 Estimation of the Statistical Distribution Parameters in Case of iid ND or 2pLND distributed Variables

This section is dedicated to the analysis of statistics gained from simulated serial systems composed of iid elements represented by ND or 2pLND variates. The simulations were performed in R (2009). First results of these simulations have already been presented in section 3.3.1. Thereby Fig. 3.14 shows the relative change of some distribution characteristics (mean, standard deviation, CoV and quantiles) in dependency of the parent distribution of iid elements $X_1 \sim$ (ND, 2pLND, 2pWD). As already mentioned, whereas the distribution function of serial systems in case of iid 2pWD elements is known analytically and irrespective of system size M, for serial systems composed of iid ND or 2pLND elements analytical expressions of the statistical distribution of serial systems are

only available in the limiting case $M \to \infty$ (see section 2.6.2 concerning EVT). Thus the first idea to come up with expressions for statistics of finite, small system sizes is to find some approximations. These approximations are analysed first to describe the relative change of statistics as function of system size M, CoV and RSDM of X_1, and secondly by discussing approximative distribution functions of finite and small system sizes.

The importance of discussing approximations for small, finite M is in particular of interest for the convergence of ND or 2pLND variables to type I of EVT.

Firstly relative changes of statistics are analysed. Due to the practical relevance of modelling elements by 2pLND the following findings are restricted to this parent distribution model. Thereby iid elements $X_1 \sim$ 2pLND are examined. Following Fig. 3.14 it is obvious that the relative changes in all statistics are characterised by a non-linear decrease with increasing M. To characterise the relationship $K_\xi = X_{M,\xi} / X_{1,\xi}$, with $X_{1,\xi}$ as specific characteristic ξ of elements (e.g. mean, standard deviation, CoV) and $X_{M,\xi}$ as specific characteristic ξ of a serial system composed of M elements, a function has to be defined which fulfills following conditions:

- $\lim\limits_{M \to 1} K_\xi \to 1$, thus $X_{M,\xi} \equiv X_{1,\xi}$;
- $\lim\limits_{M \to \infty} K_\xi \to \geq 0$, thus $X_{\infty,\xi} \equiv \mu$ according EVT type I (see section 2.6.2);
- $\lim\limits_{M \to \infty} F_{X_M}(x) \to F_{X_\infty}(x)$, with $F_{X_\infty}(x)$ = type I of EVT (see section 2.6.2);
- $\lim\limits_{M \to \infty} Var[X_M] \to 0$.

Approximative Description of the relative Changes of Statistics in Case of Serial Systems composed of iid Elements $X_1 \sim$ 2pLND

By analysing Fig. 3.14 it is obvious that in case of iid $X_1 \sim$ 2pWD and according WEIBULL (1939) a simple power model is sufficient to describe the relative change of distribution characteristics, see

$$K_\xi = \frac{X_{M,\xi}}{X_{1,\xi}} = \frac{E[X_M]}{E[X_1]} = \frac{\sigma[X_M]}{\sigma[X_1]} = \ldots = \left(\frac{1}{M}\right)^\lambda \text{, with } \xi = \mathrm{E}[X], \sigma[X], x_{\mathrm{p}}, \tag{3.92}$$

and

$$\frac{CoV[X_M]}{CoV[X_1]} = 1.00 \,. \tag{3.93}$$

Nevertheless, the simple power model is not adequate to characterise K_ξ defined as ratio between distribution parameters and characteristics of serial systems composed of iid 2pLND elements. It can be shown that changes in statistics not only depend on CoV[X_1] but also on system size M (see e.g. Fig. 3.14). Thus K_ξ has to be a function of CoV[X_1] and M. Analysis of K_ξ in dependency of M showed heuristically some logarithmic relationship. To fulfill the requirement of $X_{M,\xi} \equiv X_{1,\xi}$ at $M = 1$ a shift of function ln(M) by one is required.

In case of iid $X_1 \sim$ 2pLND and in dependency of finite and small M the analysis of statistical distribution parameters by the ratio $K_\xi = X_{M,\xi} / X_{1,\xi}$ and the distribution itself by performing a series expansion of rank statistics would be straight forward. ARNOLD ET AL. (2008) provide a general adaptable expansion of $F_X^{-1}(U_{(i)})$ in a Taylor series around the point $E[U_{(i)}] = i / (M + 1) = p_i$ in relationship to successive derivatives of kth order of $F_X^{-1(k)}(u)$ evaluated at $u = p_i$ of the inverse CDF $F_X^{-1}(u)$ given as

$$\begin{aligned} X_{(i)}|M = {} & F_{X_1}^{-1}(p_i) + F_{X_1}^{-1(1)}(p_i)\cdot\left(U_{(i)} - p_i\right) + \frac{1}{2}\cdot F_{X_1}^{-1(2)}(p_i)\cdot\left(U_{(i)} - p_i\right)^2 + \\ & + \frac{1}{6}\cdot F_{X_1}^{-1(3)}(p_i)\cdot\left(U_{(i)} - p_i\right)^3 + \frac{1}{24}\cdot F_{X_1}^{-1(4)}(p_i)\cdot\left(U_{(i)} - p_i\right)^4 + \ldots . \end{aligned} \tag{3.94}$$

Here $U_{(i)}$ is the ith order statistics of a (0, 1) uniformly distributed vector (U_1, …, U_M) with

$$U_i \overset{iid}{\sim} U(0,1), \tag{3.95}$$

and $X_{(i)} \mid M$ is the ith order statistic of the vector (X_1, …, X_M) with

$$X_i \overset{iid}{\sim} F_{X_1} \,, \tag{3.96}$$

with $X_{(1)} \mid M$ as denoted above as X_M. Following ARNOLD ET AL. (2008) the expectation and variance are approximately given as

$$E\left[X_{(i)}|M\right] \approx F_{X_1}^{-1}(p_i) + \frac{p_i \cdot q_i}{2\cdot(M+2)}\cdot F_{X_1}^{-1(2)}(p_i) + \ldots , \tag{3.97}$$

plus higher order terms in $F_X^{-1(k)}(p_i)$, and

$$Var\left[X_{(i)}|M\right] \approx \frac{p_i \cdot q_i}{M+2} \cdot \left\{F_{X_1}^{-1(1)}(p_i)\right\}^2 + \frac{p_i \cdot q_i}{(M+2)^2} \cdot \left[2 \cdot (q_i - p_i) \cdot F_{X_1}^{-1(1)}(p_i) \cdot F_{X_1}^{-1(2)}(p_i) + \right.$$
$$\left. + p_i \cdot q_i \cdot \left[F_{X_1}^{-1(1)}(p_i) \cdot F_{X_1}^{-1(3)}(p_i) + \frac{1}{2} \cdot \left\{F_{X_1}^{-1(2)}(p_i)\right\}^2 \right]\right] + \ldots, \tag{3.98}$$

with

$$q_i = 1 - p_i = \frac{M - i + 1}{M + 1}. \tag{3.99}$$

Thus the Taylor series requires the evaluation of the derivatives of $F_X^{-1}(u)$. In case of $X_1 \sim$ 2pLND this is not available in explicit form. Nevertheless, ARNOLD ET AL. (2008) provide, based on the relationships

$$F_X^{-1(1)}(u) = \frac{d}{du} F_X^{-1}(u) = \frac{dx}{du} = \frac{1}{f_X(x)} = \frac{1}{f_X\left(F_X^{-1}(u)\right)}, \tag{3.100}$$

the first two derivatives of $F_X^{-1}(u)$ in case of $X \sim$ ND, given as

$$F_X^{-1(1)}(u) = \frac{1}{f_X\left(F_X^{-1}(u)\right)}, \qquad F_X^{-1(2)}(u) = \frac{F_X^{-1}(u)}{\left[f_X\left(F_X^{-1}(u)\right)\right]^2}. \tag{3.101}$$

Formulations above can also be used for iid $X_1 \sim$ 2pLND by evaluating $\ln(X_1) \sim$ ND. Nevertheless, these equations do not provide an easy evaluation of extreme values, in particular of minimas $X_{(1)} \mid M$. They also not provide explicit insight in the change of statistical distribution parameters in dependency of M. Therefore an explicit formulation of the inverse CDF of X_1 would be required which is not available in case of $X_1 \sim$ ND or 2pLND. Thus the aim of this section is to define and analyse simple relationships for the description of distribution parameters of serial systems expressed by K_ξ on empirical basis and to provide estimators for parameters required.

Assuming that equ. (3.92) should in principal remain the same but approximately an adequate function in M a formulation is found by

$$K_\xi = \frac{X_{M,\xi}}{X_{1,\xi}} \approx \frac{1}{\left[\ln(M)\cdot \beta_\xi + 1\right]^{\alpha_\xi}}, \text{ with } \xi = \mathrm{E}[X],\ \sigma[X],\ x_\mathrm{p}. \tag{3.102}$$

Thereby K_ξ fulfills the condition $X_{\mathrm{M},\xi} \equiv X_{1,\xi}$ at $M = 1$, independent of parameters α_ξ and β_ξ.

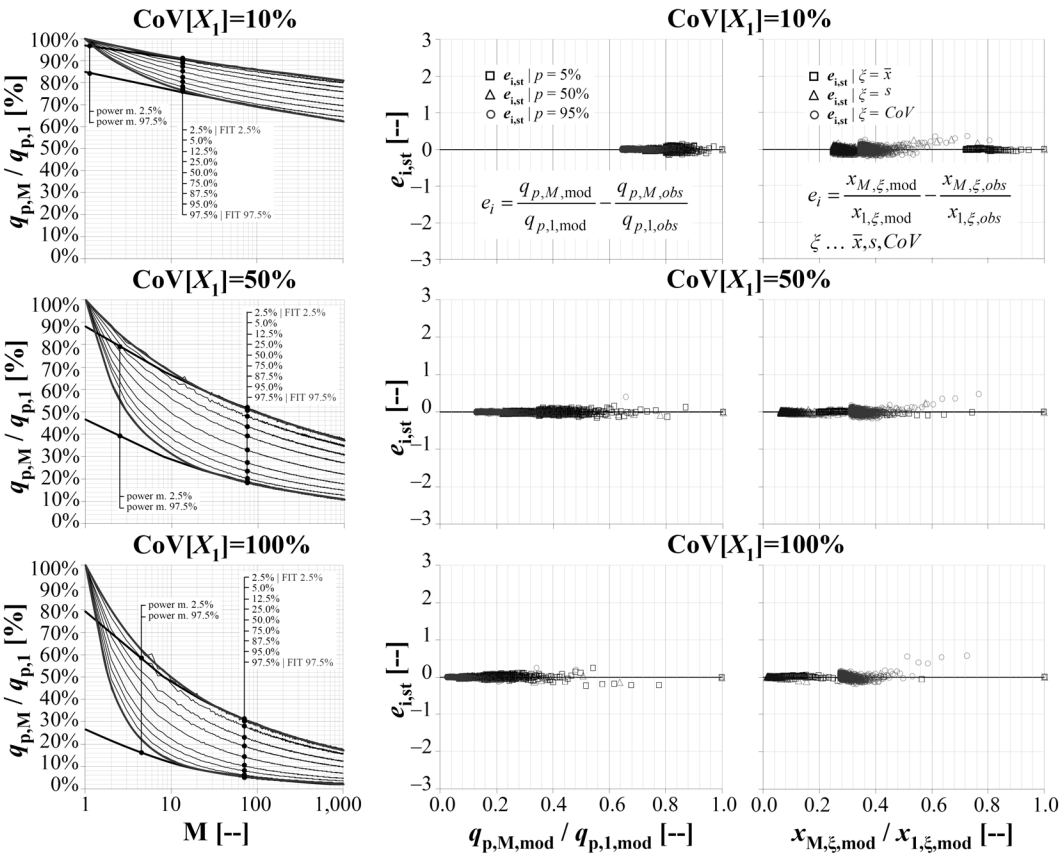

Fig. 3.16: Goodness of fit of equ. (3.102) for various relative quantiles in comparison with goodness of fit of a simple power model (left) as well as residuum plots for judgement of model fit for relative quantiles (middle) as well as relative changes of mean, standard deviation and CoV (right): comparison of model fit for various CoV[X_1]

Comparing (3.102) with the simple power model in (3.92) following equivalences are given. The system size M in (3.92) is substituded by the expression $[\ln(M)\,\beta_\xi + 1]$ in (3.102). The power parameter λ in (3.92) is substituded by the power parameter α_ξ in (3.102).

Fig. 3.16 presents exemplarily the goodness of fit between the simulated data and the simple power model in (3.92) as well as by means of the adapted model of (3.102). Therefore standardised residues $e_{i,st}$ based on $e_i = (K_{\xi,M,obs} - K_{\xi,mod})$ are given.

The standardised residues $e_{i,st}$ are defined as (see e.g. STADLOBER AND SCHAUER, 2007)

$$e_{i,st} = \frac{e_i}{s_{K_{p,M,obs}} \cdot \sqrt{1-h_{ii}}}\,, \tag{3.103}$$

with

$$e_i = K_{p,M,obs} - K_{p,M,\mathrm{mod}}\,,\ h_{ii} = \frac{1}{n} + \frac{t_i^2}{s_t^2}\,,\ t_i = x_i - \bar{x} \text{ and } s_t^2 = \sum_{i=1}^{n} t_i^2\,, \tag{3.104}$$

and h_{ii} as the diagonal element of the hat-matrix, defined for the simple linear regression model. As shown (3.102) performs perfectly in representing $q_{p,M}$, the observed values of quantiles $x_{p,M}$ of X_M, even in case of high CoV[X_1] and large system size M. Only the CoV[X_M] is less adequate in case of very high values of CoV[X_1]. This can be explained by the definition of CoV[X] as ratio $\sigma[X]$ / E[X]. Thus changes in CoV[X_M] are directly linked with E[X_M] and $\sigma[X_M]$.

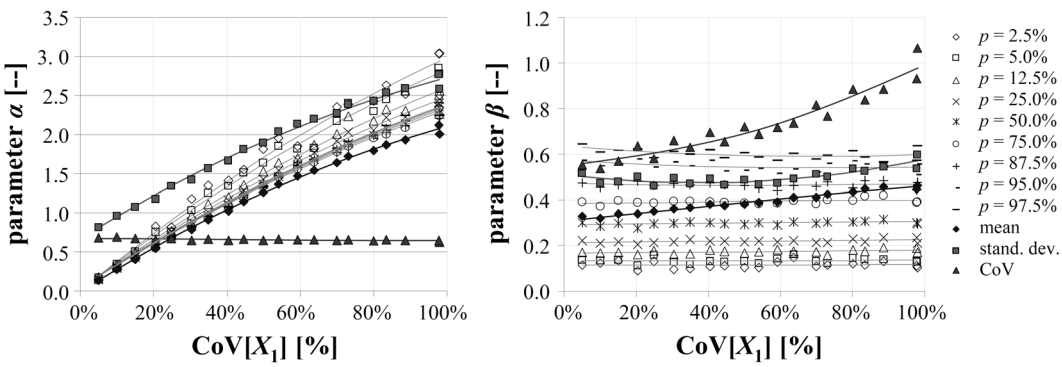

Fig. 3.17: Parameters α_ξ (left) and β_ξ (right) of equ. (3.102) vs. CoV[X_1] as best fit according LSM to simulated data and in dependency of the statistics analysed

Nevertheless, (3.102) requires the estimation of parameters α_ξ and β_ξ which itself depend on ξ. Parameter estimates for α_ξ and β_ξ found by means of the least squares method (LSM) are given in Tab. 8.1 and Tab. 8.2 in annex 8.1 and visualised in Fig. 3.17, analysing first the relationship with CoV[X_1].

Following statements can be made: Analysing first the power parameter α_ξ it can be found that α_{CoV} is nearly constant and independent of M. The parameter α_p shows to be a function of probability p and CoV[X_1]. α_σ and α_μ show also to depend on CoV[X_1] with $\alpha_\sigma \approx \alpha_\mu + \alpha_{\mathrm{CoV}}$. Furthermore, in the limiting case of CoV[X_1] → 0 it follows that $\alpha_\mathrm{p} \to 0$, $\alpha_\sigma \to \alpha_{\mathrm{CoV}}$ and $\alpha_\mu \to 0$.

Concerning parameter β_ξ it is obvious that β_p is nearly solely a function of p and minor of CoV[X_1]. Hereby β_{50} is equal to β_μ in the limiting case of CoV[X_1] → 0. In contrast to β_p parameters β_μ, β_{CoV} and β_σ suggest a dependency on CoV[X_1] and p. Furthermore, over the range of p and by comparing β_p with p = (5, 50, 95)% it can be found that β_p appears to be right-skewed distributed.

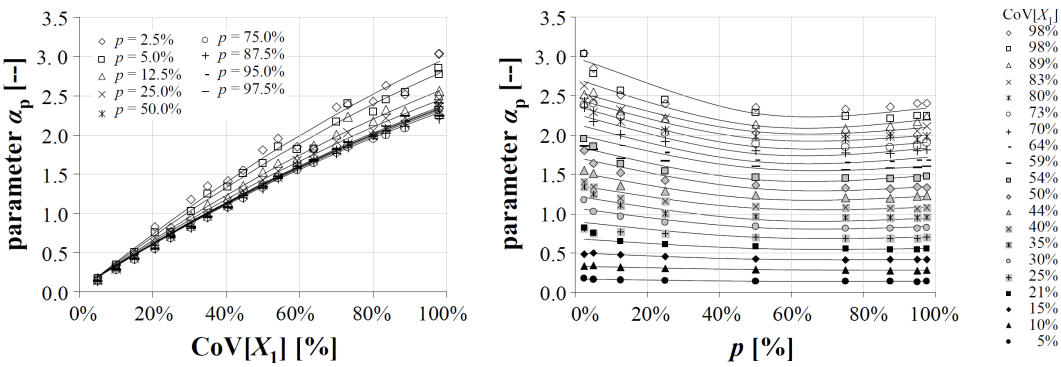

Fig. 3.18: Parameter α_p vs. CoV[X_1] (left) and vs. p (right)

Fig. 3.18 gives graphs for α_p vs. CoV[X_1] and α_p vs. p. In Fig. 3.18 (left) estimates of α_p show distinctive unsteady (irregular) behaviour, in particular in the region of CoV[X_1] = [50 ÷ 100]% and $p \leq 25\%$, which influences any kind of fitting procedure so far analytical expressions are missing. Fig. 3.18 (right) shows estimates of $\alpha_\mathrm{p}(p|\ \mathrm{CoV}[X_1])$ and α_p vs. p at given CoV[X_1]. Thereby α_p shows an asymmetric convex behaviour which diminishes with decreasing CoV[X_1]. The gradient decreases with $p \to 0$ and the level of α_p increases with increasing CoV[X_1]. Due to the fact that parameter α_p is a function of CoV[X_1] and p, in the limiting case CoV[X_1] → 0 parameter α_p converges to zero. This is trivial because at zero dispersion all x_p's are equal and thus $x_{\mathrm{p,M}}$ converges to $x_{\mathrm{p},1}$, with $\alpha_\mathrm{p} \to 0$ and CoV[X_1] → 0. Thus $x_{\mathrm{p,M}} = \mathrm{E}[X_1] = \mathrm{E}[X_\mathrm{M}]$. Of course, if X_1 is deterministic (CoV[X_1] = 0) there is by default also no stochastic serial system effect and $K_\xi = 1.0$, irrespective of ξ. Thus the description of α_p requires a function which gives $\alpha_\mathrm{p} = 0$ for CoV[X_1] = 0, independent of p, and which shows increasing α_p-values and an increase in

the asymmetric convex behaviour for increasing CoV[X_1]. Thus a function of α_p is demanded which fulfills

- $\frac{d^2}{d^2 p} f\left(\alpha_p | CoV[X_1]\right) > 0$ (increasing gradient), with $p \in [0, 1]$, CoV[X_1] $\in \mathbb{R}^+$;
- $\frac{d}{dp} f\left(\alpha_p | CoV_1[X_1]\right) = 0 < \frac{d}{dp} f\left(\alpha_p | CoV_2[X_1]\right) = 0$, with $CoV_1[X_1] < CoV_2[X_1]$;
- $\lim_{CoV[X_1] \to 0} \alpha_p \left[\frac{d}{dp} f\left(\alpha_p | CoV[X_1]\right) = 0 \right] \to 0$;
- $\alpha_p\left(CoV[X_1] \,|p = 0\right) \geq \alpha_p\left(CoV[X_1] \,|p = 1\right)$.

The simplest function capable to describe the non-linear decrease of α_p vs. CoV[X_1] and the asymmetric convex behaviour of α_p vs. p is given by a polynom of 2nd order. Mixing both functional parts gives the expression

$$\alpha_p\left(CoV[X_1]\,, p\right) = \left[a \cdot p^2 + b \cdot p + c\right] \cdot CoV^2[X_1] + \left[d \cdot p^2 + e \cdot p + f\right] \cdot CoV[X_1]\,, \qquad (3.105)$$

with $p \in [0, 1]$, CoV[X_1] $\in \mathbb{R}^+$, α_p(CoV[X_1] = 0, p) = 0 and α_p(CoV[X_1], p = 0) $\geq$ $\geq \alpha_p$(CoV[X_1], p = 1). The six model parameters a, b, …, f are found by means of LSM minimising the sum of squared differences between the observed α_p from simulations ($\alpha_{p,obs}$), and $\alpha_{p,mod}$ estimated according equ. (3.105). The parameter set is given as

a = –0.1077;	b = +0.3807;	c = –0.8714;
d = +1.5919;	e = –2.3511;	f = +3.7959.

The degree of determination for p = (2.5, 5.0, …, 95.0, 97.5)% by means of equ. (3.105) was found between $r^2 = 0.983 \div 0.999$. The residues were checked and proved qualitatively to be approximately normally distributed with $e_i \sim$ ND (0, $0.025^2 \div 0.12^2$) showing higher variation at lower p-values. A comparison of model output and best LSM estimates from simulation data is given as plot of $\alpha_{p,mod}$ vs. $\alpha_{p,obs}$ in Fig. 3.19.

The total sum of LSM is $\sum (\alpha_p)|_{LSM} = 0.722$. The overall mean difference of $\alpha_{p,obs}$ and $\alpha_{p,mod}$ is found as 0.003 and the variance as 0.004. The range R of differences decreases with increasing p, from $R = 0.42 | p = 0.025$ to $R = 0.10 | p = (0.25 \div 0.75)$ and $R = 0.17 | p = 0.975$ giving some limit of a weaker representation of α_p for extreme values

of p. Nevertheless enlargement of the model by a third-order polynom for $\alpha_p(p)$ showed only minor reduction in $\sum(\alpha_p)|_{LSM}$ to 0.616 but no significant improvement in R over the whole range analysed for p. Overall the model for α_p performs well beside the fact that differences between $\alpha_{p,mod}$ and $\alpha_{p,obs}$ are higher in case of extreme values of p.

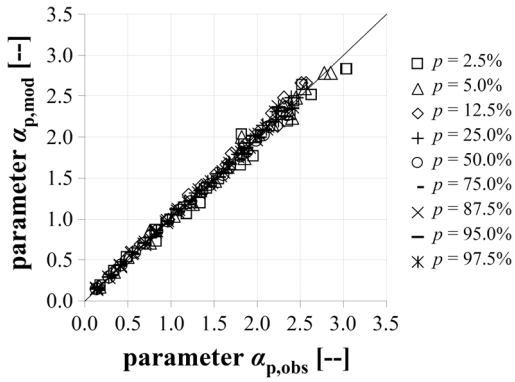

Fig. 3.19: Parameter $\alpha_{p,mod}$ vs. $\alpha_{p,obs}$ for various p-values

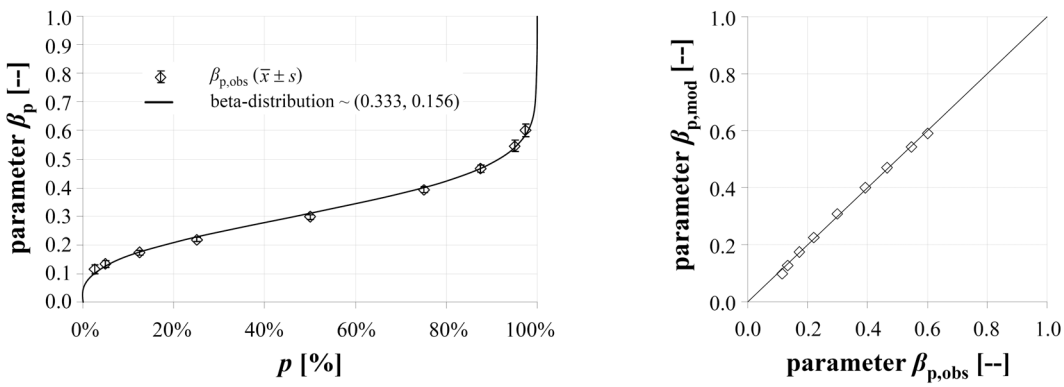

Fig. 3.20: Parameter β_p vs. p: observed values given as mean ± standard deviation; model as beta-distribution (left); $\beta_{p,mod}$ vs. $\beta_{p,obs}$ (right)

In the next step parameter β_p is analysed in more detail. As already mentioned above β_p was found to be solely a function of p and thus independent of CoV[X_1] (see Fig. 3.17). Thus mean values and variance of estimated $\beta_p|\,p$ were calculated from estimates gained from simulations (Tab. 8.2, annex 8.1). As expected, mean values vary significantly with p whereas Var[$\beta_p|\,p$] was found to be low and about 0.1% to 0.2% of $\beta_{p,mean,obs}$.

Fig. 3.20 (left) shows mean values ± standard deviation of $\beta_{p,obs}|\,p$ vs. p based on simulations. Due to the defined range of the parent distribution of iid elements $X_1 \sim$ 2pLND within [0, ∞] and the serial system characteristic X_M defined as $X_M = \min[X_i]$ over i, with $i = 1, \ldots, M$, in the limiting case $M \to \infty$ values of X_M converge to 0, the quantile value $x_{p,M}|\,p = 0$ will always be equal to zero, independent of the system size M. Thus $\beta_p \mid p = 0$ is also equal to zero. In the limiting case $p \to 1$ parameter β_p converges to one due to the fact that $\beta_p = 1$ delivers the lowest value for K performing maximum influence (reduction) of $X_{1,p}$, if β_p is bounded by ≤ 1.0 which is supported by the course of $\beta_{p,obs}$ versus p. This is conforming to the fact that the highest quantile values are mostly affected by serial system action. Thus β_p is defined within [0, 1] showing an asymmetric concave-convex behaviour within $p \in [0, 1]$. The simplest function to describe the course of $\beta_p(p) \in [0, 1]$ is a two-parameter model. Thereby the two-parameter Beta-distribution (2pBeta) which is defined within [0, 1] was identified as representative model (see Fig. 3.20, left). In general, the PDF and CDF of a 2pBeta are given as

$$f_X(x) = \frac{1}{B(p_{beta}, q_{beta})} \cdot x^{p_{beta}-1} \cdot (1-x)^{q_{beta}-1},\ x \in [0, 1];\ F_X(x) = \int_0^x f_X(z) \cdot dz, \tag{3.106}$$

with the Beta-function

$$B(p_{beta}, q_{beta}) = \frac{\Gamma(p_{beta}) \cdot \Gamma(q_{beta})}{\Gamma(p_{beta} + q_{beta})} = \int_0^1 u^{p_{beta}-1} \cdot (1-u)^{q_{beta}-1} \cdot du\,. \tag{3.107}$$

The expectation and variance of $X \sim$ 2pBeta are

$$E[X] = \frac{p_{beta}}{p_{beta} + q_{beta}} \text{ and } Var[X] = \frac{p_{beta} \cdot q_{beta}}{(p_{beta} + q_{beta} + 1) \cdot (p_{beta} + q_{beta})^2}\,. \tag{3.108}$$

For modelling of β_p parameters $p_{beta,est} \approx 0.333$ and $q_{beta,est} \approx 0.156$ were estimated by means of LSM. Thus the parameter β_p can be estimated following

$$\beta_p = \int_0^p \frac{1}{B(p_{beta}, q_{beta})} \cdot z^{p_{beta}-1} \cdot (1-z)^{q_{beta}-1} \cdot dz\,. \tag{3.109}$$

A comparison of $\beta_{p,obs}$ vs. $\beta_{p,mod}$ is shown in Fig. 3.20 (right). Besides a minor non-linear concave trend between $\beta_{p,obs}$ and $\beta_{p,mod}$ leading to underestimation of β_p in case of $p \geq 0.95$

and $p \leq 0.10$ the model performs well. The observed mean difference between $\beta_{p,obs}$ and $\beta_{p,mod}$ was –0.0004 and to observed variance 0.0003.

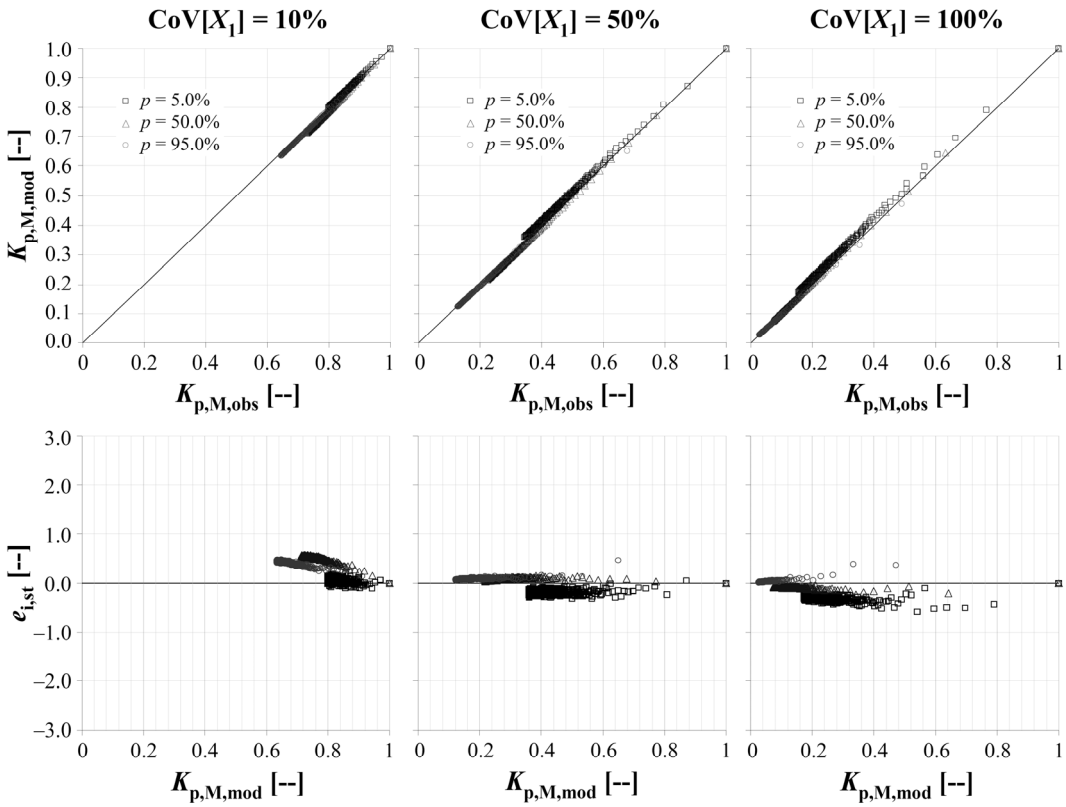

Fig. 3.21: $K_{p,M,mod}$ vs. $K_{p,M,obs}$ (above) and standardised residuum plots for $K_{p,M,mod}$ (below) for CoV[X_1] of 10% (left), 50% (middle) and 100% (right)

Having adequate models for α_p and β_p as given in (3.105) and (3.109), respectively, it is possible to give good estimates for $x_p|$ (CoV[X_1], p, M). Therefore Fig. 3.21 provides exemplarily some plots of $K_{p,M,mod}$ versus $K_{p,M,obs}$ for CoV[X_1] = (10, 50, 100)% and for p = 0.05, 0.50, 0.95. In addition plots of standardised residuals $e_{i,st}$ versus $K_{p,M,mod}$ are presented. The residual-plots show a decreasing bias of K_p with increasing p. Over all this leads to underestimation of K_p. In fact this underestimation is rather small and generates minor conservative values. Overall, the presented models behave satisfactorily and enable a very simple calculation of K_p-values. Thus the model gives good estimates for the relative change of the capacity of serial systems composed of iid lognormally distributed elements on various quantile levels. The model is in principal restricted to the examined

parameter space of $\mathrm{CoV}[X_1] = (5, \ldots, 100)\%$, $p = 0.025, \ldots, 0.975$ and $M = 1, \ldots, 1{,}000$. Nevertheless, good approximations can be also expected for $M > 1{,}000$ but not too small p-values.

In principal having an expression for calculation of x_p given p the inverse operation calculating p given x would deliver the distribution function $F_{X,M}(x)$ as function of X_1, $E[X_1]$, $\mathrm{CoV}[X_1]$ and system size M (see section 2.5). Before discussing approximations of the distribution function of serial systems some expressions for $K_{M,\mu}$, $K_{M,CoV}$ and $K_{M,\sigma}$ have to be defined.

Tab. 3.2: Regression models for parameters α_ξ and β_ξ of equ. (3.102) for mean, standard deviation and coefficient of variation of serial systems composed of iid elements $X_1 \sim$ 2pLND

regression models	r^2	$e_i \sim \mathrm{ND}(\bar{e}, s)$	
		$\bar{e}$	s
$\alpha_{\mu,mod} = -0.826 \cdot \mathrm{CoV}^2[X_1] + 2.925 \cdot \mathrm{CoV}[X_1]$	1.00	0	0.024
$\beta_{\mu,mod} = -0.005 \cdot \mathrm{CoV}^2[X_1] + 0.160 \cdot \mathrm{CoV}[X_1] + 0.309$	0.98	0	0.007
$\alpha_{\sigma,mod} = -0.806 \cdot \mathrm{CoV}^2[X_1] + 2.858 \cdot \mathrm{CoV}[X_1] + 0.681$	0.99	0	0.045
$\beta_{\sigma,mod} = 0.253 \cdot \mathrm{CoV}^2[X_1] - 0.188 \cdot \mathrm{CoV}[X_1] + 0.510$	0.78	0	0.016
$\alpha_{CoV,mod} = 0.011 \cdot \mathrm{CoV}^2[X_1] - 0.051 \cdot \mathrm{CoV}[X_1] + 0.681$	0.67	0	0.008
$\beta_{CoV,mod} = 0.326 \cdot \mathrm{CoV}^2[X_1] + 0.112 \cdot \mathrm{CoV}[X_1] + 0.555$	0.90	0	0.044

The identified regression models by means of second order polynomials are given in Tab. 3.2. Additional bias in $\beta_{CoV,mod}$ is induced by using the same functional relationship for the description of $\mathrm{CoV}[X_M]$ / $\mathrm{CoV}[X_1]$. Nevertheless, derivation of a model based on mean and standard deviation becomes more complex. In practise $\mathrm{CoV}[X_M]$ should therefore be computed based on estimates of $E[X_M]$ and $\mathrm{Var}[X_M]$.

A comparison between calculated and observed parameter values of α_ξ and β_ξ is made in Fig. 3.22. Please be aware that axis of the graphs are scaled differently. As already given in Tab. 3.2 $\beta_{CoV,mod}$ overestimates $\beta_{CoV,obs}$ by a bias of roughly 0.06 (see also Fig. 3.22). Beside that the models can be said to deliver satisfactorily estimates of α_ξ and β_ξ and therefore give a good basis for estimating $\mu[X_M]$ and $\sigma[X_M]$.

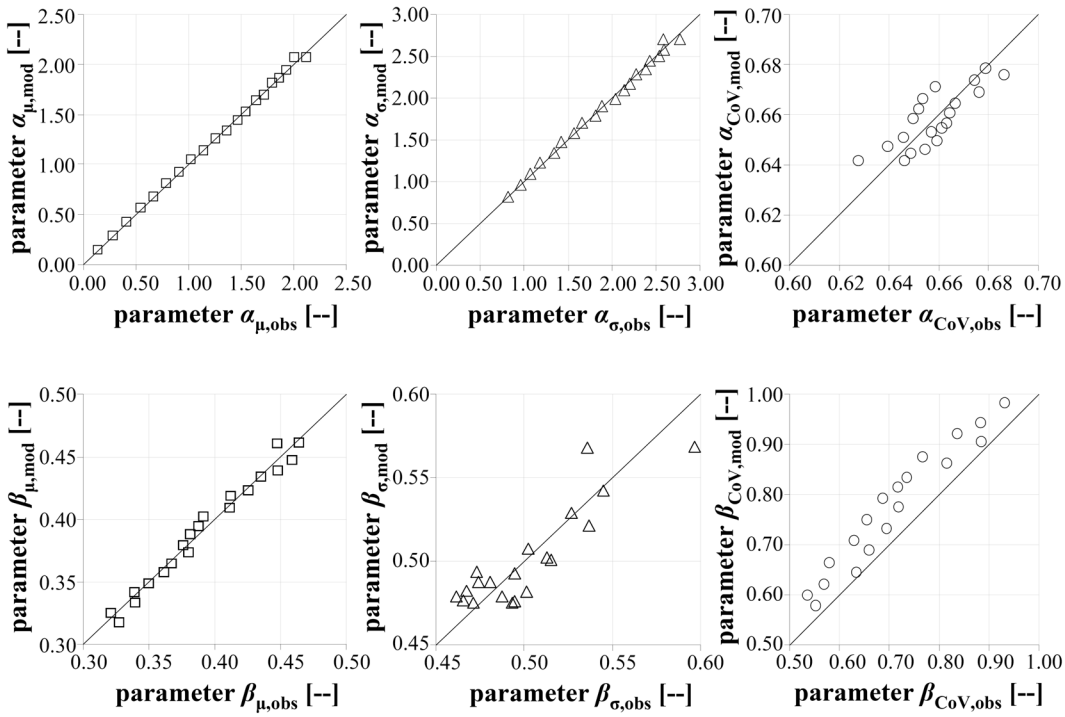

Fig. 3.22: Parameters α_ξ (above) and β_ξ (below) for ξ as mean (left), standard deviation (middle) and coefficient of variation (right): model vs. observations from simulations

Approximative Method for Distribution and Characteristics of Serial Systems composed of iid Elements X_1 ~ ND or X_1 ~ 2pLND based on Rank Statistics

Considering the definition of serial systems by means of extreme value statistics which is in general given by

$$F_{\min}(x \mid M) = 1 - \left[1 - F_X(x \mid M = 1)\right]^M , \tag{3.110}$$

with the general definition of CDF

$$F_X(x) = P[X \le x] = \int_{-\infty}^{z} f_X(x) \cdot dz . \tag{3.111}$$

By means of relations between order statistics and the distribution parameters of a normal distribution with

$$E[X] = \mu = med[X] = F_X^{-1}(0.50), \tag{3.112}$$

and

$$\sqrt{Var[X]} = \sigma_X = \frac{F_X^{-1}(0.75) - F_X^{-1}(0.25)}{\Phi^{-1}(0.75) - \Phi^{-1}(0.25)} \approx \frac{IQR}{1.349}, \tag{3.113}$$

with

$$x_p = \mu + \Phi^{-1}(p) \cdot \sigma, \tag{3.114}$$

an approximation for calculating statistics for X_M of serial systems is given. Thereby it is assumed that the distribution model for finite M, with $M \leq 1{,}000$, can be approximated by the parent distribution of X_1 but with adapted distribution parameters θ, with $\theta \rightarrow \theta\,(M) = \theta_M$.

Following equations above and in case of iid ND-variates X_1, estimates for expectation and standard deviation are

$$E[X_M] = F_{X_1}^{-1}\left(p = 1 - 0.5^{\,1/M}\right), \quad \text{with } F_{\min}\left(x = E[X_M] = med[X_M]\right) = 0.5 = 1 - \left[1 - F_{X_1}(x)\right]^M, \tag{3.115}$$

and

$$\sigma[X_M] = \frac{F_{X_1}^{-1}\left(p = 1 - 0.25^{\,1/M}\right) - F_{X_1}^{-1}\left(p = 1 - 0.75^{\,1/M}\right)}{\Phi^{-1}(0.75) - \Phi^{-1}(0.25)}. \tag{3.116}$$

In case of iid variates $X_1 \sim$ 2pLND the same formulas can be applied after X_1 was transformed to logarithmic domain, with $Y_1 = \ln(X_1)$ and $Y_1 \sim$ ND.

Fig. 3.23 and Fig. 3.24 show the relative bias between some approximated distribution characteristics and simulated data for iid $X_1 \sim$ ND and iid $X_1 \sim$ 2pLND, respectively, where parameters are derived by leaving the parent distribution model constant and independent of M but adapting its distribution parameters as function of M. For emphasising the region of M with largest deviations from simulation data the graphs are

given with a logarithmic x-axis. The graphs show changes in statistics referenced to the input parameters $\mu[X_1]$ and $\sigma[X_1]$. The random data shows partly distinctive spread. For analysing the mean bias between calculated and simulated data a trend-line for each distribution characteristic analysed versus M was fitted by means of command "nls (.)" (non-linear least squares) in R (2009) and the following function

$$y = f(M \mid \alpha, \beta) = \ln(M) \cdot M^{-\alpha} \cdot \beta^{-1}. \tag{3.117}$$

As shown in Fig. 3.23 the approximation method leads to non adequate results for characteristics of X_M if the serial systems are composed of iid elements $X_1 \sim$ ND. In particular in case of large system sizes and / or high variability a remarkable bias appears. This is due to the fact that lower quantiles as well as the expectation of X_M changes from positive to negative values as $X_1 \sim$ ND is defined within $(-\infty, +\infty)$. Furthermore, due to higher concentration of the distribution of X_M on the lower tail of the distribution of X_1 the distribution of X_M becomes heavily right skewed. The assumption that the parent distribution of X_1 can be approximately used for X_M fails in case of $X_1 \sim$ ND. Only the distribution characteristic $\sigma[X_M] = \sigma_M$ shows comparable minor bias increasing with M steadily concave and independent of CoV$[X_1]$. This is by definition strictly defined on the positive domain $\mathbb{R}^+$. Overall the approximation works poor for finite serial systems composed of iid elements $X_1 \sim$ ND. Fig. 3.24 shows results of the approximative method in case of serial systems composed of iid elements $X_1 \sim$ 2pLND. In contrast to Fig. 3.23 with $X_1 \sim$ ND the relative bias of characteristics μ_M, σ_M, CoV$[X_M]$, $X_{M,05}$ and $X_{M,95}$ is low. In contrast to ND the parent distribution 2pLND is already characterised by a right skewed shape. Thus 2pLND is already much more like the asymptotic minimum distribution type I according EVT (see section 2.6.2) even in case of small M and high varying characteristics, e.g. expressed by CoV$[X_1]$. Furthermore, 2pLND is already bounded below by zero. This prevents changes of the statistics from positive to negative domain as observable in case of $X_1 \sim$ ND. The graphs in Fig. 3.24 show also an equidistant increasing bias with increasing CoV$[X_1]$. Hence linear interpolation for estimates of bias in case of arbitrary CoV$[X_1]$ is possible. Overall, the approximation defined in equ. (3.115) and (3.116) provides usable results in case of serial systems composed of iid elements $X_1 \sim$ 2pLND. Thereby the bias of main characteristics μ_M, σ_M, CoV$[X_M]$, $X_{M,05}$ and $X_{M,95}$ can be extraxted from the graphs provided in Fig. 3.24 and used directly for correction of the calculated characteristics. In case of arbitrary CoV$[X_1]$ linear interpolation between neighboured values of CoV$[X_1]$ can be performed. In case of iid elements $X_1 \sim$ ND the approximation can be used only for small systems and low

CoV[X_1] (see Fig. 3.23). Even than the modelled statistics show remarkable bias. In all cases the results are restricted to the analysed domain in respect to CoV[X_1], DM and M.

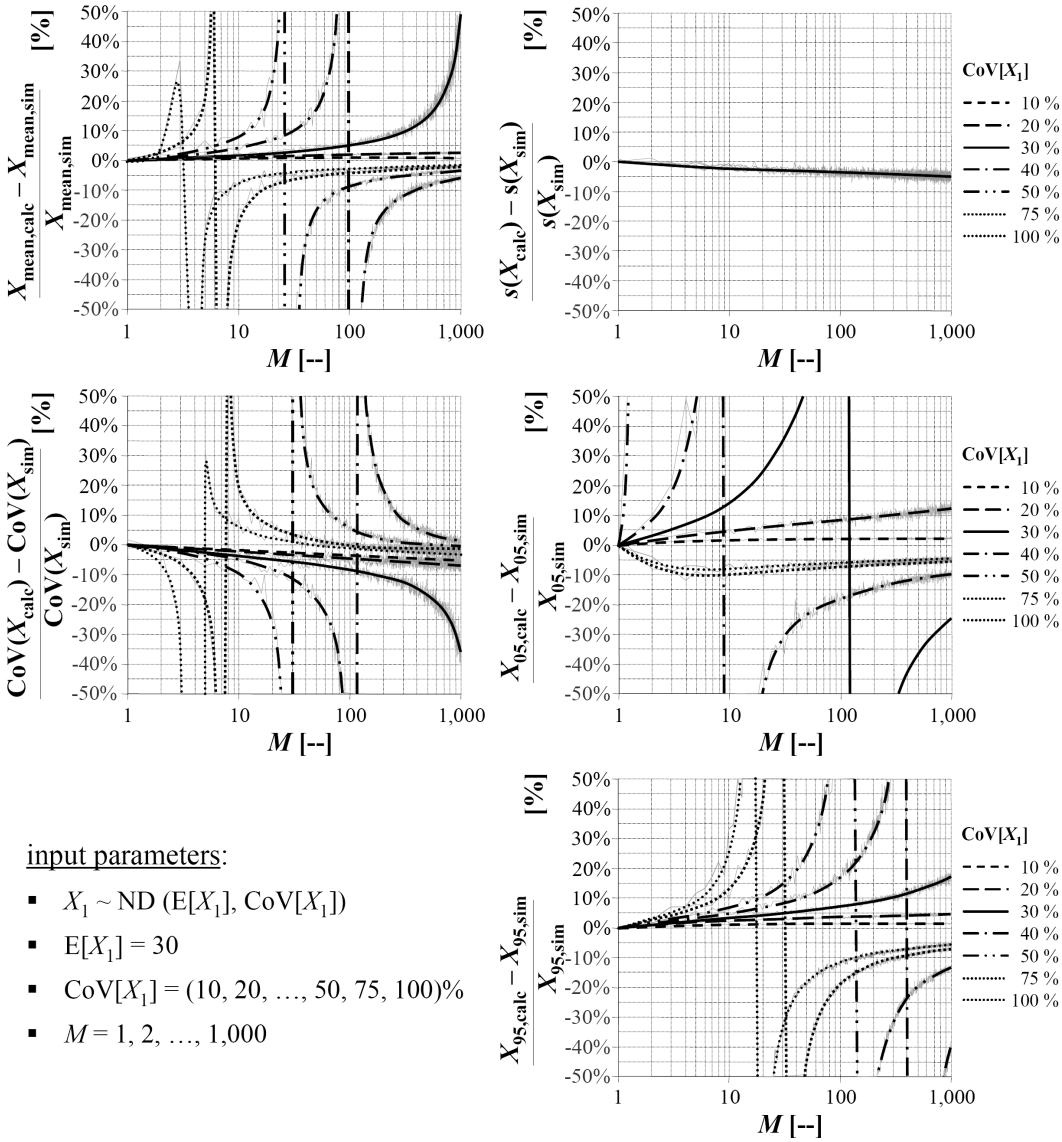

input parameters:

- $X_1 \sim$ ND (E[X_1], CoV[X_1])
- E[X_1] = 30
- CoV[X_1] = (10, 20, …, 50, 75, 100)%
- M = 1, 2, …, 1,000

Fig. 3.23: Relative bias between calculated and simulated data of characteristics E[X_M] = μ_M, σ_M, CoV[X_M], $X_{M,05}$ and $X_{M,95}$ of serial systems composed of iid elements $X_1 \sim$ ND: calculations base on rank statistic relationships as given in equ. (3.115) and (3.116)

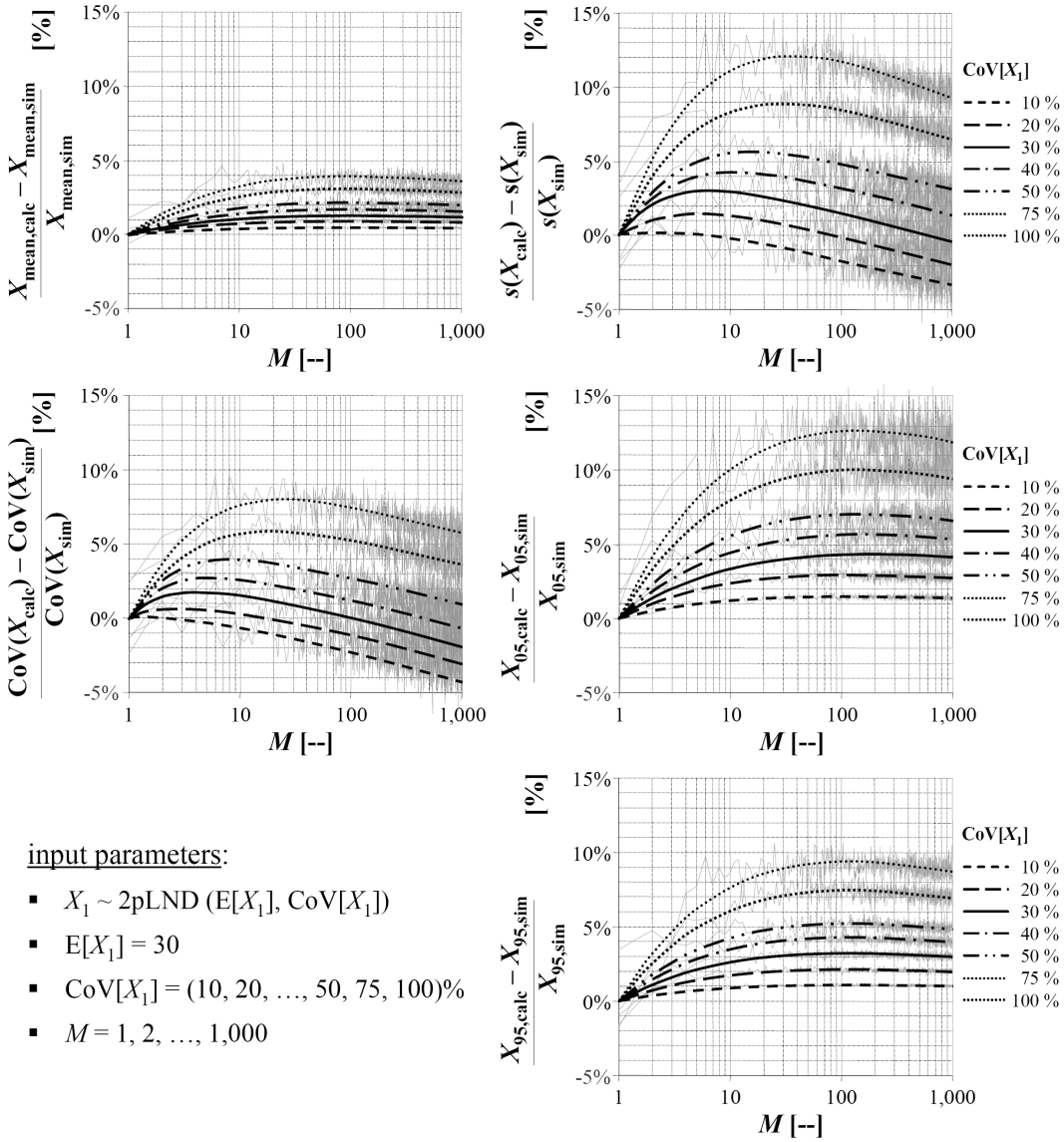

input parameters:

- $X_1 \sim$ 2pLND (E[X_1], CoV[X_1])
- E[X_1] = 30
- CoV[X_1] = (10, 20, …, 50, 75, 100)%
- M = 1, 2, …, 1,000

Fig. 3.24: Relative bias between calculated and simulated data of characteristics E[X_M] = μ_M, σ_M, CoV[X_M], $X_{M,05}$ and $X_{M,95}$ of serial systems composed of iid elements $X_1 \sim$ 2pLND: calculations base on rank statistic relationships as given in equ. (3.115) and (3.116)

Approximations for the Distribution of Minima (and Maxima) of finite sized Serial Systems following EVT Type I

The simplest way to approximate the expected value of minima and maxima of finite sized systems is given by the so called characteristic smallest and largest values. These are defined by quantiles $x_{M,p}$ and $x_{N,p}$ of X_1 corresponding to $p = 1 / M$ and $p = 1 - 1 / N$, for minima and maxima, respectively (BURY, 1975). Thus $x_{M,p}$ and $x_{N,p}$, respectively, decreases and increases with increasing sample size M and N. Thereby it is assumed that the distribution model of the system is equal or at least can be well approximated by the parent distribution model. Nevertheless, to give approximations for the whole distribution of minima and maxima more sophisticated methods are required. In case of very large and nearly infinite sized systems asymptotic distributions are provided by EVT (see section 2.6.2). For systems composed of a finite and in particular in case of a small number of elements some approximations in reference to BURY (1975) are presented and compared to the approximations discussed so far.

In case of $X_1 \sim \mathrm{ND}\ (\mu, \sigma^2)$ and CDF $F_X(x)$ BURY (1975) delivers an approximative method for the calculation of distribution parameters for the extreme value $X_{max} = X_N$ following type I EVD with $X_N \sim \mathrm{GD}\ (\mu_N, \sigma^2_N)$ in case of finite and small sample sizes N, with abreviation GD for the GUMBEL distribution. The calculations are based on the hazard function $h(x)$

$$h(x) = \frac{f_X(x)}{1 - F_X(x)}. \tag{3.118}$$

In general, a hazard function is defined as the proportion of items which fail in a certain time intervall $(x, x + \mathrm{d}x)$ divided by the proportion of survivors up to time x (BURY, 1975).

The parameters μ_N and σ_N are approximated by $\mu_{N,app}$ and $\sigma_{N,app}$, see

$$\mu_{N,app} = x_{p,N} \text{ and } \sigma_{N,app} = \frac{1}{h[x_{p,N}]}, \tag{3.119}$$

with $x_{p,N}$ as the most likely or characteristic largest value equal to mode $[X_N]$, respectively, with $p_N = 1 - 1 / N$. Thus the approximative distribution of maxima is given by $X_N \sim \mathrm{GD}\ (\mu_{N,app}, \sigma^2_{N,app})$. The expectation and variance can be calculated by means of

equ. (2.138) and (2.139) given in section 2.6.2. Nevertheless, this approximative method is limited to maxima.

Another approximation which can be applied for minima and maxima is provided by FREUDENTHAL AND GUMBEL (1956). They showed that in case of $X_1 \sim \mathrm{ND}\,(\mu, \sigma^2)$ and CDF given as $F_X(x)$ the appoximative CDFs of minima X_M and maxima X_N of X_1 are given as

$$F_{X_M}\left(x\middle|\mu,\sigma^2,M\right)=\min\left[X_i\middle|\mu,\sigma^2,M\right]=1-\exp\left[-\exp\left[+\frac{X_M-(\mu-\sigma\cdot A)}{\sigma\cdot B}\right]\right],$$
$$F_{X_N}\left(x\middle|\mu,\sigma^2,N\right)=\max\left[X_i\middle|\mu,\sigma^2,M\right]=\exp\left[-\exp\left[-\frac{X_N-(\mu+\sigma\cdot A)}{\sigma\cdot B}\right]\right], \tag{3.120}$$

with μ and σ^2 according the parent distribution of X_1 and the parameters A and B (with $M = N$) given as

$$A=\frac{2\cdot\ln(M)-0.5\cdot\ln[\ln(M)]-\ln\left(2\cdot\sqrt{\pi}\right)}{\sqrt{2\cdot\ln(M)}} \text{ and } B=\frac{1}{\sqrt{2\cdot\ln(M)}}. \tag{3.121}$$

The approximative method for minima is further called $\mathbf{MIN_{approx,ND}}$.

A possible approximation for extremes of $X \sim \mathrm{2pLND}\,(\mu, \sigma^2)$, with μ and σ^2 according the normal distribution of $Y_1 = \ln(X_1)$, is given by the WEIBULL distribution for extremes (see section 2.6.2). Thereby the distribution parameters are adapted to (BURY, 1975)

$$\alpha_M=\exp(\mu-\sigma\cdot A);\ \beta_M=\frac{1}{\sigma\cdot B} \text{ and } \alpha_N=\exp(\mu-\sigma\cdot A);\ \beta_N=\frac{1}{\sigma\cdot B}, \tag{3.122}$$

with parameters A and B according equ. (3.121). The approximative method for minima is further called $\mathbf{MIN_{approx,2pLND}}$. Thereby the calculation of $E[X_M]$, $Var[X_M]$ and $x_{p,M}$ follows the equations given in section 2.4.3 concerning 2pWD. Thus system size M is already taken into account by the parameters A and B according equ. (3.121).

Fig. 3.25 and Fig. 3.26 compare simulated data to fitted or approximative models of serial systems composed of iid elements $X_1 \sim \mathrm{2pLND}$. Thereby FIT_{2pLND} stands for a fitted 2pLND by means of the empirical statistics mean and standard deviation taken directly from the simulated data and for every system size M. The same procedure was applied by fitting GD to simulated data (FIT_{GD}). Hereby the distribution parameters were estimated

by means of equ. (2.142). For the approximative calculation of statistics for these simulated systems which base solely on the stochastic information of the elements, two methods were applied: The first method conforms to the approximation $\mathrm{MIN}_{\mathrm{approx,2pLND}}$ presented previously. The second approximation is made by applying the models for parameters of the approximative 2pLND given in Tab. 3.2. Interestingly, even for systems of up to 1,000 serial elements and $\mathrm{CoV}[X_1] \leq 100\%$ it can be found that 2pLND gives better fit to the simulated data than GD, although GD is the limiting distribution for the simulated system strength. Nevertheless, the differences between the fits of 2pLND and GD become smaller with increasing $\mathrm{CoV}[X_1]$ and M. This comparison already reflects that the approximative 2pLND gives good results if the parameters can be estimated accurately.

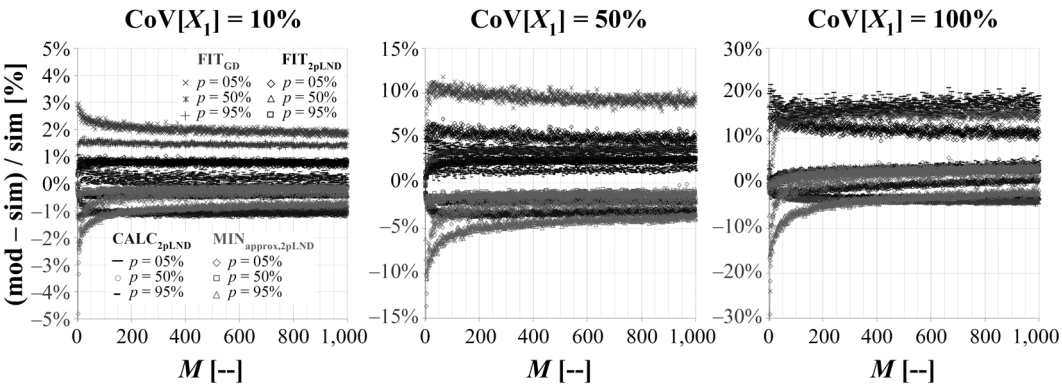

Fig. 3.25: Comparison of fitted and approximative models for minima of serial systems composed of iid $X_1 \sim$ 2pLND elements in dependency of $\mathrm{CoV}[X_1]$ and system size $M \leq 1{,}000$

Analysing the results of the two approximative models $\mathrm{CALC}_{\mathrm{2pLND}}$ and $\mathrm{MIN}_{\mathrm{approx,2pLND}}$ shows that in case of $M \to 1$ the approximation $\mathrm{CALC}_{\mathrm{2pLND}}$ fits significantly better than $\mathrm{MIN}_{\mathrm{approx,2pLND}}$ and that $\mathrm{CALC}_{\mathrm{2pLND}}$ delivers results comparable to $\mathrm{FIT}_{\mathrm{2pLND}}$. This confirms that parameters of $\mathrm{FIT}_{\mathrm{2pLND}}$ are well estimated by means of models given in Tab. 3.2. Nevertheless, power in estimation gets worse in case of very large $\mathrm{CoV}[X_1]$, e.g. $\mathrm{CoV}[X_1] = 100\%$. In contrast, the approximations based on $\mathrm{MIN}_{\mathrm{approx,2pLND}}$ gets better with increasing M and delivers always conservative estimates of analysed quantiles in case of $\mathrm{CoV}[X_1] \leq 50\%$. The approximation is also stable by delivering comparable deviations from simulated data, irrespective of $\mathrm{CoV}[X_1]$. The approximation $\mathrm{CALC}_{\mathrm{2pLND}}$ shows an increasing bias with increasing $\mathrm{CoV}[X_1]$, in particular in estimating the 5%-quantile. Nevertheless, $\mathrm{CALC}_{\mathrm{2pLND}}$ gives better results for 95%-quantiles than

$MIN_{approx,2pLND}$, irrespective of CoV[X_1] and within the whole analysed range of M, and also better results for medians in case of CoV[X_1] ≥ 50%. In particular if estimates of characteristics of small systems with $M \leq 50$ are required $CALC_{2pLND}$ enables more accurate and more stable estimations already at $M > 1$ than $MIN_{approx,2pLND}$ as CoV[X_1] ≤ 50%. At CoV[X_1] = 100% a remarkable drift in the 5%-quantile estimated by $CALC_{2pLND}$ can be observed. Focusing on a practical range of CoV[X_1] = (5 ÷ 50)% and $M \leq 50$ the approximative model $CALC_{2pLND}$ in comparison to $MIN_{approx,2pLND}$ is the better choice even if extreme quantile estimates have to be derived on estimated distribution parameters and thus not directly calculated by means of equ. (3.105) and (3.109).

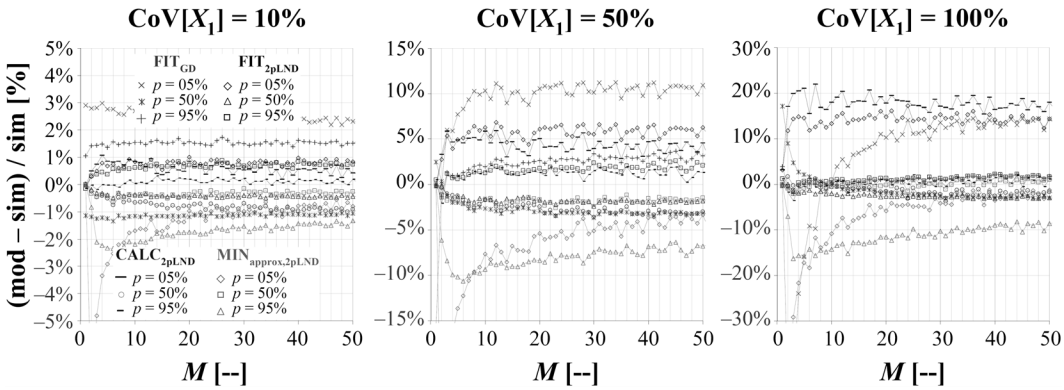

Fig. 3.26: Comparison of fitted and approximative models for minima of serial systems composed of iid X_1 ~ 2pLND elements in dependency of CoV[X_1] and system size $M \leq 50$

To conclude, in this section 3.3.2 serial systems composed of iid X_1 ~ ND and 2pLND were analysed. In particular the influences of CoV[X_1] and system size M were examined by means of simulated data with 10,000 replicates of each system. Thereby focus was on systems composed of X_1 ~ 2pLND. The reason for this is that for strength data or in general for data based on multiplicative processes distribution 2pLND automatically follows from central limit theorem. As it is not possible to define an explicit formula for calculating minima of serial systems composed of iid elements X_1 ~ 2pLND approximative models were defined, analysed and compared with simulated data. This was motivated by the observation that especially in systems of size $M < 100$ or even $M < 1{,}000$ distribution characteristics derived from the asymptotic distribution model GD according the EVT delivers inaccurate or not representative values. Based on the examinations made on serial systems composed of iid elements it can be concluded that:

- characteristics of X_M of serial systems composed of iid elements $X_1 \sim$ 2pLND and finite system size $M < 1{,}000$ can be approximated by a 2pLND; this delivers better results than GD, even in case of large systems and even if best fitted distribution parameters for GD are used;
- equ. (3.102) shows to be able to perfectly describe the dependency of characteristics on M in serial systems composed of iid elements $X_1 \sim$ 2pLND; this was proved for analysed quantiles in the range of 2.5% to 97.5% and for the characteristics mean, standard deviation, variance and CoV of X_M; nevertheless adequate parameter estimation is required;
- the approximative method worked out for 2pLND and with distribution parameters given in Tab. 3.2 shows to work well and enables simple calculation of distribution parameters of minimas dependent only on CoV[X_1] and M;
- within the range of $M \leq 50$ and CoV[X_1] $\leq 50\%$ this approximative method delivers even more accurate results than the approximative method proposed by FREUDENTHAL AND GUMBEL (1956), even if the quantile statistics are computed from transformed distribution parameters and not directly by the models worked out for quantile estimation as given in equ. (3.105) and (3.109).

3.3.3 Estimation of Statistical Distribution Parameters in Case of Serial Correlated 2pLND Variables

Within this section serial systems composed of equally correlated elements $X_1 \sim$ 2pLND are analysed. The analysis is based on data from Monte-Carlo simulations performed in R (2009). Serial systems of $M = 1, 2, \ldots, 100$, each with 10,000 independent runs, were generated by means of transformation of lognormal to normal domain and application of a multivariate normal approach. As in the previous sections E[X_1] was kept constant and equal to E[X_1] = 30 whereas CoV[X_1] varied with CoV[X_1] = (10, 30, 50)%. Calculation of lognormal distribution parameters from E[X_1] $\rightarrow \mu_{ND}$ and Var[X_1] = (CoV[X_1] · E[X_1])^2 $\rightarrow \sigma^2_{ND}$, was done according equ. (2.70). Values of the expectation vector of the multivariate normal distribution with length M were put equal to μ_X, that of the variance-covariance matrix (dimension $M \times M$) equal to σ^2_{ND}, if $i = j$, and equal to $\sigma^2_{ND} \cdot \rho_{ND}$, if $i \neq j$. The correlation coefficient ρ_{ND} was recalculated from equ. (2.89), see

$$\rho_{ND} = \frac{\ln\left[\rho_X \cdot \exp\left(\sigma^2_{ND}\right) + 1 - \rho_X\right]}{\sigma^2_{ND}}, \; 0.00 \leq \rho_X \leq 1.00. \tag{3.123}$$

It has to be noted that the correlation was well achieved on average but showed a remarkable variation from system to system. The statistics gained from simulations, as the statistics of the minimum of each simulated serial system of size M, are visualised in Fig. 3.27.

The influence of correlation on the magnitude of serial system effects is remarkable and increasing with increasing correlation. In the limiting case $\rho_X \to 1.00$ the ratio $X_{M,\xi} / X_{1,\xi}$ becomes by default 1.00, irrespective of M.

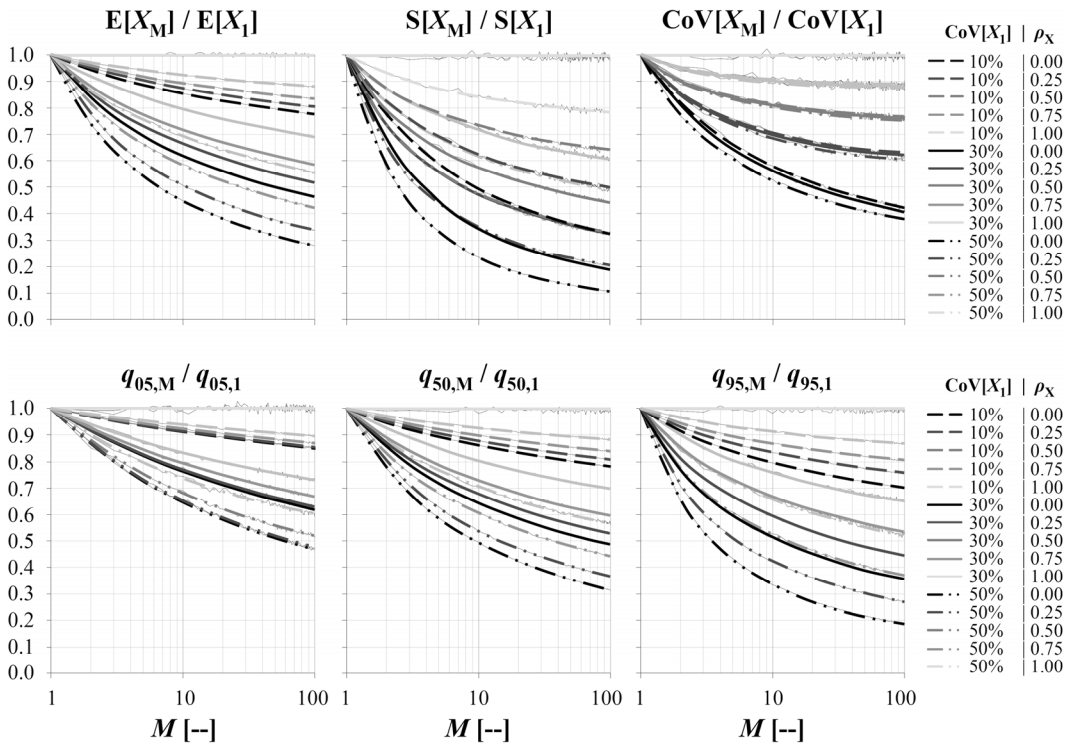

Fig. 3.27: Influence of correlation in serial systems composed of identical distributed elements $X_1 \sim$ 2pLND: relative influence on E[X_M] (left-above); S[X_M] (middle-above); CoV[X_M] (right-above); $q_{05,M}$ (left-below); $q_{50,M}$ (middle-below); $q_{95,M}$ (right-below) by variation of CoV[X_1] = (10, 30, 50)%

Due to good experiences made by fitting 2pLND to statistics of serial systems composed of $X_1 \sim$ 2pLND according equ. (3.102) and estimation of parameters α_p and β_p according equ. (3.105) and (3.109), respectively, it was verified that in principal the same formulas can also be used for serial systems composed of correlated elements. By means of

equ. (3.102) a perfect fit to the ratio $X_{M,\xi} / X_{1,\xi}$ between characteristics of simulated data was possible. Nevertheless, to account for the influence of correlation on parameters α_ξ and β_ξ an adaptation was necessary. Thereby it was observed that quantiles of simulated data were more stable than characteristics like standard deviation or coefficient of variation. Only the ratio of $X_{\text{mean,M}} / X_{\text{mean,1}}$ could be represented well by means of a simple formula.

In general, the combination of equ. (2.75) and (2.80) enables the calculation of 2pLND (μ_{ND}, σ^2_{ND}) distribution parameters based on at least two quantiles, including the median. Thus the distribution parameters are given by

$$\mu_{ND} = \ln(x_{50}),\ \sigma_{ND} = \frac{\ln(x_p) - \ln(x_{50})}{\Phi^{-1}(p)},\ \text{with } x_p \neq x_{50},\ 0.00 < p < 1.00, \tag{3.124}$$

with x_{50} as median, $x_p \neq x_{50}$ as an arbitrary quantile and $\Phi^{-1}(p)$ as operator of the inverse SND.

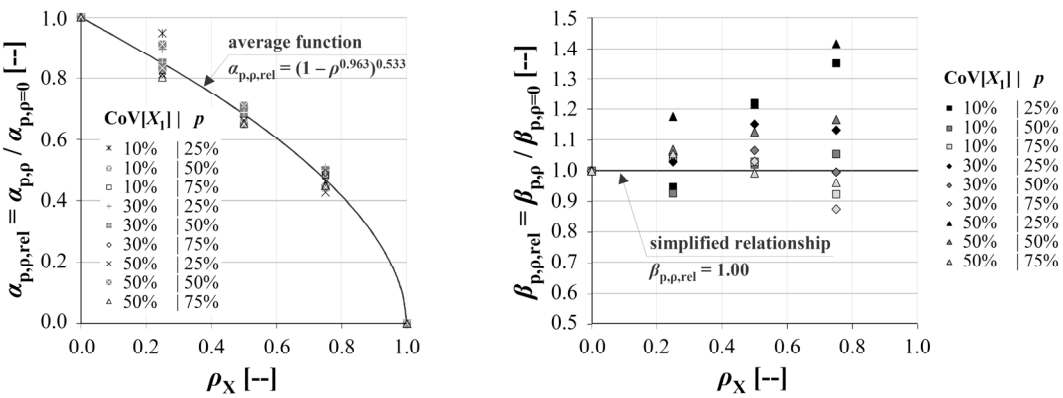

Fig. 3.28: Parameters $\alpha_{p,\rho} / \alpha_{p,\rho=0}$ vs. ρ_X (left) and $\beta_{p,\rho} / \beta_{p,\rho=0}$ vs. ρ_X (right): simulated serial systems of elements $X_1 \sim$ 2pLND, with CoV[X_1] = (10, 20, 30)%, p = (25, 50, 75)% and M = 1, 2, … 100

Fig. 3.28 shows the dependency of parameter ratios $\alpha_{p,\rho} / \alpha_{p,\rho=0}$ and $\beta_{p,\rho} / \beta_{p,\rho=0}$ on the correlation coefficient, exemplarily for p = (25, 50 75)% and CoV[X_1] = (10, 30, 50)%. From the data points it can be concluded that the ratio $\alpha_{p,\rho} / \alpha_{p,\rho=0}$ appears to be by trend dependent on p and CoV[X_1]. The ratio $\beta_{p,\rho} / \beta_{p,\rho=0}$ shows also to be influenced by CoV[X_1] and p but no clear tendency is given. Due to the fact that in principle good estimates for quantiles near the median and equal to the median are at least required for

estimating the distribution parameters $\mu_{M,ND}$ and $\sigma_{M,ND}$ a function of $\alpha_{p,\rho} / \alpha_{p,\rho=0}$ was found by means of LSM, see

$$\frac{\alpha_{p,\rho}}{\alpha_{p,\rho=0}} = \left(1-\rho_X{}^{0.963}\right)^{0.533} \approx \sqrt{1-\rho_X}\ , \tag{3.125}$$

with $R^2 \approx 1.00$ and $e_i \sim (0;\ 0.00532)$. Note: The statistics of residuum e_i and of R^2 are solely based on four values averaged for fixed ρ_X but varying CoV[X_1].

For simplification and due to the lack of a clear trend in $\beta_{p,\rho} / \beta_{p,\rho=0}$ vs. ρ_X a simplified relationship of $\beta_{p,\rho} / \beta_{p,\rho=0} = 1.00$ is used. Now the distribution parameter $\mu_{ND,M,\rho}$ can be calculated easily. For the parameter $\sigma_{M,ND,\rho}$ it is recommended to average two quantile estimates taken symmetrical to the median, e.g. $p = 45\%$ and 55% according

$$\sigma_{M,ND,\rho} = \frac{1}{2}\cdot\left(\frac{\ln(x_{45})-\ln(x_{50})}{\Phi^{-1}(45\%)} + \frac{\ln(x_{55})-\ln(x_{50})}{\Phi^{-1}(55\%)}\right)\ . \tag{3.126}$$

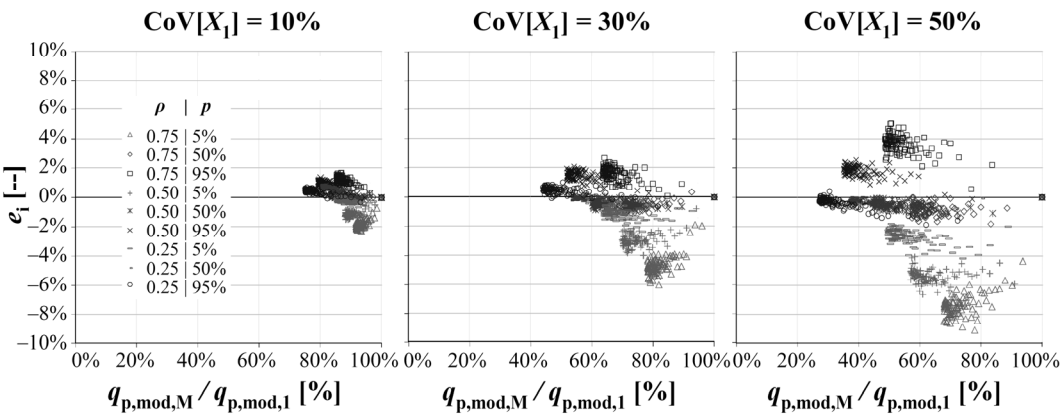

Fig. 3.29: Residue $e_i = (q_{p,M,obs} / q_{p,1,obs}) - (q_{p,M,mod} / q_{p,1,mod})$ vs. $q_{p,mod,M} / q_{p,mod,1}$: comparison between calculations based on simplified models and simulated serial systems of elements $X_1 \sim$ 2pLND, with CoV[X_1] = 10% (left); 30% (middle); 50% (right), $p = (5, 50, 95)\%$ and $M = 1, 2, \ldots, 100$

By means of the equations derived the distribution parameters were calculated solely with the information of E[X_1], CoV[X_1], M, ρ_X and 2pLND as RSDM of X_1. To verify the accuracy of the model the 5%-, 50%- and 95%-quantiles were calculated by varying M and ρ_X and on the assumption of 2pLND as RSDM even for X_M. The residue-plots are

shown in Fig. 3.29. The results are satisfying for CoV[X_1] not too large even for the extreme quantiles q_{05} and q_{95}. Nevertheless, the deviation between simulated and calculated quantiles increases with increasing CoV[X_1] and ρ_X and show at least up to 9% under- and up to 5% overestimation of the 5%- and 95%-quantiles, respectively, based on CoV[X_1] = 50% and $M = 100$. It can be concluded that these deviations are only remarkable at high variability and at a high number of serial arranged elements. Therefore, the application range of above formulas is at least restricted by the investigated domain of CoV[X_1] = (0 ÷ 50)%, $\rho_X = 0 \div 0.75$ and $M = 1 \div 100$.

As noted above a simple and well representing function of the description of the ratio $X_{mean,M} / X_{mean,1}$ vs. ρ_X could be defined for the parameter ratios $\alpha_{mean,\rho} / \alpha_{mean,\rho=0}$ and $\beta_{mean,\rho} / \beta_{mean,\rho=0}$, see

$$\frac{\alpha_{mean,\rho}}{\alpha_{mean,\rho=0}} = \sqrt{1-\rho_X} \text{ , with } R^2 \approx 1.00 \text{ and } e_i \sim (0;\, 0.0047^2), \tag{3.127}$$

and

$$\frac{\beta_{mean,\rho}}{\beta_{mean,\rho=0}} = 1.00 \text{ , with } R^2 \approx \varepsilon \text{ and } e_i \sim (0;\, 0.0152^2). \tag{3.128}$$

Note: The statistics of residue e_i and R^2 in equ. (3.127) and (3.128) above are based only on four and three values, respectively, averaged for fixed ρ_X but varying CoV[X_1].

Based on examinations above with simulated data of serial systems composed of identical distributed but correlated elements $X_1 \sim$ 2pLND following findings are given:

- all simulations were restricted to positive correlation within the range of $0.00 \le \rho_X \le 1.00$;
- the Monte-Carlo simulations performed in R (2009) were proved to work satisfactorily on average but correlation in individual systems showed remarkable variation; this is in fact a logical stochastic outcome; nevertheless as discussed in LAI ET AL. (1999) robustness of sample correlation in skewed distributions requires an unexpected high quantity of realisations to prevent bias, in bivariate 2pLND roughly three to four million; in fact the herein simulated data show only 10,000 replicants of each system, but also for multivariate 2pLND with M up to 100 which increases the robustness also;

- the characteristics calculated from simulated data show also that the influence on system effects in case of increasing correlation is non-linear, in particular convex on mean, standard deviation and on all analysed quantiles; consequently, serial systems composed of only minor correlated elements can be treated as being uncorrelated whereas systems composed of elements with $\rho_X \geq 0.50$ are remarkable influenced by correlation showing significant reduced system effects; this is in particular true for low quantiles (e.g. $q_{05,M}$) but not so distinct in higher quantiles (e.g. $q_{95,M}$); interesting but logical, the influence of correlation on CoV[X_M] is inverse, being more pronounced at low values of ρ_X near zero (see Fig. 3.27);
- as shown already for uncorrelated systems the formula presented in equ. (3.102) was again verified to be able to describe perfectly the change in all analysed statistics of correlated serial systems composed of elements $X_1 \sim$ 2pLND, as parameters α_ξ and β_ξ can be accurately determined; consequently, models for parameters $\alpha_{p,\rho}$, $\beta_{p,\rho}$, $\alpha_{mean,\rho}$ and $\beta_{mean,\rho}$ were defined;
- by means of an additionally approach presented for the determination of lognormal distribution parameters μ_{ND} and σ_{ND} based on at least two quantile values, the applicability of models for parameters $\alpha_{p,\rho}$ and $\beta_{p,\rho}$ was verified by comparing simulated data with calculated quantiles $q_{05,M}$, $q_{50,M}$ and $q_{95,M}$, derived solely on the information of E[X_1], CoV[X_1], M, ρ_X and 2pLND as RSDM of X_1;
- during verification it was shown that differences between calculated and simulated data increase with CoV[X_1] and M but deliver satisfactorily results for serial systems not too large and moderate CoV[X_1]; due to that models are restricted to the analysed scope and range of CoV[X_1] = (0 ÷ 50)%, ρ_X = 0 ÷ 0.75 and M = 1 ÷ 100.

3.4 Stochastic Effects in Parallel Acting Systems

This section is dedicated to examinations on stochastic effects in parallel acting systems. At first this section starts with a general discussion and elaboration of basic aspects. Secondly, system effects of parallel systems composed of linear-elastic and iid elements are analysed on four case studies. The systems are virtually generated by means of Monte-Carlo simulations.

In the following types of systems and differences between parallel and serial action are discussed briefly:

- ideal parallel acting systems provide full redundancy ("cold reserve"); such systems are designed according their weakest elements and consequently as perfect serial system of (iid) elements with the background knowledge that $N - 1$ elements are able to carry at least full load even after failure of the first element; this system type is not treated further in this chapter; principal findings are already given in section 3.3;
- parallel systems which are characterised by load redistribution and intermediate steady states in cumulative loading exhibit initially the same mean E-modulus as the elements but enable higher extensions or deflections with progressing system failure and thus provide the chance of load transfer to stronger system components activated by the exceedance of limits in extension or deflection; such "load sharing systems" are treated in more detail within this chapter;
- due to activated homogenisation effects, spread in characteristics is significantly reduced; the expectation of system strength can increase or decrease with increasing quantity of elements in the system, but the amount of decrease will reach that of serial systems only in limiting cases; therefore parallel systems exhibit in general a significant increase in reliability if compared to serial systems of the same size.

Further aspects were already discussed in section 3.1.

According to DANIELS (1945) parallel acting systems enable a certain amount of load redistribution after partial failure of elements. If only interested in the load bearing capacity of systems at first failure it is again a minimum value which is of interest. Of course, if the elements in the system are constraint to elongate equally or to equal load (e.g. system under tension stress in loading direction and parallel deforming infinite stiff load distribution bars providing load transfer on equally elongated elements) the minimum is not defined as the minimum strength, but by the minimum ultimate strain multiplied with the mean E-modulus of all N elements. Assuming perfect linear-elastic stress-strain relationship according HOOK's law the system strength or stress at first element failure is given as

$$f_{N,1} = \frac{1}{N} \cdot \sum_{i=1}^{N} E_i \cdot \min_N \left[\frac{f_i}{E_i} \right] = \frac{1}{N} \cdot \sum_{i=1}^{N} E_i \cdot \min_N \left[\varepsilon_{f,i} \right],\ i = 1,\ \ldots,\ N. \tag{3.129}$$

It is obvious that in parallel systems not only the interaction between the elements but in particular the relationship between strength and stiffness (stress-strain relationship) as well as the material behaviour (linear vs. non-linear; elastic vs. plastic; etc.) becomes decisive for the description of the system behaviour and in particular for computation of the mechanical potential.

These parallel acting systems are strain-constraint in contrast to being pure strength-constraint in case of serial acting systems. Consequently, in perfect brittle systems or systems under high dynamic loading were any possible load redistribution between surviving elements is prevented, the first partial system failure initiate probably a total system collaps. Therefore, system strength at first element failure serves as (conservative) estimate of systems finite but not too small.

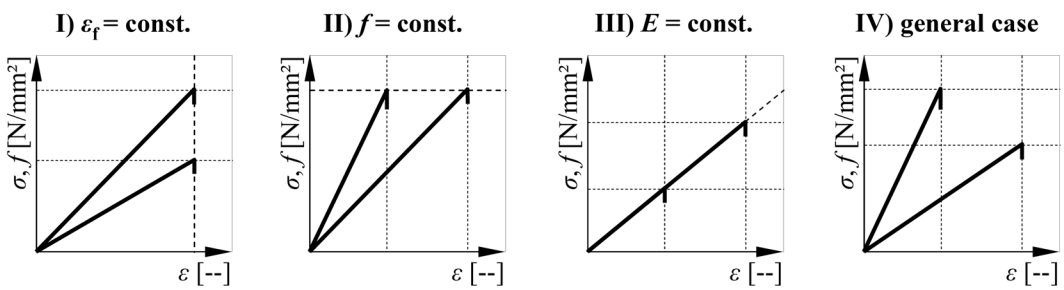

Fig. 3.30: Case studies of theoretical stress-strain relationships in case of perfect linear-elastic material behaviour with brittle failure: ideal cases with deterministic ultimate strain $\varepsilon_{f,1} = \varepsilon_f$ (case I), element strength $f_1 = f$ (case II), E-modulus $E_1 = E$ (case III) and a general relationship according HOOK's law (case IV)

As already discussed in section 3.2.4 parallel systems composed of a few elements only can act like serial systems. This is due to the simple fact that either a lack of potential surviving elements to carry the extra load is given or that CoV[f_1] is too small which makes load redistribution on survivors nearly impossible due to lack of extra load carring capacity.

Following equ. (3.129) it is obvious that the system bearing capacity is in general not defined by the average strength of the elements. Parallel system stress / strength is given

by the average of stresses in all surviving elements at given strain, in particular at the minimum strain defined by the ultimate strain of the elements which currently fail.

Over all the mechanical behaviour and stochastic nature of parallel acting systems is more complex than that of serial acting systems. This is in respect to stress-strain relationships, material behaviour, dynamics, correlation and the provided interaction between the elements (e.g. direct or indirect (matrix) stress transfer; rigid or flexible composite action). There are some more possibilities in which systems composed of parallel elements respond similar to serial systems. In contrast, serial arranged elements always act serial. Therefore additional investigations comparable to the literature are made on systems composed of elements with linear-elastic stress-strain relationship and perfect brittle failure. Hereby no softening or hardening in elements before or after fracturing or partial damage is assumed. Nevertheless, the ability to redistribute stresses after partial fracturing is allowed. These investigations are made on four case studies, see Fig. 3.30. As in general expectable the elements in the parallel system are treated iid, but the correlation between characteristics (e.g. between strength and E-modulus) within each element is considered.

Case I (Fig. 3.30, left) is defined by a deterministic ultimate strain. Given $\sigma_{\max,1} = f_1$ HOOK's law is reduced to $f_1 = E_1 \cdot \varepsilon_f$, with $\varepsilon_{f,1} = \varepsilon_f =$ constant. Thus the element and system strength depends only on E-modulus and vice versa. **Case II** (Fig. 3.30, left-middle) shows constant element strength $f_1 = f$. Thus E-modulus and ultimate strain $\varepsilon_{f,1}$ depend on each other and are given by $E_1 = f / \varepsilon_{f,1}$ and $\varepsilon_{f,1} = f / E_1$, with scalar f. In **case III** (Fig. 3.30, middle-right) a constant E-modulus $E_1 = E$ for all elements composing a parallel acting system is assumed. This is in line with the assumptions made by DANIELS (1945), see section 3.2.3. The element strength f_1 depends only on the ultimate strain $\varepsilon_{f,1}$ and is given by $f_1 = E \cdot \varepsilon_{f,1}$, with E as scalar. **Case IV** (Fig. 3.30, right) defines the element strength according HOOK's law with stochastic quantities E_1 and $\varepsilon_{f,1}$. Therefore the element strength and further the system strength depends strongly on the correlation structure between E-modulus E_1 and ultimate strain $\varepsilon_{f,1}$ as well as on the variability in both characteristics, e.g. CoV[E_1] and CoV[$\varepsilon_{f,1}$].

Within the following sections all four cases are analysed in more detail. Examinations in respect to GLS (and ELLS) and calculation of characteristics at first and final system failure are made. Whereas case I, II and III are only analysed by assuming GLS, in case IV GLS and ELLS are considered. If structures are composed of parallel arranged and rigid or flexible connected elements independency between the elements is assumed.

As already mentioned by GOLLWITZER (1986) even in case of iid parallel interacting and independently stressed elements a certain dependency structure occurs in system behaviour. Nevertheless, all elements are further treated as being iid with f_1; $E_1 \sim$ 2pLND. The focus on 2pLND is due to the lack of analysis in regard to this type of distribution model and due to the wide applicability of 2pLND in particular for models as discussed later in chapter 5. This becomes obvious by analysing equ. (3.129). The system bearing capacity of successive failures and the ultimate system strength are defined by the mean E-modulus (average E-modulus of surviving elements defined by an ultimate strain higher or equal that of already failed elements) and the minimum ultimate strain at a given system status. Consequently, ultimate strain and E-modulus are in a certain dependency due to ranking of both characteristics.

3.4.1 Analysis concerning Case I: $\varepsilon_{f,1}$ = constant

In case I a deterministic ultimate strain $\varepsilon_{f,1} = \varepsilon_f =$ constant for all N elements in a parallel acting system is given (see Fig. 3.31 and Fig. 3.32).

Due to the fact that system failure is a function of the ultimate strain the system fails immediately with reaching ε_f. Therefore no load redistribution is provided; all elements reach their ultimate strain at the same time. In that ideal case the maximum (ultimate) system strength is given by

$$f_{N,\max} = \frac{1}{N} \cdot \sum_{i=1}^{N} E_i \cdot \varepsilon_f = \frac{1}{N} \cdot \sum_{i=1}^{N} f_i = f_{N,mean}, \text{ with } i = 1, \ldots, N. \tag{3.130}$$

ad I) ε_f = const.

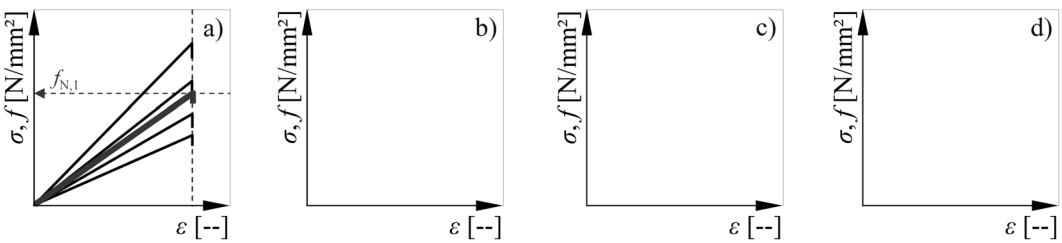

Fig. 3.31: Case I, $\varepsilon_{f,1}$ = deterministic: expected stress-strain relationship of parallel systems (bold, red graph) composed exemplarily of four elements (thin graphs) assuming in principal an element-wise failure scenario (from left to right)

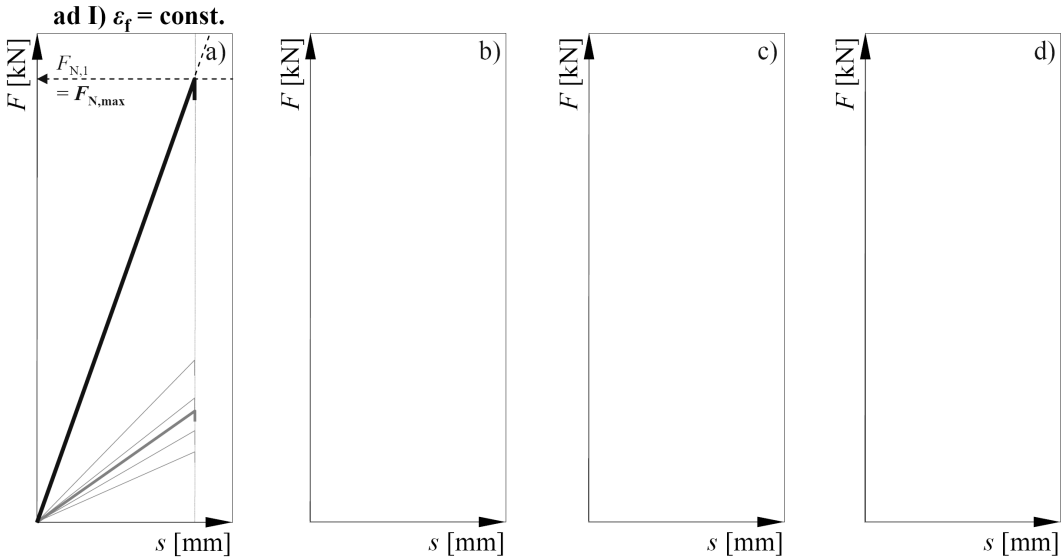

Fig. 3.32: Case I, $\varepsilon_{f,1}$ = deterministic: expected load-elongation relationship of parallel systems (bold, blue graph) composed exemplarily of four elements (thin graphs; including also stress-strain relationship) assuming in principal an element-wise failure scenario (from left to right)

As there is no possibility to redistribute stresses **GLS or LLS can not occur**. The expectation E[f_N], variance Var[f_N] and CoV[f_N] in case of iid elements are given by

$$E[f_N] = \frac{1}{N} \cdot \sum_{i=1}^{N} f_i \,,\; Var[f_N] = \frac{Var[f_i]}{N} \,,\; CoV[f_N] = \frac{CoV[f_1]}{\sqrt{N}} \,. \tag{3.131}$$

According the central limit theorem and irrespective of the parent distribution of f_1 a fast convergence of f_N to ND with increasing N is given, see Fig. 3.33 as well as section 2.6.1. Thus the distribution of system strength and E-modulus is the same as in case of perfect plastic material behaviour as discussed in section 3.2.2. Nevertheless, the system failure behaviour is different. In perfect plastic material large deformation capacity useable for monitoring of structural elements is given. These deformations offer the possibility to react before the structure gets out of control. In contrast, deterministic ultimate strain in parallel systems composed of perfect linear-elastic brittle elements leads to sudden and perfect brittle system failure without any warning in advance. Nevertheless, the parallel system in case I exhibit a remarkable increase in reliability due to a sudden decrease of spread in strength and E-modulus forced by the common action of all elements in the

parallel acting system. This is expressed by a significant homogenisation effect which is often treated as **averaging model**, in case of iid elements given as

$$E[f_N] = E[f_1],\ CoV[f_N] = \frac{CoV[f_1]}{\sqrt{N}} \quad . \tag{3.132}$$

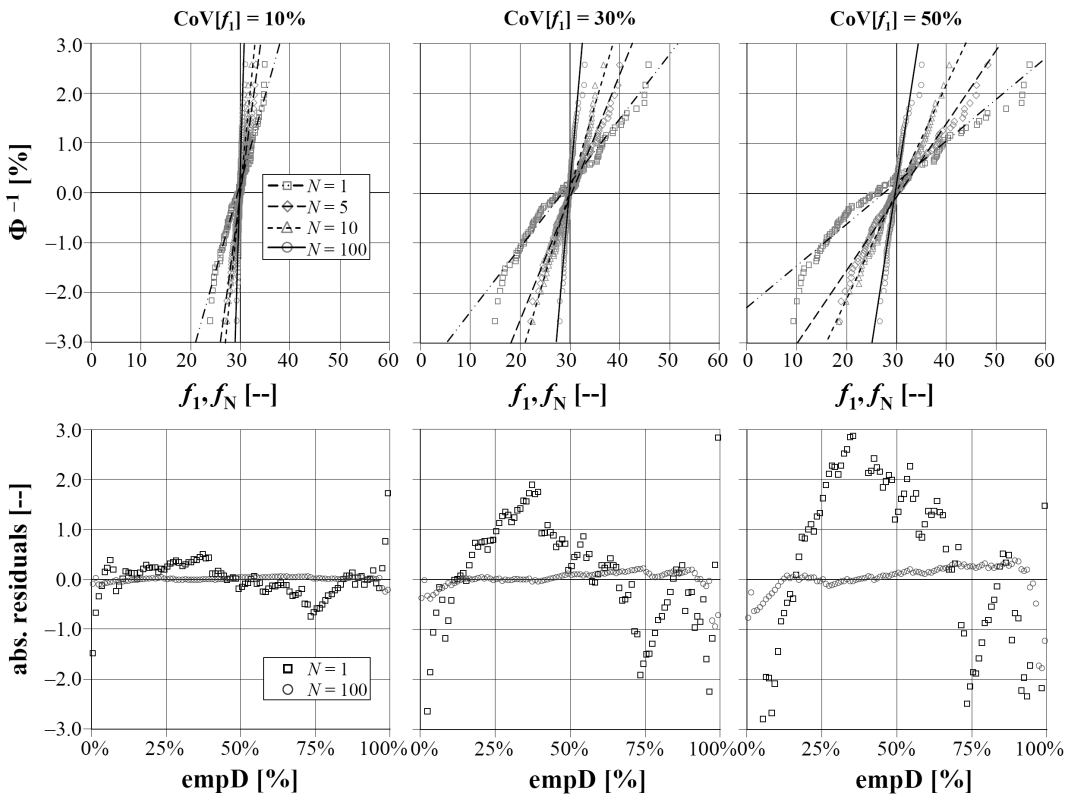

Fig. 3.33: Converging process of $f_1 \sim$ 2pLND to $f_N \sim$ ND in case of parallel systems composed of iid elements with deterministic ultimate strain ε_f: simulations with sets of $n = 100$; variation of system size N and CoV[f_1]: (above) probability paper plots of ND; (below) plots of absolute residuals between simulated data and fitted ND

Fig. 3.34 shows the relative deviations between calculated and simulated 5%- and 95%-quantiles of parallel systems composed of iid-elements $f_1 \sim$ 2pLND. The simulations were performed in R (2009) with (arbitrary choosen) E[f_1] = 30 and CoV[f_1] = (10, 30, 50)%. The ultimate and deterministic strain was fixed with $\varepsilon_f = 0.003$ and the expected E-modulus taken with E[E_1] = 10,000. The model calculations were made with E[f_N] and CoV[f_N] according equ. (3.132) and $f_N \sim$ ND or 2pLND. The plots in Fig. 3.34 show a

distinctive decrease of relative deviations with increasing N and decreasing CoV[f_1] for both distribution models, and in general a smaller bias in case of 2pLND. The fast convergence to zero deviations follows from the distinctive reduction of CoV[f_N]. Whereas in case of 2pLND deviations between calculated and simulated 95%-quantiles are larger than in 5%-quantiles vice versa is given in model ND. Consequently it is proposed to stick in principle to the parent distribution model of f_1 also for calculation of e.g. quantiles of f_N by means of expectation and variation according equ. (3.132).

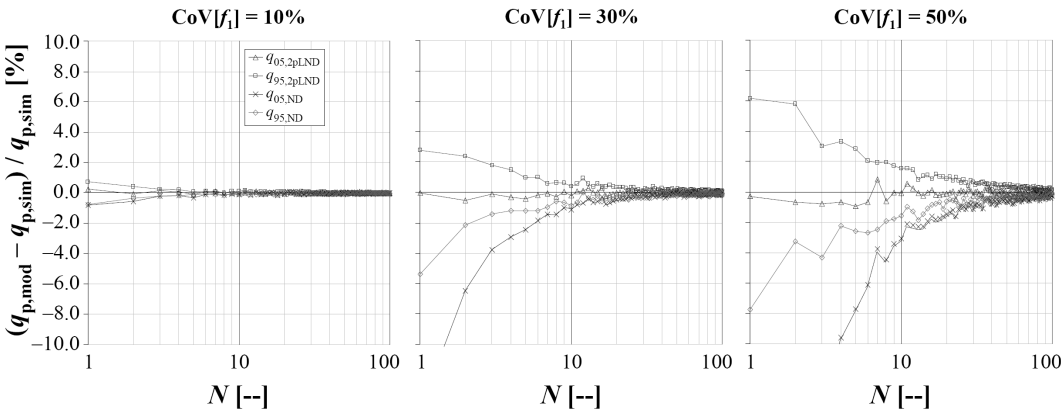

Fig. 3.34: Relative deviations between calculated and simulated 5%- and 95%-quantiles by varying CoV[f_1] = (10, 30, 50)%, left, middle, right, respectively; values of $q_{p,mod}$ are calculated with ND or 2pLND, with E[f_N] = E[f_1] and CoV[f_N] = CoV[f_1] / $\sqrt{N}$

To conclude, case I constitutes a very specific system behaviour were the first and ultimate system failure occurs at the same time. Thus the system characteristics are defined by the average of strength and E-modulus of all interacting elements. As load cannot be redistributed the system fails perfect brittle and immediately with the attainment of $\varepsilon_{f,1} = \varepsilon_f$. Nevertheless, this system arrangement leads to remarkable system effects due to a maximum of homogenisation in CoV[f_N] by leaving E[f_1] = E[f_N] unchanged.

3.4.2 Analysis concerning Case II: f_1 = constant

In this ideal case a deterministic ultimate strength $f_1 = f =$ constant for all elements within a parallel system is assumed together with a random E-modulus E_1 and random ultimate strain $\varepsilon_{f,1}$ (see Fig. 3.35 and Fig. 3.36).

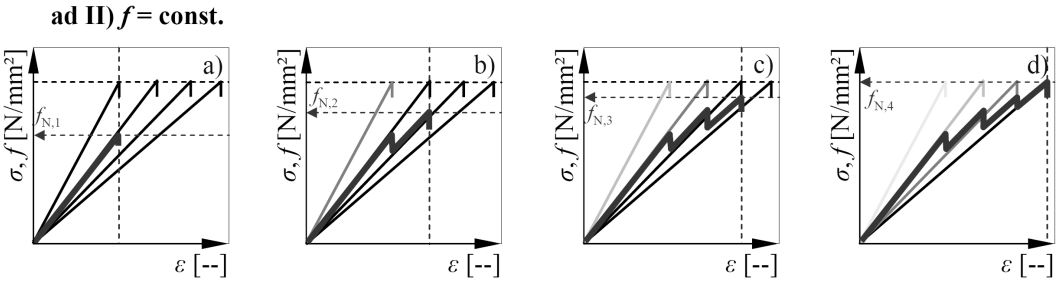

Fig. 3.35: Case II, f_1 = deterministic: expected stress-strain relationship of parallel systems (bold, red graph) composed exemplarily of four elements (thin graphs) assuming in principal an element-wise failure scenario (from left to right)

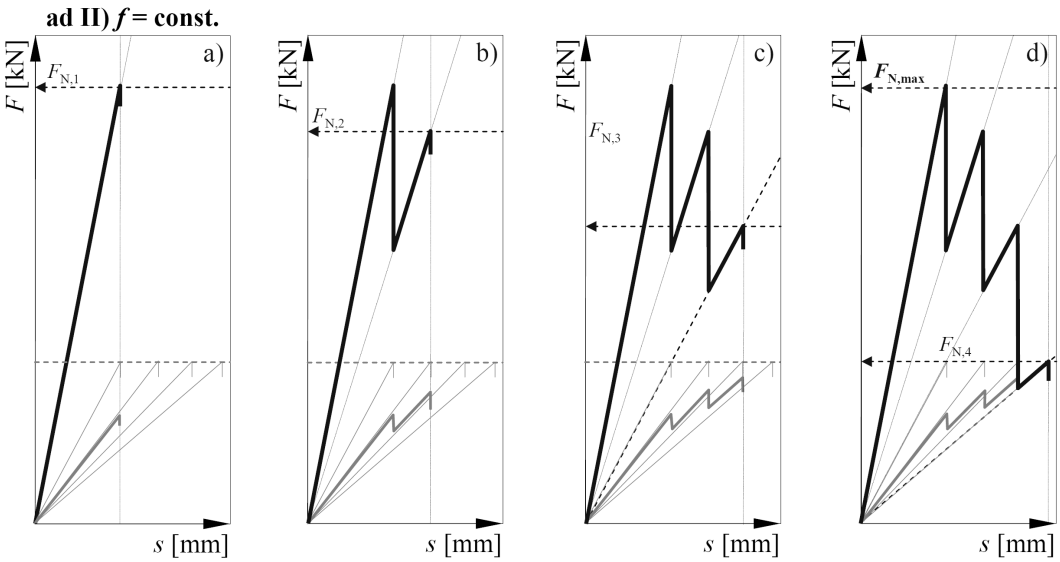

Fig. 3.36: Case II, f_1 = deterministic: expected load-elongation relationship of parallel systems (bold, blue graph) composed exemplarily of four elements (thin graphs; including also stress-strain relationship) assuming in principal an element-wise failure scenario (from left to right)

The first partial failure is caused by the element with the lowest ultimate strain according the element with the highest E-modulus and given as

$$f_{N,1} = \frac{1}{N} \cdot \sum_{i=1}^{N} \sigma_i \Big|_{\min_N(\varepsilon_{f,i})} = \frac{1}{N} \cdot \sum_{i=1}^{N} E_i \cdot \min\left[\varepsilon_{f,i}\right] = \frac{1}{N} \cdot \sum_{i=1}^{N} E_i \cdot \min\left[\frac{f_i}{E_i}\right]. \tag{3.133}$$

By ranking the elements in ascending order according their ultimate strain $\varepsilon_{f,i}$ (or descending according E_i) so that $\varepsilon_{f,(1)} \leq \varepsilon_{f,(2)} \leq \ldots \leq \varepsilon_{f,(N)}$ $(E_{(1)} \geq E_{(2)} \geq \ldots \geq E_{(N)})$ the maximum system strength in case of GLS is defined by

$$f_{N,\max} = \max_k \left[f_{N,(k)} \right] = \frac{1}{N} \cdot \max_k \left[\sum_{j=k}^{N} E_{(j)} \cdot \varepsilon_{f,(k)} \right] = \frac{1}{N} \cdot \max_k \left[\sum_{j=k}^{N} E_{(j)} \cdot \frac{f_{(k)}}{E_{(k)}} \right], \tag{3.134}$$

with $k = 1, 2, \ldots, N$ as the amount of partial failures, $(N - k + 1)$ as the amount of intact elements before partial failure and $E_{(k)}$ as E-modulus associated with $\varepsilon_{f,(k)}$.

For the analysis of such systems Monte-Carlo simulations were performed in R (2009). Thereby the iid E-modulus followed $E_1 \sim$ 2pLND, with expectation $\mathrm{E}[E_1] = 10{,}000$. The strength of the elements f_1 was taken as deterministic with $\mathrm{E}[f_1] = f_1 = 30$. Consequently, the ultimate strain of elements $\varepsilon_{f,1}$ also follows a 2pLND, with $\rho(E_1, \varepsilon_{f,1}) = -1.00$ and $\mathrm{CoV}[\varepsilon_{f,1}] = \mathrm{CoV}[E_1]$. Each system of $N = 1, 2, \ldots, 100$ elements was simulated 10,000 times. The influence of variation was analysed with a $\mathrm{CoV}[E_1] = (10, 20, \ldots, 50)\%$. As output of the simulations the system strength / stress at first failure, $f_{N,1}$, and the maximum system strength $f_{N,\max}$ together with the corresponding E-moduli ($E_{N,1}$ and $E_N \mid f_{N,\max}$) and rank of $E_i \mid f_{N,\max}$ were recorded. The output is further visualised and discussed as relative change of statistics in relationship to the corresponding input parameters of the elements.

Fig. 3.37 (left) shows the relative change of mean system strength versus system size N under variation of $\mathrm{CoV}[E_1]$. Thereby a direct comparison between $f_{N,1,\mathrm{mean}}$ and $f_{N,\max,\mathrm{mean}}$, representing the mean system strength at first failure and the maximum system strength, respectively is provided. The mean system strength decreases nonlinearly with increasing N and $\mathrm{CoV}[E_1]$. This decrease is less pronounced in $f_{N,\max,\mathrm{mean}}$. The decrease nearly diminishes in systems of $N \geq (20 \div 30)$ elements. The corresponding system size depends on $\mathrm{CoV}[E_1]$ and decreases with increasing $\mathrm{CoV}[E_1]$. Systems of only a few elements show no distinctive difference between $f_{N,\max,\mathrm{mean}}$ and $f_{N,1,\mathrm{mean}}$. This is in particular obvious in systems composed of elements with low $\mathrm{CoV}[E_1]$. Of course, a system with small N and low $\mathrm{CoV}[E_1]$ can not provide enough reserve capacity required for load redistribution in conjunction with further increase in load.

Fig. 3.37 (right) gives absolute values of $\mathrm{CoV}[f_{N,1}]$ and $\mathrm{CoV}[f_{N,\max}]$. The plotting of absolute values was necessary to prevent dividing through zero, with $\mathrm{CoV}[f_1] = 0$. Whereas $\mathrm{CoV}[f_{N,1}]$ increases up to a certain level and behaves nearly constant after that, $\mathrm{CoV}[f_{N,\max}]$ shows a much lower increase followed by a sharp decrease with increasing N.

The system size corresponding to the point were CoV[$f_{N,1}$] remains nearly constant increases with CoV[E_1]. The system size at the peak of CoV[$f_{N,max}$] decreases with increasing CoV[E_1]. This is because the variability in $f_{N,1}$, expressed by CoV[$f_{N,1}$], increases at first with increasing N because it is defined by max[E_i] or min[$\varepsilon_{f,i}$] of the system elements. Thereby $f_{N,1}$ becomes more and more correlated with $\varepsilon_{f,N,1}$. In contrast, in small systems CoV[$f_{N,max}$] behaves like CoV[$f_{N,1}$] but starts to decrease significantly with the possibility of load redistribution in combination with further stress increase. Hereby the rate of decrease in CoV[$f_{N,max}$] reaches nearly that of the averaging model, see equ. (3.132).

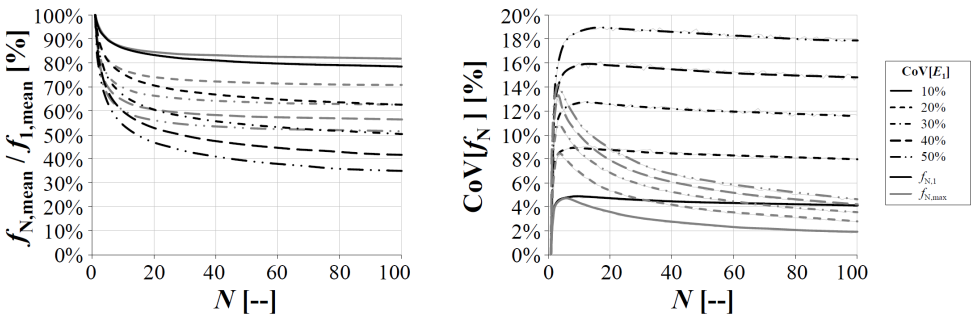

Fig. 3.37: Relative mean system strength vs. N (left) and relative CoV[f_N] vs. N (right) at first failure and at maximum system strength in dependency of CoV[E_1]

Fig. 3.38 shows the relative 5%- and 95%-quantiles of system strengths $f_{N,1}$ and $f_{N,max}$ in dependency of N and CoV[E_1]. Thereby the observable decrease is even higher in lower quantiles of system strength.

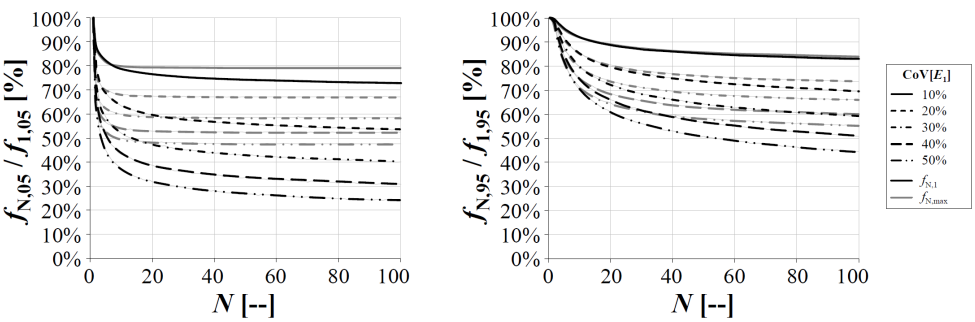

Fig. 3.38: Relative 5%- (left) and relative 95%-quantiles (right) of system strength at first failure and at maximum system strength in dependency of CoV[E_1]

The relative change in mean and CoV of the E-modulus of systems at first failure and at the point of maximum system strength is shown in Fig. 3.39. By definition $E_{N,1,mean}$ and CoV[$E_{N,1}$] follow the averaging model as given in equ. (3.132). As a consequence of GLS the mean system E-modulus $E_{N,max,mean}$ is defined as $E_{N,max,mean} \leq (E_{N,1,mean} = E_{1,mean})$. As expected the differences between $E_{N,max,mean}$ and $E_{N,1,mean}$ increase with increasing CoV[E_1] up to a certain system size which also increases with increasing CoV[E_1]. As during GLS more and more stiff elements fail and the quantity of surviving elements for calculation of the system E-modulus decreases, the relative decrease in CoV[$E_{N,max}$] decreases with increasing CoV[E_1].

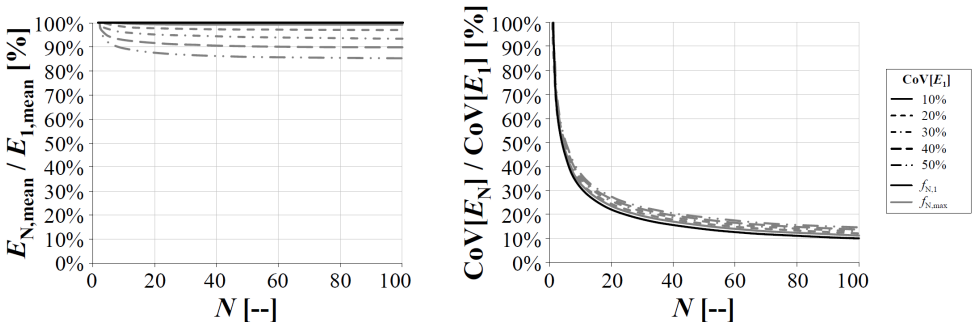

Fig. 3.39: Relative mean (left) and relative CoV (right) of E-modulus at first failure and at maximum system strength in dependency of CoV[E_1]

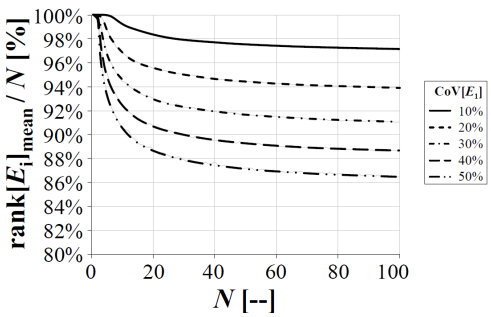

Fig. 3.40: Relative rank of E_i at given N and at maximum of system strength vs. N and in dependency of CoV[E_1]

Fig. 3.40 gives the ratio of the mean rank[E_i], at given N and at the point of maximum system strength, and of system size N. (1 – rank[E_i]$_{mean}$ / N | N; $f_{N,max}$) corresponds to the mean relative failure rate or to the share of elements which failed before reaching the maximum system strength $f_{N,max}$. The failure rates are very small and increase with

increasing CoV[E_1], for example to about 14% at CoV[E_1] = 50% and N = 100. Consequently, only a small amount of elements can fail before no further load increase is possible and the maximum system strength is reached.

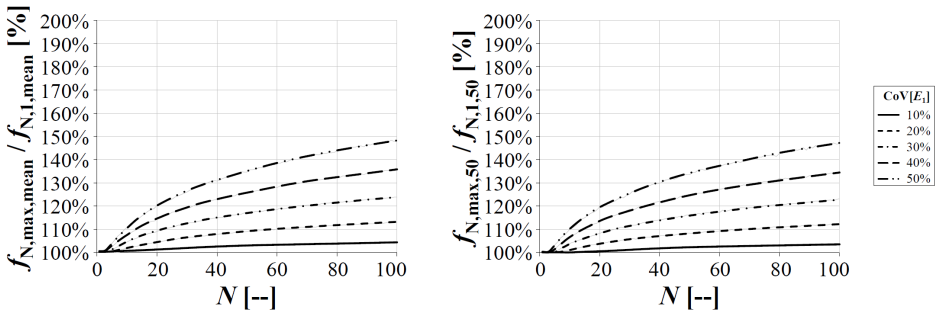

Fig. 3.41: Ratio between mean of maximum system strength and mean system stress at first failure (left) and between median of maximum system strength and median system stress at first failure (right) vs. N and in dependency of CoV[E_1]

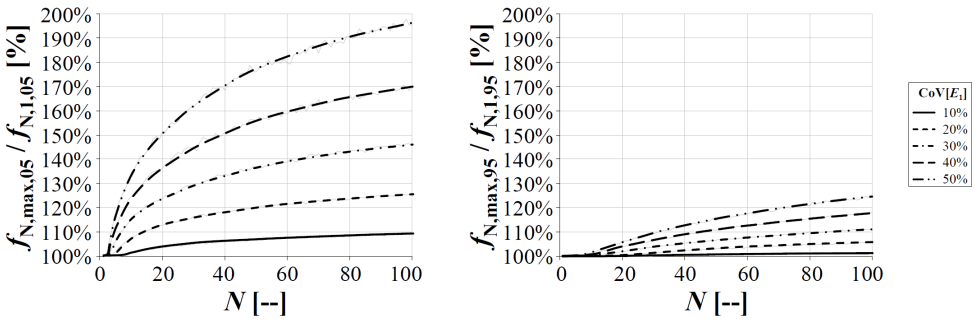

Fig. 3.42: Ratio between 5%-quantile of maximum system strength and 5%-quantile of system stress at first failure (left) and between 95%-quantile of maximum system strength and 95%-quantile of system stress at first failure (right) vs. N in dependency of CoV[E_1]

Fig. 3.41 and Fig. 3.42 visualise the extra reserves in parallel systems between the system capacity at first failure and the maximum system strength. Once again the ratios are higher the lower the analysed quantile-level. This is true in absolute and relative values.

In a next step the system reliability is examined in more detail. For simplification, both, action (A) and resistance (R) were modelled by a 2pLND.

In general, system reliability is equal to the probability of survival P_S given as

$$P_S = 1 - P_f\,, \tag{3.135}$$

with P_f as the probability of failure.

A measure for reliability in the special case of $R, A \sim$ ND is given by the reliability index β which is simply defined in relationship to P_f, see

$$P_f = \Phi(-\beta), \tag{3.136}$$

with $\Phi(.)$ as the CDF operator of the SND.

Given a limiting function

$$g = R - A\,, \tag{3.137}$$

with the events "failure" and "survival" at $g \leq 0$ and $g > 0$, respectively, and $P_f = P(g \leq 0)$ and $R, A \sim \mathrm{ND}(\mu, \sigma^2)$ the reliability index β can be simply calculated as

$$\beta = \frac{\mu_g}{\sigma_g}\,, \text{ with } g \sim \mathrm{ND}(\mu_R - \mu_A, \sigma^2_R + \sigma^2_A). \tag{3.138}$$

In case of $R, A \sim$ 2pLND the reliability index β can be in principle derived equally by means of expectation and variance of the logarithmised variables.

The advantage in analysing β or P_S instead of characteristics like mean or CoV is because these values contain information of the whole distribution.

Before the calculation procedure for β can be applied it was verified that the assumption that $f_{N,1}$, $f_{N,max}$ are iid lognormal distributed can be sufficiently secured. This verification was done successfully via qualitative judgement by means of qq-plots.

Fig. 3.43 (left) gives the ratio β_N / β_1 vs. N and analysis the resistance of systems at first failure ($f_{N,1}$) and at the point of maximum system strength capacity ($f_{N,max}$). Thereby β at $N = 1$ was fixed at 4.2 which corresponds to a probability of failure $P_f = 1.33 \cdot 10^{-5}$. A distinctive decrease in reliability is visible meaning that by equal action the reliability of the system decreases with increasing N. For the design of systems at given action the required mean system strength ($f_{N,1,mean}$ and $f_{N,max,mean}$) at given β, CoV[E_1] and Var[$f_{N,1}$] or

Var[$f_{N,max}$] to guarantee a constant reliability index of $\beta = 4.2$ was calculated. The results are shown in Fig. 3.43 (right). Compared to Fig. 3.37 the decrease of the useable percentage of $f_{N,1,mean}$ for keeping β constant is even higher. This is due to the fact that together with the mean also the variability of system strength decreases. Due to the decrease in CoV[f_N] the probability mass gets closer to the action. Consequently an additional decrease in resistance is given if not corrected properly.

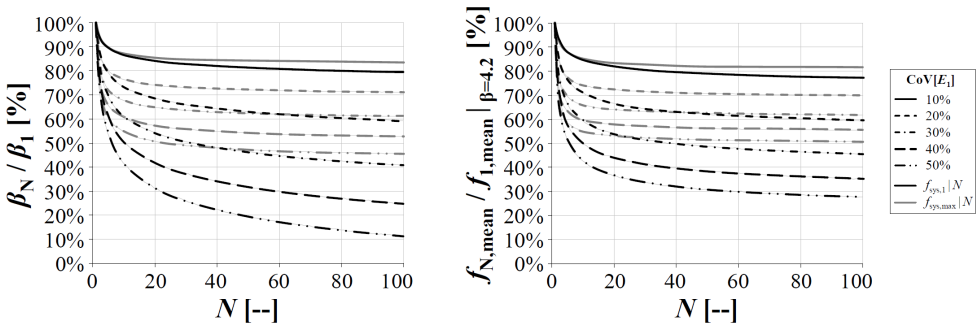

Fig. 3.43: Relative safety index β_N vs. N (left) and required ratio between mean maximum system strength and mean strength of elements for constant safety index of $\beta = 4.2$ vs. N (right) in dependency of CoV[E_1]

After the examination of relative changes in important statistics of the system strength and E-modulus it is now the aim to define and verify a model for at least the computation of system strength and E-modulus at the first failure. As already previously mentioned the system E-modulus $E_{N,1}$ follows the averaging model given in equ. (3.132). In respect to modelling of system strength $f_{N,1}$ the right hand side of equ. (3.133) can be split into two parts: The left part corresponds to the mean E-modulus of all elements in the system. This mean value follows the averaging model above mentioned. The right part represents the minimum of the ultimate strain of all elements in the system. As the ultimate strain also follows a 2pLND (see equ. (2.85)) it is possible to make use of the model defined in section 3.3.2, equ. (3.102) and Tab. 3.2. Thereby the distribution of min[$\varepsilon_{f,i}$] can be well approximated by a 2pLND. Having now estimates for min[$\varepsilon_{f,i}$] ~ 2pLND and $E_{N,1,mean}$ ~ 2pLND the distribution parameters of $f_{N,1}$ ~ 2pLND can be simply calculated by means of equ. (2.91). Thereby the correlation $\rho(E_{N,1}, \varepsilon_{f,N,1})$ has to be considered. As mentioned earlier the correlation at $N = 1$ is by default $\rho(E_1, \varepsilon_{f,1}) = -1.00$. Due to the fact that $E_{N,1}$ equals the mean value of all $E_i \mid N$ and $\varepsilon_{f,N,1}$ the minimum of all $\varepsilon_{f,i} \mid N$ the correlation fulfills the inequality $|\rho(E_{N,1}, \varepsilon_{f,N,1})| \leq |\rho(E_1, \varepsilon_{f,1})|$. This circumstance is illustrated in Fig. 3.44 (left). Thereby the transformation of the observed correlation

coefficient from simulations to normal domain is considered by use of reformulated equ. (2.89). The relationship shows a nonlinear decrease of the absolute correlation which shows also a dependency on CoV[E_1]. This nonlinear decrease was found to be roughly explainable by a simple logarithmic model given as

$$\rho\left(E_{N,1},\varepsilon_{f,N,1}\right)=k_{\rho(E,\varepsilon)}\cdot\ln\left(N\right)-1.00\,, \tag{3.139}$$

with $k_{\rho(E,\,\varepsilon)}$ as free parameter. This parameter was found to decrease approximately linearly with CoV[E_1] and can thus estimated by (see also Fig. 3.44, right)

$$k_{\rho(E,\varepsilon)}=-0.1701\cdot CoV\left[E_1\right]+0.1766\,. \tag{3.140}$$

The results of estimated $\rho(E_{N,1}, \varepsilon_{f,N,1})$ fitted to observed values of $\rho(E_{N,1}, \varepsilon_{f,N,1})$ are already given in Fig. 3.44 (left). These estimates appear sufficiently accurate for low CoV[E_1] and moderate system sizes. As the constraint $\lim_{N\to\infty}\rho(E_{N,1}, \varepsilon_{f,N,1}) \to 0.00$ is not fulfilled by equ. (3.139) in combination with (3.140) the formula may not be applied to systems with $N > 100$ and CoV[E_1] > 50%.

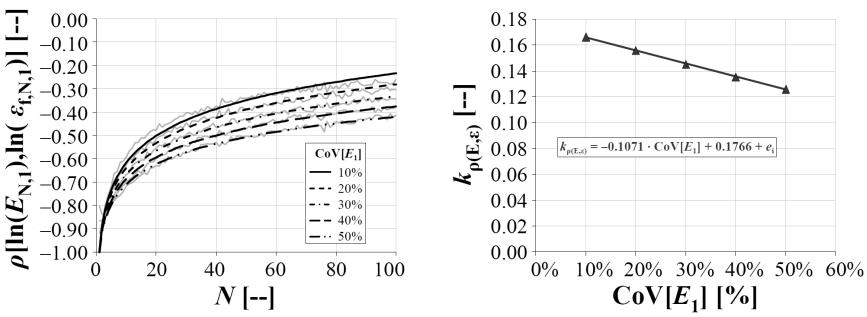

Fig. 3.44: Correlation between E-modulus and extension vs. N and in dependency of E_1 (thin graphs: simulation results; bold functions: model calculations) (left) and parameter $k_{\rho(E,\varepsilon)}$ vs. CoV[E_1] (right)

The relative deviations between the model calculations and the simulation results are visualised in Fig. 3.45 (mean and standard deviation) and Fig. 3.46 (5%- and 95%-quantiles). Overall absolute deviations increase with increasing CoV[E_1] but are not higher than 6%, despite the estimation of standard deviation of very small systems. The congruence between simulated and model results is in particular given on the mean level. Deviations in extreme quantiles are a bit higher and influenced by the bias of the

estimated standard deviation. Over all the combination of simple models enables a relatively fast and accurate estimation of the strength potential and its distribution of the analysed type of parallel systems.

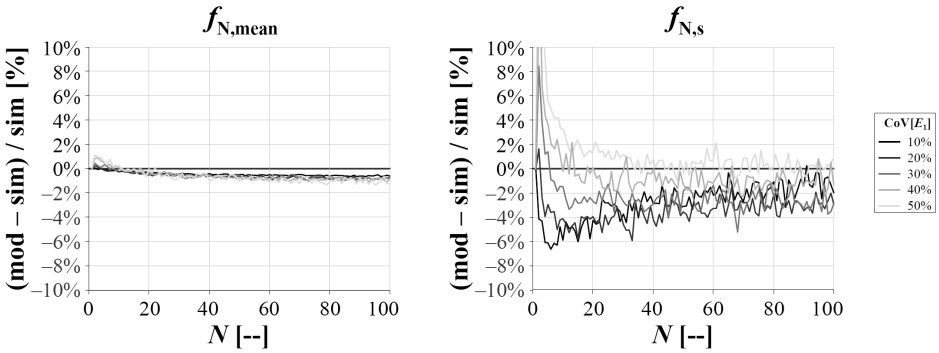

Fig. 3.45: Relative bias between model and simulation results vs. N in respect to mean system strength (left) and standard deviation of system strength (right) and in dependency of E_1

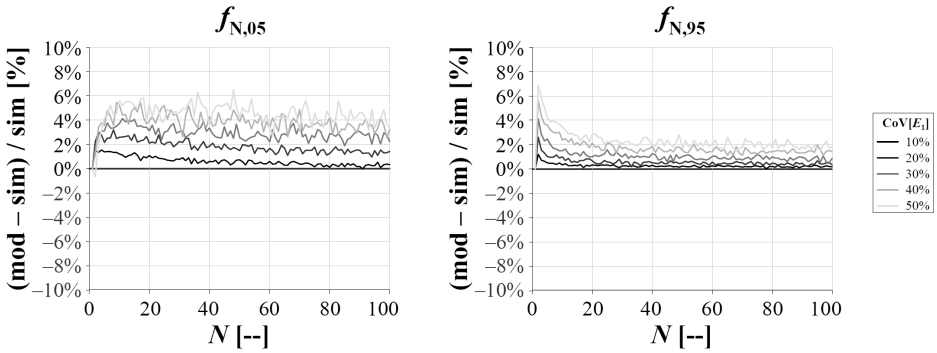

Fig. 3.46: Relative bias between model and simulation results vs. N in respect to 5%- (left) and 95%-quantile of system strength (right) and in dependency of E_1

To conclude, case II of a parallel system bounded in strength of the elements is again a very specific system type. The simulated results gained from GLS assumption show a remarkable decrease in mean strength potential with increasing N and CoV[E_1] if system failure is defined with failure of the first element characterised by max[$E_i \mid N$] or min[$\varepsilon_{f,i} \mid N$]. If system strength is defined as the maximum system stress a moderate decrease down to some kind of constant mean strength potential can be observed. A conversely behaviour can be observed in CoV[$f_{N,1}$] and CoV[$f_{N,max}$]. Of course, the share of elements in the system which are expected to fail before the maximum system strength

is reached is low. Nevertheless, the gain in bearing potential between first failure and maximum is remarkable and about 95% in the 5%-quantile of systems with $N = 100$ and CoV[E_1] = 50%. Despite this remarkable extra safety margin reliability index calculations show that in this type of system mean strength has to be reduced even more than expected from observed mean values to keep a certain safety level at increasing N. Additionally a simple model was presented which estimates system strength capacity as well as the distribution of system E-modulus at first system failure. Overall good congruence between model and simulation results could be observed.

3.4.3 Analysis concerning Case III: E_1 = constant

Case III describes the ideal situation of a parallel acting system composed of elements with random strength f_1 and random ultimate strain $\varepsilon_{f,1}$ but deterministic E-modulus $E_1 = E =$ constant assuming perfect linear-elastic material behaviour (see Fig. 3.47 and Fig. 3.48). These conditions form the basis of DANIELS (1945) analysis regarding fibre bundle models (FBMs) and his famous asymptotic result of bundle strength distribution in case of GLS (see section 3.2.3).

As already proposed by DANIELS (1945) ranking the elements in respect to strength or ultimate strain in ascending order with $(f_{(1)}, \varepsilon_{f,(1)}) \leq (f_{(2)}, \varepsilon_{f,(2)}) \leq \ldots \leq (f_{(N)}, \varepsilon_{f,(N)})$ the system strength in case of GLS is given by

$$f_{N,\max} = \max_k \left[f_{N,(k)} \right] = \frac{1}{N} \cdot \max_k \left[(N-k+1) \cdot E \cdot \varepsilon_{f,(k)} \right] = \frac{1}{N} \cdot \max \left[(N-k+1) \cdot f_{(k)} \right] , \quad (3.141)$$

with $k = 1, 2, \ldots, N$ as amount of failed elements and $(N - k + 1)$ as quantity of survivors.

In line with previous section 3.4.2 Monte-Carlo simulations were performed in R (2009) to generate data for the analysis of the system behaviour in dependency of CoV[f_1] and N and in respect to the definition of system strength, (1) as system stress at first failure, and (2) as maximum of all analysed system stresses per system. Following default settings are given: E[f_1] = 30, E[E_1] = E_1 = E = 10,000, iid $f_1 \sim$ 2pLND, CoV[f_1] = (10, 20, …, 50)%, N = 1, 2, …, 100 and n = 10,000 simulations per system configuration. The only variable parameter was CoV[f_1]. This parameter also directly determines CoV[$\varepsilon_{f,1}$]. The analysis of the simulated data is presented by the following figures.

ad III) *E* = const.

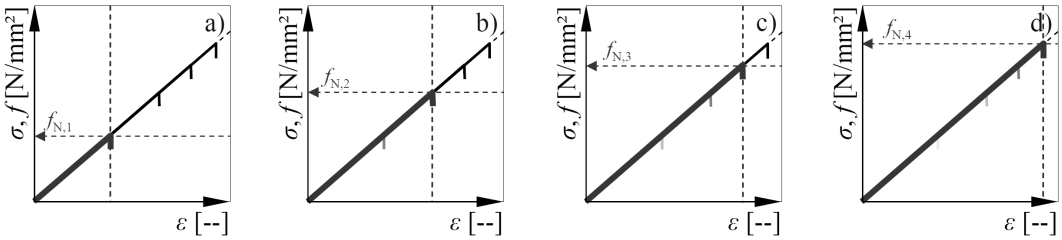

Fig. 3.47: Case III, E_1 = deterministic: expected stress-strain relationship of parallel systems (bold, red graph) composed exemplarily of four elements (thin graphs) assuming in principal an element-wise failure scenario (from left to right)

ad III) *E* = const.

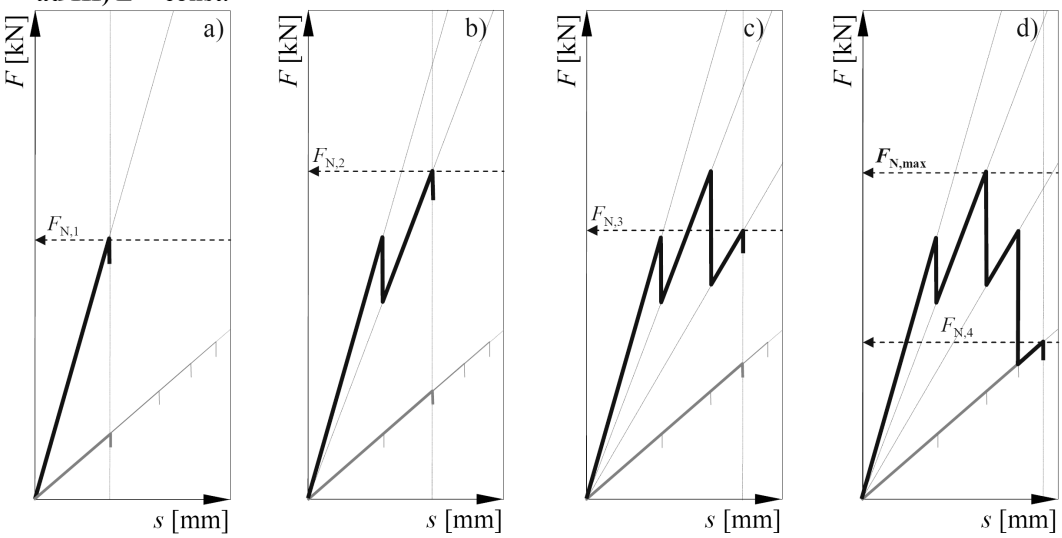

Fig. 3.48: Case III, E_1 = deterministic: expected load-elongation relationship of parallel systems (bold, blue graph) composed exemplarily of four elements (thin graphs; including also stress-strain relationship) assuming in principal an element-wise failure scenario (from left to right)

Fig. 3.49 (left) gives the relative change in $f_{N,1,mean}$ and $f_{N,max,mean}$ in dependency of N and CoV[f_1]. In comparison to Fig. 3.37 in section 3.4.2 it can be seen that the relative reduction in $f_{N,1,mean}$ is in case III even a bit higher than in case II. Nevertheless, the amount of reduction in $f_{N,max,mean}$ is in both cases comparable. The relative influence of N and CoV[f_1] on CoV[$f_{N,1}$] and CoV[$f_{N,max}$] is shown in Fig. 3.49 (rigth). Whereas CoV[$f_{N,1}$] / CoV[f_1] versus N appears to be nearly independent of CoV[f_1],

CoV[$f_{N,max}$] / CoV[f_1] versus N shows firstly a higher relative decrease and secondly a dependency on CoV[f_1] which seems to diminish with increasing CoV[f_1]. The significant higher decrease in CoV[$f_{N,max}$] if compared to CoV[$f_{N,1}$] follows from successive reduction in respect to ultimate strain or strength ordered elements before the maximum system strength is reached.

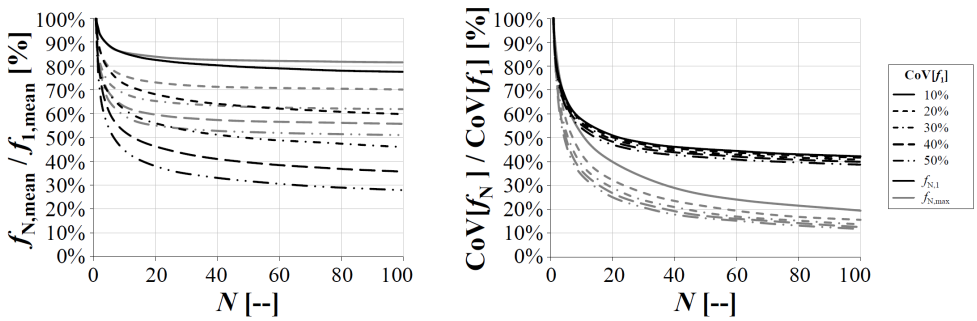

Fig. 3.49: Relative mean system strength vs. N (left) and relative CoV[f_N] vs. N (right) at first failure and at maximum system strength in dependency of CoV[f_1]

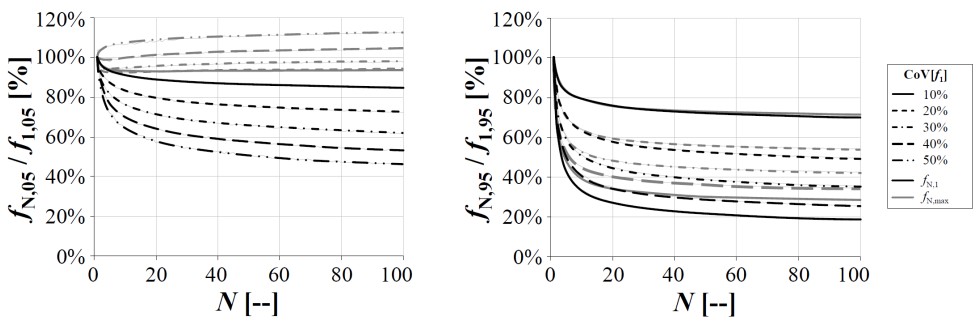

Fig. 3.50: Relative 5%- (left) and relative 95%-quantiles (right) of system strength at first failure and at maximum system strength in dependency of CoV[f_1]

Fig. 3.50 contains graphs of the relative change of 5%- and 95%-quantiles of system strength at first failure and at the point of maximum system strength. Due to the significant decrease in CoV[$f_{N,1}$] the decrease of $f_{N,1,05}$ in case III is not as high as in case II. Nevertheless, as the relative change of $f_{N,1,mean}$ is comparable in both cases the reduction in $f_{N,1,95}$ in case III is higher than in case II. Of course, these results are true if the system strength is defined by the system stress at first failure of the first element. By examination of the maximum system strength only a minor reduction and even an increase in $f_{N,max,05}$ / $f_{1,05}$ can be observed with increasing N and in particular with

increasing CoV[f_1]. This is due to the fact that despite the remarkable decrease of $f_{N,max,mean}$ this type of system offers a relatively high potential of load redistribution followed by further potential of stress increase in the remaining system. This becomes in particular obvious in Fig. 3.51 which corresponds more or less to the mean failure rate relative to N at the point of $f_{N,max}$.

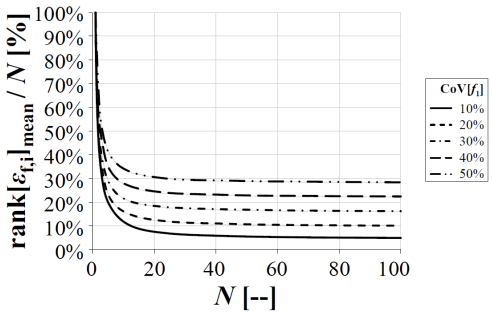

Fig. 3.51: Relative mean rank of ε_i at given N and at maximum system strength vs. N and in dependency of CoV[f_1]

Compared to Fig. 3.40 of system case II (section 3.4.2) the amount of elements which can be expected to fail before the maximum system strength is reached is more than doubled. This remarkable share of elements which are expected to fail without loss in system strength capacity leads on the one hand to an outstanding reduction in CoV[$f_{N,max}$] and on the other hand also to a remarkable increase in $\varepsilon_{f,N,max}$. The possibility of higher extensions in systems compared to elements enables e.g. monitoring for warning before a system gets out of control. Thereby the system E-modulus behaves unaffected but the stiffness decreases linearly with each further element failure.

Fig. 3.52 and Fig. 3.53 outline the additional system potential $f_{N,max} / f_1$ versus N and CoV[f_1] on the mean, median and 5%- and 95%-quantile level, respectively, and in dependency of CoV[f_1].

As introduced in the previous section 3.4.2 again the safety index β_N in relationship to $\beta_1 = 4.2$ versus N and in dependency of CoV[f_1] was calculated. Fig. 3.54 (left) shows the results for $f_{N,1}$ and $f_{N,max}$. Even if only $f_{N,1}$ is considered a slight increase in reliability of parallel systems can be achieved if N is small and CoV[f_1] is high. Furthermore, the decrease in reliability in case III is negligible if compared to that of case II and appears to be nearly independent of CoV[f_1] if CoV[f_1] $\geq$ 20%. Nevertheless, by analysing the reliability of parallel systems of type III by $f_{N,max}$ a remarkable increase can be observed

for CoV[f_1] ≥ 30%. Consequently, if a certain reliability has to be fulfilled the mean resistance of $f_{N,1}$ has to be decreased to about 70% of $f_{1,mean}$ in case of $N = 100$ and CoV[f_1] ≥ 20%, whereas $f_{N,max,mean}$ can be increased, e.g. by a factor of about 1.65 in case of CoV[f_1] = 50% and $N \geq 30$.

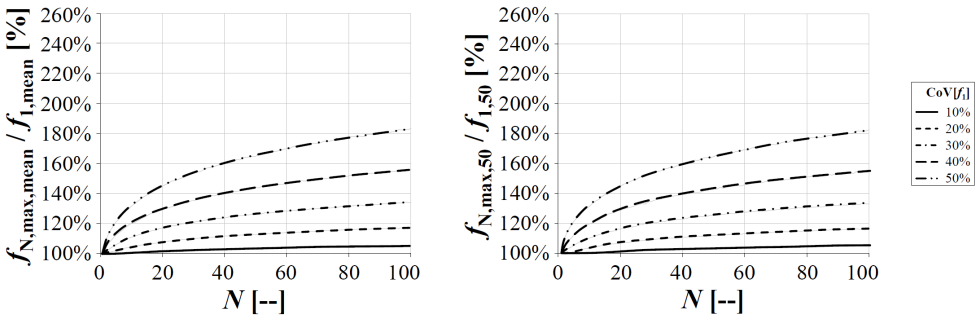

Fig. 3.52: Ratio between mean of maximum system strength and mean system stress at first failure (left) and between median of maximum system strength and median system stress at first failure (right) vs. N and in dependency of CoV[f_1]

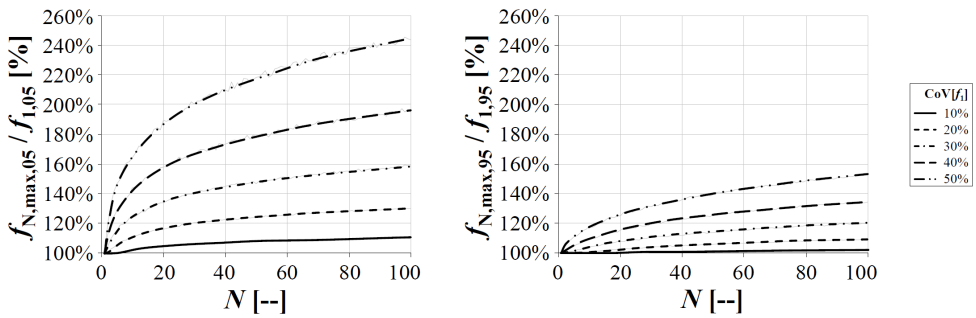

Fig. 3.53: Ratio between 5%-quantile of maximum system strength and 5%-quantile of system stress at first failure (left) and between 95%-quantile of maximum system strength and 95%-quantile of system stress at first failure (right) vs. N and in dependency of CoV[f_1]

At the end and in line with the analysis of case II a comparable model for computation of the distribution and parameters of $f_{N,1}$ in dependency of N and CoV[f_1] was formulated and verified. The model requirements are even a bit simplier because E_1 is deterministic and so the distribution of $E_{N,mean}$. Consequently, the same procedure for computation of $f_{N,1}$ as presented in section 3.4.2 can be applied but without consideration of $\rho(E_{N,1}, \varepsilon_{f,N,1})$. The output of the model as relative deviation from simulation results from mean, standard

deviation and 5%- and 95%-quantile is shown in Fig. 3.55 and Fig. 3.56, respectively. In case of larger systems ($N \geq 20$) the results of case II and case III are nearly equal.

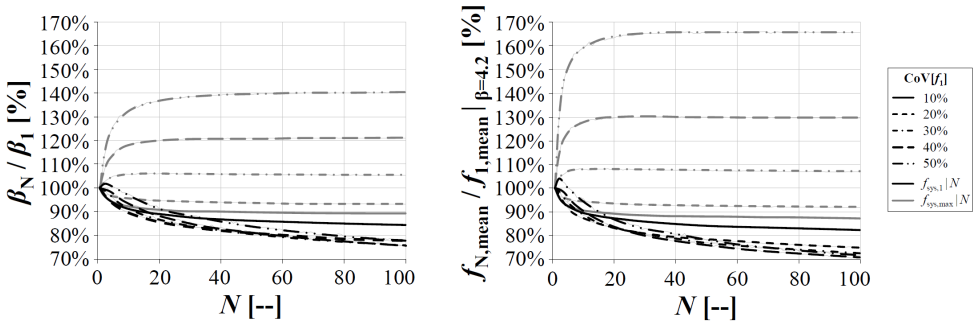

Fig. 3.54: Relative safety index β_N vs. N (left) and required ratio between mean maximum system strength and mean strength of elements for constant safety index of $\beta = 4.2$ vs. N (right) in dependency of CoV[f_1]

To conclude, the examinations in regard to case III show again a remarkable influence of CoV[f_1] which directly determines also CoV[$\varepsilon_{f,1}$]. Despite a comparable decrease in $f_{N,1,mean}$ and $f_{N,max,mean}$ but due to the significant decrease in CoV[$f_{N,1}$] and in particular in CoV[$f_{N,max}$] an increase in reliability could be verified. This increase is due to the remarkable decrease of CoV[$f_{N,max}$] which reaches nearly that of the averaging model. This decrease follows from the relatively high expectable failure rate of elements before the system reaches its maximum strength. At the end a simple model for estimating the distribution of $f_{N,1}$ was successfully verified. This model enables a fast computation with deviations from simulation data in a range comparable with case II.

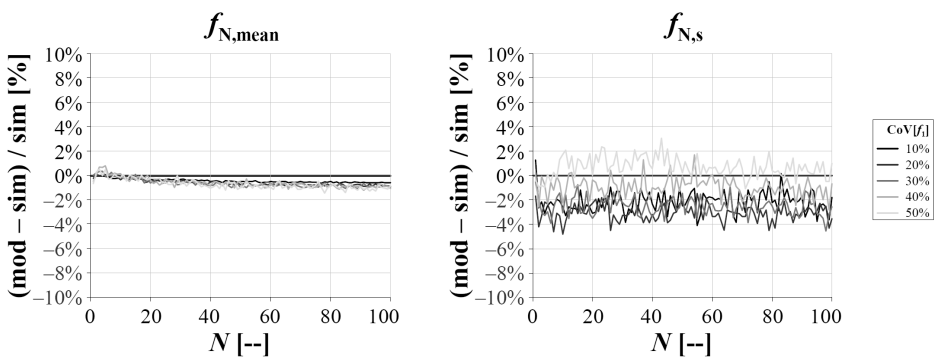

Fig. 3.55: Relative bias between model and simulation results vs. N in respect to mean system strength (left) and standard deviation of system strength (right) and in dependency of f_1

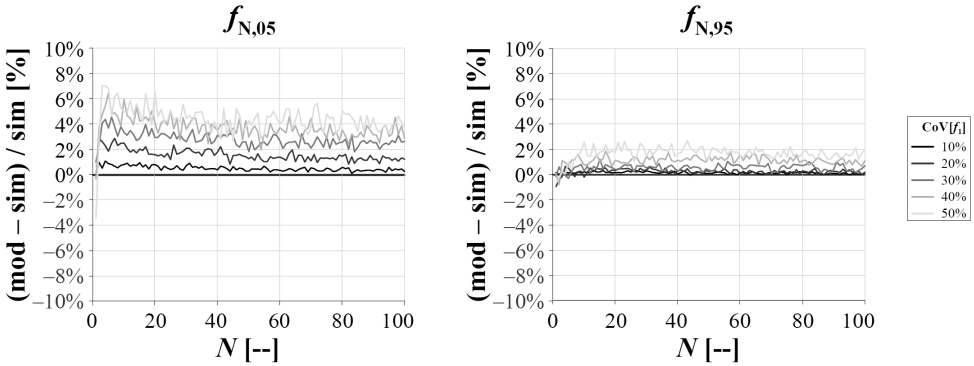

Fig. 3.56: Relative bias between model and simulation results vs. N in respect to 5%- (left) and 95%-quantile of system strength (right) and in dependency of f_1

3.4.4 Analysis concerning Case IV: General Case

Within case IV a more general behaviour of parallel systems composed of iid and perfect linear-elastic brittle elements is examined. Thereby a quasi static failure process is assumed which enables the ability of load redistribution after partial failure. Intermediate steady states in load redistribution within the system are in principle possible until it finally fails. These steady states should be reachable even under step-wise progressing load enhancements. Therefore all three parameters of HOOK's law, the element strength f_1, the E-modulus E_1 and the ultimate strain $\varepsilon_{f,1}$ are treated as random but correlated variables (see Fig. 3.57 and Fig. 3.58).

ad IV) general case

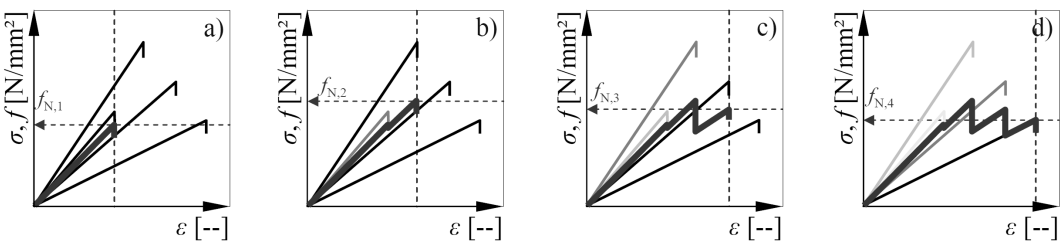

Fig. 3.57: Case IV, general case: expected stress-strain relationship of parallel systems (bold, red graph) composed exemplarily of four elements (thin graphs) assuming in principal an element-wise failure scenario (from left to right)

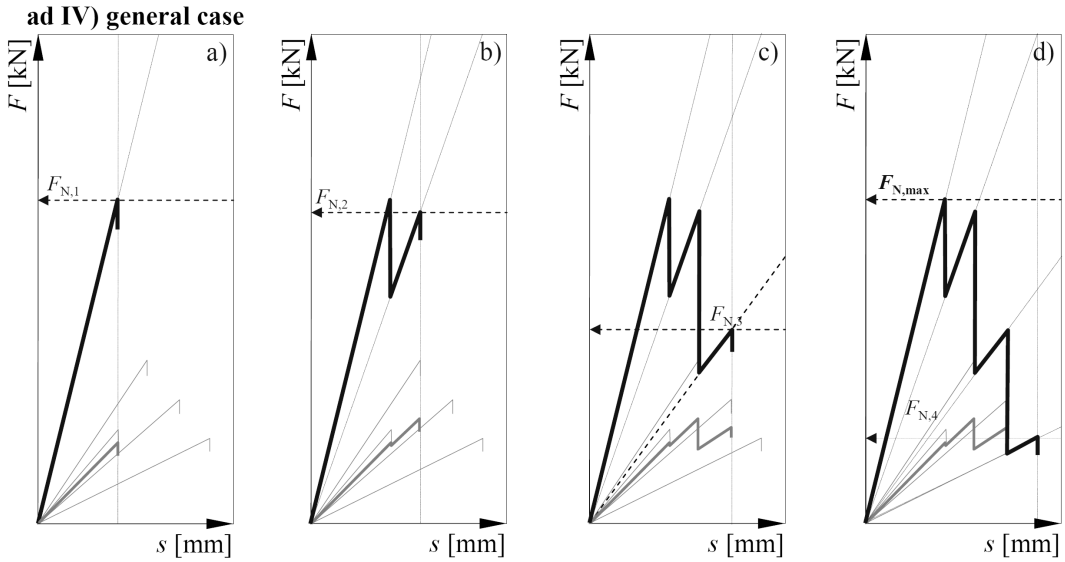

Fig. 3.58: Case IV, general case: expected load-elongation relationship of parallel systems (bold, blue graph) composed exemplarily of four elements (thin graphs; including also stress-strain relationship) assuming in principal an element-wise failure scenario (from left to right)

The first partial failure is caused by the element with lowest ultimate strain which does not necessarily confirm with the element with highest E-modulus. Consequently, if the system strength is defined as first failure strength it is given as

$$f_{N,1} = \frac{1}{N} \cdot \sum_{i=1}^{N} \sigma_i \Big|_{\min\limits_N(\varepsilon_{f,i})} = \frac{1}{N} \cdot \sum_{i=1}^{N} E_i \cdot \min\left[\varepsilon_{f,i}\right] = \frac{1}{N} \cdot \sum_{i=1}^{N} E_i \cdot \min\left[\frac{f_i}{E_i}\right]. \tag{3.142}$$

By ranking the elements in ascending order according their ultimate strain $\varepsilon_{f,i}$ (or descending according E_i) so that $\varepsilon_{f,(1)} \leq \varepsilon_{f,(2)} \leq \ldots \leq \varepsilon_{f,(N)}$ $(E_{(1)} \geq E_{(2)} \geq \ldots \geq E_{(N)})$ the maximum system strength in case of GLS is defined by

$$f_{N,\max} = \max_k \left[f_{N,(k)}\right] = \frac{1}{N} \cdot \max_k \left[\sum_{j=k}^{N} E_{(j)} \cdot \varepsilon_{f,(k)}\right] = \frac{1}{N} \cdot \max_k \left[\sum_{j=k}^{N} E_{(j)} \cdot \frac{f_{(k)}}{E_{(k)}}\right], \tag{3.143}$$

with $k = 1, 2, \ldots, N$ as the amount of partial failures, $(N - k + 1)$ as the amount of intact elements after k failures and $E_{(j)}$ as E-modulus associated with $\varepsilon_{f,(j)}$. These equations are equal to that of case II, see equ. (3.133) and (3.134).

Global Load Sharing (GLS) – Simulations and Conclusions

Within this section only the case of global load sharing (GLS) is discussed. It is assumed that the stresses released by failed elements are uniformly distributed on survivors irrespective of the relative position of survivors to failed elements. For analysis of parallel system effects in case IV and in line with previous sections 3.4.2 and 3.4.3 Monte-Carlo simulations were performed in R (2009). To examine systems in dependency of CoV[f_1] and N data sets were generated and collected for statistical analysis in respect to the definition of system strength, (1) as system stress at first failure, and (2) as maximum of all analysed system stresses per system. Following settings were used: iid element strength $f_1 \sim$ 2pLND with E[f_1] = 30 and CoV[f_1] = (10, 30, 50)%, iid E-modulus of elements $E_1 \sim$ 2pLND with E[E_1] = E_1 = E = 10,000 and CoV[E_1] = (10, 30, 50)%, correlation between strength and E-modulus with $\rho(f_1, E_1)$ = (0.00, 0.25, 0.50, …, 1.00), system size N = 1, 2, …, 100 and n = 10,000 simulations per system configuration. Default settings which were kept constant for analysis of the influence of a specific parameter are given in grey.

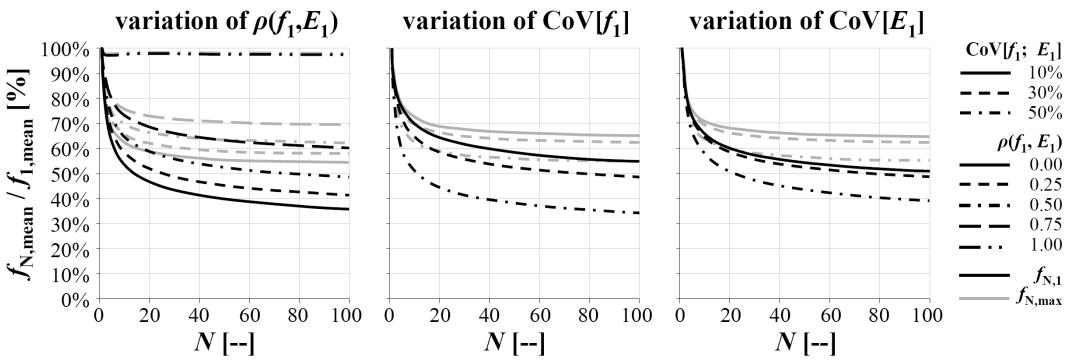

Fig. 3.59: Relative mean of system strength at first failure and of maximum system strength in dependency of $\rho(f_1, E_1)$ (left), CoV[f_1] (middle) and CoV[E_1] (right) and N; GLS

Fig. 3.59 shows the relative change in mean system strength versus system size N and in dependency of parameters $\rho(f_1, E_1)$ (left), CoV[f_1] (middle) and CoV[E_1] (right). Results for both, strength at first element failure and for the maximum system strength are given. Thereby $f_{N,mean} / f_{1,mean}$ increases progressively with increasing $\rho(f_1, E_1)$. This behaviour is more pronounced in $f_{N,1,mean}$ than in $f_{N,max,mean}$. The increase is moderate up to $\rho(f_1, E_1) \leq 0.75$ and the decrease in mean maximum system strength much lower than at first system failure. In particular at $\rho(f_1, E_1) \leq 0.50$ the influence of $\rho(f_1, E_1)$ on $f_{N,max,mean}$ is

nearly negligible. Concerning the influence of CoV[f_1] and CoV[E_1] on $f_{N,1,mean}$ and $f_{N,max,mean}$ it can be concluded that (1) the influence of CoV[f_1] is stronger than of CoV[E_1], (2) the decrease in $f_{N,1,mean}$ / $f_{1,mean}$ and $f_{N,max,mean}$ / $f_{1,mean}$ increases progressively with increasing CoV[f_1] and / or CoV[E_1], and (3) influence of CoV[f_1] is by default higher for higher variability. Consequently, the higher the correlation between E-modulus and strength of elements and the lower the values CoV[f_1] and CoV[E_1] the lower the reduction in $f_{N,mean}$ / $f_{1,mean}$.

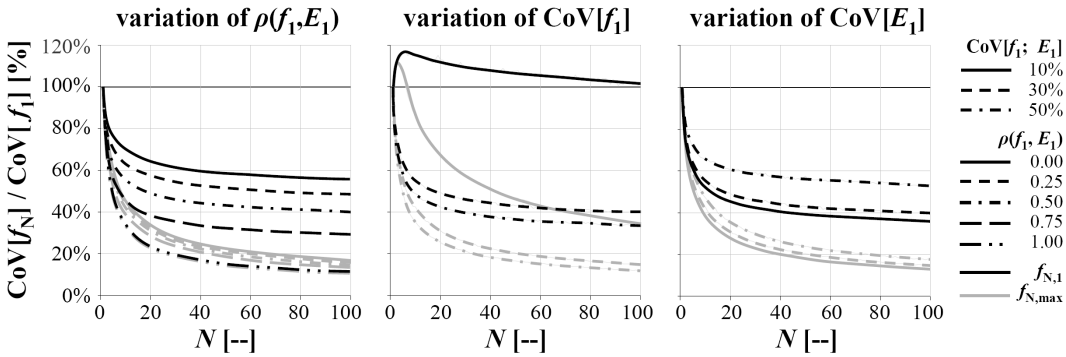

Fig. 3.60: Relative CoV of system strength at first failure and of maximum system strength in dependency of $\rho(f_1, E_1)$ (left), CoV[f_1] (middle) and CoV[E_1] (right) and N; GLS

The relative changes in CoV[f_N] are given in Fig. 3.60. Again, the influence of $\rho(f_1, E_1)$, CoV[f_1], CoV[E_1] and N on the system strength are analysed. Thereby a concave and up to $\rho(f_1, E_1) \leq 0.75$ a nearly linear progression in decrease of CoV[$f_{N,1}$] / CoV[f_1] with increasing $\rho(f_1, E_1)$ can be observed followed by a remarkable increase between $\rho(f_1, E_1) = 0.75$ and $\rho(f_1, E_1) = 1.00$. At $\rho(f_1, E_1) = 1.00$ the decrease in CoV[$f_{N,1}$] / CoV[f_1] follows the averaging model for CoV[X_N]. The influence of $\rho(f_1, E_1)$ on CoV[$f_{N,max}$] is more or less negligible. In contrast, variation of CoV[f_1] influences CoV[f_N] remarkably. In particular if CoV[f_1] < CoV[E_1] even an increase in CoV[f_N] can be observed which decreases moderately after a peak in CoV[$f_{N,1}$] and falls down suddenly in case of CoV[$f_{N,max}$]. If CoV[f_1] ≥ CoV[E_1] the influence on CoV[$f_{N,1}$] and CoV[$f_{N,max}$] is only moderate but leads to a progressive decrease of CoV[f_N], in particular of CoV[$f_{N,max}$]. This can be explained by the fact that higher variability of strength between the elements enables a higher proportion of partial failures which leads to a successive reduction in system size and thus in variability of element stresses at a given ultimate system extension. With CoV[f_1] = 50% and the rest of parameters with default settings the decrease in CoV[$f_{N,max}$] / CoV[f_1] reaches nearly that of the averaging model for CoV[X_N].

In contrast, Fig. 3.60 (right) analysis the influence of CoV[E_1] on CoV[f_N] which shows a contrary behaviour to CoV[f_1]. It can be observed that a variability in E_1 corresponds to a relative reduction in CoV[f_N]. This is in particular given for CoV[$f_{N,1}$] but minor for CoV[$f_{N,max}$]. Thereby ratio CoV[$f_{N,max}$] / CoV[f_1] reaches nearly the averaging model for CoV[X_N] at CoV[E_1] = 10%. The influence of increasing CoV[E_1] appears convex. To conclude, the higher the reduction in CoV[f_N] the higher the homogenisation effect and thus the utilisable amount of positive system effects. Thus a maximum of positive system effects are reached by combination of a high correlation $\rho(f_1, E_1)$, a high CoV[f_1] but a low CoV[E_1], in particular with the constraint that CoV[f_1] ≥ CoV[E_1].

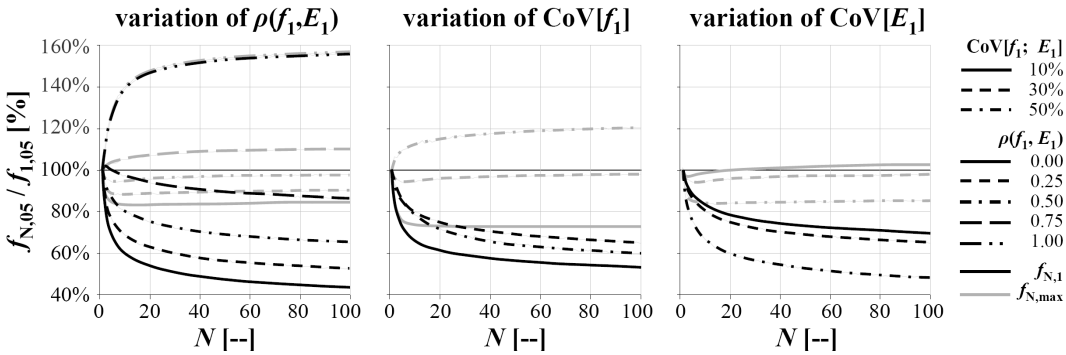

Fig. 3.61: Relative 5%-quantile of system strength at first failure and of maximum system strength in dependency of $\rho(f_1, E_1)$ (left), CoV[f_1] (middle) and CoV[E_1] (right) and N; GLS

Due to the fact that in current semi-probabilistic concepts 5%-quantiles of strength characteristics are taken as basis for design calculations the relative change of 5%-quantiles of system strength are given in Fig. 3.61 and analysed in respect to the influence of parameters $\rho(f_1, E_1)$, CoV[f_1] and CoV[E_1]. Discussing first the influence of correlation $\rho(f_1, E_1)$ on $f_{N,05}$ it can be observed that a maximal increase in $f_{N,05} / f_{1,05}$ is given at $\rho(f_1, E_1) = 1.00$. Even at $\rho(f_1, E_1) = 0.75$ an increase in $f_{N,05,max}$ with increasing N can be expected. The decrease in $f_{N,05,max}$ at lower values of $\rho(f_1, E_1)$ is moderate and not more than roughly 15%. Thereby a slight increase of $f_{N,05,max}$ at $\rho(f_1, E_1) = 0.00$ and $N \geq 5$ can be observed. Nevertheless, $f_{N,1,05}$ decreases remarkable with decreasing $\rho(f_1, E_1)$ and increasing N. Thereby a reduction of $f_{N,1,05}$ of roughly 57% at $\rho(f_1, E_1) = 0.00$ and $N = 100$ if compared to $f_{N,05}$ can be observed. In Fig. 3.61 (middle), which analysis the influence of CoV[f_1] on $f_{N,05,1}$, it can be seen that the change of characteristics in 2pLND at CoV[X] = 30% (see Fig. 3.2, right) lead to the effect that the decrease in $f_{N,05,1}$ at CoV[f_1] = 30% is lower than at CoV[f_1] = 10% or 50%. This effect is not visible in

$f_{N,05,max}$. In contrast to all beforehand discussed figures CoV[f_1] shows to effect $f_{N,05,max}$ more than $f_{N,05,1}$. Again $f_{N,05,max}$ can be increased by a CoV[f_1] > 30%, with $f_{N,05,max} / f_{1,05} \approx 1.00$ at CoV[f_1] = 30%. Parameter CoV[E_1] acts inversely to CoV[f_1] and provokes higher values of $f_{N,05,max}$ or in general a lower decrease of $f_{N,05}$ if CoV[E_1] is small. Increasing CoV[E_1] initiates a progressive and increasing effect on $f_{N,05} / f_{1,05}$. Consequently, a high correlation factor $\rho(f_1, E_1)$, high but not too high CoV[f_1] and low CoV[E_1] influence $f_{N,05}$ positively.

Fig. 3.62 shows the relative change of $E_{N,mean}$ in dependency of $\rho(f_1, E_1)$, CoV[f_1], CoV[E_1] and N. Thereby $E_{N,mean,1} = E_{1,mean}$ is by default explained by the averaging model. As a consequence of successively failing elements until the maximum strength in parallel systems is reached $E_{N,mean,max}$ is affected by $\rho(f_1, E_1)$, CoV[f_1] and CoV[E_1] and shows by default a reduction in expectation. This loss in stiffness is more pronounced at low $\rho(f_1, E_1)$ and / or low CoV[f_1] and / or high CoV[E_1]. Thereby low correlation and high CoV[E_1] enables a higher amount of partial system failures and thus a successive failure of stiffer elements. The same is true for low values of CoV[f_1] in combination with a higher CoV[E_1]. Consequently, a reduction in $E_{N,mean}$ is positive in case of parallel, redundant structures were sub-systems or system products can transfer stresses to adjacent stiffer sub-systems. This structural behaviour can be supported by activating some plastic behaviour at the hinges and perhaps utilised for advanced warning before a structure gets out of control, e.g. by exceedance of beforehand regulated deformation limits. If a reduction in $E_{N,max,mean}$ can not be allowed for some reasons it is recommended to keep $\rho(f_1, E_1)$ and CoV[f_1] high but CoV[E_1] low.

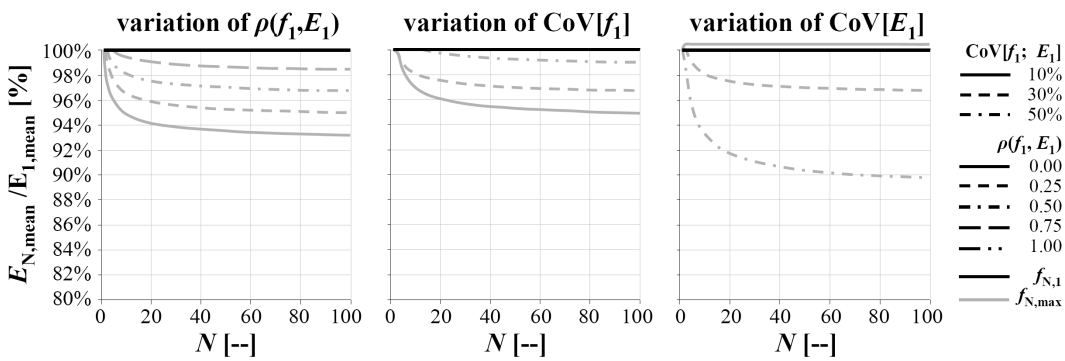

Fig. 3.62: Relative mean of system E-modulus at first failure and at maximum system strength in dependency of $\rho(f_1, E_1)$ (left), CoV[f_1] (middle) and CoV[E_1] (right) and N; GLS

In contrast to $E_{N,mean}$ parameters $\rho(f_1, E_1)$, CoV[f_1] and CoV[E_1] show only small and even negligible effects on CoV[E_N], see Fig. 3.63. In fact, CoV[$E_{N,1}$] follows analytically the averaging model for CoV[X_N] irrespective of chosen parameter sets. The minor influence of $\rho(f_1, E_1)$ and CoV[f_1] on CoV[$E_N \mid f_{N,max}$] shows to increase with decreasing parameters $\rho(f_1, E_1)$ and CoV[f_1]. The inverse is given for CoV[E_1]. Nevertheless, it can be concluded that CoV[$E_{N,max} \mid f_{N,max}$] is sufficiently represented by CoV[$E_{N,1}$]. Consequently, modelling by means of the averaging model is sufficient, so far CoV[E_1] is not too large.

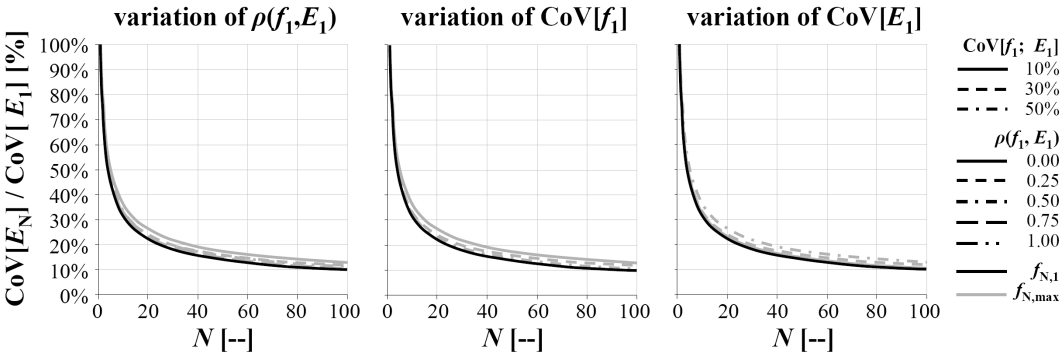

Fig. 3.63: Relative CoV of system E-modulus at first failure and at maximum system strength in dependency of $\rho(f_1, E_1)$ (left), CoV[f_1] (middle) and CoV[E_1] (right) and N; GLS

Fig. 3.64 shows the ratio between the average rank of $\varepsilon_{f,i}$ and N at maximum system strength versus N. As the elements in a given system fail in ascending order of $\varepsilon_{f,i}$ starting with the smallest (rank[$\varepsilon_{f,i}$] $\mid_{\min[\varepsilon \mid N]} = 1$) graphs in Fig. 3.64 correspond to the average failure rate of elements at the point of maximum system resistance. Simulation results reflect an increasing average failure rate with decreasing $\rho(f_1, E_1)$, e.g. of about 20% and 3% at $\rho(f_1, E_1) = 0.00$ and 1.00, respectively, and $N = 100$. This can be explained by a reduced chance for reaching a system strength above the first-failure system strength in case of $\rho(f_1, E_1) = 1.00$ due to the fact that $f_i = E_i \cdot \varepsilon_{f,i}$. A convex increasing average failure rate can be also achieved at higher values of CoV[f_1]. Thereby, a higher CoV[f_1] represents higher potential differences between the elements. These differences allow a higher amount of redistribution after partial system failures. In contrast, an increase of CoV[E_1] lowers the average failure rate because of a reduced probability of reaching a system strength above that at first failure. Nevertheless, the influence of CoV[E_1] on average failure rate is negligible small. In general, a high failure rate before achievement of the maximum system strength is of interest if the chances of redistribution, robustness and advanced warning of a structure are considered.

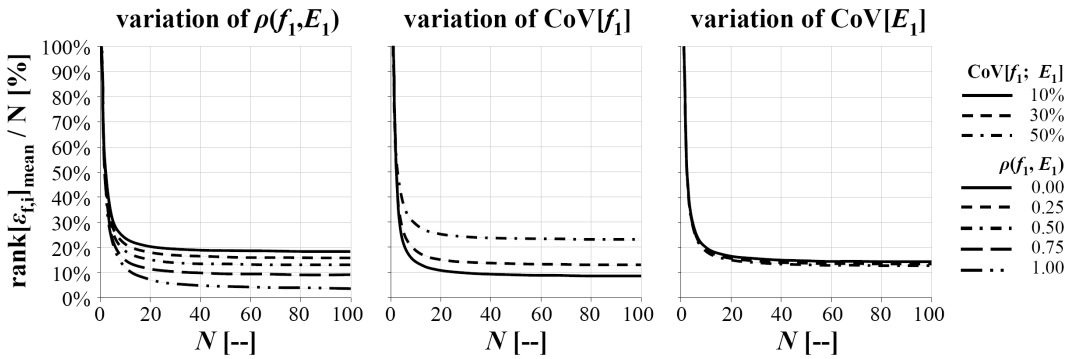

Fig. 3.64: Relative mean rank of $\varepsilon_{f,i}$ at maximum system strength in dependency of $\rho(f_1, E_1)$ (left), CoV[f_1] (middle) and CoV[E_1] (right) and N; GLS

Fig. 3.65 gives the ratio β_N / β_1 versus N. In comparison to all previous plots this is the most important one because the graphs include implicitly all system effects on expectation, variance and shape of the distribution function in dependency of input parameter sets and system size N. Fig. 3.65 (left) shows the influence of $\rho(f_1, E_1)$. Thereby, an increase in $\beta_{N,max}$ with increasing N at $\rho(f_1, E_1) > 0.25$ can be observed. Nevertheless, even in case of $\rho(f_1, E_1) \leq 0.25$ the loss in $\beta_{N,max}$ is negligible and for example amounts only about 5% at default system settings and $N = 100$ but $\rho(f_1, E_1) = 0.00$. Beside that, if load redistribution in a system after first element failure is not possible a remarkable decrease in $\beta_{N,1}$ at $\rho(f_1, E_1) < 0.50$ after an increase is given. Thereby the system size at max[$\beta_{N,1}$] increases with increasing $\rho(f_1, E_1)$, e.g. $N = 3$ and 4 in case of $\rho(f_1, E_1) = 0.50$ and 0.75, respectively. In case of $\rho(f_1, E_1) = 1.00$ a continuous concave increase of $\beta_{N,1} / \beta_1$ is given. With increasing $\rho(f_1, E_1)$ differences between $\beta_{N,1}$ and $\beta_{N,max}$ become smaller and for example in case of $\rho(f_1, E_1) = 1.00$ even zero. A significant increase in $\beta_{N,max}$ can be observed only up to about $N = 20$. Further increase of $\beta_{N,max}$ for $N \geq 20$ is nearly negligible. Parameter CoV[f_1] also remarkable affects the reliability of a system. For example, in case of CoV[f_1] $\geq$ 30% an increase even in $\beta_{N,1}$ and small N can be observed followed by a decrease afterwards. Also $\beta_{N,max}$ is significantly influenced by CoV[f_1], e.g. with $\beta_{N,max} / \beta_1 = 70\%$, 105% and 146%, respectively, at CoV[f_1] = 10%, 30% and 50% and $N = 100$. Thus the difference between $\beta_{N,1}$ and $\beta_{N,max}$ shows a positive but convex relationship with CoV[f_1]. Parameter CoV[E_1] has only a small but negative influence on β_N. Whereas loss in $\beta_{N,1}$ is significant, it is moderate in $\beta_{N,max}$ with $\beta_{N,max} / \beta_1$ between 95% and 109% at CoV[E_1] = (10 ÷ 50)%. To conclude, it can be observed that $\beta_{N,max} / \beta_1$ in case of [CoV[f_1] = 30%; $\rho(f_1, E_1) = 1.00$] versus N corresponds well with the course of [CoV[f_1] = 50%; $\rho(f_1, E_1) = 0.50$]. A similar

observation can be made for $\beta_{N,max} / \beta_1$ at [CoV[f_1] = 30%; $\rho(f_1, E_1)$ = 1.00] and [CoV[f_1] = 30%; $\rho(f_1, E_1)$ = 0.50], or for $\beta_{N,1} / \beta_1$ at [CoV[f_1] = 30%; $\rho(f_1, E_1)$ = 0.00] and [CoV[f_1] = 10%; $\rho(f_1, E_1)$ = 0.50].

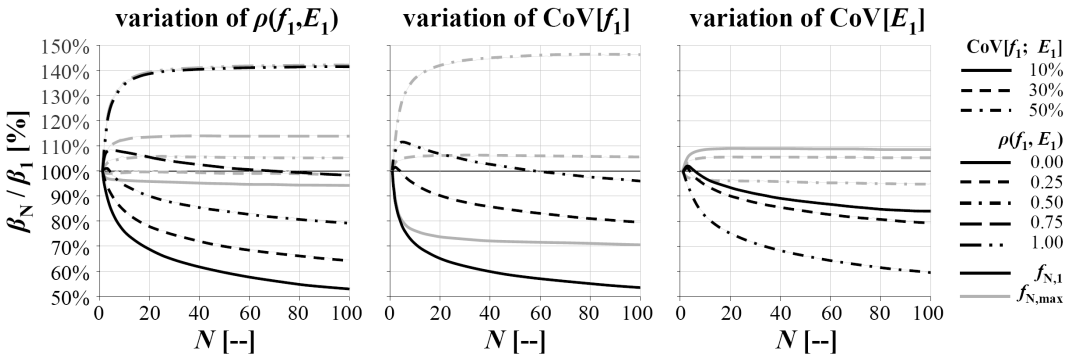

Fig. 3.65: Relative safety index β_N of system resistance against stresses at first failure and at maximum system strength in dependency of $\rho(f_1, E_1)$ (left), CoV[f_1] (middle) and CoV[E_1] (right) and N; GLS

To summarise, within this section effects on strength and E-modulus of general parallel systems composed of linear-elastic iid elements $X_1 \sim$ 2pLND with correlated strength and E-modulus were analysed. In particular the effects of parameters $\rho(f_1, E_1)$, CoV[f_1] and CoV[E_1] on distribution characteristics as well as on the reliability index β_N were examined in more detail. The findings can be seen as a first guideline for optimisation of parallel system behaviour. Nevertheless, before final conclusions and recommendations for the composition of idealised parallel systems are listed the influence of extreme local load sharing (ELLS) and plastic behaviour are discussed briefly within the next three sections.

Exteme Local Load Sharing (ELLS) – Simulations and Conclusions

In parallel systems and in case of extreme local load sharing (ELLS) the position of elements within the system and to each other becomes important. This is because ELLS is defined by load redistribution only to the direct neighboured survivors of failing elements. Consequently, also the arrangement of the parallel aligned elements, in particular if it is a 1D or 2D system, affects failure process and achievable system resistance. Thereby center elements in 2D systems are exposed to higher stresses than edge or corner elements which are only exposed to potential failing elements on three or two sides, respectively, in contrast to center elements which have a maximum of four

neighbours. Following that not only the correlation $\rho(f_1, E1)$, CoV[f_1], CoV[E_1] and the quantity of elements within the system but also the composition of the system in *y*- and *z*-direction, expressed by the quantity of elements $N_y = N$ and N_z has to be taken into account. In the following, the total system size in case of $N_z = 1$ is defined by $N = N_y$ and in case of $N_z > 1$ by $N = N_y \cdot N_z$.

According to previous sections and in particular to the last section concerning GLS again parallel systems composed of linear-elastic iid elements $X_1 \sim$ 2pLND were virtually generated in R (2009). Again, both definitions of system strength, (1) as system stress at first failure, and (2) as maximum of all analysed system stresses per system, were examined. As in the previous section the default settings were: iid element strength $f_1 \sim$ 2pLND with E[f_1] = 30 and CoV[f_1] = (10, 30, 50)%, iid E-modulus $E_1 \sim$ 2pLND with E[E_1] = $E_1 = E$ = 10,000 and CoV[E_1] = (10, 30, 50)%, correlation between strength and E-modulus with $\rho(f_1, E_1)$ = (0.00, 0.25, 0.50, …, 1.00), system size $N_y = N$ = 1, 2, …, 30 and N_z = 1, 2, …, 5, 10, 20 and n = 10,000 runs per system configuration. Default settings which were kept constant for analysing the influence of a specific parameter are given in grey.

The simulation procedure starts with the generation of correlated random vectors or matrices of length N or size $N_y \cdot N_z$ of variables f_1 and E_1. For each generated system a matrix of survivors and direct neighbours is created and updated subsequently after every partial system failure. After that the system gets stressed until the first element defined by min[$\varepsilon_{f,i}$] = $\varepsilon_{f,(1)}$ fails. It follows that stress is redistributed to direct neighbours of failed and sequential failing elements until a steady state is reached. Hereby the total system stress is kept constant. Thus the system is kept load controlled. This is logical because the system stress cannot be reduced, e.g. by loss in stiffness, before an equilibrium stress status is reached. A steady state marks an equilibrium status of the system which shows no further element failures after redistribution of stresses of sequentially failed elements.

The quantity of potential neighbours per element is given by a maximum of four, three and two, respectively for center, edge and corner elements. As the radial distance to all these neighbours is equal the released stress is transferred uniformly to potential and still surviving neighbours. In cases were no neighbours had been survived the released stress is redistributed uniformly to all surviving elements in the system, comparable to GLS. After attainment of a steady state the stress on the system is increased until the next still surviving element fails. The above mentioned procedure was repeated until the system has failed completely. During this procedure system characteristics at first system failure,

$f_{N,1}$ and $E_{N,1}$, characteristics at maximum system strength $f_{N,max}$ and $E_{N,max}$ as well as "# survivors" as the quantity of surviving system elements immediately before the final system collaps, "max[# steady]" and "max[# avalanche]" as the amount of steady states and as the maximum size of an avalanche, respectively, immediately before the final system collaps were registered and further analysed statistically. Thereby, the size of an avalanche is defined as quantity of element failures between two steady states or at least between a steady state and the final system collaps.

The following figures show the relative change of distribution characteristics of system strength and E-modulus versus N as well as the development of expectation of additional characteristics like "# survivors / N", "max[# steady] / N" and "max[# avalanche] / N". At first effects of parameters $\rho(f_1, E_1)$, CoV[f_1] and CoV[E_1] versus N on system strength and E-modulus are analysed. Results for $f_{N,1}$ and $E_{N,1}$ are by default equal to them found for GLS. The additional gains in system strength and E-modulus at maximum system strength in case of ELLS are shown in Fig. 3.66 to Fig. 3.70.

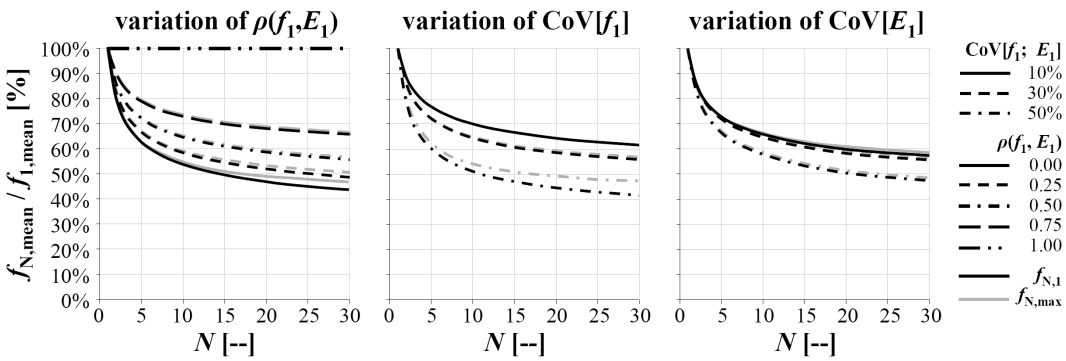

Fig. 3.66: Relative mean of system strength at first failure and of maximum system strength in dependency of $\rho(f_1, E_1)$ (left), CoV[f_1] (middle) and CoV[E_1] (right) and N; ELLS

In comparison with GLS it can be concluded that effects of parameters in case of ELLS are qualitatively the same but the gain, the difference between system strength and E-modulus at first failure and at maximum system strength is much lower and in most cases even negligible.

In a simplified manner, knowing the system characteristics at first element failure in case of ELLS is mostly sufficient for the description of system resistance. Only in cases of very low correlation $\rho(f_1, E_1) \leq 0.25$ and / or high CoV[f_1] $\geq 30\%$ a significant gain in

system reliability from $\beta_{N,1} \rightarrow \beta_{N,max}$ can be realised, see Fig. 3.70. The effects of parameters on $E_{N,max}$ are even not presented here as being absolutely negligible. For modelling of system E-modulus the averaging model approach is absolutely sufficient if the analysed parameter range is not abandoned.

To conlude, there is only a small chance that sequentiel loading and redistribution of stresses to surviving elements in case of ELLS leads to a further enhancement of system strength above that at first element failure.

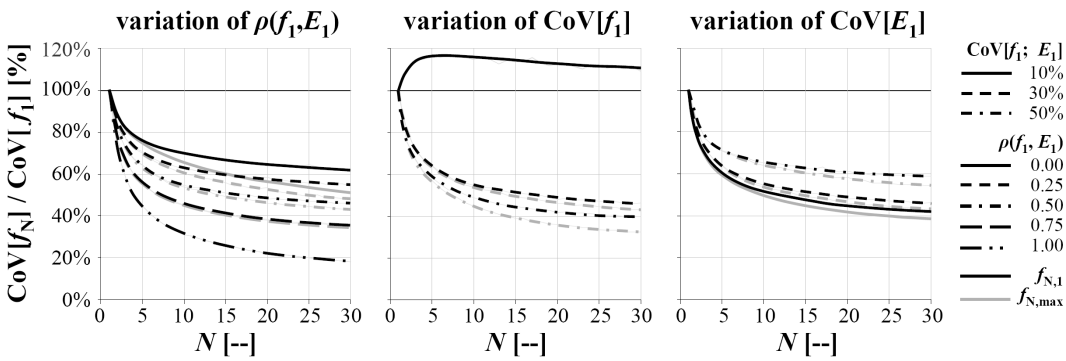

Fig. 3.67: Relative CoV of system strength at first failure and of maximum system strength in dependency of $\rho(f_1, E_1)$ (left), CoV[f_1] (middle) and CoV[E_1] (right) and N; ELLS

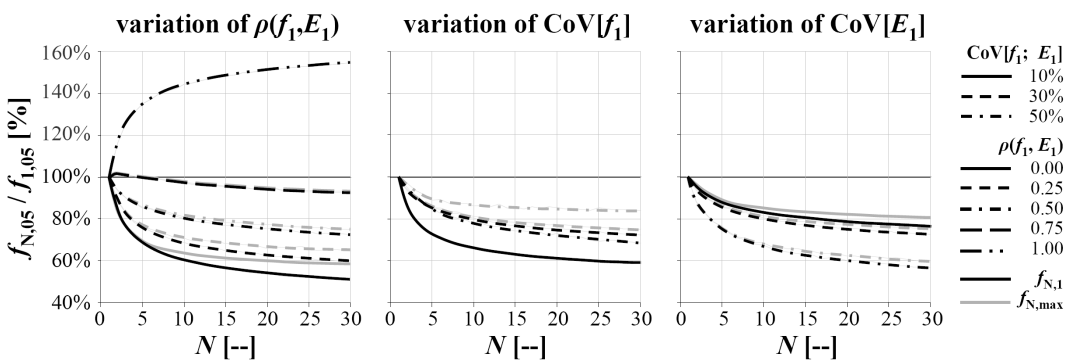

Fig. 3.68: Relative 5%-quantile of system strength at first failure and of maximum system strength in dependency of $\rho(f_1, E_1)$ (left), CoV[f_1] (middle) and CoV[E_1] (right) and N; ELLS

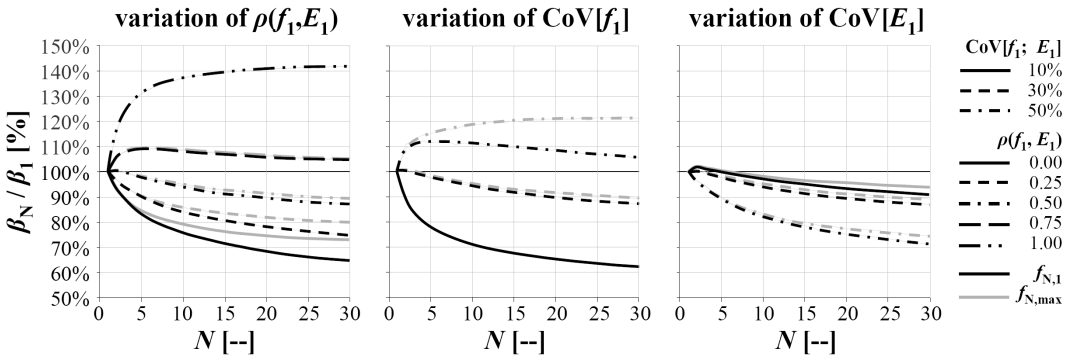

Fig. 3.69: Relative safety index β_N of system resistance against stresses at first failure and at maximum system strength in dependency of $\rho(f_1, E_1)$ (left), CoV[f_1] (middle) and CoV[E_1] (right) and N; ELLS

Fig. 3.70 shows the mean share of survivors immediately before the final system collaps. The average share decreases with increasing $\rho(f_1, E_1)$ but even at $\rho(f_1, E_1) = 0.00$ the share of survivors is about 90% meaning that on average 10% of elements fail before the system ultimately fails. This share can only be increased by CoV[f_1] ≥ 50%.

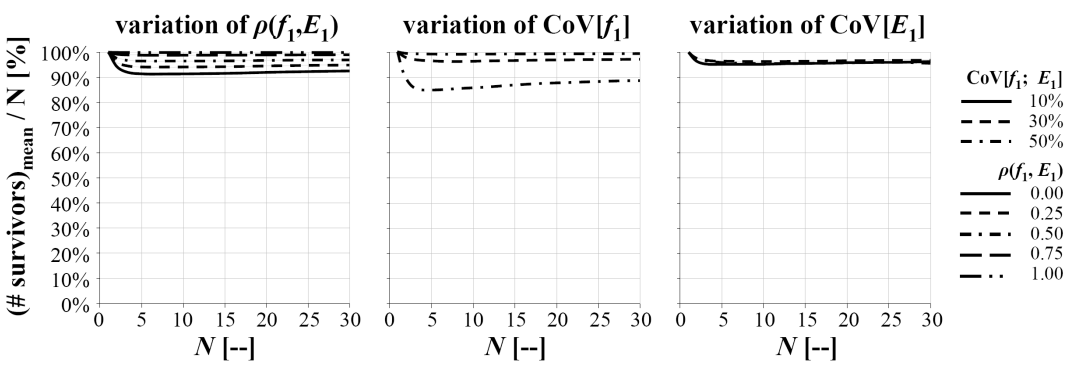

Fig. 3.70: Share of survivors at the last steady state before final system failure in dependency of $\rho(f_1, E_1)$ (left), CoV[f_1] (middle) and CoV[E_1] (right) and N; ELLS

The average amount of steady states decreases significantly with increasing N, see Fig. 3.71. This decrease can only be marginally reduced by a low $\rho(f_1, E_1)$ and / or a high CoV[f_1]. On the part of CoV[E_1] a significant influence is not given. The sharp decrease in the amount of steady states marks that in parallel systems under ELLS the amount of intermediate partial and stable system failures decreases relatively with increasing system size N. This effect is also visible in Fig. 3.70. Thereby an increase in ratio between

average amount of survivors and N after reaching a lower bound at about $N \approx 6$ can be observed. At $N \approx 6$ graphs in Fig. 3.71 show an inflexion in their course.

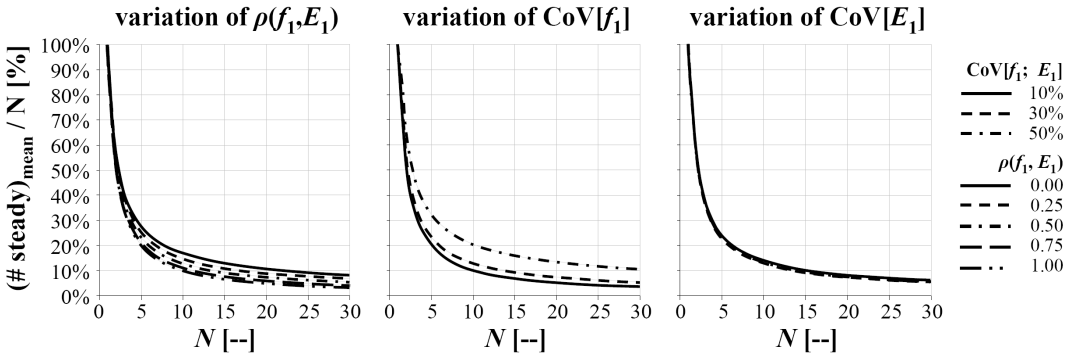

Fig. 3.71: Expectation of the ratio between the quantity of steady states and N in dependency of $\rho(f_1, E_1)$ (left), CoV[f_1] (middle) and CoV[E_1] (right) and N; ELLS

In Fig. 3.72 the relative change of average maximum avalanche versus N is illustrated. The effects of parameters $\rho(f_1, E_1)$, CoV[f_1] and CoV[E_1] on this characteristic are negligible but the relationship to parameter N has to be briefly addressed. Starting at $N \geq 1$ a fast increase of max[# avalanche]$_{mean}$ / N is given up to a peak at approximately $N = 3$ to 4. After that peak, which corresponds to an average avalanche of about 65% of system size N (corresponds to two elements at $N = 3$), a slight convex decrease can be observed, for example to about 50% at $N = 30$.

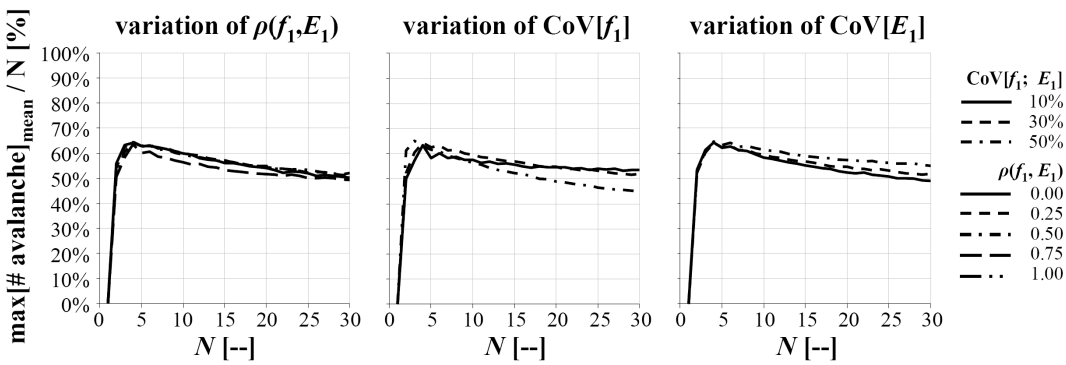

Fig. 3.72: Expectation of the ratio between the maximum avalanche size and N in dependency of $\rho(f_1, E_1)$ (left), CoV[f_1] (middle) and CoV[E_1] (right) and N; ELLS

So far only 1D parallel systems have been analysed. To examine the influence of two-dimensionality the effect of parameter N_z on $f_{N,max}$, $E_{N,max}$ and $\beta_{N,max}$ of systems with $N_z = 1, 2, \ldots, 5, 10, 20$ and $N_y = 1, 2, \ldots, 30$ was analysed in more detail. The other parameter settings were fixed at default values.

Fig. 3.73 (left) shows that the decreasing course of $f_{N,max,mean} / f_{1,mean}$ versus total system size ($N_y \cdot N_z$) becomes marginally smaller with increasing N_z. Ratio CoV[$f_{N,max}$] / CoV[f_1] versus ($N_y \cdot N_z$) in Fig. 3.73 (right) gives an increase in downward trend as N_z increases. The graphs versus N_z change between $N_z \leq 10$ and $N_z = 20$ and imply to become reverse with further increase of N_z. Significant influences of N_z on $E_{N,max}$ were not observed.

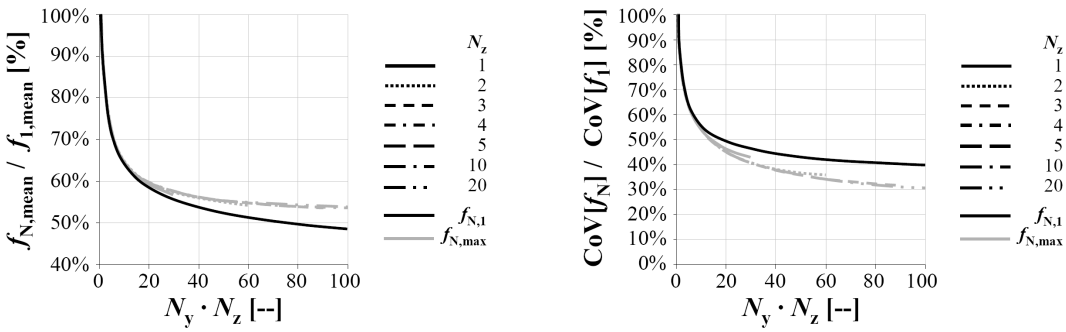

Fig. 3.73: Relative mean (left) and relative coefficient of variation (right) of system strength at first failure and of maximum system strength in dependency of system size N_z and ($N_y \cdot N_z$); ELLS

Fig. 3.74 (left) shows the relative change of the average quantity of survivors versus total system size ($N_y \cdot N_z$) and N_z. The relationship shows at first a sharp decrease at $N_z \geq 1$ to a lower bound followed by a concave increasing trend. The system size ($N_y \cdot N_z$) which corresponds to the minimum of lower bound increases with N_z whereas the magnitude of this minimum decreases up to $N_z \leq 3$ followed by an increase with increasing $N_z > 3$. The slope of the increase in average share of survivors after the peak also becomes smaller with increasing $N_z \geq 1$. Nevertheless overall effect of N_z is small. Fig. 3.74 (right) gives the relative change of average maximum avalanche versus ($N_y \cdot N_z$). As expected, the courses of these graphs are inversely and with an upper bound if compared with the characteristic discussed before. Whereby up to $N_z \leq 5$ only an increase in slope after attainment of the upper bound with constant magnitude can be observed, in case of $N_z \geq 10$ also a shift of bound and corresponding system size ($N_y \cdot N_z$) together with a minor reduction in slope is given.

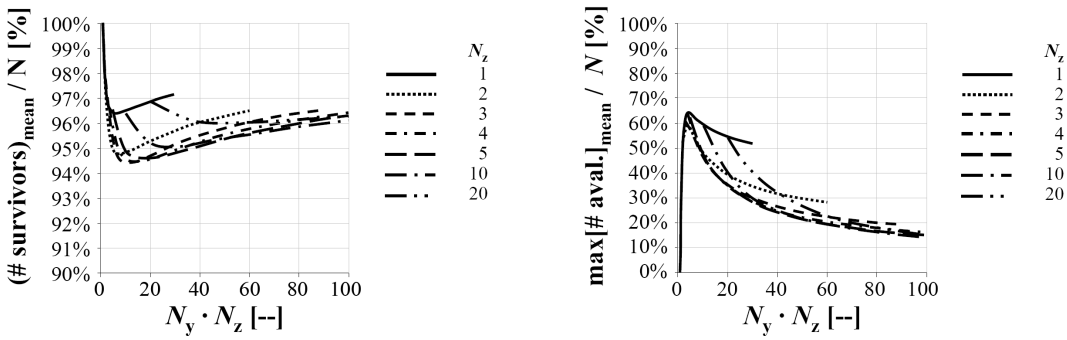

Fig. 3.74: Share of survivors (left) and expectation of the ratio between the maximum avalanche size and ($N_y \cdot N_z$) at the last steady state before final system failure (right) in dependency of system size N_z and ($N_y \cdot N_z$); ELLS

In Fig. 3.75 the ratio β_N / β_1 in dependency of N_z and versus ($N_y \cdot N_z$) is discussed. As mentioned earlier calculation of reliability indexes has the advantage that the whole distribution information is implicitely considered by only one parameter. The type of load redistribution (GLS vs. ELLS) between the elements and the arrangement of elements (1D vs. 2D) has by default no influence on $E_{N,1}$ and $f_{N,1}$. Nevertheless, it can be observed that $\beta_{N,max}$ and the slope of $\beta_{N,max} / \beta_1$ versus ($N_y \cdot N_z$) increases with increasing $N_z \leq 10$. Already at $N_z = 10$ a marginal decrease in reliability in systems of size ($N_y \cdot N_z$) ≤ 50 can be observed. At $N_z = 20$ a distinctive reduction in reliability is given in combination with a very low gradient which becomes nearly zero at ($N_y \cdot N_z$) > 60, with [β_N / β_1 | ($N_y \cdot N_z$) = 20] ≈ 91% and [β_N / β_1 | ($N_y \cdot N_z$) = 60] ≈ 90%. The change in system behaviour with higher values of N_z is due to the fact that at first the number of neighbours increases, for core elements from a maximum of two at $N_z = 1$ to three and four at $N_z = 2$ and $N_z = 3$, respectively. Thereby not only the probability that elements have to bear additional stresses from neighboured failing elements increases but also the probability that stresses can be carried by surviving neighbours. The last aspect is due to the fact that the released stresses can be shared by a higher quantity of elements. Secondly, at $N_z \geq 4$ only the shares of core elements to edge and corner elements become larger. This circumstance only marginally contributes to the ability of increased load redistribution. As already mentioned in the literature survey within section 3.2.4 failures in parallel systems under ELLS have the tendency to cluster in case of large quantities of ($N_y \cdot N_z$). Consequently, very large systems change their failure behaviour from parallel to parallel, sub-serial. Nevertheless, the influence of N_z on β_N / β_1 is small within the analysed parameter ranges and only about 3% at ($N_y \cdot N_z$) = 30. At the beginning failures of system

elements occur randomly. Thus the latter tendency of very large parallel systems under (E)LLS to act parallel, sub-serial can be explained by the increasing probability that these random failures cluster to only a few dominating failure domains. Therefore two-dimensionality is required and provokes splitting of ($N_y \cdot N_z$) systems into sub-systems. The size of such sub-systems must thereby be small enough for splitting but large enough to initiate sudden system collaps with failure of the weakest sub-system. An idea of the minimum size of such a sub-system is given at least by the average expectable failure rate, see Fig. 3.74.

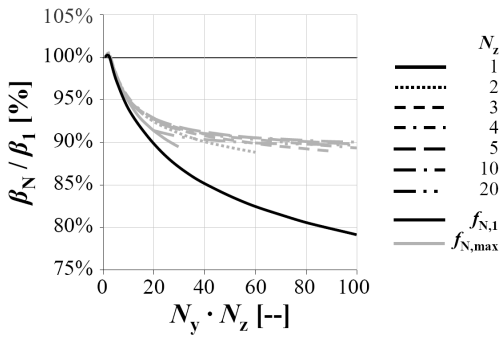

Fig. 3.75: Relative safety index β_N of system resistance against stresses at first failure and at maximum system strength in dependency of system size N_z and ($N_y \cdot N_z$); ELLS

To conclude, characteristics of parallel systems under ELLS are only marginally influenced by parameters $\rho(f_1, E_1)$, CoV[f_1] and CoV[E_1]. Only in case of very low $\rho(f_1, E_1)$ and / or high CoV[f_1] a noticeable effect on the difference between $f_{N,max}$ and $f_{N,1}$ is given. Nevertheless, two-dimensionality up to $N_z \leq 5$ nearly doubles the gain from $\beta_{N,1}$ to $\beta_{N,max}$. Higher values of N_z show a reduction in $\beta_{N,max}$ but in combination with a reduction in slope with nearly a constant ratio of $\beta_{N,max} / \beta_1$ at $N_z \geq 20$, independent of ($N_y \cdot N_z$). Overall it has to be concluded that ELLS will be seldom or even never found in real systems. Thus the results deliver a conservative lower boundary in contrast to progressive upper boundaries supported by systems under GLS. Consideration of both enables judgement of real system behaviour within at least two extreme boundaries.

Models for Calculation of System Strength and System E-Modulus at first Element Failure

As already mentioned in previous sections irrespective of the arrangement of elements in systems (1D vs. 2D) and irrespective of the way of load redistribution after partial failure

(GLS ↔ ELLS) system strength at first failure is equal and solely dependent on input parameters which are the RSDMs of strength and E-modulus and corresponding parameters like E[f_1], CoV[f_1], E[E_1], CoV[E_1], correlation $\rho(f_1, E_1)$ and system size N or ($N_y \cdot N_z$). Knowledge of predictability of system strength at first failure becomes important e.g. in (1) very dynamic system failure scenarios with a reduced probability in finding a steady state and further strength increase, (2) in first-failure systems were subsequent failure can not be tolerated, and (3) in case of ELLS were differences between $f_{N,max}$ and $f_{N,1}$ are nearly negligible. Furthermore, also GLS-systems with a high value of $\rho(f_1, E_1)$ or very low CoV[f_1] and / or N are also characterised by a ratio of $f_{N,max} / f_{N,1} \approx 1.00$. Consequently, the ability to estimate system strength at first failure is a first important step in modelling parallel systems.

Given a parallel system of N or ($N_y \cdot N_z$) linear elastic iid elements with strength $f_1 \sim$ 2pLND, E-modulus $E_1 \sim$ 2pLND and correlation between strength and E-modulus of the same element $\rho(f_1, E_1)$. In this case the system strength $f_{N,1}$ follows equ. (3.142) and thus is nothing else than a multiplication of the system E-modulus $E_{N,1}$ and the minimum ultimate strain of system elements min[$\varepsilon_{f,1,i}$], with $i = 1, \ldots, N$. Thereby, system E-modulus constitudes the average of element's E-moduli following the averaging model with E[$E_{N,1}$] = E[E_1] and CoV[$E_{N,1}$] = CoV[E_1] / $\sqrt{N}$. Based on input parameters of f_1 and E_1 and equ. (2.92) in section 2.4.2 the distribution of ultimate strain $\varepsilon_{f,1}$ follows

$$\varepsilon_{f,1} \sim 2pLND\left(\mu_{f_1} - \mu_{E_1}, \sigma_{f_1}^2 - 2 \cdot \rho(f_1, E_1)_{trans} \cdot \sigma_{f_1} \cdot \sigma_{E_1} + \sigma_{E_1}^2\right), \tag{3.144}$$

by transforming $\rho(f_1, E_1)$ by means of inverse equ. (2.89), see

$$\rho(f_1, E_1)_{trans} = \frac{\ln\left[\rho(f_1, E_1) \cdot \sqrt{\exp\left(\sigma_{f_1}^2 + \sigma_{E_1}^2\right) - \exp\left(\sigma_{f_1}^2\right) - \exp\left(\sigma_{E_1}^2\right) + 1} + 1\right]}{\sigma_{f_1} \cdot \sigma_{E_1}}. \tag{3.145}$$

For calculation of the minimum ultimate strain of system elements the serial model for minima of iid elements provided in section 3.3.2 and given by equ. (3.93) with parameter estimators in Tab. 3.2 can be applied. For multiplication of so far determined $E_{N,1}$ and min[$\varepsilon_{f,1,i}$] knowledge of correlation $\rho(E_{N,1}, \varepsilon_{f,N,1})$ is required. Correlation $\rho(E_1, \varepsilon_{f,1})$ can be derived analytically by means of the definition of PEARSON's correlation coefficient given in equ. (2.46), see

$$\rho\left(E_1,\varepsilon_{f,1}\right)=\frac{E\left[E_1\cdot\varepsilon_{f,1}\right]-E\left[E_1\right]\cdot E\left[\varepsilon_{f,1}\right]}{\sigma_{E_1}\cdot\sigma_{\varepsilon_{f,1}}}=\frac{E\left[f_1\right]-E\left[E_1\right]\cdot E\left[\varepsilon_{f,1}\right]}{\sigma_{E_1}\cdot\sigma_{\varepsilon_{f,1}}}\ . \tag{3.146}$$

After transformation of $\rho(E_1, \varepsilon_{f,1})$ to $\rho(E_1, \varepsilon_{f,1})_{trans}$ as shown for $\rho(f_1, E_1)$ in equ. (3.145) the distribution of $f_1 = E_1 \cdot \min[\varepsilon_{f,1}]$ can be rewritten as

$$f_1 = E_1\cdot\min\left[\varepsilon_{f,1}\right]\sim 2pLND\left(\mu_{E_1}+\mu_{\varepsilon_{f,1}},\sigma_{E_1}^2+2\cdot\rho\left(E_1,\varepsilon_{f,1}\right)_{trans}\cdot\sigma_{E_1}\cdot\sigma_{\varepsilon_{f,1}}+\sigma_{\varepsilon_{f,1}}^2\right). \tag{3.147}$$

Nevertheless, $\rho(E_{N,1}, \varepsilon_{f,N,1})$ is dependent on total system size given by N or $(N_y \cdot N_z)$. As no analytical formulation of the relationship $\rho(E_{N,1}, \varepsilon_{f,N,1})$ versus N is available on hand a heuristic approach gained by fitting adequate models on simulated data was formulated. Based on exact knowledge of the starting value $\rho(E_1, \varepsilon_{f,1})$ this model was searched for by analysing the ratio $\rho(E_{N,1}, \varepsilon_{f,N,1}) / \rho(E_1, \varepsilon_{f,1})$ versus N, see Fig. 3.76. Thereby effects of parameters $\rho(f_1, E_1)$, CoV[f_1] and CoV[E_1] were examined. It can be observed that up to $\rho(f_1, E_1) \leq 0.75$ only a minor but steady decrease of the ratio in combination with increasing variance of simulation results is given. At $\rho(f_1, E_1) = 1.00$ the ratio is constant and equal to one. Consequently, effects of $\rho(f_1, E_1)$ on $\rho(E_{N,1}, \varepsilon_{f,N,1}) / \rho(E_1, \varepsilon_{f,1})$ can be neglected at least up to $\rho(f_1, E_1) \leq 0.75$ and at $\rho(f_1, E_1) = 1.00$ taken as one. Fig. 3.76 (middle) gives the relationship $\rho(E_{N,1}, \varepsilon_{f,N,1}) / \rho(E_1, \varepsilon_{f,1})$ in dependency of N and CoV[f_1]. Again the relative reduction of $\rho(E_{N,1}, \varepsilon_{f,N,1})$ versus N increases non-linear convex with increasing CoV[f_1]. The other way round can be observed in Fig. 3.76 (right) which gives the effect of parameter CoV[E_1] on relative change of $\rho(E_{N,1}, \varepsilon_{f,N,1})$ versus N.

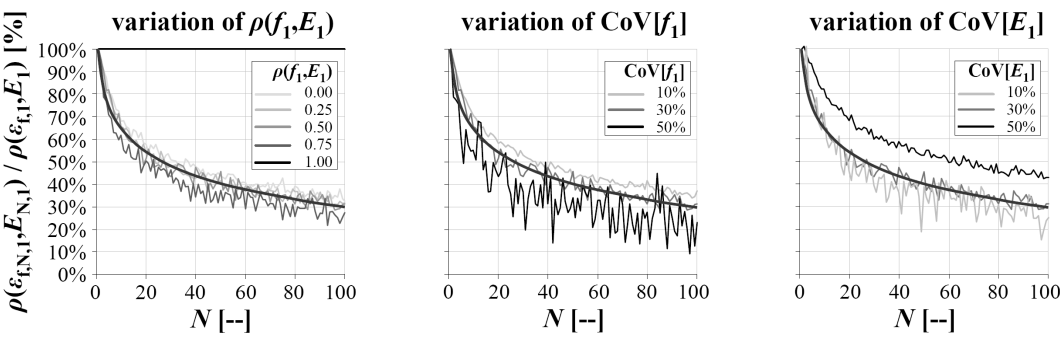

Fig. 3.76: Effect of parallel system action on correlation between E-modulus and ultimate strain at first failure: variation of $\rho(f_1, E_1)$ (left), of CoV[f_1] (middle) and of CoV[E_1] (right)

For the description of a representative non-linear model for $\rho(E_{N,1}, \varepsilon_{f,N,1}) / \rho(E_1, \varepsilon_{f,1})$ versus N two regression equations are discussed under consideration of two limiting cases

$$\lim_{N\to 1}\left[\frac{\rho\left(E_{N,1},\varepsilon_{f,N,1}\right)}{\rho\left(E_1,\varepsilon_{f,1}\right)}\right]\to 1.00 \text{ and } \lim_{N\to\infty}\left[\frac{\rho\left(E_{N,1},\varepsilon_{f,N,1}\right)}{\rho\left(E_1,\varepsilon_{f,1}\right)}\right]\to 0.00\,. \tag{3.148}$$

The two models are (1) a logarithmic and (2) a power regression model, see

$$\begin{aligned} &(1) \qquad \frac{\rho\left(E_{N,1},\varepsilon_{f,N,1}\right)}{\rho\left(E_1,\varepsilon_{f,1}\right)} = \varsigma_{\log}\cdot\ln(N)+1.00\,, \\ &(2) \qquad \frac{\rho\left(E_{N,1},\varepsilon_{f,N,1}\right)}{\rho\left(E_1,\varepsilon_{f,1}\right)} = 1.00\cdot N^{\varsigma_{power}}\,. \end{aligned} \tag{3.149}$$

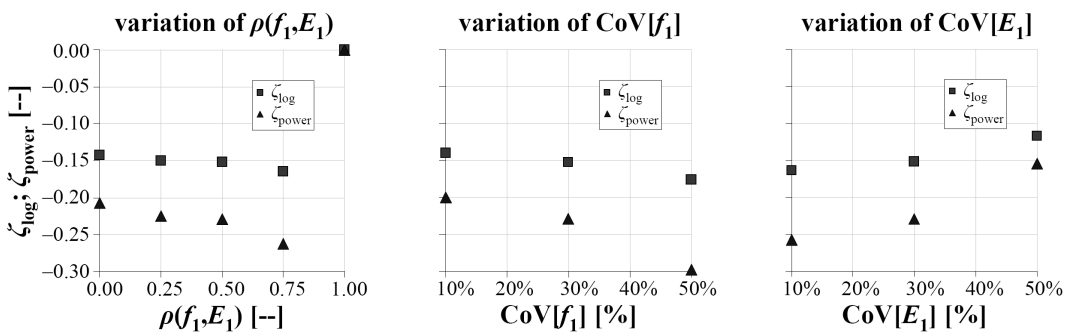

Fig. 3.77: Best fitted parameters $\zeta_{\log}$ and ζ_{power} of logarithmic and power model, respectively, for the description of $\rho(E_N, \varepsilon_{f,N}) / \rho(E_1, \varepsilon_{f,1})$ versus N: variation of $\rho(f_1, E_1)$ (left), of CoV[f_1] (middle) and of CoV[E_1] (right)

Both models fulfill the requirement for $N \to 1.00$, but only the power model is also suitable at $N \to \infty$. The results of best fitted model parameters $\zeta_{\log}$ and ζ_{power} in dependency of parameters $\rho(f_1, E_1)$, CoV[f_1] and CoV[E_1] are shown in Fig. 3.77. Parameter ζ_{power} appears to be more sensitive to variation in input parameters than $\zeta_{\log}$. Furthermore, total sum of squared deviations between simulation results and model estimates were in case of the power model always higher than by means of the logarithmic regression function. Despite the fact that the logarithmic model does not fulfill the limit constraint at $N \to \infty$ but nevertheless gives a good representation of simulation data up to $N \leq 100$ it is further preferred for modelling the ratio $\rho(E_{N,1}, \varepsilon_{f,N,1}) / \rho(E_1, \varepsilon_{f,1})$ versus N. Due to minor changes in $\zeta_{\log}$ in case of $\rho(f_1, E_1) \leq 0.75$,

CoV[f_1] ≤ 50% and CoV[E_1] ≤ 30% in modelling the parameter setting at default case $\rho(f_1, E_1) = 0.50$, CoV[f_1] = CoV[E_1] = 30% is applied only. As shown in Fig. 3.77 (right) ζ_{log} is in particular sensitive to CoV[E_1] showing a distinctive convex increase with increasing CoV[E_1].

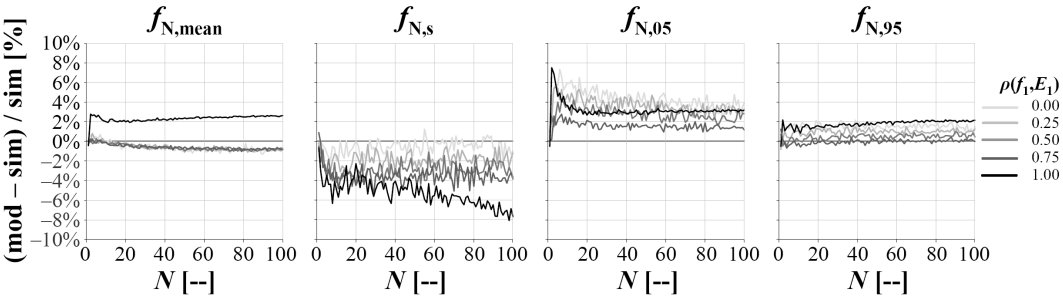

Fig. 3.78: Relative bias between model and simulation results vs. N in respect to mean system strength (left), standard deviation (left-middle), 5%-quantile (right-middle) and 95%-quantile (right) of system strength, in dependency of $\rho(f_1, E_1)$

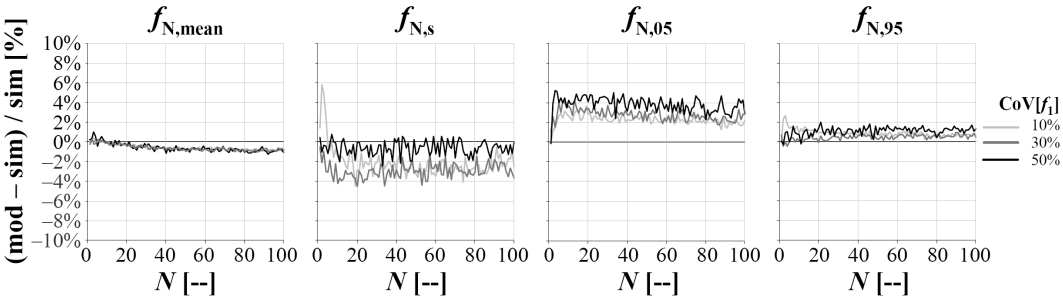

Fig. 3.79: Relative bias between model and simulation results vs. N in respect to mean system strength (left), standard deviation (left-middle), 5%-quantile (right-middle) and 95%-quantile (right) of system strength, in dependency of CoV[f_1]

The relative deviations between model calculations and simulation results versus N in dependency of parameters $\rho(f_1, E_1)$, CoV[f_1] and CoV[E_1] are given in Fig. 3.78, Fig. 3.79 and Fig. 3.80, respectively. Thereby satisfactorily results can be achieved with deviations in analysed distribution characteristics smaller than ± 4%. Despite the fact that all comparisons show a minor bias in dependency of N and / or variation in parameter settings these figures also deliver the information for direct bias correction if higher accuracy in modelling is required. Overall a good representation can be found apart from $\rho(f_1, E_1) = 1.00$ and CoV[E_1] > 30%. Nevertheless, in case of $\rho(f_1, E_1) = 1$ consequencies

of parallel action can be calculated directly by means of the averaging model. Beside that, requirements for modelling systems with CoV[E_1] > 30% will perhaps be seldom the case. Nevertheless, an estimate of $\zeta_{\log}$ for CoV[E_1] = 50% is available.

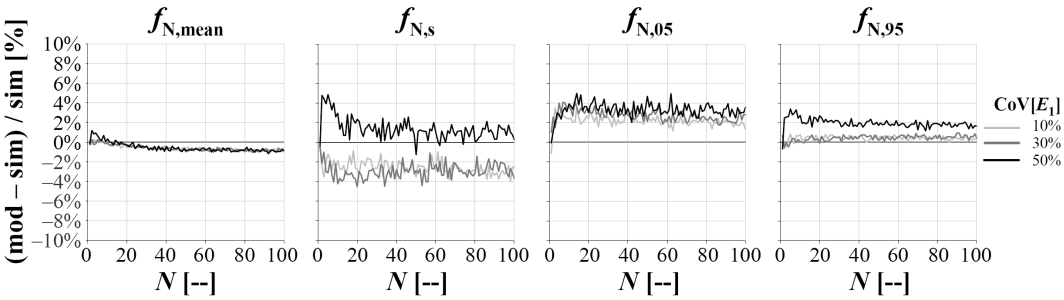

Fig. 3.80: Relative bias between model and simulation results vs. N in respect to mean system strength (left), standard deviation (left-middle), 5%-quantile (right-middle) and 95%-quantile (right) of system strength, in dependency of CoV[E_1]

To conclude, the presented model for estimation of strength and E-modulus distributions of herein discussed parallel systems shows to perform satisfactorily. It provides an easy applicable tool for judgement of parallel system behaviour and consequencies. It thereby delivers a possibility for designing high performance parallel systems under consideration of limitations in parameter settings also in conjunction with production requirements and achieveable accuracy and stability in manufacturing and / or classification of elements and system products.

Some Comments on the Effect of Plasticity

In analysing equ. (3.142) and (3.143) which give the bearing capacity at first failure and at maximum system strength, respectively, it is obvious that system strength capacity is not a direct function of element's strengths but more of the ultimate strain of elements defined explicitly by the minimum ultimate strains of all surviving and contributing elements after k failures. Consequently, even a small amount of plastic flow or ductility has a significant effect on system strength, see Fig. 3.81.

This is obvious because the possibility of elements to elongate without softening, only minor amount of softening or even hardening enables the achievement of higher capacities in all residual survivors of a system.

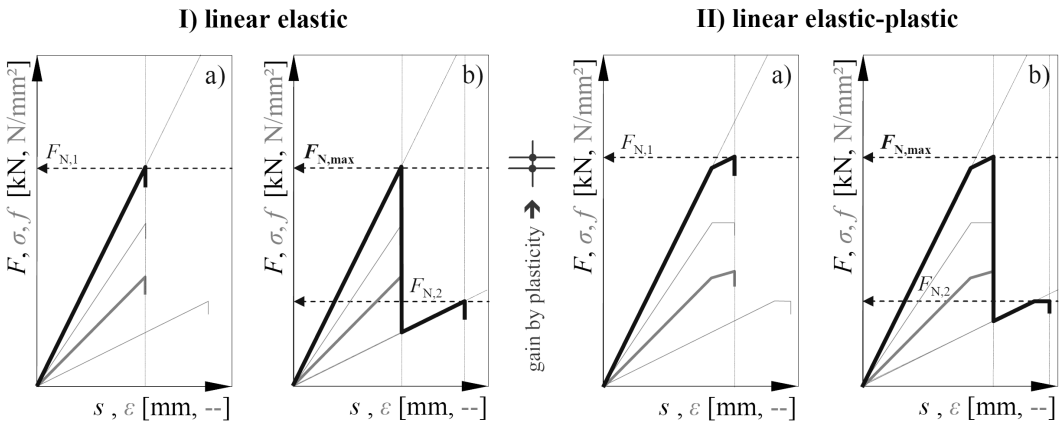

Fig. 3.81: Influence of plasticity on strength and bearing capacity of parallel systems, exemplarily composed of two elements: linear-elastic material behaviour (left) vs. linear elastic-plastic material behaviour (right)

To conclude, plastic material behaviour increases homogenisation and gains in system strength remarkably. This was already discussed for ideal linear elastic-plastic material behaviour in section 3.2.2. In this ideal case homogenisation equal to the averaging model can be reached. This was also found for ideal systems following case I. In contrast to case I plastic flow gives much better failure behaviour with the ability of advanced warning and load redistribution to stiffer components within a higher ranking structural system. Furthermore, in particular hierarchical materials can be always expected to show some amount of plastic flow due to step-wise failure processes in sub-hierarchical levels. More on that question and in particular in regard to wood and timber will be presented within the next chapter 4.

3.4.5 Parallel System Action and Effects: Findings and Recommendations

Within the last sections effects of various parallel system configurations were analysed. Thereby focus was on lognormal distributed strength and E-modulus of elements. Within the examinations effects caused by varying input parameters like CoV[f_1], CoV[E_1] and $\rho(f_1, E_1)$ as well as the arrangement of elements (1D vs. 2D) and the type of load redistribution (GLS vs. ELLS) were investigated for system strength and E-modulus at first element failure and for maximum system strength and corresponding E-modulus. Already at the end of each section a short summary and conclusions are provided. However, some additional and more general statements can be made:

- real parallel acting systems are far away from ideal parallel systems, in particular if focusing on system strength; hereby the maximum gain in system effects is seldom equal or even higher than the averaging model even in case of GLS;
- analysing failure behaviour and limits in systems but also in elements is normally done by analysing the ultimate loads and strengths; nevertheless, analysis of parallel systems, and thus also of real materials which are always something like a parallel, sub-serial composition, are definitely restricted by ultimate strain; this aspects are in particular of interest in modelling systems composed of elements with non-linear or not ideal linear-elastic brittle material; thus improvements in modelling of serial systems directly enhance the ability in modelling parallel systems;
- it could be proven and explicitly shown by the equations for $f_{N,1}$ and $f_{N,max}$ that extreme value statistics (EVT) and in particular models for calculation of minima play a decisive role in modelling parallel system behaviour with focus on strength potential;
- within previous sections and in conjunction with section 3.3.2 dealing with models of serial system strength it was shown that through the combination of heuristic and analytical expressions satisfactorily accurate modelling of system strength at first failure can be achieved even for f_1, $E_1 \sim$ 2pLND;
- the ideal assumption of GLS can be argumented to overestimate real system behaviour; nevertheless, the ideal assumption of linear-elastic and perfect brittle materials appears also a bit unrealistic and if compared to reality conservative; both effects together balance each other somehow in real life;
- discussing the expectable bearing capacities of parallel systems is also a discussion of the type of loading if it is applied deformation- or load-controlled; this discussion is directly linked with the type of load sharing, between GLS and ELLS.

Some more comments and conclusions found in analysing the special cases, case I to case III:

- concerning the special case I system strength and E-modulus can be well modelled by the averaging model approach; thus this kind of system enables a very high degree of homogenisation and in particular a maximum of homogenisation in variance of system characteristics; nevertheless this system provides no load redistribution and fails suddenly at failure of the first element;

- in the analysis of case II a remarkable decrease in mean system strength but reduced chances of load redistribution in combination with further increase of system strength is given; nevertheless, a remarkable reduction in variability of system strength $f_{N,max}$ leads to a moderate increase at least in lower quantiles, e.g. $f_{N,05,1} \rightarrow f_{N,05,max}$;
- case III shows a very high potential of redistribution after partial failures with the ability to further increase the system strength capacity; the homogenisation in CoV[$f_{N,max}$] is moderate.

Based on the analysis in previous sections the following general recommendations for optimisation of parallel system behaviour are possible:

- the reliability of parallel systems increases with increasing $\rho(f_1, E_1)$; this is due to the fact that the achievable system strength increases with a better coincidence of strength and E-modulus within elements;
- the reliability also increases with increasing CoV[f_1]; this is because a high variation in strength corresponds with high potential differences between the elements and thus with a high potential for homogenisation in conjunction with a higher potential of partial failures;
- an increase in system reliability can also be achieved with a low value of CoV[E_1]; thereby a low variation in E_1 corresponds directly with the ability of partial system failures due to restrictions in ultimate strain $\varepsilon_{f,1}$;
- to achieve a high system bearing capacity it is proposed to ensure that the ratio CoV[f_1] / CoV[E_1] is ≥ 1.00;
- in case of ELLS arrangement of elements in a two-dimensional structure shows an increase in reliability up to $N_z \leq 5$ in combination with a decreasing influence of β_N / β_1 on $(N_y \cdot N_z)$;
- even a small amount of plasticity in material behaviour affects system strength significantly; it was noted that in hierachical structured materials a certain amount of plastic flow can be always expected; if plasticity can not or not sufficiently delivered by the elements' material, plasticity can be also induced by adequate designed and performed joints between the elements;
- adequate system behaviour can not always achieved by optimising the bearing capacity or potential of advanced warning; occasionally system requirements are heavily defined by restrictions in deformations and / or partial failures or defined

by optimal stiffness and bearing potential; such behaviour is for example given in case I or in general systems with very low CoV[E_1] and CoV[f_1] in combination with a very high amount of $\rho(f_1, E_1)$.

Chapter 4

Hierachical Structure and Scaling in Wood, Timber and Timber Engineering

The term "scaling" in regard to material stands for self similarity in behaviour and characteristics over various hierarchical levels. Within this chapter general aspects concerning scaling are addressed. After a short introduction emphasise is on scaling and hierarchical levels of wood and timber (tissues). In particular the tensile properties along the hierarchical chain are discussed from molecular level up to construction timber. In a review main constituents and their functions are presented adressing each wood and timber hierarchy seperately. Analogies between natural hierarchies and in particular between natural and technical hierarchies are discussed. At the end some thoughts on consideration of scaling effects and stochastics in material modelling are presented.

4.1 General Remarks concerning Scaling

The term "scaling" is defined as self-similarity of functional relationships, shape, geometry and / or structure. It constitutes logarithmic scale invariance (e.g. WASER, 2004). Following that, functions, shapes and characteristics are in principle independent of the observed hierarchical level. Thereby scaling is not only a proportional resizing of dimensions or a transformation of a functional behaviour by volumetric resizing. It involves the whole structural system underlying each hierarchy, and shows similarity in the functional behaviour and characteristics between all these hierarchies. In some cases it is also a preservation of physical similar systems, as for example provided by Buckingham-PI-theorem (BUCKINGHAM, 1914). Scale invariance accounts for similar

structural behaviour and similar geometries of systems over all (several) hierarchical levels. Scaling itself appears dimensionless (RECHENBERG, 2000). The functional relationship exhibiting scale invarience is given by the power law

$$f(x) = y = a \cdot x^k + O(x^k), \tag{4.1}$$

with a as prefactor, k as the (universal) scale exponent (power) and $O(x^k)$ as the error term, often replaced by ε (e.g. NEWMANN, 2005). The power law satisfies

$$f(c \cdot x) \propto f(x), \tag{4.2}$$

with c as constant. Power laws are invariant functional relationships (NEWMANN, 2005). The functional relationships of logarithmic scale invariant characteristics are linear (with constant gradient) if the kernel function is transformed to logarithmic domain, see

$$f(x) = y = a \cdot x^k \xrightarrow{\ln} \ln[y] = \ln(a) + k \cdot \ln(x). \tag{4.3}$$

The logarithmised scale parameter a now functions as shift parameter $\ln(a)$ and the scale exponent k gives the slope. Re-scaling of equ. (4.1) affects the proportion but not the shape of a function. It gives a linear shift of the power model but preserves the slope in logarithmic domain (see Fig. 4.1).

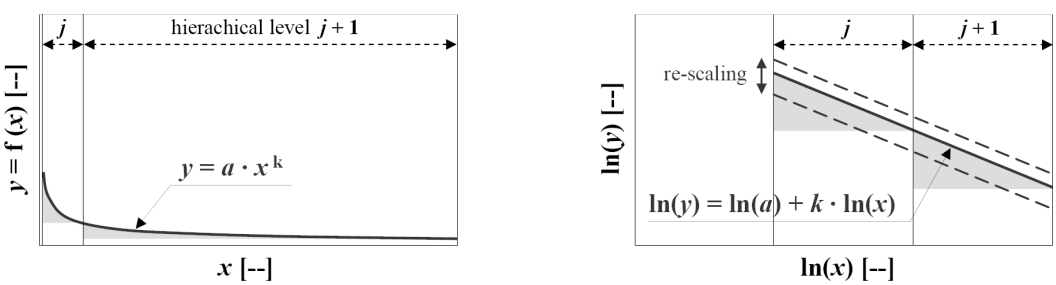

Fig. 4.1: Example of a power model: linear domain (left); logarithmised domain (right)

Power laws are often used for modelling of natural phenomena but also for modelling of phenomena in human society (e.g. physiology, sociology). For example they are used to model body sizes, diameters of volcanic craters, dimensional distribution of cities and for the distribution of words in texts (e.g. NEWMANN, 2005). Some more examples are the Gutenberg-Richter law of earthquakes, the Pareto-law or the structural scale invariance of

fractals. In the field of material research and in engineering practice many phenomena and effects are found to follow power laws, e.g. the size effect according WEIBULL (1939). WEIBULL's power model has thereby treated with caution. The reference volume or dimension for calculating the volume (size) effect on strength of an arbitrary volume can be choosen freely. The power k of the volume (size) effect (see section 3.2.1, equ. (3.33)) depends directly on the observed variability in strength. Due to material inherent system effects parameter k also depends on the dimensions or even the geometry of the reference volume and stress. Thus "size effects" have to be clearly differentiated from "scaling effects". Here "size effects" describe effects on characteristics (e.g. strength) as a consequence of changes in dimension(s) on a specific hierarchical level. In contrast "scaling effects" are in principle the outcome of changes in the material structure and / or relationships between characteristics comparing the system or the material on different hierarchical levels (e.g. SUTHERLAND ET AL., 1999; BRANDNER, 2008). For example scaling effects are observable by changing the production technique or solely by extracting a part of the total volume. Thereby the composition of the structure or mass shares of constituents is changing (SUTHERLAND ET AL., 1999). Size effects result from the influence of changed dimensions on material characteristics (e.g. strength or stiffness) without changes in the material structure. They are more related to the stochastic occurrence of flaws which influence the analysed characteristic. SUTHERLAND ET AL. (1999) conclude that material properties associated with a certain volume of produced elements and of elements cut out from a larger volume are not equal. Thus WEIBULL's power model for size effects can be used as scaling modell only if the power k and thus the variability in strength is constant on all hierarchical levels. For illustration, Fig. 4.2 shows exemplarily an exponential volumetric growth between hierarchies. Arbitrarily, in each hierarchy 18 reference volume elements form a critical cluster in scale transition. Thus the quantity of system elements on hierarchy j is generally given as $n(x, j) = x^j$, and with $x = 18$ as $n(18, j) = 18^j$. Under ideal isotropic, linear elastic and brittle material conditions with single failure criteria for system collaps according WEIBULL (1939) and power k as constant in all hierarchical levels, the system strength is given by the power law

$$\frac{f[n(x,j)]}{f[n(x,1)]} = \left(\frac{n(x,1)}{n(x,j)}\right)^k . \tag{4.4}$$

Thus exponential growth in volume results in equi-distant graduation of material hierarchies in logarithmic space of strength vs. volume (see Fig. 4.2).

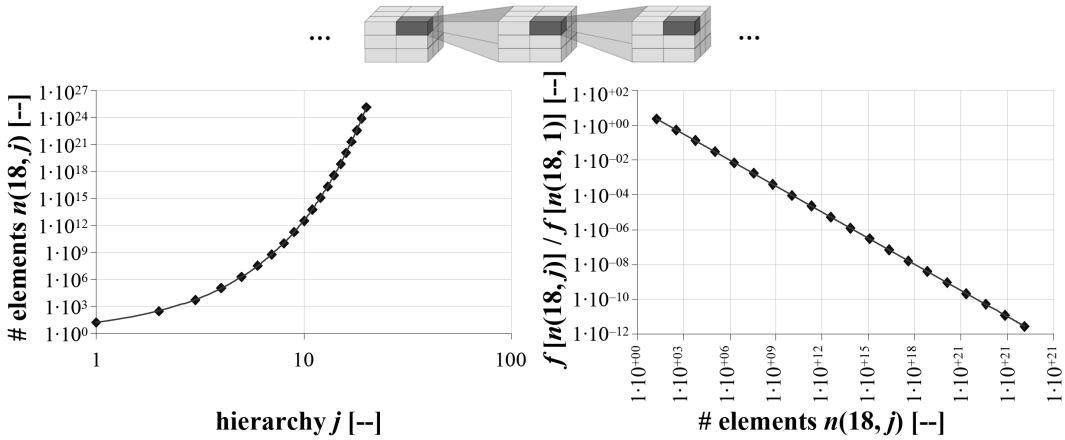

Fig. 4.2: Schematic size and scale transition: exponential volumetric growth (left); volume effect according WEIBULL (1939) assuming constant k (right)

For the analysis of systems on various hierarchical levels both, overview and detailing are required to capture the principal system behaviour. Thereby system analyses are always constrained by the system boundaries, as discussed in section 1.3. For determination of general system behaviour studying different hierarchies (sub-systems) is indispensible. At least the foregoing and the next (the neighboured) hierachical structures, additionally to the range of required hierarchy(ies), have to be analysed as well, otherwise it may occur that general or global trends are smeared by the stochastics of system behaviour within one hierarchy. This principle of analysing effects on the edges and in the center is also well known e.g. in design of experiments (DOE). Fig. 4.3 illustrates this circumstance by means of a scatter plot.

Some more examples of simple power models in material modelling are given by GIBSON AND ASHBY (1999). They modelled E-modulus and strength ratios in relation to the apparent density, given as

$$\frac{E^*}{E_S} = C_E \cdot \left(\frac{\rho^*}{\rho_S}\right)^{v_E}, \quad \frac{\sigma^*}{\sigma_S} = C_\sigma \cdot \left(\frac{\rho^*}{\rho_S}\right)^{v_\sigma}, \tag{4.5}$$

with apparent density ρ^* / ρ_S, as ratio between the density of cellular solid and the density of material (volume fraction), the power parameter v, with $v_E = 3$ in case of bending, $v_\sigma = 2$ in case of elastic buckling failure and $v_\sigma = 3 / 2$ in case of failure in plastic hinges or brittle crushing, and C_E, C_σ as factors to account for changes in the material structure.

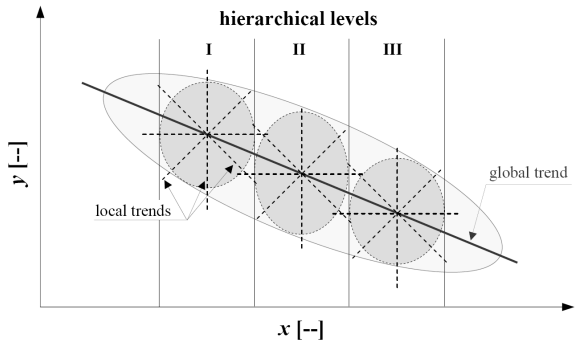

Fig. 4.3: Global vs. local trends exemplified on a schematic scatter plot: local trends based on local observations within hierarchical levels; global trend based on observations made on several hierarchical levels

It is very specific that in analysis of systems on one hierarchy all characteristics of foregoing hierarchical levels are present. Consequently, their structures, relationships and properties determine the system on the observed hierarchy. This implies that scale transition, the change from one hierarchical level to the next, can never be discontinuous or aprubt. Nature does normally not change discontinuously, not on microscopic nor on macroscopic level. Therefore scaling models have to assure continuous transition processes. Thus all materials which are composed of interacting elements on more than one hierarchy are hierarchically structured and exhibit scaling. This is also of interest if e.g. stepwise failure processes by stepwise energy release and dissolution of a material can be observed.

The definition of hierarchical levels in materials in regard to strength can be done in conformity with significant changes in type and dimension of the main failure inducing characteristics. This is in conjunction with changes in the material structure. These are clearly observable on each specific hierarchy, on nano, micro, meso and macroscopic level.

4.2 Wood and Timber (Tissues): Characteristics on Natural and Technical Hierarchical Levels

Wood and timber are naturally grown and evolutionary optimised tissues. They constitute geniously raw materials usable for a nearly infinite variety of technical applications. If sustainable cultivated and harvested, wood and timber demonstrate one of the real

answers to regulate climate unbalance, availablility of resources and energy by being CO_2-active and a renewable carbon sink until combustion. Thereby wood and timber are by nature optimised load bearing materials. They show the ability to perform dual adaptation, in shape as well as in the microstructure itself (FRATZL AND WEINKAMMER, 2007). As "biologically controlled self-assemblies" wood and timber have the ability to remodel or adapt shape and structure according changing environment. Thereby nature uses a common blueprint which is adapted to structures following local, individual needs (FRATZL AND WEINKAMMER, 2007).

Within this section characteristics of wood and timber, its constituents and dimensions are presented. As the material structures on different hierachical levels are sometimes viewed as being self-contained materials, the material structure on a higher hierarchical level constitude nothing else than a composition of sub-materials of previous levels.

Within this section the materials wood and timber are not only discussed on their natural hierarchies but also on their so called "technical hierarchical levels" (see Fig. 4.4). The difference between both scales is obvious considering the formation of materials wood and timber naturally as bottom-up process (e.g. from cell division to the tree), whereas technical hierarchies are characterised by dissolution of naturally grown structures, e.g. by the breakdown process of logs to sawn products (boards, beams, …) or further separation by mechanical and / or chemical dissolution (e.g. clear wood → flakes, strands, fibres, cellulose nanofibrils, … → bottom-down). After dissolution the tissues are formed to new agglomerations, new systems. Nevertheless, observations of materials in laboratory on natural hierarchical levels are in dependency of the technical treatment, the preparation process, and thereby always somehow influenced (e.g. BRÄNDSTRÖM, 2001; BERGANDER AND SALMÉN, 2002; ZIMMERMANN ET AL., 2007). The technical use of wood and timber with focus on load bearing purposes not only results in separation. By means of "connection techniques" (see Fig. 4.4) beforehand classified elements are positioned and joined to larger structures (systems) known as engineered wood and timber products. These are designed to fulfill specific requirements e.g. in regard to

- stress transfer (1D, 2D);
- dimensions;
- homogenisation of physical properties by reduction of naturally inherent variability (e.g. strength, stiffness, density, swelling and shrinkage);
- surface (e.g. coating, haptic features, colour, multifunctionality e.g. in acoustics).

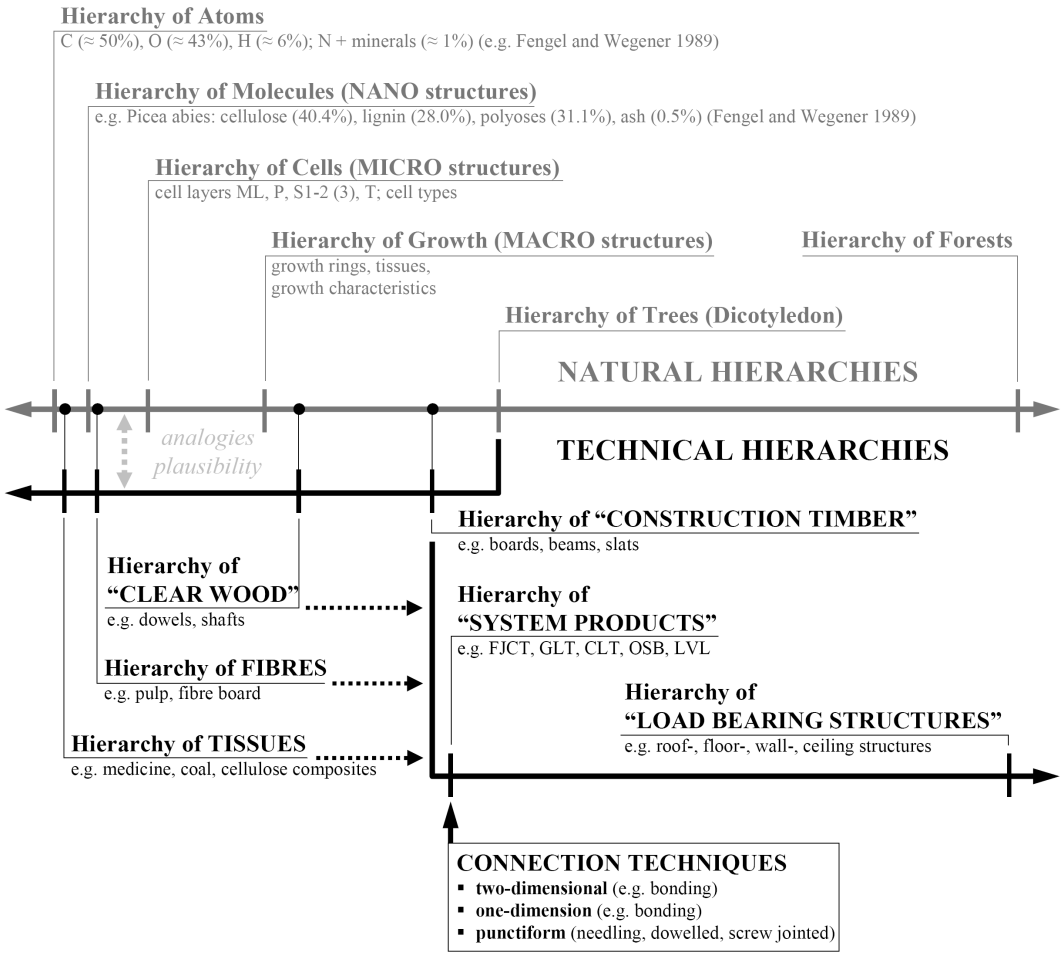

Fig. 4.4: Overview of natural and technical hierarchies in wood tissues, wood, timber and timber engineering

Following sub-sections present the main constituents and their functions on different hierachical levels. At first natural hierarchies are discussed followed secondly by the technical hierarchical levels, as illustrated in Fig. 4.4.

4.2.1 Natural Hierarchical Levels: Constituents, Functions and Models

In the following the bottom-up principle observable in natural creation of wood and timber is presented. The discussion starts at the atomistic level and ends briefly with some comments on forests.

Hierarchy of Atoms

This hierarchical level is defined within 10^{-19} to 10^{-10} m (= 1 Å). On that level e.g. quarks, neutrons, electrons and protons are the constituting elements of atoms. The atomic model consists of neutrons and protons in the core and electrons on discrete energy levels as shells of the atom. The main elements in wood and timber are carbon (C; ≈ 50%), oxygen (O_2; ≈ 43%), helium (H; ≈ 6%) and nitrogen (N) (organic agents) as well as minerals (anorganic agents). The last two are together about 1% of the mass of molecules (FENGEL AND WEGENER, 1989).

The mechanical behaviour on this hierarchical level can be studied by ab-initio calculations based on first-principle of quantum mechanics (e.g. COLUMBO, 2008).

Hierachy of Molecules

This level is defined within the range of 10^{-10} to 10^{-6} m known as "nano-level". The main molecules are cellulose (40% in Norway spruce; in general 40 ÷ 50%), hemicelluloses (polyoses) (31% in Norway spruce; in general 15 ÷ 35%), lignin (28% in Norway spruce; in general 20 ÷ 35%) as organic constituents, and about 1 ÷ 3% of anorganic substances (0.5% in Norway spruce; FENGEL AND WEGENER, 1989). The structure of wood is often viewed in analogy to reinforced concrete. Thereby cellulose acts as reinforcement and lignin as concrete (e.g. CLARKE, 1938; GOLDSTEIN, 1991). BOOKER AND SELL (1998) specify cellulose as steel reinforcement, hemicellulose as cement and lignin as rock and sand filler. Overall the wood polymer with its main constituents cellulose, hemicellulose and lignin can be best described as fibre-reinforced composite with cellulose as reinforcement and lignin and hemicelluloses as matrix material (e.g. SCHICKHOFER, 1994; SALMÉN, 2004; WATHÉN, 2006).

The **cellulose** constitutes a 1,4 β-glycosidic bonded, linear and unbranched chain-like molecule of β-D glucose. In native form it exhibits a high degree of polymerisation (DP), in the range of 10,000 to 15,000 (e.g. BLEDZKI AND GASSAN, 1999; WATHÉN, 2006). The chain consists of 89 ÷ 96% crystalline (ordered) and 4 ÷ 11% amorph (unordered) regions (FENGEL AND WEGENER, 1989). The cellobiose units with dimensions l / w / d = 1.03 nm / 0.8 nm / 0.8 nm are the basic units. These are further linked in serial to cellulose molecules.

The cellulose is anisotropic (BERGANDER AND SALMÉN, 2002) and unsolvable (FENGEL AND WEGENER, 1989; EICHHORN ET AL., 2001). Its mean density is ρ_{mean} = 1,500 kg/m³ (e.g. ROBERTS ET AL., 1995; EICHHORN ET AL., 2001; STEELE, 2007). Cellulose is highly affine to intra- and intermolecular H-bondings (WATHÉN, 2006). If stressed, two types of bindings are observable. These are C-O-C and H-H (HINTERSTOISSER ET AL., 2001). It behaves visco-elastic. In general its material characteristics are dependent on moisture, temperature and time (WATHÉN, 2006). Due to its chain-like linear structure and predominant longitudinal orientation in wood and timber cellulose primary determines the strength and stiffness characteristics in fibre direction. Interestingly, the maximum tensile strength is already reached at DP ≈ 2,000 (CLARK, 1938). The softening temperature of cellulose is given with ≥ 230 °C (WATERHOUSE, 1984).

Polyoses or **hemicelluloses** show a DP of 50 to 300 (WATHÉN, 2006). It consists of pentosis and hexosis (polysaccharides) like xylose, mannose, galactose and arabinose. The molecules are more or less branched chains (EICHHORN ET AL., 2001), anisotropic (BERGANDER AND SALMÉN, 2002) and constitute a kind of mediator between cellulose and lignin by stiffening and strengthening their interaction. Hemicellulose and lignin together form the matrix material in the fibre composite wood. They dominate the stiffness characteristics of fibres in transverse direction (SALMÉN, 2004). In particular at 10% moisture content hemicellulose and lignin together constitute an active stress transfer matrix between cellulose molecules (fibrils) (KERSAVAGE, 1973; BERGANDER AND SALMÉN, 2002). In comparison with cellulose hemicelluloses shows lower mechanical characteristics. Thereby xylose was found to be most important for strength (SPIEGELBERG, 1966; SJÖHOLM ET AL., 2000). It is assumed that hemicellulose crystallises after extraction which makes it difficult to determine reliable properties by mechanical testing (BERGANDER AND SALMÉN, 2002). The softening temperature of hemicelluloses is within the range of ≥ 150 ÷ 220 °C (WATERHOUSE, 1984).

Lignin is in particular in the later discussed middle lamella (ML) a highly branched macromolecule of phenylpropane units and assumed to be isotropic, at least if extracted (BERGANDER AND SALMÉN, 2002). Lignin is amorph and shows softening above 80 °C (SALMÉN, 2004) or at least above 124 ÷ 193 °C (WATERHOUSE, 1984). Lignin shows high resistance against compression (CLARKE, 1938). Together with hemicellulosis it acts as connector between cellulose fibrils and in particular between wood cells in the middle lamella. The lignification, an infiltration process of polysaccharides and lignin into the cell wall, starts in the middle lamella and already after the cell has reached its final size

(FENGEL AND WEGENER, 1989). SALMÉN (2004) describes lignin as material with a high degree of visco-elasticity and cellulose as well as hemicellulose as elastic. Both, cellulose and hemicellulose are hydrophil. Up to the fibre saturation point they are able to absorb four to five times the amount of water of lignin (COUSINS, 1978), with lignin being more or less hydrophob. Thereby only 20% of celluloses are able to absorb water (SALMÉN, 2004). According SALMÉN (2004) the loss of stiffness in cells up to 20% moisture content is caused by changes in hemicellulose.

Overall, for modelling of wood tissues on molecular hierarchical level a continuation of ab-inito calculations as well as the use of molecular dynamics, quantum mechanical models or empirical models based on classical physics are applied (e.g. COLUMBO, 2008).

Hierarchy of Cells

This level is dedicated to wood tissues within 10^{-6} to 10^{-3} m and is often named as "micro level". Within this level the main molecule cellulose aggregates to larger complexes. Together with hemicellulose and lignin these build up wood cells. In general a cellular structured material shows an optimised ratio of mechanical properties and weight (GIBSON AND ASHBY, 1999) and gives masterplans for an efficient use of resources. In the following firstly aggregates of cellulose molecules are discussed briefly followed secondly by the structure of the cell wall and detailed information for each wall-layer. A state-of-the-art review of cell wall mechanics serves as example of high sophisticated evolution by nature and source for transfer to technical applications.

Cellulose Aggregates

At first $30 \div 40$ parallel aligned and densely packed cellulose molecules aggregate to elementary fibrils of $3 \div 4$ nm in diameter (FENGEL AND WEGENER, 1989; SALMÉN, 2004; WATHÉN, 2006). About $18 \div 20$ of these elementary fibrils (WATHÉN, 2006) further agglomerate to microfibrils of about $10 \div 30$ nm in diameter (FENGEL AND WEGENER, 1989; EICHHORN ET AL., 2001; WATHÉN, 2006). As next these microfibrils are more or less parallel aligned in the cell wall layers and covered by strongly bonded and highly visco-elastic glucomannan. This causes an in-between distance of about $3 \div 4$ nm by being oriented in cell direction and surrounded by hemicelluloses and lignin (SALMÉN, 2004).

The Structure of Wood Cells

The cell wall consists of several layers (see Fig. 4.10, left) starting with the primary cell wall (P) followed by the secondary cell wall (S), which itself consists of S1, S2 and S3. In some timber species also a tertiary cell wall (T) is present. The cells themselves are connected by a thin middle lamella (ML). Due to its minor thickness a clear differentiation from P is difficult. Thus it is common to describe it as combined middle lamella (CML), as assembly together with the adjacent P-walls. The overall density of cell wall material is given with 1,500 kg/m³ (KOLLMANN AND CÔTE, 1968; ASHBY ET AL., 1995; EDER ET AL., 2009; MICHELL AND WILLIS, 1978; MICHELL ET AL., 1978; ORSO ET AL., 2006) and thus equal to the density of cellulose.

Tab. 4.1: Characteristics of cell wall layers of wood: shares of main constituents

cell wall [--]	**cellulose** [%] mass | volume	**hemicellulose** [%] mass | volume	**lignin** [%] mass | volume
ML	≈ 0% [1]; 12% [3]	44% [1]; 26% [3]	56% [1]; 62% [3]
P	15% [1]; 12% [3]	33% [1]; 26% [3]	52% [1]; 62% [3]
CML	16% | 11% [2]	29% | 14% [2]	55% | 75% [2]
S1	45% | 37% [2] 28% [1]; 35% [3]	33% | 35% [2] 31% [1]; 30% [3]	22% | 28% [2] 41% [1]; 35% [3]
S2	56% | 45% [2] 50% [1] [3]	28% | 34% [2] 31% [1]; 27% [3]	22% | 21% [2] 19% [1]; 23% [3]
S3	44% | 34% [2] 48% [1]; 45% [3]	34% | 36% [2] 36% [1]; 35% [3]	22% | 30% [2] 16% [1]; 20% [3]

[1] BERGANDER AND SALMÉN (2002)
[2] BURGERT (2007)
[3] FENGEL (1969) and KOLLMANN AND CÔTE (1968)

Tab. 4.1 and Tab. 4.2 give an overview of mass and volume fraction of the main molecules for each cell wall. Additionally the thickness and construction of cell walls in respect to the orientation of microfibrils relative to the cell axis, the microfibril angle (MFA) with MFA = 0° and MFA = 90° corresponding to parallel and perpendicular to cell axis, respectively, is given.

Tab. 4.2: Characteristics of cell wall layers of wood tissues: dimensions, MFA

cell wall [--]	**thickness** [1] **[µm]**	**thickness [%]** early- | latewood	**MFA [°]**	**# sub-lamellas** [3] **[--]**
ML	0.30	-- | --	--	--
P	0.10	-- | --	unordered [1]	--
CML	0.50	4.2% | 2.1% [2] 5% [3] 4.3% | 2.1% [4]	--	--
S1	0.15	12.5% | 9.0% [2] 10% [3] 12.4% | 8.8% [4]	–70 ÷ +70 [1] 50 ÷ 70 [3] [5]	4 ÷ 6
S2	1.60	78.7% | 85.4% [2] 75% [3] 79.0% | 85.8% [4]	0 ÷ 10 [1] 10 ÷ 30 [3] [5]	30 ÷ 150
S3	0.03	4.5% | 3.3% [2] 10% [3]	≈ 70 [1] 60 ÷ 90 [3] [5]	0 ÷ 6
T	--	4.3% | 3.3% [4]	--	--

[1] BERGANDER AND SALMÉN (2002)
[2] FENGEL AND STALL (1973)
[3] SCHNIEWIND (1989) and DINWOODIE (1989)
[4] FENGEL AND WEGENER (1989)
[5] HAKKILA (1998)

In the following paragraphs, the structure and function of the cell wall layers are discussed. BOOKER AND SELL (1998) studied fracture processes in cell walls with the hypothesis that they follow the path requiring lowest energy (lowest resistance). They observed that fracturing of microfibrils requires more energy than fracturing of matrix material. On that basis possible fracture paths and fracture mechanisms were analysed. Some of their results are presented for each layer.

The connecting layer between the cells, the middle lamella (ML), is a very thin and isotropic (CLARKE, 1938) layer primarily built up of lignin (≈ 60%) and hemicelluloses (≈ 30%).

The primary wall (P) is the first cell layer which is created by differentiation of a new wood cell by the secondary meristem cambium. It shows low MFA and antidromic net-like sub-layers composed of microfibrills. The P-layer consists of thin microfibrils and shows a high amount of hemicelluloses, pectin and lignin (CLARKE, 1938). The net-structure together with the high amount of branched molecules enables the P-layer to expand easily during cell differentiation in all directions, in particular transversely. Both cell layers, ML and P, play an important role in the mechanical potential and fracture mechanics of wooden cells. Following BOOKER AND SELL (1998) the combined middle lamella (CML) resists delamination of the double cell walls (interwall checking) and prevents internal checking. Additionally it is a part of the mechanism to absorb vibration energy. CLARKE (1938) report that green wood under tension stress parallel to grain fails in P or ML. GORDON AND JERONIMIDIS (1974) analysed fibre composites under tension load parallel to grain and observed fibre separation (failure initiated in P or ML) followed by tension buckling. Thereby tension buckling stands for cell folding followed by subsequent cell collaps (e.g. EDER ET AL., 2008A).

The secondary wall (S) is created after primary cell differentiation. It is responsible for stability and strength of the cell in longitudinal and transverse direction. Its structure prevents radial cell expansion (CLARKE, 1938). The secondary wall layer consists of three sub-layers S1, S2 and S3. The sub-layer S2 with a share of roughly 80 ÷ 90% of total cell wall thickness dominates clearly the characteristics of the total cell wall. It is primary responsible for its mechanical stability in longitudinal direction. Sub-layers S1 and S3 dominate cell wall mechanics in transverse direction and play an important role in explaining differences between early- and latewood (BERGANDER AND SALMÉN, 2002). The fibrils in S1 and S3 are more or less perpendicular oriented to that in S2 (BOOKER AND SELL, 1998). This activates some locking effect. In the following paragraphs each sub-layer will be outlined separately.

Compared to S2 sub-layer S1 consists of more loosely packed microfibrils. These change their orientation alternating between each sub-sub-layer from S- to Z-helix, e.g. in Norway spruce with overall MFA = 54° and MFA = 46° in early- and latewood, respectively (BRÄNDSTRÖM, 2001; FENGEL AND WEGENER, 1989). BOOKER AND SELL (1998) report that in Norway spruce the MFA changes from S-helix outside (boundary of P and S1) with MFA = 45° to a Z-helix and MFA = 70° inside (boundary of S1 and S2). Thus a nearly perpendicular orientation of fibrils from out- to inside of the cell with main orientation transverse to the cell axis can be observed. In cell wall mechanics in case of

axial compression S1 limits the maximum shear stresses in CML by limiting the expansibility of later discussed S2 sub-layer (locking effect). Due to the fact that fibrils are not tightly packed it is assumed that the constraining mechanism starts already above a certain limit. Furthermore S1 prevents interwall cracks from developing into transwall cracks (BOOKER AND SELL, 1998). Nevertheless, MARK AND GILLIS (1970) report that fracture in cell wall initiates at the boarder or within S1. This was observed experimentally by DAVIES (1968), GROZDITS AND IFJU (1969), KEITH AND CÔTE (1968), KÓRÁN (1967) and MARK (1967).

The sub-layer S2 is the dominating layer in wooden cells. The densily packed microfibrils are strongly parallel aligned in a Z-helix with a low MFA of 0 ÷ 30° (0 ÷ 20° according BOOKER AND SELL, 1998).

The orientation of microfibril aggregates transversely the cell wall is controversely discussed. KERR AND GORING (1975), CLARKE (1938), FAHLEN AND SALMÉN (2002), RUEL AND GORING (1978) and SALMÉN (2004) propose an arrangement in concentric lamellas. Thereby CLARKE (1938) states that the observable arrangement of microfibrils depends on the treatment done in preparing the specimen. SELL AND ZIMMERMANN (1993), SELL (1994), BOOKER AND SELL (1998), SCHWARZE AND ENGELS (1998) and ZIMMERMANN ET AL. (2006, 2007) confirm the observation that the observable structure depends on the treatment beforehand. In dependency of the treatment concentric, radial as well as random arrangements of microfilbril aggreagates were found. Nevertheless, a sandwich construction of with microfibril reinforced radial ribs is proposed by ZIMMERMANN ET AL. (1994). From the mechanical point of view this arrangement increases the resistance of the cell against buckling (axial compression forces), against collaps (negative pressure induced by water transport), and it increases the bending stiffness (BOOKER AND SELL, 1998). A high resistance of S2 is required because this layer is in principle responsible to support own weight as well as normal stresses imposed externally (e.g. by wind or snow) (BOOKER AND SELL, 1998). If compressed axially S2 rotates slightly due to MFA > 0° and compresses (expands) like a spring (FRATZL AND WEINKAMMER, 2007; GORDON AND JERONIMIDIS, 1974; KECKES ET AL., 2003). Thereby the compression (expansion) capacity and rotation of S2 is restricted by S1. The role of MFA is apparent. The steeper the windings the stiffer the respond of S2 against stresses. Furthermore, all cells show in principle the same helical orientation. Thus neighboured cell walls have opposite MFA which lead to a kind of reinforcement, a locking effect, between the cells. This induces shear stresses in ML and CML (e.g. KECKES ET AL.,

2003). Thereby higher branched 3D lignin is suitable to resist these shear stresses. Furthermore, it supports the damping mechanism by dissipating vibrational energy. This damping mechanism is also present within the rib-like structured microfibrill aggregates in the cross section of S2. Thereby it damps the rotation due to lignin-layers between cellulose ribs stressed under cyclic shear. S2 also remarkable resists transwall crack propagation (BOOKER AND SELL, 1998). Additionally, mechanics of S2 seems to be independent of tree species. This was observed by analysing tension tests on cell walls of Norway spruce, pine and poplar (EDER, 2007).

The structure of the third sub-layer S3 shows a MFA varying between $60 \div 90°$ (HAKKILA, 1998) and a flat helical arrangement of microfibrils (CLARKE, 1938). BOOKER AND SELL (1998) give a MFA = 70° and a Z-helix on the outside which changes to MFA = 30° and to a S-helix in the inside of S3. Following that, microfibrils at outside and inside of S3 are nearly perpendicular to each other with most fibrils oriented transversely to the cell axis. Furthermore a high variation of MFA in the range of 30° and 90° between tracheids in the innermost part of S3 is reported. In cell wall mechanics S3 strengthens the cell wall against collapse, e.g. due to hydrostatic tension forces from negative pressure as consequence of water transport. Furthermore, the sub-layer reinforces the cell wall against transwall fracturing perpendicular to grain and stiffens the cell wall decisively transversely (BOOKER AND SELL, 1998).

The tertiary cell wall layer (T) is not present in all wood species. If it is, its fibrils are in a flat and not strictly parallel arrangement. The surface is sometimes covered by warts (warty layer).

So far characteristics and mechanics of cell wall layers have been discussed. Analysing fracture processes of the whole wooden cell PAGE ET AL. (1972) and PAGE AND EL-HOSSEINY (1976) remark that the occurrence and amount of local fibre defects and MFA in S2 are the main parameters. According PAGE ET AL. (1971) failure of single fibres stressed in tension is initiated by buckling (tension buckling). JAYNE (1959) describes fibres under tension parallel to grain as viscoelastic. KERSAVAGE (1973) report that dry fibres of low MFA stressed in tension parallel to grain behave linear-elastic. FRATZL AND WEINKAMMER (2007) remark that modulation of strength and stiffness properties between layers of the cell wall create an effective crack stopping mechanism. This is due to the variation of constituents and MFA. REITERER ET AL. (1999) states that < MFA in the dominating layer S2 makes cell wall stiff and brittle whereas > MFA consequences a flexible and tough behaviour if stressed in tension parallel to grain. More generally

FRATZL AND WEINKAMMER (2007) state that during elongation of cells and decrease of MFA matrix between fibrils is sheared up to a critical point. Above this point partial and irreversible deformation is given due to successive failing bonds. After stress release a rebonding is assumed which leads to some kind of arresting of the cell in elongated position. Thus the matrix is not irreversible damaged although the cell is irreversible elongated (KECKES ET AL., 2003). This mechanism requires strong bindings between fibrils and matrix (KECKES ET AL., 2003; FRATZL ET AL., 2004). WATHÉN (2006) references HILL (1967) who observed a decreasing MFA in wood under creep stresses in tension parallel to grain. Stiffening and increase of plastic deformation was also observed in cyclic tensile tests of wood fibres by WILD ET AL. (1999), SEDIGHI-GILANI AND NAVI (2007) and EDER ET AL. (2008B).

Although the following belongs to the next hierarchy some notes on early- vs. latewood as well as juvenile vs. adult wooden fibres are already given now. These facts support the understanding of fracture processes and its influencing parameters. According MARK (1967) latewood cells are in comparison to earlywood cells not only stiffer and stronger because of their thicker cell walls but also because of a lower MFA (see also BRÄNDSTRÖM, 2001). EDER ET AL. (2008A) tested wet fibres of Norway spruce in tension parallel to grain. They report on tension buckling in cells after initial fibre folding in (thin) earlywood fibres and transverse cracking in (thick) latewood fibres. In the latter case weak zones like piths or pith fields showed to be more relevant for cracking than in thin walls. Comparing trees with different growth rates BRÄNDSTRÖM (2001) report that MFA in cells of fast growing trees is higher. MFA decreases significantly from pith to bark influenced by juvenile and adult cambium meristem, respectively.

FRATZL AND WEINKAMMER (2007) state that natural (nano) composites combine two in principle contradicting properties, namely stiffness and toughness. The stress-strain relationship shows high stiffness at lower stresses but a much softer behaviour at high stresses comparable to an elastic-plastic spring (FRATZL AND WEINKAMMER, 2007). As common in all composites also wooden fibres are joined by a thin glue layer which is loaded under shear. Thus stiffness comes from fibres whereas toughness results from plastic deformations of the glue layer (FRATZL AND WEINKAMMER, 2007).

Wood Cell Types

So far constituents, structure and function of cell wall layers were discussed. As next, the types of cells and their function in the living tree are presented. At first differentiation is

made in cell types of softwoods (coniferous tree species) and hardwoods (deciduous tree species). In regard to the evolution timeline hardwoods are younger than softwoods and are characterised by a more complex structure and cell types which are optimised for each specific function. Tab. 4.3 gives a brief overview of cell types and functions of both, soft- and hardwoods. For example Norway spruce consists of about 95.3% tracheids and 1.4 ÷ 5.8% longitudinal and 4.7% radial parenchyma cells (FENGEL AND WEGENER, 1989). In general tracheids decisively determine the physical (mechanical) properties of softwoods. The main parameters influencing the mechanical performance are

- length;
- diameter;
- cell wall thickness;
- structure of S2 (e.g. share of cellulose and MFA).

Tab. 4.3: Wood cell types and their functions in soft- and hardwoods (according FENGEL AND WEGENER, 1989)

function	softwoods	hardwoods
mechanical function (e.g. load bearing, stress transfer, stiffening)	latewood tracheids	libriform fibres fibre tracheids
conducting (transport) function	earlywood tracheids radial parenchyma (wood rays)	wood vessels (tracheae)
storage function	radial parenchyma longitudinal parenchyma (resin channels)	radial parenchyma longitudinal parenchyma (resin channels)
secretion function	epithel cells	epithel cells
local mechanical function (reaction wood)	compression wood (opposite wood)	tension wood (opposite wood)

An overview of the dimensions of tracheids is given in Tab. 4.4. In Norway spruce tracheids show a mean length of 1.7 ÷ (2.9) ÷ 3.7 mm and a diameter of 20 ÷ (30) ÷ 40 µm (FENGEL AND WEGENER, 1989). In general, the length of tracheids depends on the fusiform cambial cell (BRÄNDSTRÖM, 2001). After differentiation the cell elongates to its final shape. The length of tracheids can change afterwards to initiate some

pre-stress in tension or compression transversely (WEINKAMMER AND FRATZL, 2007; MATTHECK, 1994, 2003).

Tab. 4.4: Characteristics of tracheids of Norway spruce: dimensions in juvenile vs. adult wood as well as early- vs. latewood

	juvenile wood [1)]	**mature wood** [1)]	**earlywood**	**latewood**
tracheid length [mm]	1.3 ÷ 2.7	2.8 ÷ 4.3	--	--
tracheid diameter (rad.) [µm]	15.0 ÷ 29.0	29.3 ÷ 39.7	39.3 [2)]	13.1 [2)]
tracheid diameter (tan.) [µm]			32.7 [2)]	32.1 [2)]
tracheid wall thickness (rad.) [µm]	0.8 ÷ 4.6	2.1 ÷ 7.5	3.5 [3)]	6.2 [3)]
tracheid wall thickness (tan.) [µm]			2.9 [3)]	4.7 [3)]

1) BOUTELJE (1968)
2) FENGEL (1969)
3) OLLINMAA (1961)

Additional differences between early- and latewood as well as between juvenile and adult wood are discussed in the next section, dedicated to the hierarchy of growth.

Beside fibre tracheids libriform fibres are responsible for load bearing and stiffening in hardwoods (FENGEL AND WEGENER, 1989).

Parenchyma cells operate as storage. Radial oriented parenchyma (wood rays) act additionally as reinforcement of wood in transverse direction (FENGEL AND WEGENER, 1989; MATTHECK, 1994).

Wood vessels or tracheae are only common in hardwoods. They are one impressive proof of the evolution of wood tissue from soft- to hardwoods and the separation of conducting and transport from the mechanical function. Thereby vessels are responsible for transport of water and nutrients (FENGEL AND WEGENER, 1989).

Epithel-cells are secretion channels (FENGEL AND WEGENER, 1989).

To conclude, for cell wall mechanics it is required to have comprehensive knowledge of dimensional relationships, volume and mass fractions of constituents, geometry, MFA in layers and sub-layers and about the interaction between adjacent cells. Thereby it is recommended to model two or more cells instead of single cells or at least to study

double cell walls built up of S3, S2, S1, CML, S1, S2, S3 and empty lumen (BARBER AND MEYLAN, 1964).

Hierarchy of Growth

The hierarchy of growth is roughly defined within 10^{-3} to 10^{0} m. Thereby cells of previous mentioned types form large structures (tissues) which aggregate to wood and timber. The main structural element is the annual or seasonal growth ring as the result of secondary growth in thickness. In temperate climate zones on wood (xylem) and bark side (phloem) every year a ring of several cell rows is formed by the secondary meristem cambium. In tropical or subtropical climate the formation is linked to breaks in growth. In extreme dry and cold regions with extreme short vegetative periods sometimes only a partial growth ring is created (see e.g. *Pinus longaeva*). Nevertheless, the focus is on tree species of temperate climate zones and in particular on softwoods. Every annual growth ring consists radially of an early- and latewood zone. As given in Tab. 4.3 earlywood is primary responsible for conduction and transport whereas latewood primary provides mechanical stability. The wider the annual growth rings the wider the zones of earlywood by more or less constant thick latewood. In hardwood two distinctive different formations of cells in growth rings can be distinguished, namely ringporous species and diffuse porous species. Ringporous species create one or more rings of tracheae (vessels) in spring responsible for conduction and transport. These rings are followed by a zone of libriform fibres, tracheids and longitudinal parenchyma cells which are responsible for the mechanical stability, strength and stiffness of the tree. The wider the growth rings the thicker the latewood zones. Thereby the porous ring zone stays constant over the years. In growth rings of diffuse porous species vessels are randomly distributed and give a more regular pattern. Nevertheless, due to denser wood at the end of the growth ring they are visible macroscopically.

Back to early- and latewood of softwoods PAAKKARI AND SERIMAA (1984) observed higher MFA in early- than in latewood. Differences between both are explained with different shares of hemicelluloses (BERGANDER AND SALMÉN, 2002). Tracheids in latewood are observed to be longer than in earlywood but decrease distinctively in length at the end of the growth ring (BRÄNDSTRÖM, 2001). The cell wall thickness in latewood is also higher but decreases sharply at the end of the annual growth ring (in reference to DENNE, 1973; GINDL AND WIMMER, 2000). The cell wall thickness and the share of latewood increase with age and height of the tree (BRÄNDSTRÖM, 2001). The changing dimensions and shares in early- and latewood affect also the density. In Norway spruce it

increases from 300 kg/m³ in earlywood via 450 kg/m³ in transition wood and to 1,000 kg/m³ in latewood of nearly constant width of 0.2 mm (PERSSON, 2000).

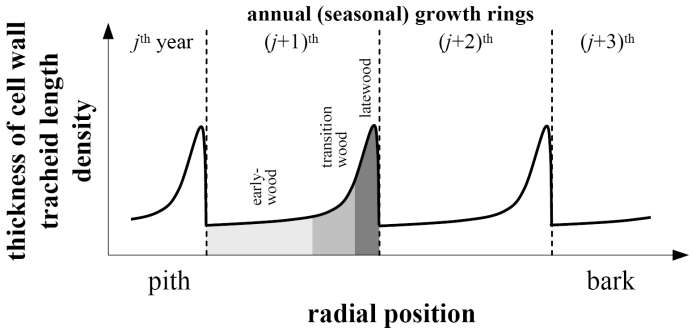

Fig. 4.5: Qualitative trend of density transversely with analogies to changes in MFA, length of tracheids and cell wall thickness

The cell diameter in tangential direction is more or less constant whereas in radial direction earlywood cells are larger e.g. BRÄNDSTRÖM, 2001; Tab. 4.4). Changes in cell diameter and wall thickness together lead to a remarkable increase of bulk material in latewood. Together with a reduced MFA an increase in strength and stiffness longitudinally is given.

With maturing of the cambium the characteristics of cells change in radial direction of the tree, from pith to bark. These changes are known as transition process from juvenile to adult wood. This transition process is in particular distinctive in softwoods but also present in hardwoods (see Fig. 4.6).

The juvenile wood zone is characterised by a sudden change of wood properties, increase e.g. in density, fibre length, cell wall thickness, strength and stiffness longitudinally, share of latewood and swelling and shrinkage transversely, as well as by a decrease e.g. of MFA and swelling and shrinkage longitudinally (see e.g. BENDTSEN, 1978; Fig. 4.7). These changes are observed to be highly variable even in the same tree species and growth region (e.g. ABDEL-GADIR AND KRAHMER, 1993). The change was also found to passing nonlinearly to adult wood zone over the transformation region. The transformation zone is often associated with an age of five to twenty years in softwoods, in Norway spruce with around 20 years. Nevertheless, the timeline of the transition process is highly variable and depends on the analysed characteristic (e.g. ZOBEL AND SPRAGUE, 1998).

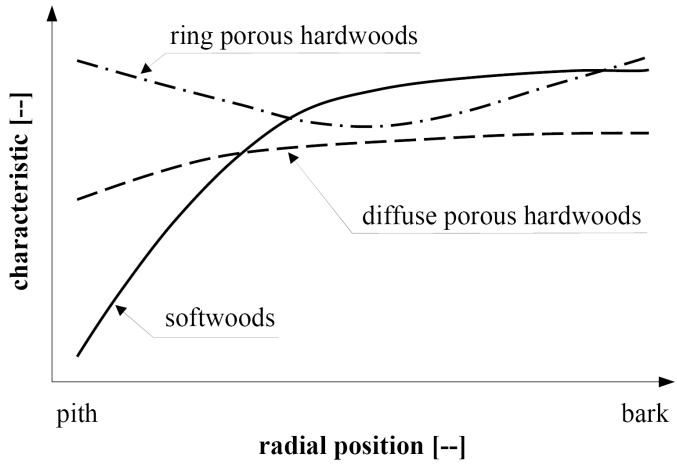

Fig. 4.6: Qualitative change in characteristics from juvenile to adult wood in softwoods as well as ring and diffuse porous hardwoods: exemplarily for density (ZOBEL AND SPRAGUE, 1998)

The adult wood is described as region of more homogeneous and nearly constant wood properties. Due to changes in fusiform cambial cells MFA in S2 in juvenile tracheids of softwoods is $20 \div 40°$ whereas adult wood shows $6 \div 10°$ (SERIMAA ET AL., 2000; LICHTENEGGER ET AL., 2000). The length of tracheids increases from $1.3 \div 2.7$ mm to $2.8 \div 4.3$ mm in juvenile and adult wood zones, respectively (BRÄNDSTRÖM, 2001). Also tracheid diameter and cell wall thickness increase, from $15 \div 29$ µm to $29 \div 40$ µm and from $0.8 \div 4.6$ µm to $2.1 \div 7.5$ µm in juvenile and adult wood, respectively (BRÄNDSTRÖM, 2001).

The zone of juvenile wood appears more or less as cylindrical volume in the core of the tree which corresponds to the age of cambium. In contrast, the radial change from sap- to heartwood, with sapwood at the outside and of constant thickness within the same tree, leads to a cone-shaped volume of heartwood in the core of the tree (see Fig. 4.8).

Sapwood represents the younger wooden part positioned adjacent to the bark zone. It consists of a certain amount of living cells, at least the parenchyma cells as well as some cells of the last annual growth ring(s). Its main functions are the transport of water and nutrients from root to top as well as the storage of sugars. Sapwood has very high moisture content, often above 100%. In contrast, heartwood is in the core of trees. It has no living cells and lower moisture content around the fibre saturation point ($u \approx 25 \div 30\%$). Physiologically heartwood is the inactive wooden part in trees

(GROSSER, 2003). It follows after a naturally, chemically transformation process in a certain age of the tree, leading in many species to more durable wood. Also in many tree species heartwood can be differentiated from sapwood by its colour. The classification of heartwood according its colour can be made in species with true heartwood (obligatory creation of distinct coloured heartwood), false heartwood (facultative occurrence of coloured heartwood), ripewood (heartwood without change in colour) and tree species with heart- and ripewood (e.g. GROSSER, 2003).

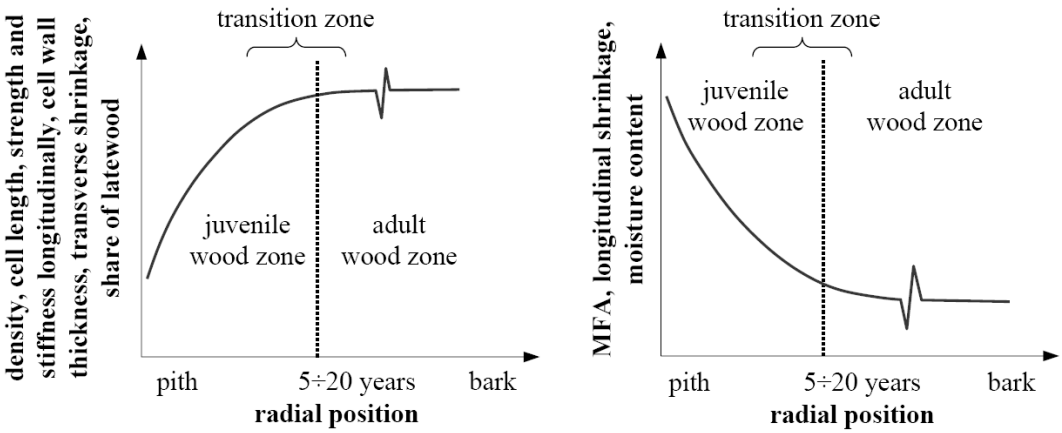

Fig. 4.7: Changes in characteristics from juvenile to adult wood in softwoods according BENDTSEN (1978): increasing characteristics (left); decreasing characteristics (right)

For local mechanical reaction on asymmetric or exeptional externally or internally applied stresses trees are able to form reaction wood in combination with opposite wood, placed radially on the other side of the pith. Softwood species create compression wood and hardwoods tension wood (see Tab. 4.3) to support the tree against local compression or tension stresses, respectively. Cells of compression wood are cylindrical in shape with a high amount of lignin (visually appearing darker in colour) (e.g. WIMMER, 2002). It stiffens the wood against compression stresses and supports with the reduction of contact area between neighboured cells, so that cells can glide more easily against each other. In case of high compressive stresses transversal expansion of cells leads to an increase of contact area and stiffness. Tension wood in hardwoods is characterised by a high amount of celluloses. The tracheids of tension wood have a gelatinous layer (G-layer) in the secondary wall of highly parallel arranged cellulose fibrils which are oriented strictly in longitudinal direction (CÔTÉ AND DAY, 1964; WIMMER, 2002).

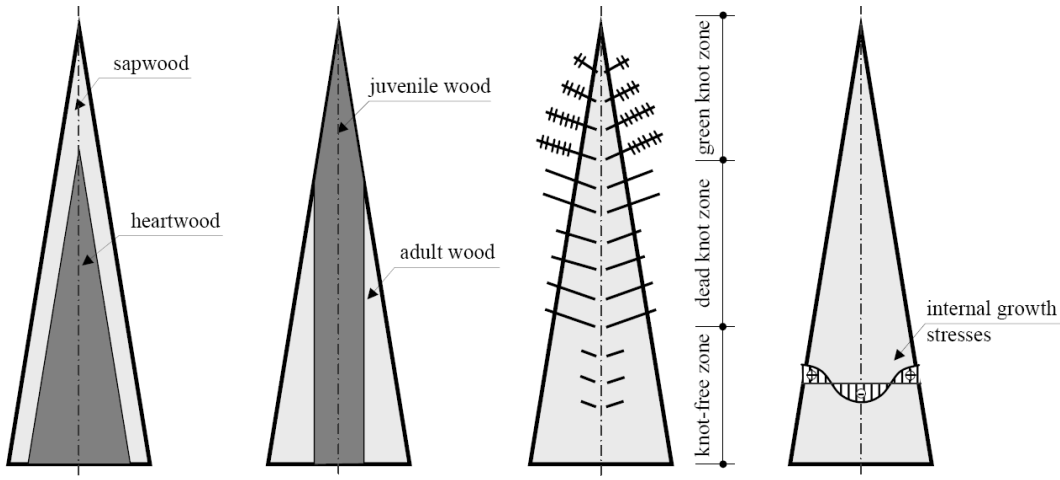

Fig. 4.8: Wood and timber zones in longitudinal and transverse direction of trunks: sap- vs. heartwood (left); juvenile vs. adult wood (left-middle); knot zones in trees observed from outside (middle-right); internal growth stresses (pre-stresses) in trees (right)

To summarise, within the hierarchy of growth several mechanical characteristics are differentiated, e.g. within the growth ring (early- vs. latewood), between juvenile and adult wood, heart- and sapwood as well as between normal and reaction wood. Many of these characteristics are a consequence of the age of the tree, the age of the secondary meristem cambium and due to the ability to respond on externally applied stresses.

Hierarchy of Trees

This hierarchical level comprises all main elements of trees, like the crown, the stem, branches and the root system, all roughly within a range of 10^0 to 10^2 m. In regard to this manuscript the focus is on the stem and branches, the latter so far it is a part of the stem. In particular these elements play a major role in classifying wood and timber for technical applications. At this hierarchical level all so far discussed elements of previous hierarchies merge to the final complex, the individual tree, as the largest living unit on earth. The complex of all constituents described previously, cellulose, hemicellulose and lignin, the different cell wall layers, cell types and their individual specifications within the growth ring and along the stem, juvenile vs. adult wood, heart- and softwood and zones with or without knots, etc., are beside their individual and local adaptability what is generally experienced as a tree.

With focus on the trunk the key element within this hierarchy are branches. They are the bearing element of the leafes which form the supply unit for taking up sun energy, CO_2 and release of O_2. The part of branches included in the stem is called knot. The longitudinal occurrence of branches appears very regular in softwoods being strongly apical dominant. In hardwoods this dominance is often not as strict as in softwoods. The formation and the age of branches in trees in longitudinal direction, from root to top, are linked to the position of the tree and its branches relative to the sunlight. In open stands branches are observable along the whole tree. In dense stands the stem of an older tree shows in principle three zones from root to top, respectively, a zone free of branches, a zone of dead branches and a zone of green leaf bearing branches (see Fig. 4.8). As branches normally arise from the pith, the innermost region of stems shows higher knot density than the outer zone. The way how branches are incorporated in the stem (see e.g. SHIGO, 1986) together with the higher knot density in the core of stems act like a reinforcing element, i.e. like dowels in case of wind loads and induced bending stresses. They increase the resistance of timber against shear in the most shear stressed inner zone and increase the resistance against bending stresses in the lateral stem region in case of being absent. The branch itself can be mechanically modelled as one-sided restraint cantilever with elastic bedding. Thereby reaction wood and opposite wood plays a major role in stabilising the branch, in particular near the stem. Higher bending resistance in the outer part of the stem is supported additionally by adult wood as well as by the pre-stressed core of the tree (see Fig. 4.8). This pre-stressing compensates the fact that due to the alignment of tracheids wood is optimised for tension but not for compression (MATTHECK, 1995). For stabilisation against wind loads, gravity and landslide on hillsides trees often show reaction wood at the root end.

Another characteristic of trees is the spiral grain. In the first years of a tree the cells wind longitudinally in a left spiral around the pith which later changes to a right helix. This helical orientation varies remarkable between and even within tree species. In particular in Norway spruce change in spiral orientation is found to be linked with the transition of juvenile to adult wood (e.g. HOFFMEYER, 1987). In sawn timber spiral grain is one reason for global grain deviation which describes the orientation of fibres in respect to the edge of prismatic sawn structural timber. The other reason for global grain deviation is the cutting process if not done parallel to the outside of the stem (which is common in standard structural timber) or not properly edging (HOFFMEYER, 1987). Global grain deviation in sawn timber not only significantly reduces strength and stiffness but also amplifies warping and twisting.

Hierarchy of Forests

This hierarchy overspans the range of 10^2 to $\geq 10^6$ m. For example, in particular in Central Europe managed forests have following four main functions:

- utility function: sustainable forest management;
- protection function: against erosion, avalanches, falling rocks, etc.;
- regeneration function: harmonising human life;
- welfare function: storage and reconditioning of water and air.

Wood and timber of each tree highly depends not only on genetics but also on local supply and climate conditions even if trees are grown in managed forests. Thus timber shows a very high variability in its characteristics, in particular in strength and stiffness, even between trees of the same forest and of the same species. This underlines the assumption that nature in principal delivers some kind of recipe for life which is every time adapted on local needs and challenges (FRATZL AND WEINKAMMER, 2007). As trees are a complex of all these individually but in context to the whole system adapted cells and tissues a high variability in characteristics consequences. This is in particular amplified by the fact that cells in trees after established and lignified are not rebuilt or adapted once conditions have changed, as it is known e.g. from bone.

4.2.2 Technical Hierarchical Levels: Constituents, Functions and Models

The aim of this section is to present or just list some utilisation examples of wood, timber and their tissues separately for each technical hierarchy. This is done in context to natural hierarchies. Technical products of these hierarchical levels are always a result of separation, starting by harvesting and trimming of tree stems up to mechanical or chemical dissolution of wood and timber to fibres and molecules (tissues). Some of the products follow from agglomeration of beforehand dissolved tissues or sawn timber products. The variety of basic elements and structures of agglomeration and the possibilities in joining creates numerous products and structures which can be engineered to be optimised for specific technical applications. Thus discussing products of technical hierarchies cannot be done without considering the external tool of joining techniques.

Hierarchy of Tissues

Products of this hierarchy are in the range of 10^{-9} to 10^{-6} m. Examples are e.g. cellulose nanofibrils for the creation of high-capacity fibre reinforced composites, tannic acids e.g. from oak for tanneries, extractives for food industry like vanillin or suggars, for medicin like acetylsalicyl acid, lignin as adhesive and much more.

Hierarchy of Fibres

This hierarchy overspans 10^{-6} to 10^{-3} m. Wood fibres are widely used, e.g. for (high, medium, low density) fibre boards (with / without additional adhesives), pulp for paper and packaging, fibres for clothes and hygienic products or for the production of wood plastic composites (WPCs).

Hierarchy of Clear Wood

Clear wood in this hierarchy is not as strict defined as e.g. in DIN 52180. It describes timber without any natural growth characteristics, e.g. like knots or checks. The hierarchy overspans roughly 10^{-3} to $\geq 10^{-1}$ m. Famous technical products on this hierarchical level are e.g. various sawn products like battens, helves, veneers or massive panels for furnitures. The characteristics of clear wood are also of interest for modelling of finger joints in structural timber which have to be placed in a clear section.

Hierarchy of Construction Timber

The range of roughly 10^{-2} to 10^{1} m of the hierarchy of construction timber overlaps in the lower region with the previous hierarchy of clear wood. Well known representatives of this hierarchy are sawn products like boards, posts and beams. For application as load bearing elements construction timber is standardised in strength and stiffness grades by classifying the timber according regulated requirements.

Hierarchy of System Products

System products or engineered timber products are typically in the range of 10^{-2} to 10^{10} m. These products are designed to fulfill special properties as e.g. mentioned in section 4.2. These products base on sawn timber or even smaller timber elements which are joined by adequate connection techniques to linear, two- or three-dimensional load bearing products of dimensions even larger than trees. In particular two- and three-

dimensional products are designed for loads in and out of plane. Some representatives of linear members are finger jointed construction timber, duo and trio beams and glued laminated timber (glulam; GLT). Products for a two-dimensional load transfer are cross laminated timber (CLT), plywood or laminated veneer lumber (LVL) and oriented strand boards (OSB). All these products base on structural timber elements which are joined rigidly by adhesives. Another possibility is to join the elements by means of mechanical fasteners, e.g. nails, screws or bolts. Well known system products in this category are nail-laminated posts or pre-stressed timber bridge decks.

All these products have in common the homogenisation of physical properties of timber. In particular cross laminated products suffer from distinctive homogenisation of swelling and shrinkage. The resulting mechanical characteristics, foremost strength properties, depend decisively on the arrangement of the elements in respect to the stress situation, i.e. if they act primarily in serial or parallel. Consequently, these products are suffering from system effects of first and even second category, $k_{sys,I}$ and $k_{sys,II}$, see section 1.1.

Hierarchy of Load Bearing Structures

This hierarchy again overlaps with the previous one. It is defined within 10^0 to 10^{10} m. It comprises all structures, e.g. roof-, floor- and wall-constructions as well as bridges. Thereby products of previous hierarchies are combined by direct joining side-by-side (e.g. folded pannels) or indirect connection via load distributing elements of a secondary or tertiary load bearing and load distributing structure. Again system effects can be utilised. These system effects can be a result of category one to three, $k_{sys,I}$ to $k_{sys,III}$, see section 1.1. A design principle in particular relevant for this hierarchy is robustness. Thereby extend of damage of a structure should be in relationship to the cause of damage and in respect to the importance of the structure and risks. In principle in case of serial and brittle acting systems or statically determined structures load transfer between structural key elements should be prevented whereas in case of redundant, parallel acting systems or statically indetermined structures or in principle in systems with ductile behaving elements the connection between elements should enable load transfer and load redistribution to prevent a dramatic (local) collaps in case of partial failure without warning in advance (e.g. by large deformations). The ability of a structure to resist static as well as dynamic loading depends in principal on the type of connection which is, as in the previous hierarchy, a key characteristic for the design of system structures.

4.3 Analogies between the Hierarchies of Wood and Timber

The term "analogy" (greek-latin) in general stands for equivalence, similarity, conformity and identity of relationships (DUDEN, 2005). The aim of this section is to discuss some analogies between several natural as well as technical hierarchies. Some analogies in structure, the influence of angle between stress and fibre direction and similarities in failure behaviour on various hierarchies are presented. In addition, the influence of stochastics in respect to size (volume) effects are presented exemplarily. Once more it is the aim to stress the hierarchical structure of wood and timber and to underline the importance to perform material research on various scales.

4.3.1 Analogies between the Structures of Wood and Timber Tissues

Wood and timber are widely described as being analog to fibre reinforced composites. Wood and timber are materials which show a distinctive relationship between physical characteristics and fibre orientation. This is in particular obvious if the rhombic anisotropic, roughly orthotropic material characteristics are considered. Summarising the structural details presented in the discussion of natural hierarchies in section 4.2.1 following similarities can be found:

- cellulose molecules of cellobiose units are polymerised to serial chains of 7,000 to 15,000 elements; these chains have crystalline and amorph sections; strong tendency of intra- and intermolecular H-bondings (sub-structures for cross-linking) imply conglomeration to elementary- and further to micro-fibrils of strictly parallel aligned cellulose molecules (see Fig. 4.9);
- the cellulose microfibrils are surrounded by branched chain molecules of hemicelluloses which act as cross-linking agent to the three-dimensional and highly branched lignin-molecules; the polymer of cellulose fibrils, hemicellulose and lignin are the basic elements in the cell wall;
- the cell wall consists of various sub-layers with sub-layer S2 as dominating layer (roughly 80 ÷ 90% of cell wall thickness) which itself consists of strictly parallel aligned and densily packed fibrils; characteristics of S2 determine the cell wall properties longitudinally whereas sub-layers like S1 and S3 stabilise S2 by cross orientation of fibrils; they influence decisively the cell wall properties transversely (see Fig. 4.10);

- the cells (in softwoods roughly 95% tracheids) are again parallel aligned and oriented longitudinally but cross-linked in serial by the middle lamella with its main constituents hemicelluloses and lignin; cells are linked in serial within the tree forming chains e.g. for transport of water and nutrients; these chains are parallel aligned but the connections between the cells are interlaced longitudinally or layered horizontally (see Fig. 4.11);
- cell complexes form radial circular growth rings which are reinforced transversely and linked by radial parenchyma (rays); branches intergrown or at least incorporated as knots in the stem reinforce wood against shear and tension as well as compression failures perpendicular to grain;
- in trees, zones with and without knots alternate longitudinally and radially.

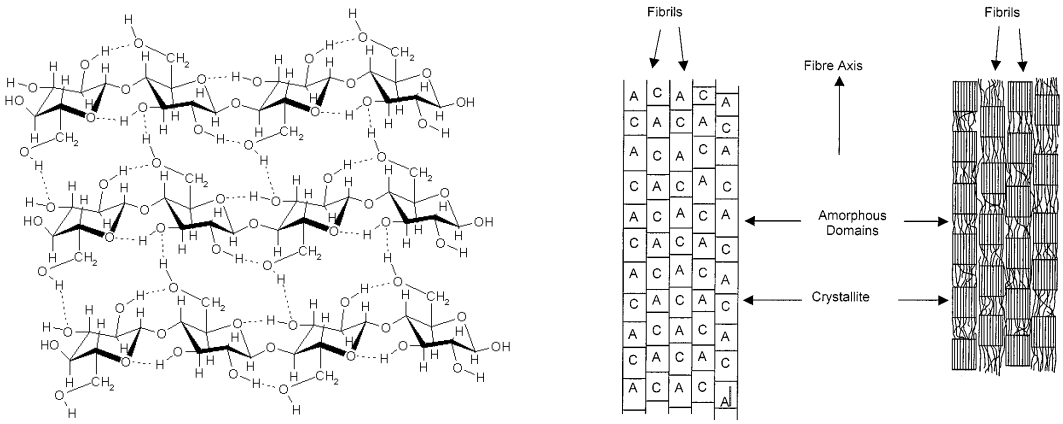

Fig. 4.9: Arrangement of cellulose molecules: chemical structure and intra- and intermolecular bondings (left; UNIVERSITY OF CAMBRIDGE, 2010); interlaced arrangement of cellulose fibrils – amorph and crystalline zones (right; EICHHORN ET AL., 2001)

Based on these considerations gained from analysis of wood and timber (tissues) over several natural hierarchies it can be concluded that wood and timber demonstrate **highly hierarchical materials**. The underlying principle in the structure of elements and interaction on several hierachical levels can be described as being **parallel, sub-serial** with a high degree of cross-linkage.

Analogies can be found also in technical hierarchies. Starting at structural timber (e.g. boards and beams) longer systems can be generated by joining these timber elements in serial, e.g. by finger joints. These systems again are sub-systems in linear system products

like duo and trio beams, glued laminated timber (GLT) or in two-dimensional products like cross laminated timber (CLT) or vertical laminated floor systems. In these products the sub-systems are parallel or partly cross arranged forming again parallel, sub-serial structures. Thereby the type of connection, the way how stresses are transferred between the sub-systems as well as between the elements play a major role. The way how the system acts in respect to the applied stresses is also decisive. The same can be found in technical products of lower hierarchical levels, e.g. one- or two-dimensional structures consisting of fibres, particles, flakes, chips, strands or veneers. These elements are further joined to products like paper and carton, fibre boards, particle boards, oriented strand board (OSB), parallel strand lumber and laminated veneer lumber (LVL).

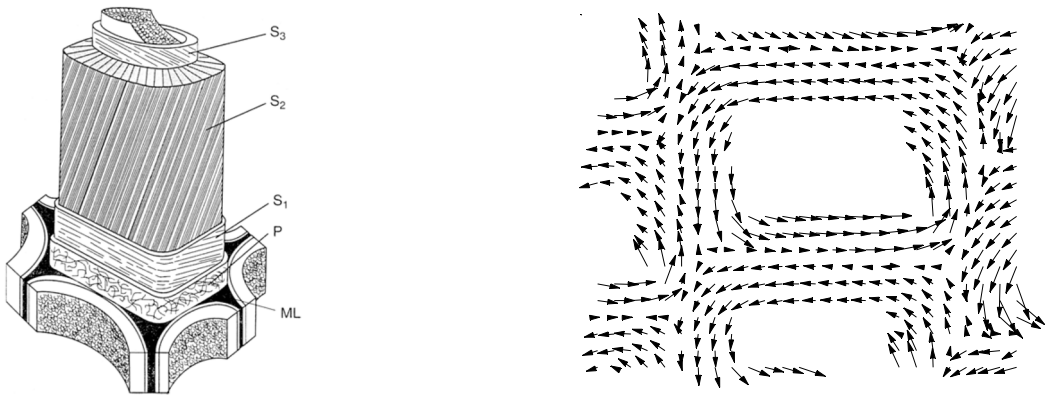

Fig. 4.10: Structure of wooden cell walls according SELL AND ZIMMERMANN (1993) (left); spiraling of cellulose fibrils (right; LICHTENEGGER ET AL., 1999)

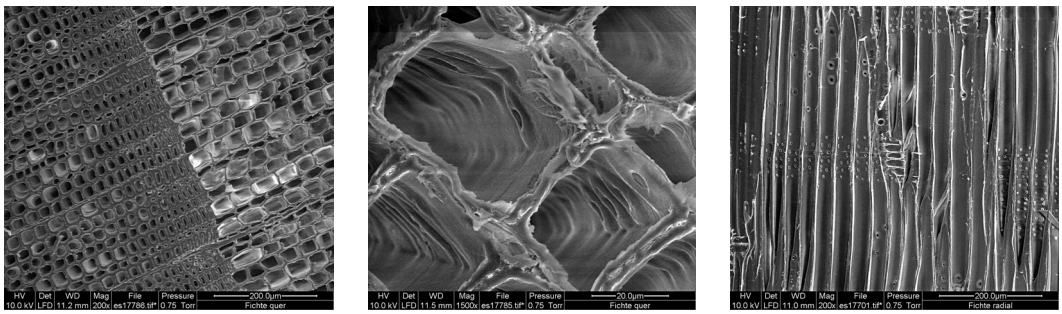

Fig. 4.11: Microscopic structure of Norway spruce (*Picea abies (L.) Karst.*) (REM_ESEM 600; INGOLIC, 2008): cross section of an annual ring (left); cross section of tracheids with boardered pits and a radial parenchyma ray (middle); radial structure showing interlaced tracheids, cross pit fields and boardered pits (right)

4.3.2 Analogies in respect to Stress and Fibre Orientation

The rhombic anisotropic, roughly orthotropic material characteristics of wood and timber are the result of the parallel, sub-serial structure as discussed in the previous section 4.3.1. Thus mechanical characteristics like strength and stiffness of wood and timber on various natural hierarchical levels are decisively influenced by the angle between stress and direction of fibres. This dependency can be observed in particular on the hierarchies of cells, growth and trees. The same can be found in the technical hierarchies of fibres, clear wood and construction timber as well as on the levels of system products and structures. Some results gained from different hierarchies are further discussed. Fig. 4.12 shows the influence of stress-fibre angle α on strength and stiffness on fibres as well as the expectable relationships for strength and stiffness of clear wood and construction timber. The results as well as the models are from PAGE ET AL. (1977), HANKINSON (1921) and WATHÉN (2006). Similar observations made on fibres can be found e.g. in CAVE (1969), REITERER ET AL. (1999) and SALMÉN (2004).

By means of classical theory of elasticity and rotation of the principal planes KEYLWERTH (1951) derived an equation for E-modulus under stress-fibre angle α, see

$$E_\alpha = \frac{1}{\left(\frac{\cos^2(\alpha)}{E_0} - \frac{\sin^2(\alpha)}{E_{90}}\right)\cdot\cos(2\cdot\alpha) + \frac{\sin^2(2\cdot\alpha)}{E_{45}}}, \tag{4.6}$$

with E_{45} as the E-modulus at $\alpha = 45°$ and E_α as the E-modulus at stress-fibre angle α.

A similar formulation for strength is more difficult to derive because up to now a definite failure hypothesis for wood in dependency of stress-fibre angle α is missing. Nevertheless ROBERTSON (1920) and STÜSSI (1946) derived equations for the strength f_α based on elementary theory of elasticity, see

$$f_\alpha = \min\left\{\begin{array}{c} \frac{f_0}{\cos^2(\alpha)} \\ \frac{f_v}{\sin(\alpha)\cdot\cos(\alpha)} \\ \frac{f_{90}}{\sin^2(\alpha)} \end{array}\right., \tag{4.7}$$

with f_v as shear strength, f_0 and f_{90} as strength parallel and perpendicular to grain, respectively.

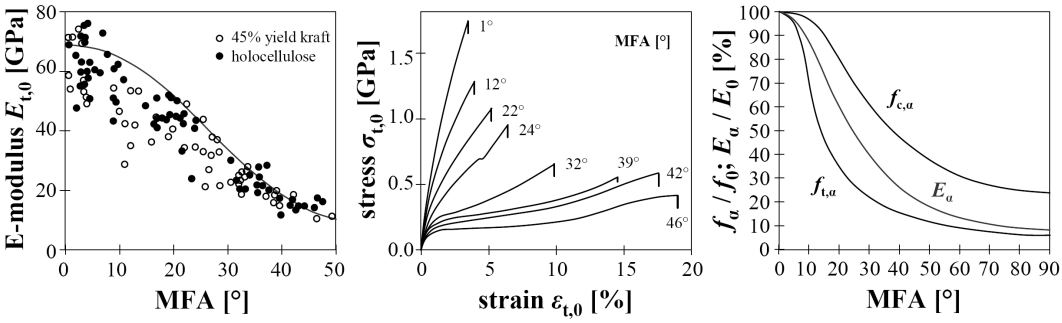

Fig. 4.12: Strength and stiffness in dependency of MFA or stress-fibre angle α: E-modulus of Norway spruce fibres vs. micro fibril angle (MFA) in S2 according WATHÉN (2006) (left; dots represent test data, curve corresponds to the model of PAGE ET AL., 1977); tensile strength of fibres of Norway spruce at different MFAs of S2 vs. strain according WATHÉN (2006) (middle); relative change of strength and stiffness of clear wood, construction timber and timber system products vs. stress-fibre angle α based on HANKINSON (1921) (right)

Based on curve fitting it was found that the transformation from longitudinal to transverse strength and stiffness characteristics follows in principle a circular formula with defined boarder values X_0 and X_{90} for the longitudinal and transverse characteristics, respectively (e.g. HAGER, 1842; HANKINSON, 1921; KOLLMANN, 1934; PAGE ET AL., 1977; PAGE AND EL-HOSSEINY, 1983). The empirical relationship was originally derived for tensile strength (HANKINSON, 1921). Nevertheless it was found to be adequate also for other mechanical characteristics. The general function is given as

$$X_\alpha = \frac{X_0 \cdot X_{90}}{X_0 \cdot \sin^\xi(\alpha) + X_{90} \cdot \cos^\xi(\alpha)}, \tag{4.8}$$

with X_α as the characteristic in dependency of angle α and ξ as power parameter fitted to the analysed mechanical characteristic. For the E-modulus HAGER (1842) (cited in GEHRI AND STEURER, 1979) and KOLLMANN (1934) found a factor of $\xi = 3.00$. In contrast GORDON AND JERONIMIDIS (1974) observed a loss of stiffness with increasing MFA proportional to $\cos^2(\alpha)$. For strength characteristics KOLLMANN (1934) proposed to use power factors in dependency of the type of loading (e.g. tension or compression). HANKINSON (1921) suggested simply a power factor of $\xi = 2.00$.

In addition BURGERT (2006) observed that ultimate strain of cells stressed in tension parallel to grain increases convex with increasing MFA of S2. He report that MFA becomes significantly reduced if fibres are strained above their (linear) elastic limit.

To conclude, the respond in strength and stiffness is highly dependent on the stress-fibre angle α. This was verified on several hierarchical levels of wood and timber and underlines once more similarities within the principal structure of wood and timber on different scales.

4.3.3 Analogies in the Failure Behaviour exemplarily for Compression parallel to Grain

In this section analogies between the failure behaviour within natural and technical hierarchies are discussed. In particular the failure behaviour in compression parallel to grain is addressed. At first the failure behaviour along the natural hierarchical levels is presented. Therefore POULSON ET AL. (1997) analysed comprehensively the failure behaviour of clear wood of Norway spruce in compression parallel to grain (l / w / d = 50 mm / 14 mm / 14 mm). They subdivided the stress-strain respond of clear wood specimen under compressive stresses in three states which describe the failure process as kinking and compression strength as a limiting mechanism (see Fig. 4.13).

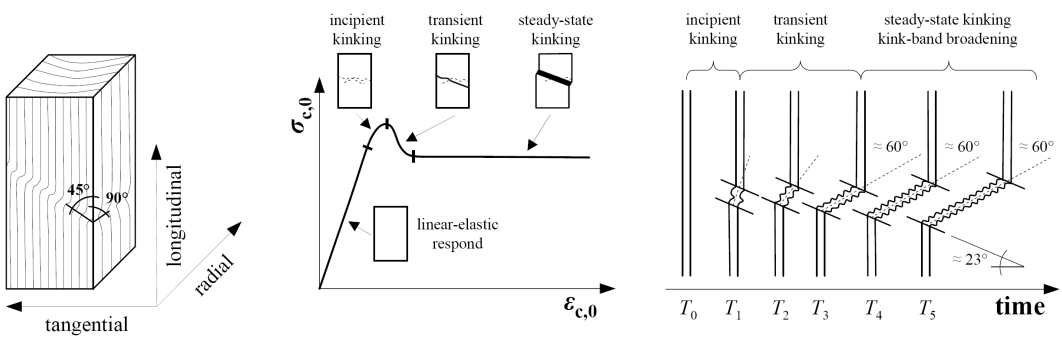

Fig. 4.13: Failure behaviour of wood and timber tissues in compression parallel to grain adapted from POULSEN ET AL. (1997): formation of shear bands in clear wood in radial and tangential direction (left); phases of compression failure as common in advanced composites (middle); schematic step-wise failure behaviour of a single fibre with phase transitions (right)

Fig. 4.14: Specimens of Tree-of-Heaven (*Ailanthus altissima (Mill.) Swingle*) which failed in compression parallel to grain: clear wood with 45° inclined shear band in tangential direction (left) and with formation of a shear wedge followed by tension failure perpendicular to grain (middle); structural timber specimen with shear band in roughly 45° in tangential direction (right)

The description of compressive failure behaviour in wood was done in analogy to compressive failure behaviour as common in advanced composites. Thereby three failure phases are given:

- incipient kinking: this starts above linear-elastic stress-strain respond (roughly at about $80 \div 90\%$ of $f_{c,0}$) and lasts till attainment of the maximum stress, the compression strength; the process is determined by longitudinal shear strength as well as by high local fibre misalignments which are intrinsic in the microstructure of wood;
- transient kinking: this describes the failure behaviour in the section between maximum stress and steady-state kinking; hereby incipient, local kinks develop to kink bands through the whole cross section;
- steady-state kinking: this state describes the failure process after a constant stress limit was reached; it is characterised by a continuous expansion of deformations; thereby kink bands broaden continuously at a steady-state stress; this stress constitutes a lower bound of the peak stress.

POULSEN ET AL. (1997) observed that incipient kinking often initiates at resin channels which occur longitudinally and radially in wood and which show a high amount of misaligned fibres (see also KUCERA AND BARISKA, 1982). Furthermore the kink-band angle was found to be constant and approximately 23° (see POULSEN ET AL., 1995 and TONNESEN ET AL., 1995). Both describe also that the kink-band is inclined in tangential

direction whereas in radial direction it is more or less transverse. The same was found by MATTHECK (2003) who argumented that radial wood rays reinforce cells in radial direction and thus prevent sliding of in transversely sheared surfaces as it can be observed in tangential direction. Furthermore MATTHECK (2003) differences between two failure scenarios: first scenario with formation of a tangential sheared layer inclined 45° to fibre direction and followed by a steady sliding, or secondly the formation of a shear wedge and subsequent sliding which induces tension failure perpendicular to grain (see Fig. 4.14). The steady state kinking process was described under a constant fibre angle of 60° which was defined as lock-up angle. At this angle densily packed latewood fibres are compressed completely and show their maximum shear resistance (see POULSEN ET AL., 1997).

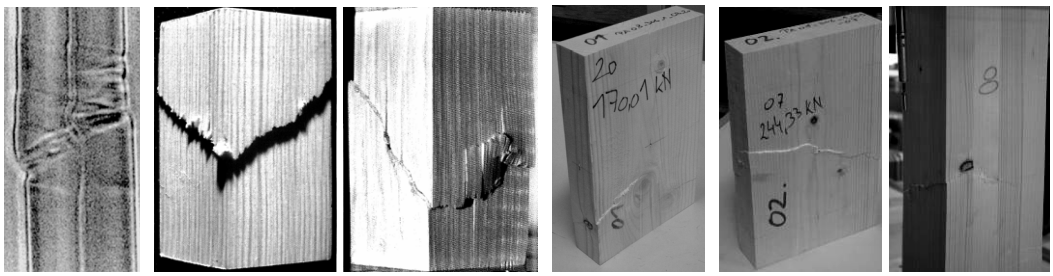

Fig. 4.15: Specimens which failed in compression parallel to grain: hemp fibre (left; kink-band angle roughly 24°; EICHHORN ET AL., 2001); clear wood (left; MATTHECK, 2003); construction timber (middle); system product, e.g. glulam (right; RULI, 2004)

This failure process, which is in general very common in composites, can be observed also at molecular level were atoms show kinking, on the hierarchy of cells and fibres (see Fig. 4.15, left) as well as on the technical hierarchies like construction timber and system products (see Fig. 4.15, middle & right).

To conclude, analogies in the failure behaviour on several natural as well as technical scales of elements were presented exemplarily in compression parallel to grain. Furthermore, equ. (4.9) and (4.10) give regression functions of density vs. compression strength parallel to grain. Again similarities between clear wood and the system product glued laminated timber can be found. The first equation originates from tests on clear wood specimen of Norway spruce with $l / w / d = 6$ mm / 12 mm / 12 mm ($u = 12\%$) made by GINDL AND TEISCHINGER (2002).

$$f_{c,0,mean} = 0.13 \cdot \rho_{12} - 14.00 \text{ , } R^2 = 0.84. \tag{4.9}$$

The second equation was gained by analysing data of glued laminated timber specimen also of Norway spruce of tests performed by RULI (2004), see BRANDNER ET AL. (2006). These specimen consisted of four lamellas and had a moisture content of $u = 12\%$ and a dimension of $l / w / d = 720$ mm / 120 mm / 160 mm. Both equations have comparable regression coefficients. The degree of determination is lower for glulam compression strength. This can be attributed to additional variability caused by growth characteristics, e.g. knots or knot clusters. Furthermore, some constraints in the failure behaviour in glulam due to reinforcement of the formation of shear bands in partly tangential and radial direction are expected.

$$f_{c,0,g,mean} = 0.10 \cdot \rho_{12} - 8.15 \text{ , } R^2 = 0.70. \tag{4.10}$$

Nevertheless, elements in load bearing structures which are loaded in compression parallel to grain are vulnerable to lateral buckling rather than to fail in compression at their peak load.

4.3.4 Analogies in respect to Size (Volume) Effects exemplarily shown for Length Effects

Size (volume) effects in particular on strength are an inherent feature of all materials. The reasons for that are at least the stochastic nature of materials and structures and the distinctive extreme nature of strengths. Consequently, variability in strength characteristics is the driving force of size effects. This was already discussed in previous chapters, e.g. chapter 1.2 & 3. Independent of the hierarchical level, size effects are the logical consequence of changes in the dimension of a structure within each hierarchy, the scale. Each scale consists of sub-structures of previous scales which influence the relationships between their constituents.

Within this section solely size (length) effects from tension tests performed on different hierarchical levels are addressed. For example KERSAVAGE (1973) observed that an increase in free length in tensile tests of single fibres lead to a significant reduction in strength. The same was found already earlier by HARDACKER (1962). PAGE AND EL-HOSSEINY (1976) also performed tension tests, in particular on sulfite pulp fibres, and confirmed a strength reduction with increasing testing length (see Fig. 4.16).

DILL-LANGER ET AL. (2003) performed tensile tests on clear wood on two different volumes and observed a distinctive reduction in strength with increasing volume. The same was already previously reported by GRAF AND EGNER (1938). They performed tensile tests on clear wood as well as on structural timber. BRANDNER ET AL. (2007A) report on tensile tests performed on finger jointed construction timber of Norway spruce with a cross section of $w / d = 160$ mm / 60 mm and variable free test length between 1,440 mm and 17,222 mm (see JEITLER ET AL., 2007). Thereby a clear reduction in tension strength parallel to grain with increasing free testing length was given. This reduction was in particular pronounced on mean level whereas on the design relevant 5%-quantile the reduction was lower thanks to distinctive reduction in variability.

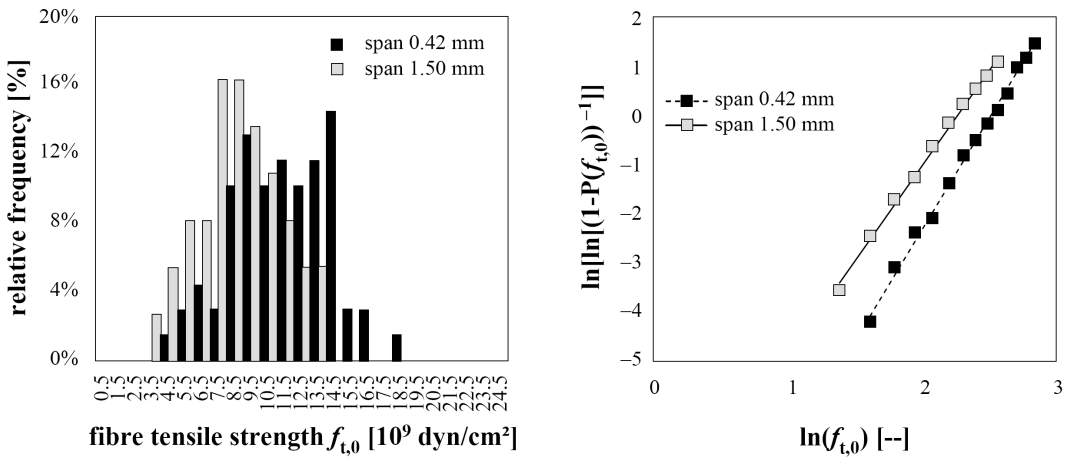

Fig. 4.16: Influence of length on tensile strength of sulfite pulp fibres adapted from PAGE AND EL-HOSSEINY (1976): histogram (left); WEIBULL probability paper (right)

More on size (volume) and in particular length effects on the technical hierarchies of wood and timber is given in the following chapter 5, in particular in section 5.1.2.

4.4 Scaling in Wood and Timber Hierarchies, exemplarily for Tensile Characteristics parallel to Grain

Within this section material characteristics of wood and timber (tissues) on several hierarchies of Norway spruce (*Picea abies Karst.*) are discussed exemplarily. Hereby focus is on strength and E-modulus in tension parallel to grain. The data base on a comprehensive literature survey on tensile characteristics of the principal molecules

cellulose, hemicellulose and lignin, cell wall and fibre, clear wood specimen as well as structural timber (see section 8.2, Tab. 8.3). All in all expectable data of four consecutive hierarchies are presented. The data, in particular of molecules and fibres, originate from tests as well as from theoretical considerations and model calculations. In that respect it has to be mentioned that partly tremendous variability in published values of the same characteristic was found. This is not estonishing if the differences in currently discussed cell wall models, the challenges in performing tests on nano- and micro-scale as well as the necessity for providing simple models capable for computation of tissues up to a certain scale are considered.

Tab. 4.5: Selected physical characteristics of wood and timber (tissues) on various hierarchical levels: reference length of destructive tests; rounded median and range of published (mean) values of density, E-modulus and strength in tension parallel to grain at a moisture content of roughly u = 12%.

	l_{ref} [mm]	ρ_{12} [kg/m³]		$E_{t,0,12}$ [kN/mm²]		$f_{t,0}$ [N/mm²]	
		median	range	median	range	median	range
lignin	--	--	--	2	2÷7	--	--
hemicellulose	--	--	--	4.8	2÷18	--	--
cellulose (crystalline, fibrils)	0.01 [2)]	1,500	--	137.8	70÷319	10,000	1,000÷19,000
cell wall & fibre	3.00 [3)]	1,500	--	25.4	0.4÷7.7	860	200÷1,450
clear wood	110 [4)]	430	400÷510	12.5	9÷16.7	95	70÷240
constr. timber [1)]	2,000 [5)]	450	410÷520	11.8	9.1÷18.1	30	15÷50

[1)] data from BRANDNER AND SCHICKHOFER (2007)

[2)] assumptions: DP = 10,000; length of cellobiose units 1.03 nm (FENGEL AND WEGENER, 1989)

[3)] mean length of tracheids of Norway spruce (*Picea abies (L.) Karst.*) (FENGEL AND WEGENER, 1989)

[4)] local free test length of clear wood specimen tested in tension parallel to grain according DIN 52188

[5)] reference free test length of boards for glued laminated timber in tension parallel to grain according EN 1194

In previous section 4.2 it was outlined clearly that sub-layer S2 of the cell wall dominates the mechanical performance of wooden cells in longitudinal direction. The cellulose as fibre-reinforcement is the main constituent of S2 and nearly solely bears the tension stresses in the cell wall composite. Consequently, strength and E-modulus of cellulose in

tension parallel to grain are seen as representative characteristics of the molecular hierarchy of wood tissues. For the hierarchy of fibres the tension characteristics of the cell wall material are used, with a density of ρ_{12} = 1,500 kg/m³ equal to that of cellulose.

Two different reference volumes are used in the literature. Some papers publish mechanical characteristics of fibres in reference to the whole fibre cross section (including the lumen). Other researchers calculate their strength and stiffness solely in reference to the cell wall geometry (volume of bulk material). Beside the fact that the single fibre constitudes the basic element of the cellular material wood and timber and the fact that both are characterised by their porosity, the mechanics of the single fibre seem to be more representative and better linked to the interacting sub-layers in the cell wall. Thus on the hierarchy of fibres characteristics of the bulk material with a reference density of ρ_{12} = 1,500 kg/m³ are used. Nevertheless in the hierarchies of clear wood and construction timber the porosity is included in the calculated mechanical characteristics. Consequently, the characteristics are automatically in conjunction with the timber species and their characteristic densities. Due to the high density of knots a 3% higher density in construction timber compared to clear wood is considered. As all tension characteristics are given in grain direction, in principle a correction of chracteristics of fibres, clear wood and construction timber according MFA would be necessary. Nevertheless, in line with common practise and not provided MFA in most of referenced literature this correction was not applied. A summary of representative statistics of all four hierarchies is given in Tab. 4.5.

Fig. 4.17 shows the characteristic tensile strength and E-modulus parallel to grain in dependency of the reference test length l_{ref}. For additional information also the reference density is given. Both, abscissa and ordinate are transformed to natural logarithmic domain. Furthermore power regression models found by least squares method are presented for both tensile characteristics. All in all representative data of in total four consecutive hierarchies is presented, starting with molecular, to fibre, clear wood and up to construction timber. In particular the tensile strength characteristics reflect a nearly perfect linear decreasing trend. The same can be observed for the E-modulus, disregarding the hierarchy of construction timber. The given power models are hereby not seen as strict quantitative and universal power laws automatically representative for tensile characteristics of wood and timber tissues. But they deliver important and more than indicative information about trends in strength and stiffness over the range of represented scales. Furthermore, the high degree of determination of R^2 = 0.99 and 0.93

for the power models of strength and E-modulus, respectively, is not surprising considering the fit to only four data points although they represent highly condensed information on the median level.

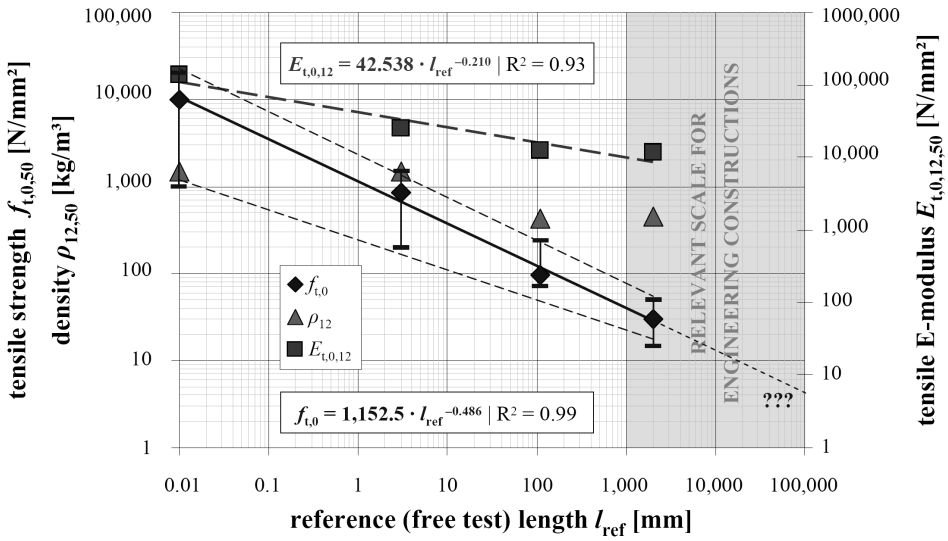

Fig. 4.17: Physical characteristics of Norway spruce (*Picea abies (L.) Karst.*) on median level in dependency of the evaluated hierarchical scale: density, tensile strength (including range) and tensile E-modulus parallel to grain

Nevertheless, considering the general definition of scaling and power laws as discussed in section 4.1, the presented hierarchical structure of wood and timber in section 4.2 as well as the analogies in structure and behaviour between natural, technical but also natural and technical hierarchical levels, it appears more than plausible that in particular for strength power laws in wood and timber are in principal inherent. Beside all that and as also presented in Fig. 4.17 dimensions of timber products used for load bearing purposes in engineered structures are at least up to two scales higher than normally tested in laboratories. The question about scaling effects in this untested dimensions as well as concerning scaling effects in wood and timber tissues in general are treated in the next section.

4.5 How to explain Scaling Effects in Wood and Timber and what can be concluded?

As already outlined in the previous section 4.4 the aim of the fitted power functions in Fig. 4.17 is not to deliver strict and universal applicable power laws. This is despite the fact that the data underlying these presented models have very high information content. Nevertheless, the aim is to present some quantified qualitative information about the general trend of tensile characteristics parallel to the grain of wood and timber tissues. The significant decrease of strength and stiffness consequences from two facts: (1) the hierarchical structure of the material, and (2) the parallel, sub-serial composition of elements to systems of material complexes. Both reasons are characteristic on every scale. The power parameter of the trend model in strength is about two times that of the power of stiffness, in particular if only the first three scales are analysed. Hereby the underlying nature of the characteristics has to be considered. Whereas the E-modulus constitutes the harmonic mean of local E-moduli, strength, irrelevant of the scale, is determined very locally by the weakest cross section. Hereby the weakest cross section is defined by the cross section with the lowest resistance against tension stresses.

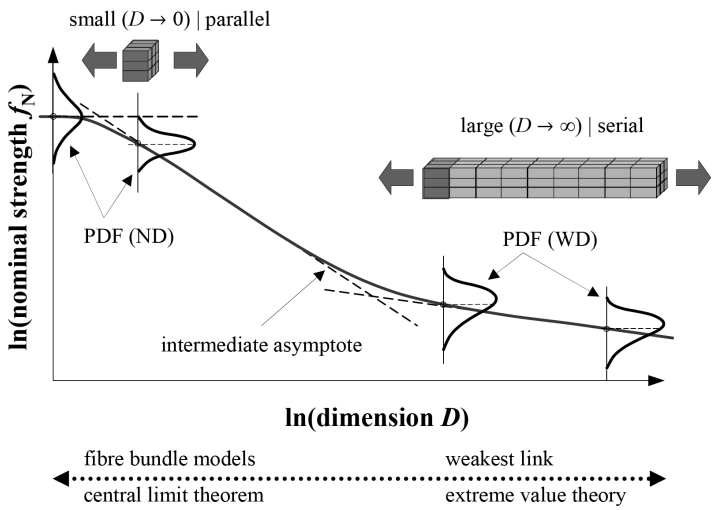

Fig. 4.18: Transformation process of system actions adapted from publications on size effects of quasi-brittle materials (BAŽANT AND CHEN, 1996; BAŽANT AND PLANAS, 1998 and BAŽANT, 2004): transformation from parallel to serial system action

The trend-functions only account for changes in material characteristics between scales. Nevertheless, scaling between hierarchies incorporates not only the output due to changes in the structure but automatically also changes in dimension within the hierarchies. Whereas E-moduli are only slightly affected by changing dimensions, in particular on the mean (median) level, strength characteristics exhibit tremendous change due to serial and parallel system effects.

The hierarchical material structure of wood and timber tissues can thereby also be described as a system of elements. Hereby the elements itself are systems of the previous hierarchy. Considering the structure as parallel, sub-serial it follows that in the zone of scale transition, which is characterised by the increasing dominant occurrence of new structural elements which determine the new hierarchical level, a primary parallel arrangement of systems of the previous hierarchy together with the new structural elements conglomerate to a new basic element representative in the next hierarchical level. Within the hierarchy changes in dimension occur primary by serial linkage of the elements which leads to significant serial system effects, as discussed in section 3.3. In case of 2pLND element strengths with a coefficient of variation CoV[f] = 30%, which is e.g. common in tensile strength of structural timber parallel to grain, the mean (median) serial system effect can be approximated locally ($M = 1 \div 10$) by a best-fitted power model with a power of 0.20 (0.19). Within hierarchies a scale transition from parallel to serial system action can be observed due to

- primarily longitudinal orientation of tissues on all hierarchies;
- transition from parallel to serial systems in case of LLS, see Fig. 3.10, section 3.2.4;
- transition in structural strength according fracture mechanics of (quasi) brittle materials, evaluated as size effects according BAŽANT AND CHEN (1996), BAŽANT AND PLANAS (1998) and BAŽANT (2004), see Fig. 4.18.

The scaling effects between hierarchies result from changes in the dominance of new strength determining elements (flaws) which become important not till then a certain dimension of the material structure is reached. Some examples are:

- <u>hierarchy of atoms → hierarchy of molecules</u>:
  - inter- and intramolecular bondings;
- <u>hierarchy of molecules → hierarchy of cells</u>:
  - crystalline and amorph regions in cellulose molecules and fibrils;

- inclusion of hemicellulose and lignin;
- agglomeration of cell-layers with different MFA and share of constituents.

Consequently, system effects within a hierarchy are responsible for roughly half of the global "scaling effect" on strength. The other half can be dedicated to a pure structural scaling effect which consequences from the before mentioned changes in the material structure. As the E-modulus behaves nearly constant within each hierarchical level it is not surprising that only the half value of the power parameter can be found in the global power trend function (Fig. 4.17).

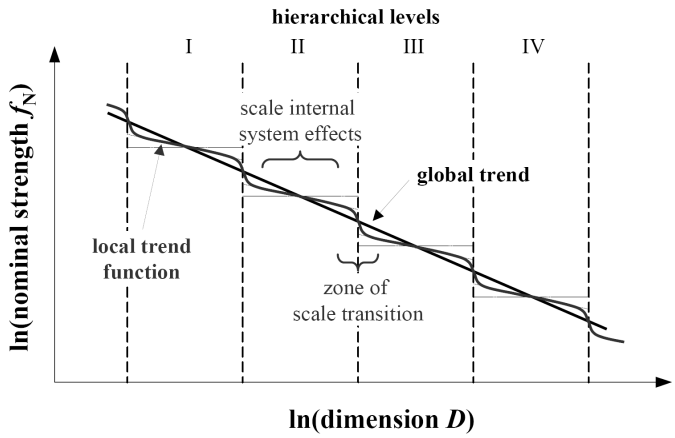

Fig. 4.19: Scaling in wood and timber tissues: global vs. local trend functions by separation of scaling effects between and system effects within hierarchical levels

A qualitative model which separates scale transition between hierarchies and system effects observable within hierarchies is shown in Fig. 4.19. For quantification the definition of the transition zones is dedicated to further research. The definition is seen as being dependent on the:

- dimension of characteristics decisive for the strength in the next hierarchy (dimension of flaws) → geometrical definition;
- scale-dependent (characteristic) fracture length → fracture mechanical definition;
- definition of RVEs on each scale which itself depend on the characteristic flaw size (see section 5.1) → stochastic definition.

Changes in the natural hierarchical structure are always accompanied by the inclusion of certain stress-transfer layers or zones (e.g. amorph regions in cellulose molecules and fibrils; lignin and hemicelluloses as matrix material surrounding cellulose as reinforcement; CML + S1 + S3 as stress-transfer layers for S2; changes in density within annual (seasonal) growth rings). These layers or zones lead to a certain reduction in E-modulus from hierarchy to hierarchy but increase the ability to (re)distribute stresses successfully within the tissues by providing a certain amount of deformability. In that respect FRATZL AND WEINKAMMER (2007) outline that glued composites become flaw-tolerant if the particles became smaller than a critical length

$$h^* \approx \pi \cdot \gamma \cdot \frac{E^P}{\sigma_{th}^2}, \tag{4.11}$$

with parameters γ as surface energy of particle material, σ_{th} as theoretical (molecular) strength and E_P as E-modulus of the particle material. This follows from GRIFFITH's law where the strength of a particle with a flaw decreases with the square-root of the flaw size. Following GAO (2006) flaw-tolerance can be imposed by a hierarchical arrangement of composites, where the stiff fibre at each hierarchical level is in fact a composite of much smaller particles which are glued together. Such a hierarchical composite structure becomes insensitive to flaws at all length scales.

So far scaling and system effects on the natural hierarchical structure were discussed. The question what can be concluded for (engineered) structural timber products of the technical hierarchies "construction timber", "system products" and "load bearing structures" still remains unanswered. Answering would necessitate extrapolation over two scales. This has to be done with caution. Consequently some key considerations on the basis of available information are figured out:

In general, if the underlying structure of a system does not change then scale transition does not occur. Only effects which are caused by the arrangement of elements, the serial and parallel system effects, have to be taken into account. If in addition a significant change in the underlying structure is given, a scale transition has to be considered as well. Such a significant change in the underlying structure automatically occurs in applying finite element method for numerical analysis of structural timber elements, system products or parts of system structures by means of a net of only a view millimeters or centimeters in one dimension. A correct and more realistic implementation necessitates the use of stochastic finite elements and in particular knowledge of all characteristics and

functions for scale transition. This to model material effects on a larger scale realistically and by consideration of serial and parallel system effects. For discussion of these general aspects each hierarchical level is further treated separately:

I: Construction Timber

If the characteristics are gained directly by full-scale tests performed on a representative material (including all flaws which are typical for this level) than the consideration of system effects is required only if the dimension(s) used deviate from the reference dimension(s). If the material characteristics are gained from clear wood effects due to scale transition as consequence of significant changes in the material structure and of failure characteristics have to be considered.

II: System Products

The necessity to consider scaling effects depends on the product itself and its basic element (e.g. structural timber, veneer, strands, flakes, particles, fibres). Every system product depends on the arrangement and connection of the elements. In case of glued elements which lead to systems composed of rigid joined elements only system effects have to be taken into account if it is secured that failures always occur in wood and timber tissues and not in the adhesive layers. The basic characteristics of each product have to be derived on the basis of the characteristics of the elements and their arrangement. The argument is that failure of the system occurs in the element and thus in the same types of flaws which cause failure of the single element. This is in particular not the case in laminated veneer lumber (LVL) where the failure characteristic of veneer layers may be significantly influenced by adhesive treatment and shakes filled with adhesive.

For an arbitrary applied joining technique and in particular in case of punctiform and / or flexible combounds not only the structural behaviour of the elements in the system product but also the failure characteristic may change. In that case also scaling effects can become relevant.

III: Load Bearing Structures

In load bearing structures element or joint failures are the two principle possibilities how a part or a whole structure can collaps. Consequently, a change in the structural behaviour is mostly present and requires in principle the consideration of both, system and scaling effects.

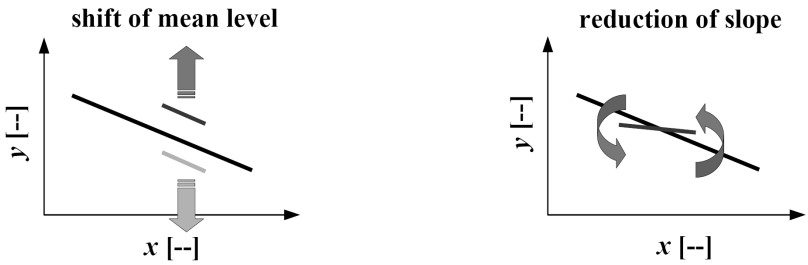

Fig. 4.20: Trivial solutions to influence system and scaling effects: shift of mean level (left); reduction of slope (right)

Nevertheless, independent of the hierarchy the two main principles (trivial solutions) to influence scaling and system effects are (see Fig. 4.20):

1) Shift of Mean Level

This can be done by classification (grading, grouping) of the elements. Nevertheless upgrading of one part of a sample automatically leads to downgrading of the rest. Classification coincides also with a reduction in variability of characteristics. This has an influence on the second trivial solution, the reduction of slope. Nevertheless, classification of timber elements in particular in regard to strength, which can be done only indirectly by means of relationships to non-destructively determinable indicating properties, has only minor influence on strength variability.

2) Reduction of Slope

In case of scale transition a reduction in slope can be achieved by a reduction of differences between existing and new flaws. In respect to system effects a reduction in slope can be achieved by a reduction of the variability. For example this can be done by the creation of smart designed system structures in conjunction with a systematic activation of system effects within one hierarchical level, e.g. by joining elements to primarily parallel acting and rigidly connected structures.

4.6 Concluding Remarks to Chapter 4

The main conclusions are:

- wood and timber tissues are highly hierarchical structured materials which are organised as parallel, sub-serial systems;

- analogies within natural, technical as well as between natural and technical hierarchies were presented exemplarily;
- serial and parallel system actions and effects are inherent in every material, in particular if the materials are structured hierarchically. Together with scaling effects, system effects lead to significant lower strengths of structural material than someone would expect if analysing the molecular strength of material tissues alone;
- with wood and timber nature provides evolutionary optimised materials which are outstanding in multifunctionality and in their physical characteristics;
- scarce raw materials and limits in costs should consequently be the driving forces to learn from nature and to adopt mechanisms to engineering practice, material and structure design;
- it was presented that global scaling trends can be separated into scaling effects between and system effects within hierarchical levels;
- it was outlined that realistic numerical modelling including stochastics requires the material characteristics on the element scale as well as the functional description of scale transitions up to the hierarchical level of the analysed system structure adapted to the dimension choosen for finite elements, in particular if continuum mechanical calculations are made.

Chapter 5

Serial and parallel acting Systems in Timber, Engineered Timber Products and Structures

This chapter is dedicated to the definition and verification of stochastic (mechanic) models representing the structural behaviour of timber, engineered timber products and structures. At the beginning the applicability of the concept of representative volume elements is briefly discussed. Proposals for reference dimensions of stochastic elements characterising spatial distributed timber properties as well as an alternative concept for structuring timber are presented. In particular data of longitudinal distribution and correlation of global and local characteristics are collected and discussed. The magnitude of correlation as well as a concept for modelling is specified. Therefore a comprehensive literature review and analysis of published data were required. After clarifying all these aspects explicit application examples of serial-parallel system considerations for timber characteristics are given and properties of timber system products are presented and supplemented by literature reviews, modelling issues, discussion of model output and verification.

5.1 Basic Considerations in Modelling of Serial and Parallel Stochastic System Effects

As already and more generally discussed in chapter 3, serial and parallel system actions result from potential differences between common acting elements. Consequently, the higher the potential differences the higher the expected system effects. Due to the hierarchical structure of timber (see chapter 4) every system composed of timber

elements of level I, II or III (see section 1.1) exhibits parallel, sub-serial system actions. These lead to significant differences between material characteristics (e.g. strength and stiffness) if compared on different hierarchical levels of the material structure (see section 4.4, Fig. 4.17).

Modelling of serial and parallel stochastic system effects requires knowledge of spatial distribution and spatial correlation of local material characteristics. Due to the heterogeneous, rhombic anisotropic, roughly orthotropic composition of wood and timber the question arises how to characterise wood and timber locally. In particular the definition of an incremental volume sub-element, as a representative basic unit for modelling of serial and parallel interactions within and between common acting timber elements, is needed. In view of the concept of so called "representative volume elements (RVEs)" known from continuum mechanics the question arises if, and how RVEs can be defined in case of timber and preceeding hierarchical levels (see section 4.2, Fig. 4.4).

In general, a representative volume element (RVE) is defined as the basic element used for continuum mechanics calculations, in particular for modelling and simulation of biomaterial behaviour, e.g. of wood and wood-based products. These biomaterials are due to their hierarchical structure over various scales and due to their local varying coordinate system far away from continuum-based representation (LANDIS ET AL., 2002). Therefore the RVE has to be in size (volume) on one side large enough to show sufficient statistical homogenisation of the microstructural heterogeneity within the material structure, and on the other side small enough to sufficiently represent the behaviour of a material on a macrostructural level. The material behaviour should be at least representative on the expected (mean) level which is enabled by ergodic periodic imaging (LANDIS ET AL. 2002; KANIT ET AL., 2003; GITMAN, 2006; ZEMAN AND ŠEJNOHA, 2007; GITMAN ET AL., 2007). Thus the definition of an RVE depends on (i) the precision required for the representation of the expected macroscopic material behaviour (preventing bias), (ii) the physical properties and volume fractions of microstructural constituents (e.g. flaws) and in particular on (iii) the physical property which has to be modelled representatively on the (observed) macroscopic level. Thus the dimension of RVEs depends on the physical characteristic in question (LANDIS ET AL., 2002; KANIT ET AL., 2003; LIU, 2005; ZEMAN AND ŠEJNOHA, 2007; GITMAN ET AL., 2007). Consequently, an RVE shall behave independent of macroscopic boundary conditions and constitutes of a large number of microscopic heterogeneities (e.g. flaws). Nevertheless the RVE must be small enough to

enable continuum mechanics calculations (KANIT ET AL., 2003) but it requires also a separation of scales in material structure (GITMAN ET AL., 2007). Beside that one has to be aware that the implementation of an RVE leads to substantial loss of information through statistical homogenisation (ZEMAN AND ŠEJNOHA, 2007). Whereas RVEs are in particular applicable in elastic material description GITMAN ET AL. (2007) question the use of RVEs in modelling of quasi-brittle materials showing softening behaviour. For example, wood and timber behave quasi-brittle combined with softening, e.g. in compression parallel to grain.

However, the introduction of a consistent definition of RVEs for all physical properties of interest is out of scope of this work. Publications which report on RVEs in continuum mechanics modelling of wooden structures on various hierarchical levels are e.g. ASTLEY ET AL. (1997) and HOFSTETTER ET AL. (2006).

As mentioned above, the definition of RVEs for each group of characteristic, e.g. strength, stiffness and density, or even for each individual characteristic of timber creates a challenge due to common occurrence and influence by discrete and continuous distributed growth features of dimensions starting at e.g. knots, knot clusters, annual growth rings and checks. These flaws are only few times smaller or even larger than structural components made of wood or timber, and sometimes larger than the volume occupied e.g. by connection technique (e.g. pin-shaped fasteners). Furthermore, the variety of growth characteristics and their influences on characteristic properties affects and hinder the definition and standardisation of e.g. representative statistical distribution models (RSDMs). In fact highly sophisticated modelling, in particular of parallel system actions, under consideration of varying timber quality and timber strength (stiffness) classes, would require the combination of individual RSDMs for each growth feature to a multi-modal RSDM which can be used for the estimation of an individual local property (e.g. tensile strength). The combination (mixing) of RSDMs is done by weighting them according their probability of occurrence, see equ. (5.1). Thereby the mixing probabilities p_X can be assumed as deterministic or as stochastic variables as well. This procedure would remarkable improve current knowledge and widen the possibilities in modelling timber products and structures.

$$f_Z(z|\theta_z) = p_1 \cdot f_1(x_1|\theta_1) + \ldots + p_i \cdot f_i(x_i|\theta_i) + \ldots + p_n \cdot f_n(x_n|\theta_n),$$

with $i = 1, \ldots, n$; $\int_{-\infty}^{\infty} f_Z(z|\theta_z) \cdot dz = 1$; $\sum_{i=1}^{n} p_i = 1$. (5.1)

Perhaps this approach would be theoretically straightforward but it fails due to desiderate stochastics and knowledge about interactions between all parameters. This lack of knowledge is in particular evident for rare characteristics like pre-broken tree tops or in compression pre-damaged local areas. However, even these characteristics often show a significant and even dominating influence on the distribution of strength, in particular in the lower distribution tail, and thus influence the characteristics required for the design of timber structures. Furthermore, growth characteristics like knots and knot clusters, which show a nearly endless variety of dimensions, possibilities of occurrence and combinations, make it nearly infeasible to account for all this diversity. Testing all these combinations is practically impossible and even testing some "representatives" is economically disastrous. Therefore modelling and simulation techniques are straightforward but require information with some degree of detailing corresponding to the model resolution required. Thus the definition of stochastic input parameters of RVEs or of elements with reference dimensions, under consideration of relationships between growth characteristics and characteristic mechanical properties (e.g. strength and stiffness), is required for a sufficiently accurate modelling of system behaviour. As long as modelling of system behaviour is not provided over all hierarchical levels the definition of RVEs and / or reference dimensions has to be done for each hierarchical level individually.

Discussing the hierarchical level "timber" the material structure can be in principle modelled as compound of wood – roughly characterised by global stochastic properties, e.g. global grain deviation and density – and spatially distributed growth features, e.g. knots and pitch pockets, which locally influence the material properties of sawn timber, in particular strength. Thus structural properties which decisively influence the material structural behaviour are subdivided into:

[1] <u>globally influencing characteristics</u>

characteristics which determine the basic (inherent) potential of sawn timber, in particular the basic material wood, with "clear wood" as one specific type of wood (e.g. DIN 52180);

[2] <u>locally influencing characteristics</u>

characteristics which locally decisively influence the basic potential of timber and consequently determine the local potential of sawn timber and thus the possibility and amount of interaction is enforced to act parallel or serial-parallel systems of rigid or even flexible connected elements and components.

Representatives of categories [1] and [2] thereby have an influence on the expectation, the statistical spread and even on the whole shape of the statistical distribution of e.g. strength and stiffness. Whereas representatives of type [1] determine the basic potential of the element and can be treated as continuously but randomly distributed over the whole dimension (e.g. length, volume), representatives of type [2] are characterised by discrete occurrence and with or without local clustering. Thus they require additional information of their dimension, their spatial distribution and correlation.

Typical characteristics which are classified to type [1] are:

- density
  measure for the amount of principle wood tissues (cellulose, lignin, polyoses) per unit volume; sometimes estimated from mean width of annual growth rings and / or radial position within the stem;
- global grain deviation including spiral grain
  as principal information of expectable properties in respect to the coordinate system of the specimen relative to grain direction.

Typical representatives of type [2] are:

- local grain deviation
  estimated by the occurrence, dimension and position of knots and knot clusters or irregular occurring growth features like pre-broken tree tops;
- in compression pre-damaged zones
  distances between affected zones correspond to the distance between distinctive knots and / or knot clusters (→ knots stiffen in compression and cause local pre-damage);
- reaction wood
- checks, splits, …
- degredation
  e.g. by funghi.

Representative parameters of type [1] are further assumed to follow longitudinally a stationary but non-ergodic stochastic process. Thus it is assumed that expectation and variance vary from log to log and between sawn timber specimens. The assumption of stationarity can be argumented by the breakdown process of logs into sawn timber performed preferable parallel to pith. Furthermore sawn timber in Central Europe has a

typical length of 4 m. Due to the presence of juvenile and adult wood zones it is assumed that radial variation of basic parameters of wood, like density and E-modulus, do not provoke longitudinal trends in spatial variation of these parameters. This is in contrast to data of e.g. LAM AND BARRETT (1992) who found some longitudinal trends in local values of $E_{m,0,i}$ of sawn timber. Nevertheless it is not clear if the observed trends are inherent in wood or a result of local characteristics of type [2]. The preclusion of ergodicity follows from the rhombic anisotropic, roughly orthotropic material structure of timber in respect to radial and tangential direction in cross section which depends on the dimension and original radial position of sawn timber within the log. An ergodic stochastic process in longitudinal direction is not expected due to the distinctive variation of spatially distributed features which vary from log to log and even within sawn timber of the same log. For example DITLEVSEN AND KÄLLSNER (2005) reported that local bending strength of sawn timber with identical longitudinal position but cut halved and symmetric to the pith showed correlation of $r \approx 0.15$ (i.e. nearly uncorrelated) whereas local bending strength of two segments of the same timber specimen showed serial pairwise equicorrelation of $r \approx 0.50$.

Representatives of type [2] are further differentiated in (i) spatially in distribution and dimension uncorrelated, arbitrary occurring characteristics, and (ii) spatial correlated characteristics with assumed correlation in distance and dimension.

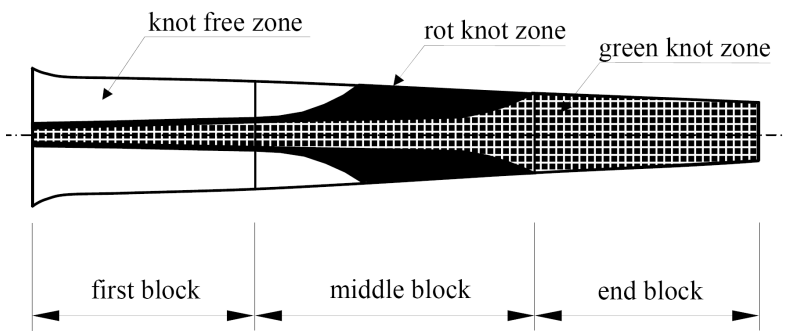

Fig. 5.1: Knot zones along the stem of a typical mature (softwood) tree; adapted from FRONIUS (1982)

Features which are assumed to be spatially uncorrelated are for example so called intermediate knots. These are single knots which occur in between the dominating, discrete in length more regularly distributed knot clusters. Thus spatial correlated characteristics are for example knot clusters. They show distinctive longitudinal

correlation. In Norway spruce (*picea Abies Karst.*) knot clusters mark the primary (longitudinal) yearly growth increment. Thereby every year a new knot cluster grows. Nevertheless, growth characteristics which show a regular pattern in occurrence in the tree must not show this pattern again in sawn timber, after the breakdown process. Thus the spatial distribution and correlation of these features in sawn timber is decisively influenced and reduced. This influence is additionally forced by changes in the type of knot zones, from "green knot zone" to "rot knot zone" to zones in the tree without visible knots at the outside ("knot free zone") due to the primary growth and changes in crown formation (see Fig. 5.1). Although these changes already occur in the living tree the breakdown process may produce sawn timber with two or even three different knot zones in longitudinal direction.

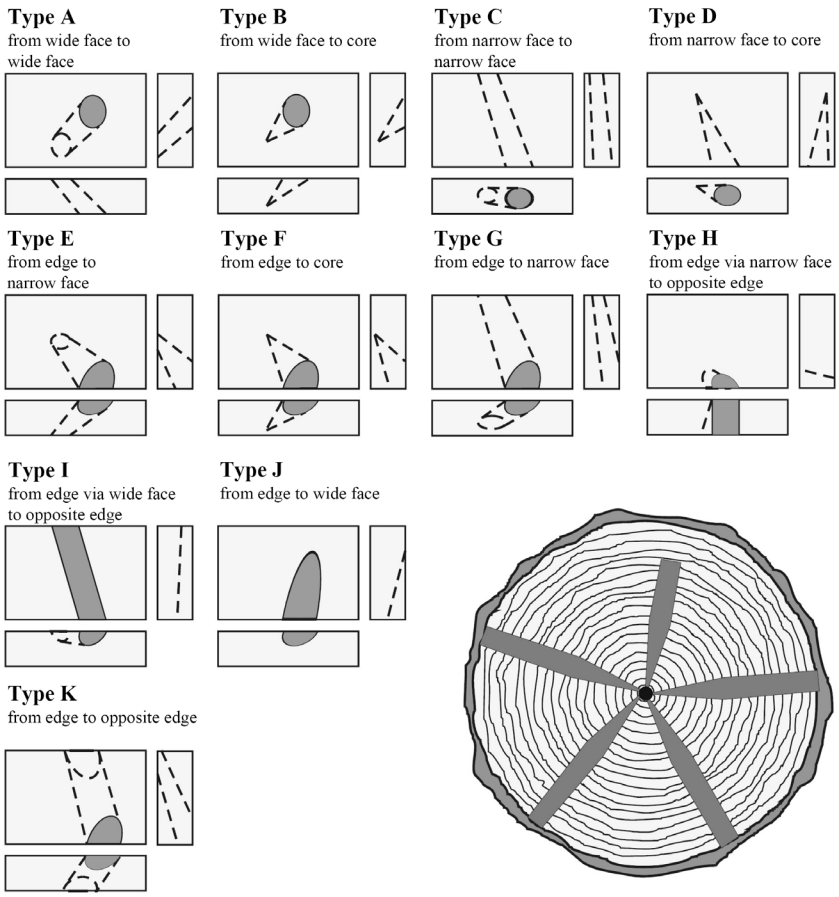

Fig. 5.2: Types of knots; adapted from AUGUSTIN (2004) and GLOS (1978)

Moreover, during the breakdown process knots and knot clusters are cut under various angles leading to numerous types in appearance (see Fig. 5.2). Due to localised grain deviation the way how a knot is cut and its position within the cross section of sawn timber determines the strength and stiffness characteristics of sawn timber, in particular if stressed non-uniformly over the cross section, as e.g. in bending.

Numerous analysis regarding the distribution of knot clusters and the influence of knots on strength (and stiffness) are available and corresponding models widely discussed in the literature (e.g. ISAKSSON, 1999; RIBERHOLT AND MADSEN, 1979; FOLEY, 1997; COLLING, 1990). In particular the longitudinal distribution of knot clusters is in focus of some authors. They used the information for modelling of length effects on strength of timber stressed in bending, tension or compression parallel to grain (e.g. ISAKSSON, 1999; RIBERHOLT AND MADSEN, 1979; KÄLLSNER AND DITLEVSEN, 1994). Thereby randomly distributed intermediate knots are not discussed and neglected due to the fact that they are not treated as being strength determining so far at least one knot cluster is given in every element. Thereby a serial system which fails with failure of the weakest sub-element represented by the biggest knot cluster is assumed. This will be further discussed in section 5.1.2. In contrast to serial systems, adequate modelling of parallel systems requires detailed information of arbitrary distributed single and intermediate placed knots and their influence on local strength and stiffness. This is to account for local interactions between adjacent elements.

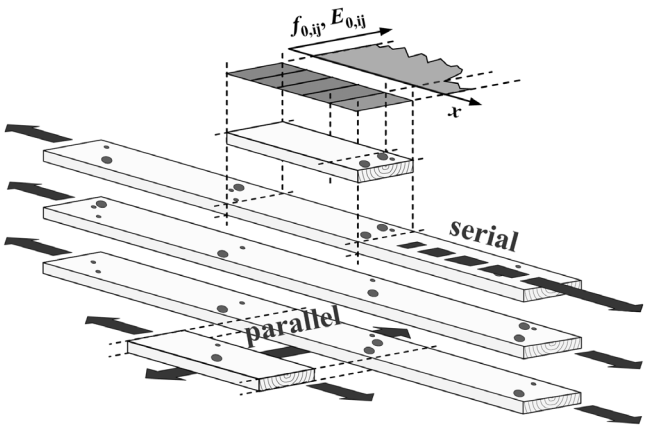

Fig. 5.3: Serial, parallel and serial-parallel system action in and between structural timber elements

Under consideration of previous statements the spatial distribution of type [2] characteristics is assumed to follow a general stochastic process whereby, to be honest, not even stationarity can be assumed. In particular in modelling local mechanical characteristics of timber the stochastic processes of both, type [1] and [2] characteristics, have to be combined. Consequently stationarity in stochastic description of spatial timber properties can generally not be assumed, in particular if representatives of type [2] exhibit some kind of irregular local clustering, for example knot clusters in longitudinal direction of sawn timber, which provokes a certain trend in longitudinal trajectories of strength, stiffness and density.

This first discussion outlines that modelling of serial and parallel systems requires further simplifications in modelling of spatial distributed and correlated characteristics. Therefore some general thoughts on spatial distribution and correlation of timber characteristics are discussed before quantitative results of spatial correlation of strength, stiffness and density within sawn timber are presented.

Just consider softwood trees, for illustrative purposes Norway spruce, which is characterised by a more or less regularly primary yearly growth increment in length direction. The basic potential and health of the tree is thereby defined by its genetics, the local conditions, e.g. soil conditions, supply of water, nutrients, sun energy and climate. From the first day on many of these parameters influence the primary and secondary growth of the tree and thus the creation of timber by cell division in the secondary meristem cambium. Some of these parameters may also vary over time, e.g. sun energy due to denser or more open stand of the tree. In temperate zones life of trees is additionally determined by alternating growth and recovery phases. Thus the rate of growth per year is to a certain amount determined by supply and growth of previous year(s). The basic parameters like genetics and local growth conditions determine the basic properties of e.g strength, stiffness and density of wood as a certain tree inherent potential. This potential is at least influenced by yearly changes in these parameters. Thus characteristics of every yearly increment are expected to have a certain common dependency on the basic parameters of each habitat. Following these statements two kinds of spatial correlation are in principle expected. First, due to yearly changes in basic growth parameters which are to a certain degree assumed to depend on the years before or at least on some foregoing cell divisions, some kind of autocorrelation or k^{th}-order Markov-chain can be expected. Thereby k has to be specified but can be expected to be within $0 < k \leq 5$. Secondly, due to the common occurrence of representatives of type [1]

and type [2], whereby the variability given for representatives of type [1] is assumed to be small compared to that of type [2], and due to the basic potentials defined by genetics and growth conditions a certain amount of in distance independent spatial correlation between increments within sawn timber can be expected as well. This kind of correlation is considered as equicorrelation. Herein a common dependency of all sub-elements within sawn timber on a specimen inherent basic potential is given. This assumption is for example supported by observations of COLLING (1990). He found distances between knot clusters as well as the diameters of dominating knots fluctuating around specimen specific average values. Furthermore, the hierarchical material structure of wood and timber indicates a hierarchical process which is per definition in conjunction with equicorrelation (see section 4.2). With some references regarding the correlation of strengths between weak zones of the same structural element WILLIAMSON (1994) mentioned some explanations why a certain amount of correlation can be expected in principle, namely,

- breakdown is the same for the whole stem and depends on each stem;
- pith (radial position) or position relative to pith is the same for the whole structural element;
- density and other basic characteristics can be assumed to be more or less deterministic in longitudinal direction (juvenile / adult wood);
- nearly the same or comparable knot characteristics can be assumed;
- structural elements origin from the same height of the tree;
- identical genetics;
- same or nearly identical characteristics in respect to moisture content.

Note: Juvenile and adult wood is constant in distance to pith (radial position) but knot characteristics change in radial position as well as longitudinally (see Fig. 4.8 and Fig. 5.1).

To conclude, common presence of auto- and equicorrelation in the spatial correlation structure of local characteristics in sawn timber can be assumed. The shares of auto- and equicorrelation are yet not known and will be further discussed. Retrospective to the findings in chapter 4 it can also be concluded that the spatial correlation observable within structural timber is decisively influenced by the characteristics of the foregoing hierarchical level of “clear wood” or wood in general. Consequently, global characteristics represented by type [1] can also be treated as the basic potential of wood,

whereas characteristics of type [2] cause the required scale transition to the hierarchical level of "structural timber". The consequences of these thoughts are discussed at the end of the next section 5.1.1 and in particular and qualitatively in Fig. 5.21.

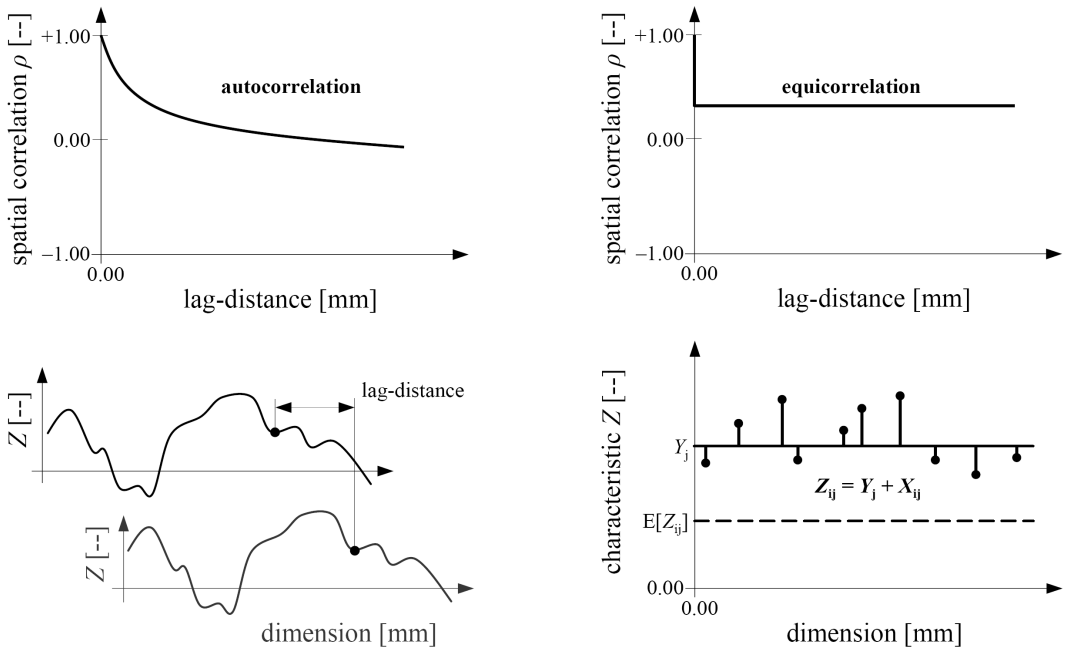

Fig. 5.4: General autoregressive stochastic process (left) vs. (2nd level) hierarchical stochastic process (right)

The next section 5.1.1 is dedicated to spatial distribution and correlation of local characteristics within structural timber. Sections 5.1.2 and 5.1.3 are dedicated to (volume) size and system effects in timber engineering. Each section starts with a general introduction for classification of (volume) size and system effects. It has to be mentioned that the term "system effect" in timber engineering and wood technology is in general only associated with effects of parallel systems. Thereby system effects are defined as multiplication factors, e.g. defined as system factor $k_{sys} = f_{N,05} / f_{1,05} \geq 1.00$, which enhance the characteristic strength potentials of parallel systems compared to that of single elements. Serial system effects are considered in conjunction with size (volume) effects. Consequently research on general system effects in wood and timber engineering is often split in either (parallel) system effects or volume (size) effects. More information on size and system effects is given in sections 5.1.2 and 5.1.3.

5.1.1 Spatial Distribution and Correlation Structure of local Characteristics within and between Structural Timber Elements

Before discussing results on spatial distribution, correlation of flaws (characteristics of type [2]) and physical properties e.g. density, stiffness and strength, some general constraints are listed: First, to the knowledge of the author examinations on local characteristics within sawn timber are restricted to the longitudinal direction. Studies on spatial variation in width or depth are expected to be scarce and not available to the author. Secondly, the definition of a representative length for analysing spatial variation of characteristics in timber is still missing and in general not even discussed in literature.

Spatial Distribution, Correlation of Growth Characteristics and Notes on Reference Volume Elements in Structural Timber

The aim to quantify length effects in sawn timber and to create a data basis for simulations of glulam beams were the driving forces to deal with longitudinal correlation within timber. Thereby the longitudinal description of local characteristics is required and generally performed for 2D simulation models (e.g. FOSCHI AND BARRETT, 1980; BENDER ET AL., 1985; EHLBECK ET AL., 1985B; FOSCHI, 1985; COLLING, 1990; FRESE, 2006). The general lack of a reference length for the description of longitudinal correlation outlines on the one hand the difficulty in specifying this representative length. This is due to the spatial variation of flaws in dimensional scales equal to the scale of timber. On the other hand it is a challenge to define a universal dimension applicable for a variety of timber species. Hereby differing primary growth features, e.g. the amount of knot clusters established each year, are observable, even if observations are restricted to softwoods.

Some publications (e.g. RIBERHOLT AND MADSEN, 1979; COLLING, 1990; ISAKSSON, 1999) provide data of dimension and spatial distribution of flaws (e.g. knot clusters, expressed by knot share parameters, see e.g. SCHICKHOFER AND AUGUSTIN, 2001). In most publications dealing with practical examinations on spatial distribution it has to be considered that the test span used was choosen without any plausible reasoning. It can be assumed that some arguments for the selection fall into the categories: (i) contraints given by the test equipment, (ii) considerations made in regard to the material and discrete distributed flaws, (iii) dimensions proportional to qualitatively comparable test configurations given in standards, or (iv) simple because the same span was used already in previous analysis and / or other authors. In particular the last argument would provide

direct comparability between test results of various sets and studies and thus enlarge the power of available results. Tab. 5.1 gives a brief summary of test spans used so far in literature.

Tab. 5.1: Summary of test spans for practical examination of the longitudinal distribution of strength and stiffness in structural timber

source	test span	characteristic(s)	species
CORDER (1965)	305 mm	$E_{m,0,i}$	Western hemlock
GLOS (1978)	180 mm	$f_{c,0,i}$	Norway spruce
HEIMESHOFF AND GLOS (1980)	137.5 mm	$f_{t,0,i}$; $E_{m,0,i}$	Norway spruce
KLINE ET AL. (1986)	762 mm	$E_{m,0,i}$	NN
TAYLOR AND BENDER (1988, 1989), TAYLOR (1988)	610 mm	$f_{t,0,i}$; $E_{m,0,i}$	Douglas Fir
SHOWALTER ET AL. (1987)	762 mm	$f_{t,0,i}$; $E_{m,0,i}$	Southern pine
LAM AND VAROGLU (1991A,B)	610 mm	$f_{t,0,i}$	Spruce-Pine-Fir
XIONG (1991), LAM AND BARRETT (1992), LAM ET AL. (1994), WANG ET AL. (1995)	152 mm	$f_{c,0,i}$; $E_{m,0,i}$	Spruce-Pine-Fir
RICHBURG AND BENDER (1992), RICHBURG (1989)	610 mm	$f_{t,0,i}$; $E_{m,0,i}$	Douglas Fir
ISAKSSON ET AL. (1994), ISAKSSON AND THELANDERSSON (1996), ISAKSSON (1998, 1999)	400 mm	$f_{m,i}$; $E_{m,0,i}$	Norway spruce
KÄLLSNER AND DITLEVSEN (1994), KÄLLSNER ET AL. (1997)	< 720 mm	$f_{m,i}$	Norway spruce
BRANDNER ET AL. (2005)	400 mm	$E_{t,0,i}$	Norway spruce
FRESE (2006)	≥ 150 mm	$f_{t,0,i}$; $f_{c,0,i}$; $f_{t,j}$; $E_{t,0,i}$; $E_{c,0,i}$	Beech
STUEFER (2011)	150 / 300 mm	$f_{t,90,i}$; $E_{t,90,i}$; ρ_{12}	Norway spruce

The motivation to deal with spatial distribution and correlation of mechanical characteristics in timber is versitale but divisible in three main aspects: The first aspect aims on the improvement of stress grading algorithms by improving strength estimation based on local $E_{m,0,i}$ instead of global $E_{m,0}$ values. The second aspect serves for deeper understanding and enhanced modelling of size (volume) effects (in particular length effects) with focus on improved design of solid and glued laminated timber. The third

aspect concentrates on the establishment of a data base to increase the significance of input parameters for stochastic-mechanic modelling and simulation of glued laminated timber products, e.g. glulam (GLT), CLT, duo and trio beams.

Mechanical tests thereby only provide discrete data of spatial distribution and correlation. Continuous or nearly continuous information is scarce and for example given for density estimated from X-ray scanning or for apparent E-modulus (including shear deformation) based on readings from machine stress rating devices. In particular the determination of local strength requires a certain test increment as "free span length" and additional length for clamping or loading devices. The introduction of load requires a certain volume (length) to guarantee that the measured load confirms with the assumptions made in calculation of stress and stiffness values. For example BOGENSPERGER (2006) showed by means of FE-analysis that a distance to the clamping device of about one times the clamping length is required to secure a uniform distribution of tensile stresses over the whole cross section of a specimen stressed longitudinally in tension. This may then conform to the theoretical assumption according the simple beam theory given by $\sigma_{t,0} = F / A$, with $\sigma_{t,0}$ as tensile stress in grain direction, F as tensile force applied in grain direction and $A = A(x)$ as cross section area. Thus the specification of a suitable test increment requires the consideration of at least two points: first to secure that the theoretically assumed stress distribution confirms sufficiently accurate with the real stresses during testing, and secondly, a certain linkage to the material structure of structural timber, e.g. in regard to the length increment (distance) between knot clusters. For example WILLIAMSON (1992) report on observations that 3 m long softwood boards of low quality contain approximately $20 \div 50$ "macroscopic" flaws (significant in their dimension in respect to the dimension of boards) whereas boards of high timber quality were found to contain also the same quantity but of "microscopic" flaws. WILLIAMSON (1992) cites BURY (1974) who stateted that ≥ 20 elements (e.g. flaws) are a sufficient quantity to use an asymptotic EVT distribution model (see section 2.6.2). Nevertheless as discussed in section 3.3 this assumption appears a bit rough and if than only applicable in case of more or less iid elements. Thereby the heterogeneity between structural timber elements and the dependency between sub-elements within the same element cause the same phenomenon but under a different perspective.

Numerous studies concentrated on the spatial distribution of knot clusters. In structural timber these are often associated as best indicators of a potential failure domain. For example RIBERHOLT AND MADSEN (1979) found that the distance between knot clusters

varies remarkably even if only one timber species, i.e. Norway spruce is considered. For example in one series Swedish and Danish spruce showed a mean distance between knot zones (*KZD*) of E[*KZD*] = (330 ÷ 360) mm, with CoV[*KZD*] = (28 ÷ 34)%. Another series on Danish spruce give an expectation of E[*KZD*] = (450 ÷ 500) mm, with CoV[*KZD*] = (50 ÷ 63)%. Beside that a positive dependency on timber grade can be expected although the presented data showed no clear tendency. The distribution of *KZD* was modelled by means of an exponential distribution as a special case of the Gamma distribution with distance of one increment. Beside the qualitatively weak representation of test data by the exponential distribution model, which was also confirmed by KS-tests performed by RIBERHOLT AND MADSEN (1979), the model was further used as basis for the definition of the so called "weak zone model" which will be discussed in more detail later. CZMOCH ET AL. (1991) report with reference to COLLING AND DINORT (1987), JÖNSSON AND ÖSTLUND (1987) and FEWELL (1991) that the mean distance between knot clusters in Norway spruce can be assumed to be roughly 500 mm and independent of grading (strength) class. KÄLLSNER ET AL. (1997) found 6 (7) weak zones over 3.5 m long boards with a cross section of w / d = 45 mm / 120 mm. ISAKSSON (1999) analysed the longitudinal distribution of knots and knot clusters by means of knot share parameter "knot area ratio" (*KAR*). This parameter is defined as the relative share of knot area projected on the cross section area. Thereby overlapping areas are only counted once. He calculated the *KAR* values of knots of Swedish spruce, w / d = 45 mm / 145 mm of 150 mm long board increments for every 10th mm. He predicted the occurence of knot clusters based on *KAR* readings and by means of two *KAR* limits of 40% and 50%. Thereby mean distances between knot cluster of 440 mm and 494 mm, respectively, were observed. The distance between weak zones was found to be independent of the strength potential of the beam. This observation corresponds to findings of CZMOCH ET AL. (1991) but contradicts results of RIBERHOLT AND MADSEN (1979). Note: This can be explained by the dependency of the distance on growth and the relative radial position of sawn timber within the stem. Thereby strength grading is regulated by limits of knot diameters but not by the distance between knot clusters. As mentioned by WILLIAMSON (1992) the dimension of flaws is reduced in higher strength grades whereas the quantity is not. Nevertheless, the mean distances determined by means of *KAR* limits correspond well with the mean distances gained from direct measurements which were in the range of (400 ÷ 600) mm corresponding to 4 ÷ 8 weak sections within (5.1 ÷ 5.4) m long boards. In agreement with RIBERHOLT AND MADSEN (1979) also ISAKSSON (1999) used a Gamma distribution for modelling the distance between weak zones. But even though not discussed but provided in ISAKSSON (1999) 2pLND shows qualitatively a distinctively

better representation of knot data than the Gamma distribution. With reference to COLLING AND DINORT (1987) *KAR*-values were found to be independent of (i) growth region (provenience), (ii) board width or (iii) grading class. Note: *KAR*-values independent of the grading class can in general not be expected as this parameter is an indicating property for strength in visual and machine grading. The mean *KZD* was found to be (450 ÷ 500) mm.

The length of knot clusters, classified as length of weak zones, is often associated with the length increment of knot accumulation parameters, e.g. *KAR* or parameters given in DIN 4074-1 like *DEB*, *DAB*, *DEK* which normally have to be determined within 150 mm long increments. Deviating from this rule RIBERHOLT AND MADSEN (1979) analysed knot share parameters within a length equal to the width of the board. Note: This specification is in dependency of geometric constraints defined during the breakdown process of logs to timber and not linked with growth features of the living tree. ISAKSSON (1999) modelled the length of weak zones by means of a Beta distribution and observed a range of (10 ÷ 380) mm.

In general, all currently available knot parameters are brought in some relationship to local strength data. This is done with the aim to find all grading relevant, but mostly only the maximum (worst flaw) associated with the lowest strength. Thereby the occurrence and ascertainable dimension of knots is merely an indicator for local grain deviation. In particular in wood with its roughly orthotropic material structure this grain deviation shows a significant and decisive impact on strength. For example in clear wood a deviation from parallel to grain of $\alpha = 10°$ leads to about 30% loss in tensile strength $f_{t,\alpha}$ if compared to $f_{t,0}$ (see HANKINSON, 1921). Based on results of comprehensive research projects (i.e. SCHICKHOFER AND AUGUSTIN, 2001; FINK ET AL., 2011) addressing the relationships between knot accumulation parameters and strength of structural timber it can be concluded that a correlation between $f_{t,0}$ and *KAR* of $r = -0.47$ (SCHICKHOFER AND AUGUSTIN, 2001) as well as $r = -0.55$ (FINK ET AL., 2011) can be expected. Beside this weak negative correlation analysing the correlation between global parameters (type [1]) like density and dynamical E-modulus (e.g. based on eigenfrequency or ultrasonic speed) to $f_{t,0}$ gives comparable or even higher positive correlation values even though no direct local information is contained (e.g. density vs. $f_{t,0}$: $r = 0.47$; dyn. E-modulus based on eigenfrequency ($E_{dyn,EF,12}$) vs. $f_{t,0}$: $r = 0.77$; FINK ET AL., 2011). In case of multiple regression analysis including global but also local characteristics of type [2] the gain on power of strength estimation models by knot parameters is negligible (*KAR* and $E_{dyn,EF,12}$

vs. $f_{t,0}$: $r = 0.80 \rightarrow +0.03$; FINK ET AL., 2011). Nevertheless, the size of knots and knot clusters give an impression and a first estimate for the extension of discrete weak zones in timber and thus a first estimate of the geometric spatial distribution of mechanical characteristics in structural timber. Note: The definition of the largest defect is linked to an estimate of the defect with the lowest strength potential or the highest impact on the strength potential of sawn timber, based on non-destructively determined properties and thus an "idea" of the local strength. For the determination of the "largest defect" a relative comparison between the estimated potentials of all weak sections within a board is sufficient but the relationship between the knot parameters and strength is generally weak.

Within the following part analysis results of dimensional and spatial distribution of knot data are presented. Therefore parallel to grain tensile test data on boards accomplished on Norway spruce (*Picea abies (L.) Karst.*) of provenience Central Europe (Switzerland: I-CH; Austria: II-AT & III-AT) taken from MISCHLER-SCHREPFER (2000) and SCHICKHOFER & AUGUSTIN (2001) (who partly cooperated during the reported projects) are presented. Tab. 5.2 contains an overview of tested dimensions and quantities as well as additional information like nominal grading classes according DIN 4074 and the type of grading, visual (vis), machine (mach) and semi-machine (semi).

The tensile tests were accomplished according the prescriptions of test standard EN 408, with a minimum free testing length of $l_{free} = 9 \cdot w$ (w as width of the board) and measurement of local elongation within the free testing length over a distance of $5 \cdot w$. In general, the free testing length was maximised to $l_{free} = 3{,}300$ mm and 2,860 mm for series I-CH and series II-AT & III-AT, respectively. Furthermore, the placement of the specimen in the tensile testing device was done randomly without visual judgement of the weakest cross section. Before testing in tension the following additional information per board were recorded:

- global density;
- dynamical E-modulus ($E_{dyn,US}$) by means of ultrasonic speed measurement device Sylvatest;
- radial position (*RP*) within the log, determined as distance between the pith and the center of board cross section;
- average annual ring width (*ARW*).

Tab. 5.2: Test data – overview of main- and sub-series, nominal grading classes, quantities and dimensions

	main- & sub-series [--]	NGC [3] [--]	quantity [--] all	quantity [--] cen. [4]	width *w* [mm]	thickness *t* [mm]	length *l* [mm]
I-CH	_1:semi:m [1]	not defined [2]	62#	46#	150	45	4,450
	_1:semi:s [1]		62#	37#			
	_1:semi:ss [1]		61#	43#		29	
II-AT	_1:vis	S10	45#	35#	150	35	3,200 ÷ 4,000
	_2:vis	S13	45#	34#			
	_3:mach	MS13	45#	39#			
	_4:mach	MS17	41#	35#			
	_5:mach	MS13	16#	12#	230		
	_6:mach	MS17	14#	6#			
III-AT	_1:vis	S10	45#	35#	110		
	_2:vis	S13	45#	34#			
	_3:mach	MS10	45#	37#			
	_4:mach	MS13	45#	32#			
	_5:mach	MS17	44#	35#			
		$\Sigma =$	615#	460#			

[1] m, s, ss denote different radial positions (*RP*) of the board (cross section center) within the log, with *RP*(m) ≈ 26.5 mm, *RP*(s) ≈ 79.5 mm and *RP*(ss) ≈ 100.0 mm

[2] pre-selected 5 m long roundwood with ultrasonic speed (Sylvatest) $v_{US} \geq 4{,}500$ m/s (corresponds to the upper 43% of all harvested logs) and mid log diameter MDM = (29 ÷ 31) cm

[3] nominal grading class (NGC)

[4] only data sets containing all required data (complete knot data; $M_{WZ} \geq 1$; failure in free testing length; fracture in a registered knot cluster)

Before testing visually detectable and measurable irregularities, especially knots and knot clusters, were registered. Hereby, every knot with a diameter $dm_{knot} \geq 5$ mm (as common) was recorded regarding its dimension and position within the entire board. In total, for the 615# boards about 40,000 knots were recorded and documented. Based on this data knot indicators, e.g. knot area ratio (*KAR*), knot density (*KD*) and others were derived (see SCHICKHOFER AND AUGUSTIN, 2001).

Tab. 5.3: Main statistics (mean and CoV) of geometrical and physical characteristics for each sub-series: statistics of all and of censored data (see Tab. 5.2)

sub-series [--]	**mean_all | mean_cen (fixed value)** CoV_all | CoV_cen				
	ARW [mm]	**RP [mm]**	**ρ_{12} [kg/m³]**	**$E_{t,0,l,12}$ [N/mm²]**	**$f_{t,0,l}$ [N/mm²]**
I_1:semi:m	4.1 | 4.1	(26.5)	404 | 403 6.3% | 6.4%	10,580 | 10,490 13.6% | 13.9%	22.7 | 22.3 33.6% | 32.8%
I_1:semi:s	2.5 | 2.5	(79.5)	442 | 440 6.6% | 7.0%	13,310 | 13,160 12.7% | 13.4%	34.0 | 33.6 32.6% | 34.5%
I_1:semi:ss	2.3 | 2.3	(100.0)	459 | 459 7.3%| 7.9%	13,720 | 13,710 14.2% | 14.1%	34.7 | 33.0 32.4% | 32.0%
II_1:vis	2.2 | 2.2	37.7 | 38.4	450 | 453 8.8% | 8.2%	10,870 | 10,910 14.0% | 11.4%	21.1 | 20.8 28.5% | 28.0%
II_2:vis	1.9 | 2.0	56.1 | 56.1	441 | 444 8.2% | 7.9%	12,720 | 12,810 18.6% | 18.5%	34.4 | 34.9 30.7% | 30.7%
II_3:mach	2.1 | 2.1	50.4 | 50.5	473 | 475 8.6% | 8.8%	13,820 | 13,800 7.3% | 7.7%	32.2 | 31.8 24.0% | 22.5%
II_4:mach	1.6 | 1.6	51.1 | 50.3	508 | 506 8.6% | 8.7%	16,390 | 16,190 10.1% | 9.9%	44.0 | 42.2 25.4% | 24.0%
II_5:mach	2.6 | 2.6	71.0 | 67.3	437 | 438 6.3% | 6.7%	13,250 | 13,230 5.4% | 5.4%	30.5 | 30.9 27.7% | 28.5%
II_6:mach	2.2 | 2.2	89.4 | 87.0	455 | 447 8.3% | 9.3%	14,340 | 13,570 14.9% | 16.3%	44.1 | 37.7 32.8% | 34.6%
III_1:vis	2.7 | 2.7	29.7 | 29.5	443 | 446 11.0% | 11.3%	10,660 | 10,680 16.3% | 15.8%	23.0 | 23.3 34.7% | 35.9%
III_2:vis	2.5 | 2.3	42.2 | 41.0	446 | 456 10.2% | 9.7%	10,290 | 10,320 11.6% | 12.1%	34.1 | 35.1 23.0% | 23.2%
III_3:mach	3.0 | 3.0	36.4 | 37.0	425 | 424 6.8% | 6.9%	10,680 | 10,640 10.9% | 11.2%	25.4 | 24.4 34.0% | 33.1%
III_4:mach	2.0 | 2.0	39.1 | 39.5	476 | 479 6.5% | 6.6%	10,760 | 10,550 14.1% | 13.3%	35.4 | 36.3 24.2% | 23.5%
III_5:mach	1.8 | 1.9	37.5 | 37.4	500 | 497 8.2% | 8.3%	14,370 | 14,180 17.7% | 18.6%	38.6 | 37.2 36.4% | 36.7%

For a joint consideration of knot and tensile test data the position of the board in the tensile testing device was recorded together with the position of the elongation measurement devices. Nevertheless, due to contradicting knot data of opposite or adjacent board sides or boards without any knot cluster (in total 101#), failure within the clamping area or missing data (50#) as well as missing values of maximum force (4#) in total only 460# boards could be utilised for further computations.

The E-modulus in tension was adjusted according EN 384 to a reference moisture content of $u = 12\%$. The size effect for adjustment of tension strength of boards to a reference width of 150 mm as given in EN 384 or additionally to a reference length of 2,000 mm according EN 1194 was not applied. The main statistics of geometrical as well as physical characteristics are given in Tab. 5.3. The comparison of test statistics over all 615# and of only 460# boards shows no significant differences, whether in mean nor in variation. This indicates that the censoring happened randomly and that the censored data set can be considered as representative as the total sample. A comparison of the empirical distribution of tension strength for each sub-series separately with a best-fitted lognormal distribution (2pLND) is presented in Fig. 5.5.

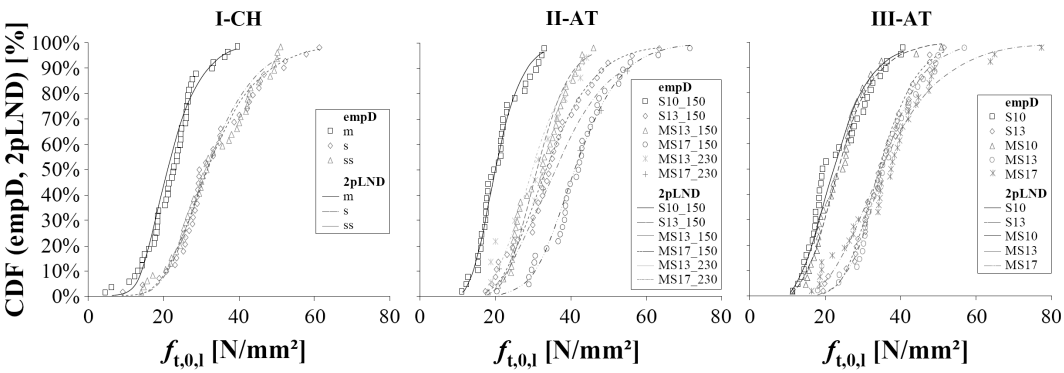

Fig. 5.5: Empirical distributions as well as best fitted 2pLND of tension strength in sub-series of I-CH (left), II-AT (middle) and III-AT (right)

Qualitative judgement of the distribution of $f_{t,0}$ for each sub-series in Fig. 5.5 shows that 2pLND as RSDM appears acceptable. Additionally, Shapiro-Wilk tests were performed in R (2009). Thereby the empirical distribution of $f_{t,0}$ was tested against ND and 2pLND, the latter taking the logarithm of $f_{t,0}$. At a confidence level of $(1 - \alpha)\% = 95\%$ in 10 of 14 and 13 of 14 sub-series the assumption of being normal or lognormal distributed, respectively, could not be rejected. The same test procedure was applied for E-modulus in

tension parallel to grain ($E_{t,0,12}$) and density (ρ_{12}). Thereby, in 11 of 14 and 10 of 14 as well as in 13 of 14 and 14 of 14 cases the assumed models ND and 2pLND could not be rejected, respectively for E-modulus and density. By counting the cases were the realised significance (*p*-value) either of the test against ND or against 2pLND was higher the ratios #ND / #2pLND of 9 / 5, 10 / 4 and 4 / 10 were found. Due to grading all sub-series contain two- or at least one-sided truncated data. This is in particular true for density and E-modulus. Both are explicit or implicit strength grading parameters. Due to truncation an increased symmetry in distribution can be expected. Nevertheless, due to physics 2pLND is preferred for representing strength and E-modulus in tension parallel to grain, even for sub-samples. The dominance of not rejected empirical distributions represented by ND was not expected. Nevertheless, already BURGER (1998B) chose 2pLND as RSDM for density. Comparable results were also found in BRANDNER AND SCHICKHOFER (2007). Consequently, 2pLND is also taken as RSDM for density.

The definition of knot clusters is of particular interest in this study. In the context of visual grading, judgement of knot clusters has to be done within a fixed segment length in longitudinal direction of the board, e.g. within 150 mm as given in DIN 4074. In this study the definition of the length for judgement of knot clusters as well as its geometrical extension in longitudinal direction was kept variable and in dependency of the size of the knots within the corresponding knot cluster. With reference to MEIERHOFER (1976) and BUKSNOWITZ ET AL. (2010) (see Fig. 5.6) the area influenced by a knot is viewed in relation to the local grain deviation around a knot. Referring to their analysis the section length of knot zones in case of single knots can be defined as the measurable knot diameter in direction longitudinal to the global grain direction plus two times the measurable knot diameter transverse to global grain direction. Following that, knot clusters are defined as a group of knots with a maximum in-between distance of one knot diameter, whereby the larger diameter of two neighbouring knots is taken into account. The section length in case of a knot cluster is defined as the length of the knot cluster itself plus the diameter of the outermost knots in both directions. These geometrical definitions of knot (cluster) zones are theoretically straighforward. Nevertheless, for comparability of the presented analysis with the literature statistics of weak zones of knot clusters (WZ) and intermediate knots (IK) are given without the additional knot diameters in longitudinal direction. A further reason is to supply statistics of the length of weak zones equal to that used for the calculation of *KAR*-values. Nevertheless, for the definition of a representative longitudinal element the influence of local grain deviation is explicitely taken into account.

The calculated *KAR*-values KAR_{WZ} which correspond to the weak (knot) zones represent the projected knot area on the cross section by considering all knots within the defined segment length. Thereby, overlapping areas are only counted once.

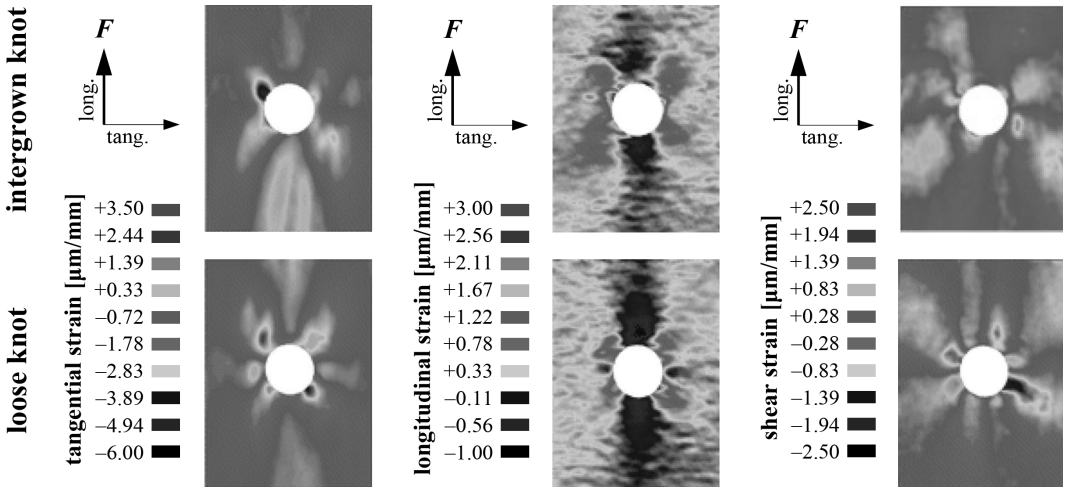

Fig. 5.6: Electronic speckle pattern interferometry (ESPI) measurements on an intergrown (above) and loose knot (below) with a diameter of 15 mm under tensile stress parallel to grain of 10 N/mm² on Norway spruce from BUKSNOWITZ ET AL. (2010): tangential strain (left); longitudinal strain (middle); shear strain (right)

In general, the expected failure inducing characteristic is given by a global or local grain deviation. Local grain deviation is ascertainable by knots or knot clusters, which significantly weaken, e.g. the tensile strength capacity parallel to the grain of a board within the affected board segment. This follows on one hand directly from the fact that clear wood tensile strength perpendicular to the grain is only about 1 / 30 of that parallel to grain. On the other hand and due to the breakdown process, knots, which are optimised for bearing the branches, leaves and live loads in the living tree appear as disturbed area in regard to grain orientation, stress and strain flow within the board.

As mentioned above, every knot with a diameter of $dm_{knot} \geq 5$ mm was recorded with regard to its dimensions and position within the board. Consequently, all knot share ratios, dimensions and other statistics in relation with knots are censored somehow. Some comments on this aspect are given later. During the tension tests fracture propagation (if detectable) and / or fracture characteristics were recorded for each specimen by reporting affected and involved knots and knot clusters. On the basis of calculated knot share ratios

under the assumption that the cross section with the highest share of knots within the fractured zone initiated the failure of the board and hence determined the tensile strength, the highest share of knots of all recorded knot zones along the fracture is associated with the tensile strength of the board. Consequently, it can be expected that all other knot zones along the free testing length show an equal or higher tensile strength as measured by the destructive test. That means that beside the quantitative information about the ultimate tension capacity tested, the qualitative information of the number of survived weak zones per board given by the number M_{WZ} as the number of elements composing a serial system, is of highest interest for the representation of the length effect on strength (see e.g. sections 3.3, 5.1.2 and 5.4).

Tab. 5.4: Statistics of weak zones: quantity (M_{WZ}), width (w_{WZ}) of and distance (d_{WZ}) between weak zones within free testing length l_{free}

sub-series [--]	M_{WZ} **[--]**		w_{WZ} **[mm]**		d_{WZ} **[mm]**		
	median	**mean**	**median**	**CoV**	**mean**	**median**	**CoV**
I_1:semi:m	4#	68	51	76%	763	709	72%
I_1:semi:s	5#	48	35	65%	681	712	70%
I_1:semi:ss	4#	43	31	68%	695	718	70%
II_1:vis	9#	47	40	57%	398	340	68%
II_2:vis	7#	38	33	50%	522	489	58%
II_3:mach	6#	47	39	54%	554	514	59%
II_4:mach	6#	40	34	49%	591	534	57%
II_5:mach	5#	56	44	69%	760	569	61%
II_6:mach	3#	58	57	48%	664	448	77%
III_1:vis	8#	44	40	48%	466	463	60%
III_2:vis	6#	37	31	48%	528	468	65%
III_3:mach	6#	52	45	50%	527	544	56%
III_4:mach	7#	41	35	56%	443	425	57%
III_5:mach	7#	40	34	49%	475	430	51%

As discussed previously in this section and as illustrated in Fig. 5.1 the distance between knot clusters corresponds to the yearly incremental longitudinal growth of the tree, depending on the position of the board within the stem and on the breakdown process.

For a reproducible determination and classification of distinctive knot clusters as potential weak zones within a given board a knot share limit has to be defined. As already discussed by ISAKSSON (1999) this is difficult but decisive for further calculations. ISAKSSON examined two limits, a 40% and a 50% limit of max[*TKAR*] of each individual specimen, whereby *TKAR* was determined for a fixed board segment of 150 mm length. The herein presented knot share ratios base on varying lengths of board segments. Consequently, a new definition of a practicable limit is required, in particular in connection with the width of the weak zone. After visually judgement of various possibilities it was decided to define the limit with $KAR_{WZ} \cdot w_{WZ} \geq 0.20$, with KAR_{WZ} as the *KAR*-value corresponding to the above defined length of the knot zone, and w_{WZ} as the longitudinal dimension (width) of the knot zone in [mm]. Tab. 5.4 gives an overview of some statistics for quantity M_{WZ} and width w_{WZ} of weak zones and (in-between center) distance d_{WZ} between the weak zones for each sub-series of series I, II and III. Due to the distinctive differences in d_{WZ} between series I-CH and II-AT & II-AT data of I-CH is excluded from further statistical analysis.

Fig. 5.7 and Fig. 5.8 contain the empirical distribution of KAR_f from fractured weak zones in comparison with the best fitted 2pLND. Over all KAR_f can be qualitatively well represented by 2pLND.

A comparison between empirical and best fitted 2pLND of variable w_{WZ} is provided in Fig. 5.9 and Fig. 5.10. According the definition of weak zones the width w_{WZ} as well as the distance d_{WZ} are bounded below (→ 3pLND). Again and despite the lower boundary a good to excellent agreement between empD and 2pLND is given.

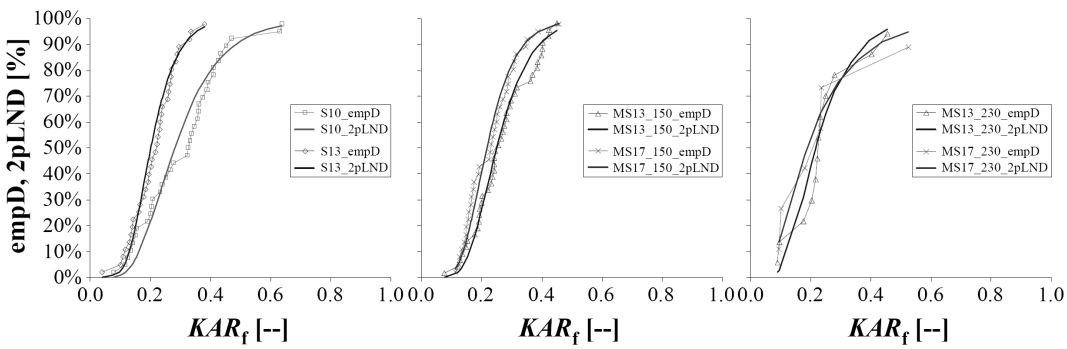

Fig. 5.7: Empirical distribution of KAR_f in fractured weak zones vs. best fitted 2pLND: Series II-AT

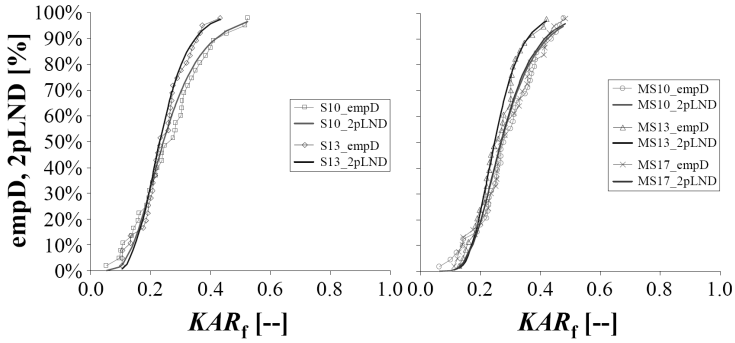

Fig. 5.8: Empirical distribution of KAR_f in fractured weak zones vs. best fitted 2pLND: Series III-AT

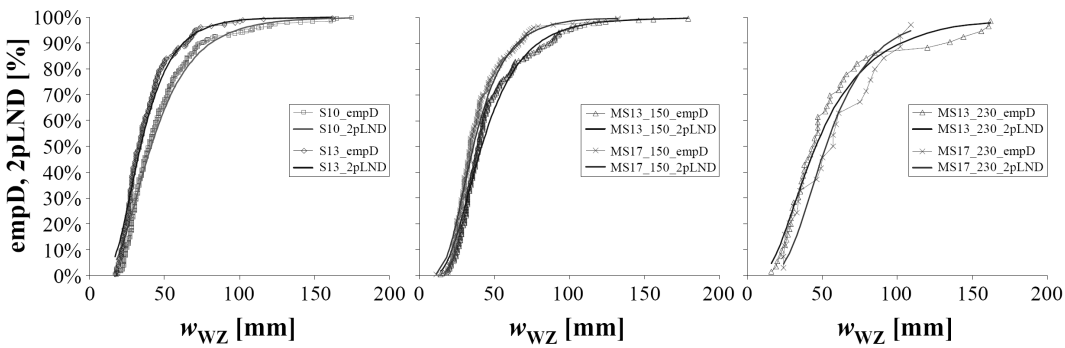

Fig. 5.9: Empirical distribution of the width of weak zones w_{WZ} vs. best fitted 2pLND: Series II-AT

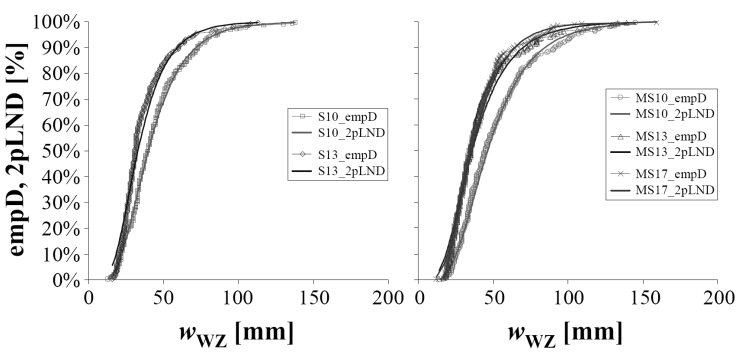

Fig. 5.10: Empirical distribution of the width of weak zones w_{WZ} vs. best fitted 2pLND: Series III-AT

Fig. 5.11 and Fig. 5.12 show the empD and best fitted 2pLND and exponential distribution, the latter in reference to literature. Despite the fact that the exponential distribution has one fitting parameter less than 2pLND overall representation of d_{WZ} is poor. Comparison of empD with 2pLND gives congruent and representative results.

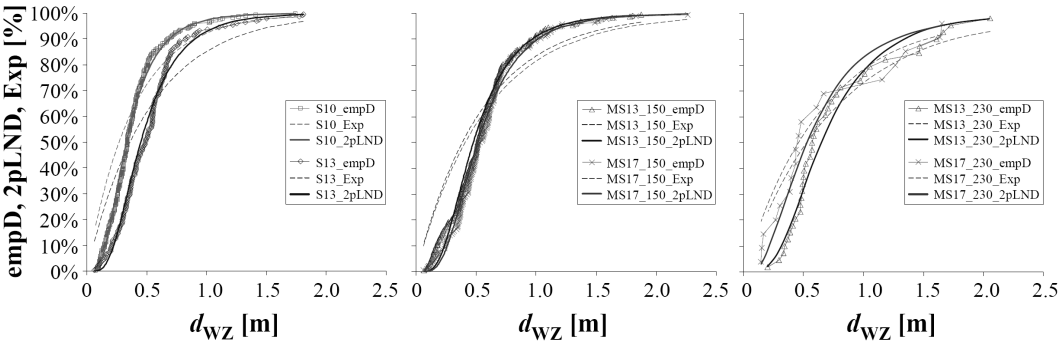

Fig. 5.11: Empirical distribution of the distance between weak zones d_{WZ} vs. best fitted exponential distribution (Exp) and 2pLND: series II-AT

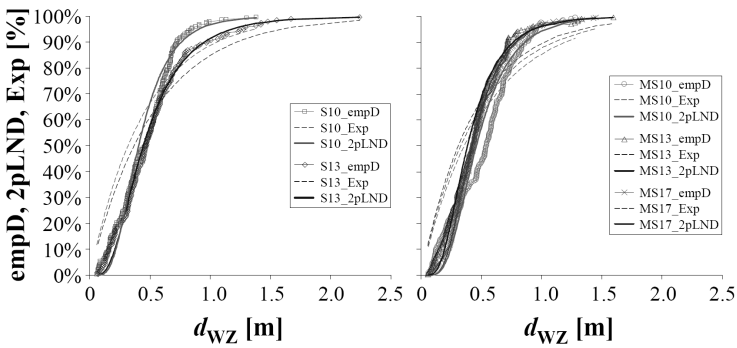

Fig. 5.12: Empirical distribution of the distance between weak zones d_{WZ} vs. best fitted exponential distribution (Exp) and 2pLND: series III-AT

For simplification of further examinations and to increase the significance of results all 14 sub-series were compared in respect to their medians. Therefore the Mann-Whitney-U test as implemented in R (2009) was applied to compare density, E-modulus and strength data of all 14 sub-series. The confidence level was again chosen with $(1 - \alpha)\% = 95\%$. The aim was to assembly sub-series not significantly different to at least three data groups which are significantly different. Thereby only data of sub-series which are assignable to

a specific group in all three analysed physical characteristics are accepted. The output of the tests lead to:

- group **g01**: II-AT_1:vis & III-AT_1:vis & III-AT_3:mach (in total 107#);
- group **g02**: II-AT_3:mach & II-AT_6:mach (in total 45#);
- group **g03**: II-AT_4:mach (in total 35#).

Statistics of the physical characteristics density, E-modulus and tension strength of grouped data are given in Tab. 5.5. Median tests performed on density, E-modulus and tension strength by means of Shapiro-Wilk test on normality and with a confidence level of $(1 - \alpha)\% = 95\%$ showed that 2pLND could be rejected in none of the groups. In four of nine cases this was also true for ND. Also for KAR_f the assumed 2pLND could not be rejected for g02 and g03. In g01 p-value was on the boarder of rejection.

Tab. 5.5: Statistics of grouped data: density, E-modulus and strength in tension parallel to grain

	ρ_{12} [kg/m³]			$E_{t,0,l,12}$ [N/mm²]			$f_{t,0,l}$ [N/mm²]		
	g01	**g02**	**g03**	**g01**	**g02**	**g03**	**g01**	**g02**	**g03**
#	107#	45#	35#	106#	45#	35#	107#	45#	35#
min	370	400	438	7,860	10,430	14,170	11.1	18.0	20.4
mean	440	471	506	10,740	13,770	16,190	22.9	32.6	42.2
median	**439**	**471**	**501**	**10,820**	**13,770**	**15,840**	**21.5**	**32.6**	**42.1**
max	567	601	615	14,160	16,600	20,810	50.8	54.9	71.6
CoV [%]	**9.3%**	**9.0%**	**8.7%**	**12.8%**	**9.0%**	**9.9%**	**33.3%**	**25.2%**	**24.0%**
X_{05}	384	413	444	8,490	12,090	14,350	13.1	21.3	28.9
X_{95}	525	551	595	12,800	16,190	19,010	35.7	45.4	58.1

A comparison of the medians of density, E-modulus and strength between the groups by means of Wilcoxon-test statistics give in all cases a rejection of the null hypotheses of equal medians on high significance level ($p < 0.01$).

Based on 2pLND as RSDM of all three physical properties, simple linear regression analysis was performed on logarithmised variables. The goodness of fit was judged qualitatively by regression analysis on normality (qq-plot of residuals on normal probability paper, leverage plot, check of homoscedasticity and residual analysis) and by a test summary provided in R (2009) based on F-test statistics. Thereby a weak

relationship between density and E-modulus with $r^2_{adj} = 0.35 \div 0.39$ was found in all three groups with high significant intercept and slope parameters. Despite the regression between E-modulus and tension strength in group g01 with $r^2_{adj} = 0.30$ no significant relationships between $E_{t,0,12}$ and $f_{t,0}$ as well as between ρ_{12} and $f_{t,0}$ were detected. The reason for contradicting data and lack in relationship is not clear. Comprehensive analysis of data sets in BRANDNER ET AL. (2012) and other literature (e.g. GLOS, 1995; JOHANSSON, 2000; JCSS:2006) shows in general weak to moderate correlation between the analysed variables, see Tab. 5.6.

Tab. 5.6: Coefficients of determination and correlation coefficients between density, E-modulus and strength in tension parallel to grain

R^2 / R	ρ_{12}	$E_{t,0,12}$	$f_{t,0}$
ρ_{12}	1.00	0.40 ÷ 0.55 [1)]	0.20 ÷ 0.30 [1)]
$E_{t,0,12}$	0.63 ÷ 0.74 [1)]; 0.60 [3)]	1.00	0.30 ÷ 0.45 [1)]
$f_{t,0}$	0.45 ÷ 0.55 [1)]; 0.50 [2)] 0.40 [3)]; 0.54 ÷ 0.62 [4)]	0.55 ÷ 0.67 [1)] 0.80 [3)]; 0.87 [4)]	1.00

[1)] BRANDNER ET AL. (2012): based on simple linear regression of logarithmised variables

[2)] GLOS (1995)

[3)] JCSS:2006

[4)] JOHANSSON (2000)

Statistics of weak zones as well as intermediate knot zones (*KAR*-values, width and distances in-between) are given in Tab. 5.7 and Tab. 5.8. On a first view a decreasing trend in $KAR_{f,50}$, $KAR_{WZ,50}$ and $w_{WZ,50}$ together with a slight decrease in variation with increasing group number and thus with increasing timber grade can be observed, whereas the in-between distance of weak zones ($d_{WZ,50}$) increases on median level. This trend was expected because the lower the quantity of weak zones per unit length and the smaller the dimension of destroyed areas in structural timber the lower the influence on strength and thus the higher the corresponding strength class or group number. Comparable but not so distinctive trends can be found in Tab. 5.8 which contains statistics of intermediate knot zones. In these statistics d_{IK} is defined as distance between the centers of intermediate knot zones. Comparison of medians between groups of weak zone statistics rejects the hypothesis of equal medians at $\alpha = 5\%$ except for $w_{WZ,50}|$g01 vs. $w_{WZ,50}|$g02 and $d_{WZ,50}|$g02 vs. $d_{WZ,50}|$g03. Test on equal variance at the same significance level by means of command "var.test" in R (2009) on logarithmised data were in general rejected for Var[KAR_{WZ}] with the exception of Var[KAR_{WZ}]|g01 vs. Var[KAR_{WZ}]|g02. In contrast, in

none of the cases the hypothetical equivalence between variance of w_{WZ} and d_{WZ} could be rejected. Comparable results were also found for the statistics of intermediate knot zones.

Tab. 5.7: Statistics of weak zones of grouped data: KAR_f, KAR_{WZ}, width w_{WZ} of and distance d_{WZ} between weak zones

	KAR_f [--]			KAR_{WZ} [--]			w_{WZ} [mm]			d_{WZ} [mm]		
	g01	**g02**	**g03**	**g01**	**g02**	**g03**	**g01**	**g02**	**g03**	**g01**	**g02**	**g03**
#	107#	45#	35#	829#	280#	197#	826#	279#	197#	719#	234#	163#
min	0.06	0.10	0.08	0.05	0.04	0.08	13	14	11	57	67	62
mean	0.29	0.26	0.23	0.23	0.21	0.17	48	48	40	447	563	591
median	**0.28**	**0.24**	**0.23**	**0.21**	**0.19**	**0.15**	**41**	**40**	**34**	**404**	**508**	**534**
max	0.88	0.53	0.46	0.88	0.55	0.46	175	179	132	1,743	1,876	2,264
CoV [%]	**45%**	**38%**	**38%**	**45%**	**45%**	**41%**	**53%**	**54%**	**49%**	**57%**	**61%**	**57%**
X_{05}	0.10	0.12	0.12	0.10	0.09	0.09	22	23	22	111	136	174
X_{95}	0.48	0.42	0.36	0.41	0.40	0.29	101	100	73	802	1,313	1,158

Tab. 5.8: Statistics of intermediate knot zones of grouped data: KAR_{IK}, width w_{IK} of and distance d_{IK} between intermediate knot zones

	KAR_{IK} [--]			w_{IK} [mm]			d_{IK} [mm]		
	g01	**g02**	**g03**	**g01**	**g02**	**g03**	**g01**	**g02**	**g03**
#	858#	174#	89#	1,248#	287#	203#	625#	126#	80#
min	0.00	0.00	0.00	5	5	5	16	16	16
mean	0.03	0.04	0.04	13	15	13	73	117	175
median	**0.02**	**0.03**	**0.03**	**7**	**11**	**8**	**54**	**78**	**145**
max	0.28	0.24	0.14	137	82	69	525	768	735
CoV [%]	**111%**	**83%**	**77%**	**101%**	**81%**	**85%**	**85%**	**96%**	**79%**
X_{05}	0.00	0.00	0.01	5	5	5	19	24	26
X_{95}	0.10	0.09	0.11	36	40	36	191	366	404

Fig. 5.13 shows the empirical distributions of weak zone characteristics KAR_{WZ}, w_{WZ} and d_{WZ} in comparison with best fitted 2pLND. Thereby an acceptable representation of data by 2pLND is observed. In line with statistics given in Tab. 5.7 the distribution of KAR_{WZ}

and w_{WZ} of group g03 show lowest variation and medians whereas d_{WZ} of g03 has the highest but nearly the same median as d_{WZ} of g02.

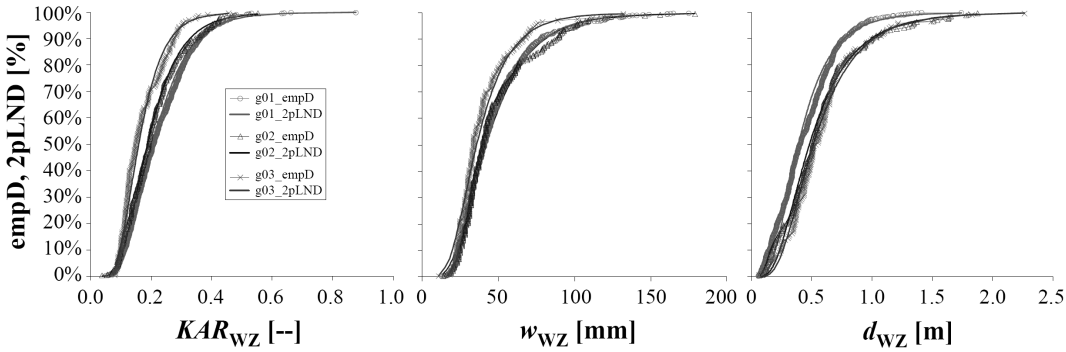

Fig. 5.13: Empirical distribution and best-fitted 2pLND of characteristics of weak zones of grouped data: distribution of KAR_{WZ} (left); width of weak zones w_{WZ} (middle) and distance between weak zones d_{WZ} (right)

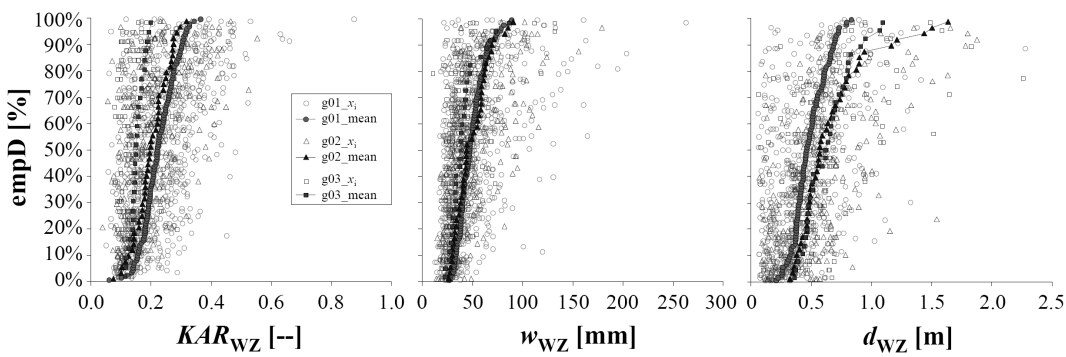

Fig. 5.14: Empirical distribution of characteristics of weak zones within structural timber elements, ordered according their mean values; grouped data: $KAR_{WZ,mean}$ (left); $w_{WZ,mean}$ (middle) and $d_{WZ,mean}$ (right) together with realisations within each structural timber element

Fig. 5.14 supports investigations concerning serial correlation between KAR_{WZ}, w_{WZ} and d_{WZ} within the same structural timber element by separate analysis of each group. Thereby all elements were ordered according the mean-values of examined characteristics and for comparison between the groups plotted as empD. It can be concluded that no distinct serial correlation can be observed. The same plots were made for KAR_{IK}, w_{IK} and d_{IK} of intermediate knot zones, see Fig. 5.15 and Fig. 5.16. The results are qualitatively

comparable to that of the weak zones, whereby the differences between the groups concerning d_{IK} are even more pronounced than in d_{WZ}.

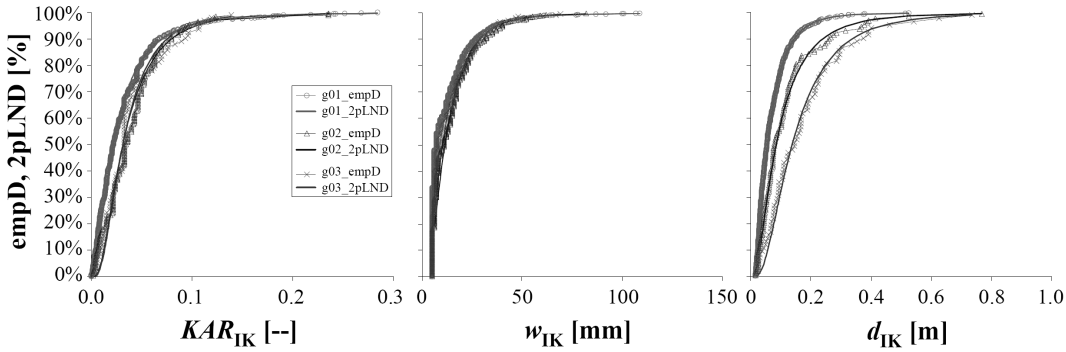

Fig. 5.15: Empirical distribution and best-fitted 2pLND of characteristics of intermediate knot (zones) of grouped data: distribution of KAR_{IK} (left); width of weak zones w_{IK} (middle) and distance between weak zones d_{IK} (right)

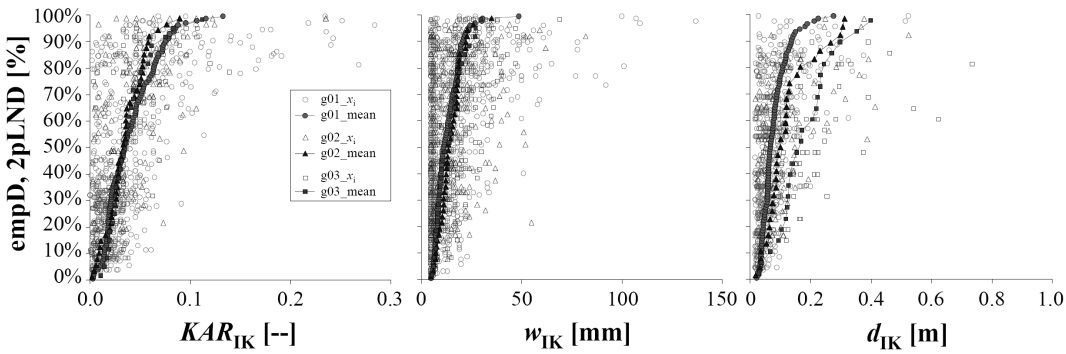

Fig. 5.16: Empirical distribution of characteristics of weak zones within structural timber elements ordered according their mean values; grouped data: $KAR_{IK,mean}$ (left); $w_{IK,mean}$ (middle) and $d_{IK,mean}$ (right) together with realisations within each structural timber element

Further analysis of statistics of weak zones given in Tab. 5.7 shows e.g. a distinctive higher $KAR_{f,50}$ in comparison to KAR_{WZ}, but unexpected equal maximum values. Also the variations are comparable. The median or mean width of weak zones is roughly 1/3 of the generally proposed increment of 150 mm whereas the maximum values are in the range of (130 ÷ 180) mm. Consequently, for a simplified judgement of weak zones in visual or machine grading the current increment length of 150 mm can be roughly confirmed. The minimum of w_{WZ} is given with $w_{WZ} \geq 10$ mm. The mean or median statistics of d_{WZ} are in

the range of (400 ÷ 600) mm and thus coincide with results of e.g. RIBERHOLT AND MADSEN (1979), COLLING AND DINORT (1987), JÖNSSON AND ÖSTLUND (1987), FEWELL (1991) and ISAKSSON (1999). In line with RIBERHOLT AND MADSEN (1979) a significant positive dependency of d_{WZ} on timber grade was found.

The statistics of $d_{IK,50}$ in Tab. 5.8 show also a positive dependency on timber grade. Overall KAR_{IK}, w_{IK} and d_{IK} are more variable than the parameters of weak zones.

So far only knot characteristics in longitudinal direction were analysed. Nevertheless, also an influence on knot characteristics given by the transverse dimension of structural timber elements can be expected. In the test data analysed three different board widths were tested: $w = 110$, 150 and 230 mm. Based on Mann-Whitney-U tests done for data grouping and with focus on not significantly different medians in tension strength the following sub-series can be compared in respect to a possible influence of width on knot zone characteristics:

- ***w* = 110 mm**: III-AT_4:mach & III-AT_5:mach;
- ***w* = 150 mm**: II-AT_3:mach;
- ***w* = 230 mm**: II-AT_5:mach & II-AT_6:mach.

The (averaged) medians of *RP* and knot characteristics of weak zones and intermediate knot zones are given in Tab. 5.9. It can be observed that KAR_f and KAR_{WZ} decrease with increasing board width, whereas the width of and the center-distance between weak zones increases. Of course, these observations have to be seen in connection with the radial position (*RP*) of the board within the stem which also increases with rising board width. This is reasonable since a larger log diameter is required to gain structural timber of larger width or depth. Based on median statistics of intermediate knot zones clear trends are not extractable.

Tab. 5.9: Median statistics of knot characteristics of weak zones as well as intermediate knot zones: classification according the board width

	RP **[mm]**	KAR_f **[--]**	KAR_{WZ} **[--]**	w_{WZ} **[mm]**	d_{WZ} **[mm]**	KAR_{IK} **[--]**	w_{IK} **[mm]**	d_{IK} **[mm]**
***w* = 110 mm**	39	0.26	0.20	35	428	0.03	7	58
***w* = 150 mm**	51	0.25	0.19	39	514	0.04	13	82
***w* = 230 mm**	77	0.22	0.18	51	509	0.02	7	78

A decrease in knot share ratios with increasing board width was also observed by BURGER (1998B; for *DAB*-values) and DENZLER (2007; for *KAR*-values). Nevertheless, in the present work the focus is on the analysis of system actions and effects as result of different arrangements of the elements in respect to each other and in respect to stresses applied externally. Thereby, for every system analysed the dimension of elements in width and thickness are treated as deterministic. Consequently, the physical characteristics of the elements at a given dimension are fixed, thus effects in width and thickness within the elements have an influence on the absolute values e.g. on strength and stiffness of the elements but not directly on the relative output of system action.

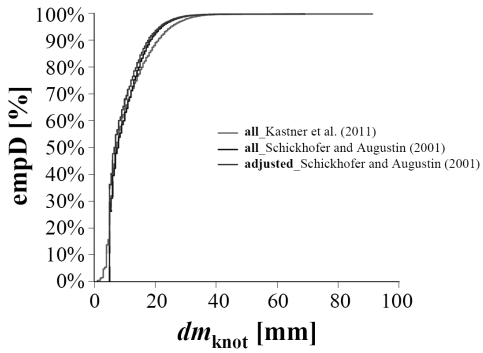

Fig. 5.17: Empirical distribution of knot diameter data taken from SCKICKHOFER AND AUGUSTIN (2001) and KASTNER ET AL. (2011)

As mentioned at the beginning of this sub-section only knots with a diameter $dm_{\text{knot}} \geq 5$ mm were taken into account. This is a very common regulation in international grading procedures. Consequently, all knot characteristics are somehow censored. To get an idea of the influence of this common procedure and some statistics for correction of geometric knot zone data the distribution of knot diameter is analysed. Fig. 5.17 shows the empirical distribution of knot diameters obtained from the data of SCHICKHOFER AND AUGUSTIN (2001). Additionally, the empirical distribution of knot diameters as found by KASTNER ET AL. (2011) is given. In the second project tension characteristics of boards of Norway spruce (*Picea abies (Karst.)*) with a cross section of w / t = 170 mm / 45 mm and strength class C24 according EN 338 were analysed. Thereby every knot, irrespective of its diameter was recorded. Despite the fact that the strength class C24 examined in KASTNER ET AL. (2011) underestimates the mean mechanical potential of the series analysed in SCHICKHOFER AND AUGUSTIN (2001) the knot data show a qualitatively comparable distribution. Interestingly, both empDs show an unexpected change in slope

at about 50% of empD. It can be assumed that the observed empD of knot diameters is a mixed distribution of more homogeneous intermediate knots, which are also smaller in diameter, and main knots, which show a wider range and thus a higher variation in diameters and a higher expected value. In line with the lower mechanical potential a higher variation of knot diameters and higher absolute values were expected in the data of KASTNER ET AL. (2011). Based on the fact that 15.6% of knots showed a diameter less than 5 mm the empirical distribution gained from the data of SCHICKHOFER AND AUGUSTIN (2001) was adjusted (see Fig. 5.17). The main statistics are given in Tab. 5.10.

Tab. 5.10: Statistics of knot diameter

	knot diameter dm_{knot} [mm]		
	SCHICKHOFER & AUGUSTIN (2001)	SCHICKHOFER & AUGUSTIN (2001); adjusted	KASTNER ET AL. (2011)
#	22,340#	--	45,264#
min	5	--	1
mean	10	--	10
median	**8**	**7**	**7**
max	69	--	91
CoV [%]	**59%**	**--**	**70%**
X_{05}	5	--	4
X_{95}	22	21	25

Interpreting the empirical distributions in Fig. 5.17 and the statistics in Tab. 5.10 it can be concluded that the distribution in knot diameter below the median level is very steep characterised by low variation. Above the median level the distribution shows remarkable higher variation. Consequently, the censoring below 5 mm does not affect the distribution too much but predominantly knots of intermediate knot zones with minor relevance for the strength of full-size structural timber elements. Nevertheless, statistics in Tab. 5.10 provide also important values for the adjustment of w_{KZ} and d_{KZ} by at least adding median or mean diameters to the mean or median statistics of w_{KZ} and d_{KZ}. This to adjust them according the advanced knot (cluster) zone definition provided at the beginning of this sub-section.

To conclude, this sub-section gives important statistics for further modelling of local characteristics within elements and for the definition of a representative longitudinal

length increment of sub-elements on the basis of data groups defined herein. The characteristics of the variables will be used to classify at least three groups of material quality. These groups deliver the basic information in further modelling procedures. Therefore connections to current European strength class systems will be also included. More on these aspects will be given at the end of this section 5.1.1.

Spatial Correlation of Strength, Stiffness and Density

After the introductory discussion of some literature on spatial distributed growth characteristics, test data and simulation results of various publications dedicated to spatial, in particular longitudinal correlation of strength, stiffness and density are presented. Tab. 5.11 provides a brief overview of all publications and data treated.

Tab. 5.11: Overview of literature sources and examined data in regard to longitudinal correlation of material inherent characteristics

source	species	*w* / *d* [mm / mm]	grade	characteristics	equi- or autocorrelated
HOFFMEYER (1978)	NN	NN	NN	$E_{m,0,i}$	equi $r \approx 0.81 \div 0.85$
RIBERHOLT AND MADSEN (1979)	Norway spruce	NN	UG	$E_{m,0,app,i}$; $f_{m,i}$; $f_{t,0,i}$	equi f: $r \approx 0.14 \div 0.49$
LEICESTER (1985)	Radiata pine	45 / 100	F7 & F8 (LQ)	$f_{m,i}$	equi, $r \approx 0.10$
LEICESTER (1985)	Eucalyptus	45 / 90	No. 1 & 2 (HQ)	$f_{m,i}$	equi, $r \approx 0.50$
SHOWALTER (1986)	NN	NN	NN	$f_{t,0,i}$	equi, $r \approx 0.63$
KLINE ET AL. (1986)	Southern pine	38 / 89 38 / 235	No. 2 KD15 (VG) 2250f-1.9E (MSR)	$E_{m,0,i}$	auto
SHOWALTER ET AL. (1987)	Southern pine	38 / 89 38 / 235	No. 2 KD15 (VG) 2250f-1.9E (MSR)	$E_{m,0,i}$; $f_{t,0,i}$	auto
TAYLOR (1988) TAYLOR AND BENDER (1988, 1989, 1991)	Douglas fir	38 / 140	L1 (VG, HQ) 302-24 (VG, HQ)	$E_{m,0,i}$; $f_{t,0,i}$	auto
MADSEN (1989A)	NN	NN	NN	$f_{t,0,i}$	equi

					$r \approx 0.48 \div 0.70$
MADSEN (1989A)	NN	NN	NN	$f_{m,i}$	equi $r \approx 0.61 \div 0.72$
RICHBURG (1989), RICHBURG AND BENDER (1992)	Douglas fir	38 / 140	6# E-rated grades (MSR) L2 & L3 (VG)	$E_{m,0,i}$; $f_{t,0,i}$	auto
LAM AND VAROGLU (1991A,B)	Spruce-Pine-Fir	38 / 89	No. 2	$E_{m,0,app,i}$; $f_{t,0,i}$;	auto
CZMOCH (1989, 1991)	Swedish pine & spruce	45 / 120 45 / 95	K 24	(stiffness) $E_{m,0,i}$	auto
XIONG (1991), WANG ET AL. (1995), LAM ET AL. (1994)	Spruce-Pine-Fir	38 / 89	2400f-2.0E (MSR) 1650f-1.5E (MSR)	$E_{m,0,app,i}$; $f_{c,0,i}$	auto
KÄLLSNER ET AL. (1997), DITLEVSEN AND KÄLLSNER (1998)	Norway spruce	45 / 120	UG	$E_{m,0,i}$; $E_{m,0,app,i}$; $f_{m,i}$	equi $r \approx 0.55 \div 0.68$
ISAKSSON (1998, 1999)	Norway spruce	45 / 145	UG	$E_{m,0,app,i}$; $f_{m,i}$	equi, $r \approx 0.54$
STICH (1998)	Norway spruce	45 / 120	UG	$E_{m,0,i}$; $f_{m,i}$	equi, $r \approx 0.50$
BRANDNER ET AL. (2005)	Norway spruce	40 / 80	S10 (VG)	$E_{t,0,i}$	equi $r \approx 0.36 \div 0.41$
STUEFER (2011)	Norway spruce	40 / 150	L25 (MSR; SQ)	$E_{t,90,i}$; $f_{t,90,i}$; ρ_{12}	equi E: $r \approx 0.42 \div 0.45$ f: $r \approx 0.42 \div 0.50$ ρ: $r \approx 0.87$

HQ … high quality; SQ … standard quality; LQ … low quality
VG … visually graded; MSR … machine graded; UG … ungraded material
xxx … no report concerning spatial correlation but examined by tests
NN … data not specified or not available

Fig. 5.18 to Fig. 5.20 show plots of serial (longitudinal) pairwise correlation of strength, stiffness and density, respectively. The correlation coefficient of PEARSON is used as adequate measure of association for continuous variables not necessarily normally distributed.

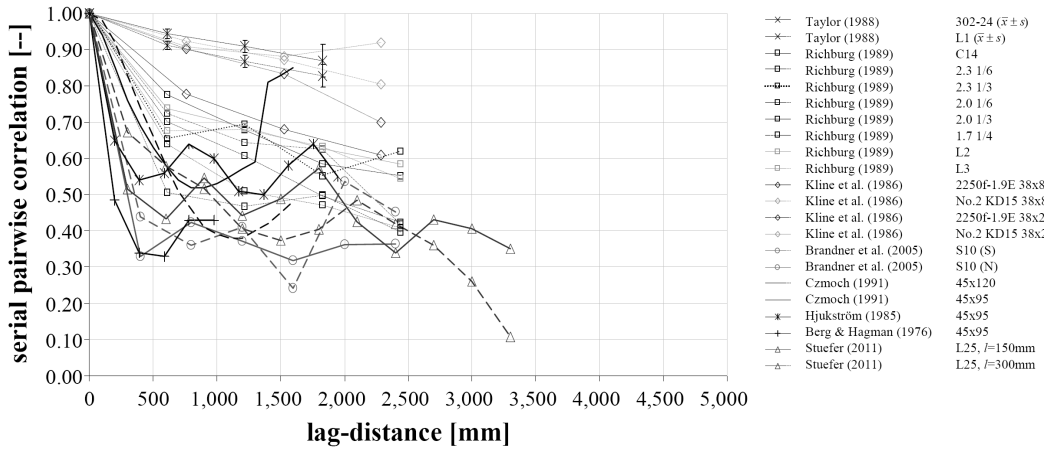

Fig. 5.18: Serial pairwise correlation according PEARSON vs. lag-distance: serial correlation of E-modulus within timber specimen; black = $E_{m,0,i}$; green = $E_{t,0,i}$; red = $E_{t,90,i}$; bold = Norway spruce

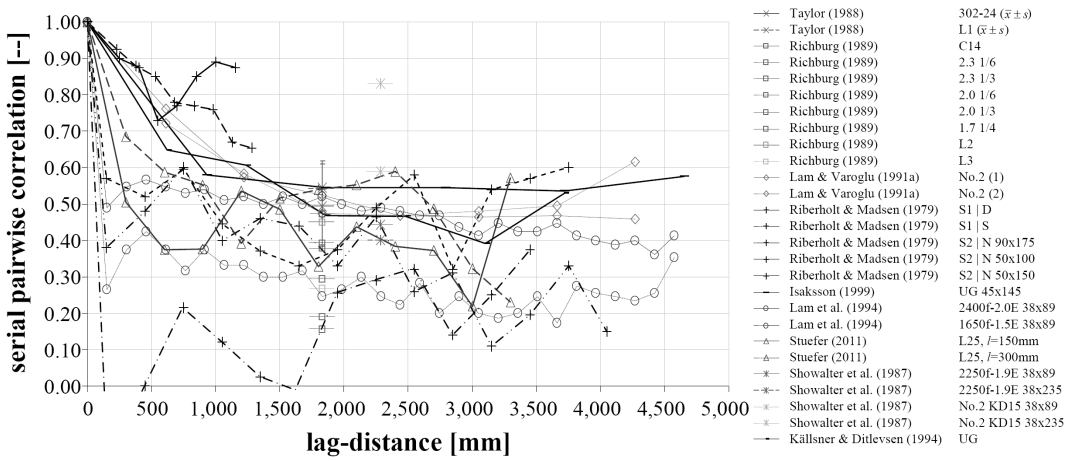

Fig. 5.19: Serial pairwise correlation according PEARSON vs. lag-distance: serial correlation of strength within timber specimen; black = $f_{m,i}$; green = $f_{t,0,i}$; red = $f_{t,90,i}$; blue = $f_{c,0,i}$; bold = Norway spruce

In addition to Tab. 5.11 further details will be discussed: RIBERHOLT AND MADSEN (1979) seem to be the first who analysed serial correlation of strength in timber. They performed bending tests on ungraded Norway spruce on three own test series and observed an overall correlation of $r \approx 0.14 \div 0.49$. The correlation trajectories showed no coherent trend with increasing distance. Based on this fact and supported by data of

HOFFMEYER (1978) who also reported on local bending strengths RIBERHOLT AND MADSEN (1979) established a two-level hierarchical model presuming equicorrelation. In addition, a positive relationship between density ρ and timber quality was found. Note: Serial correlation follows from common dependency of strength and stiffness on the material inherent potential which is primary manifested by the basic characteristics of wood, e.g. density and E-modulus. Thus the higher the strength class, the more homogeneous the material exhibiting less influences by local characteristics of type [2].

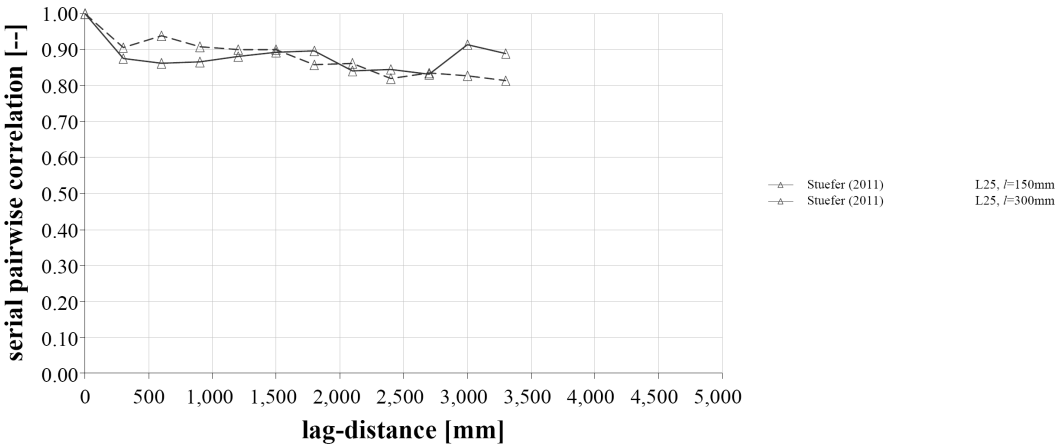

Fig. 5.20: Serial pairwise correlation according PEARSON vs. lag-distance: serial correlation of density within timber specimen; red = $\rho_{12,i}$; bold = Norway spruce

A few years later LEICESTER (1985) performed tests on low quality Radiate pine as well as on high quality Eucalyptus specimen analysing the local bending strength on two increments per board with length of 540 mm and 600 mm respectively, and a lag-distance of 2,150 mm. He supports the findings of RIBERHOLT AND MADSEN (1979) of increasing correlation with increasing timber quality, with $r = 0.10$ and $r = 0.50$ for Radiate pine and Eucalyptus, respectively. KLINE ET AL. (1986) report on local $E_{m,i}$-values determined on four consecutive increments of Southern pine on two cross sections and two strength grades. Overall they found a decreasing correlation with increasing lag-distance. SHOWALTER (1986) and SHOWALTER ET AL. (1987) continued the work of KLINE ET AL. (1986). Thereby and additionally destructive tensile tests on the first and fourth segment, tested before in local $E_{m,0,i}$, were performed. Whereas correlation of $f_{t,0,i}$ was higher for the smaller cross section and for visual grade, correlation of $E_{m,0,i}$ was also higher for visual grade but indifferent concerning the dimension of the cross section.

Later, extensive studies were made with Douglas fir. TAYLOR (1988) and TAYLOR AND BENDER (1988, 1989, 1991) determined the spatial distribution and correlation of $E_{m,0,i}$ on 4 (5) consecutive segments and $f_{t,0,i}$ on first and fourth $E_{m,0,i}$-segment on two high quality visual grades of five suppliers. Thereby significant differences in serial correlation from grade to grade and even between the suppliers were found. Hereby $E_{m,0,i}$-values showed also higher correlation at higher grades whereas results of $f_{t,0,i}$-values are contrary. RICHBURG (1989) and RICHBURG AND BENDER (1992) extended the studies of TAYLOR (1988) and TAYLOR AND BENDER (1988, 1989, 1991) and determined $E_{m,0,i}$ and $f_{t,0,i}$ on six E-rated grades and two visual grades by performing the same procedure. They found significant variation of correlation with grade. There is a tendency that higher E-grades as well as the higher visual grade show higher correlation for $E_{m,0,i}$ but no tendency for $f_{t,0,i}$. Furthermore RICHBURG AND BENDER (1992) observed similar cross correlation between $E_{m,0,i}$ and $f_{t,0,i}$ for E-rated as well as for visual grades, as reported by TAYLOR (1988). CZMOCH (1991) studied serial correlation of bending stiffness applying five different load steps. He performed tests on Swedish spruce and pine of two different cross sections. He found a higher variability of bending stiffness between specimen with CoV = 22% and CoV = 15%, respectively. Furthermore, remarkable deviating correlation trajectories were observed for the five different load steps. Thus Fig. 5.18 contains only the values of the correlation between data of the first load step. In addition comparable results of BERG AND HAGMAN (1976) and HJUKSTRÖM (1985) are cited for one cross section.

In the same year LAM AND VAROGLU (1991A,B) and XIONG (1991) published their results on serial correlation of tensile and compression strength parallel to grain. All tests were performed on two-by-four SPF specimens. LAM AND VAROGLU (1991A) performed long span tensile tests to define the minimum tensile strength of 6.1 m long boards within a free testing length of 4.88 m. Thereby the largest flaw of the board was placed within the free testing length. Then, in total $3 \div 5$ additional segments with free testing length of 610 mm got tested. Thus data of in total $4 \div 6$ incremental tensile strengths are available per each board. To analyse the correlation of the incomplete and incremental strength profiles window analysis and semivariogram were applied. They concluded, based on constant variance between segments of ≥ 1.83 m distance, that local tensile strength can be assumed being independent of each other. Note: Additionally performed and presented longitudinal correlation analysis clearly outlines a decreasing spatial (longitudinal) correlation of $r = 0.75$ for $N = 1$ (610 mm distance) to $r \approx 0.5$ for $N \geq 2$ ($\geq 1{,}220$ mm distance) which indicates autocorrelation at beginning and distinctive equicorrelation for lag-distances of roughly ≥ 2 m. XIONG (1991) analysed serial compression strength

parallel to grain as well as variation of E-modulus of strength class 2100f-1.8E. The first was analysed on 32 consecutive increments per specimen and the last based on readings of a stress grading device. Nevertheless data of serial correlation of $f_{c,0,i}$ are not published in XIONG (1991) but test results of two further strength grades can be found in WANG ET AL. (1995) and LAM ET AL. (1994). Thereby a slight decreasing trend in serial correlation can be observed with remarkable higher correlation ($\Delta \approx 0.20$) for the higher strength class.

WILLIAMSON (1992) focused on modelling of length effects in timber. Therefore he also analysed strength data of serial correlation published by SHOWALTER (1986) and MADSEN (1989A). On the basis of his statistical analysis he found a mean equicorrelation of $r \approx 0.60$ for bending and tension strength data. Although a slight decrease of serial correlation with increasing lag-distance was observed in data of MADSEN (1989A), significance tests led to no rejection of the hypothesis of equicorrelation. Two years later WILLIAMSON (1994) published results concerning serial correlation of strength gained from analysis of 15 data sets from literature (SHOWALTER ET AL., 1987; GERHARDS, 1983; MADSEN, 1992; LAM AND VAROGLU, 1991A; TAYLOR AND BENDER, 1991 and a test series performed at NZ FRI, 1992). He calculated correlation coefficients assuming equicorrelation along the sawn timber. He found a range of $r = 0.37 \div 0.72$, on average with $r_{mean} = 0.58$. Comparison of the mean value with 95 % confidence intervals of r of each test series showed that in only one test series r_{mean} was not within the confidence intervall. In his work WILLIAMSON (1994) further concluded that (i) the assumption of equicorrelation can not be rejected, (ii) the assumption of decreasing correlation with increasing lag-distance can not be supported, (iii) that higher (visual) grades tend to have a higher serial correlation, (iv) that serial correlation shows to be unaffected by the length of specimens (→ supports assumption of stationarity), and (v) that visual grades indicate higher correlation than machine graded timber. The last point is argued by the observation that density shows high correlation along the specimen. Thus visual grading focuses on knots leading to reduction of knot variability but not density, whereas machine grading focuses more on density (note: or on dynamic E-modulus which is by physics directly linked with density). Consequently visual grading enforces serial correlation due to high correlation with density, whereas machine grading reduces serial correlation by restricting density variation.

KÄLLSNER ET AL. (1997) as well as DITLEVSEN AND KÄLLSNER (1998) report on two test series for determination of local bending strength of ungraded specimen of Norway

spruce examined by KÄLLSNER AND DITLEVSEN (1994). In this context extensive studies on consecutive segments with one knot cluster each were performed. Every increment was finger jointed between two strong beams and tested under four-point bending. Despite all caution many failures occurred in finger joints or in the side-beams. Nevertheless extensive statistical analysis by means of MLE for right-censored data and under the assumption of a two level hierarchical model allowed to define equicorrelation with $r = 0.55$ and $r = 0.68$. Later, DITLEVSEN AND KÄLLSNER (2005) analysed test data of STICH (1998) under the same assumptions and found $r = 0.50$.

ISAKSSON (1999) tested 4 ÷ 8 increments of Swedish spruce. He tested over 400 mm free span and applied pure bending stress, starting with the increment containing the worst flaw, followed by the second worst and so forth. The range of local strength within each board appears roughly constant over all tested specimen. This indicates an approximately constant variance of local bending strength data within boards. Furthermore a certain dependency of local $f_{m,i}$ on mean strength potential of each beam is observable. This is indicated by a shift of $f_{m,i}$-range in comparison to others, if weaker or stronger. This is in line with observations of COLLING (1990) and his knot data analysis. Examination of longitudinal correlation was possible up to lag-5 and gave $r = 0.54$.

BRANDNER ET AL. (2005) report on tensile tests on finger jointed flanges for I-beams. Thereby local $E_{t,0,i}$-values of seven consecutive segments of 400 mm length as well as global E-modulus were determined. The position of finger joints was recorded and considered in the analysis of serial correlation. Two series of Norway spruce of nominal visual grade S10 according to DIN 4074-1 were tested, one series of provenience Styria / Austria (Central Europe; S) and the other series of provenience Scandinavia (N). Test results of strength, stiffness and density suggest to classify series (S) and (N) as C20/C22 and C27/C30, respectively. Serial correlations of both series show equicorrelation of $E_{t,0,i}$ whereby a relationship between the magnitude of correlation and the strength class was not found. Recently, STUEFER (2011) tested segments of Norway spruce in tension perpendicular to grain. He used 150 mm and 300 mm long increments but with constant lag-distance of 300 mm. He determined $f_{t,90,i}$, $E_{t,90,i}$ and $\rho_{12,i}$. Overall results of serial correlation suggest equicorrelation, whereby trajectories of strength and density show higher correlation at increment length of 300 mm than in case of 150 mm.

As shown in Tab. 5.11 models for the longitudinal correlation of local strength and stiffness values, in principle autoregressive vs. hierarchical stochastic processes, are controversial discussed in the literature. Whereas KLINE ET AL. (1986), SHOWALTER ET

AL. (1987), TAYLOR (1988), TAYLOR AND BENDER (1988, 1989, 1991), RICHBURG (1989), RICHBURG AND BENDER (1992), LAM AND VAROGLU (1991A,B), CZMOCH (1991), XIONG (1991), WANG ET AL. (1995) and LAM ET AL. (1994) postulate an autoregressive stochastic process HOFFMEYER (1978), RIBERHOLT AND MADSEN (1979), LEICESTER (1985), SHOWALTER (1986), MADSEN (1989A), KÄLLSNER AND DITLEVSEN (1994), KÄLLSNER ET AL. (1997), DITLEVSEN AND KÄLLSNER (1998), ISAKSSON (1998, 1999), STICH (1998), BRANDNER ET AL. (2005) and STUEFER (2011) or data sets of them suggest the description of spatial correlation by means of hierarchical models associated with equicorrelation. Thereby it is interesting to notice that the latest publications and test series suggest equicorrelation.

Following the discussion in section 5.1 at first both types of stochastic processes (autoregressive and hierarchical process) can be argumented. This by considering the creation processes of wood and growth characteristics like branches and the fact that the tree as a whole is one living unit. Nevertheless, the question which type of stochastic models best represents the correlation structure has to be considered in dependency of (i) the hierarchical material structure, (ii) the spatial distribution of discrete distributed material characteristics as well as (iii) the test increment choosen for the analysis of spatial correlation.

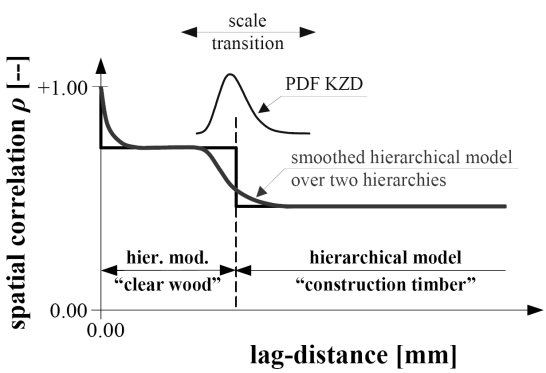

Fig. 5.21: Schematic illustration of scale transition between two hierarchical stochastic processes

For illustrative purposes an increment of one millimetre in length is considered. It can be expected that mechanical properties show distinctive serial pairwise correlation if the distance between the increments amounts only few millimeters. Otherwise, due to more or less deterministic parameters within a tree, like climate conditions or supply of nutrients, water and sun energy, it cannot be expected that there will be no residual

pairwise serial correlation after a distance of one meter or more. The critical aspect in this example is that an increment of one millimetre in length may be representative for the analysis of serial pairwise correlation in the scale of centimeters but not for meters. By comparing characteristics within one meter distance other features than within the scale of millimetres can be expected to be decisive.

In structural timber, i.e. in Norway spruce, growth characteristics like knot clusters are the determining feature of characteristics, i.e. strength and E-modulus, at long lag-distances, whereas other features are decisive on the scale of millimetres. What happens is a change in the representative length which causes an adaptation of the length increment for analysing serial pairwise correlation. This adaptation was already discussed in section 4.5 in respect to scale transition. In view of the given example a transition process from the hierarchy of "wood" to that of "structural timber" is given. Due to the fact that the features (e.g. knot clusters) itself are stochastic variables with distribution in respect to dimension and distance in occurrence, scale transition is expected as a continuous process, e.g. as a transition function between the equicorrelation observable in wood to that in timber (see Fig. 5.21). Consequently, the convergence to a certain value of equicorrelation $\rho_{\text{equi}} > 0$ depends on the distribution and influence of features relevant for the investigated characteristic.

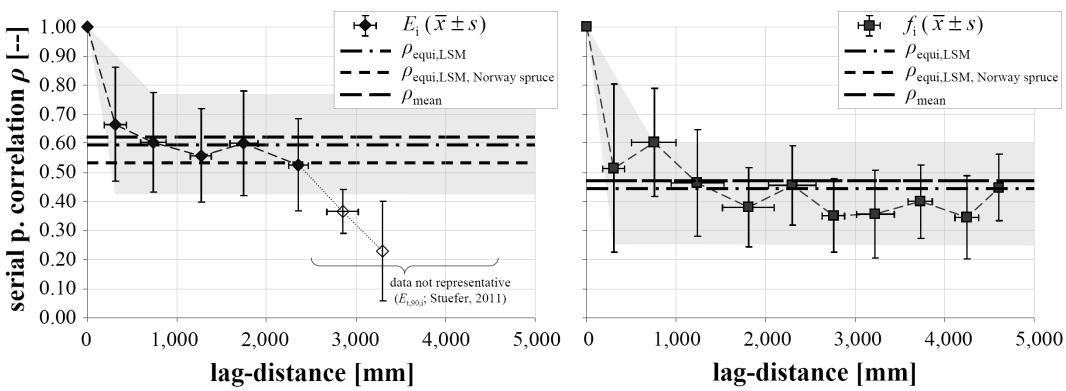

Fig. 5.22: Serial pairwise correlation vs. lag-distance of E-modulus (E_i; left) and strength (f_i; right): mean ± standard deviation of section-wise correlation as smoothed function; mean of all correlation coefficients of lag-k, $k \geq 1$ (ρ_{mean}); least squares fit (LSM) assuming equicorrelation considering all data of $k \geq 1$ ($\rho_{\text{equi,LSM}}$) and $\rho_{\text{equi,LSM,Norway spruce}}$ considering only data from Norway spruce

In particular, it can be assumed that clear wood segments (increments) show high serial correlation. It can be also assumed that knot zones show a distinctive correlation but not as high as clear wood because the variability of parameters like knot arrangement, size and position relative to cross section is very high. Thus it can be concluded that serial correlation in timber within knot-free zones (hierarchy of wood) is on a high level and equicorrelated. This is supported by the material inherent hierarchical structure of wood and timber. This high serial correlation immediately changes to a lower level if knot zones become a part of analysed segments. Following that a representative length increment for timber has to include at least one (representative) knot cluster and is thus defined by the serial distribution of knot clusters. If the length of the increment is choosen too short failure characteristics of the previous hierarchical level "wood" may become decisive. This postulate is also supported by the outcomes of the literature study as shown in Fig. 5.22. Within these plots expectable correlation functions as "mean" pairwise serial correlations in dependency of the distance between two increments are introduced.

Further analysis of spatial correlation concerning influences given by (i) timber species, (ii) cross sectional dimension, (iii) load type (bending, tension parallel or perpendicular to grain and compression) as well as (iv) length of increment tested, showed no clear tendency.

Models for the Generation of serial correlated Random Variates – Literature Review

So far experimental data and observations concerning spatial correlation of strength, stiffness and density within sawn timber have been discussed. Nevertheless, for modelling and performance of simulations by means of randomly correlated variates some constraints and simplifications have to be made. One of the main steps is the determination of RSDMs for the local physical properties. Thereby a variety of different distribution models proposed for the same characteristic can be observed. For example RICHBURG (1989) assumed a 3pLND for the representation of local $E_{m,0,i}$-values whereas KLINE ET AL. (1986) (cit. in TAYLOR, 1988) used a ND. Analyses of TAYLOR (1988) showed good representation of $E_{m,0,i}$ by 2pLND or 3pWD but overall 3pWD was preferred. The same was done by WOESTE ET AL. (1979) and TAYLOR AND BENDER (1991) but interestingly not in TAYLOR AND BENDER (1989) were a 2pWD was used for modelling $E_{m,0,i}$-values. Examination of data reported in BRANDNER ET AL. (2005) showed that 2pLND best represents local values of $E_{t,0,i}$. Thereby results of fitting data with ND, 2pLND and 2pWD were compared. Analysis of $E_{t,90,i}$-values of STUEFER (2011)

indicated preference of 2pLND and 2pWD as RSDMs. Thereby fitting results of models ND, LND and WD were analysed. The local bending strength $f_{m,i}$ was found to follow a ND (ISAKSSON, 1998; DITLEVSEN AND KÄLLSNER, 1998; KÄLLSNER ET AL., 1997) or a 2pWD (RIBERHOLT AND MADSEN, 1979). Local tensile strength values parallel to grain $f_{t,0,i}$ were modelled by means of 2pLND (SHOWALTER ET AL., 1987), 3pLND (RICHBURG, 1989), 2pWD or 2pLND (TAYLOR, 1988) and 3pWD (TAYLOR AND BENDER, 1991). STUEFER (2011) analysed the empirical distribution of $f_{t,90,I}$ in comparison with ND, 2pLND, and 2pWD. He found that 2pWD best represented his data sets.

To conclude, as discussed in section 2.4 the reduction of model parameters to an amount which is practically manageable and physically justifiable is strongly recommended. In particular the third parameters in 3pLND and 3pWD which are defined as a lower limit value $x_0 \geq 0$ can not be fixed easily and thereby are not secured in the daily production process. Therefore it is recommended to reduce the RSDMs for the local strength and stiffness values to two-parametric distribution models. Due to the multiplication process underlying in E- and G-moduli and the fact that strength is always a minimum value irrespective the size of the test increment, skewed distribution models are preferred. For E- and G-moduli the use of 2pLND as RSDM is proposed. This is in line with recommendations of JCSS (2006). For strength values the definition is not so clear and depends on the material behaviour observable at a specific stress. Therefore the use of 2pLND or 2pWD is proposed, whereby 2pLND is preferred for characteristics like $f_{t,0,i}$, $f_{m,i}$, $f_{c,0,i}$ and $f_{c,90,i}$, whereas for $f_{v,i}$ either 2pLND and 2pWD, and for $f_{t,90,i}$ the use of 2pWD is recommended.

To the author's knowledge the first who formulated a model for the stochastic process of serial correlation of mechanical characteristics in timber were RIBERHOLT AND MADSEN (1979). They created a two-level hierarchical model with equicorrelation between local strength increments. Then they discussed the occurrence of weak zones in accordance with the yearly longitudinal growth increment typical for Norway spruce. Thereby a weak zone was associated with a knot cluster. The occurrence was modelled by a Poisson-process. Thus the distance between weak zones follows an Exponential distribution. The strength between weak zones was kept constant and equal to the highest strength of the weak zones within each specific board. Thus the failure of a board can only occur at weak zones. This was suggested as assumption sufficiently accurate for modelling length effects so far every sawn timber specimen contains at least one increment, at least one weak zone. The distribution parameters for the strength of weak zones were gained from

standard tests on boards with known quantity of weak zones as well as from estimates of longitudinal local strength profiles based on non-destructively determined grading parameters like local density and local E-modulus. As already discussed in section 5.1.1 beside the fact that Poisson and Exponential distribution models failed in representing the number and distance between weak zones, respectively, RIBERHOLT AND MADSEN (1979) decided to use them in their weak zone model. From tests it was observed that the skewness of strength distribution of the weakest section within tested length (→ serial system!) is higher than that of the weak section strength itself. Note: This follows directly from extreme value theory and the concentration of minimum values in serial systems. Tests of RIBERHOLT AND MADSEN (1979) showed an overall pairwise serial correlation of $r = 0.14 \div 0.49$. In reference to DITLEVSEN (1978) who postulated that the error of an assumed independency between correlated sub-elements in case of $r \leq 0.5$ is relatively small, RIBERHOLT AND MADSEN (1979) modelled local strengths as iid.

To account for material inherent correlation, in particular for modelling length effects, LEICESTER (1985) discussed the modification of WD through adaptation of WD-shape parameter by scaling it proportional to the given correlation. In doing so he preconditions equicorrelation, with strength of two sub-elements as independent realisations but common and equal dependent on a basic value of the element itself. Thereby inconsistency is given by fitting a WD on test data assuming independency between the sub-elements but afterwards adaptation of the shape parameter by consideration of a certain amount of spatial correlation (WILLIAMSON, 1992). KLINE ET AL. (1986) modeled the longitudinal variability of local $E_{m,0,i}$-values between 762 mm long segments by means of a second-order Markov-chain. SHOWALTER ET AL. (1987) enlarged KLINE's model by inclusion of longitudinal variation in $f_{t,0,i}$. They combined KLINE's Markov-process for $E_{m,0,i}$ with the regression model given in WOESTE ET AL. (1979) to estimate $f_{t,0,i}$-values based on a weighted least squares regression. The residues of the regression model were thereby parallel modelled as a 1st-order Markov-chain.

TAYLOR AND BENDER (1988, 1989) defined a model for the generation of local strength and stiffness values. Their approach consists of several steps: At first, the variance-covariance matrix of local strength and stiffness values has to be found. Secondly, RSDMs as parent distribution models of strength and stiffness values have to be determined. In the third step SND-variates are created by means of the variance-covariance matrix from the first step. To create local strength and stiffness values the length of the expectation vector as well as the squared size of the variance-covariance

matrix are twice the length of the serial system, the quantity of increments of sawn timber. In the fourth step the correlated SND-variates are transformed to their parent distributions. This is done by calculating the inverse $F_X^{-1}(u)$ which follows a uniform distribution U (0, 1), followed by application of the inverse transformation method U (0, 1) → $F_X(x)$ to transform the variates to their parent distribution. Thereby the RSDM of each variate can be preserved completely and the correlation satisfactorily. TAYLOR AND BENDER (1991) used this approach to simulate $E_{m,0,i}$- and $f_{t,0,i}$-values of four consecutive board segments. Based on test results of $E_{m,0,i}$ of all four segments but $f_{t,0,i}$ of only the first and fourth segment missing $f_{t,0,i}$-values were generated by means of an autoregressive process, knowing the cross-correlation of $E_{m,0,i}$ and $f_{t,0,i}$. Furthermore, enlargement of the simulation model for boards composed of ten segments was enabled by estimating the additionally required but not tested serial correlation values for $E_{m,0,i}$ and $f_{t,0,i}$ of lag-k, $k > 4$ by means of an autoregressive process (AR-process) (TAYLOR AND BENDER, 1991). The suitability of the model in preserving satisfactorily also the correlation between arbitrary distributed variables was analysed by HAN ET AL. (1991). They found that correlation was well preserved if the parent distributions of all variates have either positive or negative skewness, whereas the correspondence between indicated and simulated correlation in case of variates having positive and negative skewness was weaker. The model of TAYLOR AND BENDER (1988, 1989, 1991) was also used by RICHBURG AND BENDER (1992).

LAM AND VAROGLU (1991B) modelled local tensile strength based on incomplete incremental tensile strength profiles but complete incremental profiles of $E_{m,0,app,i}$ from readings of a Cook-Bolinder SG-AF grading device. They analysed two simulation procedures: First a random process assuming independent local strength data, and secondly a random moving average process (Markov-chain) to account for serial correlation. Both stochastic models showed good performance if compared with results of a second matched sample, whereby matching was done according the $E_{m,0}$-values. Note: The satisfactorily correspondence is not surprising since the material, grading and dimension conform to the first sample used for fitting of the model parameters and the given local tensile strength correlation between $E_{m,0,i}$ and $f_{t,0,i}$.

CZMOCH ET AL. (1991) modelled local bending strengths based on the model of RIBERHOLT AND MADSEN (1979) and by means of a stationary stochastic process.

XIONG (1991) modelled $E_{m,0,i}$-values by means of a spectral approach. Values of $f_{c,0,i}$ were generated based on $E_{m,0,i}$-profiles and by means of a bivariate ND considering a stationary

process. Thereby the transformation method of TAYLOR AND BENDER (1988) was applied. The variability of $f_{c,0,i}$ was indirectly considered by the spectral approach. WANG ET AL. (1990) and WANG AND FOSCHI (1992) studied variability in glulam beams under serviceability loads by means of FEM. Thereby variability of $E_{m,0,i}$ was modelled by means of random fields in length and depth direction of a glulam beam (2D-model).

LAM AND BARRETT (1992) analysed the applicability of kriging analyses to generate local strength and stiffness values for elements smaller than the tested length of increments. Thereby kriging can be interpreted as a kind of weighted interpolation method. To secure stationarity in serial processes of local test data, trend removal techniques were applied.

WILLIAMSON (1992) modelled longitudinal distributed strength values by means of a mixed multi-modal WD or GUMBEL distribution considering autocorrelation. The mixing was done by weighting of a kernel WD or GUMBEL distribution for various strength classes (classes of weak, median or strong boards). The weighting was done according typical shares of strength classes occurring in an ungraded population. LAM ET AL. (1994) analysed the spatial distribution of $E_{m,0,i}$ and $f_{c,0,i}$. They modelled the longitudinal variation by combination of a stationary as well as a random trend process to account for the observed non-stationarity in their test data. WANG ET AL. (1995) analysed the applicability of a gain-factor model for the simulation of serial correlated $E_{m,0,i}$-values and strength profiles in standardised normal space coupled with a trend removal model and multivariate SNDs.

KÄLLSNER ET AL. (1997) modelled local strength values assuming equicorrelation between $k \geq 1$ weak cross sections per board. Thus the weak zones are reduced to discrete weak cross sections. The model of KÄLLSNER ET AL. (1997) is based on publications of RIBERHOLT AND MADSEN (1979), WILLIAMSON (1994) and ISAKSSON (1996) who all dedected equicorrelation. The model was also used by DITLEVSEN AND KÄLLSNER (2005). They enlarged the two-level to a three-level hierarchical model, with level I as variation between logs, level II as variation between beams cut from two sides of the log (opposite the pith) and level III as variation between strengths of weak cross sections of the same beam. The coefficients of variation regarding the mean of weak section strength are for the first and second level 9% and 13%, together 17%, and for the third level also 17%.

Already before this publication ISAKSSON (1999), with reference on KÄLLSNER ET AL. (1997), established a three-level hierarchical model. This model is given as

$f_{ij} = \mu + \tau_i + \varepsilon_{ij}$, if $f_{ij} \sim$ ND is assumed, or in case of $f_{ij} \sim$ 2pLND as $f_{ij} = \exp(\mu + \tau_i + \varepsilon_{ij})$. Thereby f_{ij} is defined as bending strength of a weak zone, μ as $f_{m,mean}$ of all weak zones in a population, τ_i as random difference between μ and $f_{m,mean,i}$ of all weak zones of one individual beam, and ε_{ij} as random difference between τ_i and the weak zones of this specific beam. The estimated expectations and variances are given as $E[\mu_{est}] = 57.33$, $Var[\mu_{est}] = 13.42$, $Var[\tau_{i,est}] = 10.11$ and $Var[\varepsilon_{ij,est}] = 8.86$. This corresponds to $CoV[\mu_{est}] = 23.4\%$, $CoV[\tau_{i,est}] = 17.6\%$ and $CoV[\varepsilon_{ij,est}] = 15.5\%$. According ISAKSSON AND FREYSOLDT (1997) and based on information gained from Cook-Bolinder the strength of clear wood sections between weak zones was found to follow $f_{m,CW} = -0.133 \cdot f_{m,WZ} + 16.48$ ($r^2 = 0.43$).

Intermediate Conclusions concerning spatial Correlation of Characteristics in Structural Timber

The aim of this sub-section is to define crucial parameters for the stochastic description of characteristics of structural timber. These parameters are given for three groups representing three different timber qualities: G_I, G_II and G_III. The material qualities described are on one hand in conjunction with the groups g01, g02 and g03 analysed before, and on the other hand somehow linked to the strength class system of EN 338, and thereby to C24, C30 and C40. Tab. 5.12 provides expectations and coefficients of variation of knot share parameter *KAR* for weak as well as intermediate knot zones, their geometric extension and center-distances, as well as specifications for various (equi)correlation coefficients of strength and stiffness values and density. Overall this table gives the basic information required for further modelling of system actions and related effects on density, stiffness and strength characteristics. This will be exemplarily demonstrated within the next sections.

Tab. 5.12: Expectation and coefficient of variation of selected characteristics required for the definition of groups G_I, G_II and G_III

		G_I	**G_II**	**G_III**
E[d_{WZ}]	[mm]	450	520	590
CoV[d_{WZ}]	[%]		60%	
E[w_{WZ}] [1)]	[mm]		50 + 20 = 70	
CoV[w_{WZ}] [1)]	[%]		40%	
E[KAR_{WZ}]	[--]	0.23	0.20	0.17

CoV[KAR_{WZ}]	[%]		45%	
E[d_{IK}]	[mm]	70	120	170
CoV[d_{IK}]	[%]		80%	
E[w_{IK}] [1)]	[mm]		15 + 20 = 35	
CoV[w_{IK}] [1)]	[%]		40%	
E[KAR_{IK}]	[--]		0.04	
CoV[KAR_{IK}]	[%]		90%	
$\rho(\rho_{12}; E_{t,0,12})$	[--]		0.60 ÷ 0.70	
$\rho(\rho_{12}; f_{t,0})$	[--]		0.40 ÷ 0.60	
$\rho(E_{t,0,12}; f_{t,0})$	[--]		0.55 ÷ 0.85	
$\rho_{equi}(\rho_{12})$	[--]		0.80 ÷ 0.90	
$\rho_{equi}(E_{t,0,12})$	[--]		0.50 ÷ 0.60	
$\rho_{equi}(f_{t,0})$	[--]		0.40 ÷ 0.50	

1) longitudinal extension of knot zone as defined previously; including two times the expected knot diameter (and variation) for consideration of the influence of local grain deviation

5.1.2 Volume (Size) Effects: Serial System Effects in Engineered Timber Products

In timber engineering serial system effects are often modelled according WEIBULL's "weakest link theory", also known as "strength theory of brittle materials" (WEIBULL, 1939). Beside the fact that structural timber is assumed to fail brittle in tension perpendicular and parallel to grain as well as in shear and quasi-brittle in bending, it has to be outlined that some key assumptions of WEIBULL (see section 3.2.1) are not fulfilled in structural timber. These aspects and more on quasi-brittle materials are discussed in more detail.

Discussions about serial system effects in wood and timber are in general associated with volume and size effects. These effects describe the relative change of structure resistance due to changes of volume in one, two or even three dimensions in respect to a (arbitrary choosen) reference volume. Already in 1500's LEONARDO DA VINCI observed size effects by testing cords and stated that "*... among cords of equal thickness the longest is the least strong*" (see e.g. LUND AND BYRNE, 2000). Later, explicit studies on size effects were made by GALILEO (1638), MARIOTTE (1686), GRIFFITH (1920) and many other well

known researchers. A comprehensive literature survey on the history of size effect models can be found e.g. in BAŽANT AND CHEN (1996).

In 1926 PEIRCE formulated the weakest link theory (WLT) by introduction of extreme value theory (EVT) originated by TIPPETT (1925) (see also section 2.6.2). After further developments in EVT it was WEIBULL (1939) who defined a physically driven three-parameter distribution model based on a power law for the explanation of size effects in perfect brittle materials. This model got famous as the 3pWD which reduces to 2pWD in case of $x_0 = 0$ (see e.g. section 2.4.3). This distribution model is in particular of interest because it is analytically solvable and the only model of three in EVT which formulation is in principle the same at $M = 1$ and $M \rightarrow \infty$. The WEIBULL- or WLT-model is in general associated with the term "statistical size effect" (e.g. BAŽANT, 2001; BAŽANT ET AL., 2004; BAŽANT AND PANG, 2006; BAŽANT AND YU, 2009). It was widely proved to be applicable for various types of brittle materials, e.g. ceramics and glasses. Beside that numerous researchers fitted 2pWD or 3pWD or just the power models of WLT (see section 3.2.1) also to strength data of non-brittle materials. Several publications outline explicitly the lack of representation and the violation of WEIBULL's model assumptions and constraints e.g. as being obvious in discussions on quasi-brittle materials.

Thereby quasi-brittle materials are in failure behaviour defined as being in between perfect brittle and perfect plastic. The observable behaviour depends on the stressed volume relative to a representative volume element (RVE) or characteristic dimension (e.g. characteristic length, l_c). According WEIBULL (1939) perfect brittle materials are characterised by randomly distributed microscopic flaws and consequently have no reference dimension driven by material structure. According the WLT an arbitrary complex of brittle material fails suddenly with the failure of the first, the weakest element (see section 3.2.1). In contrast, quasi-brittle materials show macroscopic flaws which are additionally seldom randomly distributed. Consequently, modelling of this type of material necessitates the definition of an RVE. The RVE or the characteristic length l_c can be defined as being two- or three-times the maximum dimension of macroscopic flaws (BAŽANT, 2001; BAŽANT ET AL., 2004; BAŽANT AND PANG, 2006; BAŽANT AND YU, 2009). Some representatives of quasi-brittle materials are e.g. concrete, rock, stiff soils, sea ice, rigid foams, fibre composites, bone and wood (e.g. BAŽANT, 2001). Whereas material structures in volume in the range of an RVE are assumed to act as plastic and like a parallel system characterised by load-redistribution and subsequent partial failure with intermediate stable crack growth, volumes which are far larger than the RVE show

more perfect brittle material behaviour by flaws which become microscopic in comparison to the analysed volume (see BAŽANT, 2001; BAŽANT ET AL., 2004; BAŽANT AND PANG, 2006; BAŽANT AND YU, 2009). Of course, these limited examinations are not solely associated with size effects. These are already associated with scale transition at changes in the hierarchical level of the material structure so far hierarchical materials are concerned (see sections 4.1 and 4.5).

BAŽANT AND YU (2009) defined six asymptotic cases which can be observed in quasi-brittle materials, namely:

- differentiation according the examined structural dimension: very small vs. very large structures;
- differentiation according the failure process: structures failing at crack initiation on a smooth surface vs. deep cracks;
- differentiation according the main cause of size effects: purely statistical (WEIBULL-type) size effects vs. purely energetic (deterministic) size effects.

In case of hierarchically structured materials and with reference on previous chapters, the first two subdivisions are at the edge of scale transition and therefore in particular of interest for comprehension of material behaviour in limiting cases within a specific hierarchical level. The last subdivision appears heavily focused on WEIBULL's WLT vs. fracture mechanics. The term "deterministic" in the energetic size effect which is discussed and defined in conjunction with load-redistribution and the definition of RVEs appears confusing. BAŽANT (2001), BAŽANT ET AL. (2004), BAŽANT AND PANG (2006) and BAŽANT AND YU (2009) describe this type of size effect as the result of intermediate stable crack growth enabled by redistribution of load as e.g. supposed by DANIELS's FBM (DANIELS, 1945). Nevertheless, if the material sub-structure would be deterministic a redistribution of load can not occur. Therefore the stochastic nature is explicitly and implicitly the driving force of size effects and the last subdivision again a discussion of the limits of serial vs. parallel system effects.

In the following a differentiation in various types of size effects or sub-effects is made (e.g. according BAŽANT AND CHEN, 1996; BAŽANT AND PLANAS, 1998; BAŽANT, 2004; BAŽANT AND PANG, 2005):

- <u>serial system effects</u>: often associated with the statistical (WEIBULL-type) size effect

    - caused by the randomness of (strength) characteristics within the material structure;
    - often described by means of WLT assuming brittle failure behaviour;
- parallel system effects together with energetic, fracture mechanics size effects:
    - redistribution of stresses by energy release together with softening and intermediate stable crack growth caused by partial structural failures by subsequent load increase;
- boundary layer size effects:
    - caused by heterogeneous internal material structure which differs from core to outer layers (e.g. distribution of aggregates in concrete, hardening processes in outside layers, characteristics influenced by sawing pattern e.g. in structural timber in respect to radial variation of characteristics like juvenile vs. adult wood; knot share; density; etc.);
- diffusion phenomena size effects:
    - caused by external influencies, the interaction with environment, e.g. (delayed) transport of chemicals like water or impregnating agents, or of temperature, degradation e.g. by funghi or sun light;
- material effects caused by inherent constraints within the material structure:
    - every material has its own inherent maximum dimension defined by the material composition (structure) and through dead load limited in resistance against external caused stresses;
    - e.g. for bone GALILEO (1700'S) stated: "*... a small dog could probably carry on his back two or three dogs of his own size; but I believe that a horse could even not carry even one of his own size.*" (TIMOSHENKO, 1983).

As already mentioned, the power of WEIBULL's WLT and the associated distribution models 2pWD and 3pWD is noteworthy but often misused. Some notes on that were already given in section 3.2.4 dealing with advances in stochastic material modelling. In the following a brief discussion on constraints of WLT in respect to size effects and with focus on quasi-brittle materials is presented. Thereby aspects of WILLIAMSON (1992) and BAŽANT (2001) are included:

- WLT assumes a homogeneous material composed of iid elements and infinite quantity of microscopic flaws without any real reference dimension; quasi-brittle

materials are characterised by a heterogeneous structure containing a finite quantity of macroscopic flaws which induce a reference volume (RVE) or characteristic dimension (l_c);

- according WLT the system suddenly fails with the failure of the weakest element; nevertheless, in quasi-brittle materials a certain amount of load-redistribution can be observed which contradicts WLT;
- the structural geometry and failure mechanisms have no influence on the result according WLT but are decisive for quasi-brittle material strengths; in particular the arrangement of (sub-)elements in respect to stress direction (serial vs. parallel) is not considered by WLT;
- according WLT size effects in two- or three-dimensional structures are equal; in contrast, deviating results are observed in tests on quasi-brittle materials;
- WLT assumes iid elements which agglomerate randomly to a system; spatial correlation within the material structure or interaction between sub-elements is not taken into account;
- according WEIBULL's WLT the coefficient of variation CoV[X_M] in case of 2pWD is directly linked with the WEIBULL shape-parameter β and treated as material inherent parameter being independent of the stressed volume; based on tests often a dependency of CoV[X_M] on the amount of stressed volume can be observed; nevertheless variable CoV[X_M] follows in case of 3pWD with $x_0 > 0$; the treshold value therefore must be independent of the stressed volume; this is again difficult to verify by tests;
- changes in volume are often associated with scaling effects, in particular if material classification rules base on geometrical constraints (e.g. knot size restrictions in structural timber);
- if according EVT the distribution of strength of a system or volume follows a WD also the strength of elements must follow a WD with equal shape parameter β; nevertheless, local strength values (e.g. of timber) are often found to be better represented by ND or LND;
- in particular in parallel acting (sub-)elements interaction between elements as load sharing due to the influence of variation of E-modulus is given; according WLT only strength characteristics are considered, the relationship between strength and stiffness is neglected.

In particular with focus on structural timber and timber system products WEIBULL's WLT theory is the basic theory for the explanation of size effects as well as of load configuration factors by means of fullness parameters as discussed in section 3.2.1. Nevertheless, with focus on structural timber all points above can be confirmed and the application of WLT can not be proposed in general. Furthermore, size effects in timber have to be in addition classified into:

- size effects as result of using a classified material in dimensions others than classified:
  - due to changes in dimension after classification (grading) of the material changes in material characteristics can be observed; hereby material inherent correlation has to be taken into account;
- size effects as result of classification of material according a specific dimension:
  - in dependency of the required dimension different size effects have to be considered;
- size effects as result of composing classified elements to larger volumes:
  - by composing of systems, e.g. by finger jointing of structural timber to serial finger jointed construction timber, iid elements can be assumed and in principle WLT can be applied.

This classification was already discussed in WILLIAMSON (1992) who comprehensively analysed length effects in structural timber.

Furthermore, as structural timber in reality can be described as quasi-brittle rather than brittle material, the following additional influences or sub-size effects are expected:

- size effects due to the classification of timber by limitation of flaw dimension and quantity;
- species dependent size effects due to species dependent distribution and dimension of flaws;
- size effects due to serial vs. parallel interaction; whereas strength distribution and spatial correlation influence serial effects, material behaviour and strength-stiffness relationships contribute decisively to parallel effects.

In the following a brief summary of the literature survey on size effects in wood and timber is presented.

For example WILLIAMSON (1992) gives a comprehensive overview of research on size effects in timber engineering starting with WEIBULL's basics and the well known publications of BOHANNAN (1966), BARRETT (1974), BARRETT AND FOSCHI (1979), MADSEN (1990) and many others. Much earlier examinations on size effects on clear wood were made. TANAKA (1909) proposed to consider size effects in bending by adjustment of the section modulus by a power factor n which should be regulated in dependency of timber species, see

$$f_m = \frac{M}{W} \xrightarrow{3pB} \frac{3 \cdot F \cdot l}{2 \cdot b \cdot h^2} \rightarrow \frac{3 \cdot F \cdot l}{2 \cdot b \cdot h^n}. \tag{5.2}$$

Congruent to him MONNIN (1932) proposed the same formalism but with power n as function of timber quality and not of species. Already before NEWLIN AND TRAYER (1924) proposed to consider size effects in bending by an additional factor multiplied on section modulus, see

$$f_m = \frac{M}{W \cdot \gamma}, \text{ with } \gamma = 1 - 0.07 \cdot \sqrt{\frac{d}{2} - 1}, \text{ with } d \text{ in [inch].} \tag{5.3}$$

YLINEN (1942) analysed the depth effect on clear wood and timber under bending stresses. He found a significant dependency of bending strength on the depth of the specimen. The depth effect in timber with a high share of knots was as double as high as in clear wood, indicating a strong dependency on timber quality. He proposed to adjust the bending strength by means of a fictive bending strength $f_{m,0}$ for $d = 0$ and parameters c_1 and c_2:

$$\frac{f_m}{f_{m,0}} = \frac{1 + c_1 \cdot d}{1 + c_2 \cdot d}. \tag{5.4}$$

SCHNEEWEIß (1962, 1964A,B) developed a modified WLT with parameter $K_2 = 1 / \beta$ and β as WD-shape parameter:

$$\begin{aligned} &\ln(f_m) = \ln(K_1) - K_2 \cdot \ln(V), \text{ in case of changes in volume;} \\ &\ln(f_m) = \ln(K_1) - K_2 \cdot \ln(d), \text{ in case of changes in depth.} \end{aligned} \tag{5.5}$$

He remarked that according WLT only linear-elastic stress-strain relationships are accepted. In compression tests parallel to grain he observed little changes in the stress-strain relationship by variation of volume but a shift of maximum stress to lower strains.

MARKWARDT AND YOUNGQUIST (1956) performed tension tests perpendicular to grain on structural timber and observed an increase in $f_{t,90,mean}$ of 23% in radial direction by halving the width of the ASTM specimen from 50.8 mm to 25.4 mm, but no significant increase in tangential direction. Further tests showed that volume effects are more pronounced in timber than in clear wood ($\beta = 4.04$ and $\beta = 6.35$, respectively) and a CoV[$f_{t,90}$] independent of volume and thus consistent to WLT. Again, a dependency of size effects on timber quality was indicated. Later, BOHANNAN (1966) stated that changes in thickness of structural timber may lead to rather parallel than serial system effects if stressed in grain direction. In his discussion of size effects in timber under bending stresses he differentiates between elements arranged in and transverse to stress direction. Thereby longitudinally arranged elements are in serial whereas elements in width and depth direction are in parallel. Despite that both are in parallel direction, their action is different. Whereas all elements in width are considered as being equally stressed (note: equally deflected and elongated), elements in depth show different stresses according the principle linear bending stress distribution in z-direction. It was observed that a complete (cascade) failure in width occurs before a subsequent failure in depth. Thereby the stress on remaining elements in width increases by the factor $N / (N - 1)$ whereas the stress increase in depth is much higher due to squared reduction of depth in the section modulus, in a rectangular cross section given by $W = w \cdot d^2 / 6$. He concluded that the probability of a low strength element increases with width but the probability of a cascade failure in width decreases due to increasing chance of load-redistribution. He assumes that the net effect of these two is negligible and proposes, supported by tests on Douglas fir, not to consider a width effect but depth and length effects in clear wood under bending stresses of comparable magnitude. BARRETT (1974) and BARRETT AND FOSCHI (1979) observed well representation of size effects according WLT in clear wood and GLT if stressed in tension perpendicular to grain or shear. MADSEN AND BUCHANAN (1985) give a comprehensive report on size effects in timber stressed in bending, tension or compression parallel to grain. They differentiate between:

- length effects within elements (single-member length effects);
- length effects for elements in series (multiple-member length effects);
- depth effects;
- width effects;
- load configuration effects: expressed as function of the proportion of tested and stressed length;

- stress distribution effects: expressed by the fullness parameter as discussed in section 3.2.1 (note: later named as load configuration factor);
- effects of grading rules.

Based on three comprehensive data sets prepared for the examination of size effects the following conclusions are given: Length effects on strength were found to be significant in tension and bending. Due to lack of data the same length effect for both stress types is proposed, with $k_{l,05} = 0.29$. The multiple-member length effect in tension members was found to be slightly higher than the within member length effect, with $k_{l,05} = 0.36$. Note: This was expected since spatial correlation within elements reduces the variability and thus the stochastic part of the size effect. A significant depth effect was not found in bending. In case of bending test configurations with a constant span / depth ratio the introduction of a length effect is proposed.

In general and in line with previous findings, an inverse relationship between length effects and timber quality was found. Furthermore, size effects were found to be in dependency of the analysed quantile, at $p = (5, 50, 95)\%$, being less distinct at $p = 5\%$. A dependency of size effects on timber species could not be found but a certain influence is indicated by test results. Note: Hereby a possible influence in particular on the length effect is supposedly due to a species dependent creation of knot clusters per year. MADSEN AND BUCHANAN (1985) also observed a species dependent knot size and quantity. In Douglas fir few but large knots were registered whereas spruce was characterised by many but small knots. They also note a certain influence by the static system, in particular if it is determined or indetermined, with the latter (three-point bending with fixed ends on both sides) characterised by simultaneous failure in three or more pieces. Note: The analysed test configuration shows three peaks in the longitudinal bending moment distribution. MADSEN AND BUCHANAN (1985) proposed a modified WLT by assignment of size effect parameters for the different material directions as well as in dependency of the applied stresses.

LAM (1987) examined length effects in tension members loaded parallel to grain by means of proof loading. He analysed three timber species (group) (Douglas fir, Hem fir, SPF), three grades (Select Structural, No. 1, No. 2), six different widths and three different free test lengths. He found a grade independent but species dependent width effect of $k_{w,05} = 0.15 \div 0.30$ and a species dependent length effect of $k_{l,05} = 0.20 \div 0.37$.

He proposed to model length and width effects solely by means of WEIBULL's power model according the WLT.

MADSEN (1988) reported on bending tests on SPF of cross section w / d = 38 mm / 140 mm. Thereby six different load configurations, three- and four-point bending (with 1/3 and 1/4 of test span as distance between the symmetrical placed loading points) were performed at spans of 1.55 m and 3.10 m. He analysed size and load configuration factors according WEIBULL's WLT and found a good correspondence between calculated and observed bending strengths on (empirical determined) 5%-quantile level. One year later MADSEN (1989B) summarised his findings for standardisation. For bending members he concluded that width effects can be neglected but length effects are significant and should be combined with load configuration factors. In elements under tension stresses he found length and width effects separately but proposed to combine both, perhaps together with a load configuration factor in case of non-constant tension stresses along the member. Length and width effects were also found in elements stressed in compression parallel to grain. MADSEN (1989B) proposed to consider these size effects in stability formulations and not in strength characteristics. Effects in thickness were not examined. In general, a decreasing quantity of flaws with increasing timber grade was found together with stress dependent size effects. Furthermore, variation in size effects along the strength distribution due to changes in failure modes was observed. He noted that the bending test procedure with explicit placement of the worst flaw in the maximum bending-tension zone leads to biased characteristics for the design of timber structures. Note: This test procedure not only delivers conservative values of E[f_m] but also of Var[f_m] which must not always lead to conservativeness in reliability of bending members or in their characteristic 5%-values. In 1990 MADSEN proposed to fit a 3pWD to the lower tail ($P(X \leq x) \leq 25\%$) of strength data to increase the representative power of statistical information for the design relevant region of strength. Note: In principle this would be a good idea and MADSEN was not the only one who proposed lower tail fitting (e.g. also done by LAM AND VAROGLU, 1990; SØRENSEN AND HOFFMEYER, 2001). Nevertheless, some questions still require further clarification: Firstly, how to guarantee the lower limit of strength according the third WD-parameter x_0, and secondly, can the 3pWD be a general applicable RSDM of timber strength data. According the first remark short term strength may be limited by means of proof loading which rejects all specimens with strength below the proof level. Nevertheless, the influence of some kind of "pre-damage" and in particular the consequences from short time proof loading on duration of load effects still needs further

clarification. Concerning the second remark, the fitting of statistical distribution models to only one part of data by means of three parameters and finite data, is perhaps not the big challenge if good to moderate fitting is required. It can be expected that not only the WD-model gives good results (in particular skewness and kurtosis information, the position of median, mode in respect to mean, etc. is missing). Beside that and under consideration of EVT for minima (see section 2.6.2) changes in serial system size lead to changes in statistical parameters and even of the distribution model, influenced by the whole distribution information of the single elements. Thus, restricted statistical information causes restricted information in regard to the expected distribution of strength values of material complexes with deviating size or volume. Beside that, WILLIAMSON (1992) observed well representation of the lower distribution tail either by WD or GUMBEL distribution. Based on his test data of bending, tension and compression tests parallel to grain performed on SPF MADSEN (1990) observed a relationship between strength level and size effect. He proposed length effect parameters of $k_{l,50} = 0.13$, 0.09 and 0.17, and $k_{l,05} = 0.22$, 0.10 and 0.22 for members stressed in tension, compression and bending, respectively. Interestingly the length effects on the 5%-level were found to be higher than on the 50%-level. Note: This contradicts EVT and WLT. The reason for that lies in the tail-fitting procedure which may induce overestimation of values in the lower distribution range. The same phenomenon was observed in LAM AND VAROGLU (1990) who performed tail-fitting to the lower 15% of test data. MADSEN (1990) also found width (depth) effects in compression parallel to grain and bending but not in tension parallel to grain. BARRETT AND FEWELL (1990) report on size effects on bending and tension strength. Based on a comprehensive literature survey equal length effects for bending and tension strength were observed with $k_l = 0.17$. Depth (width) effects in bending and tension were also found to be equal, with $k_{d(w)} = 0.23$. In case of a constant span / depth ratio a total size effect (length + depth effect) of $k = 0.40$ is proposed. A species dependent size effect could not be confirmed.

BARRETT ET AL. (1992) again examined size effects in bending, tension and compression strength and suggested to use of a modified WLT with separate size adjustments for every material direction (see section 3.2.1). They stated that variation in member width lead to changes in material structure in case the material is classified by limiting flaws, defined relative to cross section dimension. They confirmed quality dependent size effects and the influence of compression-bending yielding on bending strength, in particular in higher timber qualities. They mentioned already the idea to explain the ratio between bending and tension strength by means of WLT and under consideration of size and load

configuration factors. This idea was later executed by BURGER AND GLOS (1997) who reported on an increasing ratio of $f_{t,0} / f_m = 0.60 \div 0.80$ with increasing timber quality in machine graded timber and on a constant ratio of 0.70 in case of visual graded timber. BARRETT ET AL. (1992) proposed the same length and width factors for bending and tension strength as given in BARRETT AND FEWELL (1990). Length and width factor in compression parallel to grain were suggested to be $k_l = 0.10$ and $k_w = 0.11$, respectively.

WILLIAMSON (1992) further observed that length effects in timber stressed in bending or tension parallel to grain are higher than in compression parallel to grain. Also, in lower timber grades length effects are more pronounced than in timber of a higher strength class. Note: These observations can be explained by taking into account the expectable dispersion of strength data in bending, tension and compression, and / or by changing statistical spread from low timber quality with high local (and even global) variation of growth characteristics and basic wood properties, to lower statistical spread as consequence of a more homogeneous material structure in case of high, selected timber quality. Therefore, and as WILLIAMSON (1992) also mentioned, statistical length effects (note: as all statistical system effects) are a function of variability within and between the elements. WILLIAMSON (1992) enlarged WLT by additional consideration of spatial correlation inherent in timber elements and by adaptation of WD to better represent the distribution of real strength data. The latter was done by implementing a mixed distribution model. Thereby he sticked to the limiting models of EVT, explicitly to WD and GUMBEL distribution, but noted that spatial correlation has a decisive influence on realised length effects. Based on his analysis again a grade dependent size effect was found ($k_l = 1.11$ and 1.16 for high and low grade timber, respectively).

In regard to four-point bending tests RIBERHOLT AND MADSEN (1979) noted that the full test span should be taken as test length if the specimen was judged and the weakest zone placed within the zone of maximum moment. If the specimen is positioned randomly only the length of maximum moment zone is accepted as test length. Note: Even if specimen and their weak zones are judged beforehand by means of non-destructive methods a reliable judgement of strength, even if only relatively, is not possible. Based on own experiences the chance to find the weakest zone is nearly 50%. Also LAM AND VAROGLU (1990) remark that only $(34 \div 44)$% of the specimen stressed in tension parallel to grain failed in the grade determining flaw which was found by visual or machine judgement. Even then the length of the specimen must be larger than the required test length to guarantee that the assumed weakest section can be placed within the zone of maximum

moment. But in that case the inspected and judged zone would be usually larger as the test length.

KÄLLSNER ET AL. (1997) modelled length effects in timber by means of a discrete weak zone model in combination with a two- or three-level hierarchical process. In case of long-span timber elements with $k \geq 1$ weak zones under constant bending moment, the beam is assumed to fail with the failure of the first weak section. In the physical model system failure can only occur in a weak zone with strength $Z = X + Y$, in particular in the weakest of all weak zones (WLT) with $Z_{(1)} = X + \min[Y]$, X as random variable representing the variation between structural timber elements and Y a random variable representing the variation within structural timber as deviation from X. The bending strength of the structural timber is given as $Z_{k,(1)} = X + \min[Y_{k,i}]$. Assuming $Z_1 \sim$ ND the distribution of $Z_k \mid k$ follows

$$F_Z(z|k) = P(X + \min\{Y_1,...,Y_k\} \leq z) = \frac{1}{\sigma_X} \cdot \int \left[1 - \Phi\left(-\frac{z-x}{\sigma_Y}\right)^k\right] \cdot \varphi\left(\frac{x-\mu_X}{\sigma_X}\right) \cdot dx\,, \tag{5.6}$$

with $\varphi(.)$ and $\Phi(.)$ as standard normal density and distribution function, respectively, and μ_X, σ_X and σ_Y as the mean of X and the standard deviations of X and Y. With K as discrete random variable with realisations $k \in \{1, 2, \ldots\}$ as outcome with probability p_k, the distribution function of Z becomes

$$F_Z(z) = \sum_{k=0}^{\infty} F_Z(z|k) \cdot p_k = 1 - \frac{1}{\sigma_X} \cdot \int_{-\infty}^{\infty} E\left[\Phi\left(-\frac{z-x}{\sigma_Y}\right)^k\right] \cdot \varphi\left(\frac{x-\mu_X}{\sigma_X}\right) \cdot dx\,, \tag{5.7}$$

with expectation

$$E\left[\Phi\left(-\frac{z-x}{\sigma_Y}\right)^k\right] = \sum_{k=0}^{\infty} \Phi\left(-\frac{z-x}{\sigma_Y}\right)^k \cdot p_k\,, \tag{5.8}$$

which can be expressed by the probability generating function

$$\psi(x) = E\left[x^K\right], \tag{5.9}$$

of integer variable K. Assuming K being Poisson distributed with parameter $\lambda \cdot l$ and l as the length of the structural element than the probability generating function becomes

$$\psi(x) = \exp[\lambda \cdot l \cdot (x-1)], \tag{5.10}$$

and equ. (5.7) can be rewritten as

$$F_Z(z|l) = 1 - \frac{1}{\sigma_X} \cdot \int_{-\infty}^{\infty} \exp\left[-\lambda \cdot l \cdot \Phi\left(-\frac{z-x}{\sigma_Y}\right)\right] \cdot \varphi\left(\frac{x-\mu_X}{\sigma_X}\right) \cdot dx\,. \tag{5.11}$$

The comparison between local strength and test data of long span beams with 6 ÷ 8 weak zones under constant bending moment over 3,500 mm (cross section w / d = 45 mm / 120 mm) made by KÄLLSNER ET AL. (1997) showed that the model gives (5 ÷ 15)% higher bending strength values than observed from tests. It was concluded that size effect cannot be explained only by stochastics and that additionally energy release effects (as discussed e.g. in BAŽANT, 2001) have to be considered. This was concluded by the observation that the failure process got more progressive the longer the testing length was. Note: The deviations between predicted and realised strength values, perhaps and beside of the small number of tests, can be explained by a mixture of tension-bending failures and compression-bending followed by tension-bending failure. This was also mentioned for one series by KÄLLSNER ET AL. (1997). Compression strength in timber has normally a higher expectation and lower spread if compared with tension parallel to grain. This leads to some kind of bi-modal bending strength distribution function (see e.g. test data of MADSEN, 1990). Furthermore, the model assumes system failure according the WLT. In the tests of single weak zones, intermediate steady states and even a further increase of load after load-redistribution could be sometimes observed. In 2005 DITLEVSEN AND KÄLLSNER reported again on results concerning length effects in timber under bending stresses. Test results of KÄLLSNER AND DITLEVSEN (1994) as well as STICH (1998) were analysed. In their discussion concerning interaction effects in case of failure between adjacent weak zones they concluded that these effects can be neglected. This was found by comparing predictions and realisations of systems of more than one weak zone by means of the single weak zone model.

BURGER AND GLOS (1996) and BURGER (1998A,B) analysed the size effects on structural timber in tension parallel to grain. Based on observations which have been already reported earlier by others a systematic examination of size effects and distribution of strength determining characteristics in dependency of the dimension of structural timber was performed. Thereby BURGER (1998B) differentiated between “direct size effects” as consequence of WLT, and “indirect size effects” as result of size dependent distribution

of flaws. Strength determining characteristics as the share of knots (*DAB* ~ 2pLND), density, (~ 2pLND) annual ring width (*ARW* ~ 2pLND) and share of reaction wood (*RW* ~ Exp. + Heavyside function) were considered. Thereby an increase in E[*DAB*] and Var[*DAB*] with increasing length and decreasing width was found. E[*ARW*] and Var[*ARW*] also decreased with increasing width. The density shows a decrease in expectation but a more or less constant variance with increasing width. Based on a multiple regression model composed of modified terms of WLT together with a linear term for density and exponential terms for *DAB* and *RW*, *DAB*, density and test length were identified as the main parameters explaining about 58% of the variance of the test data on tension strength. Due to the influence of indirect size effects he found even higher length effects than predicted by WLT, a positive as well as negative width effect in dependency of timber quality (weaker or even contrary to WLT) but no influence of indirect size effects in thickness which effect was found to be negative. Nevertheless, the possibility of parallel system effects in width or thickness was not checked. He remarked the difficulty in specifying general applicable size effects because even the grading method itself (visual vs. machine grading) has a distinctive influence on them. Later, DENZLER (2007) examined by comparable principles the direct and indirect size effect on bending strength. By means of a multiple regression model the main parameters found for bending strength were density, *ARW*, *KAR*, depth and length. Nevertheless, beside the fact that only in 47% of analysed test specimen a brittle fracture was observed and in the majority a ductile or subsequent failure with further load increase was given, the modified WLT was taken as core of the multiple regression model with f_m ~ WD.

Also ISAKSSON (1999) analysed size effects on bending strength of timber. He tested in total 673 single weak zones of Swedish spruce with a cross section of $w / d =$ = 45 mm / 145 mm and by applying a constant bending moment. He observed a roughly constant variance of $f_{m,i}$ over all tested boards. Furthermore, a certain dependency between local $f_{m,i}$ and mean strength potential of each element ($f_{m,mean}$) can be observed. The test data of weak zones was split into bending-tension failures ($f_{m,mean,i}$ = 52.2 N/mm²; CoV[$f_{m,i}$] = 22.8%) and bending-compression-tension failures ($f_{m,mean,i}$ = 63.8 N/mm²; CoV[$f_{m,i}$] = 19.4%). Based on these results he formulated a two- and a three-level hierarchical model for normal or lognormal distributed bending strength with discrete distributed weak zones along the length of timber.

Intermediate Conclusions found in respect to Serial System Action and Effects

As shown by the literature survey, size effects on wood and timber strengths are preferable modelled by means of WLT and WEIBULL-distributed strengths. Of course, in some material directions perfect brittle failure behaviour can be nearly observed. Nevertheless, even in the prime example of timber stressed in tension perpendicular to grain of STUEFER (2011) in some tests there appeared partial failure followed by further load increase. As outlined at the beginning of this section, structural timber and even wood behaves quasi-brittle rather than perfect brittle. Consequently, all main model assumptions made for the derivation of WEIBULL's WLT are violated in some way or have to be at least questioned. This is in particular obvious by the numerous adaptions made to WEIBULL's WLT.

For example MADSEN UND BUCHANAN (1985) and BARRETT ET AL. (1992) used a modified WLT to account for the anisotropy of timber. BURGER AND GLOS (1996), BURGER (1998A,B) and DENZLER (2007) enlarged WLT by additional terms for strength determining characteristics. WILLIAMSON (1992) enlarged WLT by a bi-modal distribution and by inclusion of spatial correlation. Results not conforming to WLT were found by MADSEN AND BUCHANAN (1985), MADSEN (1990) and LAM AND VAROGLU (1990), whereas BARRETT (1974), BARRETT AND FOSCHI (1979), LAM (1987) and MADSEN (1988) found consistent results or at least well explanation of load configuration factors. A further indicator of lack in representation of timber strength data is given in bending. Thereby no width effect was given; see e.g. BOHANNAN (1966), MADSEN (1989B) and DENZLER (2007).

In conformity with quasi-brittle material assumptions size effects were found to be dependent on (1) <u>failure mode</u> (MADSEN, 1989B), (2) <u>timber quality</u> (YLINEN, 1942; MARKWARDT AND YOUNGQUIST, 1956; MADSEN AND BUCHANAN, 1985; MADSEN, 1989B; WILLIAMSON, 1992; BURGER AND GLOS, 1996; BURGER, 1998A,B; DENZLER, 2007), (3) <u>timber species</u> (indicated in MADSEN AND BUCHANAN, 1985; confirmed in LAM, 1987; not confirmed in BARRETT AND FEWELL, 1990), (4) <u>grading method</u> (BURGER, 1998A,B; DENZLER, 2007), (5) <u>strength level</u> (MADSEN AND BUCHANAN, 1985; MADSEN, 1990) and (6) <u>the arrangement of sub-elements relative to stress direction</u>, parallel vs. serial (BOHANNAN, 1966; MISTLER, 1979, see section 3.2.4).

It can be agreed that for some or even most applications a well fitted WEIBULL WLT delivers sufficient accurate information for the consideration of size effects in daily

design processes of timber structures. Someone may also argue that size effect dependency on timber species, grade, grading method, strength level and failure mode is not really a dependency but more a sign for model adjustments to in principle different materials. In the limiting case the same can be said against stochastics in general and in particular in materials, by discussing different (in)finite small material volumes which agglomerate to material volumes in an observable range.

In the review also a preferred use of WD for strength values of timber was observed. Also in the numerous publications of BAŽANT on quasi-brittle size effects (e.g. BAŽANT, 2001; BAŽANT ET AL., 2004; BAŽANT AND PANG, 2006; BAŽANT AND YU, 2009) WD is assumed and argumented by EVT. Nevertheless, as redistribution of load is in principle allowed in quasi-brittle materials, fracture of an element can be described as subsequent failure and step-wise separation of material structure in the failure zone. This separation process, which can be observed in destructive tests, is comparable with "the law of proportionate effect" (see GIBRAT, 1930 & 1931) which is the basis for the lognormal distribution model. It has to be outlined that the models 2pLND or 3pLND are often cited as RSDMs of strength data.

To conclude, in quasi-brittle materials strength data analysis should be made very carefully and in respect to the observed failure modes. Following GIBRAT (1930, 1931) 2pLND as RSDM of strength data of quasi-brittle materials can not be generally recommended but it is seen as a representative distribution model with physical background, in particular in materials and stresses were load-redistribution and step-wise failure can be observed. Furthermore, current discussions on size effects involve both, serial and parallel system effects. It is recommended to differentiate explicitly between both contrary system actions and effects.

5.1.3 System Effects: Parallel System Effects in Engineered Timber Products and Structures

System effects in engineered timber products and structures are versitale. They are obvious e.g. in glued laminated (solid) timber or duo and trio beams if stressed in tension or compression parallel to grain, or in the same products if the elements are stressed edgewise in bending. In detail, the hierarchical structure of the material and the arrangement of elements which itself constitude sub-systems cause that these products act mainly in parallel but also in serial. As already discussed in section 4.3.1, chapter 4 these systems can be described as being **parallel, sub-serial** (see Fig. 5.23).

Thereby, the serial segmentation of elements on a first level (hierarchy of construction timber) is given in (1) serial arrangement of boards or beam segments by finger-, butt- or scarf-joints, and (2) by the serial composition of construction timber of alternating sections with or without apparent knots or knot clusters (see section 5.1.1). Nevertheless, system effects in these products are, if at all described or regulated, treated as general system effects or considered by system or load sharing factors.

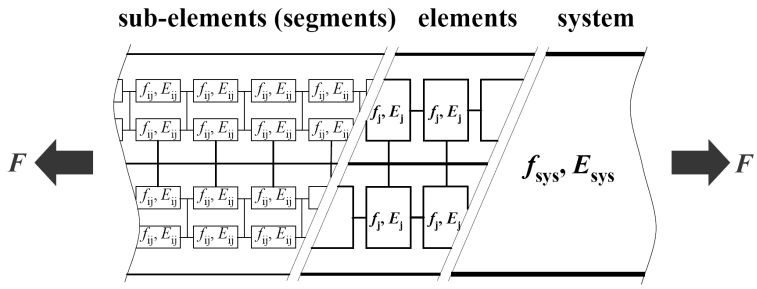

Fig. 5.23: Schematic parallel, sub-serial system structure with $N = 2$ under tension stress parallel to grain (adopted from BRANDNER, 2006)

In general, parallel systems can be differentiated according:

- <u>the distance between the elements</u>
  - elements placed in (regular) center-distance larger than the thickness of the elements; hereby the load distribution is performed by an additional primary or secondary construction element
  - elements placed side-by-side
- <u>the type and characteristics of connection</u> between side-by-side placed elements
  - without (loose) connection, theoretically even without friction
  - flexible connected (flexible composite) e.g. by means of nails, bolts or pre-stressing
  - rigid connection (rigid composite), e.g. by bonding
- <u>the type and characteristics of the load distributing element</u> in parallel systems composed of elements in (regular) center-distance larger than the thickness of the elements
  - stiffness of load distributing element, in particular in relationship to the center-distance

    - type and characteristics of connection between the load distributing element and the elements of the parallel system (possible amount of composite action)
- general characteristics, e.g. timber quality, material behaviour, type of loading, partial or full loading.

Parallel systems are often described as "load sharing systems". According BONNICKSEN AND SUDDARTH (1966) the three main characteristics of these systems are:

- redundancy (fail-safe; stand-by): the structure does not fail if one or even more elements fail;
- load sharing: each element carries actively a share of the total system load;
- load redistribution: load of failed elements after partial system failure is re-distributed on the survivors.

In general, the herein discussed **load-sharing systems are in behaviour and reliability somewhere in-between serial** (chain-type or weakest link systems) **and parallel-redundant systems** (ideal parallel systems) (e.g. BONNICKSEN, 1965). It is assumed that the load is equally distributed on all parallel interacting elements which are restricted to elongate or deflect equally. The stresses in the elements are not uniform but proportional to the (local) stiffness of the elements.

ZAHN (1970) mentioned three main stochastic effects which are observable in parallel systems:

- effect of grouping: reduction of CoV[f] equal to a serial system type (weakest link);
- mutual constraints: increase in effective strength (5%-quantile) due to load sharing between the elements proportional to their global stiffness;
- local reinforcement of flaws: increase in effective strength (5%-quantile) due to load sharing between the segments of (adjacent) elements proportional to their local stiffness.

Whereas the first two stochastic effects are the result of the variability between the elements the last effect can be traced back to variability within the elements (ZAHN, 1970).

There are numerous parameters which influence the system behaviour. A comprehensive overview of these can be found e.g. in BRANDNER (2006). Following main parameters are given:

- quantity of interacting, parallel elements N;
- stochastic characteristics of the elements including correlation structure of strength and stiffness between and within the elements and in particular the variability of strength and stiffness characteristics (e.g. CoV[f], CoV[E]);
- type of interaction (stiffness of the connection) between the elements;
- type of loading / load configuration (bending, tension, compression, etc.).

The definition of an element in a parallel system can be versitale. In general, the element is defined as the basic unit which if parallel aligned creates the described parallel system. Some possibilities are shown in Fig. 5.24 (see e.g. GEHRI, 1997 and BRANDNER, 2006).

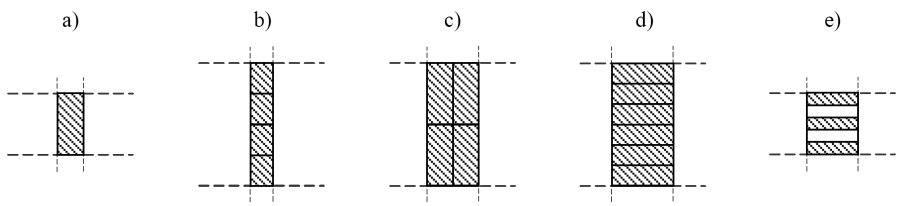

Fig. 5.24: Various types of elements (basic units) in parallel systems: a) structural timber; b) stacked structural timber; c) multi-girder; d) glued laminated (solid) timber; e) basic element of cross laminated timber

The simplest case for studying system effects in engineered timber products (ETPs) is given by linear members stressed in **tension parallel to grain**. Even in compression parallel to grain system behaviour becomes more complex due to additional infuence of stability. An overview of various types of parallel acting systems stressed in tension or compression parallel to grain is provided in Fig. 5.25.

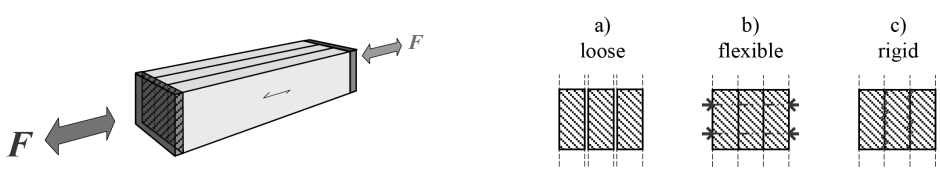

Fig. 5.25: Examples of parallel acting systems stressed in tension or compression parallel to grain: principle sketch (left); degree of connection between the elements (right)

Systems composed of parallel acting elements loaded in tension parallel to grain can be at first differentiated according the degree of connection between the elements, in loose, flexible and rigid. **If the elements are unconnected** over a certain distance in longitudinal direction or at least only clamped at the ends, the serial system size M is equal to one, if, as usual, the element strength and stiffness characteristics of the same dimension as used for the system are taken as basic (reference) characteristics for the judgement of strength and stiffness of the system. The sub-serial structure inherent in the elements has no influence on the system behaviour because it is already sufficiently considered by the element characteristics. Given the values $f_{t,0,i}$ and $E_{t,0,i}$ of the elements, which represent the minimum and the inverse harmonic mean of the serial segments of construction timber, than **the expectable system characteristics are sufficiently characterised by a parallel system behaviour** as discussed in section 3.4. Thereby the load distribution between the elements is proportional to the global E-modulus of each element and the system strength is defined by the element strengths. Consequently, additional information about within correlation of local strength and stiffness in the elements and their segments is not required. As a continuous connection between the elements is not given (except on the ends) each element can only fail once.

In contrast, the description of the behaviour of systems composed of parallel acting, continuously and rigid connected structural timber elements requires sufficient knowledge of their parallel, sub-serial structure. Load sharing ocurs very locally and on the hierarchy of segments or sub-segments. Consequently, local strength and E-moduli and their distribution within the elements are required to model the system behaviour. Therefore, the correlation structure within and between structural timber as well as further stochastic information, e.g. RSDMs of strength and stiffness of the segments (e.g. of zones with and without apparent knots or knot clusters) and the appropriate distribution parameters have to be known. The influence of the degree of connection (loose vs. rigid) is schematically demonstrated in Fig. 5.26. Thereby a straight subdivision of structural timber longitudinally in segments with and without flaws (e.g. zones with knots or knot clusters and “clear wood” zones free of flaws) is made. Fig. 5.26 (left) shows the PDF of strength of structural timber. Fig. 5.26 (right) shows a bi-modal PDF of strength in segments as expected in a single structural timber element. This bi-modal PDF is created by weighting the PDFs of zones with and without flaws according the probability of occurrence, see e.g. equ. (5.1). As both PDFs represent local strength values expectation of strength even of zones with flaws is (much) higher than that observable in standard tests on structural timber. Because of the material inherent spatial correlation it can be in

general shown that the variability is also even lower than in structural timber which includes between and within element variability. Consequently, as parallel systems composed of rigidly and continuously connected elements enforce load sharing between adjacent segments a concave increase of the expectation of system strength with increasing N can be expected. Nevertheless, as the difference in strength between the segments with and without flaws decreases with increasing timber grade the increase in mean strength potential becomes lower or even negative. This is in particular true if the variability between the elements lead to a remarkable decrease of average system strength as it is in general observable in parallel systems composed of linear-elastic, brittle failing elements. Nevertheless, system action between segments is based in principle on higher varying strength characteristics due to bi-modal density functions.

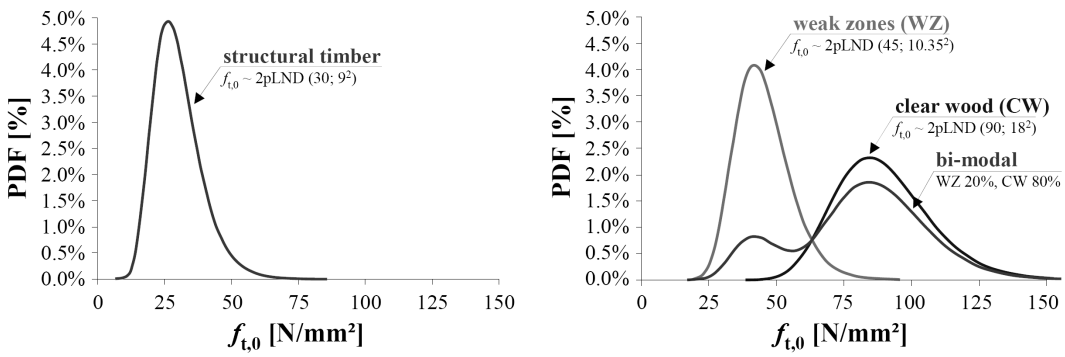

Fig. 5.26: PDF of tension strength in structural timber (including within and between strength variation; left); bi-modal PDF exemplarily for 20% probability of occurrence of weak zones (including knots) and 80% probability of occurrence of clear wood (right); all uni-modal distributions are assumed to follow 2pLND

Due to continuous connection elements can fail more than one time. In reality even partial segmential fracture can be observed in conjunction with redistribution of stresses to another position in width and / or longitudinally of the system.

Publications on parallel system behaviour composed of structural timber and stressed in tension or compression parallel to grain are scarse. One of them is the work of WESTMAN AND NEMETH (1968). They examined systems of $N = 1, 2$ components made of Douglas fir on four samples of different timber grades. Thereby the duo beams where rigidly glued together face-by-face. In all four groups significant increase of the 5%-quantile of tension strength $f_{N,t,0,05}$ was observed in comparison to $f_{1,t,0,05}$ of the single elements. This was due to the remarkable decrease in dispersion, e.g CoV[$f_{t,0}$]. Furthermore a dependency of

system strength capacity on timber grade was found, in particular on the mean level $f_{N,t,0,mean}$. Whereas $f_{N,t,0,mean}$ of the highest grade was slighly below $f_{1,t,0,mean}$ a remarkable increase of up to 107% was given in lower timber grades. A summary of the main statistics is given in Tab. 5.13.

Tab. 5.13: Main statistics of tension tests parallel to grain on parallel systems composed of Douglas fir; WESTMAN AND NEMETH (1968)

grading class ➔		**K**	**L-1**	**L-2**	**L-3**
group [--]	# [--]	$f_{t,0,mean}$ | min[$f_{t,0}$]÷max[$f_{t,0}$] | $f_{t,0,05}$ [N/mm²]			
SINGLE	42# (each)	52.5 | 22.0÷95.7 | 28.7	42.1 | 7.6÷104.4 | 19.1	25.0 | 9.6÷89.0 | 14.3	10.8 | 2.9÷21.0 | 2.9
DUO	21# (each)	50.9 | 28.7÷72.3 | 31.1	47.6 | 30.6÷76.6 | 34.4	33.2 | 22.5÷69.4 | 23.9	22.4 | 10.7÷30.1 | 13.4

Tab. 5.14: Main statistics of tension tests parallel to grain on parallel systems composed of finger jointed structural timber; BRANDNER (2006) and BRANDNER AND SCHICKHOFER (2006)

group [--]	***N*** [--]	# [--]	$\rho_{12,mean}$ (CoV) [kg/m³]	$E_{t,0,12,mean}$ (CoV) [N/mm²]	$f_{t,0,mean}$ (CoV) | $f_{t,0,05,empD}$ [N/mm²]
Z_1	1	46#	460 (6.4%)	11,900 (11.6%)	23.0 (26.8%) | 14.5
Z_2	2	41#	453 (4.5%)	11,750 (8.4%)	24.6 (17.7%) | 16.5
Z_4	4	30#	457 (3.6%)	12,380 (7.3%)	28.3 (14.6%) | 21.3

BRANDNER (2006) and BRANDNER AND SCHICKHOFER (2006) report on tests performed on systems composed of finger jointed construction timber, with $N = 1, 2, 4$. The timber was Norway spruce, graded to S10+ in accordance to DIN 4074-1 which can be allocated to strength class C24+ according EN 338. The single elements had a cross section of $w / t = 78$ mm / 60 mm. The free testing length was 4,860 mm. The elements in the systems were glued side-by-side by means of polyurethan adhesive. All elements were proof-loaded in tension parallel to grain up to a proof level of 7 N/mm². The main results and statistics are shown in Tab. 5.14. Based on these statistics it can be observed that the expectation of E-modulus and density is unaffected by N. Furthermore, CoV[$E_{t,0,12,N}$] and CoV[$\rho_{12,N}$] follow the **averaging model** given as

$$E[X_N] = E[X_1] \text{ and } CoV[X_N] = \frac{CoV[X_1]}{\sqrt{N}}. \tag{5.12}$$

Parameter CoV[$f_{t,0,N}$] is also roughly in line with the averaging model but mean tension strength increases significantly with increasing N.

Tab. 5.15: Main statistics of tension tests parallel to grain on parallel systems composed of unjointed and unconnected (ZL) and side-by-side glued elements (ZK); BRANDNER (2006)

group [--]	***N*** [--]	**#** [--]	$\rho_{12,mean}$ **(CoV)** [kg/m³]	$E_{t,0,12,mean}$ **(CoV)** [N/mm²]	$f_{t,0,mean}$ **(CoV)** [N/mm²]
ZL_1	1	21#	499 (8.8%)	16,030 (14.0%)	41.4 (30.3%)
ZL_2	2	10#	481 (4.2%)	15,610 (7.2%)	32.0 (19.5%)
ZL_3	3	7#	490 (5.0%)	15,280 (6.5%)	36.3 (17.0%)
ZL_4	4	5#	491 (5.9%)	15,290 (6.5%)	34.3 (7.8%)
ZK_1	1	26#	482 (7.3%)	15,210 (12.2%)	41.8 (30.7%)
ZK_2	2	9#	496 (5.1%)	15,760 (7.4%)	44.9 (17.7%)
ZK_3	3	7#	494 (3.8%)	16,050 (8.2%)	48.2 (27.7%)
ZK_4	4	6#	502 (6.2%)	15,800 (16.0%)	46.2 (20.4%)

BRANDNER (2006) reports on experiences made on two further tension test samples. The elements were glulam lamellas also of Norway spruce but unjointed and of grading class MS17 according DIN 4074 which can be allocated to strength class C40 according EN 338. The elements with an initial cross section of $w / t = 165$ mm / 40 mm were ripped in center-line of the width and planed to elements with a cross sections of $w / t = 78$ mm / 40 mm. Thereafter two equal sized and matched samples according their dynamical E-modulus based on ultrasonic runtime measurements ($E_{dyn,US}$) were constituted. In each sample systems of $N = 1, 2, 3, 4$ composed of elements with roughly equal $E_{dyn,US}$ were built up. The reason of equal $E_{dyn,US}$ was to eliminate the influence of differences in global stiffness. In sample ZL the elements were left unconnected. All elements were constrained to equal elongation by being clamped at the ends in the testing device. The elements in the second sample ZK were glued side-by-side by means of

polyurethane adhesive. The free testing length was 3,820 mm. Tab. 5.15 shows the main statistics of both groups.

The sample sizes are, except for $N = 1$, only small but reflect the expected differences of structural behaviour of systems composed of elements without (ZL) and of continuously rigidly connected elements (ZK). Thereby $E_{N,t,0,12}$ and $\rho_{N,12}$ again follow roughly the averaging model. Mean strength $f_{N,t,0,mean}$ of sample ZL decreases in trend with increasing N. This is in line with parallel systems composed of linear-elastic and brittle failing elements. In contrast, strength in group ZK shows in trend an increase of $f_{N,t,0,mean}$ with N. In respect to the high strength class C40 of the base material the results appear at first to be contrary to that of WESTMAN AND NEMETH (1968). Nevertheless, ripping of the base material to elements led to an increase in variability and decrease of strength due to the fact that, e.g. limits in flaw dimensions for timber grades are often in conjunction with the dimension of cross section.

To conclude, the last two groups ZL and ZK clearly underline the different system behaviour of loose and rigid connected elements. In sample ZL a decrease of $f_{N,t,0,mean}$ but a significant reduction in CoV[$f_{N,t,0}$] can be observed. This is not because of local load sharing between segments of the elements but due to an "averaging" of element strength variation. In sample ZK an increase of $f_{N,t,0,mean}$ due to local load sharing and bridging of flaws by stiffer adjacent sections can be observed. Thereby CoV[$f_{N,t,0}$] shows a minor decrease. This can be traced back to changes in the relevant basic strength distribution representative for consideration of the interaction between the segments (see Fig. 5.26). The E-modulus and the density are widely unaffected by the type of connection between the parallel elements, so far no or a rigid, stiff connection in longitudinal direction (e.g. finger joints or scarf joints) can be assured. The averaging model appears as being sufficient to account for system effects on E-modulus and density. There is an additional effect which has to be considered: Flaws in elements, in particular knots and knot clusters, cause a low local E-modulus. In case of elements under tension stresses and asymmetrical placement of flaws within the cross section moments are induced. Consequently, elements in long span tension tests are under MN-interaction which leads to an underestimation of the "real" bearing capacity of the elements in tension (see e.g. COLLING, 1990; FALK AND COLLING, 1994, 1995). This effect is also negatively dependent on timber grade, being more distinctive in lower grades which suffer from a high share of knots. If the elements are rigidly composed to systems averaging and bridging of weak zones reduces the effect of MN-interaction. Consequently, an increase

in $f_{N,t,0,mean}$ is given. In systems under compression parallel to grain (as discussed next) this effect can also be expected but to a smaller amount. Nevertheless as these systems get slender other effects, e.g. stability considerations, dominate.

In case of parallel systems composed of elements under **compression stresses parallel to grain** stability analysis has to be additionally taken into account. Once more the type of connection between the elements (degree of connection; discrete vs. continuous connection) plays a role. It determines not only the treatment of the system as solely parallel or as parallel, sub-serial, but also the expectable composite action which is decisive for the action of the system in case of instability. Two extreme cases (i) acting nearly like single elements (only constrained to equal compressive strain; no connection in between), and (ii) acting as one complex (continuous, rigid connection) are given. In particular in case (ii) slender systems which are endangered to buckle homogenisation of E-modulus gives an extra advantage.

WILSON AND COTTINGHAM (1952) present results of compression tests parallel to grain on systems of $N = 8, 11, 17$ elements. All systems had a cross section of $w / d = 135$ mm / 152 mm so that the elements got thinner with increasing N. The length of the systems was $l = 915$ mm. In the analysis three types of longitudinal joints were examined (butt-joints and scarf-joints with inclination 1:3 and 1:5) and compared with control samples of the same but unjointed material. Furthermore the influence of one single joint on the outside and that of staggered joints in neighboured elements on the outside of the systems was investigated. In total 36 samples of three replicants each were tested. On the mean level no differences between the E-modules $E_{N,c,0,mean}$ and strengths $f_{N,c,0,mean}$ of systems of unjointed (controls) or scarf-jointed elements could be found. Nevertheless, the butt joint significantly affected both characteristics, $E_{N,c,0,mean}$ and $f_{N,c,0,mean}$. This led to about 30% loss in stiffness at $N = 8$ which decreased down to roughly 0% at $N = 17$, and to about 25% loss in strength at $N = 8$ which was also reduced to roughly 10% at $N = 17$. In a further step the influence of timber grade was investigated on systems of the same length and cross section dimension and $N = 8, 17$. Thereby the elements were classified in four groups, clear wood, No. 1, No. 2 and No. 3. Each of the eight groups was tested with three replicants. A comparison between the groups of $N = 8$ and $N = 17$ shows in trend an increasing ratio of $X_{N=17,mean} / X_{N=8,mean}$ for $E_{c,0,mean}$ and $f_{c,0,mean}$ with decreasing timber grade. In particular in the group of clear wood the ratio is nearly 1.00 whereas in systems of No. 3 elements a ratio of roughly 1.30 and 1.20 can be observed for $E_{c,0,mean}$ and $f_{c,0,mean}$, respectively.

A further interesting study of system behaviour in compression is published by WINANS (2008). He analysed parallel strand lumber (PSL) of Southern pine by means of stochastic finite element analysis. He concludes that both, $E_{N,c,0}$ and $f_{N,c,0}$ follow the averaging model in expectation and variability.

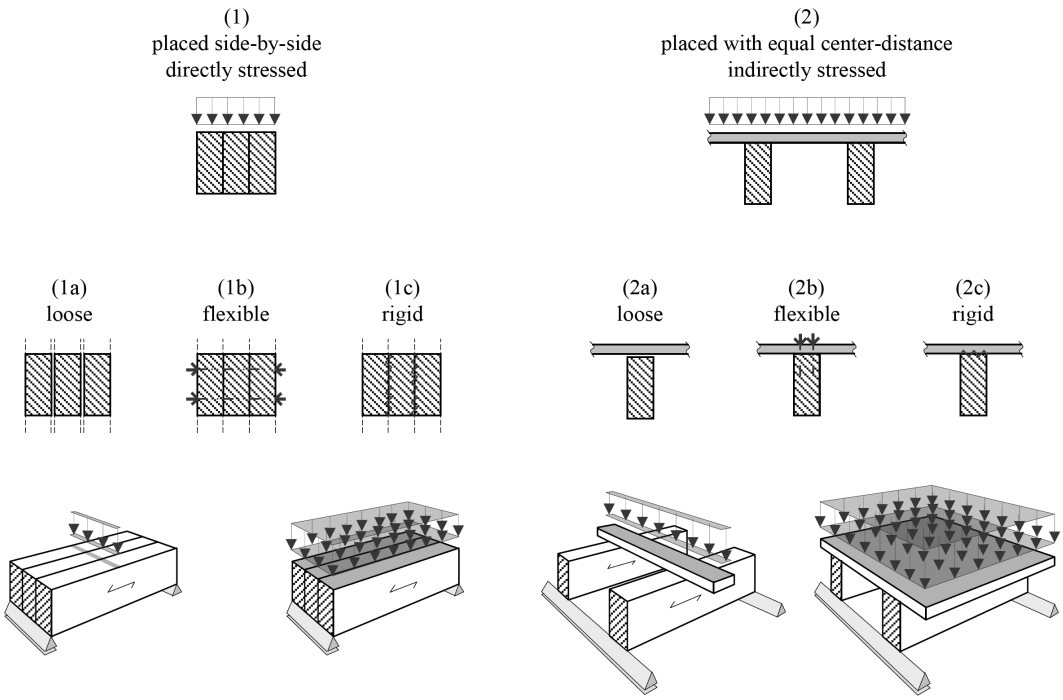

Fig. 5.27: Examples of parallel systems stressed in bending

The next important group of parallel systems are **systems under bending stresses**. Categorisation is made in systems composed of (1) directly stressed and side-by-side placed elements and (2) indirectly stressed and under (equal) center-distance larger the width of the elements placed elements. In type (1) further subdivision is made in (1a) loosely, (1b) flexibly and discretely, and (1c) rigidly and continuously connected elements. In systems of type (2) load sharing and thus the system action is decisively determined by the stiffness of the load distributing element and the connection of this element to the system elements. A deviating respond between the elements in type (1) and (2) can be expected in dependency of the connection between the elements and on the way how bending stresses are applied. This is not only because of different moment distributions but also because of the respond of the individual elements. Thereby bending

moments can be applied continuously (pure bending), by means of a distributed load per unit area or by applying line- or even point-load(s) (see Fig. 5.27).

As already discussed for parallel systems stressed in tension or compression parallel to grain, the respond and the strength potential in (1) is dependent on the degree of connection between the elements (loose – flexible – rigid) and on the longitudinal distribution of the connections (discrete vs. continuous). In type (2) the degree of connection between the system elements and the load-distributing unit decisively influences the amount of T-beam action. Nevertheless, the main effect on system strength potential is given by the stiffness of the load distributing unit as an indicator for the ability to enforce the parallel elements to equal deflection and common action as the basic concept of herein discussed parallel systems. In the case where the stiffness of the load distributing element $(E_0 \cdot I_y) \rightarrow \infty$ all elements are constrained to deflect equally. Beside the mechanical influence of T-beam action equivalent system behaviour as in type (1a) is given in principle.

In the following publications dealing with examinations on type (1) systems are discussed. For example MCALISTER (1974), who was probably the first in testing parallel aligned elements without any connection in between in bending (type 1a), examined systems of $N = 1, 2$ of Southern pine, No. 2. He compared the test results of systems with that of beams of the same cross section as the system, same species and grade. Consequently direct comparison has to be done with caution. Nevertheless, $E_{N,m,0,mean}$ and $f_{N,m,mean}$ of 12% higher and 7% lower, respectively, together with a reduced CoV[$f_{N,m}$] are given. Later, BAKHT AND JAEGER (1991) performed a stochastic simulation study on systems of type (1a) or also of type (2a) if the bending stiffness of the load distributing unit can be assumed to be $(E_0 \cdot I_y) \rightarrow \infty$. They analysed the distribution of system stress at first failure and the ultimate strength by varying the stress-strain-relationship from linear-elastic and brittle failure (case 1) to bi-linear relationship with inclination at 50% of maximum load and reduction of E-modulus of up to 65% (case 4). On the mean level a ratio of $f_{N,m,mean} / f_{1,m,mean}$ of roughly 1.0 was found for case 4. In case 1 a remarkable concave decrease up to 0.5 for $N = 20$ was given. Due to the observed non-linearity of stress-strain relationship in structural timber under bending (see SEXSMITH ET AL., 1979) a ratio of 1.0 was proposed, at least for parallel systems of type (1c) in bending, shear and tension parallel to grain.

Examinations on type (1b) are numerous. Thereby the degree of connection between the elements plays a decisive role. BONNICKSEN (1965) and BONNICKSEN AND SUDDARTH

(1966) report on tests on systems composed of $N = 1, 3$ elements of Douglas fir with $w / d = 38$ mm / 140 mm and $l = 3{,}048$ mm. The mechanical lamination was done with 30# 20d nails with spacings of 305 mm and 457 mm in the center and at the ends, respectively. The edge distance was 28.6 mm. The structural timber was delivered and kept in green condition also during testing. In the tests a subsequent failure in most of the trio beams was observed. In general, failure was initiated in bending-compression zone followed by a subsequent failure of the elements under bending-tension stresses. A sudden failure of two or three elements occurred only exceptionally. The ultimate bending strenght $f_{N,m}$ shows a slight but significant reduction in mean (–5.5%) and a remarkable reduction in CoV[$f_{N,m}$] to only 54% of CoV[$f_{1,m}$]. The reduction in variation is even slightly below the estimate according the averaging model which was accepted in a statistical test up to $\alpha = 10\%$.

Some results of MCALISTER (1974) were already mentioned in the previous group of (type 1a). Here a comparison between test results of nail-laminated duo beams and his control group of unconnected duo beams is presented. The nailing was done with 6d standard nails and spacing of 203 mm. His results indicate a slight increase in $E_{N,m,0,mean}$ and $f_{N,m,mean}$ of 2% and 4% due to activation of flexible composite action and load sharing between segments of the elements in the nail-laminated duo beams. The variability, expressed by CoV[$f_{N,m}$], was not distinctively influenced by nailing.

In the 1990ties a series of works on nail-laminated posts (type 1b) was published. For example BOHNHOFF AND MOODY (1990) performed bending tests on single and on nail-laminated, unspliced trio beams of Southern pine, No. 1 KD15. Thereby a reduction in mean bending strength of 11% by roughly constant mean E-modulus was observed. The variation of strength and E-modulus of the systems decreased significantly to 40% and 46% of that of the elements, respectivley. Later, BOHNHOFF ET AL. (1991) gave a comprehensive report on (un)reinforced and (un)spliced nail-laminated posts. Based on their research on <u>unspliced nail-laminated posts</u> they concluded that (1) the mean strength $f_{N,m,mean}$ is higher for low grade timber but nearly the same for high grades, (2) the mean E-modulus $E_{N,m,0,mean}$ is the same, regardless of grade and that (3) the CoV[X_N] of strength and stiffness follows the averaging model. Furthermore, the size, type and location of nails showed no significant influence on system strength. Based on a literature survey and finite element simulations (see BOHNHOFF, 1989) in regard to <u>staggered butt-joint spliced three-layer nail-laminated posts</u> they conclude that (1) an overall splice length has to be secured to enable an effective stress distribution in the vicinity of butt joints (at least

0.9 m are recommended), (2) high localised stresses in wood layers can only be decreased by additional nails up to a certain level, (3) the longest unjointed timber element in the center of the system defines the primary stressed element, (4) highest nail stresses are always adjacent to a butt-joint in the outer layer, and (5) system strength capacity is related to timber grade. Consequently, an efficient increase in system strength capacity is expected by (i) increase of the strength of the primary stressed center element and (ii) reinforcement of the outside butt-joints. The last one also reduces the slip and thus the stress concentration on nails. In contrast to unspliced elements the strength and stiffness of a system composed of butt-jointed elements are significantly influenced by the size, type and location of the nails. BOHNHOFF ET AL. (1991) reported on tests performed on single and trio beams. The trio beam designs included a sample of unspliced posts as well as samples of posts with staggered butt-joints with and without outside reinforcement. The reinforcement was a high-strength toothed metal plate which was applied on the outside of the spliced post. Two types of nails and nail application (gun-driven ring shank nails of 3.68 mm in diameter and $l = 102$ mm vs. machine-driven nails of 4.8 mm diameter and $l = 115$ mm) were analysed in separate samples but a significant difference could not be confirmed. Analysis of failure characteristics of single and trio beams showed in principle no difference. As expected the primary element causing failure was the longest (sub)element in the center with the longest contact length to adjacent elements. This element is exposed to a maximum of local stress concentrations and load sharing constraints. In the samples with reinforcement the bearing capacity of the reinforcement was reached already before the system failed. The reinforcement not only homogenised the stress distribution near the butt-joint. It also caused a certain lower bounding of the strength distribution by preventing early failures below a certain threshold. By comparison of the tested designs a ratio $f_{N,m,mean} / f_{1,m,mean}$ of 0.89 was found in the sample of unspliced posts whereas a ratio of $0.42 \div 0.43$ was found for spliced posts. This reduction is much higher than expected from an engineering model were at least two elements are treated as being always active in a trio beam. Nevertheless, these two elements are not at their maximum capacity at the point where the weakest element fails. This consequencies on a lower system bearing capacity as assumed by an averaging process (see BOHNHOFF ET AL., 1991) but also because load redistribution capacity in systems of $N = 3$ is limited. Furthermore, first failure is also influenced by higher local stress concentrations in elements and nails due to a certain amount of **interlayer slip** between the elements as it is common in flexible splices (e.g. BOHNHOFF ET AL, 1992), but also due to a higher variability between the elements as one element itself is composed of at least two independent sub-elements. In the samples of reinforced posts

the ratio is 0.47 ÷ 0.50. The ratio CoV[$f_{N,m}$] / CoV[$f_{1,m}$] is roughly 40% in the designs of unspliced and spliced but reinforced posts, and roughly 55% in spliced but not reinforced trio beams. A significant difference between unspliced and spliced as well as between unreinforced and reinforced post design was confirmed. The ratio of $E_{N,m,0,mean}$ / $E_{1,m,0,mean}$ is 1.09 if unspliced, 0.65 if spliced and 0.80 if spliced but reinforced. The variability in $E_{m,0}$ was only (50 ÷ 60)%, irrespective of the post design if compared to the elements. WILLIAMS ET AL. (1994) enlarged previous works on nail-laminated posts by analysing systems of $N = 1, 4$. In their survey they concluded that the load-bearing behaviour in mechanically laminated assemblies is primary dependent on (1) the interlayer shear transfer capacity, (2) the splice arrangement, (3) the splice length, and (4) the existence of a butt-joint reinforcement. In their tests the material was again Southern pine, but machine stress rated (MSR) to grade 2250f-1.9E. Tests on elements and in total on five designs of unspliced and spliced (butt-jointed) posts were made. The influence of butt-joint reinforcement, splice distance and splice-design were examined. The elements were connected by gun-driven nails with a diameter of 3.3 mm and a length of $l = 95.3$ mm. These were placed every 305 mm in the unspliced and every 76 mm and 152 mm in and near the spliced area. As expected, the failure took place primary in the center elements and near butt-joints. Also here the reinforcement buckled already before the maximum load of the system was reached. The ratio $f_{N,m,mean}$ / $f_{1,m,mean}$ is nearly 1.0 in unspliced samples, 0.30 in case of only 1.22 m splice length and 0.45 in case of 1.83 m splice length, with the tendency to decrease further in splice-designs with longer total contact length between the (sub)elements. In the group with reinforcement and 1.83 m splice length a ratio of 0.59 is realised. The ratio CoV[$f_{N,m}$] / CoV[$f_{1,m}$] is about 0.6 in the sample of unspliced and spliced elements with 1,219 mm splice length but reduced total contact length, about 0.65 in spliced posts with higher total contact length, irrespective of the splice distance, and 0.50 in the sample of reinforced butt-joints. The variability in bending E-modulus CoV[$E_{N,m,0}$] follows roughly the averaging model. The change in overall splice length from 1.22 m to 1.83 m leads to a significant increase in system bearing capacity. This is because of a more homogeneous load transfer and due to the reduction of load per nail. The reduction of the total contact length and the use of butt-joint reinforcements additionally lead to a significant increase in bearing capacity.

Based on these previous works on mechanically laminated posts BOHNHOFF (1995) proposed repetitive member factors (equivalent to $k_{sys,05}$) for the design of these systems in case of bending stresses applied edgewise on the elements (see Tab. 5.16). These factors have to be adjusted by a multiplication factor of 1.00 in case of unspliced posts

and 0.42 and 0.55 in case of spliced posts without and with butt-joint reinforcement, respectively. A further comprehensive study on nail-laminated posts was published by BOHNHOFF ET AL. (1997). They report on tests on systems composed of $N = 1, 2, 3, 4$ unspliced elements of Southern pine of visually grade No. 2 and machine grade 2250f-1.9E. Two further samples of MSR quattro beams were tested by loading only the outer elements. One of these samples had also higher nail density (nail spacing 152 mm instead of 305 mm) to increase the shear capacity against interlayer slip. The results show a concave decrease in $f_{N,m,mean} / f_{1,m,mean}$ with N. This decrease is higher in systems composed of visually graded elements. Note: Structural timber with a remarkable higher variability in its characeristics. The application of load only on the outer layers of quattro beams showed only a minor reduction (0.96 → 0.94). The sample with higher nail density showed no increase in system strength. It can be assumed that the stiffness in case of 305 mm nail spacing is already high enough to ensure sufficient load sharing among the elements. The ratio CoV[$f_{N,m}$] / CoV[$f_{1,m}$] shows a remarkable higher non-linear decrease than expected from the averaging model. In contrast, $E_{N,m,0,mean}$ increases only minor. The reduction in CoV[$E_{N,m}$] is even stronger than expected from the averaging model. Nevertheless, the application of the averaging model for system E-modulus is proposed by BOHNHOFF ET AL. (1997). In EP559 FEB03 a guideline for the design of mechanically laminated posts is published. Therein the repetitive member factors in Tab. 5.16 were used by taken into account the results of BOHNHOFF ET AL. (1997) with slight changes in the factors for posts composed of visually graded elements, with 1.35 and 1.40 for trio and quattro beams, respectively.

Tab. 5.16: Repetitive member factors for systems composed of mechanically laminated and edgewise loaded elements under bending stresses; BOHNHOFF (1995)

	DUO	**TRIO**	**QUATTRO**
visually graded	1.25	1.30	1.42
mechanically graded	1.15	1.25	1.30

As next systems of type (1c) according Fig. 5.27 are investigated in more detail. For example WILSON AND COTTINGHAM (1952) analysed various lay-ups of systems under variation of the quantity of interacting lamellas, the type of loading and the orientation of elements in respect to loading direction. In one sub-series systems of Douglas fir composed of eigth flatwise loaded and glued elements versus systems of four edgewise loaded elements were tested in shear by means of a four-point bending test configuration.

Each sample consisted of 20 specimens. All systems had a cross section of approximately w / d = 150 mm / 300 mm. In both samples only 40% to 60% of the specimen failed in shear. Consequently all test results of WILSON AND COTTINGHAM (1952) were re-evaluated to acount for the censoring in the data. Therefore the maximum likelihood method (MLE) for right-censored data was applied under the assumption of lognormally distributed characteristics. The parameters of 2pLND were found by maximising the log-likelihood function

$$\ln\left[L\left(\hat{\theta}\right)\right] = \max_{\theta} \left[\ln\left[L(\theta)\right]\right], \text{ with } L(\theta) = \prod_{i=1}^{n} f_{X_i}\left(x_i|\theta\right)^{d_i} \cdot \left[1 - F_{X_i}\left(x_i|\theta\right)\right]^{1-d_i}, \tag{5.13}$$

with indicator variable $d_i = 1$ if the event equals the target and $d_i = 0$ otherwise. The main statistics of both samples are given in Tab. 5.17. The expectation and CoV of bending characteristics are based solely on bending failures whereas statistics of shear strength are based on shear failures.

Tab. 5.17: Main statistics of shear tests on systems composed of eight flatwise loaded and four edgewise loaded elements; test data of WILSON AND COTTINGHAM (1952); re-evaluated by means of MLE for right censored data

	$E_{m,mean}$ [N/mm²]	CoV[E_m] [%]	$f_{m,mean}$ [N/mm²]	CoV[f_m] [%]	$f_{v,mean}$ [N/mm²]	CoV[f_v] [%]
8# flatwise loaded elements	15,923	7.1%	62.4	11.1%	3.4	9.2%
4# edgewise loaded elements	16,201	8.6%	60.6	18.3%	4.4	11.1%

A comparison of the statistics given in Tab. 5.17 in regard to shear strength gives in mean 29% higher shear strength in systems of edgewise loaded elements. This is in particular of interest because the number of flatwise loaded elements is twice the number used in edgewise loaded elements.

In the report of MCALISTER (1974) also test results from glued-laminated duo beams of Southern pine No. 2 are presented. Two samples, one width phenol resorcinol and the other with neopren-base adhesive were tested in four-point bending. A comparison with a control sample of unconnected duo beams shows an increase in $E_{N,m,0,mean}$ and $f_{N,m,mean}$ of (5 ÷ 8)% and (57 ÷ 58)%, respectively due to activation of rigid composite action with continuous load sharing between the segments of elements.

Tab. 5.18: Main statistics of bending tests performed on post-tensioned decks of various widths; SEXSMITH ET AL. (1979)

	Hem fir			White pine			Red pine		
	N [#]	$f_{m,mean}$ [N/mm²]	CoV[f_m] [%]	N [#]	$f_{m,mean}$ [N/mm²]	CoV[f_m] [%]	N [#]	$f_{m,mean}$ [N/mm²]	CoV[f_m] [%]
single	1#	45.9	33.0%	1#	16.0	36.0%	1#	28.0	36.0%
1 ft	6#	46.9	16.0%	6#	19.4	15.0%	6#	27.5	21.0%
2 ft	12#	43.9	9.0%	12#	21.2	7.0%	12#	29.0	14.0%
3 ft	19#	44.8	8.0%	16#	18.3	8.0%	17#	28.8	7.0%

Another comprehensive test series on parallel systems composed of rigidly connected elements is given by SEXSMITH ET AL. (1979). They investigated the load sharing behaviour of post-tensioned vertically laminated beams as for example used for timber bridge decks. Dependent on the post-tensioning this system is in real something in between (1b) and (1c). Nevertheless, due to the high amount of post-tensioning and friction between neighboured segments of the elements this type is further treated as being comparable to (1c). In their analysis three timber species (Hem fir, No. 2 and better, green condition; White pine, ungraded, $u = 19\%$; Red pine, ungraded, $u = 19\%$), three different widths of the decks (305 mm, 610 mm, 915 mm) and ten replicants per sample were tested in four-point bending. Additional bending tests on single elements with a cross section of $w / d = 38$ mm / 235 mm were performed. Based on the test results the averaging model for $E_{N,m,0,mean}$ and CoV[$E_{N,m,0}$] could again be verified. The main statistics of bending strength are given in Tab. 5.18. Based on these and with the background information that the timber quality of White pine was lower than of Hem fir and Red pine it can again be concluded that a negative dependency of system effect on the mean level on timber grade is given. Hereby the ratio $f_{N,m,mean} / f_{1,m,mean}$ is nearly always 1.00 except the samples of White pine which give a ratio in the range of $1.15 \div 1.32$, nevertheless without trend to N. In contrast, ratio CoV[$f_{N,m}$] / CoV[$f_{1,m}$] decreases non-linearly in N but irrespective of the timber species or grade, from 1.00 for $N = 1$ to $0.42 \div 0.58$ at $N = 6$, $0.19 \div 0.39$ at $N = 12$ and $0.19 \div 0.24$ at $N = 16 \div 19$. SEXSMITH ET AL. (1979) postulate the full applicability of the averaging model for the bending strength, for expectation and variability. Furthermore, only a marginal increase in ductility in systems was observed with increasing N.

WOLFE AND MOODY (1979) performed a literature survey. In reference to BONNICKSEN AND SUDDARTH (1966), NEMETH (1967) and MCALISTER (1974) they concluded that the magnitude of parallel system effects is indicated to depend on timber quality and N. Their own test results performed on high quality L1 Douglas fir, medium quality N2D Southern pine and low quality L3 Douglas fir on systems with $N = 1, 2, \ldots, 5$ elements with cross section $w / d = 38$ mm / 140 mm once again confirmed that the ratio $E_{\mathrm{N,m,0,mean}} / E_{\mathrm{1,m,0,mean}}$ can be taken equal to 1.00. Furthermore, CoV[$E_{\mathrm{N,m,0}}$] as well as CoV[$f_{\mathrm{N,m}}$] follow approximately the averaging model. In line with previous findings a negative dependency of $f_{\mathrm{N,m,mean}}$ on timber grade was observed. In all samples an increasing mean value was found, with significant increase from $N = 1 \rightarrow 2$ and $N = 2 \rightarrow 3$. In systems of $N \geq 3$ a further significant increase could be determined. Note: Also CoV[$f_{\mathrm{1,m}}$] increased with decreasing timber quality. WOLFE AND MOODY (1979) observed no differences in the failure characteristics between systems and elements. They note that systems suffer from the **edge effect** which compensates weak zones in elements by stronger, adjacent segments. They defined the power model as given by equ. (5.14) for estimating $f_{\mathrm{N,m,05}}$ in dependency of CoV[$f_{\mathrm{1,m}}$], N and timber grade. Timber grade is considered by the strength ratio (SR) which transfers the strength of clear wood $f_{\mathrm{m,mean,CW}}$ to that of structural timber of a specified grade. Following this model values of $k_{\mathrm{sys,05,N\geq 3}} = 1.50$ and $2.50 \div 3.00$ are proposed for highest and lowest timber grades, respectively.

$$f_{N,m,05} = f_{m,mean,CW} \cdot SR^{\gamma} \cdot N^{\alpha} \cdot \left[1 - 1.645 \cdot \frac{CoV\left[f_{1,m}\right]}{\sqrt{N}} \right] \text{, with } \alpha = 0.329,\ \gamma = 0.81 \qquad (5.14)$$

WRIGHT (1987) analysed the bearing capacity of trio and quattro beams composed of glued finger jointed elements in four-point-bending. The systems were made of Southern pine of grade No. 2 KD15 and tested at $u = 12\%$. Due to missing data for the single elements only a relative comparison between trio and quattro beams is possible, with cross sections $w / d = 102$ mm / 179 mm and 140 mm / 179 mm, respectively. The failure was primarily induced or in the area of finger joints. An increase in mean bending strength from $N = 3 \rightarrow 4$ of +15% and an increase in bending E-modulus of +4% was observed, together with a slight reduction in CoV[$f_{\mathrm{N,m}}$] and CoV[$E_{\mathrm{N,m,0}}$].

As previously discussed for systems (1a) BAKHT AND JAEGER (1991) proposed models for calculation of the system effect for systems of type (1c) based on simulations on system type (1a) and test results of SEXSMITH ET AL. (1979). They defined $f_{\mathrm{N,m,s}} / f_{\mathrm{1,m,s}}$ vs. N given as

$$\frac{f_{N,m,s}}{f_{1,m,s}} = \sqrt{\frac{2}{N+1}}\,, \tag{5.15}$$

by an upper bound fitting to test data, with $f_{\mathrm{N,m,s}}$ and $f_{\mathrm{1,m,s}}$ as standard deviation observed in test samples of systems and elements, respectively. The model is a shifted averaging model of variability. The ratio of $f_{\mathrm{N,m,mean}}$ / $f_{\mathrm{1,m,mean}}$ was taken equal to 1.00. Following that and based on reliability calculations by means of 2pLND for actions and resistances, system factors $k_{\mathrm{sys,N,05}}$ for OHBDC-91-01 were defined. The proposed functions and factors are thereby in dependency of timber grade, the associated CoV and the quantity of interacting parallel elements N, for systems under bending, shear or tension stresses parallel to grain.

BRANDNER (2006) and BRANDNER AND SCHICKHOFER (2006) report on various test series performed for the determination of parallel system effects on duo and quattro beams of finger jointed structural timber, glulam and cross laminated timber (CLT). The first test series was done on glulam beams (see SCHICKHOFER, 2004) composed of edgewise loaded lamellas of Norway spruce and strength class C16/C24 according EN 338. Systems of $N = 1, 2, 4, 8$ elements were tested in four-point bending. The cross section of the elements was w / d = 36 mm / 100 mm. The test results show an increase of $f_{\mathrm{N,m,mean}}$ from 4 to 5% from $N = 1$ to $N \geq 2$ and a reduction in CoV[$f_{\mathrm{N,m}}$], even higher than predicted by the averaging model. JÖBSTL ET AL. (2006) report on four-point bending tests on five-layered cross laminated timber elements of Norway spruce lamellas (strength class C24 according EN 338) with equal thickness, a depth of 110 mm and a width of the segment equal to the width of the board with w = 120 mm. Thereby systems of $N = 1, 2, 4, 8$ were examined. Again, an increase of $f_{\mathrm{N,m,mean}}$ of 3% from $N = 1$ to $N \geq 2$ and a reduction in CoV[$f_{\mathrm{N,m}}$] even a bit higher than predicted by the averaging model could be observed. A further test series on systems composed of $N = 1, 2, 4$ elements of finger jointed construction timber of Norway spruce (strength class C24 according EN338) was accomplished by BRANDNER (2006). The cross section of the systems were N-times the cross section of the elements of w / d = 80 mm / 160 mm. All elements were proof loaded in tension parallel to grain with a proof level of $\sigma_{\mathrm{t,0,pl}}$ = 7.0 N/mm². The test results show an increase in $E_{\mathrm{N,m,0,mean}}$ of about 5% and in $f_{\mathrm{N,m,mean}}$ of about 15%. The coefficients of variation CoV[$f_{\mathrm{N,m}}$], CoV[$E_{\mathrm{N,m,0}}$] and CoV[ρ_{N}] can be well estimated by the averaging model. By investigating published and own results on systems stressed in bending and tension parallel to grain BRANDNER (2006) formulated a simple model for

the estimation of the 5%-quantile of system strength $f_{N,05}$ in dependency of N and CoV[f_1] by means of

$$E[f_N] = E[f_1],\ CoV[f_N] = CoV[f_1] \cdot N^{-2 \cdot CoV[f_1]}, \tag{5.16}$$

with $f_1 \sim$ 2pLND and CoV[f_1] $\leq$ 25%.

EISER (2008) investigated the system bearing capacity of duo and trio beams composed of finger jointed glulam-lamellas of Norway spruce, w / d = 22 mm / 240 mm by testing in four-point bending. Two timber grades (C24/C30 and C35+ according EN 338) were used. Analysis of the test results shows an increase of $E_{N,m,0,mean}$ from $N = 1$ to $N \geq 2$ of (7 ÷ 10)% and 6%, and an increase in $f_{N,m,mean}$ from $N = 1$ to $N \geq 2$ of 33% and 16% in systems composed of elements C24/C30 and C35+, respectively. The unexpected high increase in $f_{N,m,mean}$ was interpreted as a consequence of not adequate grading, which was done for tensile characteristics according the requirements on glulam-lamellas and not for edgewise bending. In particular edge knots, which are not as decisive for tension as for bending, are assumed to cause low strength capacity in single elements. In systems and due to the edge effect a remarkable increase of strength in duo beams is given. Corresponding to most previous cited data sets a reduction of CoV[$f_{N,m}$], CoV[$E_{N,m,0}$] and CoV[ρ_N] according the averaging model was observed. Later, EISER ET AL. (2010) tested single elements and duo beams of Norway spruce in bending. The cross section of the elements (strength class C24+ according EN 338) was w / d = 40 mm / 245 mm, that of the duo beams 80 mm / 240 mm. The duo beams showed an increase of 5% and 21% in $E_{N,m,0,mean}$ and $f_{N,m,mean}$, respectively, and again a reduction of CoV[$f_{N,m}$], CoV[$E_{N,m,0}$] and CoV[ρ_N] according the averaging model. As in EISER (2008) the elements were again graded in tension and not according the requirements on edgewise bending. Recently, a comprehensive research project on duo or trio beams and glulam of two or three laminations of the same dimensions was accomplished and published by FAYE ET AL. (2010). Thereby, two timber species (groups) (Douglas fir, Norway spuce & fir) and three timber grades (C18, C24 and C30 according EN 338) were tested in four-point bending. In both, edgewise and flatwise loaded systems $E_{N,m,0,mean}$ was found to be on average equal to $E_{1,m,0,mean}$ of the single elements tested edgewise. In particular in the mean bending strength $f_{N,m,mean}$ of edgewise loaded systems no clear trend and no dependency on timber grade or species was dedected. If flatwise loaded a reduction in $f_{N,m,mean}$ of roughly 10% was given. The coefficients of variation CoV[$E_{N,m,0}$] and CoV[ρ_N] of flatwise and edgewise loaded systems can be well estimated by the averaging model. The

same was found for CoV[$f_{N,m}$] in case of edgewise loaded systems, whereas in flatwise stressed systems (glulam) no clear trend could be determined.

Intermediate Conclusions found in respect to Parallel System Actions and Effects

So far presentation focused on a comprehensive literature survey on parallel systems composed of elements placed side-by-side and constrained to equal elongation or deflection. Numerous publications regarding systems with a secondary load-distributing element also exist but due to the focus of this work these are not discussed further. Nevertheless, on delivered background some important conclusions can be made:

- due to the hierarchical structure inherent in wood, timber and engineered timber products and structures the material (system) structure and action can be described as parallel, sub-serial;
- it was found that concerning their reliability and their system behaviour herein discussed parallel systems are in between serial and parallel redundant systems;
- it was generally concluded, that system effects are in principle dependent on the stochastics within and between elements or even sub-elements (segments);
- the main parameters which determine system effects were identified as: (i) the type of system, (ii) the quantity of interacting elements N, (iii) the degree of connection between the elements, and (iv) the stochastic nature of the elements, in particular the variability, e.g. CoV;
- two types of systems were defined: type 1 composed of side-by-side placed elements (directly stressed) and type 2 composed of elements which are connected by a secondary load-distributing element (indirectly stressed);
- the required stochastic information depends on the degree of connection between the elements; in case of unconnected (loose) elements the system behaviour can be sufficiently characterised by the stochastics of elements; in case of rigidly and continuously connected elements comprehensive stochastic information including also the spatial correlation and distribution of local characteristics within and between the elements and segments is required;
- on the basis of a comprehensive literature survey on parallel systems stressed in tension or compression parallel to grain, in bending or shear the following statements can be made:

- the expectations of E-modulus and density $E_{N,mean}$ and $\rho_{N,mean}$ as well as their variabilities expressed by CoV[E_N] and CoV[ρ_N] follow in principle the averaging model;
- in most publications test data of strength values confirm also the applicability of the averaging model for the estimation of CoV[f_N]; this is in particular of interest as SMITH (1980) observed that CoV[X_N] in fibre bundles and in case of GLS decreases proportional to $\sim 1 / \sqrt{N}$ whereas in LLS a proportional decrease of $a / \ln(N)$, with a constant was observed; this was also confirmed e.g. by KLOSTER ET AL. (1997) (see section 3.2.4);
- the expectation of system strength $f_{N,mean}$ was found to depend on timber grade, with $f_{N,mean} / f_{1,mean} \approx 1.00$ for high grades and $f_{N,mean} / f_{1,mean} > 1.00$ for low grades;
- the expectation of system strength was also found to be significantly influenced by the grading method used for the elements if the grading procedure is not congruent with later stress situations.

5.2 System Effects on Density and their Relevance for Design Procedures

Density of wood, timber and engineered timber products is in general one of the three characteristics determining grade. For example the strength class system provided by EN 338 is based on the characteristic bending strength (5%-quantile), bending E-modulus (mean value) and density (5%-quantile).

In general, as the density of systems is nothing else than the average of the densities of elements and sub-elements composing the system, its distribution follows the averaging model, see equ. (3.132). Thereby independency between the elements but not necessarily between sub-elements can be assumed. The RSDM of global density of elements (the density determined by dividing total mass by total volume) is often assumed to be normally distributed. In general this can be expected because of the fact that already the global density is nothing else than the average of local densities. Nevertheless, comprehensive data analysis e.g. by BURGER (1998B), BRANDNER AND SCHICKHOFER (2007) and BRANDNER ET AL. (2012) showed a preference of 2pLND. The reason is seen in the distinctive equicorrelation between local densities within elements which

decisively contradicts constraints of the central limit theorem. Based on the analysis of BRANDNER AND SCHICKHOFER (2007) and BRANDNER ET AL. (2012) a relative variation of global density between the elements with CoV[ρ_{12}] = (6 ÷ 10)% can be expected. As the arrangement of elements within the system is irrelevant, decrease of variance is proportional to the number of elements ($N \cdot M$). Consequently and so far iid elements can be assumed $\rho_{12,(N\cdot M),mean}$ and CoV[$\rho_{12,(N\cdot M)}$] can be calculated as

$$\rho_{12,(N\cdot M),mean} = \rho_{12,1,mean}\,,\; CoV\left[\rho_{12,(N\cdot M)}\right] = \frac{CoV\left[\rho_{12,1}\right]}{\sqrt{(N\cdot M)}}\;. \tag{5.17}$$

The 5%-quantile can be calculated according equ. (2.80) by assuming also iid $\rho_{12,i}$ ~ 2pLND. As the median of X ~ 2pLND is smaller or equal the mean value of X the 5%-quantiles of $\rho_{12,1}$ ~ 2pLND are larger than in case of $\rho_{12,1}$ ~ ND. Nevertheless due to the low CoV[$\rho_{12,1}$] the differences are negligible and disappear with increasing number of elements.

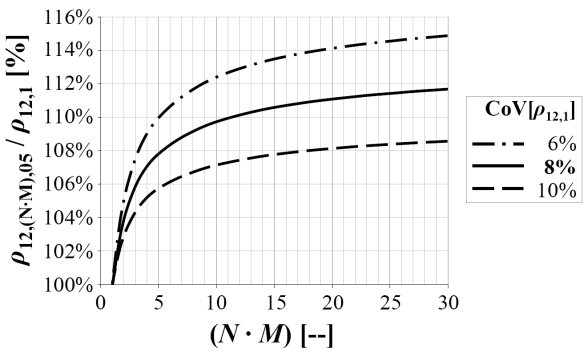

Fig. 5.28: Relative change of 5%-quantile of density of systems in dependency of the system size ($N \cdot M$) and CoV[$\rho_{12,1}$], assuming iid $\rho_{12,1}$ ~ 2pLND

Fig. 5.28 shows the relative change of $\rho_{12,(N\cdot M),05}$ in dependency of ($N \cdot M$), with iid $\rho_{12,1}$ ~ 2pLND and approximated $\rho_{12,(N\cdot M)}$ ~ 2pLND. The changes are not dramatic because of the relatively low variation in density. Nevertheless, if for example the density of glued laminated timber (GLT) with reference cross section w_{GLT} / d_{GLT} = 150 mm / 600 mm and 15 lamellas with a standard thickness of t_{lam} = 40 mm is of interest $\rho_{12,(N\cdot M),05}$ can be expected to be 10% higher than $\rho_{12,1,05}$. This circumstance is taken into account by current product standards, e.g. EN 1194 and PREN 14080. According to Fig. 5.28 it can be seen

that already the 5%-quantiles of density of duo, trio and quattro beams is expected to be about 4%, 6% and 7%, respectively, higher than that of the elements.

The characteristic density is in particular used as indicating property for estimating the bearing capacity of metal fasteners placed in wood and timber, e.g. for the embedment strength of dowel-type fasteners and for the withdrawal strength of axially loaded (self-tapping) screws. For dowel-type fasteners, primary stressed in shear, the local resistance of timber against compression stresses in an angle to grain is decisive. In contrast, the withdrawal resistance of screws, primary stressed axially, is defined by the local shear resistance of timber in an angle to grain direction.

Current regulations for both resistance characteristics as provided by EN 1995-1-1 are based on regression equations, established by fitting test data. The embedment strength parallel to grain of bolts up to a diameter of $d \leq 30$ mm is given as

$$f_{h,0,k} = 0.082 \cdot (1 - 0.01 \cdot d) \cdot \rho_k \,, \tag{5.18}$$

and the withdrawal strength perpendicular to grain as

$$f_{ax,90,k} = 3.6 \cdot 10^{-3} \cdot \rho_k^{1.5} \,. \tag{5.19}$$

Thereby diameter d and characteristic density ρ_k (lower confidence limit of the 5%-quantile) have to be inserted in [mm] and [kg/m³], respectively, to get $f_{h,0,k}$ and $f_{ax,90,k}$ in [N/mm²].

Due to the linear influence of ρ_k on the embedment strength the resistance of fasteners in timber at fixed d increases linearly with increasing ρ_k. Nevertheless, due to the non-linear influence of ρ_k on the withdrawal strength the resistance increases progressively with increasing ρ_k, e.g. with $k_N = 10\%$ and $(1 + k_N)^{1.5} = 115.4\%$ a plus of 15.4% in $f_{ax,90,k}$ is given.

Because of the local placement of fasteners it is not the global but the local density which is of interest and which decisively influences the resistance in timber. Beside this fact a common practise in designing fasteners placed, e.g. in GLT is to make use of the characteristic density of the system product, irrespective of the number of elements penetrated by the fastener. Furthermore, in most system products fasteners can be placed in different ways, e.g. in linear members like GLT perpendicular to face or edge of the

lamellas, penetrating ≥ 1 and only one lamella, respectively. Consequently, if only one element is penetrated the resistance is only determined by the local density and its variation. Thereby local variation can be very significant, e.g. if considering the change from juvenile to adult wood (see section 4.2.1) or the occurrence of knots which e.g. in Norway spruce shows a 3 ÷ 4 times higher density if compared to surrounding wood. Again, if more than one element is penetrated by a fastener at least the averaging model for calculating the characteristic density according equ. (3.132) can be applied. Thereby also the distribution of action and resistance along the axis of fasteners has to be taken into account. For example, full-threaded self-tapping screws placed transversely to grain show roughly a triangular stress distribution along the screw axis.

In addition to this aspect of a non-linear stress distribution, system effects on density as indicating property of withdrawal strength are further discussed. On one hand it was observed that already the penetration or contribution of a small knot by a self-tapping screw nearly doubles the withdrawal capacity if compared to tests on knot free specimen. On the other hand stresses in general concentrate at stiffer elements (layers) which are in particular in a porous material like wood and timber directly associated with a higher density. So, if iid elements and a homogeneous stress distribution along the screw axis can be assumed, and if a high positive correlation between local density and local stiffness characteristics is taken into account, the withdrawal strength is given by a function of the maximum density of all penetrated elements as a first-failure system can be assumed. The last assumption is adequate because of the low variability in density and related withdrawal strength which allows only minor if any load redistribution and a further increase in bearing capacity. Consequently, the indicating property of withdrawal strength ρ_{12} is given by $\max[\rho_{12,i}]$, with $i = 1, \ldots, (N \cdot M)$.

For quantification of this effect, systems of $(N \cdot M) = 1, \ldots, 100$ iid elements with densities $\rho_{12,1} \sim$ 2pLND, $E[\rho_{12,1}] = 450$ kg/m³ and $CoV[\rho_{12,1}] = (6, 8, 10)\%$ were generated in R (2009). Thereby the maximum density of elements per system with 10,000 runs each was calculated and analysed statistically. Main results like the relative changes of $E[\max[\rho_{12,i}]]$, $CoV[\max[\rho_{12,i}]]$ and $\max[\rho_{12,i}]_{05}$ are shown in Fig. 5.29. Due to powerful resuls in fitting equ. (3.101) to minima the same approach was used for the maxima system densities. The corresponding parameters are given in Tab. 5.19. Again and as already known from fitting to minima the ratio $E[\max[\rho_{12,i}]] / E[\rho_{12,1}]$ versus $(N \cdot M)$ is perfectly represented by equ. (3.101) whereas fitting to $CoV[\max[\rho_{12,i}]] / CoV[\rho_{12,1}]$ versus $(N \cdot M)$ shows minor deviations. Nevertheless, comparison of 5%-quantiles from

simulations and model calculations with the assumption that the distribution of max[$\rho_{12,i}$] can be approximated by a 2pLND gives reliable estimates, see Fig. 5.29 (right). Overall this system effect influences the 5%-quantile of density to a greater extend and thus also the withdrawal strength as expected from the averaging model. In contrast to the averaging model a remarkable effect on expectation can be observed whereas the homogenisation expressed by relative decrease of CoV[max[$\rho_{12,i}$]] is considerably lower. The increase in expectation was also observed in tests reported by REICHELT (2012). Nevertheless, before a comprehensive bearing model of self-tapping screws in timber can be proposed clarification of the influence of non-linear stress distribution along the screw axis is required.

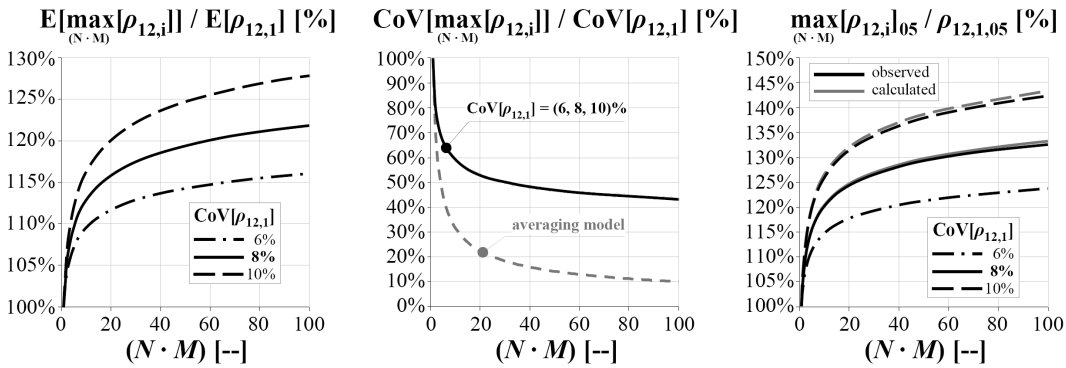

Fig. 5.29: Relative change of expectation (left), CoV (middle) and 5%-quantile (right) of density in dependency of system size ($N \cdot M$) and CoV[$\rho_{12,1}$] in case of the maximum model; additionally a comparison between CoV[max[$\rho_{12,i}$]] / CoV[$\rho_{12,1}$] based on simulations and according the averaging model (middle) & a comparison between simulated (observed) and calculated 5%-quantiles (right)

Tab. 5.19: Best fitted parameters α_ξ and β_ξ of equ. (3.101) determined by means of LSM and for expectation and CoV of max[$\rho_{12,i}$]

	ξ = max[CoV[$\rho_{12,i}$]]	ξ = E[max[$\rho_{12,i}$]]		
CoV[$\rho_{12,1}$] =	**(6, 8, 10)%**	**6%**	**8%**	**10%**
α_ξ	0.8351	–0.1616	–0.2136	–0.2705
β_ξ	0.3764	0.3281	0.3304	0.3219

Back to the variation of local density, results in section 5.1.1 showed that a very high equicorrelation of $\rho_{equi}[\rho_{12,i}] = 0.80 \div 0.90$ can be expected, e.g. between segments of 150 mm or 300 mm length (see STUEFER, 2011). Consequently, only a small proportion

of variation observable between elements origin from variation within the members. For example, given a two level hierarchical model $Z_{ij} = Y_j + X_{ij}$ with Y_j as mean of the jth element and X_{ij} as iid deviation from Y_j by sub-element i of element j, with $\mu_X = E[X_{ij}] = 0$, $Var[X_{ij}] = \sigma_X^2$, $CoVar[Y_j + X_{ij}, Y_j + X_{kj}] = Var[Y_j] = \sigma_Y^2$, $E[Z_{ij}] = E[Y_j] = \mu_Y$ and $Var[Z_{ij}] = \sigma_X^2 + \sigma_Y^2$, the equicorrelation ρ_{equi} is generally given as (see e.g. KÄLLSNER ET AL., 1997)

$$\rho_{equi} = \frac{\sigma_Y^2}{\sigma_X^2 + \sigma_Y^2} \,. \tag{5.20}$$

Thus the equicorrelation is the fraction of variance between the elements to the sum of variances between and within the elements.

Following the above defined two-level hierarchical model for density with parameters $\rho_{equi} = 0.85$ and $CoV[\rho_{12}] = (\sigma_X^2 + \sigma_Y^2)^{0.5} / \mu_Y = 8\%$ the coefficients of variation $CoV[X_{ij}]$ and $CoV[Y_j]$ are 3.1% and 7.4%, respectively. In general, hierarchical models imply a correlation independent of separation. Nevertheless, the involved volume of timber occupied by fasteners is even more locally than analysed in STUEFER (2011). Thus a scale transition has to be considered.

Concerning the above discussed homogenisation effect in characteristic densities of systems with iid elements, only a part of the observed variance between the elements, expressed by equicorrelation, can be taken into account. In the example above this is not $CoV[\rho_{12}] = 8\%$ mentioned before but $CoV[\rho_{12}] = 7.4\%$. Nevertheless, the overestimation of the ratio $\rho_{12,(N \cdot M)} / \rho_{12,1}$ using $CoV[\rho_{12}] = 8\%$ is negligible.

To conclude, the relevance of system effects and the basics of density regulations for system products in relationship to the density of composing elements were shown. A simple model for calculating the system effect in case of iid elements was provided. The influence of density on fasteners was presented and discussed in respect to current design practise and regulations in EN 1995-1-1. Furthermore, a first model for the influence of density on withdrawal strength of self-tapping screws was developed, but it needs further adaptation to account for non-linear stress distribution along screws. However, the influence of local density variation within and between elements concerning the placement of fasteners in system products and in respect to group effects between fasteners is outside the scope of this study.

5.3 System Effects on Stiffness Characteristics and their Relevance for Design

Stiffness characteristics of timber elements as well as of fasteners are relevant for a variety of designs. In the allocation process of structural timber and engineered timber products to strength classes mainly the compliance of mean E-modulus is required, but in designing timber structures also the 5%-quantile of modulus of elasticity and shear are important. In serviceability limit state design (SLS) average stiffness determines the ability to withstand deflection and thus exhibit a characteristic relevant for design. In some cases, (i) if a deflection limit has to be guaranteed for the life-time of a construction, or (ii) in case of large sliding doors or automatic racking systems in high rack warehouses, it may be indicated to design the deflections on the 5%-level by considering additionally long-term effects as creep. In ultimate limit state design (ULS) 5%-quantiles of modulus or extreme values of elasticity and shear are of relevance for calculations according theory of first or second order. This is in particular true for lateral (torsional) buckling as well as column buckling and for the calculation of internal stresses in statically indetermined structures. Therefore models which enable accurate estimation of distributions of stiffness characteristics in system products are relevant. They should reflect the dependency on the arrangement, quantity and characteristics of the elements in systems.

The following sections concentrate (section 5.3.1) on the definition of expectable stiffness characteristics in structural timber and show possibilities in modelling parallel (section 5.3.2) and serial system effects (section 5.3.3). At the end the relevance of correct modelling is shown by explicit consideration of stiffness characteristics common in timber.

5.3.1 Variation of E- and G-Modulus within and between Structural Timber Elements

Before discussing modelling of serial and parallel system effects on E- and G-modulus their expectable variations have to be defined. Therefore a literature survey was performed to clarify the variation between and within structural timber elements. For this data from publications already discussed in context with serial correlation of timber properties in section 5.1.1 is analysed.

Tab. 5.20: Variation of local E-modulus in bending: analysis based on data from TAYLOR (1988)

nom. grading class	L1	302-24
n **[#]**	498#	497#
CoV[$E_{m,0,i}$]$_{mean}$ [1] [%]	5.0%	4.0%
CoV[$E_{m,0}$]$_{mean}$ [2] [%]	16.9%	17.1%

[1] arithmetic mean of the coefficient of variation of E-moduli of sub-elements within one element; 4 sub-elements each

[2] arithmetic mean of the coefficient of variation of E-moduli of elements (including within and between variation)

Tab. 5.21: Variation of local E-modulus in bending: analysis based on data from RICHBURG (1989)

nom. grading class	C14	2.3 1/6	2.3 1/3	2.0 1/6	2.0 1/3	1.7 1/4	L2 1/3	L3 1/2
n **[#]**	189#	172#	29#	196#	180#	165#	173#	199#
CoV[$E_{m,0,i}$]$_{mean}$ [1] [%]	6.5%	5.6%	6.4%	5.8%	7.5%	6.5%	7.7%	10.8%
CoV[$E_{m,0}$]$_{mean}$ [2] [%]	12.4%	8.6%	10.4%	7.7%	9.0%	10.7%	13.7%	17.5%

[1] arithmetic mean of the coefficient of variation of E-moduli of sub-elements within one element; 5 sub-elements each

[2] arithmetic mean of the coefficient of variation of E-moduli of elements (including within and between variation)

For example TAYLOR (1988) and RICHBURG (1989) examined local variation of bending E-modulus in Douglas fir, see Tab. 5.20 and Tab. 5.21, respectively. These two tables list mean values for the coefficient of variation found for local variation of E-moduli within the same structural element as well as for the variation of E-modulus including both, within and between element variations. The statistics for within element variation are based on four and five sub-elements, respectively. Interestingly, data of TAYLOR (1988) shows slightly lower CoV[$E_{m,0,i}$]$_{mean}$ if compared to that of RICHBURG (1989), but higher CoV[$E_{m,0}$]$_{mean}$. The lower ratios of CoV[$E_{m,0,i}$]$_{mean}$ / CoV[$E_{m,0}$]$_{mean}$ in TAYLOR (1988) imply a significant higher serial correlation, see Fig. 5.18, section 5.1.1. This can be explained to a certain amount by the high strength classes of material analysed by TAYLOR (1988). Thus high homogeneous material can be expected to show high within element correlation. As expected, visually graded timber (both data sets of TAYLOR, 1988 and samples L2 1/3 & L3 1/2 of RICHBURG, 1989) shows a higher CoV[$E_{m,0}$]$_{mean}$ than machine graded timber. A clear tendency or even a trend in CoV[$E_{m,0}$]$_{mean}$ and CoV[$E_{m,0,i}$]$_{mean}$ versus grading class within a grading method (visual vs. machine) can not be confirmed. Furthermore, the number of sub-elements seems also not to have an influence on CoV[$E_{m,0,i}$]. This confirms the assumption of equicorrelation defined to be independent of separation. Overall the observed amount of variation appears rather low.

Further discussion on this issue is required and will be continued after presenting additional data from literature.

Tab. 5.22: Variation of local E-modulus in tension parallel to grain in dependency of the quantity of involved sub-elements per each element: analysis based on data from BRANDNER ET AL. (2005); source S10 (N)

# sub-elements (*M*)	**3#**	**4#**	**5#**	**6#**	**7#**
***n* [#]**	9#	12#	7#	6#	25#
CoV[$E_{t,0,i}$]$_{mean}$ [1] [%]	10.5%	16.6%	10.8%	14.9%	16.3%
CoV[$E_{t,0}$]$_{mean}$ [2] [%]	17.9%	8.3%	11.8%	21.3%	16.2%

[1] arithmetic mean of the coefficient of variation of E-moduli of sub-elements within one element

[2] arithmetic mean of the coefficient of variation of E-moduli of elements (including within and between variation)

Tab. 5.23: Variation of local E-modulus in tension parallel to grain in dependency of the quantity of involved sub-elements per each element: analysis based on data from BRANDNER ET AL. (2005); source S10 (S)

# sub-elements (*M*)	**3#**	**4#**	**5#**	**6#**	**7#**
***n* [#]**	0#	10#	18#	8#	20#
CoV[$E_{t,0,i}$]$_{mean}$ [1] [%]	--	16.4%	14.5%	19.5%	22.3%
CoV[$E_{t,0}$]$_{mean}$ [2] [%]	--	19.3%	21.8%	24.6%	18.7%

[1] arithmetic mean of the coefficient of variation of E-moduli of sub-elements within one element

[2] arithmetic mean of the coefficient of variation of E-moduli of elements (including within and between variation)

BRANDNER ET AL. (2005) report on tensile tests on finger jointed structural timber performed on Norway spruce. Thereby local E-moduli in tension parallel to grain were determined on seven successive sub-elements with a measurement increment of 400 mm by testing timber of two proveniencies. In the analysis only values of one, the longer unjointed element, were used. Consequently the output gives statistics for a variation of sub-elements involved; see Tab. 5.22 and Tab. 5.23. To summarise the results: a clear trend in CoV[$E_{t,0,i}$]$_{mean}$ and CoV[$E_{t,0}$]$_{mean}$ in dependency of the quantity of involved sub-elements can not be found. The ratio between CoV[$E_{t,0,i}$]$_{mean}$ and CoV[$E_{t,0}$]$_{mean}$ is lower than that of CoV[$E_{m,0,i}$]$_{mean}$ / CoV[$E_{m,0}$]$_{mean}$, it is on average nearly 0.90. Furthermore it can be observed that lower timber quality shows higher values of CoV[$E_{t,0,i}$]$_{mean}$ and CoV[$E_{t,0}$]$_{mean}$. This is in line with the observations made on data of TAYLOR (1988) and RICHBURG (1989).

Tab. 5.24 gives statistics obtained from test data of STUEFER (2011) who performed tension tests perpendicular to grain on four different samples including variation of test length (150 mm and 300 mm) and of radial position of the elements within the stem ("S" for side boards and "M" for near center boards but without pith). In each element (board) 12 sub-elements were tested. An influence of test length on CoV[$E_{t,90,i}$]$_{mean}$ and CoV[$E_{t,90}$]$_{mean}$ can not be observed.

Tab. 5.24: Variation of local E-modulus in tension perpendicular to grain: analysis based on data from STUEFER (2011)

sample	**150_S**	**150_M**	**300_S**	**300_M**
***n* [#]**	6#	6#	6#	6#
CoV[$E_{t,90,i}$]$_{mean}$ [1] [%]	13.8%	8.7%	9.5%	15.7%
CoV[$E_{t,90}$]$_{mean}$ [2] [%]	12.0%	14.0%	6.4%	15.8%

[1] arithmetic mean of the coefficient of variation of the E-moduli of segments within one element; 12 sub-elements each

[2] arithmetic mean of the coefficient of variation of the E-moduli of elements (including within and between variation)

Overall variation within and total variation including within and between variations of E-modulus in elements were analysed. Thereby data of elements stressed in bending, tension parallel and perpendicular to grain were taken into account. It can be concluded that CoV[E_i]$_{mean}$ is often lower than CoV[E]$_{mean}$. Beside the fact that CoV[E]$_{mean}$ includes both, within and between element variation, it has also to be considered that this value is a combination of between element variation and variation within elements, whereby serial system action between sub-elements already occured. Furthermore it was confirmed that lower timber quality induces higher variation. The same was found for visually graded timber. Hence CoV[E]$_{mean}$ seems to be more affected than CoV[E_i]$_{mean}$. Additionally, based on the analysis made in section 5.1.1 the assumption of equicorrelation can be confirmed as no dependency of separation on variation and thus on correlation between the sub-elements was found.

For discussion of the magnitude of serial and parallel system effects on stiffness in timber and in particular in regard to timber of Norway spruce, examinations of expectable variation of E- and G-modulus of elements as common in full-sized structural timber is required. For example, BRANDNER AND SCHICKHOFER (2007) found in their comprehensive data analysis a mean coefficient of variation of CoV[$E_{m,0}$] = (18 ÷ 26)% (13 data series) and CoV[$E_{t,0}$] = (10 ÷ 17)% (40 data series). A comparison between the statistics in Tab. 5.24 with that in Tab. 5.22 and Tab. 5.23 gives comparable results

between CoV[$E_{t,0}$] and CoV[$E_{t,90}$]. Thus in case of E-modulus in bending higher variation can be expected than in tension parallel or perpendicular to grain. This can be explained by the effect of edge knots or knot clusters in bending-tension zone of elements stressed in bending. These have a tremendous effect on strength, much higher than in elements stressed equally in tension parallel to grain. For comparison, JCSS (2006) proposes for the bending E-modulus a coefficient of variation of CoV[$E_{m,0}$] = 13% and the same for CoV[$E_{t,0}$], CoV[$E_{t,90}$] and CoV[G_{090}]. Furthermore, 2pLND is proposed as RSDM of E- and G-moduli. The last statement was also confirmed by own comprehensive data analysis.

Tab. 5.25: Coefficients of variation for E- and G-moduli in dependency of equicorrelation ρ_{equi} defined for a two-level hierarchical model: CoV[Z_{ij}] including within and between sub-element variation, CoV[X_{ij}] and CoV[Y_j] expressing within and between sub-element variation, respectively; stacked values per box give rounded values of the expected range considering the central 50% of coefficients of variation found in test samples (25%-quantile, mean value, 75%-quantile) for CoV[Z_{ij}] and associated values for CoV[X_{ij}] and CoV[Y_j]

		ρ = 0.50		ρ = 0.55		ρ = 0.60	
	CoV[Z_{ij}]	**CoV[X_{ij}]**	**CoV[Y_j]**	**CoV[X_{ij}]**	**CoV[Y_j]**	**CoV[X_{ij}]**	**CoV[Y_j]**
$E_{t,0}$	10%	7.1%	7.1%	6.7%	7.4%	6.3%	7.7%
$E_{t,90}$	**15%**	**10.6%**	**10.6%**	**10.1%**	**11.1%**	**9.5%**	**11.6%**
$E_{c,0}$	20%	14.1%	14.1%	13.4%	14.8%	12.6%	15.5%
$E_{m,0}$	15%	10.6%	10.6%	10.1%	11.1%	9.5%	11.6%
	20%	**14.1%**	**14.1%**	**13.4%**	**14.8%**	**12.6%**	**15.5%**
G_{090}	25%	17.7%	17.7%	16.8%	18.5%	15.8%	19.4%

Based on findings above it is proposed to consider CoV[$E_{m,0}$] of sub-elements in the range of 15% to 25%, on average with CoV[$E_{m,0}$] = 20%, and CoV[$E_{t,0}$] = CoV[$E_{t,90}$] in the range of 10% to 20%, on average with CoV[$E_{t,0}$] = CoV[$E_{t,90}$] = 15%. For shear modulus G_{090} data on structural timber are scarce. Nevertheless, results from glulam bending tests in BRANDNER ET AL. (2007B, 2008) give comparable coefficients of variation for G- and E-modulus. Thus CoV[G_{090}] = CoV[$E_{m,0}$] is a reasonable assumption. The mentioned ranges of CoV for sub-elements are thereby not much deviating from the observable range of CoV of elements. This is due to the fact that a certain amount of variation induced by errors in practical determination of local as well as global stiffness characteristics has to be considered.

As reported in STEIGER (1996) and MICHELITSCH (2011) the coefficient of variation of E-modulus in compression parallel to grain is found to be in the same range as that of tension. Thus it is further proposed that $\mathrm{CoV}[E_{c,0}] = \mathrm{CoV}[E_{t,0}]$. Based on the analysis concerning serial correlation between sub-elements in section 5.1.1 an equicorrelation coefficient with focus on Norway spruce in the range of $0.50 \leq \rho_{equi} \leq 0.60$, on average with $\rho_{equi} = 0.55$ can be expected. Furthermore, the assumption of equicorrelation in conjunction with a two-level hierarchical model $Z_{ij} = X_{ij} + Y_j$ considering both, between and within element variation, was also confirmed by the analysis. Therefore and in reference to the definitions of two-level hierarchical models in section 2.6.4 and 5.2 a summary of current findings is given in Tab. 5.25. Therein are model parameters for calculation of serial and parallel system effects on E- and G-moduli, together with segmentation in within and between relative variations. Thereby, influences by grading method and timber quality can be considered by means of upper or lower values of equicorrelation.

The results in Tab. 5.25 are the basis for discussions on serial and parallel system effects on E- and G-modulus in structural timber and engineered timber products in section 5.3.4.

5.3.2 Parallel System Action on E-Modulus of Rigid Composite Structures

Considering a structure as a system of N parallel aligned, parallel acting as well as rigidly connected elements, e.g. glulam, duo or trio beams, or elements connected with a connector as stiff as the elements (thereby the quantity of system elements has to be increased by $N-1$). In this case, the elements can be assumed to be mutually independent. Furthermore and based on data analysis in previous section 5.3.1, the lognormal distribution (2pLND) was identified as suitable RSDM of E- and G-modulus of identical elements if they are stressed, e.g. in bending, tension or compression parallel to grain. Thus the distribution of E_1 is given as

$$E_i \overset{iid}{\sim} 2pLND\left(\mu_1, \sigma_1^2\right). \tag{5.21}$$

In case of N parallel acting and rigidly connected elements the E-modulus E_N of the system follows the averaging model according equ. (5.12), with parameters

$$E[E_N] = E[E_1],\ Var[E_N] = \frac{Var[E_1]}{N} \quad \text{and} \quad CoV[E_N] = \frac{CoV[E_1]}{\sqrt{N}}. \tag{5.22}$$

Thus the mean E-modulus of parallel acting systems $E_{N,mean}$ corresponds to the arithmetic mean of the elements' E-moduli E_1.

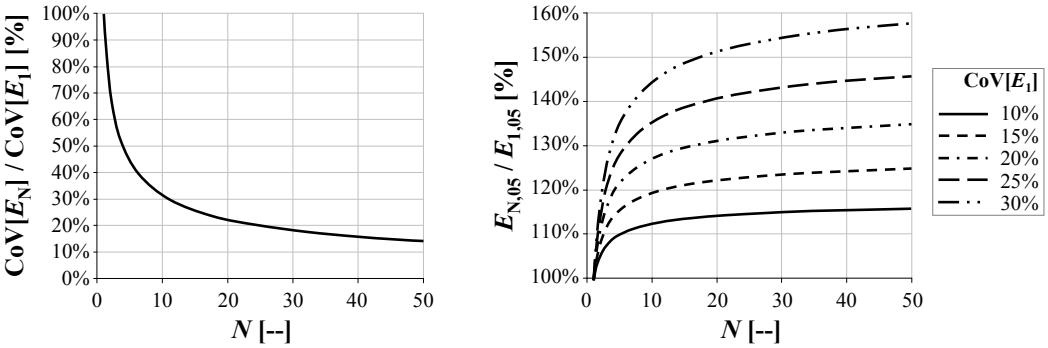

Fig. 5.30: Parallel system effect according the averaging model: CoV[E_N] / CoV[E_1] vs. N (left) and $E_{N,05}$ / $E_{N,1}$ vs. N (right); assuming iid E_1 ~ 2pLND

The interaction between the rigidly connected elements leads to a remarkable reduction of variability in system E-modulus in dependency of the number of system elements N. Therefore Fig. 5.30 exhibits graphs for CoV[E_N] / CoV[E_1] and $E_{N,05}$ / $E_{1,05}$ versus N by taking into account the expected range of CoV[E_1] of structural timber elements as defined in section 5.3.1. In particular the reduced CoV[E_N] is of interest for design situations were the whole distribution of at least the limiting value, e.g. the 5%-quantile $E_{N,05}$, is required. This is true for lateral (torsional) buckling and buckling of columns under compression loads. Further examples were already mentioned in section 5.3.1. The consideration of parallel system effects is also of importance for the examination of general observable parallel, sub-serial systems like GLT, CLT and finger jointed structural timber. Thereby, the reduction achieved in CoV[E_N] compared to CoV[E_1] decisively determines the serial effects of M in serial linked components, each of N parallel interacting elements. Before going into more detail serial effects on E-modulus are discussed within the next section 5.3.3.

5.3.3 Serial System Action on E-Modulus in Rigid Composite Structures

A serial system of M rigidly connected elements, sub-elements or joints with the same stiffness as that of the elements (in this case the quantity of the system elements has to be increased by $M - 1$) is assumed.

As in the previous section 5.3.2, 2pLND is taken as RSDM of E_1. According mechanical theory for linear elasticity and serial arranged elements, e.g. serial arranged springs, the E-modulus of the system is given as

$$\frac{1}{E_M} = \frac{1}{M}\sum_{j=1}^{M}\frac{1}{E_j} \quad \rightarrow \quad E_M = \frac{M}{\sum_{j=1}^{M}\frac{1}{E_j}}. \tag{5.23}$$

Hence, equ. (5.23) obviously expresses the harmonic mean function.

In general, there are three well known definitions of mean values, namely the arithmetic mean $X_{\text{mean,arith}} = X_{\text{mean}}$ according equ. (5.24), the geometric mean $X_{\text{mean,geo}}$ according equ. (5.25) and the harmonic mean $X_{\text{mean,har}}$ according equ. (5.26). The magnitude of mean values is thereby in the order of $X_{\text{mean,har}} \leq X_{\text{mean,geo}} \leq X_{\text{mean,arith}}$.

$$X_{mean,arith} = X_{mean} = \frac{1}{M}\sum_{j=1}^{M} X_j \tag{5.24}$$

$$X_{mean,geo} = \left(\prod_{j=1}^{M} X_j\right)^{1/M}, \; X_j > 0 \tag{5.25}$$

$$X_{mean,har} = \frac{M}{\sum_{j=1}^{M}\frac{1}{X_j}}, \; X_j \neq 0 \tag{5.26}$$

LIMBRUNNER ET AL. (2000) give some relationships between the mean values, e.g.

$$\frac{X_{mean,har}}{X_{mean}} = \frac{1}{1+CoV^2[X]}; \; \frac{X_{mean,geo}}{X_{mean,har}} = \sqrt{1+CoV^2[X]}; \; X_{mean,har} = \frac{X_{mean,geo}^2}{X_{mean}}. \tag{5.27}$$

MCALISTER (1879) shows that in case of $Y = \ln(X)$

$$Y_{mean,arith} = \ln\left(X_{mean,geo}\right). \tag{5.28}$$

For $X \sim$ 2pLND AHRENS (1954) approximated the relationship between arithmetic and geometric mean by $X_{\text{mean,arith}} / X_{\text{mean,geo}} \approx 1.15 \cdot \sigma^2$.

JENSEN ET AL. (1997) calculated the harmonic mean for $X \sim$ 2pLND and $Y = \ln(X) \sim$ ND as

$$X_{mean,har} = \exp\left(\mu_Y - \frac{\sigma_Y^2}{2}\right) = \frac{\mu_X}{1 + CoV^2[X]} = \frac{X_{mean,arith}}{1 + CoV^2[X]}. \tag{5.29}$$

This result is the same as later found by LIMBRUNNER ET AL. (2000). The ratio $X_{\text{mean,har}} / X_{\text{mean,arith}}$ according equ. (5.27) and (5.29) give the expectation of the maximum serial system effect achievable in case of iid lognormally distributed E-moduli in the limiting case $M \to \infty$. In case $M = 1$ both mean values, $X_{\text{mean,arith}}$ and $X_{\text{mean,har}}$ are equivalent. The same can be found for correlated E-moduli E_1 with $\rho = 1.00$. Nevertheless, a description of the harmonic mean in dependency of M is so far missing.

Following BARAKAT (1976) and his assumption that sums of lognormal variables again follow approximately a lognormal distribution if $M \to >>$ JENSEN ET AL. (1997) derived the distribution of the harmonic mean in dependency of M and with $X_{\text{M,mean,har}} \sim$ 2pLND ($\mu_{\text{Y,M,har}}$, $\sigma_{\text{Y,M,har}}^2$). For iid $X_1 \sim$ 2pLND expectation and variance of the harmonic mean in dependency of M are

$$E[X_{M,mean,har}] = X_{mean,har} \cdot \left(1 + \frac{CoV^2[X_1]}{M}\right), \tag{5.30}$$

$$Var[X_{M,mean,har}] = X_{mean,har}^2 \cdot \left(1 + \frac{CoV^2[X_1]}{M}\right)^2 \cdot \frac{CoV^2[X_1]}{M}. \tag{5.31}$$

In the limiting case $M \to \infty$ the variance $\text{Var}[X_{\text{M,mean,har}}]$ converges to zero and the expectation $\text{E}[X_{\text{M,mean,har}}]$ to $X_{\text{mean,har}}$ according equ. (5.29).

Equations above are valid only in case of iid $E_1 \sim$ 2pLND. They are adaptable for the description of serial system action. Identical distribution of E_1 can be assumed as being appropriate for sub-elements (e.g. board segments) of the same element (e.g. board or beam). Furthermore, identically distributed E_1 can also be assumed in case of elements of the same population, e.g. grading or strength class of structural timber. Nevertheless, the requirement of independency can only be assumed in case of serial systems composed of M elements. If serial action of sub-elements within one element is of interest dependency has to be taken into account, at least by adaptation of the variance of E-moduli of sub-elements, e.g. see section 5.1.1 concerning analysis of equicorrelation. Therefore,

covariance CoVar[E_j, E_k] between the serial linked E_j, E_k has to be taken into account. In general, the covariance is defined as

$$CoVar[X,Y] = E[(X - E[X]) \cdot (Y - E[Y])] = E[X \cdot Y] - E[X] \cdot E[Y]. \tag{5.32}$$

In case of the divisor in equ. (5.23) as a summation of inverse E_j the covariance can be derived by considering

$$CoVar[X + Y + ..., X + Y + ...] = CoVar[X,X] + CoVar[X,Y] + ... + CoVar[Y,Y] + ... \tag{5.33}$$

In case of identical distributed $X = X_j$ and consequently $X = Y$, and in dependency of M it follows that

$$CoVar\left[\sum_{j=1}^{M} X_j, \sum_{k=1}^{M} X_k\right] = M \cdot Var[X] + 2 \cdot \binom{M}{2} \cdot \rho \cdot Var[X] = Var\left[\sum_{j=1}^{M} X_j\right]. \tag{5.34}$$

Using the definition of PEARSON's correlation coefficient

$$\rho = \frac{CoVar[X,Y]}{\sqrt{Var[X] \cdot Var[Y]}} \quad \rightarrow \quad \rho = \frac{CoVar[X,Y]}{Var[X]} \quad \rightarrow \quad CoVar[X,Y] = \rho \cdot Var[X], \tag{5.35}$$

and the binomial coefficient, to consider all possible combinations of pairs of covariance which can be simplified by means of

$$\binom{M}{2} = \frac{M!}{2! \cdot (M-2)!} = \frac{M \cdot (M-1) \cdot (M-2) \cdot (M-3) \cdot ...}{2 \cdot 1 \cdot (M-2) \cdot (M-3) \cdot ...} = \frac{M \cdot (M-1)}{2}, \tag{5.36}$$

to

$$Var\left[\sum_{j=1}^{M} X_j\right] = M \cdot Var[X] + M \cdot (M-1) \cdot \rho \cdot Var[X] = M \cdot Var[X] \cdot \psi, \tag{5.37}$$

with

$$\psi = 1 + (M-1) \cdot \rho. \tag{5.38}$$

With $X = E_1$ the distribution of E_M according equ. (5.23) can be derived following a stepwise procedure and with identical distributed E_1: $E_1 \sim 2\text{pLND}(\mu_E, \sigma_E^2)$ and $\ln(E_1) \sim \text{ND}(\mu_{\ln(E)}, \sigma_{\ln(E)}^2)$, see

$$1^{st}\text{ STEP: } A = \frac{1}{E_j} \rightarrow \ln(\text{A}) \sim \text{ND}\left(-\mu_{\ln(E)}, \sigma_{\ln(E)}^2\right); \tag{5.39}$$

$$2^{nd}\text{ STEP: } B = \sum_{j=1}^{M} \frac{1}{E_j} \rightarrow E[B] = M \cdot E[A],\ \text{Var}[\text{B}] = M \cdot \text{Var}[\text{A}] \cdot \psi\ ; \tag{5.40}$$

$$3^{rd}\text{ STEP: } C = \frac{1}{\sum_{j=1}^{M} \frac{1}{E_j}} \rightarrow \ln(C) \sim \text{ND}\left(-\mu_{\ln(B)}, \sigma_{\ln(B)}^2\right); \tag{5.41}$$

$$4^{th}\text{ STEP: } E_M = \frac{M}{\sum_{j=1}^{M} \frac{1}{E_j}} \sim 2\text{pLND}\ , \tag{5.42}$$

with

$$E[E_M] = M \cdot E[C] \text{ and } Var[E_M] = M^2 \cdot Var[C]. \tag{5.43}$$

The 1st step follows directly by application of equ. (2.85). Equ. (5.40) gives the 2nd step. Hereby the approximation given in BARAKAT (1976) together with the term considering the correlation between E-moduli was used. The 3rd step is equivalent to the 1st step. The 4th step concludes with the application of simple multiplication with a scalar. During processing of this stepwise procedure special care has to be taken on computing the corresponding parameters either in untransformed or logarithmised domain. After some simplifications following equations for the expectation, variance and coefficient of variation of E_M can be derived from input parameters E[E_1], CoV[E_1], M, correlation coefficient ρ and identical distributed $E_1 \sim 2\text{pLND}$:

$$E[E_M] = \frac{E[E_1] \cdot \left[M + CoV^2[E_1] \cdot \psi\right]}{M \cdot \left(1 + CoV^2[E_1]\right)}\ , \tag{5.44}$$

$$Var[E_M] = \left[\frac{E[E_1] \cdot \left(M + CoV^2[E_1] \cdot \psi\right) \cdot CoV[E_1] \cdot \sqrt{\psi}}{\sqrt{M^3} \cdot \left(1 + CoV^2[E_1]\right)}\right]^2\ , \tag{5.45}$$

$$CoV[E_M] = \frac{CoV[E_1] \cdot \sqrt{\psi}}{\sqrt{M}} \quad . \tag{5.46}$$

The lognormal distribution parameters of E_M are obtained by transforming equ. (5.44) and (5.45) according equ. (2.70).

In case of $\rho = 0$ ($\rightarrow \psi = 1$) equ. (5.44) to (5.46) simplify to

$$E[E_M | \rho = 0] = \frac{E[E_1] \cdot [M + CoV^2[E1]]}{M \cdot (1 + CoV^2[E1])} \quad , \tag{5.47}$$

$$Var[E_M | \rho = 0] = \left[\frac{E[E_1] \cdot (M + CoV^2[E_1]) \cdot CoV[E_1]}{\sqrt{M^3} \cdot (1 + CoV^2[E_1])} \right]^2 \quad , \tag{5.48}$$

and to

$$CoV[E_M | \rho = 0] = \frac{CoV[E_1]}{\sqrt{M}} \quad . \tag{5.49}$$

Using (5.29) in (5.30) and (5.31) and simplifying confirms equivalence to the equations above.

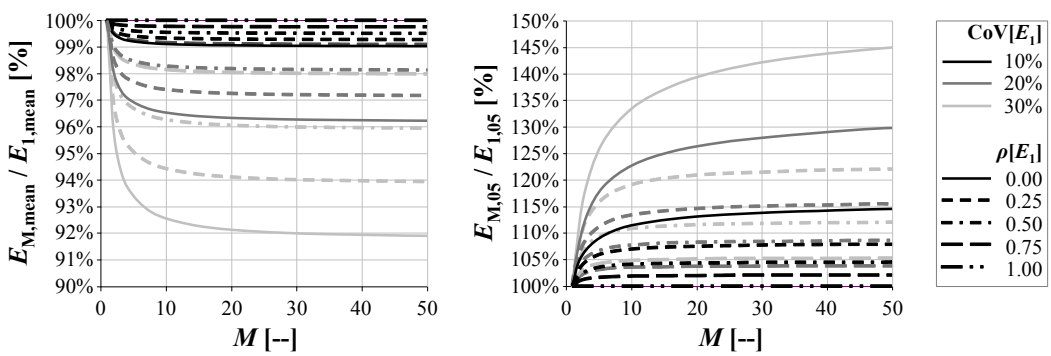

Fig. 5.31: Serial system effects on E-modulus: $E_{M,mean} / E_{1,mean}$ vs. M (left); $E_{M,05} / E_{1,05}$ vs. M (right); assuming identically distributed $E_1 \sim$ 2pLND

In case of $\rho = 1$ ($\rightarrow \psi = M$) where all elements $E_1 = E$ are equal, equ. (5.44) to (5.46) simplify to

$$E\left[E_M \middle| \rho = 1\right] = E\left[E_1\right] \ , \ Var\left[E_M \middle| \rho = 1\right] = Var\left[E_1\right] \ , \ CoV\left[E_M \middle| \rho = 1\right] = CoV\left[E_1\right] \ . \qquad (5.50)$$

The influence of parameters M, CoV[E_1] and ρ on relative mean $E_{\mathrm{M,mean}}$ / $E_{1,\mathrm{mean}}$ and 5%-quantile $E_{\mathrm{M},05}$ / $E_{1,05}$ is shown in Fig. 5.31. Both diagrams in Fig. 5.31 show a linearly decreasing serial effect in means and 5%-quantiles at increasing correlation and fixed CoV[E_1]. The serial effect on mean value $E_{\mathrm{M,mean}}$ increases progressively with increasing CoV[E_1] whereas on the 5%-quantile a linear increase is shown. Nevertheless, the influence on $E_{\mathrm{M,mean}}$ is rather low if compared with the significant increase in $E_{\mathrm{M},05}$ with increasing M, increasing CoV[E_1] and decreasing correlation. More concerning the relevance of serial effects on stiffness characteristics on the characteristics of structural timber and engineered timber products is given in the next section 5.3.4.

5.3.4 Serial and Parallel System Effects on E- and G-Modulus in Structural Timber and Engineered Timber Products

Let $E_{0,1}$ and $G_{090,1}$ be represented by a two-level hierarchical model including within and between element variation, with $E_{1,0}$ and $G_{1,090}$ as modulus of elasticity and shear of sub-elements, respectively. This model approach was confirmed in section 5.3.1. Let $E_{1,0}$ and $G_{1,090}$ be lognormally distributed (2pLND). According a two-level hierarchical model $Z_{\mathrm{ij}} = X_{\mathrm{ij}} + Y_{\mathrm{j}}$, variable X_{ij} which gives the deviation of sub-elements from elements' average is identically and independent distributed (iid) with E[X_{ij}] = 0 and Var[X_{ij}] = σ_{X}^2. Thus, if stochastic serial or parallel system effects within elements are of interest $E_{1,0}$ and $G_{1,090}$ can be treated as independent variables, with $\psi = 1$ and expectation, variance and coefficient of variation according equ. (5.47) to (5.49).

Serial System Effects of unjointed and finger jointed Structural Timber

The E-modulus of structural timber stressed in tension or compression parallel to grain depends on the length of the analysed system, see section 5.3.3. The longer the system the lower the average E-modulus and CoV[E]. Thus the reduction also depends on the reference length of elements. Based on comprehensive data analysis gained from structural timber of Norway spruce and presented in section 5.1.1, in total three groups with associated characteristics were defined as G_I, G_II and G_III, see Tab. 5.12. Furthermore, coefficients of variation given in Tab. 5.23 are associated with these length increments. If l_{ref} = 2,000 mm is taken as (deterministic) reference length of structural timber or systems composed of jointed sub-systems, as for example regulated in

EN 1194, than expectation and variance of M for all three groups can be calculated by means of equ. (2.85). The results together with input parameters are given in Tab. 5.26.

Tab. 5.26: Expectation and coefficient of variation of d_{WZ} (taken as length increment of elements) and the number of serial elements per reference length of structural timber or general serial systems given l_{ref} = 2,000 mm for group G_I, G_II and G_III

		G_I	**G_II**	**G_III**
E[d_{WZ}]	[mm]	450	520	590
CoV[d_{WZ}]	[%]		60%	
E[M]	[--]	6.04	5.23	4.61
CoV[M]	[%]		60%	

An analytically closed consideration of M as 2pLND variable based on computation of $E_{M,0}$ is not possible. Consequently, parameters like expectation and variance of $E_{M,0}$ were estimated based on 30,000 random variates generated per group and parameter set and created in dependency of input parameters E[$E_{1,0}$], CoV[$E_{1,0}$], $\rho_{equi}[E_{1,0}] = 0.55$, E[$M$] and CoV[$M$], with iid $E_{1,0}$; $M \sim$ 2pLND. At first, systems composed of serial correlated elements representing unjointed structural timber were analysed. Thus only system effects as consequence of within member variation can be observed. The ratios E[$E_{M,0}$] / E[$E_{1,0}$] and CoV[$E_{M,0,within}$] / CoV[$E_{1,0}$] as well as CoV[$E_{M,0}$] / CoV[$E_{1,0}$] are given in Tab. 5.27. Thereby CoV[$E_{M,0,within}$] gives the coefficient of variation of E- and also G-modulus of unjointed structural timber composed of M serial arranged reference elements. Thereby only variation observable within structural timber elements relative to E[$E_{M,0}$] is included. Thus CoV[$E_{M,0}$] = CoV[$Z_{M,ij}$] is given as

$$CoV\left[Z_{M,ij}\right] = \frac{\sqrt{\left(CoV\left[X_{ij}\right] \cdot E\left[Z_{M,ij}\right]\right)^2 + \left(CoV\left[Y_{ij}\right] \cdot E\left[Z_{M,ij}\right]\right)^2}}{E\left[Z_{M,ij}\right]} \quad . \tag{5.51}$$

In case of serial systems composed of finger jointed sub-systems, composed of serial arranged elements, the sub-systems can be treated as independent whereas the elements per sub-system exhibit equicorrelation. It is further assumed that the E-modulus of finger joints is comparable with that of jointed elements. Additionally and due to the short length of commonly produced finger joints of only 15 to 20 mm in comparison to average element length of 450 to 590 mm the joints are not treated as additional elements. In such a system a combination of serial system effects as consequence of within element and

total variation has to be considered. Thus, computation of E[$E_{M,0,FJ}$] and CoV[$E_{M,0,FJ}$] require E[$E_{M,0}$] and CoV[$E_{M,0}$] gained from sub-systems composed of unjointed elements.

Tab. 5.27: Ratios of expectations and coefficients of variation of serial system effects on E-modulus in case of unjointed or finger jointed structural timber; l_{ref} = 2,000 mm

			G_I	G_II	G_III
0# FJ 2)	**15% 1)**	**E[$E_{M,0}$] / E[$E_{1,0}$]**	**0.992**	**0.993**	**0.993**
		CoV[$E_{M,0}$] / CoV[$E_{1,0}$]	0.803	0.812	0.821
		CoV[$E_{M,0,intern}$] / CoV[$E_{1,0}$]	0.457	0.491	0.524
	20% 1)	**E[$E_{M,0}$] / E[$E_{1,0}$]**	**0.986**	**0.987**	**0.988**
		CoV[$E_{M,0}$] / CoV[$E_{1,0}$]	0.803	0.812	0.821
		CoV[$E_{M,0,intern}$] / CoV[$E_{1,0}$]	0.457	0.491	0.524
1# FJ 2)	**15% 1)**	**E[$E_{M,0,FJ}$] / E[$E_{1,0,FJ}$]**	**0.988**	**0.988**	**0.988**
		CoV[$E_{M,0,FJ}$] / CoV[$E_{1,0,FJ}$]	0.608	0.619	0.631
		CoV[$E_{M,0,intern}$] / CoV[$E_{1,0}$]	0.647	0.695	0.740
	20% 1)	**E[$E_{M,0,FJ}$] / E[$E_{1,0,FJ}$]**	**0.979**	**0.979**	**0.980**
		CoV[$E_{M,0,FJ}$] / CoV[$E_{1,0,FJ}$]	0.608	0.619	0.631
		CoV[$E_{M,0,intern}$] / CoV[$E_{1,0}$]	0.647	0.695	0.740
2# FJ 2)	**15% 1)**	**E[$E_{M,0,FJ}$] / E[$E_{1,0,FJ}$]**	**0.986**	**0.986**	**0.986**
		CoV[$E_{M,0,FJ}$] / CoV[$E_{1,0,FJ}$]	0.527	0.540	0.554
		CoV[$E_{M,0,intern}$] / CoV[$E_{1,0}$]	0.792	0.851	0.907
	20% 1)	**E[$E_{M,0,FJ}$] / E[$E_{1,0,FJ}$]**	**0.975**	**0.976**	**0.976**
		CoV[$E_{M,0,FJ}$] / CoV[$E_{1,0,FJ}$]	0.527	0.540	0.554
		CoV[$E_{M,0,intern}$] / CoV[$E_{1,0}$]	0.792	0.851	0.907
3# FJ 2)	**15% 1)**	**E[$E_{M,0,FJ}$] / E[$E_{1,0,FJ}$]**	**0.985**	**0.984**	**0.984**
		CoV[$E_{M,0,FJ}$] / CoV[$E_{1,0,FJ}$]	0.481	0.496	0.511
		CoV[$E_{M,0,intern}$] / CoV[$E_{1,0}$]	0.914	0.983	1.047
	20% 1)	**E[$E_{M,0,FJ}$] / E[$E_{1,0,FJ}$]**	**0.973**	**0.973**	**0.973**
		CoV[$E_{M,0,FJ}$] / CoV[$E_{1,0,FJ}$]	0.481	0.496	0.511
		CoV[$E_{M,0,intern}$] / CoV[$E_{1,0}$]	0.914	0.983	1.047

1) CoV[$E_{1,0}$] = CoV[$Z_{1,ij}$]

2) average (deterministic) number of finger joints per reference length l_{ref} = 2,000 mm

The parameters of sub-systems as well as of the total system depend on the number of finger joints per reference system length. In case of two joints the derivation of system E-modulus is based on a system composed of three iid sub-systems, each sub-system consisting of M serial arranged and equicorrelated elements, with M based on $l_{ref} / 3 = 2{,}000 / 3 \approx 667$ mm. Thereby both serial system effects, based on within and residual total variation, can be derived independently and afterwards multiplied to obtain the total serial system effect.

Results for several deterministic numbers of joints per reference length of the system are included in Tab. 5.27. Again, ratios for E[$E_{M,0,FJ}$] / E[$E_{1,0}$], CoV[$E_{M,0,within}$] / CoV[$E_{1,0}$] and CoV[$E_{M,0,FJ}$] / CoV[$E_{1,0}$] are given.

Overall, the influence of serial system action on expectation of E-modulus (and also G-modulus) is small. Due to equicorrelation between elements within sub-systems but jointing of independent sub-systems effects on expectation are a bit higher in case of jointed structural timber. In contrast, system size significantly affects CoV[$E_{M,0}$] and CoV[$E_{M,0,FJ}$], being solely dependent on M and by definition not on CoV[$E_{0,1}$].

Parallel System Effects in Structural Timber and Engineered Timber Products

As already outlined in more detail in section 5.3.2 E- and G-modulus of parallel acting systems follow the averaging model as given in equ (5.22). Thereby $E_{1,0}$ and $G_{1,090}$ are assumed to be iid lognormal distributed. Consequently, irrespective of within element correlation, e.g expressed as equicorrelation in case of a hierarchical model, the input variance for the averaging model includes both, within and between element variance. Consequently, CoV[Z_{ij}] = 15% and 20% have to be taken into account for $E_{1,t,0}$, $E_{1,t,90}$ and $E_{1,c,0}$ as well as $E_{1,m,0}$ and $G_{1,090}$, respectively, and as given in Tab. 5.23. Consequently, as the averaging model gives a significant reduction in variance proportional to $1 / N$ by leaving the expectation constant, a remarkable increase in 5%-quantiles of E- and G-modulus is given. Therefore Tab. 5.28 shows the effect of parallel action for numerous system sizes.

An increase in 5%-quantiles of E- and G-modulus is given in tension or compression parallel to grain but also for bending. Even if the elements are rigidly connected face-by-face and loaded flatwise more or less the same homogenisation in stiffness characteristics can be achieved and verified by means of rigid composite theory and stochastic input parameters. Nevertheless, for product modelling and stability design the interaction of

parallel and serial system effects is of relevance. More on this interaction is given within the next section.

Tab. 5.28: Parallel system effects on coefficient of variation and 5%-quantile of E- and G-modulus for numerous system sizes

	N =	1	2	3	4	5	10	15	20	30
CoV[X_N] / CoV[X_1] = 1 / √N =		**1.00**	**0.71**	**0.58**	**0.50**	**0.45**	**0.32**	**0.26**	**0.22**	**0.18**
CoV[X_1] = 15%	**CoV[X_N]**	15.0%	10.6%	8.7%	7.5%	6.7%	4.7%	3.9%	3.4%	2.7%
	$X_{N,05}$ / $X_{1,05}$	1.00	1.08	1.12	1.14	1.15	1.19	1.21	1.22	1.23
CoV[X_1] = 20%	**CoV[X_N]**	20.0%	14.1%	11.6%	10.0%	8.9%	6.3%	5.2%	4.5%	3.7%
	$X_{N,05}$ / $X_{1,05}$	1.00	1.11	1.16	1.19	1.21	1.27	1.30	1.31	1.33

Interaction of Parallel and Serial System Effects and the Relevance in Stability Design

System effects on stiffness characteristics of systems composed of parallel arranged sub-systems can be modelled as serial acting sub-systems of parallel acting elements. As the E- and G-modulus of parallel acting elements is nothing else than the average, the magnitude of equicorrelation between serial sub-systems is not affected by N. Consequently, interaction of parallel and serial effects can be simply computed by multiplication of both sub-effects. Nevertheless, the coefficient of variation of sub-systems has to be taken into account.

For illustration, system effects in some engineered timber products are presented here where the same reference length of l_{ref} = 2,000 mm as in serial effects is applied. Due to the decrease in coefficient of variation from CoV[X_1] to CoV[X_N] serial effects on expectation are negligible even for $N \geq 2$ and G_I, so far only unjointed structural timber is addressed.

The first example deals with modelling of duo and trio beams where system products of unjointed and jointed structural timber are addressed. Following previous sections, parallel interaction of two or three elements decreases CoV[X_N] to 71% and 58% of CoV[X_1], respectively. Subsequent serial arrangement of sub-systems to duo and trio beams with ρ_{equi} = 0.55 leads to system effects and characteristics as given in Tab. 5.29.

Tab. 5.29: System effects on stiffness characteristics of duo and trio beams composed of unjointed and jointed structural timber elements

			DUO	TRIO
			G_I, G_II, G_III	G_I, G_II, G_III
	CoV[$X_{M,N}$] / CoV[X_M]		**0.71**	**0.58**
0# FJ	**E[$X_{M,N}$] / E[X_M]**		1.00	
	$X_{M,N,05}$ / $X_{M,05}$	CoV[X_1] = 15%	1.07	1.10
		CoV[X_1] = 20%	1.10	1.14
1# FJ	**E[$X_{M,N}$] / E[X_M]**		1.01	
	$X_{M,N,05}$ / $X_{M,05}$	CoV[X_1] = 15%	1.04	1.08
		CoV[X_1] = 20%	1.08	1.11
2# FJ	**E[$X_{M,N}$] / E[X_M]**		1.01	
	$X_{M,N,05}$ / $X_{M,05}$	CoV[X_1] = 15%	1.05	1.07
		CoV[X_1] = 20%	1.07	1.10

Comparing expectation, coefficient of variation and 5%-quantiles of structural timber with that of duo and trio beams it can be observed that the relative effect on CoV[$X_{M,N}$] is independent of CoV[X_M] and solely dependent on N. The effect on expectation is negligible, but on 5%-quantile a ratio of $X_{M,N,05} / X_{M,05}$ of 7% to 14% in systems composed of unjointed structural timber can be observed, in dependency of CoV[X_1] and N. In case of a deterministic amount of finger joints per reference length of one or two comparable conclusions can be made. Nevertheless, the increase of $X_{M,N,05}$ is a bit lower than in unjointed structural timber because of a higher amount of homogenisation already in serial systems. Therefore overall differences between groups G_I, G_II and G_III are negligible.

In a second example system effects on stiffness characteristics of glued laminated timber (GLT) are analysed in more detail. Again differentiation is made between GLT composed of unjointed and jointed structural timber. The same reference length of l_{ref} = 2,000 mm is used.

According EN 1194 the reference cross section of GLT is given by w / d = 150 mm / 600 mm. In Europe the thickness of standard GLT-lamellas is 40 mm. Thus a GLT-beam in reference dimensions consists of 15 lamellas. Nevertheless, GLT is

available in dimensions up to 2,000 mm or even 3,000 mm in depth which corresponds to 50 or even 75 lamellas. Therefore system effects in GLT are discussed a bit broader.

Tab. 5.30: E-modulus of GLT in bending as well as of constituting boards in tension parallel to grain: expectation, CoV and ratio of expectations; literature survey

source	series	$E_{t,0,l}$ [N/mm²]		$E_{m,0,g}$ [N/mm²]		ratio [1)]
		E[.]	CoV[.]	E[.]	CoV[.]	
SCHICKHOFER ET AL. (1995)	MS10-h_300	10,840	12.5%	10,838	3.4%	1.00
	MS13-h_300	13,140	14.7%	12,354	4.5%	0.94
	MS17-h_300	14,620	17.5%	15,156	5.6%	1.04
	MS10-h_600	10,840	12.5%	11,005	4.4%	1.02
	MS17-h_600	14,620	15.5%	14,489	6.8%	0.99
SCHICKHOFER & RIEBENBAUER (1997)	1717_300	18,110	14.2%	16,714	5.9%	0.92
BRANDNER & SCHICKHOFER (2010)	S10_320	10,780	18.6%	10,800	9.5%	1.00
	S10_160	10,780	18.6%	11,520	9.3%	1.07
	S10+_320	12,330	20.0%	11,730	8.5%	0.95
	S13+_320	12,960	13.7%	12,580	7.3%	0.97
	GL36h_600	14,440	8.7%	14,650 (global) 15,880 (local)	3.5% (global) 3.8% (local)	1.01 (global) 1.10 (local)
RIBERHOLT (2008)	C30-12E_300	12,802	--	13,000	--	1.02
	C37-14E_300	15,102	--	15,362	--	1.02
	C37-14E_300	15,102	--	14,596	--	0.97
	VTT_M1_540	12,100	--	11,800	--	0.98
	VTT_M2_540	12,800	--	12,600	--	0.98
	VTT_M3_540	13,400	--	13,200	--	0.99
	VTT_M4_540	12,200	--	12,600	--	1.03
	SP_540	12,150	--	11,900	--	0.98
	TI_600	13,000	--	12,600	--	0.97

1) ratio = $E_{m,0,g,mean}$ / $E_{t,0,l,mean}$

Following the models in previous sections it can be concluded that for the calculation of system effects of analysed parallel, sub-serial structures it is irrelevant if sub-effects are at first derived on parallel or the serial interaction between the elements. Consequently, taken into account the ratios given in Tab. 5.27 for serial system effects, total system effects can be simply derived by multiplication with the ratios given for parallel system action in Tab. 5.28.

Effects on expectation of system stiffness can be set equal to one for $N \geq 10$ or taken as the inverse values of Tab. 5.27. This is because E-modulus of GLT is regulated on the basis of E-modulus of the constituting boards. For example, EN 1194 states that $E_{\mathrm{m,0,g,mean}} = 1.05 \cdot E_{\mathrm{t,0,l,mean}}$, with $E_{\mathrm{m,0,g,mean}}$ and $E_{\mathrm{t,0,l,mean}}$ as E-modulus in grain direction of glulam in bending and boards in tension, respectively. This is because in testing of single boards a serial system effect is given which leads to a reduction in expectation. In the system product GLT parallel system action between rigidly connected boards and lamellas initiates a significant homogenisation in sub-systems of board segments to a degree were serial effects between these sub-systems in GLT diminish. Consequently, E-modulus $E_{\mathrm{m,0,g,mean}}$ of GLT is higher than expected from testing the constituting single boards.

Nevertheless, as shown in Tab. 5.27 unjointed structural timber shows only 1% to a maximum of 2% reduction in $\mathrm{E}[E_{\mathrm{M}}]$ if compared to $\mathrm{E}[E_1]$. Even in finger jointed elements a maximum of 3% can be verified by models discussed before. For clarification of differences between calculated and regulated ratio $E_{\mathrm{M,N}} / E_{\mathrm{M}}$, Tab. 5.30 gives a survey of some test data from literature with observed ratios. Based on this data it can be concluded that over all $E_{\mathrm{m,0,g,mean}} = E_{\mathrm{t,0,l,mean}}$. Furthermore, significant reduction from $\mathrm{CoV}[E_{\mathrm{t,0,l}}]$ to $\mathrm{CoV}[E_{\mathrm{m,0,g}}]$ can be observed. Hereby all derived models can be verified, at least on average.

To conclude, effects on stiffness characteristics of systems with elements loaded axial or flatwise in bending show minor and thus negligible effects on expectation but a significant reduction in $\mathrm{CoV}[X_{\mathrm{M,N}}]$. However, if elements are loaded edgewise, as for example given in duo and trio beams and if composed of boards of a lower strength grade material also a significant increase in expectation $\mathrm{E}[X_{\mathrm{M,N}}]$ is given, with $\mathrm{E}[X_{\mathrm{M,N}}] / \mathrm{E}[X_1] \approx 1.05 \div 1.20$, see e.g. EISER (2008). This circumstance can be explained by the disproportionate effect of edge knots on bending stiffness of elements which become reinforced in case of face-to-face by adhesive rigidly connected duo and trio beams. For modelling this effect fragmentation of elements' cross section and stochastic

assignment of local characteristics would be required. Thereby and due to the common breakdown process the edgewise loaded elements' cross section acts like a composite which can be taken into account by means of rigid composite theory plus stochastic distributed properties.

Predictability of stiffness characteristics in parallel, sub-serial systems is not only relevant for product modelling, but also for stability design. Thereby two cases of stability, compression buckling (column stability) and lateral (torsional) buckling can be distinguished but both can also occur simultaneously. Following the model column method anchored for example in EN 1995-1-1 design of columns under compression stresses parallel to grain has to be verified by

$$\frac{\sigma_{c,0,d}}{\min\left[k_{c,y};k_{c,z}\right]\cdot f_{c,0,d}} \leq 1.00\,, \tag{5.52}$$

with $\sigma_{c,0,d}$ and $f_{c,0,d}$ as compression stress (action) and strength (resistance) on design level, respectively, and factor k_c which is defined in dependency of the direction of possible buckling, here exemplarily given for y-direction, as

$$k_{c,y} = \frac{1}{k_y + \sqrt{k_y^2 - \lambda_{rel,y}^2}}\,, \tag{5.53}$$

with parameter k_y, relative and geometric slenderness $\lambda_{rel,y}$ and λ_y, respectively,

$$k_y = 0.5\cdot\left[1+\beta_c\cdot\left(\lambda_{rel,y}-0.3\right)+\lambda_{rel,y}^2\right],\ \lambda_{rel,y} = \frac{\lambda_y}{\pi}\cdot\sqrt{\frac{f_{c,0,k}}{E_{0,05}}}\,,\ \lambda_y = \frac{l_k}{i_y} = \frac{l_k}{\sqrt{\frac{I_y}{A}}}\,, \tag{5.54}$$

and with parameter β_c considering pre-curvature of compression members regulated as

$$\beta_c = 0.2 \text{ in case of structural timber, and } \beta_c = 0.1 \text{ in case of LVL or GLT,} \tag{5.55}$$

I_y and i_y as moment of inertia and radius of inertia in y-direction, respectively, $f_{c,0,k}$ as characteristic (5%-quantile) compression strength and $E_{0,05}$ as 5%-quantile of longitudinal E-modulus. Consequently, buckling resistance on the part of the material can be increased by decreasing β_c and increasing of $E_{0,05}$ and $f_{c,0,k}$. Thereby a high 5%-quantile of compression strength increases on one hand and under the square root the relative

slenderness parameter $\lambda_{rel,y}$ by counteracting positive system effects on $E_{0,05}$, but on the other hand increases also directly the resistance of the material, see equ. (5.52).

In case of lateral (torsional) buckling action with or without interaction with axial compression stresses design has to fulfill

$$\frac{\sigma_{m,d}}{k_{crit} \cdot f_{m,d}} \leq 1.00 \text{, or } \left(\frac{\sigma_{m,d}}{k_{crit} \cdot f_{m,d}}\right)^2 + \frac{\sigma_{c,0,d}}{k_{c,z} \cdot f_{c,0,d}} \leq 1.00 \text{,} \tag{5.56}$$

with $\sigma_{m,d}$ and $f_{m,d}$ as design bending stress and strength, respectively, and k_{crit} given by

$$k_{crit} = \begin{cases} 1.00 & for \quad \lambda_{rel,m} \leq 0.75 \\ 1.56 - 0.75 \cdot \lambda_{rel,m} & for \quad 0.75 < \lambda_{rel,m} \leq 1.40 \\ \dfrac{1}{\lambda_{rel,m}^2} & for \quad 1.40 < \lambda_{rel,m} \end{cases} \text{,} \tag{5.57}$$

and

$$\lambda_{rel,m} = \sqrt{\frac{f_{m,k}}{\sigma_{m,crit}}} \text{, with } \sigma_{m,crit} = \frac{M_{y,crit}}{W_y} = \frac{\pi \cdot \sqrt{E_{0,05} \cdot I_z \cdot G_{090,05} \cdot I_{tor}}}{l_{ef} \cdot W_y} \text{,} \tag{5.58}$$

with $\sigma_{m,crit}$ as critical bending stress, $M_{y,crit}$ and W_y as critical bending moment and section modulus, respectively, I_z and I_{tor} as moment of inertia and torsion moment of inertia, respectively, and l_{ef} as effective length for calculation of torsional buckling resistance, which depends on support conditions and load configuration.

Again, material resistance against lateral (torsional) buckling can be increased with increase of the product ($E_{0,05} \cdot G_{090,05}$) under the square root of equ. (5.58) of $\sigma_{m,crit}$ and by increasing $f_{m,k}$. Nevertheless, a higher bending strength increases also parameter $\lambda_{rel,m}$.

Consequently, system effects which enhance the 5%-quantiles of strength and stiffness characteristics are relevant for the material part in stability design. Within this section only effects on stiffness are discussed. Starting with X_M as characteristic of unjointed or finger jointed structural timber further system effects due to parallel arrangement of rigidly and continuously connected elements can be sufficiently accurate described by $E[X_{M,N}] = E[X_1]$ and $CoV[X_{M,N}] = CoV[X_M] / \sqrt{N}$, following the averaging model in

combination with a minor correction in expectation. With $X_1 \sim$ 2pLND and iid $X_M \sim$ 2pLND the 5%-quantile $X_{M,N,05}$ can be derived directly by applying equ. (2.70) and (2.80). Due to the fact that in stability design the resistance against bending deflection is of relevance the increase in 5%-quantile of $E_{0,05}$ is by default calculated based on CoV[X_1] = 20%. Results for duo and trio beams are given in Tab. 5.31 where no significant influences of group characteristics (G_I to G_III) are visible.

Tab. 5.31: Ratios $E_{M,N,0,05} / E_{M,0,05}$ of duo and trio beams composed of unjointed or jointed structural timber

$E_{M,N,0,05} / E_{M,0,05}$	0# FJ	1# FJ	2# FJ
DUO	1.10	1.09	1.08
TRIO	1.14	1.12	1.11

Overall a system factor of 1.10 seems to be applicable to take into account the increase of $E_{M,N,0,05}$ in case of duo and trio beams. Due to homogenisation of growth characteristics and physical properties by continuous and rigid connection of structural timber also a reduced value of $\beta_c = 0.15$ or even 0.10 and thus equal to GLT can be proposed, in particular if structural components are produced and used in latter expected equilibrium moisture content.

Tab. 5.32: Ratio $X_{M,N,05} / X_{M,05}$ in dependency on N and the amount of finger joints per l_{ref} = 2,000 mm; CoV[X_1] = 20%

N =	5	10	15	50	∞
$X_{M,N,05} / X_{M,05}$ | CoV[X_M] ≈ 16% | 0# FJ	1.19	1.23	1.25	1.29	1.32
$X_{M,N,05} / X_{M,05}$ | CoV[X_M] ≈ 13% | 1# FJ	1.15	1.19	1.20	1.23	1.24
$X_{M,N,05} / X_{M,05}$ | CoV[X_M] ≈ 11% | 2# FJ	1.14	1.17	1.18	1.21	1.21

In GLT a remarkable higher homogenisation in E- and G-modulus can be observed due to the commonly higher amount of interacting lamellas. Therefore, Tab. 5.32 gives some ratios of $X_{M,N,05} / X_{M,05}$ in dependency of N and the amount of finger joints per l_{ref} = 2,000 mm. Again, the results base on CoV[X_1] = 20%. The homogenisation already achieved by serial system action within each GLT-lamella is expressed by CoV[X_M] and also included in Tab. 5.32. Interestingly, in lamellas containing on average one finger joint within 2,000 mm, which can be on average expected in Central European GLT

production lines, variability in E-modulus is given by CoV[$E_{M,0}$] = 13%. This is exactly in line with the proposal in JCSS (2006), as already referenced in section 5.3.1.

The ratio $X_{M,N,05}$ / $X_{M,05}$ is significantly determined by N but also by CoV[X_M]. Due to the fact that in EN 338, which provides a strength class system for structural timber, a CoV[X_M] = 20% is inherently supposed by $E_{0,05} = 2 / 3 \cdot E_{0,mean}$ and iid $E_{0,i}$, ratios for this remarkable higher CoV[X_M] are given in Tab. 5.33.

Tab. 5.33: Ratio $X_{M,N,05}$ / $X_{M,05}$ in dependency on N; CoV[X_M] = 20% according EN 338

***N* =**	**5**	**10**	**15**	**50**	**∞**
$X_{M,N,05}$ / $X_{M,05}$ | CoV[X_M] = 20%	1.21	1.27	1.30	1.35	1.41

Furthermore, Tab. 5.32 and Tab. 5.33 provide also ratios of $X_{M,N,05}$ / $X_{M,05}$ at $N \rightarrow \infty$ which are the same as $X_{M,mean}$ / $X_{M,05}$. These values give the maximum achievable homogenisation potential on the 5%-quantile in dependency of CoV[X_M]. Following both tables it can also be concluded that a further relative gain in system effect at $N \geq 10$ (15) is only small. Consequently it can be proposed to regulate $X_{M,N,05}$ / $X_{M,05}$ for $5 \leq N < 10$ with 1.15 and at $N \geq 10$ with 1.20. Consequently, in case of GLT and $N \geq 10$ lamellas $E_{0,05}$ in equ. (5.54) can be increased by 20%. The same can be done in equ. (5.58) for calculation of $\sigma_{m,crit}$ in case of lateral (torsional) buckling. Thereby, both, E- and G-modulus can be multiplied by 1.20. This is in particular supported by the fact that E_0 and G_{090} can be treated as independent variables, in particular in laminated products like GLT. Despite the fact that for example EN 338 regulates G_{mean} in direct relationship to $E_{0,mean}$, by $G_{mean} = E_{0,mean} / 16$, BRANDNER ET AL. (2007B; 2008) showed that the assumption of independency of both variables can be supported. Thus in case of GLT $\sigma_{m,crit}$ or l_{ef} can be increased by 20% in comparison to solid timber. Hereby l_{ef} gives the effective distance between lateral supports or bracing elements.

Nevertheless, a current proposal in PREN 14080 states that the product ($E_{0,g,k} \cdot G_{g,k}$) at $N \geq 10$ can be multiplied by a factor of 1.40, with ($E_{0,g,k}$; $G_{g,k}$) = 5 / 6 · ($E_{0,g,mean}$; $G_{g,mean}$). In fact, this factor is too high; it is even above the maximum possible homogenisation at $N \rightarrow \infty$.

To conclude, within this section and in previous sections serial and parallel system effects on stiffness characteristics were discussed. Thereby and under assumption of $X_1 \sim$ 2pLND analytical models for correlated as well as for independent elements were presented.

With focus on timber, serial equicorrelation and characteristics of CoV[X_1] were determined on the basis of data from literature and previous studies in section 5.1.1. Following that, serial and parallel system effects, their interaction in respect to modelling of product characteristics and the calculation of parameters for stability design were examined and discussed. In general, good to very good agreement between model results and test data was observed. At the end the current regulation of $X_{g,05} / X_{g,mean} = 5 / 6$ according EN 1194 can be confirmed whereas the proposal in PREN 14080 cannot be supported even in case when a higher CoV[X_M] = 20% is applied as currently inherently given in EN 338.

5.4 Serial System Effects on Tensile Strength parallel to Grain – Length Effects

Within this section serial system effects on tensile strength of timber and linear engineered timber products are addressed. As already outlined in previous sections 5.2 and 5.3 again serial correlation of timber characteristics is taken into account. Hereby a two-level hierarchical model with subdivision of total variability of strength in variability within and between elements is considered. Retrospective to section 5.2 and the definition of a two-level hierarchical model the tensile strength $f_{t,0} = R$ of a structural member composed of serial arranged sub-elements or more general of a serial system is simply given by the minimum of all involved resistances as

$$R = \min\left[Z_{ij} \middle| M = m\right] = Y_j + \min_m\left[X_{ij}\right] = Y_j + X_M \quad . \tag{5.59}$$

Thus, the distribution function $F_R(r)$ of resistance R by consideration of equ. (2.190) is given by the convolution integral

$$\begin{aligned} F_R(r) = P\left(Y_j + X_M \le r \middle| M = m\right) &= \int_0^\infty f_Y(y) \cdot \left(\int_{-\infty}^{r} f_{X_M}\left(u - y \middle| m\right) \cdot du \right) \cdot dy \\ &= \int_0^\infty f_Y(y) \cdot F_{X_M}\left(r - y \middle| m\right) \cdot dy \ , \end{aligned} \tag{5.60}$$

with

$$F_{X_M}\left(x \middle| M = m\right) = 1 - \left[1 - F_X\left(x \middle| M = 1\right)\right]^m \quad . \tag{5.61}$$

Based on results gained by modelling serial system effects in section 3.3.2 the CDF of $X_M = \min[X_{ij}]$ can be directly and well approximated by assuming $X_1, X_M \sim$ 2pLND, by means of equ. (3.102) and estimators for expectation and standard deviation as provided in Tab. 3.2. Therefore the distribution characteristics of $F_{X\,|\,M=1}(x)$ have to be known, in particular the variability of X_1, which beside M constitutes the dominating parameter in calculating serial system effects. This information is in fact challenging as results are rare according tension tests on structural timber (and in particular Norway spruce) performed in sections. Nevertheless, EHLBECK ET AL. (1985A) report on regression equations formulated for simulation of strength and stiffness characteristics of board segments with a length of 150 mm or 137.5 mm. These equations are based on comprehensive test series accomplished to gain basic knowledge for modelling of glued laminated timber (GLT) composed of Norway spruce lamellas. For this the main part was executed and reported by GLOS (1978). For tension strength and E-modulus parallel to grain the regression equations are given as

$$\ln\left(E_{t,0,ij}\right) = 8.20 + 3.13 \cdot \rho_0 - 1.17 \cdot KAR + \varepsilon_E \,, \tag{5.62}$$

with correlation coefficient $r = 0.77$ and $\sigma[\varepsilon_E] = 0.180$, and

$$\ln\left(f_{t,0,ij}\right) = -4.22 + \ln\left(E_{t,0,ij}\right) \cdot \left(0.876 - 0.093 \cdot KAR\right) + \varepsilon_f \,, \tag{5.63}$$

with correlation coefficient $r = 0.86$ and $\sigma[\varepsilon_f] = 0.187$, with $E_{t,0,ij}$ and $f_{t,0,ij}$ as tension E-modulus and strength of board segments in [N/mm²], respectively, ρ_0 as oven dry density in [kg/m³] and KAR as knot area ratio in [%].

Following the specifications for groups G_I, G_II and G_III as given in Tab. 5.12 and the basic assumption that these groups are somehow related to the strength classes C24, C30 and C40 according EN 338, the densities ρ_{12} defined at a reference moisture content of $u = 12\%$ are given as 410, 460 and 500 kg/m³, respectively for group G_I to G_III. The oven dry densities can be calculated by excluding the mass of water and consideration of a reduction in volume due to shrinkage. The reduction in volume, in particular near $u \approx 0\%$ is non-linear (chemisorption). Thus the differential ratio of shrinkage cannot be applied. Nevertheless, for the following calculations it is judged to be sufficient accurate to use the simplified approach given in EN 384 and to adapt the density by 0.5% per percent change in moisture content. A compilation of densities is given in Tab. 5.34.

Tab. 5.34: Expectations and coefficients of variation of densities; groups G_I to G_III

		G_I	G_II	G_III
$E[\rho_{12}] = \rho_{12,mean}$	**[kg/m³]**	420	460	560
$E[\rho_0] = \rho_{0,mean}$	**[kg/m³]**	396	434	472
$CoV[\rho_{12}] = CoV[\rho_0]$	**[%]**	8%	8%	8%

Furthermore, E-modulus and strength in equ. (5.62) and (5.63) are formulated in dependency of knot share parameter *KAR*. This parameter is related to 150 mm or 137.5 mm long board segments. Due to the fact that this parameter gives the share of the sum of knot area within the reference segment length projected on the cross section and the observation that the expected width of weak zones (e.g. defined by knot clusters) was found by own analysis to be $E[w_{WZ}] = 70$ mm (see Tab. 5.12) the same equations for local strength and E-modulus can be applied, even for the definition of a stochastic reference segment length. Assuming that the width of weak zones (w_{WZ}) follows a 2pLND with $CoV[w_{WZ}] = 40\%$ (see Tab. 5.12) it can simply worked out that 98.5% or at least 97.4% of all weak zones are smaller or equal to segments with a length of 150 mm or 137.5 mm.

Based on regression equations (5.62) and (5.63) it can be observed that the whole variabilities of local strength and E-modulus are represented by the errors ε_f and ε_E. It can be shown that in the examinations of GÖRLACHER (1989) and COLLING (1990) also a two-level hierarchical model and thus a partitioning of total variance in within and between variation of E-modulus and strength of board segments took place. COLLING (1990) proposed to regulate $\sigma^2[\varepsilon_E] = \sigma^2[\varepsilon_{E,X}] + \sigma^2[\varepsilon_{E,Y}]$, with iid $\varepsilon_{E,X} \sim ND(0; \sigma^2[\varepsilon_{E,X}])$ and iid $\sigma^2[\varepsilon_{E,X}] \sim ND(0.079; 0.27^2)$, as well as iid $\varepsilon_{E,Y} \sim ND(0; 0.16^2)$. This corresponds to an equicorrelation of $\rho_{equi}(E_{t,0,ij}) \approx 0.80$, which is much higher than found in section 5.1 on average (see also Tab. 5.12). The variance of tensile strength was defined as $\sigma^2[\varepsilon_f] = \sigma^2[\varepsilon_{f,X}] + \sigma^2[\varepsilon_{f,Y}]$. Both variances are iid $\sigma^2[\varepsilon_{f,X}] = \sigma^2[\varepsilon_{f,Y}] \sim ND(0; 0.13^2)$ which corresponds to $\rho_{equi}(f_{t,0,ij}) \approx 0.50$. This is in line with the results found in section 5.1.1.

Overall, application of regression equations (5.62) and (5.63) delivers basic strength and stiffness characteristics of weak zones. The results based on 10,000 randomly generated variates are shown in Tab. 5.35.

On a first view values of $E[E_{t,0,ij}]$ are 5% to 10% below the values associated with strength classes C24, C30 and C40. According EN 338 these are $E_{t,0,mean}$ = 11,000, 12,000 and 14,000 N/mm², respectively for C24, C30 and C40, although an additional reduction

of the expectations in Tab. 5.35 due to serial effects on E-modulus (see section 5.3.4) has to be taken into account. Values of CoV[$E_{t,0,ij}$] are in contrast and on average nominal 9% (relative 60%) higher than expected (see e.g. Tab. 5.25 for comparison). Judgement of E[$f_{t,0,ij}$] is currently difficult, the same is true for CoV[$f_{t,0,ij}$]. Nevertheless a comprehensive analysis of test data of boards in BRANDNER AND SCHICKHOFER (2008) showed that CoV[$f_{t,0}$] can be expected to be within the range of (30 ± 10)%. Based on randomly generated variates also a correlation coefficient between strength and E-modulus of $\rho(f_{t,0,ij}; E_{t,0,ij}) = 0.75$ can be observed. This magnitude of correlation is in line with that in Tab. 5.12.

Tab. 5.35: Expectations and coefficients of variation of tensile strength and E-modulus parallel to grain of board segments; groups G_I to G_III

		G_I	G_II	G_III
E[$E_{t,0,ij}$]	**[N/mm²]**	9,912	11,554	13,472
CoV[$E_{t,0,ij}$]	**[%]**	24.0%	23.8%	23.8%
E[$f_{t,0,ij}$]	**[N/mm²]**	39.3	45.9	53.6
CoV[$f_{t,0,ij}$]	**[%]**	31.5%	30.8%	30.2%

Based on a complete set of input parameters for strength characteristics of board segments, in general of sub-elements, and by means of equ. (5.60) for a fixed value of M it is possible to calculate serial system effects of systems composed of unjointed but serial correlated elements and sub-elements. If M itself constitutes a random variable, as indicated by the stochastic nature of the distance between knot clusters (d_{WZ}), the convolution integral of equ. (5.60) has to be adapted to

$$F_{Z_M}(z|l) = \int_0^\infty f_M(m) \cdot F_{Z_M}(z|m) \cdot dm\,, \tag{5.64}$$

with $M \sim 2\text{pLND}(\mu[l] - \mu[d_{WZ}]; \sigma^2[d_{WZ}])$ and l as the length of the analysed serial system or structural timber member. As the expectation and variance of $F_{Z_M}(z|M)$ solely depend on CoV[Z_{ij}] and M it is only required to integrate over the ratio

$$\frac{X_{M,\xi}}{X_{1,\xi}} = \int_0^\infty f_M(m) \cdot \frac{1}{\left[\ln(m) \cdot \beta_\xi + 1\right]^{\alpha_\xi}} \cdot dm\,, \tag{5.65}$$

see also equ. (3.102). This can in principle be done numerically or simply by means of random variates. Considering the second approach and the analysed ranges of parameters it can be simply demonstrated that 10^6 random variates are sufficient to derive ratios $X_{M,\xi} / X_{1,\xi}$ for ξ as expectation or standard deviation with an accuracy of at least three digits.

Based on this facts and the models serial system effects of unjointed and finger jointed structural timber members are discussed in the following sections 5.4.1 and 5.4.2, respectively.

5.4.1 Serial System Effects in unjointed Structural Timber

Following the two-level hierarchical model of previous section 5.4 it can be concluded that the magnitude of serial system effects of unjointed structural timber depends on (i) the length of the timber, (ii) the distance between weak zones and (iii) the variation of tensile strength, observable within structural timber and expressed by CoV[X_{ij}]. Based on total variation expressed by CoV[Z_{ij}] parameters CoV[X_{ij}] and CoV[Y_j] of groups G_I to G-III can be calculated directly by means of equ. (5.20) and by means of $\rho_{equi}(f_{t,0,ij}) = (0.40 \div 0.50)$ (see Tab. 5.12). The results are given in Tab. 5.36. Based on the observation made in section 5.1 that the amount of serial correlation increases with increasing timber quality the results for CoV[X_{ij}] and CoV[Y_j] in Tab. 5.36 are derived by adapting $\rho_{equi}(f_{t,0,ij})$ group-wise.

Retaining the same reference length $l_{ref} = 2{,}000$ mm as used in previous section 5.3 and expectation and variance of M as given in Tab. 5.26 the length effects and main characteristics of the tensile strength of boards, as given in Tab. 5.37, can be determined. This was done by means of 10,000 generated random variates with models and input parameters as mentioned above.

Tab. 5.36: Coefficients of variation for total, within and between element variation of local tensile strength; groups G_I to G_III

		G_I	G_II	G_III
$\rho_{equi}(f_{t,0,ij})$	[--]	0.40	0.45	0.50
CoV[Z_{ij}]	[%]	31.5%	30.8%	30.2%
CoV[X_{ij}]	[%]	24.4%	22.8%	21.4%
CoV[Y_j]	[%]	19.9%	20.7%	21.4%

Tab. 5.37: Strength characteristics and results of serial system action on unjointed structural timber; groups G_I to G_III

		G_I	G_II	G_III
$f_{t,0,mean}$ (CoV)	[N/mm²] ([%])	29.4 (8.4%)	35.7 (8.2%)	43.1 (7.9%)
CoV[$f_{t,0}$]	[%]	30.9%	30.6%	30.3%
$f_{t,0,05}$	[N/mm²]	17.1	20.9	25.3
std. dev. $f_{t,0,i\,|\,j}$ (CoV)	[N/mm²]	4.6 (21.7%)	5.4 (22.1%)	6.3 (22.5%)
CoV[$f_{t,0,i\,|\,j}$]	[%]	15.7%	15.2%	14.6%
$f_{t,0,mean}$ / $f_{t,0,ij,mean}$	[--]	0.748	0.778	0.804
$f_{t,0,05}$ / $f_{t,0,ij,05}$	[--]	0.756	0.780	0.803
$f_{t,0,k}$ acc. EN 338	[N/mm²]	14.0	18.0	24.0

If it can be assumed that the distance between weak zones (d_{WZ}) is also equicorrelated with $\rho_{equi}(d_{WZ}) \approx 0.50$ an increase in the statistics of expectation and 5%-quantile of approximately 1% can be observed. Due to this minor effect d_{WZ} is further treated as uncorrelated.

If the bias inherent in the applied model for calculating the serial system effect for the 5%-quantile, as illustrated in Fig. 3.26, is taken into account by linear interpolation between the bias at CoV[X] = 10% and 50% an overestimation of approximately 5% has to be considered. The bias-corrected values $f_{t,0,05,corr}$ are given in Tab. 5.38.

Tab. 5.38: Bias-corrected 5%-quantile estimates for group G_I to G_III

		G_I	G_II	G_III
$f_{t,0,05,corr}$	[N/mm²]	16.3	19.9	24.1

In comparison with characteristic tensile strength values for strength classes C24, C30 and C40 as anchored in EN 338 the 5%-quantiles $f_{t,0,05,corr}$ in Tab. 5.38 show overall overestimation, in particular significant for G_I and G_II. This is not surprising because of the fact that the models used for generation of random variates of $f_{t,0,ij}$ according EHLBECK ET AL. (1985A) solely base on density, (estimated) E-modulus and knot share parameter *KAR*. It is well known and easy to prove that in particular lower timber qualities are characterised by a variety of additional global (type [1], section 5.1) and local (type [2], section 5.1) growth characteristics which decisively affect the tensile strength. For example global grain deviation, which significantly affects tensile strength

parallel to grain (see e.g. section 4.3.2), is in structural timber of lower qualities not as strict regulated and more common as in timber of strength class C40. Also the amount, variety and magnitude of knot clusters, indicating local grain deviation, are more distinct in lower timber qualities. This fact is partly taken into account by higher *KAR*-values and reduced E[d_{WZ}]. Nevertheless, unsymmetrically placed knots and knot clusters induce regions of significant lower stiffness in the cross section. This causes some amount of MN-interaction during tensile testing which reduces the observable tensile strength of structural timber. This effect was e.g. published by COLLING ET AL. (1991) and FALK AND COLLING (1994, 1995) and is one major parameter for the explanation of the "laminating effect", the homogenisation effect on strength of GLT, defined by $\lambda = f_{m,g} / f_{t,0,l}$, constituting the ratio between the bending strength of GLT and the tensile strength of the board material or GLT-lamellas. This effect of restricted MN-interaction by continuous lateral support of boards as part of GLT was estimated to be up to 1.4 (see e.g. COLLING ET AL., 1991). Another growth characteristic, the reaction wood, is also more common in timber of lower quality. This timber characteristic increases the density but reduces strength. This initiates some bias in the calculation of local strength and stiffness values based on the parameter density.

As the values in EN 338 are mainly based on tests overestimation of $f_{t,0,k}$ by $f_{t,0,05,corr}$ is not surprising, in particular if the unknown uncertainties inherent in the models and parameter sets are qualitatively considered. Quantification and further validation of the magnitude of all these effects is currently not possible, even not by means of a relationship between characteristic board tensile strength according EN 338 ($f_{t,0,l,k}$) and the characteristic strength of board segments ($f_{t,0,k,sim} = f_{t,0,ij,05}$) as provided by BLAß ET AL. (2008), see

$$f_{t,0,l,k} = -10.7 + 1.261 \cdot f_{t,0,k,sim} \,. \tag{5.66}$$

This equation considers explicitly neither the influence of the discussed local and global growth characteristics nor the influence of changes e.g. in equicorrelation or distance between weak zones, associated with changes in timber quality.

Nevertheless, for a more generalised consideration of the serial system effect the influence of changes in parameters are examined. Thereby parameters CoV[$f_{t,0,ij}$] = (20, 30, 40)%, l = (1.0 ÷ 12.0) m, E[d_{WZ}] = (400, 500, 600) mm were varied, by leaving parameters CoV[d_{WZ}] = 60% and $\rho_{equi}(f_{t,0,ij})$ = 0.45 constant. The results given as relative changes in expectation and 5%-quantile are illustrated in Fig. 5.32. Again

strength characteristics at l_{ref} = 2,000 mm were taken as reference. A bias correction in the graphs as done in Tab. 5.38 is not necessary as the bias behaves approximately constant for $M \geq (5 \div 10)$ serial linked elements which is on average already widely fulfilled at l_{ref}.

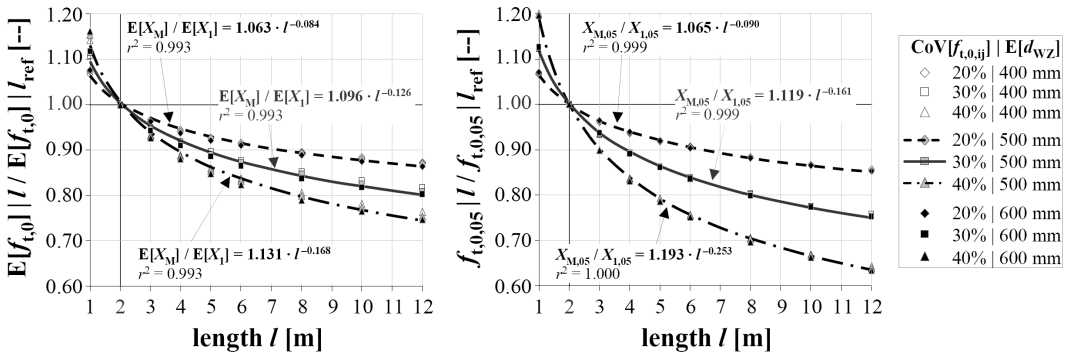

Fig. 5.32: Serial system effects on expectation and 5%-quantile of tensile strength of unjointed structural timber: influence of parameter variation CoV[$f_{t,0,ij}$], E[d_{WZ}] and length as well as best fitted power models

In contrast to the findings in section 3.3.1 where it was shown that serial system effects on 5%-quantiles are less pronounced than on expectation, the opposite can be observed in Fig. 5.32. This can be explained by the fact that serial system action in unjointed structural timber lead only to a reduction in variability within the timber elements but has no effect on the variability observable between the elements. As $\rho_{equi}(f_{t,0,ij})$ was found to be only $0.40 \div 0.50$ the magnitude of CoV[Y_j] is nearly equal ($\leq$) to that of CoV[X_{ij}]. As the expectation of strength of elements with increasing length or increasing number of serial acting sub-elements is reduced, Var[Y_j] affects the total variability of $f_{t,0}$ even more than in cases where only sub-elements are analysed. Consequently, even a minor but with CoV[Z_{ij}] increasing CoV[$f_{t,0}$] can be observed (see e.g. Tab. 5.39). Consequently, serial system action on 5%-quantiles of tensile strength of unjointed structural timber is even higher than on the mean value. Nevertheless, the increase in CoV[$f_{t,0}$] even in members multiple-times the reference length is so small that a verification by tests appears only possible by uneconomic efforts.

Power models by means of LSM were fitted to the simulation data to allow a comparison of length effects with current regulations and literature. As the influence of E[d_{WZ}] can be judged as negligible these power models were only fitted to data generated with E[d_{WZ}] = 500 mm. The fit to design relevant 5%-quantiles is even better and in total

nearly perfect than to mean-values. Overall, lack in compliance between simulation data and power models results in some conservativeness.

Based on Fig. 5.32 it becomes obvious that CoV[Z_{ij}] constitutes the dominating parameter in modelling serial system effects. This is in particular expressed by its influence on the power parameter, being 0.090, 0.161 and 0.253, respectively for CoV[Z_{ij}] = (20, 30, 40)%. Due to the fact that CoV[$f_{t,0}$] = (30 ± 10)% with E[CoV[$f_{t,0}$]] = 30% and CoV[$f_{t,0}$] ≈ CoV[Z_{ij}] at l_{ref} = 2,000 mm length effect on $f_{t,0,05}$ can be represented by a power model with power parameter $k_{l,05}$ = 0.16. If the whole range of CoV[$f_{t,0}$] is split into two groups of CoV[$f_{t,0}$] = (25 ± 5)% and CoV[$f_{t,0}$] = (35 ± 5)%, as for example proposed by BRANDNER AND SCHICKHOFER (2008), the power parameters are proposed to be $k_{l,05}$ = 0.13 and 0.21, respectively.

Tab. 5.39: Coefficients of variation of tensile strength of unjointed structural timber in dependency of CoV[$f_{t,0,ij}$] and the analysed length l

	CoV[$f_{t,0}$]		
CoV[$f_{t,0,ij}$]	**$l = l_{ref}$ = 2.0 m**	**l = 4.0 m**	**l = 8.0 m**
20%	18.7%	18.9%	19.3%
30%	29.7%	31.0%	32.6%
40%	42.2%	45.5%	49.3%

Back to the observation that the length effect on 5%-quantiles is found to be higher than on mean-level it can be stated that this observation is in principle not new. Following the literature survey in section 5.1.2 already MADSEN (1990) found for tension strength power parameters $k_{l,50}$ = 0.13 and $k_{l,05}$ = 0.22. Later and based on a literature survey, BURGER (1998) concluded with factors $k_{l,50}$ = 0.12 and $k_{l,05}$ = 0.18. Based on his own experiments, data analysis and modelling he proposed to regulate length effects with $k_{l,50}$ = 0.15 or 0.10 and $k_{l,05}$ = 0.23 or 0.20 for ungraded or visually graded unjointed structural timber. Nevertheless, BRANDNER ET AL. (2007A) report on contrary test results gained from testing structural timber elements with a free test length between l_{free} = 1,440 mm and 17,222 mm. Thereby best fitted power models gave $k_{l,mean}$ = 0.23 and for $k_{l,05}$ = 0.16. Nevertheless, whereas at l_{free} = 1,440 mm unjointed material was used, tests at l_{free} = 7,982 mm and 17,222 mm base on finger jointed structural timber. As discussed in more detail in the next section 5.4.2 this aspect has definitely an influence on the observable length effect in particular if the analysed data constitute a mixture of unjointed and jointed material.

Based on ratios $f_{t,0,mean} / f_{t,0,ij,mean}$ and $f_{t,0,05} / f_{t,0,ij,05}$ in Tab. 5.37 given for groups G_I to G_III it can be observed that serial system effects decrease with increasing timber quality. This was for example also reported by WILLIAMSON (1992) who proposed a $k_l = 0.11$ and 0.16 for high and low grade timber, respectively.

Overall it can be concluded, that the factors for $k_{l,05}$ found in modelling and simulation scenarios are within the range of published values. It can be also concluded that influences by E[d_{WZ}] are negligible. Nevertheless, CoV[$f_{t,0,ij}$] and thus CoV[$f_{t,0}$] at l_{ref} has to be known or at least regulated on a reliable basis.

The presented and discussed models enable direct consideration of within and between variation of strength characteristics but also of the stochastic nature of length and growth characteristics of single, reference elements. This allows direct reaction on changes in input parameter sets. It was outlined that the main parameters are not geometric parameters like d_{WZ}. The overall dominating parameter is represented by CoV[$f_{t,0}$]. This parameter has to be controlled by adequate methods or at least kept in a reliable range by application of adequate classification methods, e.g. the grading process of the raw material timber.

5.4.2 Serial System Effects in jointed Structural Timber

Within this section effects on finger jointed structural timber caused by serial system action are addressed. If such a member is longitudinally stressed in tension it can either fail in M elements of timber or in $(M - 1)$ finger joints. The weakest element decides about the resistance capacity of the whole member, the serial system. The jointed timber elements are further treated as iid. This is not always completely fulfilled in practise were zones which are not allowed in the aimed timber quality are trimmed out and the residual parts are jointed again. Thus it happens that parts of the same board or beam are again connected. Thereby the equicorrelation between these parts is the same as before the trimming process. This aspect is even more obvious if beams are only trimmed and jointed to reduce bow and twist to an amount acceptable for the desired timber quality and / or for the further production process. Nevertheless, the simplification to consider the parts as iid is further applied, not at least due to missing information about the distribution of joints of correlated and uncorrelated parts.

The number of finger joints per reference length $l_{ref} = 2{,}000$ mm is herein treated as deterministic. This is done because the influence of this simplification on several system

effects is judged as being small (see e.g. the influence of d_{WZ} as analysed in section 5.4.1). Furthermore, distances between finger joints vary between producers and countries. Nevertheless, explicit consideration of its stochastics can be done the same way as demonstrated for parameter d_{WZ}.

Before examinations can be performed on finger jointed structural timber it is required to regulate the performance of finger joints in relationship to that of the joining parts, the timber elements. This is done in the following sub-section.

Definition of Minimum Requirements on the Finger Joint Tensile Strength

In general, finger joints can be described as folded scarf joints. The sum of fingers provide a large surface to transfer tension stresses parallel to grain applied on structural timber in shear along the flankes of the fingers. The connection itself is done by means of a suitable adhesive system which is in general optimised for resisting shearing. Thus finger joints constitude rigid connections with a high degree of utilisation. If the tensile strength of the joint is compared to the tensile strength of structural timber a degree of utilisation of one or even above one can be reached. The reason for this outstanding performance follows from the facts that (1) finger joints have to be placed in the clear wood section of timber elements with sufficient minimum distance to adjacent knots or knot clusters to be not influenced by local grain deviation, and (2) normally it has to be secured that failure is not governed by the adhesive system but by the joining timber parts. Concerning the second point failures can be differentiated into (i) net-section failures in tension caused by the reduced cross section on the base-line of finger joints, (ii) shear failure along the flankes due to exceedance of shear strength of wood or of the adhesive system (last one has to be prevented), (iii) tension failure outside the finger joint due to a local, strength reducing characteristic, and (iv) some kind of mixture of failure types (i) to (iii). In particular failure types (i) and (ii) are decisively influenced by the geometry, the profile of the fingers. Tab. 5.40 gives a brief overview of common profiles used in Europe.

There are numerous publications dealing with stress transfer and optimisation of finger joint profiles and the interaction of finger joints in laminated products, e.g. AICHER AND KLÖCK (1990), COLLING AND EHLBECK (1992), RADOVIC AND ROHLFING (1993), GROOM AND LEICHTI (1994), SMARDZEWSKI (1995), HERNANDEZ (1998), SERRANO ET AL. (2001) and KONNERTH ET AL. (2006). Following the report of AICHER AND KLÖCK (1990) it can be concluded that the parameter $v(b_n)$ constitute one main parameter for the

optimisation of the mechanical potential of finger joints as it directly gives changes in normal stresses proportional to the loss in cross section. Concerning the parameter α, an inversely proportional reduction in stress was observed with a maximum resistance at $\alpha \approx 1 / 14$ and a significant decrease in strength at $\alpha > 1 / 10$. Due to concentration of stresses at the finger tips it was also suggested to keep the ratio $l_t / b_t > 1.00$ or even at ≥ 1.50. Furthermore it was proposed to choose the geometry of fingers such that the ratio of bond surface to net cross section complies with the ratio of shear strength and tensile strength of timber parallel to grain.

Tab. 5.40: Finger joint profiles, geometric measures and loss in cross section

l [mm]	p [mm]	b_t [mm]	b_n [mm]	l_t [mm]	α [°]	$v(b_n)$ [%]
15	3.8	0.42	0.52	0.5	5.6	13.6%
20	5.0	0.50	0.60	0.5	5.7	12.0%
20	6.2	1.00	1.11	0.5	6.0	17.8%
30	6.2	0.60	0.68	0.5	4.8	11.0%

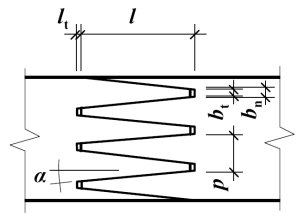

l … finger length; p … pitch; b_t … tip width; b_n … base width; l_t … tip gap; α … angle; $v(b_n)$ … loss in cross section

Overall it can be recommended to use an adhesive system which enables the production of finger joints nearly as stiff as the surrounding clear wood or even with a reduced stiffness. This is in particular of interest if finger jointed elements serve further as basic element for composing engineered timber system products of parallel aligned and continously, and by adhesive rigidly connected, parallel and common acting elements. In this case and as already intensively demonstrated in section 3.4 the stiffer an element the more stress it attracts. If a stiff finger joint is situated parallel to a weaker element the finger joint attracts the major part of stresses. If the joint is thereby as stiff as the surrounding clear wood in any case the resistance will be lower but the attracted stresses are the same. Thus it would be meaningful to reduce the stiffness of finger joints proportional to their resistance in relationship to that of clear wood of the weaker joining partner to prevent local failures. Therefore it would be required to know the performance of finger joints explicitly and in relationship to clear wood and of structural timber as the joining partners. This is in fact a challenge of its own because the performance of finger joints is decisively influenced not only by the materials wood, timber and the adhesive system but to a remarkable extend also and even more by the whole production process.

Concerning the first part, the relationship of finger joint tensile strength ($f_{t,0,FJ}$) to that of structural timber as joining partner ($f_{t,0}$) it is for example by MOODY (1970), EHLBECK ET AL. (1985B) and COLLING (1990) stated that $f_{t,0,FJ}$ is found to be related to the characteristics (e.g. strength, stiffness and density) of the weaker joining part. This is in fact reasonable so far failure takes place in the wooden part of the finger joint according a serial system in the weaker element. Thus the relationship of $f_{t,0,FJ}$ on density ρ and E-modulus $E_{t,0}$ indicates also a certain but in general very weak relationship to the tensile strength of structural timber $f_{t,0}$. This becomes obvious as $f_{t,0}$ is only to a small amount governed by the global potential of timber, e.g. expressible by parameters density and E-modulus (representatives of type [1], see section 5.1), but primarily by local characteristics of weak zones (representatives of type [2], see section 5.1). Consequently, in the following analysis finger joint tensile strength is modelled as a random variable, independent of the tensile strength of structural timber of the joining members.

Concerning the second part, the influence of production parameters on the resistance of finger joints, the following crucial parameters can be listed:

- geometry of fingers;
- service and maintenance of the production facilities, e.g. of moulder, and conveyors;
- suitability of bonding parameters, e.g.
    - adhesive system in respect to adequate joint stiffness;
    - bonding pressure;
    - adequate lateral support to prevent or at least reduce edge effects during pressing;
    - compliance of wet life, holding and curing time
    - climatic conditions, in particular temperature and moisture content of timber;
    - adequate and homogeneous application of adhesive;
    - adequate and homogeneous blend of adhesive and hardener;
- securing of adequate and homogeneous characteristics of the base material structural timber, e.g.
    - moisture content;
    - material inherent extractives;

- material inherent variability of density (in respect to bonding pressure) and of material characteristics in general (→ weakest link: in case of high potential differences a remarkable reduction of the average performance of finger joints in combination and a higher CoV[$f_{t,0,FJ}$] are given).

The huge amount of influencing production parameters and the variety of machinery developed for the finger jointing process are the reasons why this in general very complex process leads to a manufacturer individual maximum level in finger joint performance. Consequently it is proposed not to model the process itself but to regulate the demanded performance of $f_{t,0,FJ}$ by the definition of minimum requirements. These should be defined in dependency of and suitable for the demanded performance of engineered timber system products. On the basis of the assumptions made in previous section 5.4.1 and on a comprehensive data analysis following statements and assumptions are made:

- iid $f_{t,0,FJ}$ ~ 2pLND; CoV[$f_{t,0,FJ}$] = (15 ± 5)%;
- iid $f_{t,0}$ ~ 2pLND; CoV[$f_{t,0}$] = (30 ± 10)%;
- $\rho(f_{t,0}; f_{t,0,FJ}) = 0$;
- for simplicity it is assumed that the joining partners are of equal length.

In line with current regulations of strength which are based on 5%-quantiles a model is sought which relates $f_{t,0,05}$ to $f_{t,0,FJ,05}$ e.g. by

$$f_{t,0,FJ,05}(\geq) = \zeta_{05} \cdot f_{t,0,05} \cdot \tag{5.67}$$

Thereby $f_{t,0,05}$ is defined as 5%-quantile of the tensile strength parallel to grain of an unjointed structural timber element at reference length l_{ref} = 2,000 mm and $f_{t,0,FJ,05}$ as 5%-quantile of tensile strength parallel to grain of a single finger joint placed in the clear wood section of structural timber of the same population and tested with the same cross section, and ζ_{05} as parameter defined as ratio between both strength characteristics. In the following some possibilities for the definition of minimum requirements for $f_{t,0,FJ}$ are formulated:

[1] securing equal reliability of unjointed and jointed structural timber at reference length;

[2] securing equal 5%-quantiles of unjointed and jointed structural timber at reference length;

[3] securing equal failure probability of M jointed timber elements and $(M - 1)$ finger joints.

For requirement [1] a lognormally distributed action is defined with CoV = 30% and with expectation adjusted to fulfill a reliability index of $\beta = 4.2$ in dependency of the resistance of an unjointed structural timber element at $l_{ref} = 2{,}000$ mm. Hence expectation $E[f_{t,0,FJ}]$ at given $CoV[f_{t,0,FJ}]$ and $(M - 1)$ finger joints is iteratively found by complying the requirement defined in [1]. The results for the cases of one, two and three finger joints per l_{ref} are shown in Fig. 5.33. The parameter settings for the analysis are: $E[d_{WZ}] = 500$ mm, $CoV[d_{WZ}] = 60\%$, (arbitrary choosen) $E[f_{t,0,ij}] = 50$ N/mm², $CoV[f_{t,0,ij}] = (15, 20, \ldots, 45)\%$, $\rho_{equi}(f_{t,0,ij}) = 0.45$ and $CoV[f_{t,0,FJ}] = (10, 15, 20)\%$.

It can be concluded that in almost all cases the minimum requirements on $f_{t,0,FJ,05}$ to fulfill equal or higher reliability between unjointed and finger jointed structural timber elements are even lower than on $f_{t,0,05}$. Although jointing of uncorrelated elements results in qualitative higher loss in average strength due to more significant serial system action, also a higher reduction in variability and thus a reduced effect on the 5%-quantile can be observed. Furthermore, the expected coefficient of variation of $f_{t,0,FJ}$ is much lower than that of $f_{t,0}$ which further reduces the effects caused by jointing. It can be also observed that the influence by the number of finger joints per reference length on the ratio $f_{t,0} / f_{t,0,FJ}$ is small but confirms the expectation of increasing requirements on $f_{t,0,FJ}$ with increasing number of joints. The influence of $CoV[f_{t,0,FJ}]$ on the analysed ratio is negligible. Nevertheless, in case of $CoV[f_{t,0,FJ}] < CoV[f_{t,0,ij}]$ the failure of jointed structural timber is dominated by the failure of finger joints, with a failure rate of $(70 \div 100)\%$. Fig. 5.33 contains exponential regression models and their degree of determination. These models serve as suitable basis for estimating the analysed ratio in dependency of $CoV[f_{t,0}]$ given at $l_{ref} = 2{,}000$ mm.

For requirement [2] in principle the same parameter setting as for [1] was applied but with the aim to adjust $E[f_{t,0,FJ}]$ at given $CoV[f_{t,0,FJ}]$ such that the 5%-quantiles of unjointed and jointed structural timber elements at l_{ref} are equal. The results as ratio between $f_{t,0}$ and $f_{t,0,FJ}$ versus $CoV[f_{t,0}]$ are illustrated in Fig. 5.34. It can be observed that the dependency of the ratio on $CoV[f_{t,0}]$ and / or $CoV[f_{t,0,FJ}]$ is small. The relevance of this kind of definition of minimum requirements on $f_{t,0,FJ}$ can be argued by the fact that current product and design standards base on 5%-quantiles of strength values.

For requirement [3] again the same parameter setting as for [1] and [2] are applied. The results are plotted in Fig. 5.35. Hereby E[$f_{t,0,FJ}$] was adjusted at given CoV[$f_{t,0,FJ}$] to reach an equal failure probability of 50% in finger joints as well as 50% in the jointed timber elements. This can be achieved by equal medians

$$med\left[f_{t,0}\right] \equiv med\left[\min_{(m-1)}\left[f_{t,0,FJ}\right]\right] \quad . \tag{5.68}$$

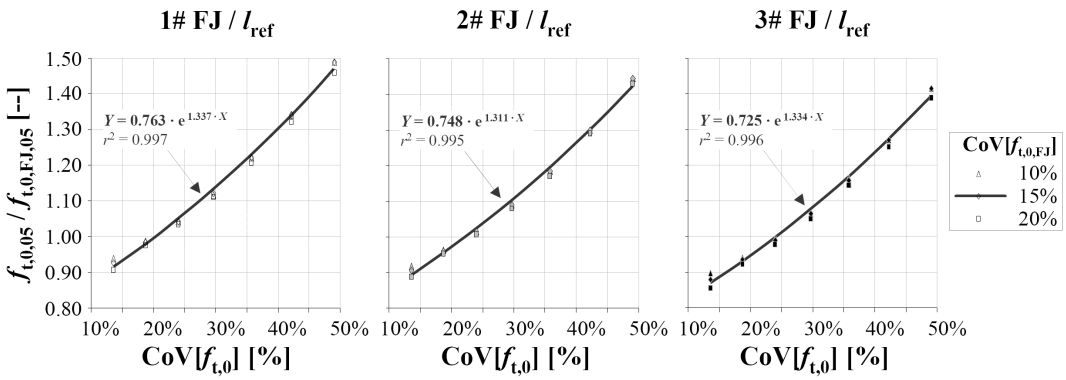

Fig. 5.33: Ratio of $f_{t,0,05}$ of unjointed structural timber at l_{ref} = 2,000 mm and of $f_{t,0,FJ,05}$ of single finger joints vs. CoV[$f_{t,0}$] and CoV[$f_{t,0,FJ}$] for the cases of 1#, 2# and 3# finger joints per l_{ref}: E[$f_{t,0,FJ}$] defined to secure equal reliability between unjointed and jointed structural timber, assuming a lognormally distributed action with CoV = 30% and β = 4.2

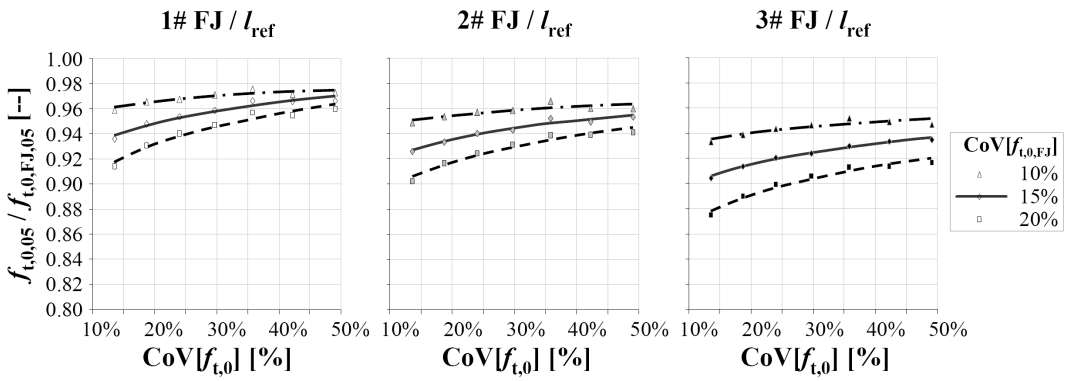

Fig. 5.34: Ratio of $f_{t,0,05}$ of unjointed structural timber at l_{ref} = 2,000 mm and of $f_{t,0,FJ,05}$ of single finger joints vs. CoV[$f_{t,0}$] and CoV[$f_{t,0,FJ}$] for the cases of 1#, 2# and 3# finger joints per l_{ref}: E[$f_{t,0,FJ}$] defined to secure equal 5%-quantiles between unjointed and jointed structural timber

Based on the graphs in Fig. 5.35 a significant influence of parameters CoV[$f_{t,0}$] and / or CoV[$f_{t,0,FJ}$] can be observed. Thereby the dependency on CoV[$f_{t,0,FJ}$] decreases as the number of finger joints per l_{ref} increases. Also the slope is slightly reduced. This is because of the reduced variability caused by min[$f_{t,0,FJ}$]. Values for parameter ζ_{05}, defined as ratio $f_{t,0,FJ,05} / f_{t,0,05}$, are listed in Tab. 5.41. Thereby the best fitted exponential regression models as shown in Fig. 5.35 are used for calculation. These models show perfect correspondence with model and simulation results. The reason for this can be explained by a theoretical example of a chain consisting of one finger joint and one structural timber element. Following this example parameter ζ_{05} is simply given as

$$\zeta_{05} = \frac{f_{t,0,FJ,05}}{f_{t,0,ST,05}} = \frac{\exp\left[\mu_{FJ} - k_{05} \cdot \sigma_{FJ}\right]}{\exp\left[\mu_{ST} - k_{05} \cdot \sigma_{ST}\right]} \ , \tag{5.69}$$

with $k_{05} = \Phi^{-1}(0.05) \approx 1.645$ and $\Phi^{-1}(.)$ as operator of the inverse SND.

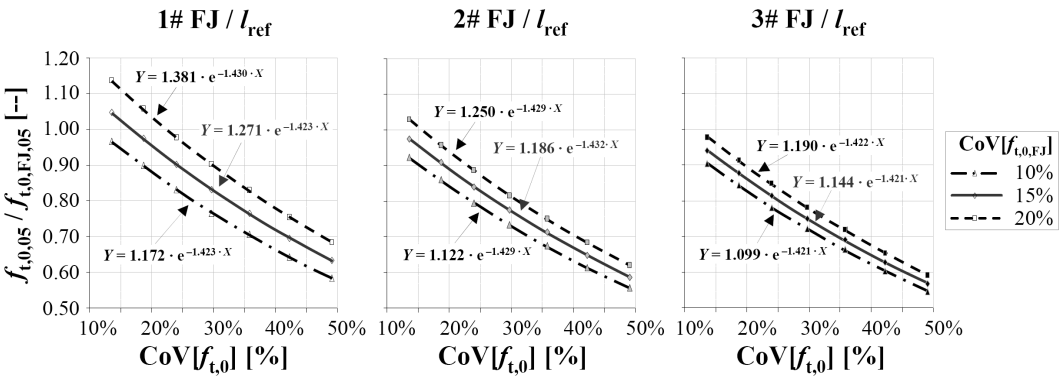

Fig. 5.35: Ratio of $f_{t,0,05}$ of unjointed structural timber at l_{ref} = 2,000 mm and of $f_{t,0,FJ,05}$ of single finger joints vs. CoV[$f_{t,0}$] and CoV[$f_{t,0,FJ}$] for the cases of 1#, 2# and 3# finger joints per l_{ref}: E[$f_{t,0,FJ}$] defined to secure equal failure probability in finger joints and timber (equal median values)

Based on the requirement given in equ. (5.68) and the general definition of the medians of a lognormally distributed variable Y defined by med[Y] = exp(μ_X) equ. (5.69) simplifies to

$$\zeta_{05} = \exp\left[-k_{05} \cdot \sqrt{\ln\left(1 + COV^2\left[f_{t,0,FJ}\right]\right)}\right] \cdot \exp\left[k_{05} \cdot \sqrt{\ln\left(1 + COV^2\left[f_{t,0}\right]\right)}\right] \ . \tag{5.70}$$

If CoV[$f_{t,0,FJ}$] is fixed the first term acts as pre-factor and the second term as exponential term in dependency of the explaining variable CoV[$f_{t,0}$]. This formulation corresponds inversely to the regression equations in Fig. 5.35.

This definition of minimum requirements is suitable for the regulation of production requirements by keeping the maximum share of finger joint failures by a balanced value of ≤ 50% which corresponds in the analysed parameter range to the fact that in most cases $f_{t,0,FJ,05} > f_{t,0,05}$ is required. Nevertheless, the presented general model for the determination of minimum requirements allows also to define values of $f_{t,0,FJ,05}$ for every probability of failure of finger joints.

Tab. 5.41: Parameter ζ_{05} in dependency of CoV[$f_{t,0,FJ}$], CoV[$f_{t,0}$] and the number of finger joints per reference length

	1# FJ / l_{ref}			**2# FJ / l_{ref}**			**3# FJ / l_{ref}**		
	CoV[$f_{t,0}$]			**CoV[$f_{t,0}$]**			**CoV[$f_{t,0}$]**		
	25%	**30%**	**35%**	**25%**	**30%**	**35%**	**25%**	**30%**	**35%**
ζ_{05} | CoV[$f_{t,0,FJ}$] = 10%	1.22	1.31	1.40	1.27	1.37	1.47	1.30	1.39	1.50
ζ_{05} | CoV[$f_{t,0,FJ}$] = 15%	1.12	1.21	1.29	1.21	1.30	1.39	1.25	1.34	1.44
ζ_{05} | CoV[$f_{t,0,FJ}$] = 20%	1.04	1.11	1.19	1.14	1.23	1.32	1.20	1.29	1.38

Having now an adequate formulation for the required finger joint strength at reference length of structural timber the next sub-section aims on studying the length effect observable in finger jointed structural timber.

Quantification of Serial System Effects on Finger Jointed Structural Timber

Within this sub-section serial system effects on finger jointed structural timber are addressed. The analysis itself is in principle equal to unjointed structural timber, as shown in Fig. 5.32. Additionally the influence of M iid jointed structural timber elements and (M – 1) iid finger joints per reference length l_{ref} = 2,000 mm are considered. Thereby and in-line with the examinations made in previous sub-section the strength characteristics of finger joints are set to fulfill equal probability of failure for finger joints and timber at l_{ref} and by assuming E[CoV[$f_{t,0,FJ}$]] = 15%. The resulting relative means and 5%-quantiles are illustrated in Fig. 5.36.

In comparison to Fig. 5.32 the length effects are even lower. Best fitted power models show a lower degree of determination which is in contrast to unjointed structural timber strength, and therefore 5%-quantiles power parameters of 0.06, 0.14 and 0.23 with CoV[$f_{t,0,FJ}$] = (20, 30, 40)%, respectively. This is true for the case of only one finger joint per l_{ref}. If this number is doubled, and thus the amount of iid serial acting elements the power parameters also increase.

Overall it can be concluded that for practical applications and in particular for the design of finger jointed structural timber members as part of a whole structural system the same power parameters than for unjointed structural timber can be applied, so far the average number of joints per reference length does not exceed three.

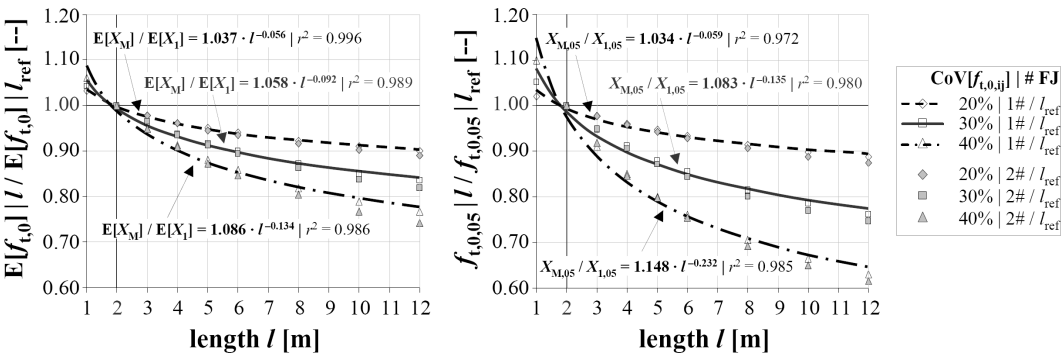

Fig. 5.36: Serial system effects on expectation and 5%-quantile of tensile strength of finger jointed structural timber: influence of parameter variation CoV[$f_{t,0,ij}$] and number of finger joints per l_{ref} = 2,000 mm as well as best fitted power models

To conclude, section 5.4 addressed serial system action on tensile strength parallel to grain of unjointed and finger jointed structural timber. Examinations focused on parameter settings which were found to be common for structural timber and finger joints. Thereby a significant length effect on expectation but more on the 5%-quantile was observed. A comparison with literature concerning unjointed structural timber showed that own results are in the range of published values.

Based on modelling and simulations also a slight increase in CoV[$f_{t,0}$] with increasing length was found. This small increase which is judged to be hardly verifyable in practical tests may be one important reason for contradicting literature data and interpretation. In particular the preference for WEIBULL's theory, as for example discussed in section 5.1.2, whose requirements and assumptions can be hardly fulfilled by materials like timber are

assumed to be caused by the fact of nearly constant CoV[$f_{t,0}$] but to be honest also by the analytical closed approach and its usability for extreme value calculations.

In contrast to current European standards which regulate length effects only for components shorter than the reference length it was found that this procedure is absolutely inadequate and physically contradicting, not justifiable nor meaningful. It prevents also to keep the reliability of engineered structures on the basic reliability level. Therefore need for action is given to adjust current regulations but also to broaden size effect regulations for strength characteristics so far not considered in European standards, like shear strength. Therefore further comprehensive examinations and models adapted to the analysed stresses are necessary.

Considering length effects on tensile strength of finger jointed structural timber it can be concluded that the power parameter positively depends on the number of finger joints per reference length. As mentioned in section 5.1.2, MADSEN AND BUCHANAN (1985) found a multiple-member factor (jointed material) of $k_{l,05} = 0.36$ which is larger than the single-member factor (unjointed material) of $k_{l,05} = 0.29$. In fact both factors are much higher than found in presented examinations. This indicates that in their examinations the variability of tensile strength in structural timber and perhaps also in that of the finger joints was much higher than normally observable. Comparison of Fig. 5.32 and Fig. 5.36 shows that the results at CoV[$f_{t,0}$] = 40% are nearly equal, irrespective if there are joints or not. Thus it can be concluded that in cases of CoV[$f_{t,0}$] > 40% and / or more than three finger joints per l_{ref} a higher length effect in finger jointed structural timber than in unjointed timber elements can be expected. As these aspects and in particular the combination of both do not correspond to the common observations of variability and expected number of finger joints per reference length it is proposed to regulate length effects of common finger jointed structural timber equal to that of unjointed structural timber.

The herein presented model allows direct consideration of the stochastic nature of strength characteristics, their longitudinal (or even three-dimensional) distribution and in particular the direct consideration of their spatial correlation structure. Hereby changes in variability and equicorrelation, as common, e.g. by changing timber quality, can be considered explicitly. The model considerations given here allow also the verification of different design approaches which are defined in dependency of the underlying design concept, e.g. deterministic, semi-probabilistic or probabilistic. It allows the characterisation of serial system effects of unjointed or jointed members more correctly.

This enhances directly the abilities in modelling and optimisation of existing linear but also two-dimensional structural members. Furthermore these tools also support the design process required for the definition of new products or judgement of new structural concepts or structures in uncommon dimensions. Nevertheless, not only serial but also parallel system actions and related effects on strength characteristics have to be known. Therefore the next section shows exemplarily parallel system effects on tensile strength parallel to grain.

5.5 Parallel System Effects on Tensile Strength parallel to Grain – System Effects

Within this section system effects of parallel arranged and common acting elements of unjointed and finger jointed structural timber members are addressed. Thereby it is assumed that the elements are only in common connected at their ends or at least in discrete distances. This allows to use the distribution characteristics of unjointed and finger jointed structural timber, found in regard to serial system action in the previous section 5.4, directly as input parameters for the examination of parallel system action. In contrast, modelling of parallel system action of continuously, flexible or rigid connected elements is a challenge and a topic of its own and hence not addressed within this section.

Tab. 5.42: Characteristics of E-modulus in tension parallel to grain of unjointed structural timber members at l_{ref} = 2,000 mm; groups G_I to G_III

		G_I	G_II	G_III
$\rho_{equi}(E_{t,0,ij})$	[--]	0.50	0.55	0.60
$E[E_{1,t,0}]$	[N/mm²]	9,698	11,343	13,263
$CoV[E_{1,t,0}]$	[%]	18.7%	19.3%	20.1%
$\rho(f_{1,t,0}; E_{1,t,0})$	[--]		0.70	

In the following parallel system effects on tensile strength parallel to grain are examined. Therefore knowledge of E-modulus, strength and their relationship are required. At first the stochastic parameters expectation and coefficient of variation are calculated. The input parameters of previously defined groups G_I to G_III, as given in Tab. 5.35, are used. These parameters were originally calculated for the length of board segments (sub-elements) and have to be now adapted to structural members with a reference length of l_{ref} = 2,000 mm. Thereby serial system effects on E-modulus as discussed in section 5.3.3

are taken into account. It is assumed that parameters of E-modulus in Tab. 5.35 are representative for the whole sub-element with a length equal to the distance between weak zones. This is in fact not true as the E-modulus of clear wood zones is for sure higher than that of zones with knots. Nevertheless it can be simply proven that a shift of E[$E_{1,t,0}$] alone has no influence on the magnitude of parallel system effects. The value of equicorrelation which is required for calculation of $E_{1,t,0}$ was taken from Tab. 5.12. Again the increasing homogeneity of the material in context with increasing timber quality was considered by adaptation of $\rho_{equi}(E_{t,0,ij})$. The results are given in Tab. 5.42.

The calculation of parallel system effects according the procedure presented in section 3.4.4 was done by assuming iid members and by considering an immediate system collaps at first partial failure. A correlation coefficient between E-modulus and tensile strength of $\rho(f_{1,t,0}; E_{1,t,0}) = 0.70$, in line with Tab. 5.12, was used. The results of these calculations are further discussed as system factor $k_{sys,\xi}$, defined as

$$k_{sys,\xi}\big|N = \frac{f_{N,\xi}}{f_{1,\xi}}, \tag{5.71}$$

with ξ = {mean, 5%-quantile} given as

$$k_{sys,mean}\big|N = \frac{f_{N,mean}}{f_{1,mean}} \text{ and } k_{sys,05}\big|N = \frac{f_{N,05}}{f_{1,05}}. \tag{5.72}$$

In section 3.4.4 it was demonstrated that model calculations are biased. The range of the number of parallel and common acting elements within the following examinations is limited by $N \leq 20$. Following Fig. 3.78 to Fig. 3.80 in section 3.4.4 it can be observed that the absolute bias up to $N \leq 10$ increases, whereas between $10 < N \leq 20$ a nearly constant bias is given. Thus in further examinations the bias, inherent in model calculations, was corrected by means of a bi-linear approach. Based on Fig. 3.78 to Fig. 3.80 the bias factors for the range of $10 < N \leq 20$ are given in Tab. 5.43. As expected a remarkable decrease in mean values can be observed whereas the reduction of 5%-quantiles is moderate. This is due to the fact that parallel system action significantly affects the variability of system strength characteristics. Overall it can be concluded that 5%-quantiles of strength of herein analysed systems composed of parallel arranged and common acting elements with $N \leq 4$ are more or less equal to the 5%-quantiles of strength of the elements. In contrast the mean values at $N = 4$ show a reduction of 20%. In comparing the results of all three groups neither a significant difference in $k_{sys,mean}$ nor in

$k_{sys,05}$ can be found. This can be explained by the fact that CoV[$f_{1,t,0}$], CoV[$E_{1,t,0}$] as well as the ratio $f_{1,t,0,mean}$ / $E_{1,t,0,mean}$ are nearly the same in all three groups. It has to be mentioned that for all groups the same correlation coefficient $\rho(f_{1,t,0}; E_{1,t,0})$ was applied. The results as $k_{sys,mean}$ and $k_{sys,05}$ in dependency of N and for groups G_I to G_III are given in Tab. 5.44.

Tab. 5.43: Bias correction factors as relative deviation of model calculations to simulated values of mean, standard deviation and 5%-quantiles

	mean	**standard deviation**	**5%-quantile**
$\rho(E_{1,t,0}; f_{1,t,0})$ = 0.60 ÷ 0.80	± 0%	– 3.75%	+ 2.0%
CoV[$f_{1,t,0}$] = (20 ÷ 40)%	± 0%	– 3.00%	+ 3.5%
CoV[$E_{1,t,0}$] = (15 ÷ 25)%	± 0%	– 3.00%	+ 3.0%

Tab. 5.44: Parallel system effects on mean and 5%-quantiles of at the ends clamped unjointed structural timber members at l_{ref} = 2,000 mm in dependency of N; groups G_I to G_III; bias corrected

0# FJ	***N* =**	**1**	**2**	**3**	**4**	**5**	**10**	**15**	**20**
G_I	$k_{sys,mean}$	1.00	0.88	0.82	0.79	0.77	0.70	0.67	0.65
	$k_{sys,05}$	1.00	1.00	0.98	0.97	0.95	0.87	0.86	0.85
G_II	$k_{sys,mean}$	1.00	0.88	0.83	0.79	0.77	0.71	0.68	0.66
	$k_{sys,05}$	1.00	1.00	0.99	0.97	0.95	0.88	0.86	0.85
G_III	$k_{sys,mean}$	1.00	0.88	0.83	0.80	0.77	0.71	0.68	0.66
	$k_{sys,05}$	1.00	1.00	0.99	0.97	0.95	0.88	0.86	0.86

To examine the influences on system action caused by parameters CoV[$f_{1,t,0}$] and $\rho(f_{1,t,0}; E_{1,t,0})$, in particular on $k_{sys,mean}$ and $k_{sys,05}$, model calculations with the following parameter settings were performed: E[$f_{1,t,0}$] = 30 N/mm², CoV[$f_{1,t,0}$] = (20, 30, 40)%, E[$E_{1,t,0}$] = 11,000 N/mm², CoV[$E_{1,t,0}$] = 15% and $\rho(f_{1,t,0}; E_{1,t,0})$ = (0.6, 0.7, 0.8). The results are shown in Fig. 5.37. Comparable to the graphs in Fig. 3.59 and Fig. 3.61 in section 3.4.4 it is once again illustrated that parallel system effects on only at their ends clamped and common acting elements mainly affect mean strength values whereas the influence on 5%-quantiles is much lower. This becomes even more obvious as CoV[$f_{1,t,0}$] increases and / or $\rho(f_{1,t,0}; E_{1,t,0})$ decreases. If CoV[$f_{1,t,0}$] is only slightly higher than CoV[$E_{1,t,0}$] and a high correlation between E-modulus and strength can be achieved even values of $k_{sys,05} \geq 1.00$ are reachable, for small N. Consequently, if parallel systems of

herein analysed types and moderate N are composed of higher quality timber associated with higher homogeneity a higher correlation can be achieved in combination with a lower variability in strength and thus a $k_{sys,05} > 1.00$ or at least a $k_{sys,05} \approx 1.00$. Thus it is in principle possible to build up a structural tension member of a cross section multiple-times that of available structural timber by this smaller sized elements and to reach resistance on the 5%-quantile of strength comparable to that of the elements so far the joint at the ends of the elements secures uniform loading of all elements. Nevertheless, if structural members are composed of elements discrete connected only in large distances of arbitrary material quality a reduction of the 5%-quantile of strength has to be considered.

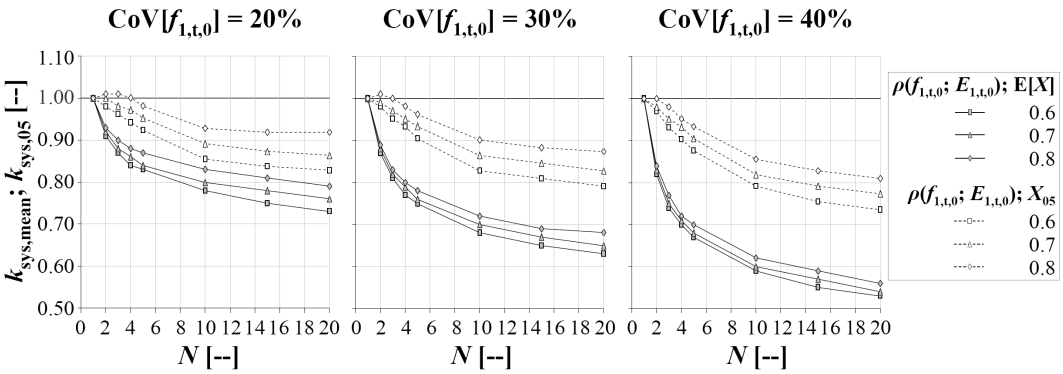

Fig. 5.37: Parallel system effects on mean and 5%-quantiles of at the ends clamped unjointed structural timber members at $l_{ref} = 2{,}000$ mm in dependency of N, CoV[$f_{1,t,0}$] and $\rho(f_{1,t,0}; E_{1,t,0})$; bias corrected

Tab. 5.45: Test results taken from BRANDNER (2006) and model calculations: a comparison

	test results						model calculations [2)]		
		$E_{t,0,12}$ [N/mm²]		$f_{t,0}$ [N/mm²]			$f_{t,0}$ [N/mm²]		
	#	mean	CoV	mean	CoV	X_{05} [1)]	mean	CoV	X_{05}
ZL_1	21#	16,030	14.0%	41.4	30.3%	24.3	41.4	30.3%	24.3
ZL_2	10#	15,610	7.2%	32.0	19.5%	22.9	36.1	22.9%	24.3
ZL_3	7#	15,280	6.5%	36.3	17.0%	27.1	33.8	20.1%	23.9
ZL_4	5#	15,290	6.5%	34.3	7.8%	30.1	32.4	18.5%	23.5

1) assuming $X \sim$ 2pLND

2) performed with E[$E_{t,0,12}$] = 15,500 N/mm²; $\rho(f_{1,t,0}; E_{1,t,0}) = 0.70$

For verification of model calculations only one test series is known. The results of main statistics together with bias corrected model calculations are given in Tab. 5.45. As the variation in N and the number of specimen within each sample are very different but overall very small the test results have to be taken with caution. Nevertheless comparison of statistics of strength values with the corresponding model values show overall good agreement. Nevertheless, as already outlined in section 5.1.3 modelling of CoV[X_N] as function of CoV[X_1] and N can also be approximated by the averaging model. This can be also confirmed for CoV of E-modulus and strength of the test series analysed.

As next step parallel effects of systems composed of finger jointed structural timber members are analysed exemplarily. Therefore basic parameters of groups G_I to G_III are used. The number of finger joints within the reference length is again modelled as deterministic, see sections 5.3 and 5.4. As before the serial system action on E-modulus in dependency of the number of finger joints and thus in dependency of the number of iid jointed elements has to be calculated. Therefore it is assumed that the E-modulus of finger joints and timber elements are identically distributed. For calculation of the tensile strength distribution of finger jointed structural members the expectation of finger joint strength was adapted to secure equal probabilities of failure in timber and joints, see section 5.4.2. Therefore CoV[$f_{1,t,0,FJ}$] was fixed with 15%. The expectations and coefficients of variation of strength and E-modulus of finger jointed structural timber members (N = 1) are given in Tab. 5.46.

Tab. 5.46: Characteristics of E-modulus and tension strength parallel to grain of finger jointed structural timber members at l_{ref} = 2,000 mm; groups G_I to G_III

			G_I	G_II	G_III
1# FJ / l_{ref}	**E[$f_{1,t,0}$]**	**[N/mm²]**	24.2	29.4	35.5
	CoV[$f_{1,t,0}$]	**[%]**	15.8%	15.7%	15.6%
	E[$E_{1,t,0}$]	**[N/mm²]**	9,535	11,139	13,007
	CoV[$E_{1,t,0}$]	**[%]**	13.2%	13.7%	14.2%
2# FJ / l_{ref}	**E[$f_{1,t,0}$]**	**[N/mm²]**	24.2	29.4	35.3
	CoV[$f_{1,t,0}$]	**[%]**	13.7%	13.7%	13.7%
	E[$E_{1,t,0}$]	**[N/mm²]**	9,480	11,071	12,921
	CoV[$E_{1,t,0}$]	**[%]**	10.8%	11.2%	11.6%

The results of model calculations are shown in Tab. 5.47 (1# FJ / l_{ref}) and Tab. 5.48 (2# FJ / l_{ref}). Overall the factors $k_{sys,mean}$ are higher than found for unjointed material whereas nearly the same or slightly lower values are found for $k_{sys,05}$. This can be explained by the fact that CoV[$f_{1,t,0}$] of finger jointed structural timber is lower than of unjointed material. Consequently system effects are lower which can be observed by a lesser reduction in $k_{sys,mean}$ but also in CoV[$f_{N,t,0}$]. Thus also the 5%-quantiles are lesser affected by parallel system action. System factor $k_{sys,05}$ evaluated at $N = 4$ and for 1# or 2# FJ / l_{ref} yields about 10% (6% ÷ 11%) reduction which is much more than the 3% found for unjointed material. Thus it can be concluded that parallel system effects in case of jointed material can be even more relevant than in unjointed material. With increasing number of finger joints this effect will be stronger but of diminishing significance.

Tab. 5.47: Parallel system effects on mean and 5%-quantiles of at the ends clamped finger jointed structural timber members at l_{ref} = 2,000 mm in dependency of N; groups G_I to G_III; 1# FJ / l_{ref}; bias corrected

1# FJ	N =	1	2	3	4	5	10	15	20
G_I	$k_{sys,mean}$	1.00	0.94	0.91	0.89	0.87	0.84	0.82	0.80
	$k_{sys,05}$	1.00	0.99	0.98	0.96	0.95	0.89	0.88	0.87
G_II	$k_{sys,mean}$	1.00	0.94	0.91	0.89	0.87	0.84	0.82	0.80
	$k_{sys,05}$	1.00	0.99	0.98	0.96	0.95	0.89	0.88	0.87
G_III	$k_{sys,mean}$	1.00	0.94	0.91	0.89	0.87	0.84	0.82	0.80
	$k_{sys,05}$	1.00	0.99	0.98	0.96	0.95	0.89	0.87	0.87

Tab. 5.48: Parallel system effects on mean and 5%-quantiles of at the ends clamped finger jointed structural timber members at l_{ref} = 2,000 mm in dependency of N; groups G_I to G_III; 2# FJ / l_{ref}; bias corrected

2# FJ	N =	1	2	3	4	5	10	15	20
G_I	$k_{sys,mean}$	1.00	0.95	0.92	0.90	0.89	0.86	0.84	0.83
	$k_{sys,05}$	1.00	0.99	0.98	0.96	0.95	0.89	0.88	0.88
G_II	$k_{sys,mean}$	1.00	0.95	0.92	0.90	0.89	0.86	0.84	0.83
	$k_{sys,05}$	1.00	0.99	0.98	0.96	0.95	0.89	0.88	0.88
G_III	$k_{sys,mean}$	1.00	0.95	0.92	0.90	0.89	0.86	0.84	0.83
	$k_{sys,05}$	1.00	0.99	0.98	0.96	0.95	0.89	0.88	0.87

Based on the findings of this section it can be concluded that even the simplest case of parallel system action on structural timber requires much more information for modelling than the examination and consideration of serial system action. In particular and beside the number of common acting elements N the ratio $\mathrm{CoV}[f_{1,t,0}] / \mathrm{CoV}[E_{1,t,0}]$ and the correlation coefficient $\rho(f_{1,t,0}; E_{1,t,0})$ affect the magnitude of system action significantly. The presented results serve also as lower limit of flexible connected elements. This aspect can be useful in design processes were the stiffness achievable by the connection is judged as being low but unknown.

Chapter 6

Conclusions

Within this chapter main findings of the overall work are briefly demonstrated and concluding remarks are made. It is the aim to provide an overview of the whole thesis and to illustrate the relevance of performed analysis as well as its impact on ongoing works and future projects. As true for every scientific work, at the end the list of open questions seems to be longer than at the beginning. In this respect an outlook with some recommendations for further relevant analysis and future research projects is given.

6.1 General Remarks

This thesis addresses stochastic system actions and related effects in regard to engineered timber products and structures. It constitutes a comprehensive work on stochastic modelling of system actions and effects, on material description with focus on wood and timber as well as their characteristics, analogies and scaling, material and product modelling. It aims on detailed examination and critical discussion of the state of the art in corresponding research fields and on extension of knowledge. The achievement of objectives is supported by extensive numerical modelling as well as extensions and elaboration of new analytical solutions. Furthermore this thesis involves comprehensively interpreted analysis and graphs for the assessment of serial and parallel system effects for various RSDMs, main distributional characteristics, load configurations and quantifies modelling bias for systems composed of uncorrelated as well as correlated elements. It exemplifies also the impact of system action on the reliability of structures. At the end this thesis focuses exemplarily on system characteristics of timber and engineered timber

system products on system levels I and II and thereby on system actions and effects on characteristics of density, stiffness and strength.

As every scientific work also this thesis constitutes an intermediate caesura of analysis and examinations but at the same time the beginning of further research projects. To reduce the effort in start-up phases of future projects on herein addressed topics this thesis aims on providing a comprehensive state of the art literature survey supported by new composition, classification, densification and discussion of available knowledge and integration of own results, comments, completed by concluding remarks. The main findings and conclusions in regard to these surveys were already and in detail outlined in the corresponding sections. In the following a brief summary of main addressed research fields and outcomes is presented.

6.2 Brief Summary and Conclusions in regard to Research Fields addressed

6.2.1 Stochastic Material Models and Advances

In chapter 3 the three main stochastic material theories, WEIBULL's weakest link theory (WLT; WEIBULL, 1939), the ideal (elastic) plastic material model and DANIELS' fibre bundle model (FBM; DANIELS, 1945) are presented. During these analyses derivation of theories together with their assumptions and constraints are discussed and their applicability are exemplarily demonstrated. Already in chapter 2 the stochastic limit theory of extremes (EVT) was introduced. Due to the limited applicability of EVT, in principle solely for systems of infinite size, efforts have been made to achieve several successful adaptations and advances of the three stochastic theories considered. These enable a more realistic mechanic-stochastic description and modelling of materials and structures. In regard to the achieved advances a comprehensive review together with several notes is provided in section 3.2.4.

It can be concluded that the three stochastic material (strength) theories constitute the fundamental basis for further development and progress. Beside the fact that all models revert to ideal material conditions they clearly express the necessity to consider stochastic approaches in material modelling. This consideration enables the examination of effects which cannot be explained by mechanics alone. The most remarkable progress in advancing the theories was made by the combination of all three approaches to serial-

parallel material models (s-p_FBMs) together with extensions in regard to material behaviour as well as explicit consideration of the interaction between system elements, over the interface of a matrix material or by friction. Furthermore, the system behaviour after partial failures, in particular the redistribution of stresses, got in focus by definition and intensive analysis of load sharing rules (GLS vs. LLS).

Obviously there are still many open questions and model constraints that require more detailed view and more detailed judgement, like the serial and parallel system behaviour in case of LND as RSDM of element strength and stiffness characteristics, the inclusion of spatial correlation in conjunction with general stochastic processes, the interaction of multi-variate and / or multi-modal RSDMs and the necessity to define some simplified equations applicable in daily and / or advanced timber engineering.

6.2.2 Stochastic Modelling of serial and parallel System Action and Effects

The main part of chapter 3, in particular section 3.3 and 3.4, are dedicated to extensive analysis of stochastic effects of systems composed of serial and / or parallel acting elements. The examinations are made by means of comprehensive stochastic simulation studies on systems composed of stochastic elements. These stochastic elements represent realisations of iid or identical but correlated random variables X_1 with RSDM ND, 2pLND or 2pWD. For iid $X_1 \sim$ WD numerous analytical solutions for the description of serial as well as parallel system actions are available. Thus the focus of this thesis is on elements X_1 following ND and in particular 2pLND.

In general, 2pLND is a very common distribution model, representative for numerous physical characteristics. According the central limit theorem 2pLND is the analytical RSDM of multiplicative processes and also very common for modelling of characteristics of hierarchically structured materials like wood and timber. Nevertheless as analytical solutions for the stochastic description of serial and parallel system actions of finite system sizes are not available the aim of these sections is not only on analysing, demonstrating and quantifying of system effects but also on the definition of an approximative setting, adequate and accurate enough for engineering purposes.

In section 3.3, dedicated to serial systems, a heuristic approach is defined and verified successfully. This approach enables perfect adaptability to distribution characteristics of serial systems composed of iid elements $X_1 \sim$ 2pLND as relative function of CoV[X_1], system size $M \leq 1{,}000$ and the analysed distribution characteristic at $M = 1$, see

equ. (3.102). As this approach only depends on two parameters great efforts were made to define adequate estimators by considering the limiting behaviour of this proposal, see Tab. 3.2. A benchmark analysis with approximative methods for minimas taken from literature shows that the derived approach works adequately and even better than its competitors, even for extreme quantiles, provided that $M \leq 50$ and $\mathrm{CoV}[X_1] \leq 50\%$.

The same approach is also applied for modelling of serial systems composed of identical but correlated elements $X_1 \sim$ 2pLND, see section 3.3.3. Again and with the adaptations for parameter estimations provided by equ. (3.127) and (3.128) satisfactory results for system strength distributions can be easily derived so far $\mathrm{CoV}[X_1] \leq 50\%$, $0.00 \leq \rho_X \leq 0.75$ and $M \leq 100$.

In section 3.4, which addresses parallel systems, again the same approach is applied, adapted and successfully verified for arbitrary system configurations of linear-elastic and iid elements with correlated strength and E-modulus following 2pLND. Hereby the conservative case of system strength associated with the first partial failure was analysed, see in particular section 3.4.4.

Overall, the new modelling approach and corresponding parameter estimators are proven to be successful and suitable for the computation of strengths of serial and parallel systems. Furthermore, numerous graphical displays provide the ability to perform bias correction if higher accuracy in model calculations is required.

6.2.3 Hierachical Structure of Wood and Timber

A review and examinations regarding the hierarchical structure of wood and timber as natural materials are the focus of chapter 4. At the beginning of this chapter basics of scaling and hierarchically organised systems are presented and interpreted. The core of this chapter focuses on a comprehensive introduction to materials wood and timber. By means of a new developed concept of classification into natural and technical hierarchies it was aimed to provide a comprehensive summary of literature together with own interpretations, relevant for each hierarchy, the understanding of the material structure and interaction of tissues and growth characteristics. As a consequence the complexity but also the material inherent organisation and structure become clearer. This aspect is in particular intensified by some brief studies on analogies between hierarchies. Hereby different topics like structure, organisation, failure behaviour but also system actions are addressed. Especially the relevance of differentiation in effects due to scaling (scale

transition) and in effects due to changes in the system structure and action within the same scale or hierarchy is outlined. Therefore scaling on tensile characteristics parallel to grain on wood and timber (tissues) is exemplified and the required differentiation in effects within (system effects) and between hierarchies (scaling effects) is demonstrated qualitatively and quantitatively. At the end the relevance of these examinations is again shown for all three system levels by following the definitions made in chapter 1, namely level I: material, level II: system products, and level III: system structures.

Overall, this chapter provides essential knowledge for a comprehensive understanding of the material structure and performance of wood and timber. Furthermore the information serves as basis for the examination of material parameters (e.g. growth characteristics) and assessment of their relevance for modelling of physical properties of the material on a certain hierarchy, e.g. system products and structures. The notes, discussions and interpretations serve also as basis for a more general understanding of hierarchical structured materials, the genius of nature, as support for understanding of fracture behaviour, for dedection of preferred stresses, and for finding of optimised combinations and activation of these tissues, appropriate for current products as well as the design of new system products and load bearing structures.

6.2.4 Serial and parallel System Effects on Timber and Engineered Timber System Products

Conclusions and final remarks in this section are taken from chapter 5. This chapter can be regarded as the core part of this thesis. It is dedicated to exemplarily demonstrate system actions and effects as inherent in the material structure or utilisable by the design of (smart) engineered timber system products and structures. Therefore at first the definition of a basic unit as (representative) element and its geometry and physical properties is required.

Starting at the natural hierarchies of wood and timber differentiation in global (type [1]) and local growth characteristics (type [2]) is made. Not only the spatial distribution, with focus on knots and knot clusters, but also the spatial correlation of growth characteristics as well as physical characteristics like density, E-modulus and strength properties are extensively examined. Based on a comprehensive data analysis of own and literature results together with data preparation allowing common analysis it was not only possible to define RSDMs of geometric and physical properties but also to quantify their stochastic nature. This is done by providing distribution parameters, correlation

coefficients for the description of relationships between different properties and by the description of spatial correlation structure with focus on longitudinal direction. Thereby also the influence of scale transition on spatial correlation is briefly discussed.

For preparation of the analysis and for demonstration of the state of the art concerning serial and parallel system effects in timber engineering literature surveys are presented. They include introductory lessons and classification as well as evaluation and discussion of data from literature which results in classification schemas. These surveys are provided for serial (volume) and parallel (system) effects separately, see section 5.1.2 and 5.1.3, respectively.

Section 5.2 is dedicated to system effects on density. This physical property mainly concerns the computation of bearing capacity of local placed fasteners like self-tapping screws or dowel-type fasteners. A simple model based on probability theory is demonstrated to work perfect for evaluation of the density of system products or as input parameter for derivation of the resistance of fasteners simply by considering global density as arithmetic (weighted) mean of interacting and involved elements. In brief also the relevance of density as indicating property for estimating the local bearing behaviour of fasteners and consideration of stress distribution of fasteners along their axis if placed in laminar products is demonstrated and discussed.

The analysis of the impact of serial and parallel system action on stiffness characteristics is dedicated to section 5.3. Descriptions of arithmetic and harmonic means are presented and the last one adapted also for correlated random variables. Based on this theoretical background serial and parallel system effects on stiffness characteristics and their interaction are analysed for unjointed as well as finger jointed structural timber and engineered timber system products (level I & II). A two-level hierarchical model associated with material inherent equicorrelation is considered. Thereby results relevant for material modelling as well as for stability design are derived and critically analysed also in respect to current regulations and published recommendations.

In sections 5.4 and 5.5 serial and parallel system effects on the tensile strength parallel to grain of unjointed and finger jointed structural timber and engineered timber system products are addressed. Based on a stochastic model which includes not only the equicorrelation of a two-level hierarchical model but also the stochastics of the longitudinal distribution and extension as well as representation of weak zones is presented and further developed by means of the modelling approaches established in

chapter 3. Strength and stiffness characteristics of boards, derived by means of published regression equations for board segments and consideration of system effects by herein derived models, are critically compared with current regulations and publications. Size factors for unjointed as well as finger jointed structural timber members are deduced and simplified power models are presented. Three different definitions for minimum requirements on finger joint tensile strength are examined. One of them is proposed for general application and further used for the examination of parallel system effects on unjointed and finger jointed structural timber members which are clamped at the ends.

Overall, chapter 5 represents an important chapter for material and product modelling. Several times it demonstrates the inclusion of stochastic nature and its impact on specifying material and product characteristics. The comprehensive analysis of published and own data delivers the required input for stochastic characterisation of the material and supports background knowledge for the assessment of relationships between material characteristics and timber quality. The stochastic parameters presented are provided if possible with parameter ranges and support of additional information on their relationship to material quality. Examinations and examples are demonstrated with the aim to give an approach overall and general applicable to material and structure modelling. Thereby the stochastic theory elaborated and provided in chapter 2 is applied. The overall approach is not restricted to longitudinal characterisation of the material although this is of primary interest in timber engineering.

6.3 Recommendations for System Products and Structures with Focus on Engineered Timber System Products

In the following sections some aspects relevant for design of serial and parallel systems are briefly demonstrated.

6.3.1 Recommendations in regard to serial Systems

- serial acting elements can be arranged only one-dimensional;
- the material behaviour (elastic vs. plastic; brittle vs. ductile) has no influence on serial system action;
- in case of density the statistical distribution of global density of systems follows the averaging approach, irrespective of the arrangement and interaction of elements;

- in case of E-modulus serial system action can be described by means of the harmonic mean following the principle of serial acting springs;
- concerning system strength the main parameters influencing serial system action are (i) the variability of element's strength, expressed e.g. by CoV[X_1], (ii) the number of serial acting elements, (iii) the serial system size M and (iv) the correlation, if relevant;
- it is recommended to approximate the distribution of strength of serial systems composed of iid or identical distributed but correlated elements $X_1 \sim$ 2pLND by means of $X_M \sim$ 2pLND but adapted distribution parameters; it is shown that EVT by means of GD gives higher bias even if $M = 1{,}000$;
- simulation data of serial systems composed of correlated elements $X_1 \sim$ 2pLND showed that system strength in case of $\rho_X \leq 0.5$ is only minor, but in case of $\rho_X \geq 0.5$ remarkable affected by correlation; in case of minor correlation ($\rho_X < 0.5$) these serial systems can be approximated by means of uncorrelated elements;
- for serial effects of unjointed timber members or in general of unjointed materials characterised by equicorrelated characteristics it was demonstrated that the impact of serial action on 5%-quantiles of strength is even higher than on the average values so far equicorrelation is low; this is due to the fact that variability between timber elements is unaffected by serial action which only influencies the variability within timber elements;
- for serial effects of finger jointed timber members or in general of jointed materials characterised by equicorrelated characteristics it was demonstrated that the number of joints per reference length has to be considered; thereby serial system action affects both, the variability within elements and the variability between jointed members; in case of strength as well as in cases were stiffness characteristics of joints and jointed materials are different also a mixing of distributions has to be considered.

6.3.2 Recommendations in regard to parallel Systems

- modelling of parallel system actions and effects is much more complex than that of serial systems;
- parallel acting elements can be arranged one- or two-dimensional;

- parallel system action and thus the interaction between parallel arranged and acting elements is decisively influenced by the correlation of strength and stiffness of each element;
- the material behaviour has a remarkable influence on parallel system action;
- in case of density the statistical distribution of global density of systems follows the averaging approach, irrespective of the arrangement of elements;
- in case of E-modulus parallel system action can be described by means of the averaging approach;
- the crucial parameters influencing parallel system action on strength are again (i) the variability of element's strength, expressed e.g. by CoV[X_1], (ii) the number of parallel acting elements, (iii) the parallel system size N, (iv) the arrangement of the elements (one-dimensional / two-dimensional), (v) the correlation between strength and stiffness of the elements expressed by $\rho(f_1, E_1)$, (vi) the amount of plasticity, (vii) the material fracture or yielding behaviour in general and, if any, (viii) the correlation between parallel acting elements (but here taken equal to zero);
- parallel system action on ultimate system strength is decisively determined by the amount of load sharing between the elements after partial failures, with the extreme cases GLS and ELLS; hereby also differentiation in load and deformation controlled stressing of systems is required;
- strength characteristics of real parallel acting systems differ remarkably from ideal parallel systems, in particular if focusing on strength;
- maximum gain in system effects in parallel systems composed of identical distributed elements is rarely equal or higher than predicted by the averaging model, even in case of GLS;
- maximum resistance of parallel systems is restricted by the minimum of ultimate strains of still surviving elements;
- the higher the correlation between strength and stiffness within elements and thus the closer the coincidence of both characteristics the higher the gain in system effects or the lower the loss in system strength;
- elements with a high variability in strength and thus with a high amount of potential differences show a high potential of homogenisation and thus a remarkable gain in strength characteristics or a lesser decrease in strength in case

of parallel system action; this also coincides with a high number of partial failures with the potential of redistribution and further increase in resistance;

- an increase on 5%-quantiles of strength due to parallel system action does not always coincide with an increase in reliability, in particular if the expectation of system strength in comparison to that of the elements has remarkable decreased, shifting the mass of resistance closer to the action;
- a low variation in E-modulus, expressed e.g. by a low CoV[E_1], increases the amount of system effects, see e.g. DANIELS's FBM and the assumption that CoV[E_1] = 0; this aspect is in particular of interest as the effort in classification of material according stiffness and thus also in securing a certain amount of CoV[E_1] is relatively low;
- it was shown that the requirement of CoV[f_1] / CoV[E_1] ≥ 1.00 has to be secured to prevent an increase of variation in system strength in case of small N and in general to design systems efficiently in regard to parallel system action;
- even a small amount of plasticity increases the achievable system strength significantly; this is due to the fact that by same or comparable strength or maximum stress an increase in ultimate strain raises the potential of increased stress transfer before the first or further partial failures;
- strength of two-dimensional parallel systems significantly affects the gain in system effects, on one hand by providing edge and corner elements extra neighbours for stress redistribution but on the other hand by increasing the ability that neighboured elements fail and induce extra stress transfer in particular in case of ELLS and mainly on affecting core elements;
- it was observed that the expectation of system E-modulus E[$E_{N,max}$] at the point of maximum system strength is only marginally smaller than E[E_1] = E[$E_{N,1}$];
- in real materials and structures and in particular in hierarchical organised materials and structures parallel, sub-serial systems have to be considered; thereby the system arrangement (one- or two-dimensional in parallel plus one-dimensional in serial), the type and amount of connection between the elements (rigid vs. flexible; discrete vs. continuously) and the way how the system is stressed (parallel or perpendicular to the main axis; tension compression, shear or bending; stress distribution in all three dimensions) have to be considered.

6.4 Recommendations for further Research Projects

In the following some recommendations for the accomplishment of further continuing or intensifying research projects in respect to timber engineering and system levels I, II and III are listed:

- so far only parallel system actions on tensile strength parallel to grain and elements clamped at the ends were analysed; it is recommended to enlarge these analysis to continuously connected elements by considering a multi-modal approach for accounting the composition of reference structural timber segments of weak zones, zones with intermediate knots and knot free (clear wood) zones, as well as by considering the probability of occurrence of these zones in parallel; furthermore it is recommended to apply the same procedure for systems stressed in compression parallel to grain or in shear;
- based on recommendations above it is suggested to analyse the interaction of parallel, sub-serial systems stressed in tension, compression and shear as e.g. given in case of bending;
- based on models above it is recommended to enlarge stochastic material descriptions to residual stress configurations, e.g. tension and compression perpendicular to grain as well as stresses applied on orthogonal or arbitrary layered laminar products;
- as already outlined in the preface and chapter 1 of this thesis the examined system considerations are also helpful and applicable to model the system behaviour of bearing structures and / or of joints composed of a system of connectors;
- it may be also of importance and interest for future research projects to verify the suggestions and qualification / quantification of system and scaling effects in regard to scaling and hierarchical modelling of wood and timber tissues.

Literature

7.1 Papers, Books, etc.

Abdel-Gadir A Y, Krahmer R L (1993) **Estimating the age of demarcation in juvenile and mature wood in Douglas fir**. *Wood Fiber Science*, 25:242-249 (cit. in Zobel and Sprague, 1998)

Ahrens L H (1954) **The lognormal distribution of the elements (2)**. *Geochimica et Cosmochimica Acta*, 6:121-131

Aicher S, Klöck W (1990) **Spannungsberechnungen zur Optimierung von Keilzinkenprofilen für Brettschichtholz-Lamellen**. *Bauen mit Holz*, 92(5):356-358, 360-362 (in German)

Aitchison J, Brown J A C (1981) **The lognormal distribution – with special reference to its uses in economics**. Cambridge University Press, ISBN 0-521-04011-6, 176 p.

Ander P, Burgert I, Frühmann K (2003) **The possible relationship between dislocations and mechanical properties of different spruce fibres: A single fibre study**. COST E20 – Wood Fibre Cell Wall Structure, Program and Proceedings of the Final Workshop "Building a Cell Wall", Helsinki, Finland, p. 66-67

Ashby M F, Gibson L J, Wegst U, Olive R (1995) **The mechanical properties of natural materials. I. Material property charts**. *Proceeding of the Royal Society London A*, 450:123-140

Astley R J, Harrington J J, Stol K A (1997) **Mechanical modelling of wood microstructure, an engineering approach**. *IPENZ Transactions*, 24(1):21-29

Augustin M (2004) **Eine zusammenfassende Darstellung der Festigkeitssortierung von Schnittholz**. Diploma-thesis, Chair of Timber Engineering, Institute of Steel, Timber and Shell Structures, Graz University of Technology, 259 p. (in German)

Azizi-Samir A S, Alloin F, Paillet M, Dufresne A (2004) **Tangling Effect in Fibrillated Cellulose Reinforced Nanocomposites**. *Macromolecules*, 37(11):4313-4316 (cit. in Gindl and Keckes, 2005)

Bakht B, Jaeger L G (1991) **Load sharing in timber bridge design**. *Can. J. of Civil Engineering*, 18:312-319

Barakat R (1976) **Sums of independent lognormally distributed random variables**. *J. Opt. Soc. Am.*, 66(3):211-216 (cit. in Jensen et al., 1997)

Barber N F, Meylan B A (1964) **The anisotropic shrinkage of wood**. *Holzforschung*, 18:146-156 (cit. in Booker and Sell, 1998)

Barrett J D (1974) **Effect of size on tension perpendicular to grain strength of Douglas fir**. *Wood and Fiber*, 6(2):126-143

Barrett J D, Foschi R O (1979) **On the application of brittle fracture theory, fracture mechanics and creep rupture models for the prediction of reliability of wood structural members**. Proceeding of the 1st International Conference on Wood Fracture, Forintek, Canada (cit. in Williamson, 1992)

Barrett J D, Fewell A R (1990) **Size factors for the bending and tension strength of structural timber**. International Council for Building Research Studies and Documentation, Working Commission W18 – Timber Structures, 23rd Meeting, Lisbon, Portugal, CIB-W18A / 23-10-3

Barrett J D, Lam F, Lam W (1992) **Size effects in visually graded softwood structural lumber**. International Council for Building Research Studies and Documentation, Working Commission W18 – Timber Structures, 25th Meeting, Åhus, Sweden, CIB-W18 / 25-6-5

Bažant Z P, Chen E P (1996) **Scaling of structural failure**. Scandia Report SAND96-2948, UC-703

Bažant Z P, Planas J (1998) **Fracture and size effect in concrete and other quasibrittle materials**. Library of Congress Cataloguing-in-Publication Data, ISBN 0-8493-8284-X, United States of America, 617 p.

Bažant Z P (2001) **Probabilistic modelling of quasibrittle fracture and size effect**. Structural Safety and Reliability, Corotis et al. (eds.), Sweets & Zeitinger, ISBN 90-5809-197-X

Bažant Z P (2004) **Scaling theory for quasibrittle structural failure**. *PNAS*, 101(37):13400-13407

Bažant Z P, Pang S D, Vořechovský M, Novák D, Pukl R (2004) **Statistical size effect in quasibrittle materials: computation and extreme value theory**. In: Li V C, Willam K J, Leung C K Y, Billington S L (Eds.), 5th International Conference on

Fracture Mechanics of Concrete and Concrete Structures (FraMCoS), Vol. 1, Colorado, USA, 189-196 (cit. in Vořechovský and Chudoba, 2006)

Bažant Z P, Pang S D (2006) **Mechanics-based statistics of failure risk of quasibrittle structures and size effect on safety factors**. *PNAS*, 103(25):9434-9439

Bažant Z P, Vořechovský M, Novák D (2007) **Asymptotic prediction of energetic-statistical size effect from deterministic finite element solutions**. *Journal of Engineering Mechanics*, 133(2):153-162 (cit. in Vořechovský and Chudoba, 2006)

Bažant Z P, Yu Q (2009) **Universial size effect law and effect of crack depth on quasi-brittle structure strength**. *Journal of Engineering Mechanics*, ASCE, 78-84

Beecher J F (2007) **Wood, trees and nanotechnology**. *Nature Nanotechnology*, 2:2

Bender D A, Woeste F E, Schaffer E L, Marx C M (1985) **Reliability formulation for the strength and fire endurance of glued-laminated beams**. USDA Forest Service Research Paper FPL 460, U. S. Forest Products Laboratory, Madison, WI

Bendtsen B A (1978) **Properties of wood from improved and intensively managed trees**. *Forest Products Journal*, 28:61-72 (cit. in Zobel and Sprague, 1998)

Berg P, Hagman O (1976) **Determination of lengthwise variation of bending stiffness in lumber**. Chalmers University of Technology, Division of Structural Design (cit. in Czmoch, 1991; in Swedish)

Bergander A, Salmén L (2000) **Variations in transverse fibre wall properties: relations between elastic properties and structure**. *Holzforschung*, 54:654-660

Bergander A, Salmén L (2002) **Cell wall properties and their effects on the mechanical properties of fibers**. *Journal of Material Science*, 37:151-156

Blaß H J, Frese M, Glos P, Denzler J K, Linsenmann P, Ranta-Maunus A (2008) **Zuverlässigkeit von Fichten-Brettschichtholz mit modifiziertem Aufbau**. Karlsruher Berichte zum Ingenieurholzbau, Band 11, Universität Karlsruhe, Lehrstuhl für Ingenieurholzbau und Baukonstruktionen, 188 p. (in German)

Bledzhi A K, Gassan J (1999) **Composites reinforced with cellulose based fibres**. *Prog. Polym. Sci.*, 24:221-274

Bodig J, Jayne B A (1982) **Mechanics of Wood and Wood Composites**. Van Nostrand Reinhold, New York (cit. in Bergander and Salmén, 2002)

Bogensperger T (2006) **Elastische Spannungsverläufe unter einer Zugprüfung**. Institute of Timber Engineering and Wood Technology, Graz University of Technology, 38 p. (in German)

Bohannan B (1966) **Effect of size on bending strength of wood members**. Forest Products Laboratory, Forest Service, U.S. Department of Agriculture, Madison, WI, RP-FPL 56, 30 p.

Bohnhoff D R, Cramer S M, Moody R C, Cramer C O (1989) **Modelling vertically mechanically laminated lumber**. American Society of Civil Engineers, *Journal of Structural Engineering*, 115(10):2661-2679 (cit. in Bohnhoff et al., 1991)

Bohnhoff D R (1990) **Laminated post design – bending strength and stiffness**. Agricultural Engineering Light-Frame Building Conference, University of Illinois, Champaign, Illinois, 33 p.

Bohnhoff D R, Moody R C (1990) **Strength and stiffness of spliced nail-laminated posts**. Proceeding, International Timber Engineering Conference, Tokyo, Japan, 715-722 (cit. in Bohnhoff et al., 1991)

Bonhoff D R, Moody R C, Verrill S P, Shirek L F (1991) **Bending properties of reinforced and unreinforced spliced nail-laminated posts**. Forest Products Laboratory, Forest Service, U.S. Department of Agriculture, RP-FPL 503, 24 p.

Bohnhoff D R, Moody R C, Manbeck H B (1992) **Solid-sawn and laminated posts**. In: Walker J N, Woeste F E, eds. Post-frame building design. ASAE Monograph, American Society of Agricultural Engineers, chapter 7, 105-137

Bohnhoff D R (1995) **Mechanically laminated post engineering practice**. *Research & Technology*, FBN, 36-39

Bohnhoff D R, Chiou W-S, Hernandez R (1997) **Load sharing in nail-laminated assemblies subjected to bending loads**. ASAE Meeting, Minneapolis, Minnesota, Paper No. 974090

Bonnicksen L-R W (1965) **Structural reliability of vertically laminated wood beams**. PhD-thesis, Purdue University, 134 p.

Bonnicksen L-R W, Suddarth S K (1966) **Structural reliability analysis of a wood load-sharing system**. *Journal of Materials*, 1(3):491-508

Booker R E, Sell J (1998) **The nanostructure of the cell wall of softwoods and its functions in a living tree**. *Holz als Roh- und Werkstoff*, 56:1-8

Boutelje J (1968) **Juvenile wood, with particular reference to northern spruce**. *Svensk Papperstidning*, 71:581-585 (cit. in Brändström, 2001)

Brandner R, Frühwald K, Unterwieser H, Jeitler G (2005) **P05 grading – Gurtlamellen: Prüfbericht**. Report, Competence Centre holz.bau forschungs gmbh, Graz, Austria, 26 p. (in German)

Brandner R (2006) **Systemeffekte von aus Konstruktionsvollholz aufgebauten Querschnitten**. Salzburg University of Applied Sciences, Studiengang Holztechnik und Holzwirtschaft, diploma thesis, 304 p. (in German)

Brandner R, Schickhofer G (2006) **System effects of structural elements – determined for bending and tension**. 9th World Conference on Timber Engineering (WCTE), Portland, Oregon, 8 p.

Brandner R, Schickhofer G, Ruli A, Halili Y (2006) **Leistungspotential von Brettschichtholz: Beanspruchung auf Längsdruck und Querdruck**. Internal Research Report, Non-K_{Ind} B_S_H, Competence Centre holz.bau forschungs gmbh, Graz, Austria, 109 p. (in German)

Brandner R, Bogensperger T, Jeitler G, Schickhofer G (2007a) **Size effect considerations for linear structural elements of timber**. COST E55: Modelling of the performance of timber structures, 2nd Workshop and 4th MC Meeting, Eindhoven University of Technology, Eindhoven, Netherlands, 19 p.

Brandner R, Schickhofer G (2007) **Mechanical potential of boards of spruce for glulam production**. Internal Research Report, Competence Centre holz.bau forschungs gmbh, Graz, Austria, 34 p.

Brandner R, Gehri E, Bogensperger T, Schickhofer G (2007b) **Determination of modulus of shear and elasticity of glued laminated timber and related examinations**. International Council for Building Research Studies and Documentation, Working Commission W18 – Timber Structures, 40th Meeting, Bled, Slovenia, CIB-W18 / 40-12-2

Brandner R (2008) **Scaling – Betrachtung von Skalenebenen in der Materialstruktur Holz in Verbindung mit der Anwendung von Modellansätzen**. 7. Grazer Holzbau-Fachtagung (7.GraHFT'08) Modellbildung für Produkte und Konstruktionen aus Holz – Bedeutung von Simulation und Experiment, Graz, B1-B48 (in German)

Brandner R, Schickhofer G (2008) **Glued laminated timber in bending: new aspects concerning modelling**. *Wood Science and Technology*, 42(5):401-425

Brandner R, Freytag B, Schickhofer G (2008) **Determination of Shear Modulus by means of standardized Four-Point Bending Tests**. International Council for

Building Research Studies and Documentation, Working Commission W18 – Timber Structures, 41th Meeting, St. Andrews, Canada, CIB-W18 / 41-21-1

Brandner R, Schickhofer G (2010) **Glued laminated timber: thoughts, experiments, models and verification**. World Conference on Timber Engineering (WCTE), Riva del Garda, Italy, 11 p.

Brandner R, Stadlober E, Schickhofer G (2012) **Stochastische Beschreibung von Brettware der Holzart Fichte auf Zug parallel zur Faser: Statistische Aus- und Bewertung der Daten aus dem Projekt INTELLIWOOD (2000-2001)**. Research Report, COMET-K Project MMSM 2.2.1 stoch_mod, Competence Centre holz.bau forschungs gmbh, Graz (in German; in progress)

Brändström J (2001) **Micro- and ultrastructural aspects of Norway spruce tracheids: a review**. *IAWA Journal*, 22(4):333-353

Buckingham E (1914) **On physically similar systems: illustrations of the use of dimensional equations**. *Bureau of Standards*, 4(4):345-376

Buksnowitz C, Hackspiel C, Hofstetter K, Müller U, Gindl W, Teischinger A, Konnerth J (2010) **Knots in trees: strain distribution in a naturally optimised structure**. *Wood Science and Technology*, 44:389-398

Burger N, Glos P (1996) **Effect of size on tensile strength of timber**. International Council for Building Research Studies and Documentation, Working Commission W18 – Timber Structures, 29th Meeting, Bordeaux, France, CIB-W18 / 29-6-1

Burger N, Glos P (1997) **Strength relationships in structural timber subjected to bending and tension**. International Council for Building Research Studies and Documentation, Working Commission W18 – Timber Structures, 30th Meeting, Vancouver, Canada, CIB-W18 / 30-6-1

Burger N (1998a) **Modification of brittle fracture theory for the determination of size effects in timber strength**. 5th World Conference on Timber Engineering, Montreux, Switzerland, 183-190

Burger N (1998b) **Einfluss der Holzabmessungen auf die Zugfestigkeit von Schnittholz unter Zugbeanspruchung in Faserrichtung**. PhD-thesis, Fakultät für Bauingenieur- und Vermessungswesen, Technische Universität München, Shaker Verlag, ISBN 3-8265-4376-9 (in German)

Burgert I, Frühmann K (2003) **Micromechanics of wood – structure-function relationships at the tissue and fiber level**. In: ESWM (ed. Salmén) Second

International Conference of the European Society for Wood Mechanics, Stockholm, Sweden, p. 85-94 (cit. in Eder, 2007)

Burgert I, Gierlinger N, Zimmermann T (2005a) **Properties of chemically and mechanically isolated fibres of spruce (Picea abies [L.] Karst.). Part 1: Structural and chemical characterisation**. *Holzforschung*, 59(2):240-246 (cit. in Orso et al., 2006)

Burgert I, Eder M, Frühmann K, Keckes J, Fratzl P, Stanzl-Tschegg S (2005b) **Properties of chemically and mechanically isolated fibres of spruce (Picea abies [L.] Karst.). Part 3: Mechanical characterisation**. *Holzforschung*, 59:354-357 (cit. in Orso et al., 2006)

Burgert I (2006) **Exploring the micromechanical design of plant cell walls**. *American Journal of Botany*, 93(10):1391-1401

Burgert I (2007) **The cell wall – some unresolved problems**. Presentation, COST E35 Meeting, 11-12 October, Stockholm

Bury K V (1975) **Statistical models in applied science**. John Wiley & Sons Inc., ISBN 0-471-12590-3

Calard V, Lamon J (2004) **Failure of fiber bundles**. *Composites Science and Technology*, 64:701-710

Carrington H (1923) **The elastic constants of spruce**. Phil. Mag., 45:1055-1057 (cit. in Persson, 2000)

Casella G, Berger R L (2002) **Statistical Inference**. 2nd ed., Library of Congress Cataloging-in Publication Data. ISBN 0-534-24312-6

Cave I D (1969) **The longitudinal Young's modulus of Pinus radiata**. *Wood Science and Technology*, 3(1):40-48 (cit. in Salmén, 2004)

Cave I D (1978) **Modelling moisture-related mechanical properties of wood; Part I: Properties of the wood constituents**. *Wood Science and Technology*, 12(1):75-86 (cit. in Neagu and Gamstedt, 2007)

Chou T W (1992) **Microstructural Design of Fibre Composites**. *Cambridge University Press, U.K.* (cit. in Ibnabdeljalil and Curtin, 1997)

Chudoba R, Vořechovský M, Konrad M (2006) **Stochastic modelling of multi-filament yarns. I. Random properties within the cross-section and size effect**. *International Journal of Solids and Structures*, 43:413-434

Clarke S H (1938) **Fine structure of the plant cell wall**. *Nature*, 3603:899-142

Colling F, Dinort R (1987) **Die Ästigkeit des in den Leimbaubetrieben verwendeten Schnittholzes**. Holz als Roh- und Werkstoff, 45:23-26 (in German)

Colling F (1990) **Tragfähigkeit von Biegeträgern aus Brettschichtholz in Abhängigkeit von den festigkeitsrelevanten Einflußgrößen**. PhD-thesis, Versuchsanstalt für Stahl, Holz und Steine, Universität Fridericiana in Karlsruhe, Germany (in German)

Colling F, Ehlbeck J, Görlacher R (1991) **Glued laminated timber: contribution to the determination of the bending strength of glulam beams**. International Council for Building Research Studies and Documentation, Working Commission W18 – Timber Structures, 24th Meeting, Oxford, United Kingdom, CIB-W18 / 24-12-1

Colling F, Ehlbeck J (1992) **Tragfähigkeit von Keilzinkenverbindungen im Holzleimbau**. *Bauen mit Holz*, 94(7):586-593 (in German)

Colombo L (2008) **Introduction to quantum physics**. Additional lecture course in: Brittle Fracture and Plastic Slip – From the Atomistic to the Engineering Scale. Centre International des Sciences Mécaniques (CISM), Udine, Italy, 26-30 May 2008

Corder S E (1965) **Localized deflection related to bending strength of lumber**. 2nd Symposium on Nondestructive Testing of Wood, Washington State University, USA, 461-473

Côte W A, Day A C (1964) **Anatomy and ultrastructure of reaction wood**. In: Cellular Ultrastructure of Wood Plants, Ed. Côte W A, Syracuse University Press (cit. in Hoffmeyer, 1987)

Cousins W J, Armstrong R W, Robinson W H (1975) **Young's modulus of lignin from a continuous indentation test**. *Journal of Material Science*, 10:1655–1658 (cit. in Salmén, 2004)

Cousins W J (1976) **Elastic modulus of lignin as related to moisture content**. *Wood Science and Technology*, 10:9–17 (cit. in Bergander and Salmén, 2002; Salmén, 2004)

Cousins W J (1978) **Young's modulus of hemicellulose as related to moisture**. *Wood Science and Technology*, 12(3):161-167

Crow E L, Shimizu K (1988) **Lognormal distributions: Theory and applications**. Library of Congress Cataloging-in-Publication Data, Marcel Dekker, Inc., New York, USA, ISBN 0-8247-7803-0

Czmoch I (1989) **Randomness of rigidity of timber beams: Statistical study based on experimental data**. Chalmers University of Technology, Division of Structural Design, 11, 112 p.

Czmoch I (1991) **Lengthwise variability of bending stiffness of timber beams**. International Timber Engineering Conference, London, UK, 2.158-2.165

Czmoch I, Thelandersson S, Larsen H J (1991) **Effect of within member variability on bending strength of structural timber**. International Council for Building Research Studies and Documentation, Working Commission W18 – Timber Structures, 24th Meeting, Oxford, UK, CIB-W18 / 24-6-3

Daniels H E (1945) **The Statistical Theory of the Strength of Bundles of Threads. I**. *Proceedings of the Royal Society A*, 183:405-435

Daniels H E (1974) **The Maximum Size of a Closed Epidemic**. *Advances in Applied Probability*, 6(4):607-621

Daniels H E, Skyrme T H R (1985) **The maximum of a random walk whose mean path has a maximum**. *Advances in Applied Probability*, 17:85-99 (cit. in Daniels, 1989)

Daniels H E (1989) **The Maximum of a Gaussian Process whose Mean Path has a Maximum, with an Application to the Strength of Bundles of Fibres**. *Advances in Applied Probability*, 21(2):315-333

Davies G W (1968) **Microscopic observations of wood fracture**. *Holzforschung*, 22:177-181 (cit. in Mark and Gillis, 1970)

Denne M P (1973) **Tracheid dimensions in relation to shoot vigour in Picea**. *Forestry*, 46: 117-124 (cit. in Brändström, 2001)

Denzler J K (2007) **Modellierung des Größeneffektes bei biegebeanspruchtem Fichtenschnittholz**. PhD-thesis, Fakultät Wissenschaftszentrum Weihenstephan für Ernährung, Landnutzung und Umwelt, Technische Universität München, 157 p. (in German)

Dill-Langer G, Hidalgo R C, Kun F, Moreno Y, Aicher S, Herrmann H J (2003) **Size dependency of tension strength in natural fiber composites**. *Physica A*, 325:547-560

Dinwoodie J M (1989) **Wood: Nature's cellular, polymeric fibre-composite**. The Institute of Metals, London, UK

Ditlevsen O (1978a) **Generalized Second Moment Reliability Index**. *J. Struct. Mech.*, ASCE, 7(4):435-451 (cit. in Gollwitzer, 1986)

Ditlevsen O (1978b) **Narrow Reliability Bounds for Structural Systems**. *J. Struct. Mech.*, ASCE, 7(4):453-472 (cit. in Gollwitzer, 1986)

Ditlevsen O, Källsner B (1998) **System effects influencing the bending strength of timber beams**. Working Conference on Reliability and Optimization of Structural Systems, IFIP 8th WG 7.5, Krakow, Poland, 8 p.

Ditlevsen O, Källsner B (2005) **Span-dependent distributions of the bending strength of spruce timber**. *Journal of Engineering Mechanics*, ASCE, 131(5):485-499

Duden (2001, 2005) **Fremdwörterbuch**. 7., neu bearbeitete und erweiterte Auflage, Band 5, Dudenverlag, Mannheim-Leipzig-Wien-Zürich, ISBN 3-411-04057-2 (in German)

Durrett R (1994) **The Essentials of Probability**. Duxbury Press, Wadsworth Inc., ISBN 0-534-19230-0

Duxbury P M, Leath P L (1994) **Failure Probability and Average Strength of Disordered Structures**. *Physical Review Letters*, 72(17):2805-2808

Eberhardsteiner J (2002) **Mechanisches Verhalten von Fichtenholz: Experimentelle Bestimmung der biaxialen Festigkeitseigenschaften**. Springer Verlag, Wien, New-York, ISBN 3-211-83763-9, 178 p. (in German)

Eder M (2007) **Structure, properties and function of single wood fibres of Norway spruce (Picea abies [L.] Karst.)**. PhD-thesis, Universität für Bodenkultur, Institut für Physik und Materialwissenschaften, Department für Materialwissenschaften und Prozesstechnik, Wien

Eder M, Stanzl-Tschegg S, Burgert I (2008a) **The fracture behaviour of single wood fibres is governed by geometrical constraints: in-situ ESEM studies on three fibre types**. *Wood Science and Technology*, 42(8):679-689

Eder M, Terziev N, Daniel G, Burgert I (2008b) **The effect of (induced) dislocations on the tensile properties of individual Norway spruce fibres**. *Holzforschung*, 62(1):77-81

Eder M, Jungnikl K, Burgert I (2009) **A close-up view of wood structure and properties across a growth ring of Norway spruce (Picea abies [L.] Karst.)**. *Trees – Structure and Function*, 23(1):79-84

Ehlbeck J, Colling F, Görlacher R (1985a) **Influence of finger-jointed lamellae on the bending strength of glulam beams: input data for the computer model**. *Holz als Roh- und Werkstoff*, 43:369-373 (in German)

Ehlbeck J, Colling F, Görlacher R (1985b) **Influence of finger-jointed lamellae on the bending strength of glulam beams: development of a computer model**. *Holz als Roh- und Werkstoff*, 43(8):333-337 (in German)

Eichhorn S J Baillie C A, Zafeiropoulos N, Mwaikamabo L Y, Ansell M P, Dufresne A, Entwistle K M, Herrera-Franco P J, Escamilla G C, Groom L, Hughes M, Hill C, Rials T G, Wild P M (2001) **Review – Current international research into cellulosic fibres and composites**. *Journal of Materials Science*, 36:2107-2131

Epstein B (1948) **Application of the Theory of Extreme Values in Fracture Problems**. *Journal of the American Statistical Association*, 43(243):403-412

Eiser A (2008) **Untersuchung von DUO- und TRIO-Trägern sowie des Grundmaterials als BSH-Ersatz für Schottland**. Internal Research Report, Project 2.1.6 separate, Competence Centre holz.bau forschungs gmbh, Graz, Austria, 47 p. (in German)

Eiser A, Jeitler G, Kastner E, Schickhofer G (2010) **Untersuchung des mechanischen Potenzials von Balkenbindern, aufgebaut aus übereinander geschichteten DUO-Balken, hinsichtlich ihrer Festigkeit und Steifigkeit**. Internal Research Report, Project 2.1.4 multigirder, Competence Centre holz.bau forschungs gmbh, Graz, Austria, 54 p. (in German)

Fahlén J, Salmén L (2002) **On the lamellar structure of the tracheid cell wall**. *Plant Biol.*, 4:339-345

Falk R H, Colling F (1994) **Glued-laminated timber: Laminating effects**. PTEC 94, 618-625, Gold Coast Australia, Australia

Falk R H, Colling F (1995) **Laminating effects in glued-laminated timber beams**. *Journal of Structural Engineering*, 121(12):1857-1863

Faye C, Rouger F, Garcia P (2010) **Experimental investigations on mechanical behaviour of glued solid timber**. International Council for Building Research Studies and Documentation, Working Commission W18 – Timber Structures, 43rd Meeting, Nelson, New Zealand, CIB-W18 / 43-12-4

Fengel D (1969) **The ultrastructure of cellulose from wood. Part 1: Wood as the basic material for the isolation of cellulose**. *Wood Science and Technology*, 3:203-217 (cit. in Persson, 2000; Brändström, 2001)

Fengel D, Stoll M (1973) **Variation in cell cross-sectional area, cell-wall thickness and wall layers of spruce tracheids within an annual ring**. *Holzforschung*, 27:1-7 (cit. in Brändström, 2001)

Fengel D, Wegener G (1989) **Wood – Chemistry, Ultrastructure, Reactions**. Walter de Gruyter, Berlin, New York, ISBN 3-11-012059-3

Fewell A R (1991) Personal communication (cit. in Czmoch et al., 1991)

Fink G, Deublein M, Köhler J (2011) **Assessment of different knot-indicators to predict strength and stiffness properties of timber boards**. International Council for Building Research Studies and Documentation, Working Commission W18 – Timber Structures, 44th Meeting, Alghero, Italy, CIB-W18 / 44-5-1

Fisher R A, Tippett L H C (1928) **Limiting forms of the frequency distribution of the largest or smallest member of a sample**. *Proc. Cambridge Philos. Soc.*, 24:180-190 (cit. in Kotz and Nadarajah, 2000)

Foley C (1997) **Strength predictions in structural timber: State of the art report and analytic discussion**. PhD-thesis, Department of Structural Engineering, Lund University of Technology

Foschi R O, Barrett J D (1980) **Glued-laminated beam strength: a model**. *Journal of the Structural Division*, Proceedings of ASCE 106(ST8):1735-175 (cit. in Richburg, 1989)

Foschi R O (1985) **AITC GLULAM: A simulation model for strength and stiffness of g1ued-1aminated beams**. Unpub1ished research report, AITC, Vancouver, WA (cit. in Taylor, 1988)

Fratzl P, Burgert I, Gupta H S (2004) **On the role of interface polymers for the mechanics of natural polymeric composites**. *Phys. Chem. Chem. Phys.*, 6:5575-5579 (cit. in Fratzl and Weinkammer, 2007)

Fratzl P, Weinkammer R (2007) **Nature's hierarchical materials**. *Progress in Materials Science*, 52:1263-1334

Frese M (2006) **Die Biegefestigkeit von Brettschichtholz aus Buche: Experimentelle und numerische Untersuchungen zum Laminierungseffekt**. PhD-thesis, Lehrstuhl für Ingenieurholzbau und Baukonstruktionen, Universität Karlsruhe, Germany (in German)

Freudenthal A M, Gumbel E J (1956) **Physics and statistical aspects of fatigue**. *Journal of Advanced Mechanics*, Vol. 4 (cit. in Bury, 1975)

Fronius K (1982) **Arbeiten und Anlagen im Sägewerk; Band 1 – Der Rundholzplatz**. ISBN 3-87181-331-1, DRW-Verlag, 94 p. (in German)

Galileo G L (1638) **Discorsi I Demostrazioni Matematiche interno à due Nuove Scienze**. Elsevier, Leiden, English transl. By T Westen, London (1730), p. 179-181 (cit. in Bažant and Chen, 1996; in Italian)

Gao H J (2006) **Application of fracture mechanics concepts to hierarchical biomechanics of bone and bone-like materials**. *International Journal of Fracture*, 138:101-37 (cit. in Fratzl and Weinkammer, 2007)

Gehri E, Steurer T (1979) **Holzfestigkeit bei Beanspruchung schräg zur Faser**. Schweizerische Arbeitsgemeinschaft für Holzforschung (SAH), Bulletin 7/2 (cit. In Hoffmeyer, 1987; in German)

Gehri E (1997) **System strength**. Comments to prENV 1995-2, section 6.3.1 (version 1997-01-14), ETH Zurich, 9 p.

Gibrat R (1930) **Une Loi Des Repartitions Economiques: L'effet Proportionelle**. *Bulletin de Statisti-que General*, France, 19, 469 p. (cit. in Crow and Shimizu, 1988 ; in France)

Gibrat R (1931) **Les Inégalités Économiques**. Paris, Librairie du Recueil Sirey (cit. in Crow and Shimizu, 1988 ; in Fance)

Gibson L J, Ashby M F (1999) **Cellular solids, structure and properties**. 2nd ed. Cambridge, Cambridge University Press, p. 510 (cit. in Fratzl and Weinkammer, 2007)

Gillis P P (1969) **Effect of hydrogen bonds on the axial stiffness of crystalline native cellulose**. *Journal of Polymer Science A*, 2(7):783-794

Gindl W, Wimmer R (2000) **Relationship between lignin content and tracheid morphology in spruce**. Proceedings of 3rd Plant Biomechanics Conference, Freiburg, Germany, 163-168 (cit. in Brändström, 2001)

Gindl W, Teischinger A (2002) **Axial compression strength of Norway spruce related to structural variability and lignin content**. *Composites: Part A*, 33:1623-1628

Gindl W, Schöberl T (2004) **The significance of the elastic modulus of wood cell walls obtained from nanoindentation measurements**. *Composites A*, 35:1345-1349 (cit. in Orso et al., 2006)

Gindl W, Gupta H S, Schöberl T, Lichtenegger H C, Fratzl P (2004) **Mechanical properties of spruce wood cell walls by nanoindentation**. *Applied Physics A*, 79:2069-2073 (cit. in Orso et al., 2006)

Gindl W, Keckes J (2005) **All-cellulose nanocomposite**. *Polymer*, 46:10221-10225

Gitman I M (2006) **Representative Volumes and Multi-Scale Modelling of Quasi-Brittle Materials**. PhD-thesis, Delft University of Technology, ISBN 90-64641-22-6

Gitman I M, Askes H, Sluys L J (2007) **Representative volume: Existence and size determination**. *Engineering Fracture Mechanics*, 74:2518-2534

Glos P (1978) **Zur Bestimmung des Festigkeitsverhaltens von Brettschichtholz bei Druckbeanspruchung aus Werkstoff- und Einwirkungskenngrößen**. PhD-thesis, Berichte zur Zuverlässigkeitstheorie der Bauwerke, Heft 35, Technische Universität München (in German)

Glos P (1995) **Festigkeitssortierung**. Beitrag A6, STEP 1, Arbeitsgemeinschaft Holz e.V., Düsseldorf, 9 p. (cit. in Augustin, 2004; in German)

Glos P (1999) **The great potential of wood as a building material for the next century**. 1st International RILEM Symposium of Timber Engineering, Stockholm, Sweden, *RILEM Publications S.A.R.L*, ISBN 2-912143-10-1, 10 p.

Goldstein I S (1991) **Overview of the Chemical Composition of Wood**. Chapter 1, In: *Wood Structure and Composition* (ed. Lewin M and Goldstein I S), Marcel Dekker Inc., New York, NY, USA, p. 1-5 (cit. in Wathén, 2006)

Gollwitzer S (1986) **Zuverlässigkeit redundanter Tragsysteme bei geometrischer und stofflicher Nichtlinearität**. PhD-thesis, Institut für Bauingenieurwesen III, Lehrstuhl für Massivbau, Technische Universität München, 215 p. (in German)

Gollwitzer S, Rackwitz R (1990) **On the reliability of Daniels Systems**. *Structural Safety*, 7:229-243

Gollwitzer S, Rackwitz R (1983) **Equivalent Components in First-Order System Reliability**. *Rel. Eng.*, 5:99-115 (cit. in Gollwitzer, 1986)

Gordon J E, Jeronimidis G (1974) **Work of fracture of natural cellulose**. *Nature*, 252:116

Görlacher R (1989) **Klassifizierung von Brettschichtholzlamellen durch Messung von Longitudinalschwingungen**. PhD-thesis, Fakultät für Bauingenieur- und Vermessungswesen, Universität Karlsruhe (cit. in Colling, 1990; in German)

Graf O, Egner K (1938) **Über die Veränderlichkeit der Zugfestigkeit von Fichtenholz mit der Form und Größe der Einspannköpfe der Normenkörper und mit der Zunahme des Querschnitts der Probekörper**. *Holz als Roh- und Werkstoff*, 1(10):384-388 (in German)

Griffith A A (1920) **The phenomenon of rupture and flow in solids**. *Philos. Trans. Roy. Soc. London A*, 221:163-198 (cit. in Kotz and Nadarajah, 2000)

Groom L H, Leichti R J (1994) **Effect of adhesive stiffness and thickness on stress distributions in structural finger joints**. *Journal of Adhesion*, 44:69-83

Grosser D (2003) **Die Hölzer Mitteleuropas. Ein mikrophotografischer Lehratlas**. Reprint der Originalausgabe von 1977 (ehem. Springer-Verlag), Verlag Dr. Kessel, Remangen, ISBN 3-935638-22-1 (in German)

Grozdits G A, Ifju G (1969) **Development of tensile strength and related properties in differentiating coniferous xylem**. *Wood Science*, 1(3):137-147 (cit. in Mark and Gillis, 1970)

Grün B (2009) **Stochastische Prozesse und Zeitreihenmodelle**. Script, chapt. 12, Department of Statistics and Mathematics, Wirtschaftsuniversität WU Wien, http://statmath.wu-wien.ac.at/courses/gwa, 80 p. (in German)

Guers F, Rackwitz R (1987) **Time-variant reliability of structural systems subjected to fatigue**. *Proc. ICASP 5*, Vancoucer, Vol. I, p. 497-505 (cit. in Gollwitzer and Rackwitz, 1990)

Gurvich M R, Pipes R B (1995) **Probabilistic analysis of a multi-step failure process of a laminated composite in bending**. *Composites Science and Technology*, 55:413-421

Gücer D E, Gurland J (1962) **Comparison of the statistics of two fracture models**. *Journal of Mechanics Physics and Solids*, 10:365-373 (cit. in Smith, 1982)

Hakkila P (1998) **Structure and properties of wood and woody biomass**. Chapter 4, In: Forest Resources and Sustainable Management (ed. Kellomäki S), Book 2, In: Papermaking Science and Technology, Fapet Oy, Jyväskylä, Finland, p. 116-185 (cit. in Wathén, 2006)

Han M B, Bender D A, Taylor S E (1991) **Computer generation of highly skewed correlated random variables**. *American Society of Agricultural Engineers*, 34(5):2279-2281

Hansen A, Hemmer P C (1994) **Critical in fracture: the burst distribution**. *Trends in Statistical Physics*, Research Trends, Trivandrum, India (cit. in Zhang and Ding, 1994)

Hankinson R L (1921) **Investigation of crushing strength of spruce at varying angles of grain**. U.S. Air Service Information Circular, Vol. 3, No. 259, Washington, DC, US Air Service, Materials Section Paper No. 130

Hardacker K W (1962) **The automatic recording of the load-elongation characteristics of single papermaking fibers**. *Tappi*, 45(3):237-246 (cit. in Mott, 1995)

Harlow D G, Phoenix S L (1978a) **The chain-of-bundles probability model for the strength of fibruous materials I: Analysis and conjectures**. *J. Composite Materials*, 12:195-214 (cit. in Smith, 1983)

Harlow D G, Phoenix S L (1978b) **The chain-of-bundles probability model for the strength of fibruous materials II: A numerical study of convergence**. *J. Composite Materials*, 12:314-334 (cit. in Smith, 1983)

Harlow D G, Phoenix S L (1981a) **Probability distributions for the strength of composite materials I: Two-level bounds**. *Internat. J. Fracture*, 17:347-372 (cit. in Smith, 1983)

Harlow D G, Phoenix S L (1981b) **Probability distributions for the strength of composite materials II: A convergence sequence of tight bounds**. *Internat. J. Fracture*, 17:601-630 (cit. in Smith, 1983)

Harlow D G, Phoenix S L (1982) **Probability distributions for the strength of composite materials under local load sharing I: Two level failure**. *Advances in Applied Probability*, 14:68-94 (cit. in Smith, 1983)

Harlow D G, Smith R L, Taylor H M (1983) **Lower Tail Analysis of the Distribution of the Strength of Load-Sharing Systems**. *Journal of Applied Probability*, 20(2):358-367

Hartung J et al. (2002) **Statistik: Lehr- und Handbuch der angewandten Statistik**. 13. unwes. Veränd. Aufl., München, Wien, Verlag Oldenburg, ISBN 3-486-25905-9 (in German)

Hassler U (2002) **Stochastische Prozesse in Finanzierung und Ökonometrie**. Script, Empirische Wirtschaftsforschung und Makroökonometrie, Technische Universität Darmstadt, WS 2002/03, 54 p. (in German)

Hearmon R F S (1948) **The elasticity of wood and plywood**. *Forest Products Research Special Report*, No. 7, HMSO London (cit. in Persson, 2000)

Hedgepeth J M, Van Dyke P (1967) **Local stress concentrations in imperfect filamentary composite materials**. *J. Composite Materials*, 1:294-309 (cit. in Smith, 1983)

Heimeshoff B, Glos P (1980) **Zugfestigkeit und Biege-E-Modul von Fichten-Brettlamellen**. *Holz als Roh- und Werkstoff*, 38:51-59 (in German)

Hemmer P C, Hansen A (1992) **The Distributions of Simultaneous Fiber Failures in Fiber Bundles**. *Journal of Applied Mechanics*, 59(4):909 (cit. in Zhang and Ding, 1994)

Hernandez R (1998) **Analysis of strain in finger-jointed lumber**. 5th World Conference on Timber Engineering, Montreux, Switzerland, Vol. 1, 145-151

Hidalgo R C, Kun F, Herrmann H J (2001) **Bursts in a fibre bundle model with continuous damage**. *Physical Review E*, 64(066122):1-9

Hidalgo R C, Moremo Y, Kun F, Herrmann H J (2002) **Fracture model with variable range of interaction**. *Physical Review E*, 65(046148):1-8

Hill R L (1967) **The creep behaviour of individual pulp fibers under tensile stress**. *Tappi*, 50(8):432-440 (cit. in Wathén, 2006)

Hinterstoisser B, Åkerholm M, Salmén L (2001) **Effect on fiber orientation in dynamic FTIR study on native cellulose**. *Carbonhydrate Research*, 334(1):27-37 (cit. in Wathén, 2006)

Hitchon J W, Phillips D C (1978) **The effect of specimen size on the strength of CFRP**. *Composites*, 9:119-124 (cit. in Sutherland et al., 1999)

Hjukström A (1985) **Size effect and lengthwise variability for modulus of elasticity**. Chalmers University of Technology, Division of Structural Design (cit. in Czmoch, 1991; in Swedish)

Hoffmeyer P (1978) **Moisture content – strength relationship for spruce lumber subjected to bending, compression and tension along the grain**. IUFRO – Timber Engineering, Vancouver, Canada, 71-91

Hoffmeyer P (1987) **The role of grain angle, knots, tension wood, compression wood, and other anomalies on the mechanical properties of wood**. Technical Report, No. 183/87, Technical University of Denmark, Building Material Laboratory

Hofstetter K, Hellmich C, Eberhardsteiner J (2006) **Continuum micromechanics estimation of wood strength**. *PAMM Proceeding of Applied Mathematics and Mechanics*, 6:75-78

Hohenbichler M (1980) **Zur zuverlässigkeitstheoretischen Untersuchung von Seriensystemen**. Berichte zur Zuverlässigkeitstheorie der Bauwerke, SFB 96, Technische Universität München, Heft 48 (cit. in Gollwitzer, 1986; in German)

Hohenbichler M, Rackwitz R (1981) **On structural reliability of parallel systems**. *Reliability Engineering*, 2:1-6

Hohenbichler M, Rackwitz R (1983) **Reliability of parallel systems under imposed uniform strain**. *Journal of Engineering Mechanics*, 109(3):896-907

Hubrig C, Herrmann P (2005) **Lösungen in der Schule: Systemisches Denken in Unterricht, Beratung und Schulentwicklung**. Carl-Auer Systeme Verlag, Heidelberg, 1. Aufl., ISBN 13: 978-3-89670-454-2 (in German)

Ibnabdeljalil M, Curtin W A (1997) **Strength and reliability of fibre-reinforced composites: localized load-sharing and associated size effects**. *Int. J. Solids Structures*, 34(21):2649-2668

Ingolic E (2008) **FFG_Forschungsprojekt "Götterbaum – Ailanthus altissima" – Lichtmikroskopie Axioplan mit CCD Camera von Polaroid, REM _ESEM 600**. Internal report, Zentrum für Elektronenmikroskopie Graz (ZFE), Graz University of Technology, Verein zur Förderung der Elektronenmikroskopie und Feinstrukturforschung (FELMI), 21 p. (in German)

Isaksson T, Thelandersson S, Moller-Pedersen T (1994) **Within member variability of bending strength of timber**. Pacific Timber Engineering Conference, Gold Coast Australia, Timber Research and Development Advisory Council, 634-641

Isaksson T, Thelandersson S (1996) **Variability and prediction of bending strength of timber**. International Wood Engineering Council, IWEC, Lousiana, USA, 2:422-429

Isaksson T, Freysoldt J (1997) **Load carrying capacity of timber beams with narrow moment peaks**. International Council for Building Research Studies and Documentation, Working Commission W18 – Timber Structures, 30th Meeting, Vancouver, Canada, CIB-W18 / 30-10-4

Isaksson T (1998) **Length and moment configuration factors**. International Council for Building Research Studies and Documentation, Working Commission W18 – Timber Structures, 31st Meeting, Savonlinna, Finland, CIB-W18 / 31-6-1

Isaksson T (1999) **Modelling the Variability of Bending Strength in Structural Timber**. PhD-thesis, Lund, Sweden, Report TVBK-1015, ISSN 0349-4969

Jayne B A (1959) **Mechanical properties of wood fibers**. *Tappi*, 42(6)461-467 (cit. in Mott, 1995)

Jeitler G, Bogensperger T, Brandner R, Schickhofer G (2007) **Versuchstechnische Ermittlung des Längeneffektes auf die Zugfestigkeit von stabförmigen Holzprodukten**. Internal research report, Competence Centre holz.bau forschungs gmbh, Non-K_{Ind} P03_qm online II, 38 p. (in German)

Jensen J L, Thomas S D, Corbett P W M (1997) **On the bias sampling variation of the harmonic average**. *Mathematical Geology*, 29(2):267-276

Johansson C-J (2000) **Grading of timber with respect to mechanical properties**. Timber Advanced Course 2000, Lunds Tekniska Högskola, Lund, Sweden, 28 p. (cit. in Augustin, 2004)

Johnson N L, Balakrishnan N, Kotz S (1994) **Continuous Univariate Distributions 1**. 2nd Edition, John Wiley & Sons, New York (cit. in Thomopoulos and Johnson, 2004)

Jones R M, Miller K S (1966) **On the multivariate lognormal distribution**. *J. Ind. Math.*, 16:63-76 (cit. in Hohenbichler and Rackwitz, 1981)

Jöbstl R A, Bogensperger T, Moosbrugger T, Schickhofer G (2006) **A Contribution to the Design and System Effect of Cross Laminated Timber**. International Council for Building Research Studies and Documentation, Working Commission W18 – Timber Structures, 39th Meeting, Florence, Italy, CIB-W18 / 39-12-4

Jönsson R, Östlund L (1987) **Säkerhetsproblem för träkonstrutioner**. TVBK-3026. Department of Structural Engineering, Lund University (cit. in Czmoch et al., 1991; in Swedish)

Kanit T, Forest S, Galliet I, Mounoury V, Jeulin D (2003) **Determination of the size of the representative volume element for random composites: statistical and numerical approach**. *International Journal of Solids and Structures*, 40:3647-3679

Källsner B, Ditlevsen O (1994) **Lengtwise bending strength variation of structural timber**. IUFRO – Timber Engineering, S 5.02, Sydney, Australia, 333-352

Källsner B, Ditlevsen O, Salmela K (1997) **Experimental verification of a weak zone model for timber in bending**. IUFRO S 5.02 – Timber Engineering, Copenhagen, Denmark, 17 p.

Kastner E, Schickhofer G, Brandner R, Unerwieser H (2011) **Untersuchung der Auswirkung des längsweisen Auftrennens auf das mechanische Potenzial von Brettschichtholzlamellen und daraus aufgebauten Brettschichtholzträgern, hinsichtlich ihrer Festigkeit und Steifigkeit**. COMET-K Project APTM 2.1.6 separate, Competence Centre holz.bau forschungs gmbh, Graz (in German)

Keckes J, Burgert I, Frühmann K, Müller M, Kölln K, Hamilton M, Burghammer M, von Roth S, Stanzl-Tschegg S, Fratzl P (2003) **Cell-wall recovery after irreversible deformation of wood**. *Nat. Mater.*, 2:810-812

Keith C T, Côte W A (1968) **Microscopic characterisation of slip lines and compression failures in wood cell walls**. *Forest Products Journal*, 18(3):67-74 (cit. in Mark and Gillis, 1970)

Kerr A J, Goring D A I (1975) **The ultrastructural arrangement of the wood cell wall**. *Cell. Chem. Technol.*, 9:563-573

Kersavage P C (1973) **Moisture content effect on tensile properties of individual Douglas-fir latewood tracheids**. *Wood and Fiber*, 5(2):105-117 (cit. in Wathén, 2006; Mott, 1995)

Keunecke D, Hering S, Niemz P (2008) **Three-dimensional elastic behaviour of common yew and Norway spruce**. *Wood Science Technology*, 42(8):633-647

Keylwerth R (1951) **Die anisotrope Elastizität des Holzes in Lagenhölzern**. VDI-Forschungsheft, No. 430, Deutscher Ingenieur-Verlag (cit. in Hoffmeyer, 1987; in German)

Kim C Y, Page D H, El-Hosseiny F, Lancaster A P S (1975) **The mechanical properties of single wood pulp fibers. III The effect of drying stress and strength**. *Journal Applied Polymer Sciences*, 19:1549-1561 (cit. in Waterhouse, 1984)

Kirchner F (1907) **Wörterbuch der philosophsichen Grundbegriffe**. www.textlog.de/kirchner_woerterbuch.htm (in German)

Kline D E, Woeste F E, Bendtsen B A (1986) **Stochastic model for modulus of elasticity of lumber**. *Wood and Fiber Science*, 18(2):228-238

Kloster M, Hansen A, Hemmer P C (1997) **Burst avanlanches in solvable models of fibruous materials**. *Physical Review E*, 56(3):2615-2625

Kollmann F F P (1934) **Die Abhängigkeit der Festigkeit und der Dehnungszahl der Hölzer vom Faserverlauf**. *Der Bauingenieur*, No. 19/20 (cit. In Hoffmeyer, 1987; in German)

Kollmann F F P, Côte W A (1968) **Principles of wood science and technology, 1. solid wood**. Springer-Verlag, Berlin, Germany (cit. in Persson, 2000)

Konnerth J, Valla A, Gindl W, Müller U (2006) **Measurement of strain distribution in timber finger joints**. *Wood Science and Technology*, 40:631-636

Kórán Z (1967) **Electron microscopy of radial tracheid surfaces of black spruce separated by tensile failure at various temperatures**. *Tappi*, 50:60-67 (cit. in Mark and Gillis, 1970)

Kotz S, Nadarajah A (2000) **Extreme Value Distributions: Theory and Applications**. Imperial College Press, ISBN 1-86094-224-5, 185 p.

Köhler J (2007) **Reliability of Timber Structures**. PhD-thesis, ETH Zurich, Institut für Baustatik und Konstruktion, Switzerland, IBK-Bericht Nr. 301

Kroon-Batenburg L M, Kroon J, Norholt M G (1986) **Chain modulus and intramolecular hydrogen bonding in native and regenerated cellulose fibers**. *Polym. Commun.*, 27:290-292 (cit. in Salmèn, 2004)

Kucera L J, Bariska M (1982) **On the fracture morphology in wood, Part 1**. *Wood Science and Technology*, 16:241-259 (cit. in Poulsen et al., 1997)

Kun F, Zapperi S, Herrmann H J (2000) **Damage in fiber bundle models**. *The European Physical Journal B*, 17:269-279

Lai C D, Rayner J C W, Hutchinson T P (1999) **Robustness of the sample correlation – the bivariate lognormal case**. *Journal of Applied Mathematics & Decision Sciences*, 3(1):7-19

Lam F (1987) **Length effect re tension and compression: addendum**. Forintek Canada Corp., Western Region

Lam F, Varoglu E (1990) **Effect of length on the tensile strength of lumber**. *Forest Products Journal*, 40(5):37-42

Lam F, Varoglu E (1991a) **Variation of tensile strength along the length of lumber. Part 1: Experimental**. *Wood Science Technology*, 25:351-359

Lam F, Varoglu E (1991b) **Variation of tensile strength along the length of lumber. Part 2: Model development and verification**. *Wood Science Technology*, 25:449-458

Lam F, Barrett J D (1992) **Modelling lumber strength spatial variation using trend removal and kriging analyses**. *Wood Science and Technology*, 26:369-381

Lam F, Wang Y-T, Barrett J D (1994) **Simulation of correlated nonstationary lumber properties**. *Journal of Materials in Civil Engineering*, 6(1):34-53

Landis E N, Vasic S, Davids W G, Parrod P (2002) **Coupled Experiments and Simulations of Microstructural Damage in Wood**. *Experimental Mechanics*, 42(4):389-394

Landwehr J M, Matalas N C, Wallis J R (1979) **Probability weighted moments compared with some traditional techniques in estimating Gumbel**

parameters and quantiles. *Water Resource Res.*, 15:1055-1064 (cit. in Kotz and Nadarajah, 2000)

Law A M, Kelton W D (2000) **Simulation Modelling and Analysis**. 3rd McGraw-Hill Higher Education, Boston (cit. in Thomopoulos and Johnson, 2004)

Leicester R H (1985) **Configuration factors for the bending strength of timber**. International Council for Building Research Studies and Documentation, Working Commission W18 – Timber Structures, 18th Meeting, Beit Oren, Israel, CIB-W18 / 18-6-2

Lichtenegger H, Reiterer A, Tschegg S E, Fratzl P (2000) **Microfibril angle in the wood cell wall: mechanical optimization through structural variation?** COST Action E20, Proceedings of Workshop Fibre Wall & Microfibril Angle, May 11-13, Athens, Greece, 4 p. (cit. in Wathén, 2006)

Limbrunner J F, Vogel R M, Brown L C (2000) **Estimation of harmonic mean of a lognormal variable**. *Journal of Hydrologic Engineering*, 5(1):59-66, ISSN 1084-0699/00/0001-0059-0066

Limpert E, Stahel W A, Abbt M (2001) **Log-normal Distributions across the Sciences: Keys and Clues**. *BioScience*, 51(5):341-352

Liu C (2005) **On the Minimum Size of Representative Volume Element: An Experimental Investigation**. Society for Experimental Mechanics, *Experimental Mechanics*, 45(3):238-243

Lowery M D, Nash J E (1970) **A comparison of methods of fitting the double exponential distribution**. *J. Hydrol.*, 10:259-275 (cit. in Kotz and Nadarajah, 2000)

Lund J R, Byrne J P (2000) **Leonardo da Vinci's tensile strength tests: implications for the discovery of engineering mechanics**. *Civil Engineering and Environmental Systems*, 00:1-8

Madsen B, Buchanan A H (1985) **Size effects in timber explained by a modified weakest link theory**. International Council for Building Research Studies and Documentation, Working Commission W18 – Timber Structures, 18th Meeting, Beit Oren, Israel, CIB-W18 / 18-6-4

Madsen B (1988) **Length effects in timber**. Proceeding of the International Conference on Timber Engineering, Seattle, Washington, USA, Vol. 1, ISBN 0-935018-41-7

Madsen B (1989a) **Size effects in lumber. Are they important?** 2nd Pacific Timber Engineering Conference, Aukland, New Zealand, 28-31 (cit. in Williamson, 1992)

Madsen B (1989b) **Proposal for including size effects in CIB W18A timber design code**. International Council for Building Research Studies and Documentation, Working Commission W18 – Timber Structures, 22nd Meeting, Berlin, German Democratic Republic, CIB-W18A / 22-100-2

Madsen B (1990) **Length effects in 38 mm spruce-pine-fir dimension lumber**. *Canadian Journal of Civil Engineering*, 17:226-237

Madsen B (1992) **Structural Behaviour of Timber**. Timber Engineering Ltd., North Vancouver, British Columbia., Canada, ISBN 0-9696162-0-1 (cit. in Williamson, 1994)

Mariotte E (1686) **Traité due movement des eaux**. Posthumously edited by M de la Hire, engl. Transl. by J T Desvaguliers, London (1718), p. 249; also Mariotte's collected works, 2nd ed., The Hague (1740) (cit. in Bažant and Chen, 1996; in France)

Mark R E (1967) **Cell wall mechanics of tracheids**. Yale University Press, New Haven, CT. (cit. in Mark and Gillis, 1970; Booker and Sell, 1998; Waterhouse, 1984)

Mark R E, Gillis P P (1970) **New models in cell-wall mechanics**. *Wood and Fiber*, 2(2):79-95

Mark R E (1983) **Handbook of physical and mechanical testing of paper and paperboard**. Vol. 1, Marcel Dekker Inc. (cit. in Waterhouse, 1984)

Mark R E (2002) **Mechanical properties of fibers**. Chapter 14 in Handbook of Physical Testing of Paper (ed. Mark R E, Habeger C C, Borch J, Lyne M B), 2nd Ed., Revised and expanded, Marcel Dekker, New York, NY, USA, Vol. 1, p. 727-869 (cit. in Wathén, 2006)

Markwardt L J, Youngquist W G (1956) **Tension test methods for wood, wood-base materials, and sandwich constructions**. USDA Forest Service, Forest Products Laboratory, Madison, WI, RP-FPL 2055

Matsuo M, Sawatari C, Imai Y (1990) **Effect of orientation distribution and crystallinity on the measurement by x-ray-diffraction of the crystal-lattice moduli of cellulose-I and cellulose-II**. *Macromolecules*, 23(13):3266-3275 (cit. in Persson, 2000)

Mattheck C, Breloer H (1994) **Handbuch der Schadenskunde von Bäumen: Der Baumbruch in Mechanik und Rechtssprechung**. Rohmbach Wissenschaft: Reihe Ökologie, Bd. 4, 2. Aufl., ISBN 3-7930-9085-X (in German)

Mattheck C (1994) **Holz: Die innere Optimierung der Bäume**. *KFK-Nachrichten 4/94*, Kernforschungszentrum Karlsruhe, p. 232-239 (in German)

Mattheck C, Kubler H (1995) **The internal optimization of trees**. Berlin: Springer-Verlag

Mattheck C (2003) **Warum Alles kaputt geht: Form und Versagen in Natur und Technik**. 1. Auflage, mit Beiträgen von Bethge K, Tesari I und Kürschner W, Forschungszentrum Karlsruhe GmbH, ISBN 3-923704-41-0 (in German)

Matthies M (2002) **Einführung in die Systemwissenschaft**. Script, 2002 / 2003, Universität Osnabrück, Germany, 130 p. (in German)

Meierhofer U (1976) **Der Ast als qualitätsbeeinflussendes Strukturmerkmal**. *Bulletin*, 4/2, Schweizer Arbeitsgemeinschaft für Holz, Lignum, Zurich (in German)

McAlister D (1879) **The law of the Geometric Mean**. *Proceeding of the Royal Society of London*, 29:367-376

McAlister R H (1974) **Strength characteristics of two-ply vertically laminated beams of southern pine**. *Forest Products Journal*, 24(8):39-43

McCartney L N, Smith R L (1983) **Statistical theory of the strength of fiber bundles**. *ASME Journal of Applied Mechanics*, 105:601-608 (cit. in Calard and Lamon, 2004)

Michelitsch M K (2011) **Statistische Prüfauswertung von Fichtenholz auf Längsdruck**. Master-project, Institut of Timber Engineering and Wood Technology, Graz University of Technology, 29 p. (in German)

Michell A J, Willis D (1978) **Cellulosic fibres for reinforcement**. *Appita*, 31(3):347-354 (cit. in Bledzhi and Gassan, 1999; Eichhorn et al., 2001)

Michell A J (1989) **Wood cellulose-organic polymer composites**. *Composite Asia Pacific*, Adelaide, 89:19-21 (cit. in Bledzki and Gassan, 1999)

Miner M A (1945) **Cumulative damage in fatigue**. *Journal of Applied Mechanics*, 12(3):A159-164 (cit. in Smith et al., 2003)

Mischler-Schrepfer V (2000) **Der Einfluss der Waldlagerung von Fichten-Rundholz auf die Längs-Zugeigenschaften des Schnittholzes**. PhD-thesis, ETH Zurich, No. 13857, 242 p. (in German)

Mistler H L (1979) **Die Tragfähigkeit des am Endauflagers unten rechtwinkelig ausgeklinkten Brettschichtträgers**. PhD-thesis, Lehrstuhl für Ingenieurholzbau und Baukonstruktionen, Technische Hochschule Karlsruhe (in German)

Monnin M (1932) **L'essai des bois**. Proceeding, Intern. Verband f. Materialprüfung, Zurich, No. H, p. 85-108 (cit. in Schneeweiß, 1969; in Fance)

Moody R C (1970) **Tensile strength of finger joints in pith-associated and non-pith-associated southern-pine 2 by 6's**. USDA Forest Service, FPL 138, Madison, Wisconsin (cit. in Colling, 1990)

Mott L (1995) **Micromechanical properties and fracture mechanisms of single wood pulp fibers**. PhD-thesis, The Graduate School, University of Maine, 218 p

Navi P, Rastogi P K, Gresse V, Tolou A (1995) **Micromechanics of wood subjected to axial tension**. *Wood Science and Technology*, 29: 411-429 (cit. in Eder, 2007)

Neagu R C, Gamstedt E K (2007) **Modelling of effects of ultrastructural morphology on the hygroelastic properties of wood fibres**. *Journal of Material Science*, 42:10254-10274

Nemeth L J (1967) **Determination of allowable worlink stresses for vertically laminated beams**. *Forest Products Journal*, 17(4):23-30

Newlin J A, Trayer G W (1924) **Form Factors of Beams Subjected to Transverse Loading only**. Natl. Advisory Com. Aeronaut, Report, No. 181 (cit. in Schneeweiß, 1969)

Newman M E J (2005) **Power laws, Pareto distribution and Zipf's law**. *Contemporary Physics*, 46(5):323-351

Niemz P (1993) **Physik des Holzes und der Holzwerkstoffe**. DRW-Verlag, Leinfelden Echterdingen (in German)

Nishino T, Takano K, Nakamae K (1995) **Elastic modulus of the crystalline regions of cellulose polymorphs**. *Journal of Polymer Science Part B: Polymer Physics*, 33(11):1647-1651 (cit. in Nishino et al., 2004)

Nishino T, Matsuda I, Hirao K (2004) **All-Cellulose Composites**. *Macromolecules*, 37:7683-7687

Ollinmaa P J (1961) **Study on reaction wood**. *Acta Forestalia Fennica*, 72:1-54 (cit. in Brändström, 2001; in Finnish)

Orso S, Wegst U G K, Arzt E (2006) **The elastic modulus of spruce cell wall material measured by an in situ bending technique**. *Journal of Material Science*, 41:5122-5126

Paakkari T, Serimaa R (1984) **A study of the structure of wood cells by x-ray diffraction**. *Wood Science and Technology*, 18(2):79-85 (cit. in Wathén, 2006)

Page D H, El-Hosseiny F, Winkler K (1971) *Nature*, 229:252 (cit. in Gordon and Jeronimides, 1974)

Page D H, El-Hosseiny F, Winkler K, Bain R (1972) **The mechanical properties of single wood-pulp fibres. Part I: A new approach**. *Pulp. Pap. Mag. Can.*, 73(8):72-77 (cit. in Wathén, 2006)

Page D H, EI-Hosseiny F (1976) **The mechanical properties of single wood pulp fibers; Part 4: The influence of defects**. *Svensk Papperstidning*, 14:471-474 (cit. in Mott, 1995)

Page D H, El-Hosseiny F, Winkler K, Lancaster A P S (1977) **Elastic modulus of single wood pulp fibers**. *Tappi*, 60(4):114-117 (cit. in Waterhouse, 1984)

Page D H, El-Hosseiny F (1983) **The mechanical properties of single wood pulp fibres. Part VI. Fibril angle and the shape of the stress-strain curve**. *Journal of Pulp and Paper Science*, 9:1-2 (cit. in Eder et al., 2009)

Palmgren A (1924) **Die Lebensdauer von Kugellagern**. *Verein Deutscher Ingenieur*e, 68:339-341 (cit. in Smith et al., 2003; in German)

Paramonova A, Kleinhof M, Paramonov Y (2006) **Normal, Lognormal, Weibull of P-sev Distribution of ultimate Strength of Strands and Composite Specimens**. Proceedings of the 5th International Conference RelStat'05, *Transport and Telecommunication*, 7(1):50-59

Peirce F T (1926) **Tensile tests for cotton yarns v. 'the weakest link' – Theorems on the strength of long and of composite specimens**. *J. Textile Inst. Tran.*, 17:335 (cit. in Kotz and Nadarajah, 2000; Daniels, 1945; Epstein, 1948)

Persson K (2000) **Micromechanical modelling of wood and fibre properties**. PhD-thesis, Structural Mechanics, Department of Mechanics and Materials – Structural Mechanics, LTH, Lund University, Lund, Sweden, ISBN 91-7874-094-0, 215 p.

Phoenix S L, Taylor H M (1973) **The Asymptotic Strength Distribution of a General Fiber Bundle**. *Advances in Applied Probability*, 5(2):200-216

Phoenix S L (1979) **The asymptotic distribution for the time to failure of a fibre bundle**. *Advances in Applied Probability*, 11(1):153-187

Phoenix S L, Ibnabdeljalil M, Hui C Y (1997) **Size effects in the distribution for strength of brittle matrix fibrous composites**. *International Journal of Solids and Structures*, 34(5):545-568

Poulsen J S, Tonnesen M, Byskov E (1995) **Localized Failure in Clear Wood**. In: Proceeding of the 15th Canadian Congress of Applied Mechanics, CANCAM95, University of Victoria, Victoria, British Columbia, p. 200-201 (cit. in Poulsen et al., 1997)

Poulsen J S, Moran P M, Shih C F, Byskov E (1997) **Kink band initiation and band broadening in clear wood under compressive loading**. *Mechanics of Materials*, 25:67-77

Pradhan S, Chakrabarti B K (2008) **Failure properties of fiber bundle models**. *International Journal of Modern Physics B*, 18 p.

Prager W, Hodge P G (1954) **Theorie ideal plastischer Körper**. Translated to German by F Chmelka, Springer Verlag Wien, 274 p. (in German)

Prager W (1959) **An Introduction to Plasticity**. Addison-Wesley, The Addison-Wesley Series in the Engineering Sciences, 148 p., ISBN 978-0201059403

Rackwitz R (1978) **Close Bounds for the Reliability of Structural Systems**. Berichte zur Zuverlässigkeitstheorie der Bauwerke, SFB 96, Technische Universität München, Heft 29 (cit. in Gollwitzer, 1986)

Radovic B, Rohlfing H (1993) **Über die Festigkeit von Keilzinkenverbindungen mit unterschiedlichem Verschwächungsgrad**. *Bauen mit Holz*, 3:196-201 (in German)

Ranta-Maunus A, Denzler J K (2009) **Variability of strength of European spruce**. International Council for Building Research Studies and Documentation, Working Commission W18 – Timber Structures, 42nd Meeting, Duebendorf, Switzerland, CIB-W18 / 42-6-1

R Development Core Team (2009). **R: A language and environment for statistical computing**. R Foundation for Statistical Computing, Vienna, Austria, ISBN 3-900051-07-0, http://www.R-project.org

Rechenberg I (2000) **Über Größe und Leistung Optimierung in der Natur (III)**. Vorlesung Bionik I, WS 00/01, Teil 7, TU Berlin (in German)

Reichelt B (2012) **Der Einfluss der Sperrwirkung auf den Ausziehwiderstand selbstbohrender Holzschrauben – eine vergleichende Betrachtung zwischen**

BSP und BSH. Master-thesis, Institute of Timber Engineering and Wood Technology, Graz University of Technology (in German)

Reiterer A, Lichtenegger H, Tschegg S, Fratzl P (1999) **Experimental evidence for a mechanical function of the cellulose microfibril angle in wood cell walls**. *Philosophical Magazine A*, 79(9):2173-2184 (cit. in Fratzl and Weinkammer, 2007; Eder, 2007)

Riberholt H, Madsen P H (1979) **Strength distribution of timber strutures – measured variation of the cross sectional strength of structural lumber**. Structural Research Laboratory, Technical University of Denmark, No. R 114

Riberholt H (2008) **Nordic glulam – Mechanical properties: Final Draft 2008-09-02**. SP Technical Research Institute of Sweden, Building Technology and Mechanics, SP Report 2008:32, Version 2-A, ISBN 978-91-85829-49-1, 40 p.

Richburg B A (1989) **Modelling localized properties of E-rated laminating lumber**. PhD-thesis, Texas A&M University of Florida, 184 p.

Richburg B A, Bender D A (1992) **Localized tensile strength and modulus of elasticity of E-rated laminated grades of lumber**. *Wood and Fiber Science*, 24(2):225-232

Roberts R J, Rowe R C, York P (1995) **The relationship between the fracture properties, tensile strength and critical stress intensity factor of organic solids and their molecular structure**. *International Journal of Pharmaceutics*, 125:157-162

Robertson A (1920) **Report on Materials of construction used in aircraft and aircraft engines**. Aeronautical Research Committee, London (cit. in Hoffmeyer, 1987)

Rohling H (2007) **Stochastische Prozesse**. Script, Institut für Nachrichtentechnik, Technische Universität Hamburg-Harburg (TUHH), 226 p. (in German)

Ruel K F, Goring D A I (1978) **Lamellation in the S2 layer of softwood tracheids as demonstrated by scanning transmission electron microscopy**. *Wood Science and Technology*, 12:287-291

Ruli A (2004) **Längs und quer zur Faserrichtung auf Druck beanspruchtes Brettschichtholz**. Diploma-thesis, Institute of Timber Engineering and Wood Technology, Graz University of Technology, 111 p. (in German)

Sachsse H (1984) **Einheimische Nutzhölzer und ihre Bestimmung nach makroskopischen Merkmalen**. Verlag Paul Parey, Hamburg und Berlin (in German)

Sacurada I, Nukushina Y, Ito T (1962) **Experimental determination of the elastic modulus of the crystalline region of oriented polymers**. *Journal of Polymer Science*, 57:651-660 (cit. in Persson, 2000)

Salmén L (2004) **Micromechanical understanding of the cell-wall structure**. *C. R. Biologies*, 327:873-880

Scherrer W (2009) **Einführung in stochastische Prozesse und Zeitreihenanalyse**. Script, Institut für Wirtschaftsmathematik, Forschungsgruppe Ökonometrie und Systemtheorie, Technische Universität Wien, 240 p. (in German)

Schickhofer G (1994) **Starrer und nachgiebiger Verbund bei geschichteten, flächenhaften Holzstrukturen**. PhD-thesis, Institut for Steel, Timber and Shell Structures, Graz University of Technology (in German)

Schickhofer G, Pischl R, Seiner C, Steinberger A, Gehri E, Mauritz R (1995) **Development of efficient glued-laminated timber with the application of mechanical stress-graded timber**. Summary, FFF-Research Project, Graz-Zurich-Vienna, 36 p.

Schickhofer G, Riebenbauer J (1997) **Expertenpaket Brettschichtholz basierend auf Leistungsniveau und EU-Standard als Grundlage für die Schaffung neuer Märkte**. Final Report, FFG-Project 6/872, Lignum Research, 21 p. (in German)

Schickhofer G, Augustin M (2001) **Project INTELLIWOOD Working Package 3: „Strength Correspondence“ – Final Report**. Report LR 9808 / 4, Lignum Research, 82 p.

Schickhofer G (2004) **Holzbau – Der Roh- und Werkstoff Holz**. Skriptum S-4-01A/2004, Kapitel 3.3.3: Ermittlung des Systembeiwertes k_{sys} aus Versuchen. Institute of Timber Engineering and Wood Technology, Graz University of Technology (in German)

Schneeweiß G (1962) **Die Berechnung der Biegefestigkeit aus den Festigkeiten der einachsigen Versuche**. *Österr. Ing.-Archiv.*, 17(1):3-31 (cit. In Schneeweiß, 1969; in German)

Schneeweiß G (1964a) **Druckfestigkeit und Stempelhärte**. *Holz als Roh- und Werkstoff*, 22(7):258-264 (cit. In Schneeweiß, 1969; in German)

Schneeweiß G (1964b) **Der Einfluß von Belastungsart, Auflagerentfernung und Querdruckfestigkeit auf die Biegefestigkeit**. *Holz als Roh- und Werkstoff*, 22(11):418-423 (in German)

Schneeweiß G (1969) **Influence of dimensions on the bending strength of wooden beams**. *Holz als Roh- und Werkstoff*, 27(1):23-29 (in German)

Schniewind A P (1989) **Concise Encyclopedia of Wood and Wood-based Materials**. *Pergamon Press*, Oxford, UK (cit. in Smith et al., 2003)

Schwarze F W M R, Engels J (1998) **Cavity formation and the exposure of peculiar structures in the secondary wall (S-2) of tracheids and fibres by wood degrading basidiomycetes**. *Holzforschung*, 52(2):117-123

Sedighi-Gilani M, Navi P (2007) **Experimental observations and micromechanical modelling of successive-damaging phenomenon in wood cells' tensile behaviour**. *Wood Science and Technology*, 41:69-85

Sell J, Zimmermann T (1993) **Radial fibril agglomerations of the S2 on transverse-fracture surfaces of tracheids of tension-loaded spruce and white fir**. *Holz als Roh- und Werkstoff*, 51:384 (cit. in Zimmermann et al., 2006)

Sell J (1994) **Confirmation of a sandwich-like model of the cell wall of softwoods by the light microscope**. *Holz als Roh- und Werkstoff*, 52:234

Sen P K, Bhattacharyya B B (1976) **Asymptotic normality of the extremum of certain sample functions**. *Wahrscheinlichkeitstheorie und verwandte Gebiete*, 34:113-118 (cit. in Gollwitzer and Rackwitz, 1990)

Serimaa R, Andersson S, Saranpää P, Saren M P, Peura M, Paakari T, Pesonen E (2000) **The structure of cell wall of Norway spruce and Scots pine by x-ray scattering methods**. COST Action E20, Proceedings of Workshop Fibre Wall & Microfibril Angle, May 11-13, Athens, Greece, p. 30-31 (cit. in Wathén, 2006)

Serrano E, Gustafsson P J, Larsen H J (2001) **Modelling of finger-joint failure in glued-laminated timber beams**. *Journal of Structural Engineering*, 127(8):914-921

Sexsmith R G, Boyle P D, Rovner B, Abbott R A (1979) **Load sharing in vertically laminated, post-tensioned bridge decking**. Forintek Canada Corp., Western Forest Products Laboratory, Vancouver, British Columbia, Technical Report No. 6, ISSN 0708-6172, 18 p.

Sharpe M J (2004) **Lognormal model for stock prices**. Script notes, Course Mathematics of Finance, University of California, San Diego (UCSD), Department of Mathematics, http://math.ucsd.edu/~msharpe/stockgrowth.pdf

Shigo A (1986) **A new tree biology: Facts, photos and philosophies on trees and their problems and proper care**. Shigo and Trees, Associates, Durham, New Hampshire, USA

Showalter K L (1986) **The effect of length on tensile strength parallel-to-grain in structural lumber**. Master-thesis, Virginia Polytechnic Institute and State University, Blacksbury, VA (cit. in Williamson, 1992)

Showalter K L, Woeste F E, Bendtsen B A (1987) **Effect of length on tensile strength in structural lumber**. United States Department of Agriculture, Forest Products Laboratory, Madison, WI, FPL-RP-482, 9 p.

Sjöholm E, Gustafsson K, Norman E, Reitberger T, Colmsjö A (2000) **Fibre strength in relation to molecular weight distribution of hardwood kraft pulp: Degradation by gamma irradiation, oxygen/alkali or alkali**. *Nord. Pulp Pap. Res. J.*, 15(4):326-332 (cit. in Wathén, 2006)

Smardzewski J (1996) **Distribution of stresses in finger joints**. *Wood Science and Technology*, 30:477-489

Smith R L (1980) **A probability model for fibrous composites with local load sharing**. *Proceeding of the Royal Society London, Series A*, *Mathematicl and Physical Sciences*, 372(1751):539-553

Smith R L, Phoenix S L (1981) **Asymptotic distributions for the failure of fibrous materials under series-parallel structure and equal load-sharing**. *Journal of Applied Mechanics*, 48:75-82 (cit. in Gollwitzer and Rackwitz, 1990)

Smith R L (1982) **The Asymptotic Distribution of the Strength of a Series-Parallel System with Equal Load-Sharing**. *The Annals of Probability*, 10(1):137-171

Smith R L (1983) **Limit Theorems and Approximations for the Reliability of Load-Sharing Systems**. *Advances in Applied Probability*, 15(2):304-330

Smith I, Landis E, Gong M (2003) **Fracture and Fatigue in Wood**. John Wiley & Sons, Chichester, ISBN 0-471-48708-2

Sonderegger W, Niemz P (2004) **The influence of compression failure on the bending, impact bending and tensile strength of spruce wood and the evaluation of non-destructive methods for early dedection**. *Holz als Roh- und Werkstoff*, 62:335-342

Sørensen J D, Hoffmeyer P (2001) **Statistical analysis of data for timber strengths**. Research Report, Department of Building Technology and Structural Engineering, Aalborg University, Vol. R0132, No. 206, 61 p.

Spiegelberg H L (1966) **The effect of hemicelluloses on the mechanical properties of individual pulp fibers**. *Tappi*, 49(9):388-396 (cit. in Wathén, 2006)

Stadlober E (2005) **Wahrscheinlichkeitstheorie und Stochastische Prozesse – für Studenten der Telematik, Informatik und Softwareentwicklung-Wirtschaft**. Script, 3. Auflage, Technische Universität Graz, Institut für Statistik, 177 p. (in German)

Stadlober E, Schauer J (2007) **Statistik: Bakkalaureat Techn. Mathematik**. Script, Institute for Statistics, Graz University of Technology (in German)

Stadlober E (2011a) **Wahrscheinlichkeitstheorie für Informatikstudien**. Script, Institute for Statistics, Graz University of Technology (in German)

Stadlober E (2011b) **Stochastische Simulation**. Handout, Institute for Statistics, Graz University of Technology (in German)

Stapel P, van der Kuilen J W, Rais A (2010) **Influence of origin and grading principles on the engineering properties of European timber**. International Council for Building Research Studies and Documentation, Working Commission W18 – Timber Structures, 43rd Meeting, Nelson, New Zealand, CIB-W18 / 43-5-2

Steele B (2007) **Cellulose Nanofibers from Wheat Straw for High-value Green Nanocomposite Materials Applications**. Presentation, NDSU, MBI International, 18 p.

Steiger R (1996) **Mechanische Eigenschaften von Schweizer Fichten-Bauholz bei Biege-, Zug-, Druck und kombinierter M/N-Beanspruchung: Sortierung von Rund- und Schnittholz mittels Ultraschall**. PhD-thesis, Institut für Baustatik und Konstruktion (IBK), Eidgenössische Technische Hochschule Zürich (ETH), 182 p. (in German)

Steinebach J (2006) **Stochastische Prozesse**. Script, Mathematisches Institut, Universität Köln, www.mi.uni-koeln.de/~jost/lehre.html, 64 p. (in German)

Stich T (1998) **Bending strength of structural timber with respect to the interaction between weak zones**. L-report 9806038, Swedish Institute for Wood Technology Research, Stockholm, Sweden (cit. in Ditlevsen and Källsner, 2005; in German)

Stuefer A (2011) **Einflussparameter auf die Querzugfestigkeit von BSH-Lamellen**. Diploma-thesis, Institute of Timber Engineering and Wood Technology, Graz University of Technology, 141 p. (in German)

Stüsse F (1946) **Holzfestigkeit bei Beanspruchung schräg zur Faser**. *Schweizerische Bauzeitung*, 128(20):251-252 (cit. In Hoffmeyer, 1987; in German)

Sutherland L S, Shenoi R A, Lewis S M (1999) **Size and scale effects in composites: I. Literature review**. *Composites Science and Technology*, 59:209-220

Tanaka F (1909) Intern. Verband f. d. Materialprüfungen d. Technik. V. Kongreß, Kopenhagen 1909. Rückblick auf den Kongreß. 11. Abt.: Die Kongreßverhandlungen, 190-191 (cit. in Schneeweiß, 1969)

Tashiro K, Kobayashi M (1991) **Theoretical calculation of three-dimensional elastic constants of native and regenerated celluloses: role of hydrogen bonds**. *Polymer*, 32(8):1516-1526 (cit. in Salmèn, 2004)

Taylor S E (1988) **Modelling spatial variability of localized lumber properties**. PhD-thesis, Texas A&M University of Florida, 283 p.

Taylor S E, Bender D A (1988) **Simulating correlated lumber properties using a modified multivariate normal approach**. American Society of Agricultural Engineers, *Transactions of the ASAE*, 31(1):182-186

Taylor S E, Bender D A (1989) **A method for simulating multiple correlated lumber properties**. *Forest Products Journal*, 39(7/8):71-74

Taylor S E, Bender D A (1991) **Stochastic model for localized tensile strength and modulus of elasticity in lumber**. *Wood and Fiber Science*, 23(4):501-519

Thoma K H (2004) **Stochastische Betrachtung von Modellen für vorgespannte Zugelemente**. PhD-thesis, ETH Zurich, Switzerland, No. 15660, 119 p. (in German)

Thomopoulos N T, Johnson A C (2004) **Some Measures on the Standard Bivariate Lognormal Distribution**. Decision Sciences Institute Proceedings, Boston, 7 p.

Tiago de Oliveira J (1963) **Decision results for the parameters of the extreme value (Gumbel) distribution based on the mean and the standard deviation**. *Trabajos Estadística*, 14:61-81 (cit. in Kotz and Nadarajah, 2000)

Timoshenko S P (1983) **History of strength of materials**. Dover Publications Inc., New York, ISBN 0-486-61187-6

Tipett L H C (1925) **On the extreme individuals and the range of samples**. *Biometrika*, 17, p. 364 (cit. in Bažant and Chen, 1996)

Tonnesen M, Poulsen J S, Byskov E (1995) **Strain Localization in Clear Wood in Compression**. Computational Mechanics '95, Proceedings of the International Conference on Computational Engineering Science, Hawaii, USA, p. 1785-1790 (cit. in Poulsen et al., 1997)

van der Put T A C M, van de Kuilen J W G (2010) **Derivation of the shear strength of continuous beams**. *Eur. J. Wood Prod.*, DOI 10.1007/s00107-010-0473-3, http://www.springerlink.com/content/g65uj13tn1747m71/fulltext.pdf

van Hauwermeiren M, Vose D (2009) **A Compendium of Distributions**. Vose Software, Ghent, Belgium, www.vosesoftware.com

Vořechovský M, Chudoba R (2006) **Stochastic modelling of multi-filament yarns. II. Random properties over the length and size effect**. *International Journal of Solids and Structures*, 43:435-458

Voß W u. a. (2004) **Taschenbuch der Statistik**. Autorenkollektiv, 2. Auflage, Fachbuchverlag Leipzig, ISBN 3-446-22605-2 (in German)

Wagenführ R (2006) **Holzatlas**. Carl Hanser Verlag GmbH & CO. KG, 6., neu bearbeitete und erweiterte Auflage, ISBN 978-3446406490 (in German)

Wang Y T, Foschi R O, Filiatrault A (1990) **Random modelling of material properties in reliability studies of laminated beams**. Proceeding, International Timber Engineering Conference, Science University of Tokyo, Tokyo, Japan, 1:279-286 (cit. in Lam et al., 1994)

Wang Y T, Foschi R O (1992) **Random field stiffness properties and reliability of laminated wood beams**. *Journal of Structural Safety*, 11:191-202 (cit. in Wang et al., 1995)

Wang Y-T, Lam F, Barrett J D (1995) **Simulation of correlated modulus of elasticity and compressive strength of lumber with gain factor**. *Probabilistic Engineering Mechanics*, 10:63-71

Waser A (2004) **Eine kurze Einführung in die Global Scaling Theorie**. Raum-Energie-Forschung GmbH i.m. Leonard Euler, Wolfratshausen, Deutschland, AW-Verlag, 66 p. (in German)

Watanobe U, Norimoto M (2000) **Three dimensional analysis of elastic constants of the wood cell wall**. *Wood Research*, No. 87, 7 p.

Waterhouse J F (1984) **The ultimate strength of paper**. *IPC Technical Paper Series*, No. 146, The Institute of Paper Chemistry, Appleton, Wisconsin, USA, 37 p.

Wathén R (2006) **Studies on fiber strength and its effect on paper properties**. PhD-thesis, KLC communications, No. 11, University of Technology, Helsinki, Finland, ISSN 1457-6252, 97 p.

Weibull W (1939a) **A statistical theory of the strength of materials**. IVA, Handling Nr. 151, Royal Swedish Institute for Engineering Research

Weibull W (1939b) **The Phenomenon of Rupture in Solids. IVA**, Handling Nr. 153, Royal Swedish Institute for Engineering Research

Weibull W (1951) **A Statistical Distribution Function of Wide Applicability**. *ASME Journal of Applied Mechanics*, 51(A-6):293-297

Westman E F, Nemeth L J (1968) **Single ply vs. 2-ply laminated tension values**. *Forest Products Journal*, 18(8):41-42

Wild P M, Provan J W, Guin R, Pop S (1999) **The Effects of Cyclic Axial Loading of Single Wood Pulp Fibres at Elevated Temperature and Humidity**. *Tappi*, 82(4):209-215 (cit. in Eichhorn et al., 2001)

Wilker H (2004) **Weibull-Statistik in der Praxis: Leitfaden zur Zuverlässigkeits-ermittlung technischer Produkte**. Band 3, ISBN 3-8334-1317-4 (in German)

Williams G D, Bohnhoff D R, Moody R C (1994) **Bending properties of four-layer nail-laminated posts**. Forest Service, Forest Products Laboratory, U.S. Department of Agriculture, RP-FPL 528, 16 p.

Williamson J A (1992) **Statistical models for the effect of length on the strength of lumber**. PhD-thesis, Department of Civil Engineering, University of British Columbia, 270 p.

Williamson J A (1994) **Statistical Dependence of Timber Strength**. IUFRO – Timber Engineering, S 5.02, Sydney, Australia, 353-363

Wilson T R C, Cottingham W S (1952) **Tests of glued laminated wood beams and columns and development of principles of design**. Forest States Department of Agriculture, Forest Service, Forest Products Laboratory, Madison, Wisconsin, RP-FPL R1687

Wimmer R, Lucas B N (1997) **Comparing mechanical properties of secondary wall and cell corner middle lamella in spruce wood**. *IAWA Journal*, 18(1):77-88

Wimmer R (2002) **Werkstoffkunde Holz: Allgemeine Botanik**. Skriptum, Holztechnikum Kuchl (in German)

Winans R (2008) **Measurement and computational modelling of the mechanical properties of parallel strand lumber**. Master-thesis, Graduate School of the University of Massachusetts, 100 p.

Winkler G (2000) **Stochastische Prozesse in der statistischen Modellierung**. Script, GSF – Forschungszentrum für Umwelt und Gesundheit GmbH, IBB – Institut für Biomathematik und Biometrie, www.gsf.de/ibb, 161 p. (in German)

Woeste F E, Suddarth S K, Galligan W L (1979) **Simulation of correlated lumber properties data – a regression approach**. *Wood Science*, 12(2):73-79

Wolfe R W, Moody R C (1979) **Bending strength of vertically glued laminated beams with one to five plies**. Forest Products Laboratory, Forest Service, U.S. Department of Agriculture, RP-FPL 333, 20 p.

Wright B W (1987) **Allowable strength and durability of preservative treated glue laminated timber construction posts**. Master-thesis, Pennsylvania State University (cit. in Bohnhoff, 1990)

Xiong P (1991) **Modelling strength and stiffness of glued-laminated timber using machine stress rated lumber**. Master-thesis, Faculty of Graduate Studies, Department of Forestry, University of British Columbia, 200 p.

Ylinen A (1942) **Über den Einfluß der Probenkörpergröße auf die Biegefestigkeit des Holzes**. *Holz als Roh- und Werkstoff*, 5(9):299-304 (in German)

Zahn J J (1970) **Strength of multiple-member structures**. Forest Products Laboratory, Forest Service, U.S. Department of Agriculture, RP-FPL 139, 44 p.

Zeman J, Šejnoha M (2007) **From random microstructures to representative volume elements**. *Modelling and Simulation in Materials Science and Engineering*, 15:S325-S335

Zhang S D, Ding E J (1994) **Burst-size distribution in fiber-bundles with local load-sharing**. *Physics Letters A*, 193:425-430

Zimmermann T, Sell J, Eckstein D (1994) **Rasterelektronenmikroskopische Untersuchungen an Zugbruchflächen von Fichtenholz**. *Holz als Roh- und Werkstoff*, 52:223-229 (in German)

Zimmermann T, Thommen V, Reimann P, Hug H J (2006) **Ultrastructural appearance of embedded and polished wood cell walls as revealed by atomic force microscopy**. *Journal of Structural Biology*, 156:363-369

Zimmermann T, Richter K, Bordeau N, Sell J (2007) **Arrangement of cell-wall constituents in chemically treated Norway spruce tracheids**. *Wood and Fiber Science*, 39(2):221-231

Zobel J, Sprague J (1998) **Juvenile Wood in Forest Trees**. Springer-Verlag, ISBN 3-540-64032-0

Zupan D, Turk G (2004) **Characteristic value determination for arbitrary distribution**. WIT, Southhampton, UK, C.A. Brebbia, 503-512

Zweben C, Rosen B W (1970) **A statistical theory of material strength with application to composite materials**. *Journal of Mechanical Physics and Solids*, 18:189-206

7.2 Standards, Codes, Approvals, etc.

EP559 FEB03:2003 Design Requirements and Bending Properties for Mechanically Laminated Columns. ANSI / ASAE

DIN 4074-1:2008 Strength grading of wood – Part 1: Coniferous sawn timber

DIN 52180:1977 Testing of wood: sampling and cutting, principles

DIN 52188:1979 Testing of wood: determination of ultimate tensile strength parallel to grain

EN 338:2009 Structural timber – Strength classes

EN 384:2004 Structural lumber – Determination of characteristic values of mechanical properties and density

EN 1194:1999 Timber structures – Glued laminated timber: Strength classes and determination of characteristic values

EN 1995-1-1:2004 Eurocode 5: Design of timber structures – Part 1-1: General – Common rules and rules for buildings

pr**EN 14080**:2011-03 Timber structures – Glued laminated timber and glued solid timber

EN 14358:2006 Timber structures – Calculation of characteristic 5-percentile values and acceptance criteria for a sample

JCSS:2001 Joint Probabilistic Model Code. Part 3.02: Resistance Models: Structural Steel. Joint Committee on Structural Safety

JCSS:2006 Joint Probabilistic Model Code. Part 3.05: Resistance Models: Timber. Joint Committee on Structural Safety

OHBDC-91-1:1991 Ontario Highway Bridge Design Code. Ministry of Transportation of Ontario, Canadian Standard

Z-9.1-0623:2005 **Balkenschichtholz Duomax – Triomax**. Allgemeine bauaufsichtliche Zulassung, Deutsches Institut für Bautechnik (DIBt), Berlin, Germany (in German)

Z-9.1-0440:2009 **Duo-Balken und Trio-Balken (Balkenschichtholz aus zwei oder drei miteinander verklebten Brettern, Bohlen oder Kanthölzern)**. Algemeine bauaufsichtliche Zulassung, Deutsches Institut für Bautechnik (DIBt), Berlin, Germany (in German)

7.3 Weblinks

University of Cambridge (2010) **The structure of wood (I)**. www.doitpoms.ac.uk/tlplib/wood/structure_wood_pt1.php (2011-11-11)

Annex

8.1 Additional Data to Chapter 3

Tab. 8.1: Estimates of parameter α_ξ for various characteristics of serial systems composed of iid elements $X_i \sim$ 2pLND based on simulation results (see section 3.3.2)

CoV[X_1]$_{obs}$	***p*-values**									**mean**	**stand. dev.**	**CoV**
	0.025	**0.050**	**0.125**	**0.250**	**0.500**	**0.750**	**0.875**	**0.950**	**0.975**			
05.1%	0.178	0.168	0.160	0.150	0.143	0.140	0.139	0.138	0.139	0.138	0.812	0.679
10.0%	0.341	0.342	0.323	0.306	0.292	0.285	0.281	0.280	0.281	0.279	0.958	0.686
15.0%	0.490	0.502	0.482	0.454	0.427	0.416	0.417	0.417	0.419	0.409	1.074	0.675
20.5%	0.825	0.758	0.651	0.615	0.585	0.556	0.546	0.547	0.554	0.545	1.181	0.659
24.8%	0.816	0.758	0.772	0.752	0.707	0.693	0.688	0.693	0.703	0.670	1.337	0.676
30.4%	1.179	1.030	0.966	0.888	0.840	0.819	0.815	0.816	0.825	0.791	1.422	0.654
34.9%	1.345	1.253	1.109	1.004	0.966	0.948	0.948	0.953	0.961	0.912	1.569	0.667
40.5%	1.412	1.341	1.200	1.159	1.097	1.078	1.069	1.068	1.082	1.023	1.662	0.652
44.5%	1.551	1.513	1.356	1.290	1.233	1.204	1.200	1.225	1.230	1.148	1.814	0.665
50.0%	1.807	1.643	1.525	1.428	1.363	1.329	1.318	1.343	1.332	1.257	1.889	0.650
54.0%	1.957	1.855	1.636	1.545	1.462	1.452	1.449	1.454	1.473	1.362	2.038	0.663
59.2%	1.856	1.816	1.700	1.670	1.607	1.557	1.578	1.592	1.602	1.467	2.137	0.661
63.7%	1.817	1.824	1.864	1.773	1.677	1.651	1.662	1.682	1.677	1.543	2.200	0.657
69.9%	2.352	2.172	2.007	1.918	1.804	1.775	1.769	1.807	1.815	1.644	2.272	0.646
73.1%	2.386	2.407	2.231	2.027	1.887	1.850	1.841	1.869	1.906	1.719	2.388	0.659
80.0%	2.431	2.296	2.173	2.059	1.986	1.958	1.986	1.951	1.984	1.799	2.425	0.640
83.4%	2.633	2.449	2.320	2.215	2.075	2.009	2.025	2.057	2.111	1.866	2.535	0.655
88.7%	2.520	2.550	2.305	2.221	2.139	2.087	2.112	2.175	2.240	1.935	2.588	0.649
97.9%	3.036	2.781	2.567	2.454	2.289	2.241	2.210	2.247	2.242	2.009	2.582	0.628
97.7%	3.041	2.851	2.511	2.397	2.356	2.331	2.362	2.407	2.405	2.120	2.772	0.646

Tab. 8.2: Estimates of parameter β_ξ for various characteristics of serial systems composed of iid elements $X_i \sim$ 2pLND based on simulation results (see section 3.3.2)

CoV[X_1]$_{obs}$	***p*-values**									**mean**	**stand. dev.**	**CoV**
	0.025	**0.050**	**0.125**	**0.250**	**0.500**	**0.750**	**0.875**	**0.950**	**0.975**			
05.1%	0.116	0.138	0.170	0.221	0.302	0.391	0.475	0.573	0.643	0.328	0.515	0.553
10.0%	0.124	0.134	0.168	0.211	0.286	0.372	0.456	0.547	0.609	0.321	0.473	0.537
15.0%	0.133	0.138	0.169	0.215	0.299	0.398	0.464	0.555	0.617	0.340	0.481	0.569
20.5%	0.091	0.111	0.162	0.206	0.278	0.390	0.482	0.577	0.622	0.339	0.501	0.635
24.8%	0.130	0.160	0.177	0.213	0.296	0.387	0.464	0.543	0.583	0.350	0.461	0.580
30.4%	0.097	0.129	0.163	0.217	0.298	0.395	0.472	0.563	0.612	0.362	0.495	0.660
34.9%	0.098	0.119	0.165	0.226	0.303	0.394	0.466	0.548	0.601	0.367	0.471	0.630
40.5%	0.111	0.130	0.180	0.219	0.302	0.392	0.474	0.572	0.620	0.380	0.493	0.695
44.5%	0.114	0.128	0.175	0.220	0.296	0.390	0.465	0.526	0.584	0.376	0.465	0.656
50.0%	0.104	0.130	0.168	0.216	0.292	0.385	0.464	0.529	0.606	0.381	0.487	0.720
54.0%	0.105	0.123	0.172	0.219	0.301	0.382	0.453	0.537	0.585	0.388	0.467	0.687
59.2%	0.128	0.143	0.184	0.218	0.289	0.387	0.440	0.515	0.574	0.392	0.474	0.717
63.7%	0.148	0.160	0.177	0.222	0.305	0.397	0.462	0.534	0.602	0.412	0.494	0.736
69.9%	0.108	0.133	0.173	0.215	0.298	0.385	0.460	0.521	0.578	0.412	0.513	0.816
73.1%	0.115	0.123	0.158	0.214	0.304	0.400	0.480	0.558	0.595	0.426	0.502	0.767
80.0%	0.122	0.145	0.181	0.230	0.305	0.396	0.452	0.569	0.615	0.436	0.537	0.885
83.4%	0.114	0.139	0.175	0.218	0.306	0.415	0.484	0.557	0.586	0.448	0.527	0.837
88.7%	0.132	0.141	0.192	0.236	0.315	0.420	0.484	0.545	0.566	0.459	0.545	0.884
97.9%	0.105	0.130	0.169	0.211	0.297	0.391	0.477	0.556	0.635	0.464	0.597	1.066
97.7%	0.111	0.133	0.188	0.236	0.303	0.389	0.445	0.508	0.573	0.447	0.536	0.931

8.2 Additional Data to Chapter 4

Tab. 8.3: Characteristics of wood and timber (tissues) on different hierarchical levels: literature survey

source [--]	tissue [--]	u [%]	$E_{t,0}$ [N/mm²]	$E_{t,90}$ [N/mm²]	G_{090} [N/mm²]	$f_{t,0}$ [N/mm²]
lignin						
BERGANDER AND SALMÉN (2002)	theor.; orthotropic	12%	2,000	1,000	600	--
COUSINS (1976); BODIG AND JAYNE (1982)	tests; isotropic	12%	2,000	2,000	800	--
COUSINS (1976); COUSINS ET AL. (1975)	tests; isotropic	dry	5,500	3,100	1,200	--
PERSSON (2000)	--	12%	2,750	2,750	--	--
BURGERT (2007); SALMÉN (2004)	--	10÷20%	2,000	1,000	600	--
hemicellulose						
BERGANDER AND SALMÉN (2002)	theor.	12%	5,500	2,150	1,400	--
CAVE (1978)	model parameters	--	--	3,400	--	--
COUSINS (1978)	tests	12%	7,500	--	--	--
PERSSON (2000)	--	12%	16,000	3,500	1,500	--
BURGERT (2007)	--	dry	4,000	800	1,000	--
SALMÉN (2004); $E_{t,0}$: OLSSON (2003)	softened model p.	12%	2,000	800	1,000	--
cellulose, crystalline (cellulose I; native cellulose)						
ASHBY ET AL. (1995)	--	--	100,000	--	--	1,000
AZIZI-SAMIR ET AL. (2004)	theor.	--	--	--	--	10,000
BLEDZKI AND GASSAN (1999)	--	--	250,000	--	--	17,800
CAVE (1978)	model p.	--	--	18,000	--	--
CAVE (1978); MARK (1967); TASHIRO AND KOBAYASHI (1991)	molecular model	--	--	17,700÷27,000	--	--

source [--]	tissue [--]	u [%]	$E_{t,0}$ [N/mm²]	$E_{t,90}$ [N/mm²]	G_{090} [N/mm²]	$f_{t,0}$ [N/mm²]
GILLIS (1969)	theor.	--	246,000	--	--	--
GILLIS (1969)	theor.	--	175,000	--	--	--
KROON-BATENBURG ET AL. (1986)	crystalline model	--	319,000	--	--	--
GLOS (1999)	--	--	--	--	--	7,500
KROON-BATENBURG ET AL. (1986)	tests; I + II	--	134,000÷136,000	--	--	--
MARK (1967); TASHIRO AND KOBAYASHI (1991)	molecular model		--	--	4400÷5100	--
MARK (1983)	theor.	--	250,000÷300,000	--	--	--
MARK AND GILLIS (1970)	--	--	137,000	27,700	4,490	--
MATSUO ET AL. (1990) ; NISHINO ET AL. (1995); SAKURADA ET AL. (1962); TASHIRO AND KOBAYASHI (1991)	tests	--	135,000÷140,000	--	--	--
MATSUO ET AL. (1990); NISHINO ET AL. (1995); SAKURADA ET AL. (1962); TASHIRO AND KOBAYASHI (1991)	molecular model	--	168,000	--	--	--
MICHELL (1989)	--	--	250,000	--	--	--
NISHINO ET AL. (2004)	--	--	--	--	--	17,800
NISHINO ET AL. (1995)	tests	--	128,000 (138,000)	--	--	--
NISHINO ET AL. (1995)	--	--	138,000	--	--	--
PERSSON (2000)	model parameter	--	130,000÷170,000	15,000÷20,000	3,000÷6,000	--
ROBERTS ET AL. (1995)	--	--	--	--	--	--
SAKURADA ET AL. (1962)	theor. est.	--	134,000÷137,000	--	--	--
WATERHOUSE (1984)	theor.	--	--	--	--	19,000

source [--]	tissue [--]	u [%]	$E_{t,0}$ [N/mm²]	$E_{t,90}$ [N/mm²]	G_{090} [N/mm²]	$f_{t,0}$ [N/mm²]
SALMÉN (2004); BURGERT (2007); MARK (1967); WATANOBE AND NORIMOTO (2000)	molecular model & tests	12÷20%	134,000	27,200	4,400 (13,000)	--
TASHIRO AND KOBAYASHI (1991)	molecular model	12%	120,000÷170,000	1,800÷30,500	3,000÷5,100	--
cellulose, amorph						
WATANOBE AND NORIMOTO (2000)	--	--	110,000	22,300	10,700	--
cellulose, fibrils						
BEECHER (2007)	--	--	145,000	--	--	7,500
MARK (2002)	--	--	140,000	14,000÷46,000	--	--
MICHELL (1989)	--	--	70,000	--	--	--
STEELE (2007)	--	--	150,000	--	--	10,000
cell wall						
EDER ET AL. (2009)	early- & latewood; adult wood	--	22,000	--	--	400÷900
GINDL AND SCHÖBERL (2004); GINDL ET AL. (2004)	S2; $E_{c,0}$	15%	13,500÷21,300	--	--	--
ORSO ET AL. (2006)	--	dry	28,000	--	--	--
ORSO ET AL. (2006)	--	12%÷wet	20,000÷30,000	--	--	500÷1,000
ORSO ET AL. (2006)	$E_{m,0}$; cantilever	--	26,000÷29,000 (8÷13%)	--	--	--
WIMMER AND LUCAS (1997)	S2	--	19,700 (15%)	--	--	--
WIMMER AND LUCAS (1997)	CML	--	6,890 (21%)	--	--	--
fibre						
ASHBY ET AL. (1995)	--	--	35,000	--	--	--

source [--]	tissue [--]	u [%]	$E_{t,0}$ [N/mm²]	$E_{t,90}$ [N/mm²]	G_{090} [N/mm²]	$f_{t,0}$ [N/mm²]
ANDER ET AL. (2003)	kraft pulp; latewood	--	27,425	--	--	899÷1,452
BLEDZKI AND GASSAN (1999)	pulp	--	40,000	--	--	--
BURGERT AND FRÜHMANN (2003)	RL-cut slices	12%	6,000	--	--	42
BURGERT AND FRÜHMANN (2003)	TL-cut slices	12%	2,000÷10,000	--	--	--
BURGERT ET AL. (2005A); BURGERT ET AL. (2005B)	--	15%	12,000÷31,000	--	--	--
EDER ET AL. (2008A)	earlywood; adult wood	wet	--	--	--	553 (6%)
EDER ET AL. (2008A)	transition wood; adult wood	wet	--	--	--	706 (17%)
EDER ET AL. (2008A)	latewood; adult wood	wet	--	--	--	799 (23%)
EDER ET AL. (2008B)	earlywood; sapwood	wet	31,800 (24%)	--	--	760 (26%)
EDER ET AL. (2008B)	latewood; sapwood	wet	25,700 (14%)	--	--	861 (12%)
EDER ET AL. (2009)	earlywood; adult wood	--	2,500÷6,000	--	--	50÷200
EDER ET AL. (2009)	latewood; adult wood	--	16,000	--	--	600
GLOS (1999)	tracheids	--	--	--	--	1,200
KIM ET AL. (1975)	tests	--	--	--	--	1,130
MICHELL ET AL. (1978); MICHELL AND WILLIS (1978)	softwood; kraft-pulp	--	40,000	--	--	1,000
NAVI ET AL. (1995)	Sitka spruce; TL-cut slices	12%	1,200÷4,100	--	--	--
PAGE ET AL. (1977)	tests	--	76,900	--	--	--
PERSSON (2000)	earlywood	--	--	--	--	--

source [--]	tissue [--]	u [%]	$E_{t,0}$ [N/mm²]	$E_{t,90}$ [N/mm²]	G_{090} [N/mm²]	$f_{t,0}$ [N/mm²]
PERSSON (2000)	transition wood	--	--	--	--	--
PERSSON (2000)	latewood	--	--	--	--	--
WATERHOUSE (1984)	theor.	--	175,000	--	--	1,350
WATHÉN (2006)	earlywood	--	14,800	--	--	604
WATHÉN (2006)	latewood	--	19,684	--	--	1,045
WATHÉN (2006)	paper; zero-span-strength	--	--	--	--	155÷205 (7÷10%)
clear wood						
ASHBY ET AL. (1995)	--	--	9,000	--	--	240
BLEDZKI AND GASSAN (1999)	--	--	10,000	--	--	--
CARRINGTON (1923); HEARMON (1948)	--	12%	13,500÷16,700	400÷900	100÷850	--
DILL-LANGER ET AL. (2003)	--	12%	--	--	--	139(14%)
DILL-LANGER ET AL. (2003)	--	12%	--	--	--	128 (11%)
EBERHARDSTEINER (2002)	--	12%	10,000÷15,000	--	--	70÷100
EBERHARDSTEINER (2002)	--	--	11,000÷15,000	--	--	70÷100
GLOS (1999)	--	--	--	--	--	100
KEUNECKE ET AL. (2008)	--	12%	12,800 (9%)	397 (tan) 625 (rad) (10÷20%)	587÷617	--
NIEMZ (1993)	--	12%	10,000	--	--	90
SACHSSE (1984)	--	12%	10,800	--	--	88
SONDEREGGER AND NIEMZ (2004)	--	12%	14,510 (30%)	--	--	95 (21%)
WAGENFÜHR (2006)	--	12%	11,000	--	--	90